

BIUST Research & Innovation Symposium 2019 (RDAIS 2019)

Botswana International University of Science and Technology
Palapye, Botswana
4 - 7 June 2019

ISSN: 2521-2292

BIUST Research and Innovation Symposium 2019 (RDAIS 2019)
Botswana International University of Science and Technology
Palapye, Botswana, 4 - 7 June 2019
ISSN: 2521-2292

Copyright ©2019 by Botswana International University of Science and Technology (BIUST). All rights reserved.

Copyright and Reprint Permission:
Reproduction is permitted with credit to Botswana International University of Science and Technology.

Other copying, reprint, or reproduction requests should be addressed to Office of the Deputy Vice-Chancellor for Research, Development and Innovation, Botswana International University of Science and Technology, Palapye, Botswana.

ISSN: 2521-2292

BIUST Contact Information:
Phone: +267-493-1226
Email: balikim@biust.ac.bw

BIUST Research and Innovation Symposium 2019 (RDAIS 2019)
Botswana International University of Science and Technology
Palapye, Botswana, 4 - 7 June 2019
ISSN: 2521-2292

Preface

This volume is the Proceedings of BIUST Research and Innovation Symposium 2019 (RDAIS 2019) held on June 4-7, 2019 at Botswana International University of Science and Technology in Palapye, Botswana. It contains full papers and abstracts of submissions presented in three tracks comprising: Poster, Oral Presentation, and Innovation. The Symposium is a biennial event; the first was RDAIS 2017. The present volume constitutes Proceedings of our second Symposium.

In this Symposium, there were a total of 150 submissions at an acceptance rate of 89%. The reviews were performed based on the submitted abstracts in all three tracks. We received a total of 589 reviews from 88 reviewers, mostly BIUST academics. There were four topics, namely, Infrastructures, geology, and mining with 11 presentations, Life sciences, environment, and energy with 36, Chemistry, material science, and physics with 41, and Computations, electrical, and industries with 45. On the average, each submission was subject to four reviews, with a maximum of eight reviews given to a single submission. There were 269 authors from Botswana, and the rest of 38 authors were from Austria, Germany, India, Kenya, Mali, Nigeria, Oman, Philippines, Romania Russia, South Africa, United Kingdom, United States, and Zimbabwe. Of the 133 accepted submissions there were 57 Posters, 68 Oral presentations, and 8 Innovations. Full papers and final abstracts were submitted and compiled to the present Proceedings, that was based on the accepted abstracts from the reviews. No further reviews were performed on the full papers or final abstracts.

I would like to acknowledge the help that was supplied by many members to make the work of the Program Committee successful. First, to the reviewers who tirelessly volunteered to extend their time to perform the review. We are sincerely grateful, most especially to those reviewers who were assigned many more reviews than everyone else. Second, to the members of the Program Committee for providing me with the much needed help to complete the entire task that the committee was assigned to do. Particularly, many thanks to: Kebadiretse Lefatshe, Naledi Kefitile, Dineo Sebuso, and Wiseman Ruwona. And lastly, I would like to thank EasyChair with its free version that greatly helped us to automate the process of the review and generate the Proceedings of the Symposium.

June 4, 2019
Palapye, Botswana

Professor Rodrigo S. Jamisola, Jr.
RDAIS 2019
Program Chair

BIUST Research and Innovation Symposium 2019 (RDAIS 2019)
Botswana International University of Science and Technology
Palapye, Botswana, 4 - 7 June 2019
ISSN: 2521-2292

Welcome Message



As a Research-Intensive University, BIUST continues to strategically engage in initiatives that strengthen and highlight its core mission of Research, Development and Innovation. The Research and Innovation Symposium is one such initiative, intended to provide a collaborative platform amongst researchers, innovators and industry for sharing knowledge, showcasing innovative products and demonstration of latest achievements as well as exploration of other possible benefits that will further strengthen and advance our President's vision of transforming Botswana from a natural resources economy to a knowledge-based economy. As BIUST, we are committed to a call of coming up with products and services that will transform the lives of Batswana.

June 4, 2019
Palapye, Botswana

Professor Otlogetswe Totolo
BIUST Vice-Chancellor

BIUST Research and Innovation Symposium 2019 (RDAIS 2019)
Botswana International University of Science and Technology
Palapye, Botswana, 4 - 7 June 2019
ISSN: 2521-2292

Welcome Message



I would like to convey my immense pleasure to all the participants to the 2nd Research and Innovation Symposium in welcoming them and congratulating them for their contributions to the Symposium. The enthusiastic response to the call to contribute to this Symposium is very encouraging for the future of research in Botswana. I am sure the participants will find the presentations and the discussions exciting and very informative and will take full advantage of the networking opportunities.

This event has already carved a niche to serve as a beacon of advanced research platform in Botswana. In the years to come I have no doubt that it will develop further into a prominent platform of research initiatives and idea exchange among the Southern African nations, and I would hope far beyond as well, leading to a significant boost of the regional economies.

I would like to congratulate the organizers as well for the fantastic job they have done. I wish to all a very fruitful and satisfying few days.

June 4, 2019
Palapye, Botswana

Distinguished Professor Dennis A. Siginer
BIUST Provost & Deputy Vice-Chancellor
Academic Affairs

BIUST Research and Innovation Symposium 2019 (RDAIS 2019)
Botswana International University of Science and Technology
Palapye, Botswana, 4 - 7 June 2019
ISSN: 2521-2292

Welcome Message



This is the second symposium held by the Botswana International University of Science and Technology (BIUST) to showcase the institution's responsibility as a driver of change. Eight invited speakers will honor this event and several plenary speakers from within and outside BIUST will grace this event. My simple task is to welcome all our invited speakers, plenary speakers and all who have come from our schools and universities to be a part of this great event.

I wish everyone a very happy, fruitful and memorable symposium.

June 4, 2019
Palapye, Botswana

Professor Edward Lungu
BIUST Deputy Vice-Chancellor
Research, Development and Innovation

ISSN: 2521-2292

Welcome Message



Welcome to the Research, Development and Innovation Symposium (RDAIS 2019) of Botswana International University of Science and Technology (BIUST). In this, the second edition of the RDAIS, we combine efforts with the STEM Festival, which encourage young talents meet with experienced researchers and create forums for discussion and exchanging ideas of science, research and technology. More than 150 contributions to science and numerous inventions will be on display during the Symposium.

Development of Botswana into a knowledge-based economy requires education at all levels that is initiated by promoting interest to science among our young members of society. Experience gained from RDAIS 2017 shows us that ingenuity is there to be facilitated and to be exploited. We are looking forward to meeting you at BIUST where you can meet with postgraduate students and international reputed scientists to learn more about research, innovation and scientific methodology.

Organizing this Symposium and the STEM Festival was possible only to the continued effort of staff, students and international participants. The Organizing Committee extends our sincere gratitude for your work and support given to making this event a success.

June 4, 2019
Palapye, Botswana

Professor Jens E.T. Andersen
Overall Chair
RDAIS 2019

BIUST Research and Innovation Symposium 2019 (RDAIS 2019)
Botswana International University of Science and Technology
Palapye, Botswana, 4 - 7 June 2019
ISSN: 2521-2292

Table of Contents

Preface **v**
RDAIS 2019 Program Chair Professor Rodrigo S. Jamisola, Jr. . . . . .

Welcome Message **vi**
BIUST Vice-Chancellor Professor Otlogetswe Totolo . . . . . .

Welcome Message **vii**
BIUST Deputy Vice-Chancellor for Academic Affairs Distinguished Professor Dennis A. Siginer . . . . . .

Welcome Message **viii**
BIUST Deputy Vice-Chancellor for Research, Development and Innovation Professor Edward Lungu . . . . . .

Welcome Message **ix**
RDAIS 2019 Overall Chair Professor Jens E.T. Andersen . . . . . .

Table of Contents **x**
. . . . . .

Full Papers **1**
. . . . . .

Sustainability in Grid Computing **2**
Suresh Shanmugasundaram . . . . . .

Interaction Design Principles in Virtual Learning Tool **7**
Suresh Shanmugasundaram . . . . . .

Productivity Improvement using Value Stream Mapping in a Beef Abattoir **12**
Babedi Kufigwa and Norman Gwangwava . . . . . .

Potential of Agro-waste Briquetting for Domestic Heating and Cooking as an Environmental Management strategy in Rushinga, Zimbabwe. **18**
Gordon Tinaye Madamombe, Elia Chipfupi, Beaven Utete and Abel Olajide Olorunnisola . . . . . .

Thermal Performance Assessment of a Parabolic Trough Collector Prototype System in Palapye, Botswana **23**
Ndakidzilo Nthoiwa and Einax Mario . . . . . .

SMART Energy Meter **30**
Tshepang Letshwiti, Mompati Molibe, Patrick Mapulane and Nonofo Ditshego . . . .

Active Role of Learning Institutions in Promoting Fourth Industrial Revolution (4IR) **37**
Norman Gwangwava . . . . . .

Effect of Deposition Temperature on the Wear Behavior of WC-Co Coated Mild Steel Substrate **42**
Resego Phiri, O. P. Oladijo and E. T. Akinlabi . . . . . .

ISSN: 2521-2292

Development of a Dual Axis Solar Tracking Concept using Morphological Analysis **46**
Emmanuel Karabo Mpodi, Zeundjua Tjiparuro and Oduetse Matsebe . . . . . .

IGZO TFT versus MOSFET **54**
Unopa Matebesi, Nonofo Ditshego and Gofaone Mogosetso . . . . . .

Two Stage Stochastic Bilevel Programming using Stochastic Systematic Evolutionary(SSE) Method **59**
Natnael Goshu and Semu Kassa . . . . . .

Classification of E-Commerce Online Auctions and Prediction of Seller Reputation **65**
Valarmathi B, Kavish Pandit, Charan Kumar Pyla, Chellatamilan T and Abid Yahya

Classification of Patients Data to Predict Signs of Diabetic Retinopathy **71**
Utsav Gupta, Valarmathi B, Santhi K and Abid Yahya . . . . . .

Optimizing Cognitive Radio Deployment in Cooperative Sensing for Interference Mitigation **76**
Temitope Fajemilehin, Abid Yahya, Kibet Langat and Jayeola Opadiji . . . . . .

Airblast Prediction in Blasting Operation using Artificial Intelligence Technique **82**
Kesalopa Gaopale, Rodrigo S Jamisola Jr and Itumeleng Seitshiro . . . . . .

Application of Artificial Neural Networks to Predict Blast-Induced Ground Vibration in a Diamond Mine **88**
Kesalopa Gaopale, Rodrigo S Jamisola Jr and Itumeleng Seitshiro . . . . . .

Design of a Solar Charge Controller for DC Load Output **94**
Patrick Kandjise, Kesego Petso, Pelonomi Tito and Bokani Mtengi . . . . . .

Energy Requirement Analysis for the Design of Solar Photovoltaic Micro-grids in Botswana – A Study of Jamataka Village **101**
Kealeboga Motladiile, Tobias Bader, Mervyn Smyth, Adrian Pugsley and Jayanta Mondol . . . . . .

Lamellipodial Motility of a Squared Shaped Cell - Mathematical Model **107**
Matlhogonolo Rakakae and Sachin Shaw . . . . . .

A Smart Borehole Water Pumping System **116**
Mpho David and Mmoloki Mangwala . . . . . .

Regulated Photovoltaic for Rural Electrification **122**
Kennedy Motswedi, Otsile James Mabutho, Gosatla Kelebogile Ramontsho and Samikannu Ravi . . . . . .

Machine Learning for Maximum and Minimum Temperature Analytics and Prediction at Local Level **126**
Tsaone Swaabow Thapelo and Rodrigo S. Jamisola . . . . . .

Anti-Poaching System using Wireless Sensors **135**
Karabo Bogaisang, Odirile Gamoshe, Dennis Maina and Abid Yahya . . . . . .

ISSN: 2521-2292

Numerical Fluid Mechanics Study of Effect of Rear Slant Length on the Drag of an Idealized Road Vehicle **138**
Pollard Pako Mogotsi, Thato Phologolo and N Subaschandar . . . . . .

Study of Effect of Tailgates on the Drag of an Idealised Road Vehicle using Numerical Fluid Mechanics **143**
Kenneth Bogatsu, Thato Phologolo and N Subaschandar . . . . . .

Autonomous Trash Collector Robot with Wireless Charging System in a Campus Environment **147**
Analene Montesines-Nagayo, Bindu Pv, Mazna Said Hamdan Al Saidi, Ammar Said Al Hosni, Ali Khamis Al Kharusi and Rodrigo Jamisola Jr . . . . . .

A Smart and Solar-Powered Solid Waste Segregator with Cloud-Based Wireless Monitoring System in a School Campus **154**
Analene Montesines-Nagayo, Eugene Vega, Omar Rashid Al Maqbali, Ammar Yousuf Al Farsi and Rodrigo Jamisola Jr . . . . . .

Book of Abstracts **161**
. . . . . .

On the Sphere Bundle on Grassmannians **162**
Oteng Maphane and Jean Baptiste Gatsinzi . . . . . .

Optimal Portfolios for an Investor who Receives Stochastic Income **163**
Kebareng Moalosi-Court and Edward Lungu . . . . . .

Assessing the Impact of Wastewater Irrigation on Antibiotic Resistance Dynamics and Bacteria Species Diversity using Soil Microcosm Experiments **164**
Onthatile Onalenna and Teddie Rahube . . . . . .

Impact of the Stress Jump and Slip Conditions on the Dispersion During Nanoparticles Based Drug Delivery -Two Phase Model **165**
Annah Janet Moitoi and Sachin Shaw . . . . . .

The Role of Epidemic Plasmids in Antibiotic Resistance Dissemination across Different Environments **166**
Juliet Eze and Teddie Rahube . . . . . .

Production of Biodiesel from Scinzionphyton Rautanenii (Manketti) Nut Oil by a Heterogeneous Catalyst **167**
Keene Mmusi and Sebusi Odisitse . . . . . .

Automatic Dog Feeder **168**
Seth Kurusa, Aobakwe Kenyaditswe, Obakeng Odumetse and Nonofo Ditshego . . . .

GC-ECNI-MS and Quantum Chemistry Application: Effects of Substituents on the Stability of P-Benzoquinone **169**
Nonofo Samuel, Kwenga Sichilongo and Foster Mbaiwa . . . . . .

Chalcones: Towards the Synthesis of Bioactive Heterocyclic Compounds **170**
Lesego Lilian Masutlha and Ofentse Mazimba . . . . . .

Polyphenols and Antiparasitic Activity from Rangelands Plants **171**
Olekile Tibe, Baghali Guys Mathapa and Othusite Madibela . . . . . .

ISSN: 2521-2292

Total Phenolic Content and Antioxidant Activity of Cowpea Leaves (Vigna Unguiculata (L) Walp) in Botswana **172**
Olekile Tibe, Baghali Guys Mathapa and Bakang Tiro . . . . . .

Significance of Contact and Mating on the Long Term Dynamics of Devil Facial Tumour Disease. **173**
Morelyn Sigauke and Hatson John Boscoh Njagarah . . . . . .

Fermentative Microbiota of Khadi, a Traditional Wine of Botswana **174**
Koketso Motlhanka, Kebaneilwe Lebani and Nerve Zhou . . . . . .

A Dual -Arm Robotic Nurse(DARN) for Assistance in Healthcare Facilities **175**
Tlamelo Makati, Dimpho Kgosiemang and Tagala Smarts . . . . . .

Integrated Solar and Wind Hybrid System with Remote Monitoring **176**
Jeet Parikh, Tariku Alemayehu, Janardan Yadav and Ravi Samikannu . . . . . .

Developing a Miniature Train to Deliver Medicines and Documents in Hospitals **177**
Leaname Thaolang, Tapologo Chigocha and Kebalebile Oteng Telekelo . . . . . .

The Physico-chemical Properties and Geochemical Mass Balance of Two Weathering Soil Profiles in Letlhakeng **178**
Yvette Matshameko and Peter N Eze . . . . . .

Estimating the LS Factor of the Rusle Model in a Gis Based Environment for Two Semi Arid Watersheds **179**
Thatayaone Popego and Peter Eze . . . . . .

In Silico Evaluation of Phytocannabinoids as Peroxisome Proliferator-Activated Receptors (PPARs) Agonists for Type 2 Diabetes Mellitus Therapy. **180**
Keagile Bati and Tebogo E. Kwape . . . . . .

Design and Implementation of Electronic Variable Speed Number Counting Game for Young Learner using PIC 16F887 Microcontroller **181**
Phalaneng Maphane . . . . . .

Surface Water Demand and Supply of Gaborone City and Surrounding Areas: Response to Climate Change and Population Increase **182**
Bosa Mosekiemang and Gizaw Mengistu Tsidu . . . . . .

Extraction and Characterization of Croton Gratissimus Leaf Essential Oil from Botswana **183**
Eniah Serame, Tshepo Pheko-Ofitlhile and Wellington Masamba . . . . . .

Development of a Clean Energy Driven Autonomous Vehicle Designed for All-Terrain Drive and Beauty **184**
Thabo Malete, Maikano Vryburg, Bakang Mokgethe and Kagiso Moilwa . . . . . .

Impact of Stress Jump Condition and Heterogeneous Reaction on Velocity, Temperature and Concentration During Bio-fluid Flow Through a Permeable Microvessel. **185**
Godfrey Bashaga and Sachin Shaw . . . . . .

ISSN: 2521-2292

Modelling Substance Abuse in Botswana in Presence of Multiple Amelioration Stages and Outpatient Rehabilitation **186**
Thatayaone Lucas Gasebonno and Hatson John Boscoh Njagarah . . . . . .

Assessment of the Sensitivity of Primary Cells and Cell Lines to the Southern African Territories (SAT) Serotypes in the Diagnosis of Foot-and-Mouth Disease Virus **187**
Tshephang Iris Kabelo, Kebaneilwe Lebani and Elliot Fana . . . . . .

Environmental Biotechnology of Extremophiles: Application of Alkaliphiles for the Biological Treatment of Industrial Effluents **188**
Amare Gessesse . . . . . .

Viscosity Type Douglas-Rachford Splitting Methods for a Zero of the Sum of a Finite Family of Maximally Monotone Mappings in Hilbert Spaces **189**
Getahun Bekele, Habtu Hailu and Boikanyo Oganeditse . . . . . .

Spatio-Temporal Drought Analysis under a Changing Climate over Botswana using Standardized Precipitation Evapotranspiration Index **190**
Onneile Nomsa Keitumetse and Gizaw Mengistu Tsidu . . . . . .

Synthesis and Characterization of Ruthenium (II/III) Polypyridyl Complexes with Anti-microbial Properties. **191**
James T.P. Matshwele, Sebusi Odisitse and Florence Nareetsile . . . . . .

RU(II/III) Complexes of Polypyridyl Ligands with Anti-bacterial Properties. **192**
Lebogang Julius, Daphne Mapolelo and Florence Nareetsile . . . . . .

Improving Energy Efficiency in Botswana's Hotel Sector – a Systematic Review of Energy Audit and Management Principles and Previous Findings **193**
Bao Motshwanaesi, Botsogo Kefalotse, Thebe Kgare, Tsotlhe Leshetla and Tobias Bader

Review of Solar Cooling and Air-conditioning **194**
Taboka Motlhabane and Tobias Bader . . . . . .

A Review: DNA Recombination Technology and Different Expression Systems used in the Production of Recombinant Proteins. **195**
Keletso Gorata Masisi and Goabaone Gaobotse . . . . . .

The Role of Nickel and Cobalt Nano-particles on Biogas Production from Abattoir Wastewater **196**
Mpho Radipodi and Gofetamang Ditalelo . . . . . .

Feasibility Study on the Utilization of Solar-photovoltaic Technology for Water Pumping and Electrification of an Agro-pastoral Farm **197**
Godiraone Gaedupe, Michelle Matlapeng, Kamogelo Lesole, Ketshephaone Keisang and Tobias Bader . . . . . .

Autism Meltdown Detection Device **198**
Tshiamo Tsheole and Pearl Nthusang . . . . . .

Review on performance and processing of natural fibers for thermal insulation purposes **199**
Nametso Linda Moumakwa, Eyitayo Olatunde Olakanmi and Tobias Bader . . . . . .

ISSN: 2521-2292

A Study of Energy Performance of Hotel Buildings in Botswana **200**
Mushabi Pule, Segolame Phegelo and Tobias Bader . . . . . .

Preservation Methods for Herbarium Specimens in Botswana **201**
Jakob Michael, Tobias Schrag and Tobias Bader . . . . . .

Bat Guano and the Risk of Contacting Histoplasmosis on BIUST campus **202**
Lefang Leo Chobolo, Monamodi Kesemang, Modise Goodwell, Emmanuel Sekopo, Leungo Daddie Mukoka, Galaletsang Makgarebe Dintwe, Naledi Gonnye, Precious Mpofu, Nerve Zhou and Tharina Louise Bird . . . . . .

Optimization of Ultrasound Assisted Extraction Method for HPLC-DAD UV/VIS Determination of Flavonoids in Medicinal Plants and Evaluation of Ace Inhibition Activity **203**
Katso Binang and David Takuwa . . . . . .

Quality of Water with Respect to Carbonyl Compounds in Selected Water Bodies in Botswana **204**
Neo Mogatsaseno and Kwenga Sichilongo . . . . . .

Making Silver Incarcerated Microporous Ceramic Membranes for Water Purification **205**
Bogadi Pako Letsile, Gorata Pearl Morake and Rachel Utlwang Bikimane . . . . . .

Wireless Sensor Networks Based Localization and Tracking: Roadside Livestock Monitoring System **206**
Lone Godfrey Future Kolobe, Adamu Murtala Zungeru and Joseph Chuma . . . . . .

A Biopsy Needle Detection Tool for 3D Ultrasound Imaging **207**
Nayna Ann Moni, Bakary Diarra and Boyce Sigweni . . . . . .

Development of Analytical Methods for Determination of Efavirenz using GC-MS and HPLC for Applications in Forensic, Clinical and Environmental Analysis **208**
Wangu Masenga, Kwenga Sichilongo and Giacomo Paganotti . . . . . .

Dunaliella Salina Microalgae Medium Optimization for Lipid Production using Response Surface Methodology. **209**
Kevin Nyoni, Leungo Kelebopile and Lesedi Lebogang . . . . . .

Characterization of Selected Honey from Different Floral and Geographical Origins including Botswana **210**
Tumelo Padiso and Kwenga Sichilongo . . . . . .

Drone Forensics: How the Growing use of Drone Creates New Challenges for Digital Forensics Investigation **211**
Peter Gblorso . . . . . .

Structural and Optical Properties of Ce-doped CuO Nanoparticles Prepared by Hydrothermal Synthesis **212**
Romang Bosigo, Lucia Lepodise and Cosmas Muiva . . . . . .

Design and Simulation of a Human Lower-Limb Enhancement and Rehabilitation Exoskeleton **213**
Olebogeng Mbedzi and Zimele Gwebu . . . . . .

ISSN: 2521-2292

SolaNetwork - Integrated and Affordable Solar Energy Access Solutions for Socioeconomically Diverse Rural Communities in Botswana **214**
Adrian Pugsley, Samikannu Ravi, Mervyn Smyth, Tobias Bader and Jeet Parikh . . .

Enhanced Peroxidase-like Activity of Silver Nanoparticles Doped Magnetic Nanoparticles for Sensitive Detection of L-cysteine **215**
Micode Mazhani, Melisew Tadele Alula and Davison Murape . . . . . .

Comparison of Measured Global Solar Radiation to Estimated Global Radiation Using the Liu and Jordan Method for the Locality of Gaborone, Botswana **216**
Bashi Thipe . . . . . .

Leveraging Indigenous Knowledge in Rural Botswana through Grass Roots Innovation **217**
Thabiso Mashaba . . . . . .

Analysis of the Impacts of Livestock Sedentarism on Soil Carbon Fluxes in the Kalahari Ecosystem **218**
Mooketsi Bitsang, Oagile Dikinya, Bothepha Mosetlhi and Boago Moganane . . . . . .

Density Based Traffic Light Control System **219**
Kaloso Mpho Tlotleng, Lame K Mosoboloko, Otlaatla Marumo and Moses Mosate . .

A Secured SMART Home Switching System Based on Wireless Sensor Networks **220**
Jwaone Gaboitaolelwe, Adamu Murtala Zungeru, Nonofo Ditshego and Joseph Chuma

Analysis of Energy Consumption Patterns in Tourist Lodges forImproved Energy Efficiency - The Case of Kwadiwa Lodge in Botswana **221**
Katlego Seleofeng Rahube, Tshepho Letshwenyo, Boitumelo Elizabeth Makatane, Tshepiso Mokoka and Tobias Bader . . . . . .

Variations in Kinetics of Coal Pyrolysis at Different Size Ranges and Heating Rates using a TGA **222**
Mmoloki Makoba, László-Zsolt Szabó and Paul Serban Agachi . . . . . .

Survival, Growth and Heavy Metal Accumulation of Vetiver in Different Mine-Affected Soils as Influenced by Fly Ash and Compost Amendments **223**
Oarabile Lefadola, Trust Manyiwa and Venecio Jr Ultra . . . . . .

Status of Renewable Energy in Botswana - Part 1: Conventional Energy Supply, Solar Potential & Framework **224**
Tobias Bader . . . . . .

Status of Renewable Energy in Botswana – Part 2: Higher Education, Research and Trends **225**
Tobias Bader . . . . . .

Using Drones for Warehouse Management and Quelea Birds Control **226**
Kenaleone Sebikiri, Oteng Sephiri, Bernum Masu and Gaopalelwe Tsima . . . . . .

Resistivity Surveying in Geothermal Exploration at a Hot Spring in Kasane Region, Northwest of Botswana. **227**
Calistus Ramotoroko, Anneke Thiede, Andreas Junge and Elisha Shemang . . . . . .

ISSN: 2521-2292

Survival and Growth of Vetiver in Heavy Metal Contaminated Mine Tailings Amended with Cow Manure and Mycorrhizal Fungi **228**
Kushatha Pabalinga July and Venecio U. Jr Ultra . . . . . .

Temporal Dynamics of Heavy Metals from Different Mine Tailings and Contaminated Soils as Influenced by Soil Amendments Based on Lysimeter Studies **229**
Trust Manyiwa and Venecio Ultra Jr . . . . . .

Forensic Science Practice in Botswana: Prospects and Challenges **230**
Paul Ogbole Peter . . . . . .

Heavy Metal Speciation and Availability in Soils from the Vicinity of Bamangwato Concessions Ltd (BCL) Mines as Influenced by Fly Ash and Compost Amendments **231**
Boitshwarelo Setuwe, Ultra Venecio and Serwalo Mokgosi . . . . . .

Design of a Recycling Waste Plastic Mini Plant **232**
Thabo Mokomo, Emmanuel Kootswetse and Albert Ude . . . . . .

Characterization of Individual Atmospheric Particles in the Gaborone Urban Aerosol, using Scanning Electron Microscopy-Energy Dispersive X-ray Spectroscopy (SEM-EDX/EDS) **233**
Douglas Gobe Phuthego . . . . . .

Design of a GSM-Based Fingerprint Access Control System **234**
Keene B. Ntesang, Lefika Molebatsi, Mothusi Lebogang and Adamu Murtala Zungeru

PGEs in chromitite concentrated by exsolution? **235**
Alexander Proyer . . . . . .

Gem diamond growth caused by exsolution? **236**
Alexander Proyer . . . . . .

From Fundamental to Applied Sciences: A Potential New Type of Batteries and Sensors Based on Stress in Crystal Structures **237**
Alexander Proyer . . . . . .

Diamond genesis: The ultimate challenge for a petrologist **238**
Alexander Proyer . . . . . .

Peridotite Xenoliths from Letlhakane mine: A Comparison of Geothermobarometers **239**
Alexander Proyer, Christoph Hauzenberger and Lukas Belohlavek . . . . . .

Generation of Artificial Waves Optimized for Surfing in a Water Pool **240**
Lucky Odirile Mohutsiwa, Tiro Gaogape, Mmilili Thibedi and Maemo Rathedi . . . .

Morphological Classification of Radio Galaxies Using Machine Learning **241**
Tselanngwe Seleka and Rodrigo Jamisola . . . . . .

A Framework for Enhancing Security for IOT Enabled Banking Services **242**
Pendukeni Phalaagae, Adamu Murtala Zungeru, Boyce Sigweni and Joseph Chuma . .

ISSN: 2521-2292

Software Defined Radio (SDR) Based Visible Light Communication (VLC) System **243**
Gaopalelwe Sefako, Lame Matsuokwane and Naledi Maniki . . . . . .

Nutritive Value of Silage from Maize and Sorghum Inoculated with Urea or Saccharomyces Cerevisiae **244**
Mmoloki Thuto, Othusitse Madibela, Moemedi Legodimo and Fiona Nermark . . . . .

Optimal Constraints Considerations of Energy Harvesting System for Seismic Nodes **245**
Dauda Duncan, Adamu Murtala Zungeru, Mmoloki Mangwala, Bakary Diarra and Joseph Chuma . . . . . .

Autonomous Quadrotor Risk Minimization for Law Reinforcement Applications **246**
Onalethata Maswabi . . . . . .

Biometric Fingerprint Recognition in Forensic Science; A SMART Approach **247**
Botho Modukanele and Onalethata Maswabi . . . . . .

High-Level Density of K-states in Neutron-Rich Tantalum Nuclei **248**
Nyaladzi Palalani . . . . . .

The Technical and Economic Feasibility Study to Produce Chemical Fertilizers in Botswana **249**
Bokamoso Phuthego and Paul Agachi . . . . . .

A Comparative Study of the High Fluence Neutron Irradiation Effects on the Optical and Structural Properties of Blue and Green Emitting Plastic Scintillators. **250**
Gaogalalwe Mokgatitswane and Chamunorwa Oscar Kureba . . . . . .

Anticancer Activity of Ruthenium Complexes **251**
Sumbikane Gasebonwe, Florence Nareetsile, Daphne T Mapolelo, Melvin M Leteane and David O Nkwe . . . . . .

Evaluation of Safflower Genotypes for Growth, Yield Components and Seed Yield **252**
Maatla Korononeo . . . . . .

Evaporative Cooling for Botswana: A Case Study **253**
Pradeep Sahoo . . . . . .

Program of Activities **254**
. . . . . .

Opening Programme **255**
. . . . . .

Program of Activities, Tuesday, 4 June 2019 **256**
. . . . . .

Program of Activities, Wednesday, 5 June 2019 **257**
. . . . . .

ISSN: 2521-2292

Program of Activities, Thursday, 6 June 2019 **260**

Closing Programme **263**

Appendices **264**

Reviewers for Topics 1& 2 **265**

Reviewers for Topics 3& 4 **266**

RDAIS 2019 Working Committee **267**

Author Index **268**

BIUST Research and Innovation Symposium 2019 (RDAIS 2019)
Botswana International University of Science and Technology
Palapye, Botswana, 4 - 7 June 2019
ISSN: 2521-2292

Full Papers

BIUST Research and Innovation Symposium 2019 (RDAIS 2019)
Botswana International University of Science and Technology
Palapye, Botswana, 4 - 7 June 2019

ISSN: 2521-2292

Sustainability in Grid Computing

Suresh Shanmugasundaram
Professor, Department of Engineering
Botho University, Gaborone, Botswana
Email: srec_suresh@yahoo.com

***Abstract*— Grid computing are integrated environments in which software and hardware resources are pooled in ways that give any user the impression of working with a single fast computer. This paper examines the current advances in grid computers from the point of view of their structures, global attention and support. With the advancement of technology, the working of grid based computations have been simplified where each computer's resources are shared with every other computer in the system. The major resources that are considered to be vital in the grid computing platform are the processing power, memory and data storage. These are treated as communal resources rather than as individual resources and thus promoting resource sharing for all the authorized users. This provision helps to perform on-demand services over the Internet and supports a wide variety of applications that requires huge processing power and heavy storage for data. One of the challenges due to this sharing platform that provides services on adhoc basis is to maintain sustainability. The main goal of this paper is that discuss a model that is at the conceptual level and directing it for further research.**

Keywords—Grid Computing; Sustainability; Energy; Resource usage; conceptual model

I. INTRODUCTION (*HEADING 1*)

The grid architecture comprises of Fabric layer, Connectivity layer, Resource layer, Collective layer and Application layer. The grid architecture is also well known for its large scale geographical heterogeneous distribution and the major challenge in resource sharing from this large sale consumer and provider scheme is the usage of energy and administration of resource sharing. To solve this challenge of having to maintain a grid computational efficacy, a large number of researchers proposed resource management policies, algorithms and architectures but energy-efficiency is still a challenge and there is lot of scope for future researchers. One proposed solution to overcome one of the issue is to have a fuzzy logic based SVM approach to secure a collision free path avoiding multiple adhoc obstacles [1] to handle dynamic resource scheduling. This Fuzzy logic based approach takes care of dynamic resource sharing while the major challenge is due to the security issues and inability to sustain itself due to its scalable nature. Handling both sustainability and energy-efficiency simultaneously can solve new open challenges existing in the resource scheduling. Different geographical weather and climatic scenarios may also be considered to take the advantage of temperature setting available for having a coolant system. Grid computing offers an effective administration of resources, which conserves or limits energy usage by curtailing the quantity of physical servers. Additionally, it lessens the administrative and management charges and offers added flexibility and scalability for commercial development. This paper includes a review of current trends in grid computing and available options; creation of awareness of the importance of grid computers; and conceptual model for sustainable grid framework.

II. CURRENT TREND IN GRID COMPUTING

A. Resource Discovery and Utilization:

The growth rate in network bandwidth is progressing at a faster pace than that of CPU speed which means that the way to make best use of computing power is to grid the computers in a efficient way conserving the energy [2]. Grid Computing is realized as the indispensable computing technology allowing the progression of all sciences. The components of grid computing architecture comprise of possibly remote, dynamic, heterogenous, untrusted computing resources. For a seamless provision of grid services, the processes such as authentication that takes care of the genuine nature of the user identification, authorization that allows the users to access certain resources (Virtual Organization), Resource Access that allows authorized users to remotely access resources and Resource Discovery that enables a way to determine and identify the remote resources that they can use, are considered vital. Each process as it has to comply over the remote infrastructure, is quite challenging an requires various means to economically sustain as the challenges in deployment on such a large scale is unavoidable. Grid Economics has been in detailed discussion for years and several researches have put forth several models. One such model has been proposed for the blade servers [3], where the blade servers are considered to be akin to grid computer nodes this incentive based model that could help motivate the resource providers to come forward as they get some incentives. The performance analysis for blade operations in a commercial platform is depicted in figure 1.

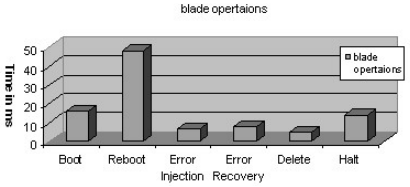


Figure 1: Performance Analysis

Owing to the performance gained, this concept is acquisitioning acceptance intended for their numerous advantages in their performance parameters such as fast

ISSN: 2521-2292

computing, compact nature, effortlessness of management, energy efficiency etc and these parameters are akin to the grid architecture in the internet backbone.

B. Grid Economics

An incentive based system has been proposed [4] to motivate the resource providers for the provision of the spare CPU time and this global billing system attempts to have precision by maintaining the track of CPU time used, CPU time provided by the resource providers and also the transactions pertaining to the incentives. However, in order for a world-wide billing system to work, there will need to be some way of accurately keeping track of the CPU time used, the CPU time provided by each user and a way of transferring incentives among the users. The system [4] proposed is scalable and also trusted that makes this framework doable. VO-wide resource allocation scheme to minimize cost [4] in order to meet a user's job and increase the mutual-reliability among the users of the GRID. However, the challenge here is in terms of the revenue generation to provide these incentives. For example, if an application is run in micro seconds through grid resources rather than taking up seconds to complete, the charge could be anywhere between 10 currency units to 100 currency units or even more depending upon the resources that were deployed and their geographical location. Some of the algorithms proposed takes care of using resources that costs minimal and certainly in the above example, there are means to allot resources that cost 10 currency units and not 100 units. One such procing paradigm is the Dynamic Pricing for multi-products in Grids [5]. While the costing can be calculated based on the ISP charges, the challenge lies in the sustainability factor of this framework. Furthermore, this model computes the optimum pricing by identifying locally available resources, where the demand is given exogenously. As it is a well known fact, dynamic users who join and leave the Virtual organization is common and the resource consumer who leaves the VOs without payment is quite possible and hence this might lead to failure of the framework. Hence a model is required that could provide this grid framework in a sustainable way. This conceptual is possible as Internet of Things is advancing day by day.

III. Grid Computer Framework

A. Cost Factors

Grid computing provides a flexible computing ambience through virtual organisations with internet as the primary backbone. In the previous section, one of the cost factor, the charges proposed by Internet Service Providers has been described. However, there are several other cost factors that play a critical role and contribute to the costing in the framework, such as, energy that is required to run the processors, type of applications and their design, storage that is required to save and retrieve records from the database management system.

B. Energy consumption

It is well known fact that energy is hugely consumed for computations based in a grid computing environment as stated in the preceding section. Consider figure fig 2 which illustrates a typical computation that is carried out in a grid platform. The applications that are run could be analytical, transactional or mere report generation. However, it requires an extensive integration of collaborative execution of tasks, coordination of resources with load balancing as well critical intelligent management of data that consumes huge amount of power both by resources provider and resource consumer and in some cases also by the Broker as there is utilization of processor, storage, memory, network and coolants.

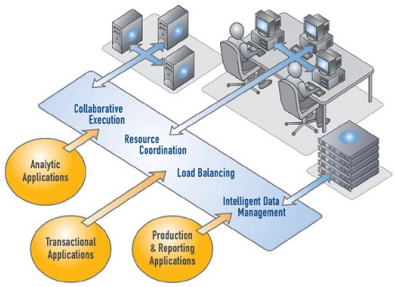


Figure 2: Computations in Grid Platform

In grid, the energy consumption varies as per the grid component. Figure fig 3 illustrates the energy consumption of different components in grid.

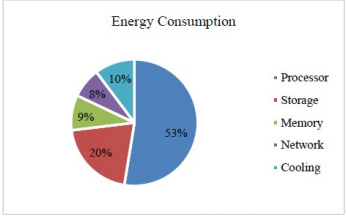


Figure 3: Energy Consumption of different parameters

ISSN: 2521-2292

One of the sustainable development goals[6] is to "Ensure access to affordable, reliable, sustainable and modern energy for all" which is classified as goal 7: affordable and clean energy and this calls for conserving energy and also to consume it sensibly and this applies to the Grid computing architecture as the trend is moving towards Greening the computations. Either it be a static or dynamic energy consumption, the energy management technique handles resource consolidation and resource management. Proactive management administers the resource management based on the future prediction and this could be based on the fuzzy logic and also recognizing the process pattern.

C. Cooling Mechanisms

For data grids, racks of database servers are placed to serve the queries that are from remote nodes and thus this needs a constant usage of servers that easily gets heated up. Hence the heat generation process can be regulated through cooling management system and this management system must ensure that the cooling mechanism is improvised as well as conserve the energy used for cooling. Scheduling that is based on the ambient temperature as well as the servers computational duration can be taken into account for this and the parameters that could be optimized by this are the execution time, energy cost, energy consumption, internet bandwidth cost, energy consumption and power cost and all this are operable in the heterogeneous workloads with reliability of service and increased security without compromising the environment sustainability.

D. Metrics used for Energy and power cost

An energy reduction and conservation technique require a metric to measure the energy consumed at a given point of time and also must provide a cumulative pattern. Some critical metrics[7]that are required are Power Usage Efficiency(PUE), Total Cost of Ownership(TCO) and Coefficient of Performance (CoP). Avoid combining SI and CGS units, such as current in amperes and magnetic field in oersteds. This often leads to confusion because equations do not balance dimensionally. If you must use mixed units, clearly state the units for each quantity that you use in an equation.

Expression 1:

$$PUE = \frac{\text{Total Energy Usage by ICT devices}}{\text{Energy Consumed by all the Devices(IT and non-IT)}}$$

Expression 2:

$$TCO = \text{Indirect Cost} + \text{Direct Cost}$$

Expression 3:

$$CoP = \frac{\text{Removed Heat}}{\text{Work done for heat removal}}$$

Expression 4[8] :

$$\textit{Carbon Usage Effectiveness (CUE)} = \frac{\text{Total CO2 emissions produced}}{\text{Energy IT equipment}}$$

Expression 5[9]:

$$\textit{Water Usage Effectiveness(WUE)} = \frac{\text{Annual Water Usage}}{\text{IT Equipment Energy}}$$

The above expression provide means to measure sustainability aspects of carbon, energy and water and the units of WUE is measure in litres per kilowatt-hour.

E. Conceptual Model for Sustainable Grids:

The above challenges must be addressed to have a long term benefit from the grid architectural framework. This also motivates the resource providers to come forward for sharing resources and thus having a world-wide integration of resources. The major components of this conceptual model is the Grid architecture, Database repository, Green Computing Resource Manager & Coolant System and User Interface via IoT. All the components are interlinked and provide inputs to others for mutually recognizing the pattern and thus attempt to achieve a long term self-sustained benefits.

F. Layered Architecture of Grid Computing System:

Consider the four-layer model of grid computing system[10] with node and interconnection layer, node system software layer, Grid system software layer and application layer. Interconnection layer consists of high performance of computer, large-scale database server, largescale file server, computer cluster, large communication equipment and high-speed interconnection network connecting these resources. Nodes system software layer includes operating system software, large-scale database system software, large-scale file system software, cluster system software, network connection protocol large equipment driver etc. Resource management, data management, user management, task management, information services, authentication and authorization are implemented in Grid system software layer. Figure 4 depicts the grid computing architecture with four layers. Additionally, a fifth layer could be added for integrating for security policies that would cater for the authentication and authorization of user nodes in the grid.



Figure 4: Layered Grid Computing Architecture

ISSN: 2521-2292

G. Database Repository Grid:

A Database Repository Grid is an assortment of low-cost sectional storage arrays integrated and retrieved by the nodes in the Grid. With the Database Repository Grid, building up a pool of system resources is possible, and this can be accomplished dynamically, that is, allocating and deallocating the resources on demand basis which is determined by the computational priorities. Figure 5 exemplifies the Database Repository Grid in a Grid enterprise computing environment and this is linked up with the grid architecture. The incoming user workload are also managed at this layer which is transferred to the grid manager for further action.

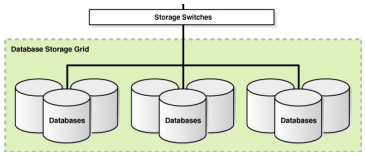


Figure 5: Database Repository

H. Green Computing Resource Manager & Coolant System:

The green computing and coolant system are primary modules of the infrastructure and they are administered by the Manager. This layer has the information pertaining to grid datacentres. The power management unit and automatic transfer Switch are used combinedly to manage the energy coming from both renewable and non-renewable sources. The provision of renewable source is to back up when the non-renewable could not generate power that would suffice. Figure 6 illustrates the infrastructure module that has both Green computing and coolant system manager. Thermal profiling and thermal scheduling is taken care at the coolant system that is integrated to the green computing unit. The ambient temperature and also the nodes temperature are all monitored by the thermal sensors. This has the significant role to switch between renewable and non-renewable source.

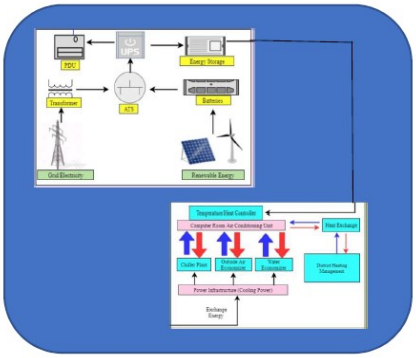


Figure 6: Infrastructure Module

I. User Interface via IoT

As the interactions via internet are becoming smaller and cheaper, and other technological advancements like IPv6, flash memory chips, smart phones usage, evolution of Internet of Things(IoT) has become prominent and thus has opened up prospects for interesting integration of applications to substantially meeting the needs in the underlying technology. The IoT paradigm is not only seen efficient, scalable, reliable, secure and trustworthy which are required for the sharing resources with in the virtual organizations of the grid architecture but also seen as the one of the module that could become indispensable for any advanced distributed paradigm such as the grid or cloud. The mobile applications and also the mobile processors, storage can also be utilized for this through a single touch of the screen. Also, the weather conditions during the mobility could change variably and this could be an added advantage for energy conservation and thus could provide inputs to the other modules such as the cooling manager and the infrastructure module. Technically the mobile nodes can also act as mobile sensors. Figure 7 exemplifies the application of IoT in Grid Computing framework.

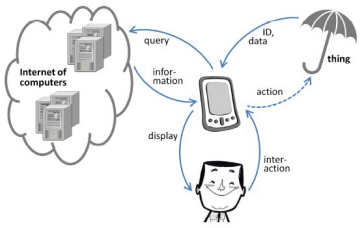


Figure 7: IoT Paradigm

IV. Integration of the Modules:

As explained in the previous segments, the integration of the modules is the key to derive the proposed conceptual model for Grid Computing framework to achieve sustainability. The integration could provide sustainable and reliable service in the grid ambience. It is also believed that through this integrated model, capacity planning, usage of renewable energy where possible and utilization of waste heat generated will certainly be improvised offering the users a reliable service while the infrastructure remains sustainable and this is shown in figure 8.

ISSN: 2521-2292

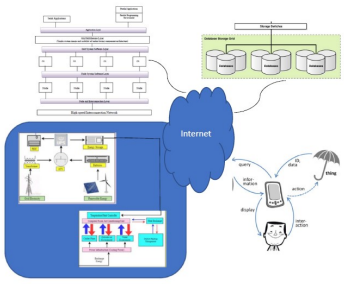


Figure 8: Integrated model for Sustainable Grid Computing

The objective of reducing power consumption certainly affects the reliability of grid services and this is could be prevented by the enhanced energy-aware resource management that needs tight integration among the four modules that could provide the amount of energy consumed from various sources and thus could conserve energy wherever possible and also without compromising the quality of grid services. The workloads that require constant power could be use the non-renewable source of energy while the workload that require minimal time duration can always switch to renewable source.

V. Conclusion

In this paper, a conceptual model for sustainable grid computations is proposed by analysing existing methods and approaches that could be applied in primary parameters such as application, energy, scheduling and internet of things paradigm. Each of the parameters were analysed with their advantages and limitations. The model also allows the provider to have the flexibility to a certain degree to allocate these jobs according to his resource utilization. Future work on this topic is required that allows to have improvised approaches that could enhance the performance of the service has been considered in this model, hoping that a detailed taxonomy for this model will be analysed that could propose various future research directions.

References

[1] Shanmugasundaram Suresh, Jeeva Poornaselvan, Chidambaram Divya Preya, "OPTIMAL PATH PLANNING APPROACH TO GRID ENVIRONMENT", POLLACK PERIODICA, An International Journal for Engineering and Information Sciences, DOI:10.1556/Pollack.6.2011.1.12, Vol. 6, No. 1, pp. 131–140 (2011), www.akademiai.com

[2] D. Laforenza. Grid programming: some indications where we are headed. ACM Parallel Computing Special Issue: Advanced environments for parallel and distributed computing, pages 1733–1752, 2002.

[3] Shanmugasundaram Suresh, "Availability Analysis of Dynamic Blade Servers in Ecommerce Platform", International Journal of Emerging Technology and Advanced Engineering Website: www.ijetae.com (ISSN 2250-2459, ISO 9001:2008 Certified Journal) Volume 5, Special Issue 2, April 2015.

[4] Suresh, S., Gayathri, C.G. and Birahadish, P. "Incentive-based Scheduling Framework for Grid Computing", Proc. of the International Conference on Software Engineering and applications (SEA 2007), Cambridge, USA, pp. 596-602,November 19-21, 2007.

[5] Arun Anandasivam and Dirk Neumann, "Managing revenue in Grids", Proceedings of the 42nd Hawaii International Conference on System Sciences, 2009

[6] United Nations, "The Sustainable Development Goals Report – 2017", available at https://unstats.un.org/sdgs/files/report/2017/TheSustainableDevelopmentGoalsReport2017.pdf

[7] Sukhpal Singh Gill and Rajkumar Buyya, "A Taxonomy and Future Directions for Sutainable Cloud Computing: 360 Degree View", Sustainability Clouds 2017.

[8] Dan Azevedo, M. Patterson, J. Pouchet, and R. Tipley. "Carbon usage effectiveness (CUE): a green grid datacenter sustainability metric." The green grid (2010).

[9] Dan Azevedo, Symantec Christian Belady, and J. Pouchet. "Water usage effectiveness (WUE™): A green grid datacenter sustainability metric." The Green Grid (2011).

[10] M. K. Singh & S. Pal, "Five Layer Security Architecture & Policies for Grid Computing System", International Journal of Computer Science and Information Technologies (IJCSIT), Vol. 2 (3) , 2011, 1312-1314

BIUST Research and Innovation Symposium 2019 (RDAIS 2019)
Botswana International University of Science and Technology
Palapye, Botswana, 4 - 7 June 2019

ISSN: 2521-2292

Interaction Design Principles in Virtual Learning Tool

Suresh Shanmugasundaram
Professor, Department of Engineering
Botho University, Gaborone,
Botswana
Email: srec_suresh@yahoo.com

ABSTRACT

As e-learning methods in Universities continue to grow, it becomes significant to recognize the usability challenges that are linked with the tools like Blackboard. Blackboard is being used in Botho University, so it is essential that the usability of its user-interface is assessed. This paper presents the outcome of assessment towards adherence of Design Principles in Blackboard from the student user perspective at Botho University, Botswana. As the University is shifting from conventional teaching mode to the contemporary blended mode a slow progress in using Blackboard is observed among the learners. It is critical to increase the usability by addressing imbalances, that are observed during this study. The challenges and frustration that these user groups experience when using the Blackboard system for learning purpose cannot be ignored as it has a severe impact on the usability and user experience. Addressing this issue to have an increased effective usage can be seen as main agenda in the Learning, Teaching & Assessment Strategy (LTA) of Botho University. For this, gathering the learners' opinion is critical to this agenda, who learn, a specific module under a programme that could be offered under any of the Faculties. The study used Blackboard as a VLE tool to get the participants' opinion in terms of their ability to acclimatize various components in Blackboard that is related to the design principles. The study is performed by using evaluation questionnaires collected from students, who are the users of Blackboard. It is found that users are more satisfied with some more expectations concerning the tool's usage. The study identified issue of low internet bandwidth as a primary hinderance to use Blackboard and the need for more trainings and this has been recommended to increase and enhance the accessibility and usability of the software.

Keywords

Blackboard; Interaction Design; Design Principles; E-Learning.

1. INTRODUCTION

Computers have now become indispensable gadgets available to everyone who can afford them irrespective of any social differences and is available in almost parts of the world [1]. In Botswana, there has been a significant adaptation of computers and computing systems that has resulted in having more interactive systems in education and training. Students at Botho University have been using Blackboard for self-learning purposes. It also helps them to respond to formative assignments that would provide an evaluation on their performance during the course of study. The notion that such a tool can be used only for distance learners has been disproved and all students of different learning modes use the Blackboard platform at Botho University. Apart from downloading learning materials, the students also use the discussion forum where they share and learn with their peers. Several reasons could influence the usability and the user experience of Blackboard. In this study, the design principles for Interaction Design are examined and each of them is evaluated to see the extent to which the existing design principles are working and where there are challenges. This research project primarily intends to explore and examine user experience and usability factors when it comes to the relationship between a computing system(Blackboard) and humans (students).

2. RESEARCH AIMS

2.1 Problem Statement

Blackboard in Botho University has been deployed for inculcating independent learning amongst students. Before the deployment of Blackboard, the lecturers relied on email to share the learning materials. The study guides and assignments were also posted in File Transfer Protocol (FTP) server. However, as more programmes were introduced, many learners had to be given different privileges to access the modules that were registered by them. Hence there was a need to deploy a better learners management system. Botho University believed that there will be a better learner experience thus improvising the student performance. However, the users at Botho University often do not explore the features to the full and this is evident from the usage report dated 19 February 2018 shown in table 1. The user activity overview for the days between 5 February and 19 February clearly indicates that the "Average Login Time Per User Per Day in Hours" was 0.10 hours and the "Average Logins" was 6.47 while the total number registered users were 5105 and the total number of modules were 627. The design principles [2] play a critical role in achieving the usability and user experience goals and hence a thorough evaluation of Blackboard by using these principles will help us to measure the effectiveness to a certain extent. Understanding any software application and its features by the users relies on the design of the application's interface. Blackboard, a tool that is primarily used by teachers and students has been consistently recording less usage at Botho University. It is anticipated that evaluation of Blackboard on the aspect of design principle will help the University to alleviate this issue.

ISSN: 2521-2292

Table 1. Blackboard Usage report Source: System Usage Activity Blackboard

User Activity Overview

Course	All Available Courses
Availability	
Nodes	All Nodes
Terms	All Terms
Number of Courses	627
Number of Users	5105
Date Range	02/05/2018 - 02/19/2018

Activity is shown for enrolled users only.

User Activity Overview

User Activity by Day

02/05/2018 - 02/19/2018

Average Login Time Per User Per Day in Hours	0,10 Hours
Average Logins	6,47

2.2 Research Objectives & Questions

The evaluation of a virtual learning system like the Blackboard is an important exercise to recognize the requirements of the learner; the challenges faced by different user groups and thus provide ways of improved usage. As such, the aim of the study is to assess the current level of usability of Blackboard at Botho University among various student groups. The main objectives of this study are, to:

i) Explore the heuristic design principles of the Blackboard platform at Botho University.
ii) Investigate the perceptions of different user groups on the effectiveness of Blackboard design principles being used.
iii) Identify the challenges faced by different users arising from the design principles and recommend ways to achieve greater satisfaction of learning.

Following from the stated objectives, the research questions for this study are:

a)What are the heuristic design principles used on the Blackboard platform at Botho University?
b)What key challenges do users face resulting from the heuristic design principles?
c) How can the heuristic design principles be improved upon to achieve greater effectiveness, efficiency and satisfaction in learning?

3. LITERATURE REVIEW

3.1 Background

Interaction Design is the discipline that helps the application developers to plan the interface as per the behavior of human-computer systems like the Blackboard Learners Management system. The official ISO 9241-11 [3] definition of usability is "the extent to which a product can be used by specified users to achieve specified goals with effectiveness, efficiency and satisfaction in a specified context of use" [4]. Interaction design also focuses on improving User-experience goals [2] by developing interactive products that are "satisfying, enjoyable, fun, entertaining, helpful, motivating, aesthetically pleasing, supportive of creativity, rewarding and emotionally fulfilling" and these are equally important as efficiency and productivity at work.

3.2 Design Principles of the Blackboard

Design principles framed by Norman provide heuristic guideline that are relevant in designing any interactive product. The design principles that are relevant for Blackboard are visibility, feedback, constraints, mapping and consistency. Each of the principles are defined in the section that follow. The adherence of those principles in Blackboard is also explained along with the challenges identified.

3.2.1 Visibility

Visibility is the rudimentary principle emphasizing that more noticeable an element is in the interface, the more probable the users will be aware of them and how to use them.

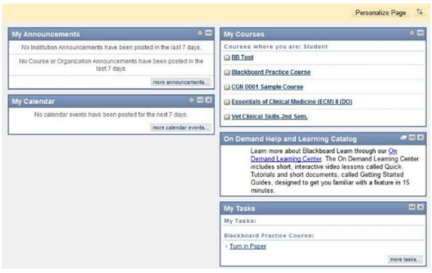


Figure 1. Blackboard Visibility

In Figure 1, the Blackboard provides good visibility of all the required components. The ability to apply this principle is realizing that not everything can be made visible, because it'll ultimately clutter the interface but instead need to rank the interface elements in terms of relevance and place them.

3.2.2 Feedback

Feedback is one of the design principle of making it understandable to the user on what action has been taken and what actions have been achieved and this could be an error message or simple label that guides the user to accomplish a task in Blackboard such as assignment creation, submission, grading of marks.

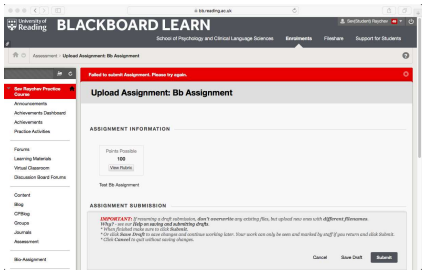


Figure 2. Blackboard Feedback

Figure 2 shows the error messages and pop up dialogs that guides the user on how to proceed further. The key challenge while adhering to this principle is that the lecturers sometimes may not use appropriate settings that could validate the actions of their learners and this eventually leaves the user assuming on what action they have taken and the repercussion of doing so ensuing in user frustration.

3.2.3 Constraints

Constraints is one of the design principles that puts an emphasis on restricting the range of options to interact for the user that simplifies the interface and direct the user to the relevant subsequent actions. Blackboard provides the feature to set various constraints by the instructional designers for their respective batch of students as shown in Figure 3. The adaptive release feature provides the facility of setting various constraints to the student groups.

ISSN: 2521-2292

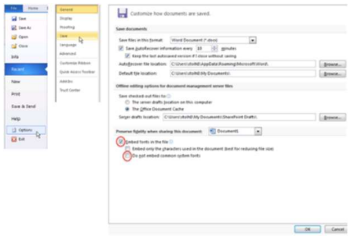


Figure 3. Blackboard Setting Constraints

3.2.4 Mapping

The design principle mapping defines on having a clear association between controls and the outcome they have on the real world. Blackboard uses sets of known icons and controls that enables the users to have easy navigation.

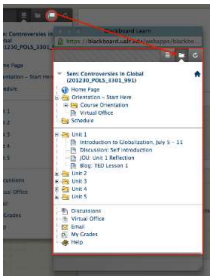


Figure 4. Blackboard Mapping

3.2.5 Consistency

The design principle consistency states the emphasis on evenness in having comparable operations and comparable elements for achieving similar tasks. An instructional designer, by providing consistent elements all over the interface, will make the learners' experience far easier to use. Blackboard interface provides similar elements for all the users in order to make it easily usable in their respective domains. The key elements that are available for ease of access are illustrated in the figure 5. Element A marked in figure 5 is "My Blackboard" and the user menu that are available everywhere in Blackboard Learn and gives the users a personalized view of the online environment. Element B displays relevant course data from all of the users'. Element C shows all the Modules on the "My Institution" stub and this controls which modules to appear on student page. Element D is the "Add Module" that is used to see the list of modules offered in a semester. Element E is the "Personalize Page" that enables the users to customize their page by allowing them to change the color scheme of the page and this provides an instructional designer to have good designs. It is often observed that both interface design of the blackboard and the instructional design plays a critical role to empower the students and facilitating learning.

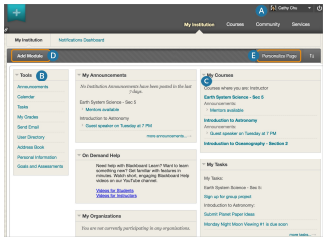


Figure 5. Blackboard Consistency

3.3 Student Attitudes about Technology

Applying technology in academia becomes effective only after an active usage by the students. The present generation of students use social networking sites with utmost convenience and that would certainly support the students to appreciate and apply the online educational tools for their learning process. Despite this fact, the assessments regarding the appreciation of students to apply educational technologies and the evaluation pertaining to the usability and user experience for VLEs like Blackboard are still under research in Botswana [5] and this is similar in other parts of the world [6]. One of the studies[5], elucidate that many learners could use Blackboard effectively when they were given clear guidance. Young university Batswana graduates who have easy access to internet are often unenthusiastic to use the educational tools. It is important to note that "Digital Competence is both a requirement and a right of citizens, if they are to be functional in today's society[7]." The current issues that prevail could challenge the usage of Blackboard discussion forums and the effective usage of VLE at Botho University.

3.4 Interaction Design & Evaluation

A main aim of interaction design to redress the gap between the interactive products which was engineered as a system which perform a set of functions and how the system was used by the real people by bringing usability into the design process. Virtual teaching tools such as the Blackboard and most of the learning activities in electronic mode necessitates familiarization of the interface of the application and its navigability and the scholars who may not have acceptable computing skills could become unwilling to learn using these web tools [8]. Heuristic evaluation is a usability review procedure initially created and established by Jakob Nielsen and team [9][10], where the design professionals, directed by a collection of usability principles known as heuristic, assess if the design interface components, such as dialog boxes, menus, navigability features, online help etc., confirm the required norms. The above theory of heuristic evaluation is carried out, to understand the successful implementation of heuristic principles with the main focus on the Blackboard users who may knew the benefits of Blackboard system and yet struggle to use due to unforeseen issues in interactivity [11].

4. RESEARCH METHODOLOGY

4.1 Research Methods

The research method used for conducting this study was the survey of students who use the Blackboard at Botho University that was carried out through the use of questionnaires. A comparison was also made between various groups of users. This data collected and analysis done were based on the questionnaires filled.

4.2 Population and sample selection

The study was conducted in all the Faculties of Botho University, namely the Faculty of Computing(FOC), Faculty of Business and Accounting(FBA), Faculty of Health & Education (FHE), Faculty of Engineering & Applied Sciences(FEAS) and Faculty of Hospitality & Sustainable Tourism (FHST). A target population describes a group of individuals, objects and aspects that may contribute through the amount of valid information they could provide (Kahane, 1992). The target population for this research study were those who are using Blackboard at Botho University for learning purposes. The population for the study consisted of around 1000 students who enrolled with "active" status in Botho University and a number of registered users of Blackboard VLE,

ISSN: 2521-2292

for the modules taught from June 2015 onwards June 2018. As per the Blackboard usage report generated on 19-Feb-2018, there were typically 418 Module Batches that use Blackboard for instruction. For this study, the total number of student participants were 136 valid responses.

4.3 Methods of data collection

For the survey, Evaluation of Blackboard Design Principles for Students Questionnaire (EBDPSTUQ) for students was developed. The questionnaires were created using Google forms and copies were distributed to all the users through email with a brief description of the study and clear instructions on how to fill them. The procedure then required the completion and signing of a waiver and ethical clearing documents, the participants were allowed to respond to the questionnaire. The questionnaires were structured in a way to enable the participants to respond to each question based on their own experience with Blackboard and the impact of the usability and user experience as a barrier to use Blackboard. The questionnaires also had sections that allowed for descriptive comments. Closed-ended questions were included and structured in a manner that participants could only respond them in a pre-defined section or by choosing from the predefined options. These were typically entry level questions which do not require long descriptive answers. The questionnaire was pilot tested before the actual data collection process by sending it to a small group of students. The feedback received from the group was used to rephrase the questions to avoid anomalies. Google forms also had the feature to download real-time questionnaire responses in multiple formats (e.g. excel) which was then coded and analyzed using SPSS. The 'analysis' feature in SPSS allowed the researcher to perform reliability testing including the missing data by applying the Cronbach Alpha to measure the internal consistency and further analysis was done only after verifying if the acceptable reliability value was close to 0.6.

4.4 Ethical Considerations

In any research project and particularly where humans are invited to participate, there should be procedural means to guard those who actively participate and the information they may divulge (Broome 1984). All the ethical considerations that is required to conduct this study was adhered to and as a first step, an application to the research permit was made to the Department of Research, Science and Technology, Botswana and the permit was received on June 14, 2018 and this enabled the researcher to proceed with administering the questionnaires. The researcher disclosed his full identification to the participants before starting the data collection process. The consent forms had been signed by participants and each participant had received an electronic copy of the statement of interest from the researcher. The form was designed in a way that if a potential member failed to complete and sign the consent form, the questionnaire will not proceed to the next section and hence data will not be collected.

5. Discussion, Interpretation of Results and Recommendations

5.1 Interpretation

The interpretations of the outcome of the survey are discussed in relation to the research questions, as set out in section 2.3. Table 2 shows the percentage of student participation from various programmes. Students pursuing Bachelors programme had the highest participation with 61%, followed by students pursuing Masters programme with 21.3%. The remaining contribution were from students pursuing Professional Diploma with 10.3%, Diploma with 2.2 %, post graduate certificate with 1.5% and post graduate diploma with 3.7%.

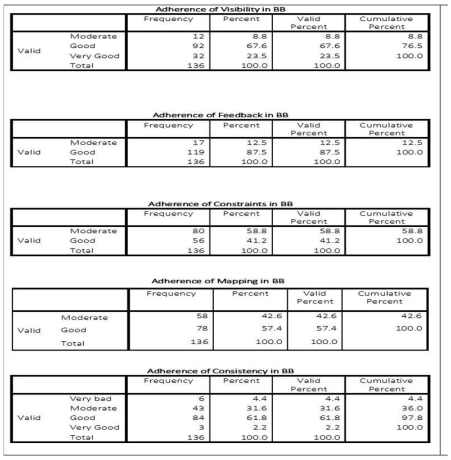
Table 2. Programme Level Participation of Students

		Frequency	Percent	Valid Percent	Cumulative Percent
Valid	Bachelors	83	61.0	61.0	61.0
	Masters	29	21.3	21.3	82.4
	Professional Diploma	14	10.3	10.3	92.6
	Diploma	3	2.2	2.2	94.9
	Post Graduate Certificate	2	1.5	1.5	96.3
	Post Graduate Diploma	5	3.7	3.7	100.0
	Total	136	100.0	100.0	

5.1.1 What are the heuristic design principles used on the Blackboard platform at Botho University?

The first and foremost research question for this study was to determine the design principles that are being adhered in Blackboard being used by students at Botho University. Evidence from this study suggests that students have a positive opinion on the adherence of design principles in Blackboard. From table 3, it is observed that 91.1% of student participants felt that Blackboard interface adhered to the 'Visibility' Design principle and 8.8% of the participants rated moderate for this statement. For the design principle 'Feedback', 87.5% of student participants had rated as 'good' while 12.5% rated it as moderate.

Table 3. Adherence of DP in Blackboard



Adherence of Visibility in BB

		Frequency	Percent	Valid Percent	Cumulative Percent
Valid	Moderate	12	8.8	8.8	8.8
	Good	92	67.6	67.6	76.5
	Very Good	32	23.5	23.5	100.0
	Total	136	100.0	100.0	

Adherence of Feedback in BB

		Frequency	Percent	Valid Percent	Cumulative Percent
Valid	Moderate	17	12.5	12.5	12.5
	Good	119	87.5	87.5	100.0
	Total	136	100.0	100.0	

Adherence of Constraints in BB

		Frequency	Percent	Valid Percent	Cumulative Percent
Valid	Moderate	80	58.8	58.8	58.8
	Good	56	41.2	41.2	100.0
	Total	136	100.0	100.0	

Adherence of Mapping in BB

		Frequency	Percent	Valid Percent	Cumulative Percent
Valid	Moderate	58	42.6	42.6	42.6
	Good	78	57.4	57.4	100.0
	Total	136	100.0	100.0	

Adherence of Consistency in BB

		Frequency	Percent	Valid Percent	Cumulative Percent
Valid	Very bad	6	4.4	4.4	4.4
	Moderate	43	31.6	31.6	36.0
	Good	84	61.8	61.8	97.8
	Very Good	3	2.2	2.2	100.0
	Total	136	100.0	100.0	

For adherence of the 'Constraints' design principle, 41.2% rated as good and 58.8% rated as moderate. For the design principle 'Mapping', 57.4% of student participants had rated as 'good' while 42.6% rated it as moderate. For adherence of the 'Consistency' design principle, 64% rated as good or very good, 31.6% rated as moderate and 4.4% rated as bad. It is observed that the student participants felt that the adherence to all design principles except 'Consistency' were rated as either moderate or good. However, for consistency, few (4.4%) felt that this design principle was not adhered to. The reason could be perhaps, a student might be doing various modules in a semester, and each instructional design might vary as per the nature of the module and hence an inconsistency could have been observed by the participants. Other than this principle, the students rated towards positive range. It is also important to note that a significant percentage of student respondents have opted for "moderate" responses in this section and this indicates that students could not clearly express if that specific design principle is adopted in

ISSN: 2521-2292

Blackboard. The other point of significance which is worthwhile to record is that the students at Botho University from various Faculties were learning through blended mode, that is, mix of both face-to-face classes (guided learning) and independent learning through Blackboard and the lecturers may have instructed students in class on how to use Blackboard that could have led towards this positive rating.

5.1.2 What key challenges do users face resulting from the heuristic design principles?

For the questions pertaining to 'identifying the completion of task like uploading assignment' and 'achieving the objective when participating in discussion forums' in Blackboard, 30.9% and 42.6% of students indicated 'easy' respectively. When the students were asked to list one positive aspect that they liked the most, 44.9% of them stated that Blackboard is user friendly and 22.5% of them responded that it is simple. It can be observed that only 6.6% have appreciated the discussion forums. When the students were asked to list the negative aspect of Blackboard from their experience that could hinder them to use blackboard, 33.8% of students expressed that 'face to face' teaching is better when compared to the online discussions and 27.2% of them claimed that internet bandwidth is not adequate to use it effectively.

5.1.3 How can the heuristic design principles be improved upon to achieve greater effectiveness, efficiency and satisfaction in learning?

The student participation from various Faculty groups in Botho University, the Faculty of Computing shows a high percentage of participation with 50.7% followed by 41.9% from Faculty of Health and Education. The remaining percentage of student participation was from Faculty of Engineering & Applied Sciences and Faculty of Business and Accounting with 2.9% each, with the Faculty of Hospitality and Sustainable Tourism having 1.5%. The results might vary if other Faculties contributed equally as that of the students from the Faculty of computing as they have good appreciation of software tools and this could have influenced the rating. However, with the collected data, it is clear that the users from all groups must come forward to use the tool, so as to achieve greater effectiveness, efficiency and satisfaction in learning.

6. CONCLUSION

From the view of students, Blackboard allows peer learning, independent learning and easy uploading of assignments and hence found it to be useful tool. With the overall rating being above average, the following recommendations that are based on the inferences were derived. Though the issue of the internet is not related to the design principles, the researcher appreciates the need for good bandwidth to reduce user frustration when using Blackboard and thus recommends that the Blackboard Administration Team should resolve this issue at the earliest possible time. The Blackboard Administration team must provide extensive training to both students and staff in terms of usage. Also, a specific training on achieving consistency through instructional design must be conducted for the staff on a regular basis. An extensive study to compare various tools that are being used at different institutions in Botswana will be useful as Botswana Government is moving towards new regulations and outcome-based education, and it is believed that such research would certainly emphasize the shift of teaching and learning practice from user-centered design to learner-centered design.

7. ACKNOWLEDGEMENTS

My sincere thanks to the Ministry of Education and Skills Development, Botswana for permitting to undertake this study and to the management, colleagues and friends at Botho University who gave me the support to carry out this study.

8. REFERENCES

[1] Madrigal, D. and McClain, B.(2010). *Do's and Don'ts of Usability Testing* [Online]. UX Matters Archive. Available from:https://www.uxmatters.com/mt/archives/2010/03/dos-and-donts-of-usability-testing.php.

[2] Rogers, Y., Preece, J., & Sharp, H. (2015). *Interaction Design: Beyond Human-Computer Interaction*. 4thEdn, London: Wiley publications.

[3] ISO (International Standard Organization) (2017) ISO 9241-110. *Ergonomics of Human-System Interaction*. London: ISO.

[4] Garrett., J.J. (2010). *The Elements of User Experience: User-Centered Design for the Web and Beyond*. 2nd Edn. Berkeley: New Riders, Peachpit a division of Pearson Education.

[5] Uziak,J.(2009). Acceptance of Blackboard Technology by Mechanical Engineering Students at the University of Botswana. *International Journal of Engineering Education* [Online], 18(3), 19-23. Available from: http://ubrisa.ub.bw/jspui/retrieve/1819

[6] Johnson, D., & Johnson, R. (2003). *Joining together: Group theory and skills*. Needham Heights, MA: Allyn & Bacon.

[7] Ferrari, A. (2012). *Digital Competence in Practice: An Analysis of Frameworks*. Joint Research Centre of the European Commission. Report number: EUR 25351 EN.

[8] Alelaiwi,A., & Hossain, M. S., (2015). Evaluating and Testing User Interfaces for E-Learning System: Blackboard Usability Testing. *Journal of Information Engineering and Applications*. 2224-5782. 5(1).

[9] Nielsen,J.,& Molich, R.(1990). Heuristic evaluation of user interfaces. *Proceedings of the SIGCHI Conference on Human Factors in Computing Systems*01 - 05 April **1990**, Seattle, Washington, USA.

[10] Nielsen, J.(1994). Technology Transfer of Heuristic Evaluation and Usability Inspection.Keynote presentation at: *International Conference on Human-Computer Interaction*, June 25-291994, Lillehammer, Norway.

[11] Ojha, S.R.,Jovanovic, M., Giunchiglia, F.(2015). Entity-centric visualization of open data. *Proceedings of Interact 2015 Conference*, September 14-18. Bamberg, Germany. Verlag: Springer, pp. 149-166.

[12] Kahane, H. (1992). *Logic and Contemporary Rhetoric*. Belmont. CA: Wadsworth.

[13] Broome, J. 1984. Uncertainty and fairness. *The Economic Journal* 94(375):624–632.

BIUST Research and Innovation Symposium 2019 (RDAIS 2019)
Botswana International University of Science and Technology
Palapye, Botswana, 4 - 7 June 2019

ISSN: 2521-2292

Paper Title: Productivity improvement using value stream mapping in a beef abattoir

[1]Babedi Kufigwa *, [2]Norman Gwangwava

Babedi Kufigwa (corresponding author)
Department of Mechanical, Energy and Industrial Engineering
Botswana International University of Science and Technology (BIUST)
Palapye, Botswana
babedi.kufigwa@studentmail.biust.ac.bw /
bdecah@gmail.com

Norman Gwangwava
Department of Mechanical, Energy and Industrial Engineering
Botswana International University of Science and Technology (BIUST)
Palapye, Botswana
gwangwavan@biust.ac.bw

Abstract— **Beef abattoirs continue to face challenges of improving productivity, in order to remain successful in a highly competitive industry. As every input cost goes higher year on year, it is important to provide better products, processes and services at lower costs to the end user by improving process cycle time efficiency of the plant. The aim of this paper is to illustrate the implementation of value stream in a beef abattoir to improve productivity. This study started with conducting site visits, touring the plant, conducting interviews, direct observation and conducting time study for the existing current production process. Current process was mapped to identify problems and bottlenecks within the beef abattoir. Long manufacturing lead time, waiting or delays within the production and too much time spent on handling the carcass. In order to address these productivity inefficiencies in a beef abattoir; future state map, estimated calculated process improvements and suggestions were proposed on how value adding time can be improved. These proposed improvements and calculated process cycle time efficiency could lead to a better system for the organization under study. The contribution highlights 21-23% process cycle time improvements and efficiency.**

Keywords: beef abattoir; cycle time efficiency; process improvement; value stream mapping

Introduction

Beef abattoir in Botswana are impeded by production inefficiency, long manufacturing lead time and unoptimized business process. In today's competitive world, productivity is one of the components that lead to successful industrial organizations. Increase in productivity can reduce the cost of work or increase in output. Productivity depends on various factors such as labour, machinery, raw materials and quality. To reduce these production inefficiencies and remain competitive with other companies, meat processing industry and other abattoirs, companies use a variety of different methods. One of the main methods is lean manufacturing. Main aim of lean manufacturing tools is to reduce waste in an operation, such as long lead time, production inefficiencies, waiting, defects and waiting. Value Stream Mapping is a lean tool that visual display where waste occurs in the process. Value stream mapping are often used assess current manufacturing processes as well as create ideal and future state processes. For this research paper, an abattoir was chosen as an industry to work with. This study is to illustrate the implementation of value stream mapping in an abattoir to improve productivity is mainly focused on the production of carcass, that is from the cattles are received from the abattoir building up until now the carcass is delivered to the customer. The focus of this study is to illustrate the implementation of value stream mapping in an abattoir to improve productivity. Current value stream with the help of time study and observations were made to identify bottlenecks in the process. Conclusion and proposed improvements were made based on the data accumulated from observations and time study analysis.

I. Literature Review

This section of the report provides a brief background on the documents, literatures sources and other documentary reports that were used to solve productivity and production inefficiencies through value stream mapping. Productivity, lean manufacturing and value stream in an abattoir were crucial topics to consider when studying this research area. Value stream mapping is a lean manufacturing tool which originated from Toyota Production System (TPS) and uses techniques of lean manufacturing to analyze and evaluate certain work processes in a manufacturing operation [1]. Value stream mapping (VSM) is used to find waste in the value stream of a product. Once waste is identified, then it is easier to decide to eliminate it and the purpose of VSM is process improvement at the system level [2]. The key benefit

ISSN: 2521-2292

to value stream mapping is that it focuses on the entire value stream to find system wastes and try to eliminate the pitfall [3]. Value stream mapping in a product or a service as a flow of sequence of activities from the beginning to end in a form of visual representation accompained with lead times [4]. The authour adds that this tool is a core element of lean transformation because it gives a basi blueprint for various changes needed to move from from a disconnected, dysfunctional flow kind environment one where material flows smoothly from one process to the next to the next, rather than making isolated improvements to individual activities within a larger value adding process. Value stream mapping provides an overall structure for applying other tools and kaizens, and for seeing beyond the symptoms of wastes to real root causes [5]. Furthermore the author stated that there are three essential parts in a value stream map, which information, material flow map and lead time ladder.

Information flow- depicts the current state of the value stream map, observing the flow of data or infrormation at the top of the map. Here the customer communicates daily requirements to the production control section via fax, verbal, email or through phone call.

Material flow- depicts the movement of product from raw material to finished product

Lead time ladder- summarizes the cycles times(i.e value adding time in each process) per piece and it is contrasted with total time spent in the value stream.

[1 - 5]stated that value stream mapping can be created simply using a pen or pencil, nevertheless more advanced maps are created using microsoft visio as well as excel. Moreover, the author further statedd that VSM is divided into five basic steps which are identifying the product, creating a current VSM, evaluating the current map by identifying problem areas, creating a future state VSM and lastly implemting the final plan. The first step in value stram mapping is choosing a specific product the VSM will focus on, then followed by creating an initial VSM current process [6]. Atter the current map has been completed; the team evaluates the process and the process and the steps involved. All this data is then compiled on a map and analysis is performed. Furthermore the author stated that parameters such as cycle time, Takt -time, work-in progress (WIP), set up time, down time, number of workers, and scrap rate are included in each step. Non value adding time will be shown at each step [1 - 6]. Moreover , the author stated that problem areas is identified after analysing and evaluating the current process of the product so as to create the final VSM state [6] .Final state is created after the current process has been changed and the problem areas has been minimized [6]. The last step of the value stream mapping process is to implement new ideas and thus turning a more efficient lean manufacturing process [6]. Benefits of value stream map were stated by [1 – 6] as it helps to visualize more than the single process level, links material and information flow, provides a blueprint for implementation, and it ties together lean concepts and techniques.

A. Background of beef industry in Botswana

Most Botswana families own cattle and are a potential stakeholder in government support to the beef value chain [7]. According to [8] cattle are both a production good that is being a draught power, transport and calves and consumption good (as milk, meat & hides) and a form of saving for future consumption and production. Cattle production in Botswana is highly cyclical, depending upon rainfall and pricing structures [9]. Farmers sell animals during droughts, flooding the market with poor-quality animals and driving prices down, and they rebuild their herds when rainfall is good reducing the number of animals for sale and driving up prices [8 – 9]. Productivity is the relationship between the outputs generated from a system and the inputs that are used to create those outputs. It is concerned with the efficiency and effectiveness with which goods and services are produced. Productivity are very essential in making sure inputs are utilized in an efficient way when they are being processed by machines into final product. Efficiency measures the resources expected to be consumed to the resources consumed (actual) and effectiveness measures what the system sets out to accomplish with what was accomplished (actual); plan vs actual [10]. Productivity in abattoirs is investigated through use of time study, determination of standard times, standardized work, takt – time (or drum-beat) production smooth flow, process mapping, value stream analysis and other necessary measurements for productivity such as labor productivity and efficiency [11].

II. METHODOLOGY

Methodology of paper relied on secondary research(such as reviewing available literature and data), informal qualitative approaches (such as engagement discussions, consultative meetings) and formal qualitative research(such as face to face interviews, direct observation, case studies, audits, site tours and plant tours).It explores application of value stream mapping in a meat processing industries (an abattoir). Value stream mapping has not been applied in beef industries rather a value chain was evaluated for a beef value chain. Site visits, company audits, engagement discussions, consultative meetings and plant tours were done to understand and investigate the flow of materials and information required to bring a service to the customer. The methods are further explained;

ISSN: 2521-2292

A. *Face to face interviews*

Face to face interviews were used to develop a common understanding of the current process. Production manager, three-line supervisor and twelve-line operators were interviewed to understand the relationship of the process steps, a true picture of the process to create a baseline for process measure.

B. *Plant tour and site visits*

Botswana Private Abattoir was mapped during site visits after consultation with the process users, production manager, and line supervisor and production team to give the actual current business process. The company currently uses batch production layout system in which workstations, machines and equipment used are arranged in a line but carcass is processed in batches. The carcass and cattle are physical moved or manually moved though rails by workers using trolleys, hands or semi-automated machines. The production system is designed in such a way that a small amount of the total work is added along as the carcass is moved along the production line and the stunned cattle's are moved in batches which encourages delays and more queuing time. It is also categorized by high production volume and low variety as of the abattoir is only cattle / small stock (usually goats) of any size. Farmers are the ones that bring their cattle's or small stock in the abattoir and documents are checked at the receiving gate. These documents include verification from the Department of Veterinary Services, kgotla, and police officers. The company receives cattle a day before they are slaughtered and it's mandatory for them to spend a night before they are slaughtered. Receiving days are Mondays to Thursdays during weekdays from 0600 hours till 1900 hours. Killing of cattle's takes place from Tuesday to Friday from 0700 hours till 1600 hours operating nine hours (in one shift). If the cattle have all the requirements, it is allowed in the building, if it does not have all the necessary documents it is sent back to the owner at the owner's expense. Cattle are then offloaded, and lair aged in holding pens according to their holding capacity. Before there are lair aged there are branded for identification. This identification is helpful for the production manager to prepare killing agenda. The cattle are then inspected often known as ante mortem inspection, where they are checked for fitness. If the cattle are not fit, it is verified by the veterinary inspect to be stunned at the emergency stunning box. If the cattle are fit and fine, it is sent to the stunning box where it is slaughtered.

Halaal checking takes place after stunning, then the slaughtered cattle are hoisted using mechanized hoist machine. The carcass is hoisted above the ground, creating less chance of contamination of carcass by filth and blood on the blood. Platform is a system that operators use for movement. Upon hoisting, skinning of heads takes place and they are tagged systematically in a trolley where they will be inspected by a meat inspect during production. Dressing takes place, then tagging of carcass takes place. Splitting takes place after the carcass has been tagged. Evisceration then takes place where the offal's will be separated and removed. Post mortem inspection takes place and done by meat inspector and veterinary officer. A report is made after the post mortem inspection has been done and it is awarded by a veterinary specialist inspect. In that report the veterinary specialist verifies whether the carcass and its offal's are good for human consumption. If there are not good for human consumption, the products are either detained in a chiller for some days or they are thrown away. If the report states that the carcass and its products are good for human consumption it is passed along the production system. All documents are then checked which includes report by an inspector. If all documents are fine, an establishment stamp is issued. The carcass is weighed, loaded, invoiced and delivered to the end user. Furthermore, activities in the plant are categorized in three sections which are gate receiving section, lair aging and the production shop floor.

C. *Time study*

Time study was also used to collect data for a process. Time study was used to measure the current state steps and to create a baseline measure. First a process was selected, which illustrates how cattles enter the building, then all involved stakeholders were engaged and made aware of the project task. After awareness was made to employees, cattle slaughtering was directly observed in order to familiarize oneself with the process. All process steps were noted down. Process cycle time was considered from the time the of cattles enters the building up until they are loaded in refridgerated trucks for delivery to the designated customer. Three cycles were performed on three consecutive working days for the nine hours working shift. Stop watch technique was used with direct observation of the operator while timming the duration of the activity. When using this technique actual times required to perform different activities were recorded in their elemental form and according to the steps involved in the slaughering of cattle. Random operators of two per each operation were timed. Reason was that the supervisor allocate task according to the availability of work content. For example, if there is more work content in dressing, one operator would be shifted to that section to add labor intensity. Tools used for conducting time study are digital and electronics stop watch, board for holding time study sheet, video camera recorder, observation time study sheet and stationary such as pen, pencil, eraser and calculator. After actual times were recorded, data was analyzed so as to obtain the time necessary to carry out a specified job at a specified level of performance rating and specified allowance such personal, fatigue and delay

ISSN: 2521-2292

(abbreviated as PFD allowance). Performance rating was taken to be 100% and PFD was taken as 15% as stated by International Labour Organization (O'Rourke, 2003). A sample size of 5 beasts and five cycles were selected and recoded their times for accuracy.Five observed cycle times were recorded and averaged. The average cycle time helped to determine how well the current operation is doing in relation to the TAKT time. TAKT time is the total available time divided by the number of units in demand for that day, see Equation (1) for calculation.

D. Data Analyzing tools

When analyzing results collected; pareto graph, computer software's (Microsoft Visio), and other forms of visualized data were used; such as process maps, and images.
Below in Table 1 summarizes tools used in order to map the value stream of the cattle slaughtering production line.

Table 1: Data analyzing tools used

Problem issue	**Data analyzing tools**
Long manufacturing lead time	-Microsoft Visio -Stop watch technique -CCTV surveillance camera analyzing -Minitab -SIMO (Simultaneous Motion Chart) -MOST (Maynard Operating Sequence Technique) Index parameter -Two hand process chart -Process flow chart

III. RESULTS AND DISCUSSION

This chapter illustrates value stream that was identified during site visits, plat tour, direct observation, workstudy and interviews. Current value stream map was identified, and from the value stream; current cycle time was identified as shown in Figure 1. Current value stream map was identified through direct observation, site visits and plant tour. Current value stream shows that the production lead time is 50 cattle's for 9 hours. Microsoft Visio was used to map the current value stream map with the help of time study conducted and motion study observed. Current state map was created using process mapping symbols and others. Based on the current state map shown in Figure 1; waiting time is far greater than the value-added time, thus increasing the lead time and operating costs due to higher levels of carcass queuing for a long period of time. Based on the available work identified through work measurement and customer demand, Takt time was identified as illustrated in Equation 1 and it was found to be 463 seconds. Takt time means that in order to meet customer demands, Botswana Private Abattoir need to produce a carcass every 10.8 minutes. This is a reference number defined by the customer and it should improve processes to match this time considering downtimes, changeovers and defects. The existing current value stream map of Botswana Private Abattoir that was mapped and is shown in Figure 1. The data learned through the design of the current map is overall lead time which spans from when the customer delivers the cattle to be slaughtered through gate receiving section, Lairaging, production and delivery of the carcass to the customer. Currently the company has a production time of nine hours, working one shift. Out of the nine hours, only 4.12 hours is value added time. Non-value adding time is 4.88 hours.

Therefore, the company has a lot of waste activities that needs to be eliminated. For a production holding capacity of 70 cattle per day, the company can only slaughter 50 herds of cattle with a total lead time of 9 hours. Each process in the value stream produce a batch and push the product to the forward process as planned by the production control as opposed to what the next process really needs. This creates carcass queue at the next process and some defects can remain hidden until it gets noticed the product is inspected at the loading bay in this next process. The time for adding value to the product is less but it takes long time to get through the value chain. The significant problem in the value chain of cattle slaughtering is more non-value adding activities, unnecessary movements and other defects such as mixture and missing of carcass which leads to reassessing, wait, and defects. Table 2 shows non value adding activities identified in the existing value stream

$$\text{Takt time} = \frac{Net\ availble\ time\ (\ in\ minutes)}{Customer\ demand}$$

$$= \frac{540\ minutes}{50\ cattles} \quad (1)$$

= 10. 8 minutes

From the current study, rollers were proposed to be used to reduce delays experienced when an operator transport some carcass and skinned heads by their backs. Recommendation were made to the research company to consider using pull manufacturing which encourages smooth flow of carcass and reduces some delays within the production line; rather than the batch production that the company is currently using. Future state was mapped and is shown in Appendix A.

ISSN: 2521-2292

Table 2: Non value adding activities

	People/ workers	Machine	Material
Non Value Adding (NVA)	waiting for machine	setup time	handling carcass
	waiting for carcass	unscheduled maintenance	moving carcass
	searching for tools		Transporting carcass
	unbalanced work load		sorting cattle's
	sorting condemned carcass		inspecting carcass
	inspecting product		
	fixing equipment		

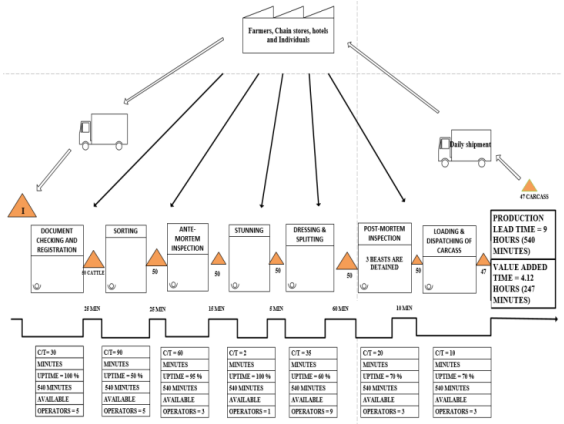


Fig. 1: Current state map

IV. CONCLUSION

This paper has examined application of value stream mapping in a beef abattoir. Current value stream was mapped with the help of time study to better understand the process cycle time. The study relived that more time is wasted in handling the carcass within the production line hence possible opportunities can also be explored in better methods of carcass handling such as use of rollers. By doing so it is feasible to improve cycle time efficiency of a projected 21- 23% process cycle time improvement. Value stream mapping has proven to be effective way to analyze abattoir's current production state and point out problem areas.

ACKNOWLEDGMENT

Sincere thanks and gratitude given to Industrial and Manufacturing supervisor and lecturer, Norman Gwangwava (Dr. Eng.) and co-mentor, Richard- Ardo Tenkorang (Dr. Eng.), for providing guidance and helping to find a company to use for my research case study. My sincere gratitude is also due to the Botswana Private Abattoir staff; director, (Mr Badiredi Phampa), and production manager, (Mr Mmelesi), for allowing me to carry out my research at their company

REFERENCES

[1] Apel, W., Li, J. Y., & Walton, V. (2007). *Value stream mapping for Len Manufacturing Implementation.* Hong Kong: Worcester Polytechnic Institute & Central Industrial Supply.

[2] Tyagi, S., Choudhary, A., Cai, X., & Yang, K. (2015). Value stram mapping to reduce the Lead Time of a Product Development Process. *International Journal of Production Economics*, 202-212.

[3] Hill, J. (2009). The use of cold storage as a scheduling aid in bedding plant production. *Journal of scheduling bedding plant in production*, 112-120.

[4] Grassi, Co.Accountants, & Consultants, S. (2014). *The Principles and Practices of Lean Manufacturing: An overview.* New York: Long Island Forum Publication.

[5] QAD Enterprise Application. (2012). Training guide (1 Ed.). California: QAD Inc.

[6] Hines, P., & Nich, N. (2001). *The seven value stream map tool*. New York: LLC Press.

[7] BEDIA, B. (2007, January 7). Botswana: The beef industry. *Botswana Powerpoint presentations*, 1-45.

[8] Engelen, V. A., Malope, P., Keyser, J., & Neven, D. (2013). *Botswnan Agrifood value chain project: Beef value Chain study.* Rome: FAO(Food and Agricultur Organization of the United Nation) and Ministry of Agriculture, Botswana.

[9] Mulale, K. (2002). *The challenges to sustainable beef production in Botswana: Implications on rangeland management.* Iowa State University, Department of Sociology: Unpublished paper.

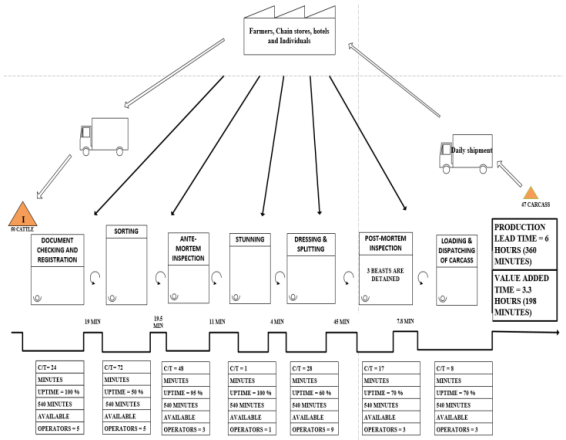
[10] Timothy, J., Dodla, S. P., Christopher, J. O., & George, E. (2005). *An introduction to efficiency and productivity Analysis.* USA: Springer.

[11] Barber, M., Etchells, J., Meltcalf, T., & Jakeman, G. (2012). *A economic impact assessment of the proposed AAco Darwin beef processing facility.* ACIL Tasman Pty Ltd: ACIL Tasman Economics Policy Strategy.

APPENDIX

APPENDIX A: FUTURE STATE MAP

ISSN: 2521-2292



BIUST Research and Innovation Symposium 2019 (RDAIS 2019)
Botswana International University of Science and Technology
Palapye, Botswana, 4 - 7 June 2019
ISSN: 2521-2292

Potential of agro-waste briquetting for domestic heating and cooking as an environmental management strategy in Rushinga, Zimbabwe.

MADAMOMBE Gordon Tinaye
Life and Earth Science Institute
Pan African University
Ibadan, Nigeria
gtmada@gmail.com

CHIPFUPI Elia
Manicaland University of Applied Sciences
Mutare, Zimbabwe

UTETE Beaven (Dr)
Department of Wildlife Ecology and Conservation
Chinhoyi University of Technology
Chinhoyi, Zimbabwe

OLORUNNISSOLA Abel O (Prof)
Department of Wood Products Engineering
University of Ibadan
Ibadan, Nigeria

ISSN: 2521-2292

***Abstract*— Deforestation and pollution are externalities produced by agriculture and natural resources exploitation economic activities. The rate of deforestation in Zimbabwe is very high relative to other SADC countries. This is due land clearance for agriculture, fuel-wood for processing of agriculture produce and fuel wood for domestic heating. With agriculture being the main source of rural livelihoods, substantial amounts of crop residue remain behind after harvesting and post-harvest processes. The practice of burning crop residue in the fields and homesteads is common and results in the dissipation of energy into the environment. To this end, this study seeks to ascertain the possibility of producing biomass briquettes from agro-residue for domestic heating and cooking as an environmental management strategy. The pre-survey established the baseline conditions and agro-residues available in the study area. Groundnut shells were selected as the briquetting feedstock while paper was used as a binder. A manual press was then used to mould briquette at the ratio of 3:1 (paper:biomass). Formed briquettes were distributed in the community after which a post-survey was conducted to evaluate the willingness to pay for and use of briquettes. Results showed that the communities were willing to pay $10 per month on briquettes, thus a binder costing less that USD$10 would be ideal for briquetting.**

Keywords*— *Briquettes, agro-residues, biomass, binder)

I. INTRODUCTION AND BACKGROUND

Agriculture is a paramount source of livelihoods in Sub-Saharan African [1]. Most of the developing countries' economies are hinged on agriculture as it is the major source of revenue [2]. Increased environmental and sustainability concerns put developing countries at a dilemma of choices in resource allocation and use especially in agriculture [3]. Deforestation and pollution are externalities produced by agriculture and natural resources exploitation economic activities [4]. In the third world, one of the major problems is the issue of the environmental degradation [5]. Forests and trees account for 23% of global carbon stored in forests, and deforestation and forest degradation account for 30% of Africa's GHG emissions [6] thus contributing to climate change. The extensive removal of tree cover for dry-land farming, overgrazing, and the disproportionate cutting of wood resources for fuel purposes are the main causes of deforestation in arid and semi-arid environments [7].

Currently, biomass provides only about 15-20% of global energy needs. In developing countries biomass provides 20-33% of total energy demand [8]. The main sources of energy used in Zimbabwe comprise coal, wood fuel, electricity and petroleum fuels. According to the Ministry of Energy and Power Development, Zimbabwe [9], wood fuel provides the bulk (61%) of the total energy supply, followed by liquid fuels (18%), electricity (13%), and coal (8%). Thirty-seven per cent of households in Zimbabwe have access to electricity that is connected via power lines. In urban areas 83 per cent of households have electricity, compared with 13 per cent in rural areas [9]. Rural communities meet 94 per cent of their cooking energy requirements from traditional fuels, mainly firewood, and 20 per cent of urban households use wood as the main cooking fuel [10].

Vision 2030 is the aspiration of Zimbabwe that they attain upper middle class economy status by the year 2030. This would translate to the re-industrialization and increased capacity utilization of industries. Regardless of the low capacity utilization of industries which affords the grid to supply domestic needs, electricity supply is erratic and demand for fuel wood is high. Thus, if Vision 2030 is realized, the industrial demand for electricity from the grid would mean that domestic supply would be more erratic than currently experienced culminating in the high demand of wood fuel, resulting in increased deforestation rates. A majority of urban households use electricity for cooking (73%); in contrast, only 6 per cent of rural households use electricity for this purpose [10]. With the current erratic electricity supply from the power utility and limited off-grid and distributed electricity supply, very high cost of LPG, low uptake of solar technologies, it is highly probable that the dependence on wood for domestic heating and cooking has increased in both rural and urban areas.

During the period 2000 – 2010, forest in Zimbabwe was declining at a rate of 1.78% against the average of 0.48% for the Southern Africa region [6]. During this period [11], the capacity utilisation of industries declined rapidly from 33.8% in 2006 to 10% in 2008. The UN Food and Agriculture Organization (FAO) [12] listed Zimbabwe as being among 10 countries that recorded the largest forest cover loss between 1990 and 2010 (losing 327,000 hectares of forest cover per year). Cutting down trees for wood fuel has been identified by Chipika and Gowero (2000) as one of the major drivers for deforestation in Zimbabwe [13]. As in most developing countries, Zimbabwe is lagging behind in terms of global trends of renewable energy, especially in biomass densification through briquetting.

Access to energy is not homogeneous with the energy matrix in urban areas comprising of a number of energy sources against that of rural folks who depend largely on wood fuel. Statistics from the Ministry of Energy, Zimbabwe [9], reveals that 94% of the people in the rural areas use fuel wood and most of the rural areas are facing wood fuel shortage as a result of inter alia, the clearing of land for agriculture and unsustainable firewood harvesting. Demand for wood fuel already exceeds supply in Manicaland, Mashonaland Central, Mashonaland East, the Midlands and Masvingo provinces [9]. Most of the people in the rural areas depend on crop farming for sustenance and produce agriculture waste which has the potential to be used as a fuel energy source. It is against this backdrop that this research seeks to assess the viability of agro-waste densification for use in domestic cooking. This paper investigates Potential of agro-waste briquetting for domestic heating and cooking as an environmental management strategy in Rushinga, Zimbabwe.".

ISSN: 2521-2292

In Zimbabwe, biomass accounts for about 47% of the energy supply in Zimbabwe (Ministry of Energy and Power Development 2012). The structure of energy supply in Zimbabwe in relation to the African continent and the world is shown in Table 1. Like in most parts of the developing world, fuel is the most widespread used energy source in rural communities.

Energy supply sources in %	Energy supply source			
	Biomass	Electricity	Coal	Petroleum
Zimbabwe	47	13	19	21
Africa	59	8	4	25
World	14	16	7	44

Source: Shonhiwa C. (2013) [13]

Biomass briquettes from agro-waste can be a biofuel substitute to wood fuel and charcoal. They are a renewable source of energy and avoid adding fossils carbon and sulphur to the atmosphere. Carboniferous material can be briquetted either without a binder under high pressure or by the aid of a binder at lower pressure. This study is therefore aimed at investigating the agro-waste densification (briquetting) using binders for domestic cooking as a substitute or compliment for fuel wood.

The rate of deforestation in Zimbabwe is very high relative to other SADC countries. Forest loss contributes significantly to Zimbabwe's green-house gas emissions as industries capacity utilisation is very low. The practice of burning crop residue in the fields and homesteads is common among rural and urban areas. In doing this, crop residues combust inefficiently polluting the environment and dissipating heat/energy which if harnessed could help reduce the dependence of people on fuel wood. Thus, briquetting will go a long way in anthropogenic CO2, enhance energy security among the vulnerable (women and children as they are the ones who fetch fuel wood), reduce pollution and provide affordable renewable energy.

II. Methodology

This paper seeks to ascertain the techo-economic feasibility of briquetting agro-waste residues for domestic heating and cooking. Qualitative research tools were utilized in the collection of data. A pre-survey was conducted to ascertain the types of crop residue that is found in the area. During this period, Key Informant Interviews were used to assess the practices of crop residue handling, utilization and disposal. Informants were chosen from community and extension workers, community leaders, farmers and child councilors. Groundnut shells were selected to be the biomass based on abundance and calorific value while waste paper was chosen as

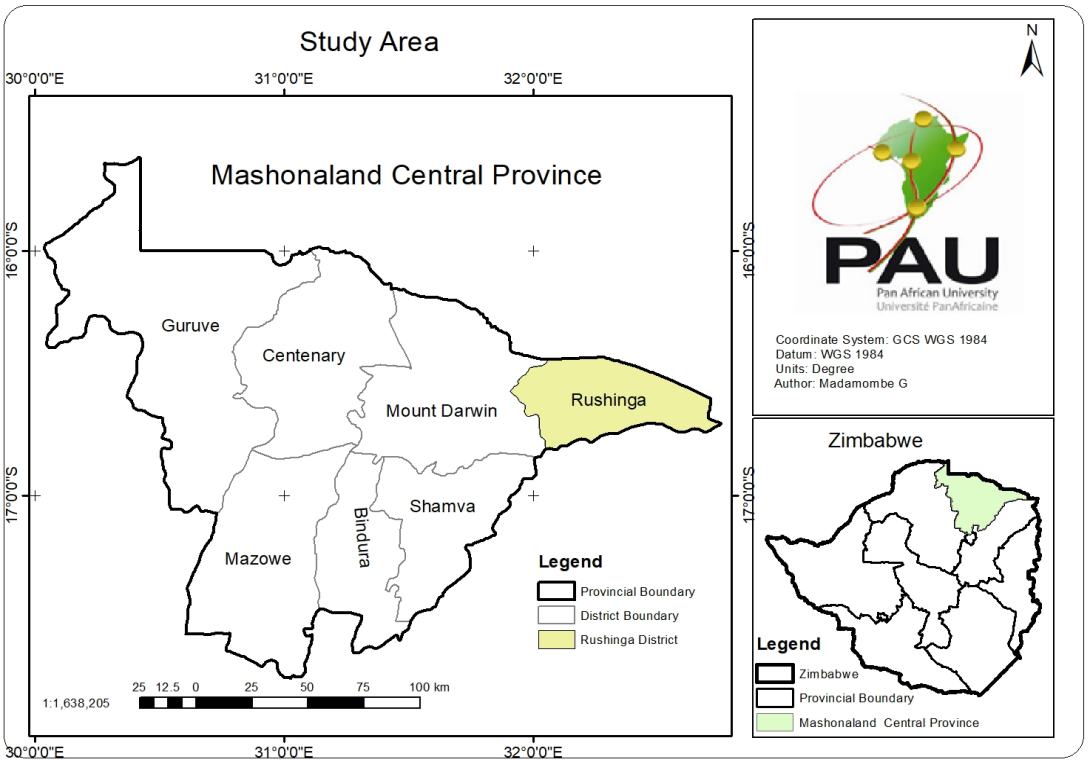


Figure 1: Location of Study Area

ISSN: 2521-2292

binder based on convenience to the researcher.

Paper was mashed in water to make a paste which was used as the binder to the biomass. Excess water was drained during the molding of the briquettes by the use of a manual hand-press. The molded briquettes were sundried for a period between 3-7days. Participants in the study then used the dried briquettes intermittently for a period stretching three months. After three months, a structured questionnaire was administered among 30 households to assess a number of things among which willingness to pay was extrapolated, contemporary fuel source, cooking practices and amounts of other fuels used. All interviewed households had stayed for at least a decade in the district. Participants were chosen based on the consent from the participants and amount of groundnut shells within the vicinity of the homestead or willingness of the participants to carry briquettes from a homestead meeting the first two conditions.

The questionnaires were printed in English and the enumerator would translate to the local Shona dialect were the respondents needed clarifications. To ratify the results from the questionnaires, enumerators would do additional checks on the amount of wood collected together with the participants as enumerators were drawn from the study area. Fig 1 shows the location of Rushinga District in Zimbabwe.

III. Results and Discussion

This section of the paper presents and discusses the results of the study. Only one member of a household participated in the questionnaire survey. On average, a family comprised of five members. Fig. 2 and Fig. 3 show the characteristics of the sample respondents from the sampled households.

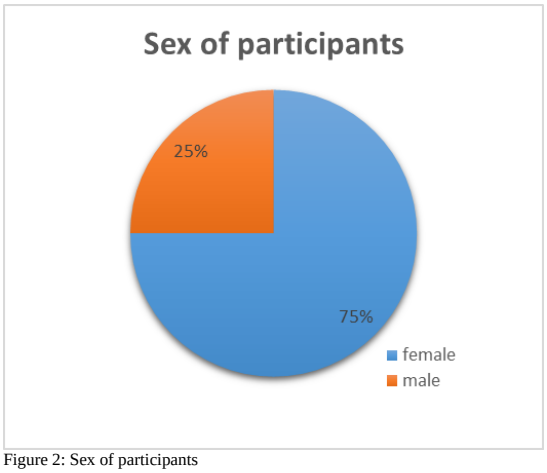


Figure 2: Sex of participants

Women are the ones mostly involved in cooking and most domestic chores. As such, 75% of the respondents were females while 25% were males. From this study alone, one cannot conclude that women are the ones mostly involved in the use of energy as the study did not cover the whole year.

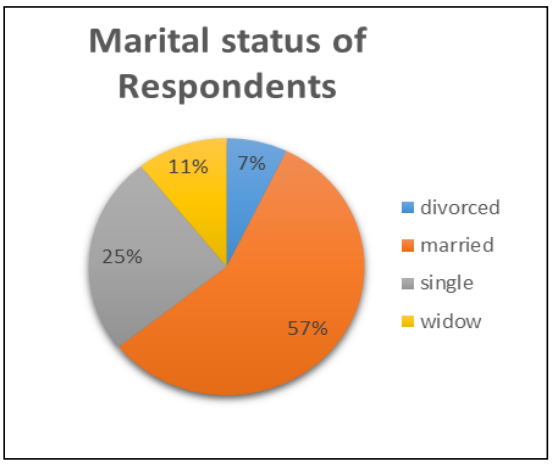


Figure 3: Marital Status of Respondents

During some seasons, in the study area, men would be engaged in beer brewing for rituals such that if the study was to be carried out during this period, the results would be different. Figure three shows the marital status of the participants. It is worth to note that participants who were single were out of school youths who were either staying with their parents or guardians.

Rushinga District lies in the arid north-east part of Zimbabwe (Fig. 1) which is sparsely vegetated. It has been noted from the participants that people in the area are aware of the consequences of the relying much on wood as the primary source of energy. 75% of the respondents considered using briquettes on the basis of curbing deforestation and increasing energy security. 30% highlighted health concerns as the motivation to using briquettes as they perceived wood as causing more pollution than briquettes. A fifth of the participants were reluctant to adopt briquettes are they did not perceive an energy crisis as was by the four fifths who were concerned about a perceived energy crisis due to shortage of wood.

ISSN: 2521-2292

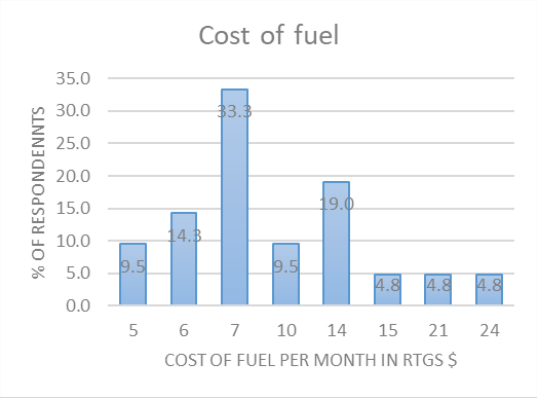


Figure 4: Cost of fuel

The results indicated that people use an average of RTGS$10 per month (at the time the study was conducted the parallel market exchange rate of USD$ to RTGS$ was at 1:2.5). From this, at the time of conducting of the research a person would be using RTGS$ 2 on wood fuel per month.

The cost of wood differed with location with a cart costing RTGS$6 and RTGS$7 while a wheelbarrow load costed between RTGS $3 and RTGS$5. The expenditure of the respondents on fuel is shown in Fig. 4. The quantities of wood used varied as with the cost as shown in Fig 5.



Figure 5: Quantity of fuelwood used per month

IV. Conclusion and Recommendations

The study results have shown that there is a proportion of people in Rushinga district who are willing to make, use and pay for briquettes made from agro-residues. With a considerable percentage viewing briquetting as means to curb deforestation thus also GHG emissions due to forest loss, policy makers may consider promulgating policies that promote briquetting. Rural communities are likely to embrace briquetting not only for harnessing energy from loose biomass, but also for managing solid waste. There is need for further research on the optimization of briquette making at community level and the developing of low cost briquetting equipment suitable for using feedstock available in the area.

Acknowledgment

We thank Dr. A. Phiri from the Environmental Management, Renewable Energy and Climate Change Research Centre of the Harare Institute of Technology who provided insights that greatly assisted in the research. Our sincere gratitude to World Vision Zimbabwe, Rushinga Area Programme (the Manager and her staff members) for affording the researchers the opportunity to utilize the community structures they work with in the collection and collation of data. We greatly appreciate the Rural District Council and the District Administrator for their unwavering support to this study.

References

[1] Rukuni M and Eicher C. K. (1994). Zimbabwe's Agricultural Evolution, University of Zimbabwe, Harare, Zimbabwe

[2] Keyser J. C. (2002). The costs and profitability of tobacco compared to other crops in Zimbabwe. Health, Nutrition and Population (HNP) Discussion Paper 1, Economics of Tobacco Control, World Bank, Washington, DC, USA.

[3] Chivuraise, C., Chamboko, T., & Chagwiza, G. (2016). An Assessment of Factors Influencing Forest Harvesting in Smallholder Tobacco Production in Hurungwe District, Zimbabwe: An Application of Binary Logistic Regression Model. Advances in Agriculture, 2016.

[4] Pearce D and Brown K (1994). Saving the world tropical forests. The Economics and Statistical Analysis of Factors Giving Rise to the Loss of the Tropical Forest, pp. 2–26, UCL Press

[5] Benhin J. K. A. (2006). Agriculture and deforestation in the tropics: a critical theoretical and empirical review. Ambio, vol. 35, no. 1, pp. 9–16

[6] Bromhead, M. (2012). Forest, Trees, and Woodlands in Africa: An Action Plan for World Bank Engagement.

[7] Hassan R. M. and Hertzler G. (1988). Deforestation from the overexploitation of wood resources as a cooking fuel: a dynamic approach to pricing energy resources in Sudan. Energy Economics, vol. 10, no. 2, pp. 163–168, 1988.

[8] Ministry of Energy and Power Development, Zimbabwe (2009). Energy Balance.

[9] ZIMSTAT (2010), Demographic and Health Survey.

[10] Zimano, D., & Kaseke, N. (2014). Turnaround strategies choice and effectiveness: The case of the manufacturing sector in Zimbabwe.

[11] Zimano, D., & Kaseke, N. (2014). Turnaround strategies choice and effectiveness: The case of the manufacturing sector in Zimbabwe.

[12] Chipika, J. T., & Kowero, G. (2000). Deforestation of woodlands in communal areas of Zimbabwe: is it due to agricultural policies?. Agriculture, ecosystems & environment, 79(2-3), 175-185.

[13] Shonhiwa C. (2013) An assessment of biomass residue sustainably available for thermochemical conversion to energy in Zimbabwe. Biomass and Bioenergy;52:131-8.

BIUST Research and Innovation Symposium 2019 (RDAIS 2019)
Botswana International University of Science and Technology
Palapye, Botswana, 4 - 7 June 2019

ISSN: 2521-2292

Thermal performance assessment of a Parabolic Trough Collector prototype system in Palapye, Botswana

Ndakidzilo Nthoiwa
Department of Physics and Astronomy
BIUST
Palapye, Botswana
ndakidzilo.nthoiwa@studentmail.biust.ac.bw

Einax Mario
Department of Physics and Astronomy
BIUST
Palapye, Botswana
einaxm@biust.ac.bw

***Abstract*— A parabolic trough collector (PTC) prototype was fabricated and tested at Palapye (22.59404 ºS and 027.12455 ºE) in Botswana. A stainless steel sheet lined with an adhesive Mylar film of high reflectivity (≥ 0.94) was used as the collector with area 3.001 m^2 and a copper tube of 15 mm external diameter and length 2.440 m coated with silicone 250 selective coating as the receiver. The performance of the coated receiver tube was compared to that of a 2.0 m long commercial receiver without any modification of the collector. The highest outlet temperature of 75.8 ºC was achieved, with inlet water and ambient temperatures of 26.1 and 28.0 ºC, respectively. The effect of the wind speed, mass flow rate of the water and the irradiation on the thermal efficiencies of the system were studied. An increase in the average wind speed from 2.8 to 4.4 m/s resulted in both the Carnot and thermal efficiency decreasing from 61.1 to 54.1 % and 20.3 to 7.7 %, respectively. At constant wind speed, a decrease in the flow rate from 0.0036 to 0.0012 kg/s resulted in an increase in the Carnot efficiency from 43.9 to 54.1 % due to an increase in the outlet temperature, while the thermal efficiency dropped by half. The wind speed had no influence on the commercial receiver outlet temperature because of the vacuum insulation.**

Keywords— Solar energy; Parabolic trough collector; Thermal efficiency; Carnot efficiency

I. INTRODUCTION

Parabolic trough collector (PTC) is the mostly adopted and mature of all the four concentrating solar power technologies (CSPT), constituting over 90 % of the total world installed concentrated solar power plants [1]. A PTC is made of three components; the receiver, collector and the support structure. A collector is a parabolic shaped sheet lined with a reflective material, which focuses all the irradiation falling on its surface to the focal line. A commercial receiver or a pipe coated with a solar selective paint is placed at the collector`s focal line to absorb the heat and raise the temperature of the fluid passing through it. Nine solar power plants established between 1985 and 1991 and known as the solar energy generating systems (SEGS) in the Mojave desert, southern California with a combined power of 354 MWe are the pioneers of concentrated solar power (CSP). It remains the biggest commercial and combined operational plants which have adopted the use of parabolic trough collectors (PTCs) [2].

The idea of harnessing solar radiation using this technique was triggered by the surging oil prices around 1979 [3], but in 1990 the prices dropped, resulting in a break from the investment in solar thermal technologies up to the year 2000 [1]. An additional 780 MWe of CSP was added between 2007 and 2010, with over half being commissioned in 2010 alone hence increasing the global total to 1095 MWe. By 2015 the global total of installed CSP had increased to 4950 MWe from 4534 MWe the previous year [4]. Africa has also adopted the technology with countries such as South Africa, Morocco, Egypt and Algeria having operational plants ranging from 20 MWe to 160 MWe. By end of 2019, South Africa is expected to generate 700.1 MWe from its eight power plants, five of which adopted the PTC technology. Morocco has also set a very ambitious milestone of achieving 2 GW of solar renewables by 2020; 42 % of the country`s energy mix [5]. On the contrary, Botswana is yet to construct the first CSP plant, with a projected capacity of 50 MWe in Jwaneng and Maun.

The daily irradiation in Botswana is enough to drive CSP stations to produce more than enough electricity to sustain the current 669 MW peak power demand. On average the country experiences over 320 clear sky days annually, receiving an average horizontal insolation of 21 MJ/m^2 per day on a flat surface. But surprisingly, Botswana is still reliant on coal powered Morupule B power station, the giant power producer in the country. Diesel generators of 70 MW and 105 MW at Orapa and Matshelagabedi respectively, have also been deployed to augment the projected power demand at a peak of 669 MW in winter [6]. Importation of power from neighboring South Africa and Mozambique on a firm and non-firm basis is also ongoing.

This paper reports on the performance of the first parabolic trough collector prototype system constructed locally and tested at a site in Palapye. This is the first prototype to be built and tested locally and it will serve as a source of information and proof of concept for scientists, entrepreneurs and the government when deciding whether or not to invest in solar thermal technologies either for industrial applications, water desalination, generation of steam for sterilization and even power generation.

ISSN: 2521-2292

II. METHODOLOGY

The PTC prototype shown in Fig. 1 was fabricated at a local metal workshop called "Supu Metal Clinic" with the help of a local craftsman using locally available materials.

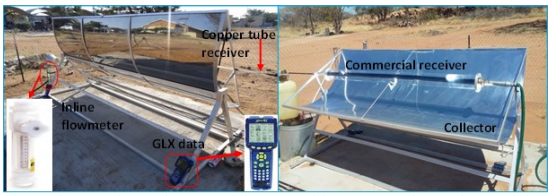


Fig. 1 The experimental set-up of the PTC with a copper tube receiver and the commercial receiver with a glass envelope.

A mirror finish-stainless steel was curved into a trough and held into the desired position with the support structures. A copper pipe of external was used as the receiver and it was drilled near both ends to insert Xplorer GLX temperature probes and the holes sealed with Pratley putty. The pipe was then coated with a selective solar paint (Thurmalox 250), which has low emissivity of 52 % and high absorptivity of 96 % in the solar spectrum range (wavelengths between 0.3 µm to 3.0 µm). The prototype was then mounted on a concrete slab, at geographical coordinates 22.59404 ˚S and 027.12455 ˚E and an altitude of 973 m. The specific dimensions and properties of the various characteristics of the prototype are given in Table 1.

Table 1 Key features of the parabolic system using two types of receivers.

Description	**PTC system with copper receiver**	**PTC system with commercial receiver**
Collector length l_a	2.440 m	2.000 m
Collector area	3.001 m^2	2.460 m^2
Aperture area	2.616 m^2	2.144 m^2
Rim angle φ_r	90 °	90 °
Focal distance f	0.268 m	0.268 m
Receiver diameter (External) D_{oa}	15.0 mm	38.0mm
Receiver diameter (Internal) D_{ia}	13.4 mm	-
Collector width w_a	1.072 m	1.072 m
Concentration ratio C	22.7	9.0
Absorber absorptivity α_a	0.96	0.94
Absorber emissivity ε_a	0.52	0.06
Mylar reflectance, ρ	0.97	0.97
Glass envelope transmittance τ_g	-	0.95
Mode of tracking	Manual	Manual

A polytetrafluoroethylene (PTFE) inline flowmeter was connected between the tap (water supply) and the inlet to the receiver pipe to regulate and monitor the flowrate during the experiment. Two Xplorer GLX data loggers were used to record the inlet and outlet water temperatures as shown in Fig. 1. This was done at time intervals of 1 minute between 0900 hours and 1600 hours on several days while tracking the movement of the sun by manually rotating the system to remain in focus. The flow rate of the water was varied to investigate its influence on the output temperature and thermal efficiency of the system. The ambient temperature, wind speed and global irradiation values for the specific days were obtained from the Mahalapye meteorological weather station, 70 km away. In another set of experiments, the copper tube receiver was replaced by a commercial receiver purchased from SUNDA solar (China). The key features of the two systems are summarized in Table 1.

III. THEORETICAL BACKGROUND

The optical efficiency of the system is the ratio of the energy absorbed by the receiver to that incident on the aperture. It is dependent on the system`s optical properties such as the reflectance of the concentrator, transmittance of the glass envelope of the receiver, absorption of the receiver`s surface, intercept factor, concentrator`s geometry and construction defect errors. The optical efficiency of a PTC system is given by [7]

$$\eta_o = \left(\rho_a \tau_g \alpha_r \gamma\right) K(\theta_i) X_{END} \quad (2)$$

where ρ_a is the collector reflectivity, τ_g is the glass transmittance, α_r is the receiver absorptivity, γ is the intercept factor, $K(\theta_i)$ the incidence angle modifier, θ_i is the angle of incidence in degrees and X_{END} is the end error losses.

Incidence angle modifier $K(\theta_i)$ is the ratio between the optical efficiency at a given incident angle and the efficiency at an incident angle of zero. Assuming a maximum incidence angle of 15 ° (equivalent to one hour of the sun`s motion), the incidence angle modifier as per the LS-2 collector is given by [8]

$$K(\theta_i) = \cos\theta_i + 0.000884(\theta_i) + 0.00005369(\theta_i^2) \quad (3)$$

The end loss error X_{END} for a parabolic trough collector refers to losses occurring as a result of the position of the sun when the incidence angle is not equal to zero. Part of the length of the receiver is not illuminated at incident angles more or less than zero. Fig. 2 shows a schematic diagram on the occurrence of the end losses.

ISSN: 2521-2292

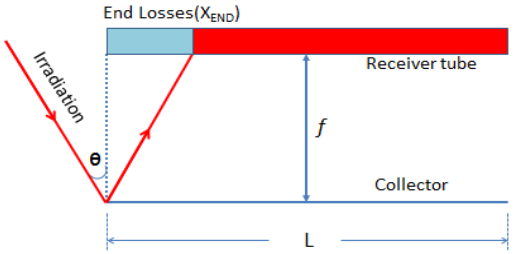


Fig. 2 The end loss effect on a parabolic trough collector

The amount of the loss in irradiation due to the effect is given by [8]

$$X_{END} = 1 - \frac{f}{L}\tan(\theta) \quad (4)$$

The instantaneous thermal efficiency is the useful heat gain Q_u supplied per unit area, A_a per the incident direct irradiation, G_b [9]. It is thus given by

$$\eta_{th} = \frac{\dot{m}c_p(T_o - T_i)}{G_b A_a} \quad (5)$$

where $\dot{m}$ is the mass flow rate of the fluid, c_p is the specific heat capacity of the fluid, and T_o and T_i are the fluid outlet and inlet temperatures respectively. The useful heat absorbed by the receiver tube, Q_u is equivalent to $\dot{m}c_p(T_o - T_i)$. It can also be presented according to thermal and optical heat losses as [9]

$$Q_u = \eta_o G_b A_a - U_L(T_r - T_a)A_r \quad (6)$$

where η_o is the optical efficiency of the system, U_L is the heat loss coefficient, T_r is the receiver temperature, T_a is the ambient temperature, while A_r is the receiver surface area .

The thermal efficiency η_{th} for a concentrating system operating under steady state condition as stipulated by the ASHRAE 1986 [10] is obtained by incorporating Eq. (6) into Eq. (5)

$$\eta_{th} = F_R\eta_o - \frac{F_R U_L}{C}\left(\frac{T_i - T_a}{G_b}\right) \quad (7)$$

Carnot efficiency is the ratio of the work done by a heat engine to the heat drawn out of the high temperature reservoir of the engine. The thermodynamic efficiency limit for a PTC system depends on the fluid inlet temperature (cold reservoir) and the fluid outlet temperature (hot reservoir) as shown in Eq. (8). Therefore the thermal efficiency of a PTC is always equal or less than the Carnot efficiency

$$\eta_c = 1 - \frac{T_i}{T_o} \quad (8)$$

IV. RESULTS AND DISCUSSIONS

A. Optical efficiency

Using parameters in Table 1, the optical efficiencies for the coated copper tube and the commercial receivers were calculated as 76.75 % and 80.34 %, respectively. The intercept factors (γ) for the coated copper tube and the commercial tube were determined as 0.876 and 0.996, respectively by using the approach of Gee et al which is based on the Gaussian approximation [11].

B. Thermal efficiency of the coated copper tube receiver

The water inlet (T_i) and outlet (T_o) temperatures were measured at intervals of 1 minute each day from 0900 hours to 1600 hours. Ambient temperature (T_a) and the global horizontal irradiation (GHI) were obtained from meteorological data provided by the Mahalapye station, 70 km away. The T_i, T_o, T_a and *GHI* as a function of time for three different days are shown in Fig. 3.

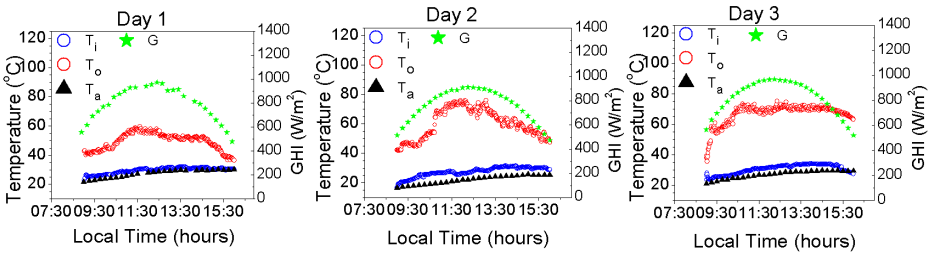


Fig. 3 The inlet, outlet and ambient temperatures and GHI as a function of time for the PTC prototype using coated copper pipe receiver on three different days

ISSN: 2521-2292

The values of the Carnot efficiency η_c given as calculated from Eq. (8) are shown in Fig. 4 for the three days. The average Carnot efficiency η_o for day one was 38.5 % with maximum values of 50.3 % obtained at 1115 hours. The efficiency dropped gradually to 16.5 % at 1600 hours due to a decrease in the GHI. On day two, the efficiency reached a maximum of 64.8 % at 1145 hours, with an average of 53.6 %. The efficiency then dropped to a minimum of 39.9 % at 1600 hours. Day three showed a much higher average Carnot efficiency of 54.1 % with the highest value of 60.4 % achieved at 1045 hours then decreasing by an average of about 6.4 % and remaining constant at 54.0 %. This shows the highest thermal efficiency that can be reached by the PTC for conditions on those particular days.

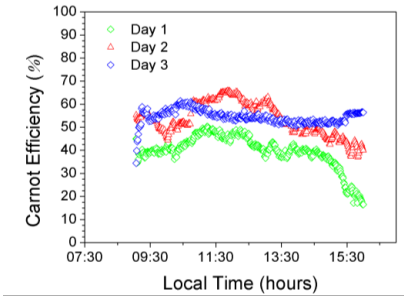


Fig. 4 Carnot efficiency of the PTC prototype when using a coated copper pipe receiver for three different days

When the instantaneous thermal efficiency η_{th}, calculated from Eq. (5) is plotted against the loss in temperature difference $(T_i - T_a)/G_b$, a straight line is obtained if the heat loss coefficient U_L is kept constant. The vertical intercept represents $F_R\eta_o$ while the gradient of the graph is equivalent to $U_L F_R/C$. Fig. 5 shows the thermal efficiency for the three different days using a coated copper pipe of external diameter 15.0 mm.

The thermal efficiency was calculated using values obtained between 1130 hours and 1330 hours where the GHI was at the highest. For this work, the GHI was used to calculate the efficiency because of lack of a Pyrheliometer to measure DNI directly on sight. It is worth noting that the efficiencies obtained therefore gives the lower limit because the GHI value used is greater than the actual DNI absorbed by the system`s receiver.

The line of best fit through the plotted data for day one in Fig. 5 could be described by Eq. (9)

$$\eta_{th} = 0.1490 - 2.009\left(\frac{T_i - T_a}{G}\right) \quad (9)$$

From Eq. (9), we have $F_R\eta_o$ = 0.1490 and $F_R U_L/C$ = - 2.009 W/°Cm^2. Because the geometric concentration, C is 22.7, $F_R U_L$ becomes - 45.60 W/°Cm^2, according to Eq. (7). From Eq. (2), the optical efficiency of the system η_o = 76.8 %, thus resulting in a heat removal factor F_R = 0.194. This in turn gives an overall heat loss coefficient U_L of - 235 W/(°Cm^2). The negative sign shows that heat is given out of the system. The average thermal efficiency calculated using Eq. (5) amounted to 14.96 % and compares well with the value 14.90 % obtained using Eq. (9).

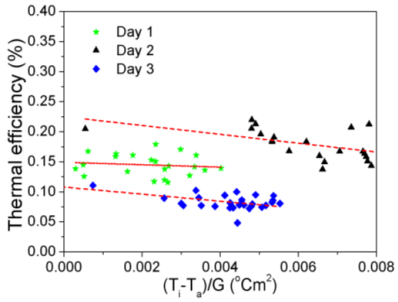


Fig. 5 Thermal efficiency of the PTC using the coated copper tube as a receiver on three different days

For day two the thermal efficiency shown in Fig. 5 is given by the expression

$$\eta_{th} = 0.2251 - 7.362\left(\frac{T_i - T_a}{G}\right) \quad (10)$$

Eq. (10) gives $F_R\eta_o$ = 0.2251 and $F_R U_L/C$ = - 7.362 W/°Cm^2. When the value of C is substituted, $F_R U_L$ becomes – 167.12 W/°Cm^2. From Eq. (2), the optical efficiency of the system η_o = 76.8 %, resulting in a heat removal factor of F_R = 0.293. This in turn gives an overall heat loss coefficient U_L of - 570.38 W/(°Cm^2). The average thermal efficiency calculated using Eq. (5) was 17.48 % and compares well with the value of 22.51 % obtained using Eq. (10).

Thermal efficiency for day three is represented by the expression

$$\eta_{th} = 0.1129 - 6.919\left(\frac{T_i - T_a}{G}\right) \quad (11)$$

which gives $F_R\eta_o$ = 0.1129 and $F_R U_L/C$ = - 6.919 W/°Cm^2. From Eq. (2), the optical efficiency of the system remain η_o = 76.8 %, giving a heat removal factor F_R = 0.147 and hence the overall heat loss coefficient U_L becomes - 1068.62 W/(°Cm^2). The average thermal efficiency calculated using Eq. (5) was 7.65 % and compares well with the value of 8.24 % obtained using Eq. (11). The results of the performance of the coated copper receiver system on the three days are summarized in Table 2.

The wind speed on day 1 and day 3 were the same but according to Eq. (5) the thermal efficiency on day 1 was twice that of day 3 because the mass flow rate for day 1 was thrice that of day 3 despite the larger temperature change on day 3. The thermal efficiency was highest on day two probably because of the higher change in temperature and lower wind speed coupled with the relatively lower GHI value. The influence of the wind speed on the outlet temperature and hence

ISSN: 2521-2292

thermal efficiency can be seen for day 2 when compared to the other days.

Table 2 A summary of the performance parameters for the coated copper receiver system for the three days.

Day	1	2	3
GHI (W/m^2)	923.8	895.4	953.5
T_i (°C)	30.6	27.6	32.3
T_a (°C)	28.6	22.7	28.0
T_o (°C)	54.6	71.2	70.3
ΔT (°C)	24.0	43.6	38.0
Mass Flow (kg/s)	0.0036	0.0026	0.0012
Carnot Efficency η_c (%)	43.91	61.06	54.06
Thermal Efficiency η_{th} (%)	14.96	19.60	7.65
Optical Efficiency η_o (%)	76.8	76.8	76.8
Wind speed (m/s)	4.4	2.8	4.4

C. Thermal efficiency of the commercial receiver

The inlet, outlet and outlet temperatures as well as the GHI obtained with the 2.00 m long commercial receiver having glass envelope insulation are shown in Fig. 6.

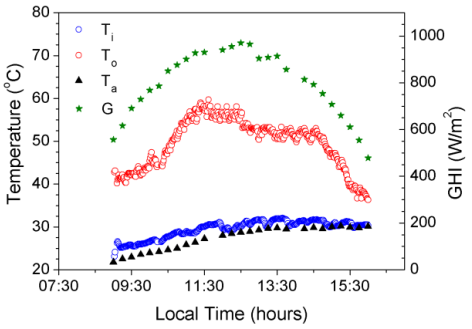


Fig. 6 The inlet, outlet, ambient temperatures and GHI as a function of local time for the PTC with a commercial receiver

On this day, the mass flow rate was set at 0.0036 kg/s. The highest temperature of the water at the outlet was about 60 °C, which is slightly higher than 54.6 °C obtained with the coated copper receiver on a day with a similar mass flow rate.

Carnot and thermal efficiency of the system using the commercial receiver are shown in Fig. 7 as a function of the local time and $(T_i - T_a)/G$, respectively. The average Carnot efficiency for the commercial receiver was found to be 45.67 % with the maximum obtained as 53.26 % at 1230 hours and the lowest being 22.0 % at 1545 hours. The thermal efficiency of the commercial receiver can be described by a linear fit given by

$$\eta_{th} = 0.2776 - 18.242\left(\frac{T_i - T_a}{G}\right) \quad (12)$$

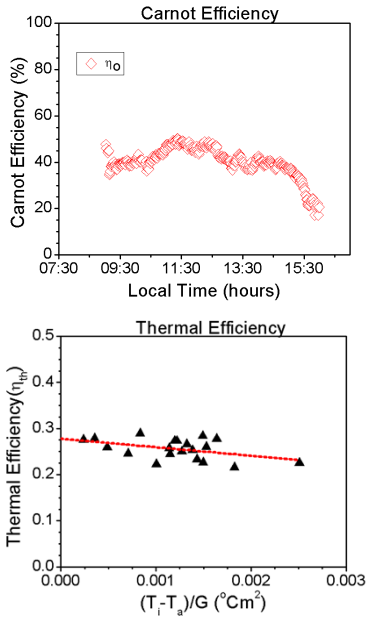


Fig. 7 a) Carnot and b) thermal efficiency of the commercial receiver

This gives $F_R\eta_o$ = 0.2776 and $F_R U_L/C$ = - 18.242 W/°Cm^2. Substituting for the concentration ratio, C = 9.0 gives the value of $F_R U_L$ as - 164.178 W/°Cm^2. The optical efficiency for the commercial receiver was computed using Eq. (5) to be 80.3 %, thus resulting in a heat removal factor F_R = 0.346. The overall heat loss coefficient is thus equivalent to - 474.50 W/(°Cm^2). The average thermal efficiency calculated using Eq. (5) was 26.61 % and compares well to the value of 29.24 % obtained using Eq. (12). The performance parameters obtained for the commercial receiver have been summarized in Table 3.

The performance of the commercial receiver and that of the coated copper tube receiver in this work cannot be compared directly due to the difference in their concentration ratios of 9.0 and 22.7, respectively. The output temperatures achieved in this work show that the PTC can be used for application in industrial process heating especially in food industry where the temperatures needed lie in the range of 60 - 180 degrees [12]. The outlet temperatures from this work are higher than 47.3 °C reported by Macedo-Valencia et al for a PTC of length 0.98 m, width 0.58 m, a concentration ratio 67.17 and a rim angle of 90 ° [13]. Jaramillo et al [14] and Rizwan et al [15] reported higher outlet temperatures of 107.5 °C and 106 °C, with input temperatures of 25 °C and 30 °C respectively. The mass flow rates used by Jaramillo et al and Rizwan et al were 0.0000694 kg/s and 0.0003400 kg/s, respectively while for this work the flow rates were relatively higher at 0.0012 kg/s

ISSN: 2521-2292

up to 0.0036 kg/s. the performance of the PTC prototype reported in this work, is therefore comparable to others tested elsewhere.

Table 3 Measured parameters and calculated efficiencies for the commercial receiver

GHI (W/m²)	1050.2
T_i (ºC)	30.0
T_a (ºC)	36.9
T_o (ºC)	77.8
ΔT (ºC)	47.8
Mass Flow (kg/s)	0.0036
Carnot Efficency η_c (%)	51.10
Thermal Efficiecy η_{th} (%)	26.61
Optical Efficiency η_o (%)	80.3
Wind speed (m/s)	2.8

V. CONCLUSION

A PTC prototype was constructed and tested under terrestrial conditions of Botswana for the first time at Botswana International University of Science and Technology. The results show very high optical efficiencies close to 80 % although the thermal efficiencies were below 50 % for the coated copper tube. The highest thermal efficiency was achieved on day two where the wind speed was the lowest at 2.8 m/s. It is clear that the wind has a strong effect on the thermal efficiency of the PTC. The performance of the system with a commercial receiver was different because of the different (lower) concentration ratio; therefore we cannot compare the performance of the two systems. With these results, the performance of the prototype can be improved by improving on the concentration ratio of the commercial system.

VI. ACKNOWLEDGMENT

This work was supported and financed by the Botswana International University of Science and Technology (BIUST).

VII. REFERENCES

[1] J. Sawin and E. Martinot, “Renewable Energy World,” The World's #1 Renewable Energy Network for News, Information, and Companies, 29 September 2011. [Online]. Available: http://www.renewableenergyworld.com. [Accessed 19 March 2019].

[2] D. Gielen, “Cost analysis series; concentrating solar power vol 1: power sectors, issue 2/5,” IRENA, Europe, 2012.

[3] S. Kraemer, “Renewable Energy World,” The World's #1 Renewable Energy Network for News, Information, and Companies., 29 March 2016. [Online]. Available: http://www.renewableenergyworld.com. [Accessed 28 April 2019].

[4] IRENA, “CSP Plaza, tracking the world csp industry,” cspplaza, 29 January 2016. [Online]. Available: http://en.cspplaza.com. [Accessed 18 February 2019].

[5] Wiston and Strawn, “LEXOLOGY,” Globe Business Media Group, 10 August 2016. [Online]. Available: http://www.lexology.com. [Accessed 24 April 2019].

[6] B. Benza, “MmegiOnline,” 02 June 2016. [Online]. Available: http://www.mmegi.bw. [Accessed 25 April 2019].

[7] A. V. Arasu and T. Sornakumar, “Performance characteristics of Parabolic Trough Solar collector system for hot water generation,” *International Energy Journal,* vol. 7, no. 2, pp. 137-145, 2006.

[8] V. E. Dudley, G. Kolb, A. R. Mahoney, T. R. Mancini, C. W. Matthews, M. Sloan and D. Kearney, “Test results: SEG ls-2 solar collector,” Sandia National Laboratories, Albuquerque, New Mexico, 1994.

[9] S. Kalogirou, “Parabolic triugh collector system for low temperature steam generation: Design and performance characteristics,” *Applied Energy,* vol. 55, no. 1, pp. 1-19, 1996.

[10] S. 9. ASHRAE, “Method of testing to determine the thermal performance of solar collectors.,” American society of heating, refrigeration and air-conditioning engineers, Atlanta, GA, 1986.

[11] R. Gee, R. Brost, G. Zhu and G. Jorgensen, “ReflectechSolar,” 2010. [Online]. Available: http://www.reflectechsolar.com. [Accessed 19 February 2019].

[12] A. G. Bhave, “Industrial process heat applications of solar energy,” *International Journal of Modern Engineering Research,* vol. 2, no. 5, pp. 3800-3802, 2012.

[13] J. Macedo-Valencia, J. Ramirez-Avila, R. Acosta, O. A. Jaramillo and J. O. Aguillar, “Design, construction and evaluation of parabolic trough collector as demostrative prototype,” *Energy proceedia,* vol. 57, pp. 989-998, 2014.

[14] O. A. Jaramillo, E. Veneges-Reyes, J. O. Aguilar, R. Castrejon-Garcia and F. Sosa-Montemayor, “Parabolic trough concentrators for low enthalpy processes,” *Renewable Energy,* vol. 60, pp. 529-539, 2013.

[15] M. Rizwan, A. R. Junaid, M. Suleman and M. A. Hussain, “Experimental verification and analysis of solar parabolic

ISSN: 2521-2292

collector for water desalination," *International Journal of enegineering research,* vol. 3, no. 10, pp. 558-593, 2014.

BIUST Research and Innovation Symposium 2019 (RDAIS 2019)
Botswana International University of Science and Technology
Palapye, Botswana, 4 - 7 June 2019

ISSN: 2521-2292

Smart Energy Meter

Patrick Mapulane , Tshepang Letshwiti, Mompati Molibe, Oagile Gaogane, Keaboka M. Sethebe, N.M.J. Ditshego
Electrical, Computer and Telecommunications Engineering Department, FET,
Botswana International University of Science and Technology (BIUST), BIUST Research and Innovation Centre,
Private bag 16, Palapye, Botswana
Email: patrick.mapulane@studentmail.biust.ac.bw, tshepang.letshwiti@studentmail.biust.ac.bw,
mompati.molibe@studentmail.biust.ac.bw

***Abstract*— This paper presents a smart energy meter for automatic metering and billing system. The integration of a mircocontroller and GSM short message service (SMS) provides the meter reading system with automatic functions that are predefined. The GSM module requires a SIM (Subscriber Identity Module) card just like mobile phones to activate communication with the network. Direct current (DC) components are used to control alternating current (AC) loads. To isolate these components from each other, relays with a network of resistors and diodes are used. Users can recharge and control loads remotely. Utility companies also have remote access to the system such as fault diagnosis and communicating with clients. The proposed energy meter system (EMS) transmits data like consumed energy in kWh and generates a bill over a GSM mobile network. Other advantages include that the system provides domestic power consumption accurately, safely and with a relatively fast update rate.**

***Keywords*—SMART energy meter, mircocontroller, GSM short message service (SMS), energy meter system (EMS), remote access, direct current (DC), alternating current (AC)**

I. INTRODUCTION

Energy meter billing is an important part of energy distribution [1]. The use of manual systems is undesirable. Due to human errors at utility companies, it is a problem for users to get them corrected; that is, customers have to stopover at the company offices, stand in a queue and get it corrected. There is a need to improve the accuracy of the bills. To avoid human intervention in the billing process, an automatic reading meter system can be used [2—6]. Currently, those imported into the country can only measure and monitor electricity but do not allow remote access. The other problems with the sytem is that it requires a lot of manpower; it is time-consuming and prone to errors. "Smart energy meter" can solve these issues by providing services to the consumer through SMS along with other inbuilt features such as tamper-proof, fault detection, etc. The energy meter utilizes a GSM module to monitor energy consumed for the authority [2—6].

Similarly, the utility company can use the GSM service so as to send feedback. The GSM technology used enables the consumer to receive messages about the consumption of power (in KW), and when low, it automatically alert the consumer to recharge. This technology holds good for all electricity distribution companies, private communities, IT parks and self-contained housing projects. The implementation of this project will help in better energy management, conservation of energy and also in doing away with the unnecessary hassles of incorrect billing. The billing system will keep track of consumption and solve any disagreements on consumption and billing [7—11].

Electricity theft is also a common issue. The main disadvantage of the 'ordinary' meter is that it is less reliable, less accurate and non-tamper proof. Even the present day electronic energy meters are not completely tamper-proof. The proposed energy meter has features of detecting faults in the distribution system, which is done by checking the status of supply at a distribution transformer [11—19].

Smart meters are the future because they have vast merits for both the consumers and the producers or suppliers. The main aim is to make the smart meters locally thus improving the number of electronic gadget's manufactured or made locally. The smart meters will, therefore, be able to counteract if not all, most of the demerits of the 'ordinary' meters, for instance; it must allow for remote access and be user-friendly, hence indicating if the amount of electricity used is high or low which leads to regulations and in turn saving energy. A microcontroller and the contactor will be the heart of the design.

II. EXPERIMENT

The smart energy meter circuits will be made by various softwares and components explained within this section. A microcontroller and the contactor will be the heart of the design as shown in figure 1 and 2. The smart meter is designed to give feedback on regular bases. Two main softwares were used: Proteus 8.6 SPO and Arduino software. Proteus was used to design and simulate the circuit. Arduino software was used to to program the microcontrollers. Sample code shown in figure 5 was written using the software and then also used to insert the code in the microchip in the circuit on figure 3 [11—19]. ATMEGA 328 is a high performance, low power AVR 8-bit microcontroller. It has advanced RISC Architecture: up to 20 MIPS throughput at 20 MHz, 32 x 8 general purpose working registers. The device also has high endurance. It controls the entire circuit. All actions the circuit does are monitored by the microchip [11—19].

ISSN: 2521-2292

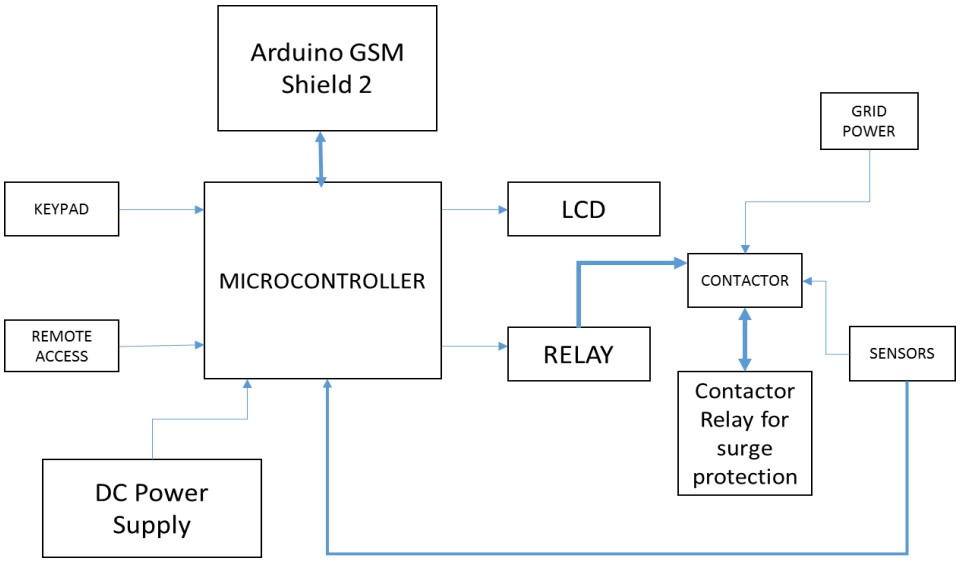


Fig. 1: block diagram

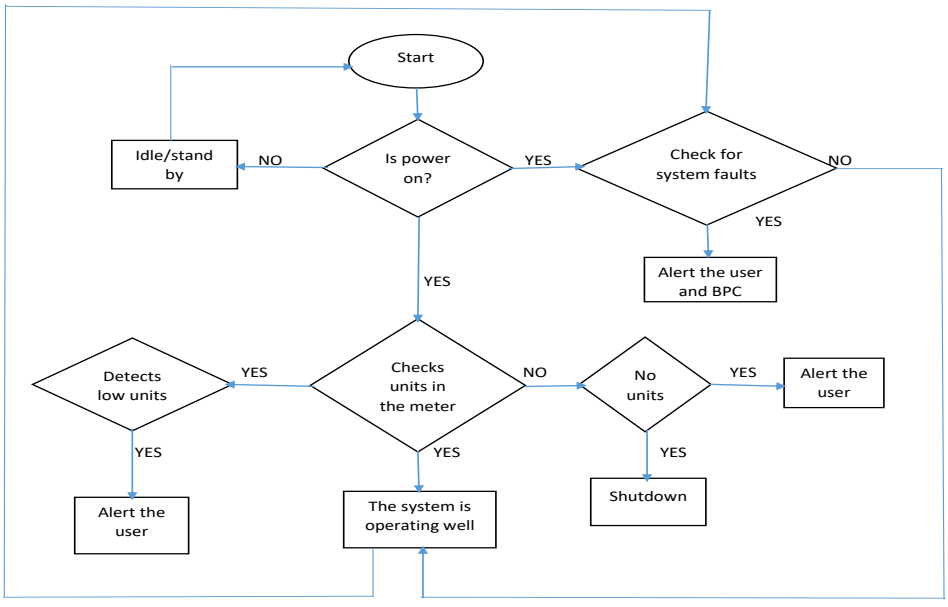


Fig. 2: flow chart

ISSN: 2521-2292

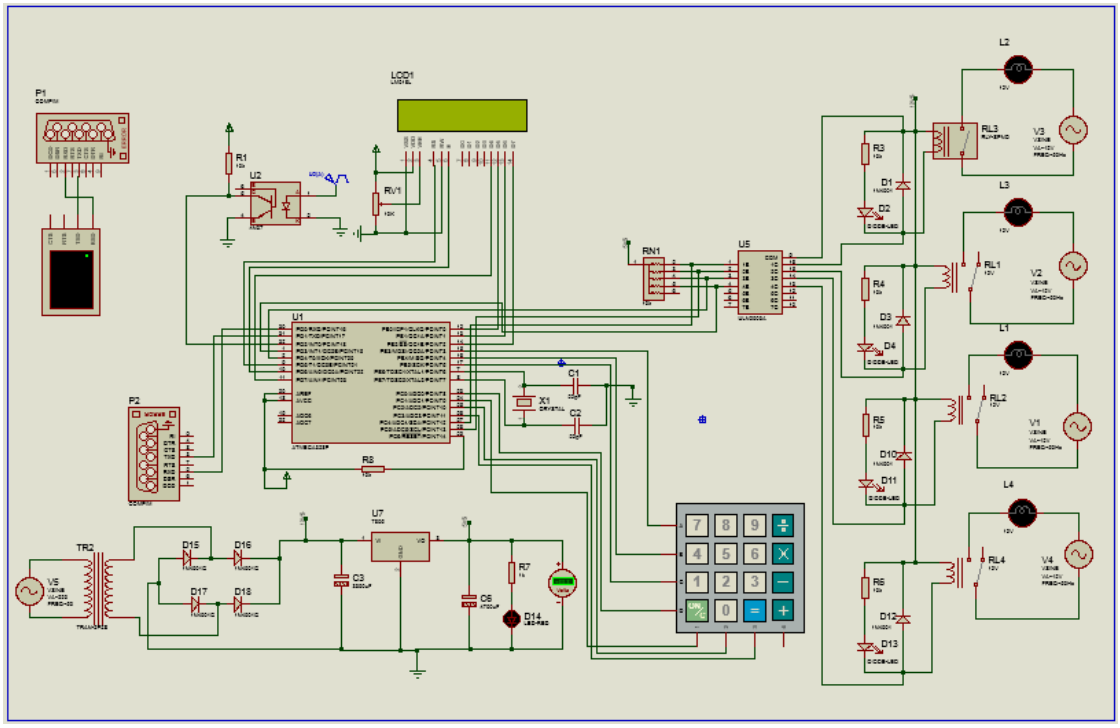


Fig. 3: Circuit diagram

```
#include <LiquidCrystal.h>
#include <TimerOne.h>
// defining library for making working keypad
#include <Password.h>
#include <Keypad.h>


//lcd(RS, E, D4,D5,D6,D7);
LiquidCrystal lcd(5, 6, 7, 8, 9, 10);

float x = 9.9;

#define Pin "pin"
#define ok "OK"
#define ERROR_str "ERROR"
#define Connected "Connected"
#define Connecting "connecting"
#define CLCC "+CLCC:"
#define atCLCC "AT+CLCC"
#define CMGF "AT+CMGF=1"
#define CMGL "+CMGL:"
#define CMGS "AT+CMGS=\""
#define CMGD "AT+CMGD="
#define UNREAD "AT+CMGL=\"REC UNREAD\""
#define CMGDA "AT+CMGDA=\"DEL ALL\""
#define CNMI "AT+CNMI=0,0,0,0"
```

Figure 5: Sample code

The COMPIMs and the virtual terminals allow wireless communication between the user and the meter. Virtual terminal COM1 represent a cell phone used by the user and COM2 is the GSM connected to the circuit. The Arduino GSM Shield 2 allows an Arduino board to connect to the internet, make/receive voice calls and send/receive SMS messages. One of the aims of the project is to allow for remote access as such the shield will help accomplish that as the system will be able to send/or receive text [1]. The function of the power source together with the AC to DC convertor circuit is to provide electrical energy to components which are connected to it [11—19].

The USB cable was used to connect computers to peripheral devices. USB cables are ‘Hot Pluggable’, in other words, you can connect and disconnect the cables while the computer is running without fear of freezing the computer. USB cables carry power as well as signals. This allows for "USB powered" gadgets as well as recharging batteries in USB peripherals. Figure 3 also shows a 16-button keypad that provides a useful human interface component for microcontroller projects. Convenient adhesive backing provides a simple way to mount the keypad in a variety of applications [11—19].

ISSN: 2521-2292

The meter-pulse regulates the rate at which the electrical units in the meter are consumed depending on usage. i.e. high pulse is for high consumption and vice versa. Connecting wires allows an electrical current to travel from one point to another because electricity needs a medium through which to move. In case of computers, wires are embedded onto circuit boards, carrying pulses of electricity that are interpreted as binary signals of zeroes and ones [11—19]. Various capacitors were used which are marked in a variety of ways. The actual format of the capacitor code or marking depends upon the type of capacitor. There are different codes used depending upon whether it is a traditional leaded component, or surface mount and/or type of capacitor dielectric or technology. Size also plays a major part as it determines the space available for the marking. The function of the electrolytic capacitor is to offer high capacitance value on to the circuit board [11—19].

Resistors play an important role to limit the current and provide only the required biasing to the vital active parts like the transistors and the ICs. The crystal oscillator provides a very stable signal. The device can be used in radio for tuning to a specific wavelength or providing that wavelength signal. They can also be used to determine an unknown signals frequency. Any time a very precise signal is required, a crystal oscillator is used. The circuit also has a potentiometer of 10K. In electrical engineering parlance, the term "potentiometer" is used in either one of two ways. It may refer to an instrument that measures an unknown emf or voltage by comparing it to a standard emf. In this instance, it is functioning as a null instrument; it permits precise measurement by adjusting the value of a circuit element until a meter reads zero. Alternatively, "potentiometer" may refer to an electronic component that is used to vary the resistance in a circuit [11—19].

The relays used are electromagnetic devices used to isolate two circuits electrically and connect them magnetically. They are very useful devices and allow one circuit to switch another one while they are completely separate. They are often used to interface an electronic circuit (working at a low voltage) to an electrical circuit which works at very high voltage. The LCD (Liquid Crystal Display) screen used is an electronic display module and finds a wide range of applications. A 16x2 LCD is a very basic module and is very commonly used in various devices and circuits. These modules are preferred over seven segments and other multi-segment LEDs. The reasons being: LCDs are economical; easily programmable; have no limitation of displaying special characters [11—19].

III. RESULTS AND DISCUSSION

When the circuit is simulated, the LCD displays as in figure 6. After GSM connecttion, the LCD then displays as in FIGURE 7. Either the keypad or the cellphone can be used to access the meter. When using the keypad, 0 is used to move down the menu interface while 2 is used to move up. The equal sign (=) is used to select the option the user wants, either recharge or start and (*) is used as back. To input units in the meter, the recharge option should be selected and the meter units' number inputted using the keypad. The LCD should then display the new balance. These can also be done using the phone. After recharging, the user can escape the recharge interface and enter start to show electric consumption. The LCD shows the remaining units in the meter, i.e. the meter counting down. The phone can also be used to switch on/off loads. There are unique alphabets the user needs to input to switch on/ off a certain load. Here are the results of the outputs when they are controlled by the virtual/real cellphone.

Table 1: output results

INPUT	Output controlled	Effects
Pressing a Pressing b	L1	Turns the bulb ON Turns the bulb OFF
Pressing c Pressing d	L2	Turns the bulb ON Turns the bulb OFF
Pressing e Pressing f	L3	Turns the bulb ON Turns the bulb OFF
Pressing g Pressing h	L4	Turns the bulb ON Turns the bulb OFF

Results of when controlling the system using a keypad as an input device are shown below.

Table 2: Keypad results

INPUT	Output controlled	Effects
Pressing 0 Pressing 1	L1	Turns the bulb ON Turns the bulb OFF
Pressing 2 Pressing 3	L2	Turns the bulb ON Turns the bulb OFF
Pressing 4 Pressing 5	L3	Turns the bulb ON Turns the bulb OFF
Pressing 6 Pressing 7	L4	Turns the bulb ON Turns the bulb OFF

For the GSM to be connected to the circuit it must be switch-on which is indicated by a light and this should be pressed immediately after it is powered up. It is indicated by figure 5 below. The lights are a confirmation that the GSM is switched on and/or that the GSM is connecting.

ISSN: 2521-2292

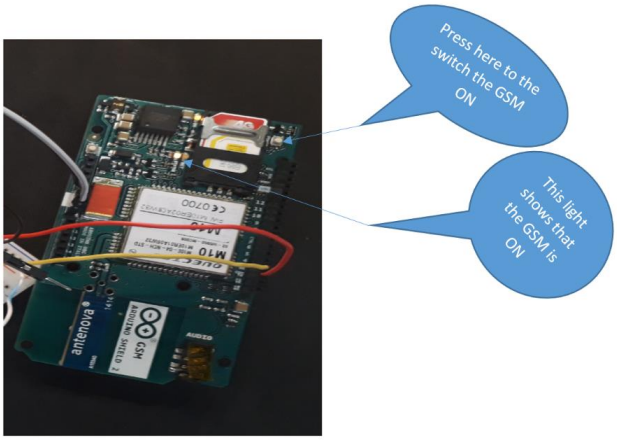


Fig. 5: Setup of the GSM



Fig. 6: GSM connecting to the system

After the GSM is connected, it will then wait for a call (communication with a mobile-phone) for configuration. It should be noted that only one number, for now, can be configured. This is relevant because it is crucial in allowing for user interaction with the system. The mobile-phone is the one which will be used to communicate with the system. Figure 8 shows the system waiting for a call to configure the number.



Fig. 7: GSM connected



Fig. 8: System waiting for call

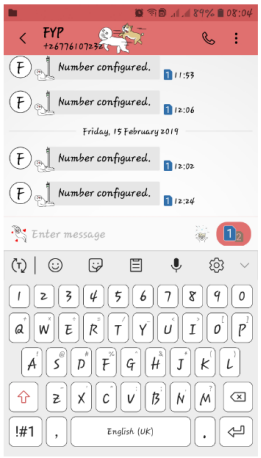


Fig. 9: configuration of the cellphone number

After the GSM received a call, it then sends a configuration message to the number that was used to call the system. Figure 9 shows the number configuration confirmation. Once the

ISSN: 2521-2292

configuration is done, the user will now be able to use the system.

The display shown in figure 10 below is for recharging, which allows users to enter recharge numbers. A particular number entered will recharge the system with particular monetary value and power units depending on the amount used to buy the recharge number.



Fig. 10: recharge of 50 units below.

Since the system is user friendly, it allows for checking of available units after or before recharge. Therefore, the figure below is relevant because it shows the available units after recharge.

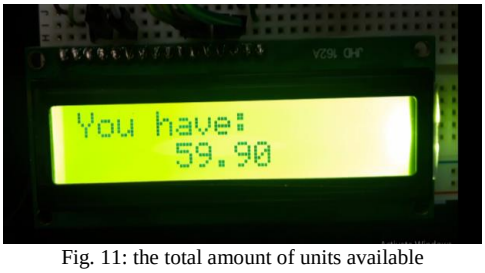


Fig. 11: the total amount of units available

IV. CONCLUSION

Some of the research aims were met, for instance, to allow the meter to be able to send messages to a mobile-phone and to allow for remote access, this was enabled by the Arduino GSM shield 2. Also, the smart meter can be recharged. Problems were experienced with the microcontroller having fewer ports than anticipated. The number of outputs were reduced to address the problem together with some modifications to the circuit. The system also depended for 3G sim cards which are no longer in use. These sim-cards have been faced out in Botswana. The only resort was to change the SIM800A GSM module to GSM shield 2 which allowed for the use of 4G sim card.

V. REFERENCES

[1] O. A. O. N. C. A, "Design and Testing of a Smart Energy Metering System Based on GSM modem," European Journal of Engineering and Technology, Vols. 3, no.4, no. 2056-5860, pp. 35-56, 2015.
[2] Arduino, “Arduino GSM Shield 2 (Integrated Antenna)”, [Online]. Available: https://store.arduino.cc/arduino-gsm-shield-2-integrated-antenna. [Accessed 24 January 2019].
[2] Arduino, “Arduino Mega 2560 Rev3”, [Online]. Available: https://store.arduino.cc/arduino-mega-2560-rev3. [Accessed 24 January 2019].
[3] “Electronic Components”, Engineers Garage, [Online]. Available: www.engineersgarage.com. [Accessed 30 November 2018].
[4] C. Fritz, "Hunker," [Online]. Available: https://www.hunker.com. [Accessed 2 December 2018].
[5] Kushagra, "Electronic Components," Engineers Garage, [Online]. Available: https://www.engineersgarage.com. [Accessed 2 December 2018].
[6] S. M. S. Praveen Vadda, "Smart Metering for Smart Electricity," Master Thesis Electrical Engineering, pp. 3-7, 2013.
[7] Giri Prasad .S, "IoT BASED ENERGY METER," International Journal of Recent Trends in Engineering & Research (IJRTER), no. 2455-1457, pp. 61-62, 2017.
[9] M. J. Jubi.K, "Prepaid Energy Meter with GSM Technology," American International Journal of Reaserch in Science, Technology, Engineering and Mathematics, no. 2328-3580, p. 195, 2013.
[10] Saddam, "Prepaid Energy Meter Using GSM and Arduino," Circuit Digest, 6 February 2016. [Online]. Available: https://circuitdigest.com/microcontroller-projects/prepaid-energy-meter-using-gsm-and-arduino. [Accessed 10 February 2019].
[11] Svsembedded, "GSM based Energy Meter Billing with Load Control using Arduino," Youtube, 29 November 2017. [Online]. Available: https://www.youtube.com/watch?v=Su97JLExmHE. [Accessed 5 February 2019].
[12] F. B. M. N. B. M. Y. S. A. C. A. Win Adiyansyah Indra, "GSM-Based Smart Energy Meter with Arduino Uno," International Journal of Applied Engineering Research, vol. 13, no. 0973-4562, p. 3950, 2018.
[13] C. McNally, "ARDUINO BASED WIRELESS POWER METER," Master of Electrical Engineering Program Cornell University Design Project Report, pp. 18-27, 2010.
[14] E. E. Queen, "Smart Meters and Smart Meter Systems: A Metering Industry Perspective," Edison Electric Institute, Washington, D.C, 2011.
[15] R. R. P. N. K. K. R. A. V. J. A. Geetha B, “Smart Energy Meter Load Control,” International Journal of Advanced Research in Electrical, Electronics and Instrumentation Engineering, vol. 2, no. 8, p. 7, 2013.
[16] Y. Y. B. S. P. Z. Sandhya Shinde, "IoT Based Smart Energy Meter," International Journal of Trend in Scientific Research and Development (IJTSRD), vol. 1, no. 6, p. 3, 2017.
[17] Muhammad Ansar, “Prepaid Energy Meter Billing VIA SMS | Arduino and GSM Based Smart Energy Meter”, Youtube, 22 January 2019. [Online]. Available: https://www.youtube.com/watch?v=Sxg0jkP6AtY. [Accessed 7 May 2019].

ISSN: 2521-2292

[18] Nevon Projects, “Power Meter Reader Plus Load Control Using GSM”, Youtube, 2 July 2015. [Online]. Available: https://www.youtube.com/watch?v=EeUO3SZtRd8. [Accessed 7 May 2019].
[19] Vipul Deshbhratar, “Smart Energy Metering with Real-time Power Analysis and Auto Monthly Billing”, Youtube, 7 March 2017. [Online]. Available: https://www.youtube.com/watch?v=-0frwbl4G40. [Accessed 7 May 2019].

BIUST Research and Innovation Symposium 2019 (RDAIS 2019)
Botswana International University of Science and Technology
Palapye, Botswana, 4 - 7 June 2019

ISSN: 2521-2292

Active Role of Learning Institutions in Promoting Fourth Industrial Revolution (4IR)

Norman Gwangwava
Dept. Mechanical, Energy and Industrial Engineering
Botswana International University of Science and Technology
Palapye, Botswana
gwangwavan@biust.ac.bw

***Abstract*—Industrial revolution has gone through four phases denoted as the 1st industrial revolution (industry 1.0) through the 4th industrial revolution (4IR or industry 4.0). The 4th industrial revolution is taking place in the digital and knowledge based economy. The major enablers of 4IR are integrated technologies that include Internet of Things (IoT), Cyber Physical Systems (CPS), and Cloud Computing (CC). University campuses and other learning institutions play an important role in promoting creativity and innovation among student and professional communities. Such efforts range from boot camps to winter school programs. They promote rapid catching up with fast-changing technology, in collaborative, unique and inspiring environments. Extra curricula activities administered to multi-disciplinary groups are more effective compared to traditional individual centered assignments. The article looks at the role that the Botswana International University of Science and Technology (BIUST) plays in creating an environment conducive to promote 4IR. A qualitative approach is used to study the engineering education initiatives since the inception of the university. Currently BIUST uses the winter school model for enrolled engineering students. The program allows second year students to undergo various engineering workshop practices, gaining essential hands-on skills. The BIUST engineering workshop houses more than twenty laboratories. In order to promote 4IR, the laboratories are equipped with state-of-the-arts machinery for thermal processes, advanced manufacturing, meteorology, and many other disciplines. Other initiatives being mooted to promote 4IR are targeted infrastructure, skills development, financing models, and promoting partnerships between public and private sector (3Ps) through MOUs.**

Keywords: : Fourth Industrial Revolution, 4IR, Industry 4.0, Technology Transfer, Innovation, Engineering Education, Active Learning

I. Introduction

The term Fourth Industrial Revolution (4IR), also known as Industry 4.0, was pioneered in Germany [1-2]. Industry 4.0 refers to the fourth industrial revolution. The 4IR calls for a dynamic transformation of how all aspects of business and production are done. As 4IR continues to change the world, new challenges arise. Successful implementation of the 4IR requires a new digital culture, training, clear vision, support the executives and management, and investment in digital technologies. Organisations must recruit and developing new talent, and be prepared to change [3-4].

The 4IR brings a paradigm shift in education. New trends drift towards less standardised and more personalised (education anywhere and anytime), with particular emphasis on creativity, collaboration, knowledge production and sharing, complex problem solving, flexibility, innovation, adaptiveness, resilience, and leadership skills [5-7]. Citizens of the 4IR need to possess vital and urgent basic and transversal digital literacy skills in order to live, share, communicate, work, learn and actively participate in the 4IR era. The 4IR era is characterized by speed, complexity, hyper-connected and increasingly knowledge-based society. Digital literacy skills for the 4IR include information literacy skills, media literacy skills, and Information and Communication Technologies (ICT) literacy skills.

Under the 4IR, business and industry takes a global focus. Advanced technologies makes globalization a reality since all supply chains can be visible across the world. Connectivity brings agility and visibility in all phases of business execution. Every country and every national becomes a global citizen, actively participating in the global economy. This broad scope of participation requires critical thinking and problem solving skills. The education system of the 4IR must nature global citizens with requisite attributes and abilities. There should be no boundaries in skills and participation.

II. Redesigning Engineering Education

A. Fourth Industrial Revolution

Industrial development has gone through four (4) revolutions in historic times. Shwab [8] gives an illustration to help understand how the industrial revolutions changed across time. During the 1st IR, water and steam were used to mechanize production. During the 2nd IR, electric power was used to create mass production. During the 3rd IR, electronics and information technology were used to automate production [9]. The humankind has been at the center stage of evolving the technology and resources used to make products. Necessity is the push factor that stretches the human mind to

ISSN: 2521-2292

become innovative. As highlighted in the introduction, humankind cannot endure discomfort indefinitely. In times of need for better production means, advanced machinery is launched, whilst a threatening scarcity triggers optimization or substitution of resources. The phases of industrial revolution are denoted as 1st industrial revolution (industry 1.0) through 4th industrial revolution (4IR).

The current level of industrial revolution, industry 4.0, is anchored on integrated technologies that include Internet of Things (IoT), Cyber Physical Systems (CPS), and Cloud Computing (CC) [10 - 12]. Cyber-physical systems (CPS) are physical and engineered systems, whose operations are monitored, coordinated, controlled and integrated by a computing and communication core [13]. CPS can be considered to be a confluence of embedded systems, real-time systems, distributed sensor systems and controls. CPS-enabled smart factories have a network of intelligent objects linking products and assets with information from the internet, as well as capturing context information. Many factors contribute to the progression of manufacturing trends through to the current phase (industry 4.0) and beyond. Some of them include shorter product life cycles, increasing product variation (mass customization), volatile markets, cost reduction pressures, scarce resources, cleaner production, lack of skilled workforce and aging community [14]. Cyber Physical Systems (CPS) and Internet of Things (IoT) technologies such as RFID, wired and wireless sensor networks, and embedded systems enable the digitization and virtualization of shared resources and capabilities in the services, manufacturing and supply chain management for access through the cloud resource pool. These technologies extend the internet into the real world, embracing everyday objects. Cloud Computing is a model for enabling ubiquitous, convenient, on-demand network access to a shared pool of configurable computing resources (e.g., networks, servers, storage, applications, and services) that can be rapidly provisioned and released with minimal management effort or service provider interaction [15]. Individuals and corporate end users access the cloud through internet and access spans over different enterprises and platforms. Cloud services are based on technologies such as HTTP, HTML, XML, JavaScript, or other protocols. CC makes it possible to deliver enterprise information systems (EISs) where each party can contribute to the establishment of the advanced system, while delivering superior integration capabilities with any party's legacy systems and web-based intranets applications.

The 4IR requires the world to produce a new kind of worker—a knowledge worker. Industry leaders, managers and workers must possess skill sets to adapt, to manage their operations in the 4IR. Critical thinking, problem solving, innovation, and communication are some crucial skills required under the 4IR. Change does not wait for anyone. Business, educators, and governments must be innovative in training and retraining the 4IR compliant workforce. Without appropriate models, the future will lack an ill-prepared generation and incapable workforce.

B. Marker Spaces

Makerspaces are being embraced in the education sector as an important development for engineering design education. University campuses and other training institutions are phasing out traditional machine shops, combining the traditional equipment with digital design and manufacturing tools to establish creative communities [16]. Educational makerspace communities support academic, extracurricular and personal design activities under the watch of schools, university faculties, staff, and students. Although makerspaces generally fall under one umbrella definition, different institutions craft out unique focus that drives the identity of the institutions. Various initiatives have been pioneered to promote creativity and innovation among student and professional communities. Such efforts range from boot camps to winter school programs. They promote rapid catching up with fast-changing technology, in collaborative, unique and inspiring environments. Unlike the formal education curricula which contributed to official assessments, these activities are extra curricula and administered to multi-disciplinary groups who are self-motivated to go an extra mile. The approach generates a significant multiplier effect where more interested individuals continue to join the movement.

Engineering education curriculum is centred on solving societal problems by using proven science to design products and systems. Because of the ever-growing complexity of the modern world, design is gaining more attention. Makerspaces are more useful in promoting engineering design because they shorten the time taken to launch new ideas into physical designs. They support iteration of ideas until better solutions are achieved. The culture of the maker movement promotes hands-on learning, openness to new ideas, diversity within problem-solving teams, sharing of techniques and results, teamwork, and multi-disciplinary approach. People use makerspaces for socializing and learning. Individuals with diverse backgrounds and skills come together, self-organize according to their needs and take decisions collectively on issues that appear throughout a project's life (Moilanen, 2012). Through activities such as workshops, software and hardware development, prototyping of new products and processes or improvement of existing ones; the overall aim is to facilitate collective discovery and experimentation, enabling the community to participate actively by peer to peer learning and horizontal knowledge exchange [17].

C. Learning Factories

Engineering education curriculum is centered on solving societal problems by using proven science to design products and systems. Because of the ever-growing complexity of the modern world, design is gaining more attention [18 - 20]. University campuses and other training institutions are

ISSN: 2521-2292

phasing out traditional machine shops, combining the traditional equipment with digital design and manufacturing tools to establish creative communities [21]. Various initiatives have been pioneered to promote creativity and innovation among student and professional communities. Such efforts range from boot camps to winter school programs. They promote rapid catching up with fast-changing technology, in collaborative, unique and inspiring environments. Unlike the formal education curricula which contributed to official assessments, these activities are extra curricula and administered to multi-disciplinary groups who are self-motivated to go an extra mile. The approach generates a significant multiplier effect where more interested individuals collaborate.

A learning factory (LF) is an idealized replica of the real world value chain industry that supports formal and informal learning through interdisciplinary hands-on engineering design projects with strong links and interactions with industry [22-23]. The LF concept was pioneered by a group of universities from the United States in 1995, led by Penn State University [24, 25]. Later on the European government and other states adopted the LF initiative to enhance education of engineers. LFs bring the real world into engineering education. Engineering graduates are exposed to the real life product life cycle – conception, design, prototyping, manufacturing and distribution. LF facilities consist of modern manufacturing facilities – CAD/CAM, CNC and manual machine centers, 3D printing, welding, and metrology.

D. Education 4.0

The fourth Industrial Revolution (4IR) has broad impacts on education. New skills demanded by the 4IR workforce pushes the education sector to innovate and become ready to produce required expertise. 4IR is controlled by artificial intelligence and digital physical frameworks that make human-machine interface more universal. Quick revolution in innovation has delivered another model of education for the future – Education 4.0 [26]. The new vision of learning promotes learners to learn not only skills and knowledge that are needed but also to identify the source to learn these skills and knowledge (Fisk, 2017). In education 4.0, teachers assume the role of facilitators and tracking of learners' performance is done through data-based customization. The new future of education promises a system that:

- responds to the needs of "industry 4.0" or the fourth industrial revolution, where man and machine align to enable new possibilities,
- harnesses the potential of digital technologies, personalised data, open sourced content, and the new humanity of this globally-connected, technology-fueled world,
- establishes a blueprint for the future of learning – lifelong learning – from childhood schooling, to continuous learning in the workplace, to learning to play a better role in society.

Some initiatives of Education 4.0 include Active Blended Learning (ABL). ABL provides a learning environment for students to play an active role. Students are given an opportunity to engage in a variety of ways in and outside the classroom, in the field, in the lab, in the studio and in the workplace.

Chatbots can also be used to help students. Other initiatives in higher education include exchange of students and staff, which is enabled through global and regional networks, and consortium of higher education institutions. Curriculum delivery and technology transfer also make the communities be mindful of the benefits and risks brought about by the 4th Industrial Revolution [27].

III. Practical Engineering Skills Training at BIUST

A. Winter School Prgramme

Winter school and Summer school are educational programmes that offer a range of short courses to boost practical competences among students. These extra curricula programmes are run outside the main academic calendar. Other institutions make use of boot camps to achieve similar purposes. BIUST has been running the winter school programme since its inception. The winter school is offered to engineering students.

B. Enrollment Statistics

BIUST has an annual enrollment of at least 100 students in the Faculty of Engineering and Technology (FET). Upon inception, the university was offering eleven (11) engineering programmes. However, some of the programmes have since been merged due to a number of constraints. The year 2016 had the highest number of students (four hundred and six – 406) who participated in the winter school. The group has was very large and presented several challenges to the institution in terms of efficient teaching. As a young institution, infrastructure is not yet adequate to handle large numbers. There is also a challenge of sustainable student-teacher ratios. These lessons contributed to a new resolution to limit enrollment to 25 students per programme. Fig 1 shows the enrollment statistics.

ISSN: 2521-2292

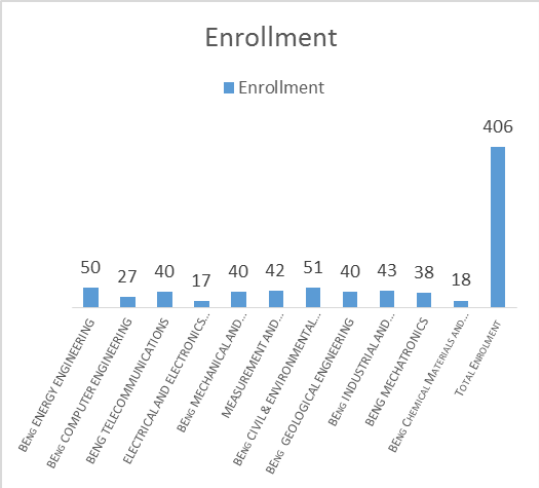


Fig. 1. Winter school enrollment for 2016

The winter school exposes students to a number of practical engineering skills. These range from the use of software programmes for engineering design, modeling, analysis, to workshop practice in fabrication, and other electrical-electronic engineering skills. BIUST has a number of engineering labs equipped with states of the arts software and industrial scale machines for imparting relevant engineering skills to students. Industrial scale machines include CNC lathes, CNC laser cutting, CNC plasma cutting, Water jet cutting, Flexible manufacturing center equipped with a robot. The labs are not only used for learning purposes, but are also used to carry out private jobs from industry. Fig 2 shows the distribution of students who enrolled in specific short courses during the year 2016 winter school programme.

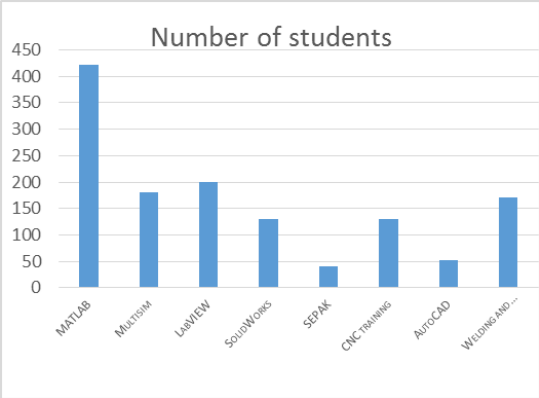


Fig. 2. Number of students who enrolled in specific courses in 2016

IV. CONCLUSION

The fourth industrial revolution (4IR) is changing the world. Components of the 4IR - Artificial intelligence (AI), robotics, big data, internet of things (IoT), and Cloud Computing (CC) impacts on jobs and industry. The workforce of the 4IR perform intellectually intensive jobs which require innovative training through cross cutting education models. Education initiatives to bridge the gap between expectations of the 4IR and current practice include winter school programmes, boot camps, staff and student exchanges, industry-academia linkages, and academics attachment in industry. Full utilization of advanced technologies brought through the 4IR converges to an Education 4.0 experience. Students can only be better prepared for the 4IR jobs when they are exposed to industry technology in the classroom. Technology is changing fast and old education models where students experience real work after finishing four-five year programmes is no longer effective.

REFERENCES

[1] Kagermann, H., Wahlster, W. and Helbig, J., 2013. Securing the future of German manufacturing industry: Recommendations for implementing the strategic initiative INDUSTRIE 4.0. Final report of the Industrie, 4(0).

[2] Shatrevich, V. and Strautmane, V., 2015. Industrialisation factors in post-industrial society. Entrepreneurship and Sustainability Issues, 3(2), pp.157-172.

[3] Ślusarczyk, B., 2018. Industry 4.0: are we ready?. *Polish Journal of Management Studies*, *17*.

[4] Hariharasudan, A. and Kot, S., 2018. A Scoping Review on Digital English and Education 4.0 for Industry 4.0. *Social Sciences*, *7*(11), p.227.

[5] Brailas, A., Avani, S., Gkini, C., Deilogkou, M., Koskinas, K., & Alexias, G. (2017). Experiential Learning in Action: A Collaborative Inquiry. The Qualitative Report, 22 (1), 271-288. Retrieved from https://nsuworks.nova.edu/tqr/vol22/iss1/15

[6] Brailas, A., Koskinas, K., & Alexias, G. (2017). Teaching to emerge: Toward a bottom-up pedagogy. Cogent Education, 4 (1), 1377506. https://doi.org/10.1080/2331186X.2017.1377506

[7] Tsekeris, C., 2019. Surviving and thriving in the Fourth Industrial Revolution: Digital skills for education and society. *Homo Virtualis*, *2*(1), pp.34-42. doi:http://dx.doi.org/10.12681/homvir.20192

[8] Shwab, K. (2016). The Fourth Industrial Revolution: what it means, how to respond. Accessed from https://www.weforum.org/agenda/2016/01/the-fourth-industrial-revolution-what-it-means-and-how-to-respond

[9] Hussin, A.A., 2018. Education 4.0 Made Simple: Ideas For Teaching. *International Journal of Education and Literacy Studies*, *6*(3), pp.92-98.

[10] Baena F, Guarin A, Mora J, Sauza J, Retat S. Learning factory: The path to industry 4.0. Procedia Manufacturing. 2017 Jan 1;9:73-80.

[11] Posada J, Toro C, Barandiaran I, Oyarzun D, Stricker D, de Amicis R, Pinto EB, Eisert P, Döllner J, Vallarino I. Visual computing as a key enabling technology for industrie 4.0 and industrial internet. IEEE computer graphics and applications. 2015 Mar;35(2):26-40.

[12] Kagermann H, Helbig J, Hellinger A, Wahlster W. Recommendations for implementing the strategic initiative INDUSTRIE 4.0: Securing the future of German manufacturing industry; final report of the Industrie 4.0 Working Group. Forschungsunion, 2013.

[13] Rajkumar R, Lee I, Sha L, Stankovic J. Cyber-physical systems: the next computing revolution. In: Design Automation Conference. 2010 Jun 13 (pp. 731-736). IEEE. Available from:

ISSN: 2521-2292

http://dl.acm.org/citation.cfm?id=1837461. [Accessed: 2014-05-16]

[14] Gwangwava N, Mpofu K, Mhlanga S. Big Data and Data Modelling for Manufacturing Information Systems. In: Big Data: Concepts, Methodologies, Tools, and Applications. 2016 (pp. 116-138). IGI Global. DOI:10.4018/978-1-4666-9840-6.ch007

[15] Mell P, Grance T. The NIST Definition of Cloud Computing. National Institute of Standards and Technology (NIST). 2011

[16] Wilczynski, V. (2015). Academic Makerspaces and Engineering Design. American Society for Engineering Education Annual Conference Proceedings.

[17] Smith, A., Fressoli, M., Abrol, D., Arond, E., & Ely, A. (2017). Grassroots Innovation Movements. London: Routledge.

[18] Gwangwava N, Ude AU, Ogunmuyiwa EN, Addo-Tenkorang R. Social Communities of Design and Makers and their Impact on Learning. International Journal of E-Entrepreneurship and Innovation (IJEEI). 2018 Jan 1;8(1):42-61. DOI:10.4018/IJEEI.2018010103

[19] Male SA, Bush MB, Chapman ES. Perceptions of competency deficiencies in engineering graduates. Australasian Journal of Engineering Education. 2010 Jan 1;16(1):55-68. DOI: 10.1080/22054952.2010.11464039

[20] Litzinger T, Lattuca LR, Hadgraft R, Newstetter W. Engineering education and the development of expertise. Journal of Engineering Education. 2011;100(1):123–150.

[21] Wilczynski V. Academic maker spaces and engineering design. American Society for Engineering Education. 2015 (Vol. 26, p. 1).

[22] Abele E, Metternich J, Tisch M, Chryssolouris G, Sihn W, ElMaraghy H, Hummel V, Ranz F. Learning factories for research, education, and training. In: Procedia CiRp. 2015 Jan 1;32:1-6.

[23] Tisch M, Hertle C, Abele E, Metternich J, Tenberg R. Learning factory design: a competency-oriented approach integrating three design levels. International Journal of Computer Integrated Manufacturing. 2016 Dec 1;29(12):1355-75. DOI: 10.1080/0951192X.2015.1033017

[24] Jorgensen JE, Lamancusa JS, Zayas-Castro JL, Ratner J. The learning factory. In: Proceedings of the Fourth World Conference on Engineering Education, St. Paul, Minneapolis, USA. October 15-20, 1995. Available from: http://citeseerx.ist.psu.edu/viewdoc/download?doi=10.1.1.89.6057&rep=rep1&type=pdf [Accessed: 2019-04-06]

[25] ElMaraghy, H, ElMaraghy, W. 2014, Learning Factories for Manufacturing Systems. In: Proceedings of the 4th Conference on Learning Factories, Royal Swedish Academy of Sciences (IVA) and KTH, Stockholm, 27-28 May, 2014.

[26] Shahroom, A. A., & Hussin, N. (2018). Industrial Revolution 4.0 and Education. International Journal of Academic Research in Business and Social Sciences, 8(9), 314–319.

[27] Fisk, P. (2017). Education 4.0 … the future of learning will be dramatically different, in school and throughout life. Retrieved from http://www.thegeniusworks.com/2017/01/future-education-young-everyone-taught-together

BIUST Research and Innovation Symposium 2019 (RDAIS 2019)
Botswana International University of Science and Technology
Palapye, Botswana, 4 - 7 June 2019

ISSN: 2521-2292

Effect of Deposition Temperature on the Wear Behavior of WC-Co coated Mild Steel Substrate

R.R.Phiri & O.P. Oladijo
Department of Chemical, Materials & Metallurgical Engineering
Botswana International University of Science & Technology
Palapye, Botswana
Resego.phiri@studentmail.biust.ac.bw

E.T. Akinlabi
Department of Mechanical Engineering Science
University of Johannesburg, Auckland Park, Kingsway Campus
Johannesburg, South Africa

***Abstract*— Mild steel offers versatile properties at relatively lower cost. Therefore, the alloy has a large application base in the industry, nonetheless mild steel still possesses application limitations required by the increasing complexity and severity of service environments. Atomic-scale surface microstructure modification by rf magnetron sputtering deposition presents a technological solution to improve material properties and performance for a wide range of industrial applications. The focus of this work was to investigate and comment on the wear behavior of surface modified mild steel surfaces subjected to different deposition temperatures. The effect of deposition temperature on the surface morphology of the material is also reported and correlated to the wear performance. The results showed that resistance to dry sliding wear of mild steel increased with increasing deposition temperature as well as decreasing roughness.**

Keywords—mild steel; rf magnetron sputtering; wear perfomance

I. INTRODUCTION

Mild steel is widely utilized in a vast number of engineering application such as construction, nuclear, mining and oil industries amongst many others. This is due to its low cost, good formability and excellent weldability [1]. Mild steel is a material of choice for a variety of engineering applications, but its properties present a setback for applications in extreme operating environments because it is lacking in the simultaneous wear resistance at the surface and tend to break easily upon impact during operations [2]. To improve such properties, surface modification techniques can be employed such that the application of the alloy is broadened.

Sputter deposition of tungsten carbide thin film on the mild steel surface is one of the surface modification method that shows prospect to improve the alloys wear performance and compressive strength to eliminate or minimize its limitations in industry. The WC thin film is opted due to its extreme hardness, good corrosion and wear performance [3-5].

The classification of different surface treatment and film deposition techniques are shown in Fig 1. The choice of the technique depends on the aims and objectives of the project.

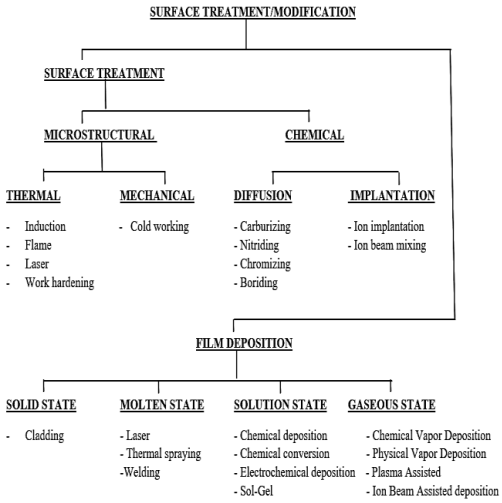


Fig 1. Classification of surface treatment and film deposition n techniques [6]

Sputter deposition is a thin film deposition method which is based upon ion bombardment of a source material (target) to transfer its atoms to the surface of the substrate material [7]. Film forming process parameters such as temperature and sputtering power have a substantial influence on the morphology, quality and properties of WC thin films. [8]. Previous study from Thomton et al [8] indicated that the changes in deposition temperatures directly affect the mobility of adatoms governing the structure evolution. Therefore, it is of great scientific and practical significance to study the effect of deposition parameters on film properties.

Wear is defined as the irreversible loss of interacting surfaces that induces gradual removal or deformation of solid surfaces [9], this surface deterioration eventually leads to material failure or loss of functionality and thus ultimately incur large and undesired economic losses. The combination of material hardness and strength plays a significant role in the wear performance of materials.

ISSN: 2521-2292

The solemn purpose of this study is to specifically investigate the wear behavior of surface coated mild steel synthesized under various deposition temperatures.

II. METHODOLOGY

RF Magnetron sputtering was used to deposit WC-Co thin films onto five mild steel substrates varying temperatures 44°C,70°C,80°C,90°C and 110°C. Samples were then sectioned to 10mm x 5mm dimensions, ultrasonically cleaned in ethanol for 10 minutes and mounted in the Bruker contour GT profilometer to determine the roughness. Wear performance was investigated using a multifunctional tribometer (Rtec-instruments). The equipment can perform tribology test utilizing its inbuilt imaging modules such as interferometer, microscope and AFM spectrometer which was used to produce micrographs and surface profiles of the wear scar. The wear tests were conducted at room temperature under dry conditions. The wear test parameters used are shown in Table 1.

Table 1. Wear test parameters

Item	***Parameter***
Wear Test	Reciprocating, ball on block
Sliding velocity	2 mm/s
Normal Load/Force	10N
Lubrication	Unlubricated/Dry
Ball material	E52100 Alloy steel, grade 25
Ball size diameter	6.350mm
Stroke Length	5mm
Test Duration	5 minutes

III. RESULTS AND ANALYSIS

A. Surface Roughness

Three-dimensional visuals of surface roughness on different sample surfaces are presented in Fig 2 and the roughness properties of the film presented in Table 2. From the surface images, the increase in temperature decreases the surface roughness. This trend has been observed for several thin films and is attributed to the evolution of the microstructure in the structure zone model from zone 1 to zone T [10]. At lower temperatures there is low mobility of adatoms resulting in a rougher film consisting of voids in between tapered column film structure, as the temperature increases, adatom mobility and diffusion increases and coarsening occurs in the early stages of growth thereby forming a smoother crystallographic texture. Further increase beyond 110°C would result in the growth of columnar grains due to bulk diffusion and surface roughness would be expected to increase.

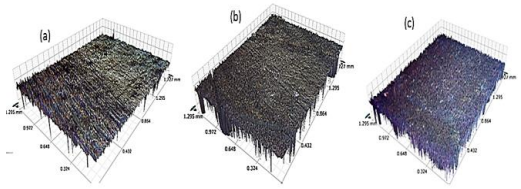


Fig 2. Three-dimensional images of surface roughness for samples deposited at substrate temperatures (a)70°C, (b)90°C and (c)110°C.

Table 2. WC thin film surface roughness properties

	Roughness Properties				
Sample	***Sa(nm)***	***Sku***	***Sp(nm)***	***Sq (nm)***	***Ssk***
44○°C	136.6±24	89.5±40	3808.2±549	201.1±23	1.2±1.9
70°C	263.2±31	22.6±4	4456.8±174	429.4±66	-2.5±0.9
80°C	204.1±54	62.5±25	4349.8±109	313.6±75	-2.23±0.5
90°C	252.2±21	5.8±0.1	4128±369	337.8±26	-0.26±0.1
110°C	310.4±2	5.49±0.3	4351.5±133	402.23±2	-0.124±0.09

B. Tribological Perfomance

The wear performance was investigated on the WC coated samples. The results of the coefficient of friction were shown in Fig 3. The results revealed that as the deposition temperature is increased, the coefficient of friction also increases. This implies that higher resistance to the sliding motion is experienced at elevated deposition temperatures as expected. Hence at higher temperatures there is an increase in film crystallinity. However, the fluctuations of friction coefficients observed at the top of the CoF curve in Fig 3, this is due to the debris influence as well as the continuous breakage and detachment of the hard tungsten carbide layer [11].

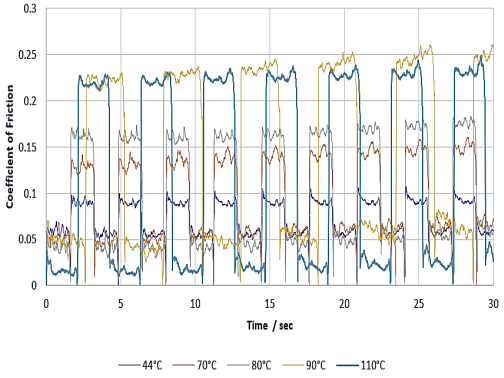


Fig 3. Influence of deposition temperature on the coefficient of friction.

The cross sections of the wear scar profiles are depicted in Fig 4 and their worn surface morphology presented in Fig 5 respectively. The profound ploughed grove observed implies prominent occurrence of abrasive wear. This is expected since the E52100 alloy steel ball used for the test is relatively harder

ISSN: 2521-2292

than the mild steel substrate, the hard tungsten carbide thin coating eventually gets scrapped off during the test exposing the soft mild steel susceptible to ploughing. The surface profiles indicate improved wear performance with increase in temperature. The corresponding 3D images of the wear scar in Fig 5 also show decrease in wear degradation with increasing deposition temperature. This is attributed to the increased crystallite quality of the film due to higher adatom kinetic energy resulting in the formation of preferred growth orientation of the hard WC-Co thin coating on the surface of the mild steel substrate.

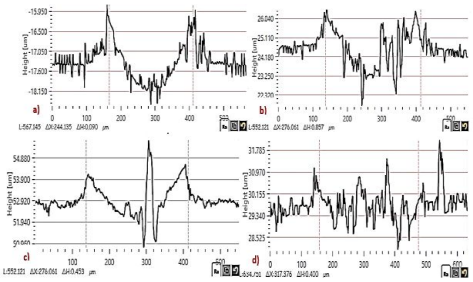


Fig 4. Cross-section of wear scar profile of the coated samples deposited at the temperatures of; (a) 44°C, (b)70°C, (c) 90°C and (d)110°C under constant 10N load.

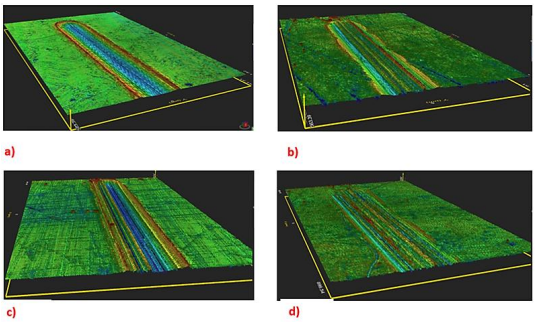


Fig 5. 3D images of coated samples wear scar for deposition temperature variation; (a) 44°C, (b)70°C, (c) 90°C and (d)110°C under constant 10N load.

Investigation was further extended to the volume loss of the film coating. It is thought that the amount of material volume loss on a surface (due to abrasion, erosion or other types of wear) can be used to describe the wear behavior of that material. The wear volume is extrapolated from the measure wear scar geometries and presented in Table 3 and Fig 6. The calculated wear volume decreases with increasing deposition temperature; however, the trend is not perfectly linear. The influence of impurities, the environmental conditions as well as the transformation of the material phases due to thermal effects during the test may be the cause of the observed offsets. The calculated wear volume is governed by the following equation [12];

$$V = \frac{\pi h}{6}\left[\frac{3}{4}d^2 + h^2\right],\ h = \frac{D}{2} - \frac{1}{2}[D^2 - d^2]^{1/2} \quad (1)$$

Where V is the wear volume, h is the scar depth, D is the ball diameter and d is the wear scar width.

Table 3. Wear scar geometries for the determination of wear volume

Sample (Parameter)	*Wear Depth (µm)*	*Wear Width (µm)*	*Wear Volume ($µm^3$)*
WC 1 (44°C)	0.585	244.1	13694
WC 2 (70°C)	0.392	281.7	12221
WC 3 (80°C)	0.345	276.1	10332
WC 4 (90°C)	0.357	262.9	9694
WC 5 (110°C)	0.199	317.4	7876

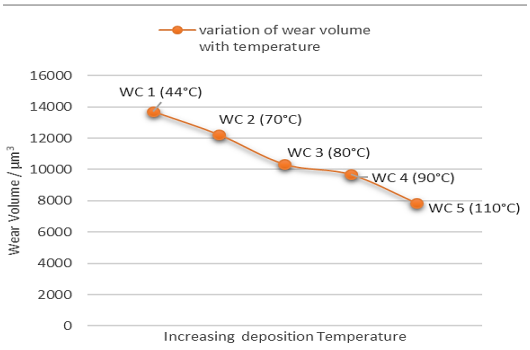


Fig 6. Effect of temperature on wear volume of the WC-Co thin film.

IV. CONCLUSION

The influence of deposition temperature on the surface topography and the wear behavior of tungsten carbide coated mild steel substrate was studied. The surface roughness of the alloy decreases with increasing temperature. better tribological performance is achieved by increasing the deposition temperatures, that is at higher deposition temperature the coated mild steel has a higher coefficient of friction and lower wear volume have more resistant to the sliding motion. The surface modification of mild steel through thin film deposition of tungsten carbide improves the material surface properties.

ACKNOWLEDGMENT

Authors would like to extend their gratitude to the following:

1. Botswana International University of Science and Technology for their financial and technical support.
2. Siam photon synchrotron light research institute, Thailand for their generous technical support and services.
3. Lightsources for Africa, the Americas, Asia and Middle East Project (LAAAMP) for the financial support and opportunities throughout the project.

ISSN: 2521-2292

REFERENCES

[1] G. Tosun, "Ni–WC Coating on AISI 1010 Steel Using TIG: Microstructure and Microhardness", Arabian Journal for Science and Engineering, pp. 2097-2106, 2014.

[2] M.A. Abdulrahaman, O.A. Abubakre, S.A. Abdulkareem, J.O. Tijani, A. Aliyu, A.S. Afolabi, "Effect of Coating Mild Steel with CNTs on its Mechanical Properties and Corrosion Behavior in Acidic Medium", Advances in Natural Sciences: Nanoscience and Nanotechnology, Vol. 8, p. 015016, 2017.

[3] S. Stadler, R.P. Winarski, D.L. Ederer, J. Maclaren, J. Van Ek, and A. Moewes, "The Electronic Structure of Tungsten Carbide", Computer (Long. Beach. Calif), 2001.

[4] T. Tavsanoglu, C. Begum, M. Alkan, M.and O. Yucel, "Deposition and characterization of tungsten carbide thin films by DC magnetron sputtering for wear-resistant applications", Jom, vol. 65, no. 4, pp. 562–566, 2013.

[5] A.M. Venter, O.P. Oladijo, L.A. Cornish, & N. Sacks, "Characterization of the residual stresses in HVOF WC-CO coatings and substrates". Materials Science Forum, 768–769, 280–285, 2013.

[6] B. Podgornik, J. Vižintin, "Tribology of thin films and their use in the field of machine elements", Vacuum, 68(1), pp. 39–47, 2002.

[7] D. Depla, S. Mahieu, J.E. Greene, "Sputter Deposition Processes. [book auth.] P, M Martin. Handbook of Deposition Technologies for Films and Coatings" (Third Edition) Science, Applications and Technology. Burlington : Elsevier, pp. 2-7, 2010.

[8] M.A Lieberman, A.J. Litchtenberg,A,J. "Principles of Plasma Discharges and Materials Processing", 2nd ed. Hoboken : Wiley. pp. 308-310, 2005

[9] K. Kato, and K. Adachi, "Wear Mechanisms, " Mod. Tribol. Handbook. Vol 1, p. 28, 2001,

[10] J.E. Greene, "Thin Film Nucleation, Growth, and Microstructural Evolution: An Atomic Scale View", Third Edit. Elsevier Ltd, 2010.

[11] R.R. Phiri, O.P. Oladijo, N. Maledi, E.T. Akinlabi, E. T. (2018) "Effect of Coating Thickness on Wear Performance of Inconel 625 coating", IOP Conference Series: Materials Science and Engineering, 423(1), pp. 3–7, 2018.

[12] S.M. Hsu.and M.C. Shen, M. C. "Wear Mapping of Materials." Wear – Materials, Mechanisms and Practice, John Wiley & Sons, Ltd, 2005.

BIUST Research and Innovation Symposium 2019 (RDAIS 2019)
Botswana International University of Science and Technology
Palapye, Botswana, 4 - 7 June 2019

ISSN: 2521-2292

DEVELOPMENT OF A DUAL AXIS SOLAR TRACKING CONCEPT USING MORPHOLOGICAL ANALYSIS

Emmanuel Karabo Mpodi, Zeundjua Tjiparuro and Ouduetse Matsebe
Department of Mechanical, Energy and industrial Engineering,
BIUST, Palapye, Botswana
emmanuel.mpodi@studentmail.biust.ac.bw

***Abstract*— Solar energy is an abundant and clean resource. However, solar energy applications face the main dual challenges of low efficiency and high capital investment due to complexity in design. To mitigate low efficiencies, electro-mechanical trackers that follow the sun path to enhance reception of solar energy are used. Usually these devices are complex. The aim of this paper is to come up with a simpler and more efficient system by advancing previous work by the authors that reviewed existing dual-axis solar trackers and collated the fundamental functional objectives embodied in the most efficient ones. The fundamental functional objectives are used, in this paper, to generate different design alternatives with the aid of a morphological analysis technique. The alternatives are evaluated using a five-point Likert scale to select a simpler, more efficient, and practical dual axis photovoltaic solar tracking concept. The selected concept is to be prototyped and tested in another future investigation.**

Keywords*— *dual axis, solar tracking, morphological chart, conceptual design, functional objectives.

I. INTRODUCTION

The morphological chart is a combinatory creative design tool used to aid in generating design concepts. As a design tool, the morphological chart has found application in different multidimensional fields such as astronomy, engineering design (design of jet and rocket propulsion), social policy, etc. [1]-[2]. The power of the morphological chart lies in its bottom-up approach, whereby an overall design solution is configured from very few sub-solutions which are combined in many ways to cause an explosion of many possible solutions [3]. The most suitable one is then selected after an appropriate evaluation process.

II. METHODOLOGY

The conventional approach for generating a morphological chart was used in this study as discussed below.

- *Morphological Chart*

A list of functions collated from studying the embodiment designs of the most efficient dual axis tracking devices were used. Journal, books, catalogues, fliers, internet etc. were used in an extensive search for new and existing ideas for achieving each stated function. In searching for an idea a hint search/key word or sentence for a specific function was used. For instance, for the function; **To accurately determine sun position**, search/key words such as [sun+position+sensor, etc.] were used. To guide the search process so that suitable alternatives are generated, the design checklist given in Table I was developed, complete with the set of: requirements, constraints, and functions to be met; suitable components; and evaluation criteria. The generated requirements and constraints were balanced against design requirements of an existing solar plant at Phakalane (Botswana) obtained through a field interview conducted by the author.

The above helped to generate the four main evaluation criteria of: serviceability, availability, interfacing, and reliable in cloudy weather, that were used in the five-point Likert scale developed to select the most suitable design from the morphological chart of Table II. Each alternative was scored against all the criteria. Then points scored by each alternative were aggregated. Alternatives scoring high points were ranked first choice and selected.

- *Alternatives evaluation*

The alternatives evaluation criteria from the preceding section are based on the 3Ps (people, profit and planet) approach, as illustrated in fig. 1. This method was incorporated in this study because it assigns appropriate measures to profit, social (people) and environment (planet) aspects of a product, such that customer needs and profitability are met without causing any destruction to the environment.

Lastly a concept was developed from the highest scoring

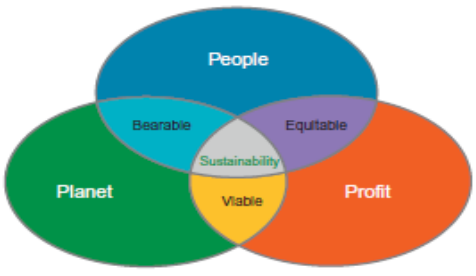


Fig. 1. Venn diagram defining sustainability [4]

selected alternatives. To further enchance the concept, supplimentary components were added at the interfaces of selected components. These components include power storage devices (battery for electrical power) and air compressor to store and supply pressurised air to the pneumatic system

ISSN: 2521-2292

Some of the design measures that are normally used for evaluation of concepts are as defined below.

- *Serviceability/ maintainability*

  This attribute describes the timeliness, relative cost and availability of skilled personnel in the local areas to carry out replacement and/or repair of the component.

- *Reliability*

  The ability to maintain an expected functional behavior at all time and specific conditions

- *Interfacing/ compatibility*

  This measure describes various ways in which a component can be applied (i.e. configurations and strategies) in order to achieve a specific function.

- *Scalability*

  The ability of a component to be re-sized for a specified application.

- *Cost*

  The price value of a component will affect the total cost of device hence its economic feasibility.

- *Availability*

  Ease of access locally or less difficulties in sourcing the component

ISSN: 2521-2292

Table I A map of design checklist, requirements, constraints, functions, components and evaluations measures

CHECKLIST QUESTIONS	REQUIREMENTS	CONSTRAINTS	FUNCTIONS	COMPONENTS	EVALUATION MEASURES
FUNCTIONAL ASPECTS					
What defines a best performing solar tracking devices?	• Should have low tracking error. • Should consume minimum energy as possible.	• Environmental disturbance (cloudiness, wind, rain etc.). • Internal disturbance (interfacing of components). • Power consumption.	• To accurately determine sun position • To precisely calibrate positioning mechanism • To rotate the panel towards the sun using low amount of energy	• Sensors • Control unit • Support structure • Actuator • Energy recycling	• Reliable in Cloudy conditions. • Accuracy and precision of control • High response rate • Power consumption
How is the solar tracking going to be operated i.e. manually, semi-automatic automatic?	Should be fully automated.	Technical know-how of operator	• To monitor the tracking effects • To precisely calibrate positioning mechanism	•Control unit •User`s interface	Adaptability to different control techniques.
In which environmental conditions is the device going to operate?	Should be robust to extreme weather and instant changes.	Environmental conditions Cost	To monitor the tracking effects	Feedback sensors Wind, rain and cloud sensors Support structure	Reliability
Is the device profitable (i.e. what is it payback)?	Should be at an optimum profit return	Financial budget for production	All functions	All components	Cost
What level of maintenance and repairing is required?	• Should be made of components available within the locality of operation. • Should be easy for locals to repair or maintain.	Technical know-how of operator	All functions	All components	Maintainability (cost and timeliness)
What type of technology is required to operate the device?	Should not be obsolete or too advanced for local uses.	Available technological aspect	All functions	All components	Scalability Availability Assemble-ability
NON-FUNCTIONAL ASPECTS					
• What method of waste disposal will be used after product life cycle? • How will the operation of the device after wildlife, birdlife and water sources?	• Should be environmentally friendly (reduced water, wild and birdlife pollutant) • Should be made of material easy to reuse and recycle	Environmental regulations	All components		Sustainability
What size of land is available of the system?	Should cover minimal land as possible	Available land	N/A	Support structure	Land coverage ratio
What level of aesthetics is required for the system?	Should be appealing to consumers	Budget Time	N/A	All components	Versatility (different application of the device e.g. car parks, roof top etc.)

ISSN: 2521-2292

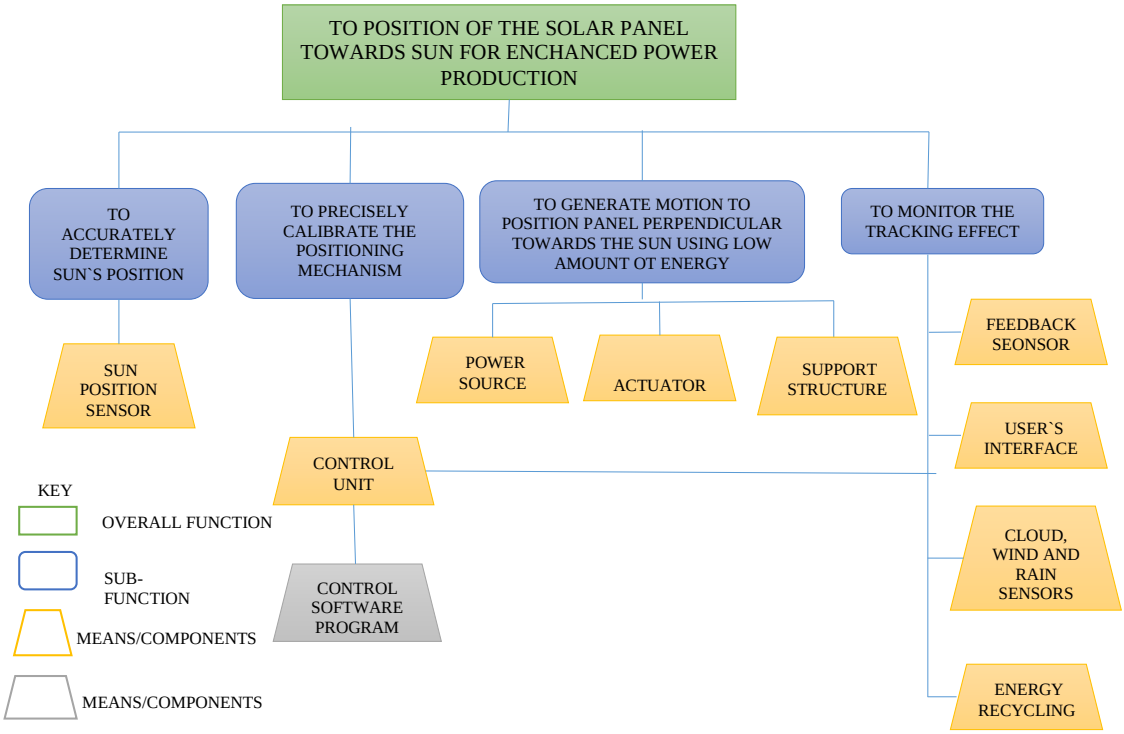


Fig. 2. Function-Means Tree of a solar tracking device

III. MORPHOLOGICAL CHART OF DUAL AXIS SOLAR TRACKING SYSTEM

Previous work by the authors, see Mpodi et al (2019) [5], identified four main modules as very important in the design of an efficient dual tracking system. Fig.2 shows the four main functions and the appropriate means/components needed to achieve them. Sun position sensor determines the change in sun position and sends a signal to a control unit. Then control unit which is equipped with a software program then calculates the output signal and calibrates the motion generating components (i.e. power source, actuator and support structure) to start the positioning of the PV panels towards the sun. Also the control unit measures the tracking effects by monitoring the following components; energy recycling module which reduces energy consumptions by using passive energy form when necessary. Feedback sensor measures the position of the support structure and panel while referencing the desired position of the structure. User`s interface is an interaction platform between the user and the machine. Rain, cloud and wind sensors detects change in environmental conditions that are not conducive for tracking (e.g. unbearable storms).

Table II presents possible practical design alternatives (marked: ALT 1, 2…) for each main function. Equation (1) was used to compute the number of possible solutions, where M denotes the number of alternatives, for each function; N. For this work, the number of possible solutions is equal to: 4, 147, 200.

$$\text{Possible combinations} = \prod_{i=1}^{n} M = 5 \times 2 \times 3 \times 4 \times 4 \times 2 \times 5 \times 4 \times 4 \times 2 \times 3 \times 2 = 4,147,200 \quad (1)$$

Table II Morphological chart of dual axis solar tracking

FUNCTION (FUNC.)	**ALTERNATIVES (ALT.)**				
	ALT 1	***ALT 2***	***ALT 3***	***ALT 4***	***ALT 5***
Sun position sensor (Sun Pos.)	Photo sensors	Real time clock (RTC)	Camera	Global positioning system device (GPS)	(RTC+ photo sensor)
Power source (elec.)	Mini PV panel	Grid electricity			

ISSN: 2521-2292

Power source (mech.)	Solar engines	Spring system	Gravity engines		
Control unit (CU.)	Micro controller	Personal computer (PC)	Programmable Logic controller (PLC)	Field Programmable Gate Array (FPGA)	
Actuator (Act.)	Hydraulic cylinder	Pneumatic cylinder	Motor and gearbox	Stepper motor	
User`s interface (UI.)	Keypad and LCD screen	Safety switch and LED flash light			
Support structure (SS.)	Cable mount	Parallel kinematics device (PKD)	Rotating platform (RP)	Polar mount	Counter balance mount (CBM)
Energy recycling system (ER.)	Spring system	Piezoelectric system	Spring return fluid power actuators	Energy recovery wheel (ERW)	
Feedback sensor (FS.)	Inclinometer	Accelerometer	Magnetometer	Gyroscope	
Wind sensor (WS.)	Electronic Anemometry (EA)	Air flow sensors			
Rain sensor (RS.)	Weighing precipitation gauge (WPG)	Optical rain gauge	Water Sensors		
Cloud sensor (CS.)	Optical sensor	Ceilometer			

Table III Evaluation of design alternatives

FUNC.	**CRITERIA**	**Alt 1**	**Alt 2**	**Alt 3**	**Alt 4**	**Alt 5**
Sun Pos.		Optical sensor	RTC	Camera	GPS	RTC+photo sensors
	Serviceability	4	5	1	3	4
	Availability	5	5	1	3	4
	Interfacing	4	5	1	3	3
	Reliable in cloudy weather	3	2	4	1	5
	Point scored	16	17	7	10	16
	Rank	2	1	4	3	2
Electric.		Mini PV panel	Grid			
	Serviceability	5	4			
	Availability	5	5			
	Reliability	4	3			
	Points scored	14	12			
	Rank	1	2			
Mech.		Solar engines	spring system	gravity engines		
	Serviceability	5	5	4		
	Availability	4	5	2		
	Reliability	5	2	2		
	Points scored	14	12	8		
	Rank	1	2	3		
Act.		Hydraulic cylinder	Pneumatic cylinder	Motor and gearbox	stepper motor	
	High response	3	4	2	5	
	Controllability	4	4	2	4	
	Interfacing	4	5	2	3	
	Minimal energy consumption	3	4	3	5	
	Compatible to support structure	5	5	3	4	
	Points scored	19	22	12	21	
	Rank	2	1	3	2	

ISSN: 2521-2292

FUNC.	CRITERIA	Alt 1	Alt 2	Alt 3	Alt 4	Alt 5
CU.		Micro controller	PLC	FPGA	PC	
	Interfacing	5	3	2	3	
	Accuracy and Precision	3	5	4	4	
	Availability	5	4	3	5	
	Serviceability	5	4	2	2	
	Adaptability to control	4	5	5	5	
	Point scored	22	21	16	19	
	Rank	1	2	4	3	
UI.		Keypad and LCD screen	LED and switch			
	Accessibility of information	5	3			
	High alarm rate	4	4			
	compatibility	5	4			
	Points scored	14	11			
	Rank	1	2			
SS.		Cable mount	Polar mount	Parallel kinematics devices	CBM	RP
	optimal land coverage	4	3	2	5	1
	Versatile utility	3	4	2	5	1
	Assemble-ability	5	3	1	5	3
	Optimal material consumption	5	3	1	4	2
	Robust mechanical	1	4	5	3	5
	Points scored	18	17	11	22	12
	Rank	2	3	4	1	5
ER.		Springs	Piezoelectric	Spring load cylinders	ERW	
	compatibility to control	5	3	5	1	
	ease of use	4	1	5	2	
	Maintainability	5	2	4	1	
	Availability	4	2	5	1	
	Points scored	18	8	19	5	
	Rank	2	3	1	4	
FS.		Accelerometer	inclinometer	Magnetometer	Gyroscope	
	Interfacing	4	5	1	2	
	Cost	5	5	1	1	
	Availability	5	5	2	2	
	Points scored	14	15	4	5	
	Rank	2	1	4	3	
WS.		Electronic anemometry	Air flow sensor			
	Interfacing	4	4			
	Availability	3	5			
	Scalability	3	4			
	Cost	4	5			
	Points scored	14	18			
	Rank	2	1			
RS.		WPG	optical gauge	water sensor		
	Interfacing	1	1	5		
	Availability	2	3	5		
	Scalability	2	4	5		
	Cost	2	1	5		
	Point scored	7	9	20		
	Rank	3	2	1		
CS.		Optical sensor	Ceilometer			
	Interfacing	5	2			
	Scalability	4	3			

ISSN: 2521-2292

FUNC.	CRITERIA	Alt 1	Alt 2	Alt 3	Alt 4	Alt 5
	Availability	5	1			
	Cost	5	1			
	Points scored	19	7			
	Rank	1	2			

IV. DEVELOPMENT OF CONCEPT

From the evaluation, a simpler and more efficient design should embody a real time clock, and a mini-PV cell. The PV cell is used to supply power to a sensor that marks the change in sun position, and also to detect the shade due to cloud cover. The power supplied is stored in a battery to also supply other subsystems. Equations (2) and (3) which calculate the sun azimuth (α_s) and elevation (γ_s) are programmed in a micro-controller to compute the position of the sun. In the equations, where (δ), denotes solar declination angle. It describes the angle between the equatorial plan and the line to the sun or the inclination of the earth axis to an orbit of about 23.45˚. Its value oscillates with the period of a year between 23.45˚ and -23.45˚. Whereas (φ) is Latitude coordinate of geographical location of the tracking devices. Lastly, (h) is the solar time based on the apparent angular motion of the sun across the sky.

$$\alpha_s = \sin^{-1}[\sin\delta \ \sin\varphi + \cos\delta\cos\varphi\cos h] \quad (2)$$

$$\gamma_s = \cos^{-1}\left[\frac{\sin\delta\cos\varphi - \cos\delta\sin\varphi\cos h}{\cos\alpha_s}\right] \quad (3)$$

The output of the process is used to control the direction and speed of the pneumatic actuator which is powered by fluid power system, through solar engine. The solar engine runs the air compressor which drives the pneumatic cylinder to smoothen operations as the power source generate varying power. As the orientation of PV attached to the support structure reaches the maximum azimuthal position at sunset or maximum tilt during winter season, a spring system within the pneumatic actuator is engaged to return the sunset position or the minimum tilt orientation during the summer season. In case of unfavorable weather conditions the air and rain sensors will send signals to the controller to switch the operating mode into safe mode, i.e. the tracking will stop. Table IV and fig.3 illustrate the components and working principle of the proposed concept respectively.

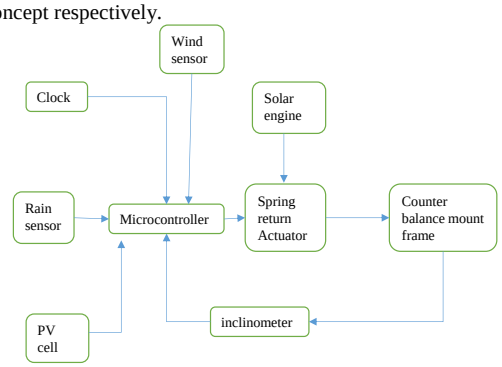


Fig. 3. Solar tracker concept embodiment

Table IV Diagrammatic sketch of a simple and efficient dual-axis tracker

FUNC.	ALT. ALT 1	ALT 2	ALT 3	ALT 4	ALT 5
Sun Pos.	Photo sensors	RTC	Camera	GPS	RTC+ photo sensor
elec.	Mini PV panel	Grid electricity			
mech.	Solar engines	Spring system	Gravity engines		
CU.	Micro controller	PC	PLC	FPGA	
Act.	Hydraulic cylinder	Pneumatic cylinder	Motor and gearbox	Stepper motor	
UI.	Keypad and LCD screen	Safety switch and LED flash light			
SS.	Cable mount	Parallel kinematics device	RP	Polar mount	CBM
ER.	Spring system	Piezoelectric system	Spring return fluid power actuators	ERW	
FS.	Inclinometer	Accelerometer	Magneto meter	Gyroscope	
WS.	EA	Air flow sensors			
RS.	WPG	Optical rain gauge	Water Sensors		
CS.	Optical sensor	Ceilometer			

V. CONCLUSION

In this study the diagrammatic design of simple and more efficient solar tracking concept was developed through the use of morphological analysis. Over 4 million design ideas were found to be possible. After an evaluation process a simpler and practical concept of dual axis solar tracking system was developed. The proposed tracker is a hybrid system with passive solar power. In a future study, the concept will then be modelled, prototyped, and further investigated.

ACKNOWLEDGMENT

Partial funding for this work was from Research Initiation Grant.

REFERENCES

[1] Álvarez, A., & Ritchey, T. (2015). Applications of general morphological analysis. Acta Morph. Gen, 4(1).

[2] Andersson, F., Sutinen, K. & Malmqvist, J., (2003). Product model for requirements and design concept management: Representing design

ISSN: 2521-2292

alternatives and rationale. In 3th Annual International Symposium INCOSE 2003.

[3] Dartnal, J., & Johnston, S. (2005). Morphological analysis (MA) leading to innovative mechanical design. In DS 35: Proceedings ICED 05, the 15th International Conference on Engineering Design, Melbourne, Australia, 15.-18.08. 2005.

[4] Johnson, A., & Gibson, A. (2014). Sustainability in engineering design. Academic Press.

[5] Mpodi, E. K., Tjiparuro, Z., & Matsebe, O. (2019). Review of dual axis solar tracking and development of its functional model. International Conference on Sustainable Materials Processing and Manufacturing, SMPM 2019. Sun City: Elsevier.

BIUST Research and Innovation Symposium 2019 (RDAIS 2019)
Botswana International University of Science and Technology
Palapye, Botswana, 4 - 7 June 2019

ISSN: 2521-2292

IGZO TFT versus the MOSFET

Unopa Matebesi, Gofaone Mogosetso, Caspar K. Lebekwe, N.M.J. Ditshego
ECT, CET, Botswana International University of Science and Technology (BIUST), Private bag 16, Palapye, Botswana
Email: unopa.matebesi@studentmail.biust.ac.bw

W.H.Khoo, S.M.Sultan
School of Electrical Engineering, Universiti Teknologi Malaysia, 81310 UTM Skudai, Johor Darul Takzim, Malaysia
Email: suhanasultan@utm.my

Abstract: Indium gallium zinc oxide thin film transistor (IGZO TFT) characteristics are investigated, improved and then compared with the standard metal-oxide semiconductor field-effect transistor (MOSFET). The device tends to operate with a negative threshold voltage which is undesirable as it means the device is 'ON' at 0.0 V. For the device to be an effective CPU switch, it needs to operate with voltage values between 0.0 V and 5.0 V where the lower value means it is completely 'OFF' with no leakage currents. Negative fixed charge was introduced to help turn the device 'OFF' whereas the MOSFET had negligible values. The TFT was driven at a drain voltage of 1.0 V whereas the MOSFET was at 0.1 V. This made the two devices comparable with similar threshold voltage of 0.6 V and an ideal subthreshold swing of 60 mV/decade. The experiment shows that the subthreshold voltage for the IGZO TFT is excellent at lower drain currents but degrades at higher currents. The quick degradation observed on the subthreshold region can also be attributed to short channel effects (SCEs).

Keywords: Indium gallium zinc oxide thin film transistor (IGZO TFT), metal oxide semiconductor field effect transistor (MOSFET), scaling, short channel effects (SCE)

I. INTRODUCTION

The metal-oxide semiconductor field-effect transistor (MOSFET) has been around for over six decades [1]. Of late the device has failed to meet the technological demands due to poor scaling properties. Ideally all dimensions are normally reduced by a factor 'k', whereas the doping is the opposite and increases by the same factor. But that has not been the case for the MOSFET, the device width and wiring dimensions have not been scaled as fast as the channel lengths. In addition, the device does not allow for voltage scaling due to subthreshold slopes, off currents, and built-in potentials that need to be maintained to avoid device degradation [1─2].

Several techniques have been developed to reduce short channel effects (SCE) which are as follows:

a) Gate (dual work function, low resistance, and tight dimensional control),
b) Insulator (very thin dimensions, reducing defect density, reducing tunnelling current, using substitute material),
c) Channel (making them shallow, strained layer to enhance mobility) [1─7].

High-K dielectrics have been introduced to replace the conventional SiO_2 which should help maintain acceptable-scalable dielectric thickness while keeping gate leakage currents low [1─2]. Even with so many improvements being made on the device, the limits of MOSFET scaling keep approaching. The thickness of the oxide (t_{ox}) cannot be less than 1nm due to higher tunnelling current and significant operational variation. The substrate doping is also very high which creates leakage and tunnelling currents that are unacceptable to device operation. The greatest physical limit in further scaling the MOSFET is the inner distance of atoms in silicon crystals which is around 0.3nm. Thus, up to a certain point, further scaling will not be realised [1─7].

Due to this scaling limit, there has been an introduction of new material and heterojunction structures as alternative to MOSFET device [2]. This paper presents indium gallium zinc oxide (IGZO) planar bulk thin film transistor (TFT) as an alternative to the MOSFET. The device has been around for over two decades [2]. The success of the device in meeting the technological demands has largely been dominated by the shrinking size of its physiognomies and junctionless (no p-n junctions) properties [1]. The junctionless property gives it an advantage over the MOSFET device especially concerning to scaling.

IGZO has practical advantages that make it an attractive semiconductor from an industrial point of view. It has low costs, abundant, non-toxic, transparent, large excitonic binding energy of 60 meV, soluble, compatible with intercellular material, and wide and direct band gap of 3.2 eV making it highly sensitive. The larger the band gap, the better is the semiconductor able to switch states and to insulate leakage currents. IGZO permittivity is 11.9 whereas ZnO permittivity is 8.12 which makes it even more preferred form of material. The higher the permittivity, the higher the output currents. The material allows for low-temperature processing of around 180°C ─ 210°C compared to 850°C ─ 1100°C for silicon. With low-temperature fabrication processes, high-quality devices can be fabricated using conventional processing technology, thereby making it suitable for low-cost mass-production [2─14].

Currently, the main commercial application for IGZO (and/or ZnO) material is in displays, with companies like Sharp and Samsung putting IGZO into mobile phone displays [9─11].

ISSN: 2521-2292

IGZO displays out-perform other semiconductor displays such as amorphous silicon and organic semiconductors by providing improved resolution and reduced power consumption. This is possible because IGZO has x20 to x50 times higher mobility than amorphous silicon and polymers, which allows for device scaling without affecting performance [9–11]. Higher mobility values can also be achieved with amorphous silicon technology, but it needs to be laser annealed which incur more cost in the fabrication process [9–11].

II. SIMULATION PROCEDURE

Three Silvaco products were used: Athena, DevEdit [15] and Atlas [16]. Figure 1 shows the two (2) device structures that were developed using Athena and DevEdit, whereas electrical characteristics and bias conditions were simulated through Atlas. Athena is used mainly to develop and show the fabrication steps in virtual environment of a device whereas DevEdit is more of an integrated circuit (IC) layout editor. DevEdit is excellent at mesh specification, refinement and mask viewing. Both tools produce same results in terms of structures. The TFT structure is assumed to have a single crystal IGZO channel with parameters as stated in Table 1 and compared to the MOSFET.

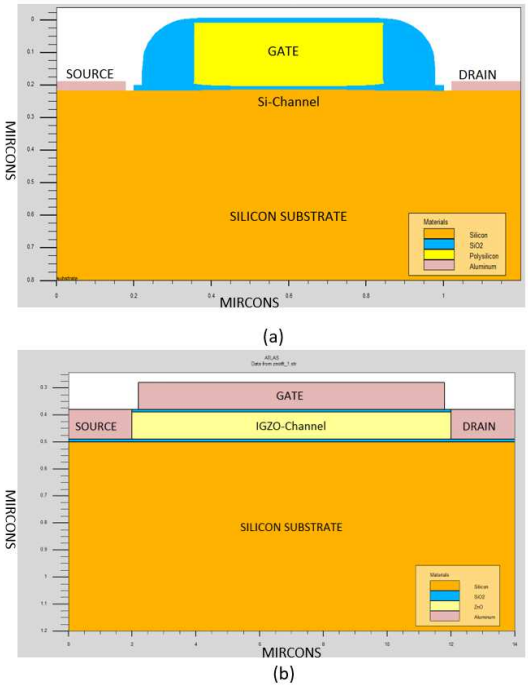


Fig. 1: Structures simulated (a) MOSFET (b) IGZO TFT

Under ATLAS, the physical model used is the Boltzmann model which is sufficient in this case because the other models are for specific situations such as heavily doped regions, low temperatures that tend to freeze the carriers, and for bipolar transistors. For mobility models, Atlas used the default values which are entirely isotropic in nature and there is no directional component. IGZO is a new material and ATLAS software does not provide for IGZO mobility models. For recombination models, the Shockley-Read-hall (SRH) model was utilized as it is the most general model for simulating new materials [10, 16–18].

Table 1: Parameters used for IGZO TFT Simulation; All simulation parameters were defined to be the same as the experimental device.

No.	Physical Parameter	MOSFET	IGZO TFT	Units
1	Si Substrate Doping	$1.32x10^{15}$	$1.32x10^{15}$	cm^{-3}
2	L = Length of channel	$0.5x10^{-6}$	$10.0x10^{-6}$	m
3	T_{ZnO} = Thickness of channel	$0.3x10^{-6}$	$0.1x10^{-6}$	m
4	W = Z = Width of channel	$1.0x10^{-6}$	$1.0x10^{-6}$	m
5	SiO_2 Insulator thickness (d)	$0.05x10^{-6}$	$10.0x10^{-9}$	m
6	Si Substrate thickness	$0.6x10^{-6}$	$0.7x10^{-6}$	m

III. RESULTS AND DISCUSSION

Figure 2 shows the $I_{DS} – V_{GS}$ plot of the TFT structure. It was observed that the IGZO TFT tends to operate with negative voltage based on its subthreshold region. This is undesirable as it means the device is 'ON' at 0.0 V. For the device to be an effective CPU switch, it needs to operate with voltage values between 0.0 V and 5.0 V where the lower value means it is completely 'OFF' with no leakage currents. Negative fixed charge was introduced to help turn the device 'OFF'. Figure 2 shows that increasing negative fixed charge from -3.0 x 10^{10} cm^{-2} to -1.0 x 10^{12} cm^{-2} slowly minimizes the leakage currents and brought the device into desired operational voltage. This change comes with unintended consequences of decreasing the maximum currents as shown in Figure 2(a) and degrading the subthreshold slope (shown in Figure 2b). The quick degradation observed on the subthreshold region can also be attributed to short channel effects (SCEs). This is because SCEs tend to negatively impact the current and also weaken the subthreshold slope [7].

Change in drain voltage was then used to mitigate the unintended consequences of introducing negative fixed charge. Figure 3 shows that the values were changed from 0.1 V to 1.5 V in steps of 0.2 V. The effects are highly desired as drain current was increased without adverse consequences (all other traits remain constant). An increase in drain voltage is desired and must be done with caution to minimize overheating of the device. Overheating degrades the maximum current of the device and damages it over time.

ISSN: 2521-2292

Figure 4 shows the comparison of drain current against gate voltage between IGZO TFT with the standard MOSFET. The graphs depict linear and subthreshold regions. As noted, the MOSFET is simulated under ideal conditions, therefore it has ideal characteristics. To achieve results similar to the ideal MOSFET, the TFT is driven at 1.0 V whereas it is at 0.1 V. This is a disadvantage for the TFT as it is desirable to drive devices with low voltage which can produce high currents. The IGZO TFT also has high fixed charge of -2.0 x 10^{11} cm^{-2} whereas the MOSFET has an ideal value of -3.0 x 10^{10} cm^{-2}. The two devices have a similar threshold voltage of roughly 0.6 V and an ideal subthreshold voltage 60 mV/decade. Figure 4(a) shows that the MOSFET linear region is bending and is starting to saturate whereas the IGZO TFT shows strength in continuing the linear region further. Figure 4(b) shows that the subthreshold voltage for the IGZO TFT is excellent at lower drain currents but degrades at higher currents.

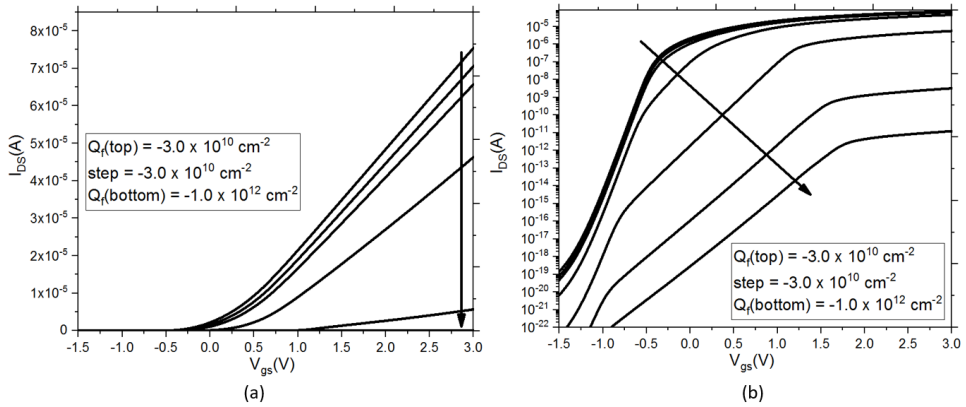


Fig. 2: A plot of drain current versus gate voltage showing the effect of the IGZO TFT fixed charge as it is varied from 3.0 x 10^{10} cm^{-2} to 1.0 x 10^{12} cm^{-2} in steps of 3.0 x 10^{10} cm^{-2}: (a) in the linear region (b) in the subthreshold region.

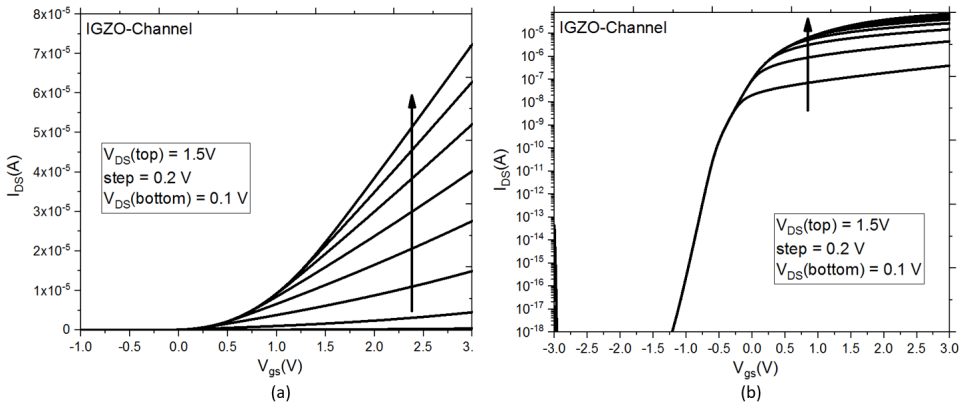


Fig. 3: A plot of drain current versus gate voltage showing the effect of the IGZO TFT drain voltage as it is varied from 0.1 V to 1.5 V in steps of 0.2 V: (a) in the linear region (b) in the subthreshold region. The fixed charge is at -1.0 x10^{12} cm^{-2}.

ISSN: 2521-2292

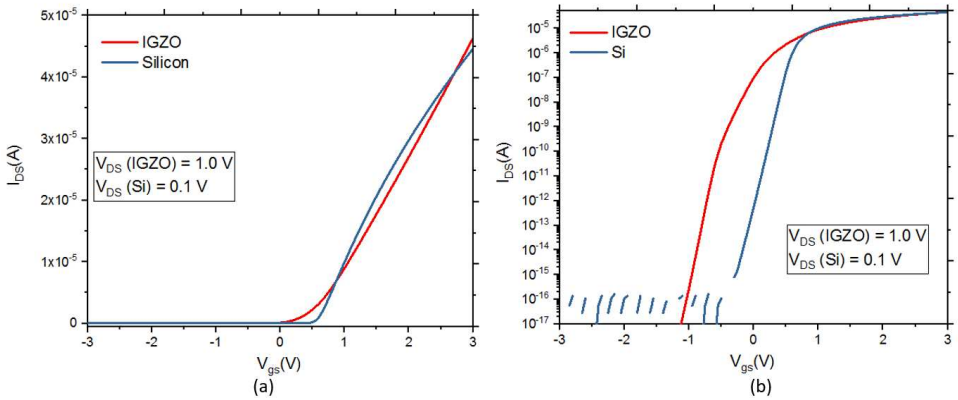


Fig. 4: A plot of drain current versus gate voltage comparing IGZO TFT with the standard MOSFET. The MOSFET is driven at a lower voltage of V_{DS} =0.1 V whereas the TFT is being driven at a higher voltage of V_{DS} = 1.0 V. The graphs depict (a) in the linear region (b) in the subthreshold region

.

IV. CONCLUSION

In summary, IGZO TFT performance has been investigated, improved and then compared with the standard MOSFET. The subthreshold swing of IGZO TFT degraded quickly when negative fixed charge increased from -3.0 x 10^{10} cm^{-2} to -1.0 x10^{12} cm^{-2} due to short channel effects. At an oxide fixed charge of 2.0 x 10^{11} cm^{-2} and at V_{DS} = 1 V, the IGZO TFT exhibits similar threshold voltage of ~0.6V and subthreshold swing of ~60 mV/decade with standard MOSFE at V_{DS} =0.1V. With further scaling, the device can compete with the FinFET and nanowire-FET silicon devices.

V. REFERENCE

[1] Laszlo Balogh, "Fundamentals of MOSFET and IGBT Gate Driver Circuits", Applications Report, Texas Instruments Incorporated, SLUA618A, March 2017

[2] C. Klingshirn, J. Fallert, H. Zhou, J. Sartor, C. Thiele, F. Maier-Flaig, D. Schneider, and H. Kalt, "65 years of ZnO research - old and very recent results," *Phys. Status Solidi*, vol. 247, no. 6, pp. 1424–1447, Apr. 2010.

[3] U. Özgür, Y. I. Alivov, C. Liu, a. Teke, M. a. Reshchikov, S. Doğan, V. Avrutin, S.-J. Cho, and H. Morkoç, "A comprehensive review of ZnO materials and devices," *J. Appl. Phys.*, vol. 98, no. 4, p. 041301, 2005.

[4] M. D. McCluskey and S. J. Jokela, "Defects in ZnO," *J. Appl. Phys.*, vol. 106, no. 7, p. 071101, 2009.

[5] A. Janotti and C. G. Van de Walle, "Fundamentals of zinc oxide as a semiconductor," *Reports Prog. Phys.*, vol. 72, no. 12, p. 126501, Dec. 2009.

[6] D. Hofstetter and H. Morkoc, "ZnO Devices and Applications : A Review of Current Status and Future Prospects," 2010.

[7] M. A. Riyadi, J. E. Suseno, R. Ismail, "The future of non-planar nanoelectronics MOSFET devices: a review", Journal of applied sciences 10(18): 2136-2146, 2010

[8] Arjav Bavarva, Tejas Bavarva, "QLED AnD IGZO: The Future Of Television Display Technology", Electronics For you, May 2018

[9] R. Triggs, "Display technology explained: A-Si, LTPS, amorphous IGZO, and beyond," (Android Authority), [online] July 2014, http://www.androidauthority.com/amorphous-igzo-and-beyond-399778/, (Accessed: 01 March 2015).

[10] J. Hruska, "The perils and promise of high-resolution displays," (Extreme Tech), [online] April 2012, http://www.extremetech.com/electronics/126519-the-perils-and-promise-of-high-resolution-displays, (Accessed: 01 March 2015).

[11] S. Anthony, "IGZO display tech finally makes it to mass market: iPad Air now, high-res desktop display soon," (Extreme Tech), [online] November 2013, http://www.extremetech.com/computing/170970-igzo-display-tech-finally-makes-it-to-mass-market-ipad-air-now-high-res-laptops-and-desktops-next, (Accessed: 01 March 2015).

[12] T. E. Murphy, J. O. Blaszczak, K. Moazzami, W. E. Bowen, and J. D. Phillips, "Properties of electrical contacts on bulk and epitaxial n-type ZnO," *J. Electron. Mater.*, vol. 34, no. 4, pp. 389–394, Apr. 2005.

[13] D.-J. Lee, J.-Y. Kwon, S.-H. Kim, H.-M. Kim, and K.-B. Kim, "Effect of Al Distribution on Carrier Generation of Atomic Layer Deposited Al-Doped ZnO Films," *J. Electrochem. Soc.*, vol. 158, no. 5, p. D277, 2011.

[14] D. Hofstetter and H. Morkoc, "ZnO Devices and Applications : A Review of Current Status and Future Prospects," 2010.

[15] SILVACO International, "DevEdit.manual - DevEdit_users.pdf," (Silvaco International) [Online] May 2010. Available: http://www.silvaco.co.uk/content/kbase/DevEdit.pdf. [Accessed: 28-May-2015].

ISSN: 2521-2292

[16] SILVACO International, “atlas_umv1.book - atlas_users.pdf,” (Silvaco International) [Online] December 2006. Available: http://ridl.cfd.rit.edu/products/manuals/Silvaco/atlas_users.pdf. [Accessed: 28-May-2015].

[17] N.M.J. Ditshego ⇑, K. Sun, I. Zeimpekis, P. Ashburn, M.R.R. de Planque, H.M.H. Chong, "Effects of surface passivation on top-down ZnO nanowire transistors," Microelectronic Engineering (MNE), vol. 145, pp. 91–95, March 2015

[18] N. M. J. Ditshego, N. A. B. Ghazali, M. Ebert, K. Sun, I. Zeimpekis, P. Ashburn, M. R. R. de Planque, and H. M. H. Chong, “ZnO nanowire-FET for charge-based sensing of protein biomolecules,” in 2015 IEEE 15th International Conference on Nanotechnology (IEEE-NANO), 2015, pp. 801–804.

BIUST Research and Innovation Symposium 2019 (RDAIS 2019)
Botswana International University of Science and Technology
Palapye, Botswana, 4 - 7 June 2019

ISSN: 2521-2292

Two Stage Stochastic Bilevel Programming using Stochastic Systematic Evolutionary(SSE) Method

Natnael Nigussie Goshu & Semu Mitiku Kassa
Department of Mathematics and Statistical Sciences
Botswana International University of Science and Technology
Pvt Bag 16, Palapye, Botswana
natnael.goshu@studentmail.biust.ac.bw, kassas@biust.ac.bw

Abstract

Stochastic bilevel programming is a bilevel program having some form of randomness in the problem definition. The main objective is to optimize the leader's (upper level) stochastic programming problem, where the follower's problem is assumed to be satisfied as part of the constraints. Evaluation of the solution requires its corresponding lower level optimal reaction for each leader's action. In addition, due to the existence of randomness property, the problem is computationally so expensive and challenging. In this paper, we considered a two stage stochastic bilevel program and we proposed a new algorithm for solving such kind of problems and the algorithm is checked using constructed test problem. This algorithm is a meta-heuristic type algorithm based on systematical partitioning of upper level decision space for searching the optimal reaction for leader's action from its own decision space and applying particle swarm optimization for searching a better follower's reaction. The result of the numerical simulations of the algorithm is very much promising. The algorithm can be used to solve complex stochastic bilevel programming problem.

Key Words: Two stage stochastic programming, bilevel programming, Stackelberg equilibrium, sample average approximation.

1 Introduction

Stochastic bilevel programming, whose underlying principles have been laid out by Patricsson and Wynter[16] in 1999 for addressing a problem on structural programming, is a bilevel program in which randomness property is involved in the problem definition. The program finds many application, in transportation network[1], energy market modeling[10], traffic model[15], structural mechanics[6, 16], network pricing[17], energy bidding[8], retail market[5], duopoly price fixation[7], telecommunication[2, 21] and multi product pricing[14]. However, due to the existence of randomness property and its hierarchical structure, the problem is computationally so expensive and challenging even for the linear deterministic bilevel program which is the simplest one among the bilevel programming family. Some authors [3, 19] have shown that bilevel linear program is strongly non-deterministic polynomial-time hard problem.

Some of the methods which are used for solving stochastic bilevel programming are stochastic quasi-gradient algorithm[21], and approximation strategies and genetic algorithm[1]. Those proposed methods are limited to some special assumptions like linearity and convexity property for the objective function of follower's problem. The search for solution methods still continues, especially for non-linearity, non-convexity, non-differentiation and other undesirable property involved in the problem. The main objective of this paper is solving two stage stochastic bilevel programming(TS-SMLP) using our proposed algorithm. The algorithm is derivative free meta heuristic type, which is a combination of systematic sampling at each level's decision space and nature inspired particle swarm optimization. Particle swarm optimization was developed by Kennedy and Eberhart[11, 12] in 1995, based on swarm behavior such as schooling of fish and flock of bird in nature and uses real number randomness and global communication among the swarm particles[9, 23].

The rest part of the paper is organized as follows.

ISSN: 2521-2292

Introduction about two stage stochastic bilevel programming is presented in section 2. In section 3, solution procedures is discussed. In addition, numerical examples are presented in section 4. Finally, some remarks on two stage stochastic bilevel programming are made in section 5.

2 Two Stage Stochastic Bilevel Programming

Consider a probability space $(\Omega, \mathscr{F}, P)$, where Ω is a non empty set of all random events, $\mathscr{F}$ the set of all subsets of Ω and P is a probability measure. In addition, consider a finite realizations ξ of $\omega \in \Omega$ and its support function Ξ. A continuous known probability distribution can be represented by a finite set of independent and identically distributed realization samples ξ, which is identified using sample average approximation or sequential bound approximation. The optimal solution and value of the approximated problem is convergent under a suitable condition like convexity[4, 13, 18].

Two stage stochastic programming problem is mathematically expressed as

$$\begin{aligned} &\min_{x}\{F(x) + \mathbb{E}[Q(x,\omega)]\} \\ &\text{subject to } G_i(x) \leq 0, i = 1, \ldots, p \end{aligned} \tag{1}$$

where

$$Q(x,\omega) = \begin{cases} \inf\limits_{\bar{x}} & \bar{F}(x,\bar{x},\omega) \\ \text{subject to} & \bar{G}_{\bar{i}}(x,\bar{x},\omega) \leq 0, \bar{i} = 1, \ldots, \bar{p} \end{cases}$$

with x representing first stage decision variable named as *"here and now variable"* and $\bar{x}$ representing the random second stage decision variable named as *"wait and see variable"* but after the first stage decision, the outcomes of the first stage decision could be affected by random events. So, a second stage decision (recourse) need to be made to compensate for possible violation of constraints and its value function $Q(x,\omega)$ is called the recourse, cost of compensation, or second stage value function.

Two stage stochastic bilevel programming is formulated as

$$\begin{aligned} &\min_{x_1} F_1(x_1,x_2) + Q(x_1,x_2) \\ &\text{subject to } G_1(x_1,x_2) \leq 0, \text{ where } x_2 \text{ solve} \\ &\qquad \min_{x_2} F_2(x_1,x_2) \\ &\qquad \text{subject to } G_2(x_1,x_2) \leq 0 \end{aligned} \tag{2}$$

where $Q(x_1,x_2) = \mathbb{E}_\xi[\Phi(x_1,x_2,\xi)], \xi : \Omega \to R^n$, $n \in \mathbb{N}$ and, for any outcome $\xi(\omega) \in \Xi$,

$$\Phi(x_1,x_2,\xi(\omega)) = \begin{cases} \min\limits_{\bar{x}_1(\omega)} \bar{F}_1(\bar{x}_1(\omega),\bar{x}_2(\omega),\omega) \\ \text{subject to } \bar{G}_1(\bar{x}_1(\omega),\bar{x}_2(\omega),x_1,y_1,\omega) \leq 0, \\ \qquad \text{where } \bar{x}_2 \text{ solve} \\ \qquad \min\limits_{\bar{x}_2(\omega)} \bar{F}_2(\bar{x}_1(\omega),\bar{x}_2(\omega),\omega) \\ \qquad \text{subject to} \\ \bar{G}_2(\bar{x}_1(\omega),\bar{x}_2(\omega),x_1,x_2,\omega) \leq 0 \end{cases}$$

with x_1 and x_2 are first stage decision variables which are decided before observing the random outcome at the second-stage, and $\bar{x}_1$ and $\bar{x}_2$ are second stage decision variables which are supposed to be decided after all randomness property has been removed. In problem (2), assuming that $Q(x_1,x_2,\omega)$, $\bar{F}_1(x_1,x_2,\bar{x}_1(\omega),\bar{x}_2(\omega))$, $\bar{F}_2(x_1,x_2,\bar{x}_1(\omega),\bar{x}_2(\omega))$, $\bar{G}_1(x_1,x_2,\bar{x}_1(\omega),\bar{x}_2(\omega))$ and $\bar{G}_2(x_1,x_2,\bar{x}_1(\omega),\bar{x}_2(\omega))$ are measurable functions, then one and two stage stochastic programming problems are equivalent[1]. So, problem (2) can be reformulated as a standard stochastic bilevel program in the following mathematical form

$$\begin{aligned} &\min_{x_1,\bar{x}_1} F_1(x_1,x_2) + \mathbb{E}_\xi[\bar{F}_1(\bar{x}_1(\xi),\bar{x}_2(\xi),\xi)] \\ &\text{subject to } G_1(x_1,x_2) \leq 0 \\ &\qquad \bar{G}_1(\bar{x}_1(\omega),\bar{x}_2(\omega),x_1,x_2,\omega) \leq 0, \forall\omega \in \Omega, \\ &\qquad \text{where } x_2 \text{ and } \bar{x}_2 \text{ solve} \\ &\qquad \min_{x_2,\bar{x}_2} F_2(x_1,x_2) + \mathbb{E}_\xi[\bar{F}_2(\bar{x}_1(\xi),\bar{x}_2(\xi),\xi)] \\ &\qquad \text{subject to } G_2(x_1,x_2) \leq 0 \\ &\qquad\qquad \bar{G}_2(\bar{x}_1(\omega),\bar{x}_2(\omega),x_1,x_2,\omega) \leq 0, \\ &\qquad\qquad \forall\omega \in \Omega \end{aligned} \tag{3}$$

Therefore, the TS-SBLP in (3) can be rewritten as

$$\begin{aligned} &\min_{x_1,\bar{x}_1} \mathbb{F}_1(x_1,\bar{x}_1,x_2,\bar{x}_2) \\ &\text{subject to } (x_1,\bar{x}_1(\omega),x_2,\bar{x}_2(\omega)) \in \mathbb{S}_1, \ \forall\omega \in \Omega \\ &\qquad \text{where } x_2, \ \bar{x}_2 \text{ solve} \\ &\qquad \min_{x_2,\bar{x}_2} \mathbb{F}_2(x_1,\bar{x}_1,x_2,\bar{x}_2) \\ &\qquad \text{subject to } (x_1,\bar{x}_1(\omega),x_2,\bar{x}_2(\omega)) \in \mathbb{S}_2, \ \forall\omega \in \Omega \end{aligned} \tag{4}$$

where $\mathbb{F}_i(x_1,\bar{x}_1,x_2,\bar{x}_2) = F_i(x_1,x_2) + \mathbb{E}_\xi[\bar{F}_i(\bar{x}_1(\xi),\bar{x}_2(\xi))]$ and

$$\begin{aligned} \mathbb{S}_i = \{&(x_1,\bar{x}_1(\omega),x_2,\bar{x}_2(\omega)) : \\ &G_i(x_1,x_2) \leq 0, \bar{G}_i(x_1,\bar{x}_1(\omega),x_2,\bar{x}_2(\omega)) \leq 0\}, \\ &\forall\omega \in \Omega \end{aligned}$$

at i^{th} level of the decision hierarchy, $i \in \{1,2\}$.

Consider TS-SBLP in (4) and the decision variable space R^m, such that $(x_1,\bar{x}_1(\omega),x_2,\bar{x}_2(\omega)) \in X_1 \times \bar{X}_1 \times X_2 \times \bar{X}_2 = \mathbb{S}(\neq \emptyset) \subseteq R^m$, where $X_i \subseteq R^{m_i}$, $\bar{X}_i \subseteq R^{\bar{m}_i}$, $\sum\limits_{i=1}^{2}(m_i + \bar{m}_i) = m$, $\mathbb{S}^i = \prod\limits_{j=i}^{2}(X_j \times \bar{X}_j)$ and $\mathbb{S}_i$ is the i^{th} level constraint set. Assume that decisions or actions are made from first level decision maker who has control over a vector $(x_1,\bar{x}_1(\omega)) \in X_1 \times \bar{X}_1$ and then reaction is made

ISSN: 2521-2292

from the 2^{nd} decision maker, this process continues sequentially until they achieve Stackelberg equilibrium. Now, let us see some important TS-SBLP definitions.

Definition 2.1. *The following definitions are associated to TS-SBLP problem.*

1. *The constraint region for problem (4) is given by:*

$$\Psi = \{(x_1, \bar{x}_1(\omega), x_2, \bar{x}_2(\omega)) \in \mathbb{S} : (x_1, \bar{x}_1(\omega), x_2, \bar{x}_2(\omega)) \in \mathbb{S}_1 \cap \mathbb{S}_2\}, \ \forall \omega \in \Omega$$

   where $\mathbb{S} = X_1 \times \bar{X}_1 \times X_2 \times \bar{X}_2$.

2. *For each given vector* $(x_1^\circ, \bar{x}_1^\circ(\omega)) \in X_1 \times \bar{X}_1$, *the feasible region of lower levels is given by:*

$$\Psi(x_1^\circ, \bar{x}_1^\circ(\omega)) = \{(x_2, \bar{x}_2(\omega)) \in X_2 \times \bar{X}_2(\omega) : (x_1^\circ, \bar{x}_1^\circ(\omega), x_2, \bar{x}_2(\omega)) \in \mathbb{S}_2\}, \ \forall \omega \in \Omega$$

3. *Projection of* Ψ *on to the* 1^{st} *level decision space is given by:*

$$\Psi(X_1, \bar{X}_1) = \{(x_1, \bar{x}_1(\omega)) : \exists (x_2, \bar{x}_2(\omega)), (x_1, \bar{x}_1(\omega), x_2, \bar{x}_2(\omega)) \in \Psi\}, \ \forall \omega \in \Omega$$

4. *For each* $(x_1^\circ, \bar{x}_1^\circ) \in \Psi(X_1, \bar{X}_1)$, *the rational reaction set of the lower order level is given by:*

$$\Phi(x_1^\circ, \bar{x}_1^\circ) = \{(x_2^\circ, \bar{x}_2^\circ) \in \operatorname{argmin}\{\mathbb{F}_2(x_1^\circ, \bar{x}_1^\circ, x_2, \bar{x}_2)\} : (x_2, \bar{x}_2(\omega)) \in \Psi(x_1^\circ, \bar{x}_1^\circ(\omega))\}, \ \forall \omega \in \Omega$$

5. *The induced region at* 1^{st} *level is defined as:*

$$\Upsilon = \{(x_1, \bar{x}_1(\omega), x_2, \bar{x}_2(\omega)) \in \mathbb{S}_1 : (x_1, \bar{x}_1(\omega)) \in X_1 \times \bar{X}_1, (x_2, \bar{x}_2(\omega)) \in \Phi(x_1, \bar{x}_1(\omega))\}, \forall \omega \in \Omega \quad (5)$$

6. *Using the set* Υ, *one can describe TS-SBLP equivalently as a single level problem of the form:*

$$\min_{\substack{(x_1, \bar{x}_1(\omega), x_2, \bar{x}_2(\omega)) \in \Upsilon \\ \forall \omega \in \Omega}} \mathbb{F}_1(x_1, \bar{x}_1, x_2, \bar{x}_2) \quad (6)$$

   Therefore, because of this equivalence any optimal solution of problem (6) is called a Stackelberg solution for TS-SBLP.

3 SSE Method for TS-SBLP

Assumption 3.1. *Assume* $\mathbb{F}_1$ *and* $\mathbb{F}_2$ *are continuous and measurable in* ω, $\mathbb{S}_1$ *is convex with respect to* x_1 *and* $\bar{x}_1$, *and* $\mathbb{S}_2$ *is convex with respect to* x_2 *and* $\bar{x}_2$, *respectively. In addition, the decision variables are bounded.*

From Assumptions 3.1, $\mathbb{F}_1$ has corresponding to any choice $(x_1, \bar{x}_1(\omega))$ of the leader there is at least one reaction $(x_2^\circ, \bar{x}_2^\circ(\omega))$. But, we can possibly select one of the elements from a set Φ in a unique way, say $\Phi^\circ(x_1, \bar{x}_1(\omega))$. Hence, $\forall (x_1, \bar{x}_1(\omega)) \in X_1 \times \bar{X}_1$, $\Phi^\circ(x_1, \bar{x}_1(\omega))$ contain a unique point and then problem (6) is equivalent to

$$\min_{x_1, \bar{x}_1} \mathbb{F}_1(x_1, \bar{x}_1, \Phi^\circ(x_1, \bar{x}_1(\omega))) \quad (7)$$
$$\text{subject to } (x_1, \bar{x}_1(\omega)) \in X_1 \times \bar{X}_1$$
$$\forall \omega \in \Omega$$

Therefore, due to continuity assumption in Assumption 3.1 over compact set and Weierstrass Theorem, there exist a solution for problem (7).

The randomness property which is involved in the TS-SBLP problem is approximated using sample average approximation method. Then, the next step is partitioning of first level decision space x_1 and $\bar{x}_1(\omega)$ using a step size value β into $a_1^j = \frac{d_1^j}{\beta}$, $\forall j \in \{1, \ldots, m_1\}$, and $\bar{a}_1^j = \frac{\bar{d}_1^j}{\beta}$, $\forall j \in \{1, \ldots, \bar{m}_1\}$, where d_1^j and $\bar{d}_1^j$ are the range of decision variables on the first level dimension space for x_1 and $\bar{x}_1$. Then, merge the first odd ($a_1^j(1)$ or $\bar{a}_1^j(1)$) and even ($a_1^j(2)$ or $\bar{a}_1^j(2)$) partition together as $b_1^j(1)$ for decision space x_1 and $\bar{b}_1^j(1)$ for decision space $\bar{x}_1$ and also merge the remaining partition as $b_i^j(p) = a_i^j(2p-1) + a_i^j(2p)$ and $\bar{b}_i^j(p) = \bar{a}_i^j(2p-1) + \bar{a}_i^j(2p)$, where p indicates partition number. In addition, partition each cell $a_1^j(1)$ and $\bar{a}_1^j(1)$ into maximum number of iteration (MaxIter) using a step size value β° for selecting one distinct point at each iteration to avoid repetition, where

$$\beta^\circ = \frac{\beta}{\text{MaxIter}} \quad (8)$$

Here, select γ^{th} first sub-interval and $(\text{MaxIter} - \gamma + 1)^{th}$ second sub-interval from the first partition ($b_1^j(1)$ or $\bar{b}_1^j(1)$) of j^{th} dimension leader's decision space and distribute it to the remaining first level decision space using systematic sampling approach with a step size β, where γ is a unique random natural number between 1 and MaxIter in each iteration. Then, after representatives are chosen, leader's action from his/her own space $X_1 \times \bar{X}_1$ is sent to search good reactions from $X_2 \times \bar{X}_2$ using particle swarm optimization.

Let $(x_2^\lambda, \bar{x}_2^\lambda)$ and $(v_2^\lambda, \bar{v}_2^\lambda)$ be the position vector and velocity for particle λ, where $\lambda \in \{1, \ldots, q\}$. Each particle is attracted towards current global best position $(x_2^G, \bar{x}_2^G)$ and its own best location $(x_2^P, \bar{x}_2^P)$ in history, while at the same time it has a tendency to move randomly. Therefore, the new velocity vector is determined by

$$(v_2^\lambda, \bar{v}_2^\lambda)^{t+1} = w(v_2^\lambda, \bar{v}_2^\lambda)^t + \alpha_1 r_1((x_2^G, \bar{x}_2^G) - (x_2^\lambda, \bar{x}_2^\lambda)^t) + \alpha_2 r_2((x_2^P, \bar{x}_2^P) - (x_2^\lambda, \bar{x}_2^\lambda)^t) \quad (9)$$

ISSN: 2521-2292

where r_1 and r_2 are two random numbers, and each entry taking the values between 0 and 1, α_1 and α_2 are called acceleration coefficients and $\alpha_1 \approx \alpha_2 \approx 2$[12]. In addition, $w(v_2^\lambda, \bar{v}_2^\lambda)^t$ is said to be inertia term, $\alpha_1 r_1((x_2^G, \bar{x}_2^G) - (x_2^\lambda, \bar{x}_2^\lambda)^t))$ is social component and $\alpha_2 r_2((x_2^P, \bar{x}_2^P) - (x_2^\lambda, \bar{x}_2^\lambda)^t)$ is cognitive component. So, the new position should be updated by

$$(x_2^\lambda, \bar{x}_2^\lambda)^{t+1} = (x_2^\lambda, \bar{x}_2^\lambda)^t + (v_2^\lambda, \bar{v}_2^\lambda)^{t+1} \tag{10}$$

If a particle find a location that is better than any previously found locations, then update it as the new current best for particle λ. The aim is to find global best among all the current best solutions until a certain number of sub-iterations, then send $(x_2^\circ, \bar{x}_2^\circ(\omega)) := (x_2^G, \bar{x}_2^G)$ as an optimal response for the upper level problem.

Finally, for each distinct and selected leader's action there is optimal reaction which is in the induced region and this continues until we find a better solution based on leader's problem using equation (7). However, we may not be sure that the current solution for a given iteration is the best. Due to this we should formulate a new solution in each iteration and use the following two definitions which are taken from [22] for comparition of results at each iteration.

Definition 3.2. *A given point* $(x_1^\circ, \bar{x}_1^\circ, x_2^\circ, \bar{x}_2^\circ)$ *is an* ϵ*-approximate Stackelberg solution in problem (4) if*

$$\mathbb{F}_i(x_1^\circ, \bar{x}_1^\circ, x_2^\circ, \bar{x}_2^\circ) \leq \mathbb{F}_i(x_1^\star, \bar{x}_1^\star, x_2^\star, \bar{x}_2^\star) + \epsilon_i(1 + |\mathbb{F}_i(x_1^\circ, \bar{x}_1^\circ, x_2^\circ, \bar{x}_2^\circ)|)$$

where, $\epsilon = (\epsilon_1, \epsilon_2)$, $(x_2, \bar{x}_2(\omega)) \in \Phi(x_1, \bar{x}_1(\omega))$, $\forall i \in \{1, 2\}$ *and* $\forall \omega \in \Omega$.

Definition 3.3. *A point* $(x_1^\circ, \bar{x}_1^\circ, x_2^\circ, \bar{x}_2^\circ) \in \Psi$ *is said to be an* ϵ*-better solution in problem (4) than* $(x_1^\nabla, \bar{x}_1^\nabla, x_2^\nabla, \bar{x}_2^\nabla)$ *if*

1. $(x_1^\nabla, \bar{x}_1^\nabla, x_2^\nabla, \bar{x}_2^\nabla) \notin \Psi$, *or if the following two statements hold true.*
2. $\forall \delta = (\delta_1, \delta_2)$ *such that* $(x_1^\nabla, \bar{x}_1^\nabla, x_2^\nabla, \bar{x}_2^\nabla)$ *is a* δ*-approximate Stackelberg solution,* $\exists \epsilon = (\epsilon_1, \epsilon_2)$ *such that* $\epsilon_i \leq \delta_i$, $\forall i \in \{1, 2\}$ *but at least one component is* $\epsilon_i < \delta_i$ *and* $(x_1^\circ, \bar{x}_1^\circ, x_2^\circ, \bar{x}_2^\circ)$ *is an* ϵ*-approximate Stackelberg solution.*

If number of iterations increases to infinity, then ϵ-approximate Stackelberg solution approaches to Stackelberg solution. The following pseudo code is the algorithm for SSE method ,to solve TS-SBLP.

- Step 1: Consider TS-SBLP with bounded decision variables.
  Input: m_i, $\bar{m}_i$, l_i^j, u_i^j,$l_i^{\bar{j}}$, $u_i^{\bar{j}}$, $\mathbb{S}_i$, $\mathbb{F}_i$, d_1^j, $\bar{d}_1^{\bar{j}}$, $\xi \in \Xi$, where $\xi(\omega) \to R^N$, $\{\xi_i\}_{i=1}^{100}$,$\forall j \in \{1, \ldots, m_j\}$ and $\forall \bar{j} \in \{1, \ldots, \bar{m}_j\}$.
  Algorithm parameters: $a_1^j = 2 \cdot \text{ceil}(\frac{d_1^j}{2\beta})$, $\bar{a}_1^j = 2 \cdot \text{ceil}(\frac{\bar{d}_1^j}{2\beta})$, b_1^j, $\bar{b}_1^j$, ϵ, $\beta^\circ = \frac{\beta}{\text{MaxIter}}$, k and perm = randperm(MaxIter)
- Step 2: Set iteration $IT = 1$
- Step 3: Partitioning of random space and decision space
  - Step 3.1: Partition the random space using the probability distribution
    $$\xi = \mu + \text{ rand}(1, n)\sigma$$
    where μ is mean, σ is variance and n is the number of realization, and then use sample average approximation.
  - Step 3.2 Partition the space of the *"here and now variables"* on the interval $[l_1^j, u_1^j]^{m_1}$ for leader's problem
    $x_1^j(1) = l_1^j + (\text{perm}(IT) - 1)\beta^\circ + \text{rand}(1)\beta^\circ$
    $x_1^j(2) = l_1^j + \beta + (\text{MaxIter} - \text{perm}(IT) + 1)\beta^\circ + \text{rand}(1)\beta^\circ$
    for $q = 3 : 2 : 2b_1 - 1$
    $x_1^j(q) = x_1^j(q-2) + 2\beta$
    $x_1^j(q+1) = x_1^j(q-1) + 2\beta$
    end for
    do Step 3.2 again for the space of the *"wait and see variables"* on the interval $[\bar{l}_1^j, \bar{u}_1^j]^{\bar{m}_1}$ for leader's problem
- Step 4: Find optimal reaction $(x_2^\circ, \bar{x}_2^\circ) \in X_2 \times \bar{X}_2$, for each $(x_1^\star, \bar{x}_1^\star) \in X_1 \times \bar{X}_1$, using particle swarm optimization from the second level decision space
  - Step 4.1: Input: q number of particles, maximum number of iterations, α_1, α_2, w
  - Step 4.2: Initialize locations $(x_2^\lambda, \bar{x}_2^\lambda)$ and velocity $(v_2^\lambda, \bar{v}_2^\lambda)$ for each λ, where $\lambda \in \{1, \ldots, q\}$
  - Step 4.3: Find $(x_2^P, \bar{x}_2^P)^{t=0}$ from argmin$\{\mathbb{F}_2(x_1^\star, \bar{x}_1^\star, x_2^\lambda, \bar{x}_2^\lambda)\}$
  - Step 4.4: For loop($t = t + 1$ pseudo time or iteration counter)
    for loop over all q particles and $m_i + \bar{m}_i$ dimensions
    Generate new velocity $(v_2^\lambda, \bar{v}_2^\lambda)^{t+1}$ using equation (9)
    Calculate new locations $(x_2^\lambda, \bar{x}_2^\lambda)^{t+1}$ using equation (10)

ISSN: 2521-2292

Evaluate objective functions at new locations $(x_2^{\lambda}, \bar{x}_2^{\lambda})^{t+1}$
Find the current best for each particle $(x_2^P, \bar{x}_2^P)$
end for
Find the current global best $(x_2^G, \bar{x}_2^G)$
end for

– Step 4.5: Output the final results $(x_2^G, \bar{x}_2^G)$ and let $(x_2^\circ, \bar{x}_2^\circ) := (x_2^G, \bar{x}_2^G)$

- Step 5: Select approximate solution using leader's problem from equation (7),

$$\mathbb{F}_1(x_1^\circ, \bar{x}_1^\circ, x_2^\circ, \bar{x}_2^\circ) \leq \mathbb{F}_1(x_1, \bar{x}_1, x_2^\circ, \bar{x}_2^\circ)$$

and then set a solution, $(x_1, \bar{x}_1, x_2, \bar{x}_2)$ for iteration IT.

- Step 6: If $IT > 1$, update ϵ-approximate Stackelburg solution using Definition 3.2 and equation

$$\epsilon_i(IT) = \frac{1}{IT} \cdot \frac{k(4\beta^2)^{\frac{1}{2}}}{1 + |\mathbb{F}_i(x_1^\circ, \bar{x}_1^\circ, x_2^\circ, \bar{x}_2^\circ)|}$$

- Step 7: Terminate, if IT = MaxIter, else set $IT = IT + 1$ and go to step 3.

- Step 8: Out put: $(x_1, \bar{x}_1, x_2, \bar{x}_2)$

4 Simulation Results

TS-SBLP problem (4) can be reduced to a deterministic problem or a finite number of deterministic problems when either the random variables which are provided in the problem are fixed by a single or finite number of realization ξ. In any case, we will check the effectiveness and competitiveness of our proposed algorithm using deterministic bench mark Stackelberg problem from literature[20] in Example 4.1. Moreover, we construct TS-SBLP problem which is in Example 4.2 for testing our new algorithm.

Example 4.1. *[20].*

$$\begin{aligned}
&\min_{x_1} x_1^2 + (x_2 - 10)^2 \\
&\textit{subject to } \mathbb{S}_1 = \{(x_1, x_2) : -x_1 + x_2 \leq 0\}, \\
&\qquad \textit{where } x_2 \textit{ solves} \\
&\qquad \min_{x_2} (x_1 + 2x_2 - 30)^2 \\
&\qquad \textit{subject to } \mathbb{S}_2 = \{(x_1, x_2) : x_1 + x_2 \leq 20\} \\
&\qquad\qquad x_1 \in X_1 = [0, 15],\ x_2 \in X_2 = [0, 20]
\end{aligned}$$

After implementing the SSE algorithm using MATLAB©software, we let it run 10 independent times, where each run has 50 iteration and $\beta = 0.25$. So, we obtain optimal values to be $\mathbb{F}_1 = 99.989$ and $\mathbb{F}_2 = 2.7439e^{-006}$, with optimal solution $(9.9994, 9.9994)$ is appeared at 6^{th} iteration. Whereas the optimal value and solution on the literature[20] are $\mathbb{F}_1 = 100.0001$ and $\mathbb{F}_2 = 5.5e^{-011}$, with optimal solution $(10.0009, 9.9993)$. Therefore, according to equation (5), the solution method SSE is competitive and very promising.

The following example is for TS-SBLP in normal (N) probability distribution.

Example 4.2.

$$\begin{aligned}
&\min_{x_1, \bar{x}_1} x_1^2 + (x_2 - 10)^2 + \mathbb{E}[\omega \bar{x}_1 + (\bar{x}_2 + \omega)^2] \\
&\textit{subject to } \mathbb{S}_1 = \{-x_1 + x_2 \leq 60, x_1^2 + \bar{x}_1 + 2\bar{x}_2 - \omega \leq 20\}, \\
&\qquad \textit{where } x_2 \textit{ and } \bar{x}_2 \textit{ solves} \\
&\qquad \min_{x_2, \bar{x}_2} (x_1 + 2x_2 - 30)^2 + \mathbb{E}[2\omega \bar{x}_1^2 + \omega \bar{x}_2] \\
&\qquad \textit{subject to } \mathbb{S}_2 = \{2x_1 + x_2 \leq 20, \\
&\qquad x_1 + \bar{x}_1 + 2\bar{x}_2 - \omega \leq 10\} \\
&\qquad\qquad x_1 \in X_1 = [0, 15],\ x_2 \in X_2 = [0, 20] \\
&\qquad\qquad \bar{x}_1 \in \bar{X}_1 = [0, 10],\ \bar{x}_2 \in \bar{X}_2 = [0, 6] \\
&\qquad\qquad \forall \omega \in \Omega, \omega \sim N(2, 3)
\end{aligned}$$

After implementing the algorithm the optimal values are $\mathbb{F}_1 = 33.8243$ and $\mathbb{F}_2 = 0.47757$, with optimal solution $(0.408675, 0.401272, 14.7957, 0)$ which is appeared at 18^{th} iteration, where $\beta = 0.5$.

5 Conclusion

In this paper TS-SBLP is considered and a new type of derivative free meta-heuristic algorithm so-called SSE method is proposed for solving our problem. The algorithm is constructed based on systematic partitioning of upper level decision space for searching the optimal reaction for each leader's action on its own decision space and applying particle swarm optimization for searching a better response from lower level reaction. These updating responses for each leader's action will continue iteratively using an ϵ-approximate Stackelberg solution definition. The proposed algorithm is compared with other methods using bench mark problem from literature. The result of the numerical simulations of the algorithm is very much promising. The algorithm can be used also to solve complex stochastic multilevel programming. In addition, it is a useful new addition topic for stochastic multilevel program.

Acknowledgments. This work was supported by the research initiation grant of the office of the DVCRI of Botswana International University of Science and Technology (DVC/RDI/2/1/161(34)).

ISSN: 2521-2292

References

[1] Alizadeh, M., Marcotte, P. and Savard, G. [2013], 'Two stage stochastic programming over a transportation network', *Elsevier* **Part B**(58), 92–105.

[2] Audestad, A., Gaivoronski, A. and Werner, S. [2006], 'Extending the stochastic programming framework for the modeling of several decision makers : pricing and competition in the telecommunication sector', *Annals of Operations Research* (142), 19–39.

[3] Ben-Ayed, O. [1993], 'Bilevel linear programming', *Computer and Operations Research* .

[4] Birge, R. and Louveaux, F. [2011], 'Introduction to stochastic programming', *Springer* .

[5] Carrion, M., Arroyo, M. and Conejo, J. [2009], 'A bilevel stochastic programming approach for retailer futures market trading', *Power Systems, IEEE Transactions on* **24**(3), 1446–1456.

[6] Christiansen, S., Patriksson, M. and Wynter, L. [2001], 'Stochastic bilevel programming in structural optimization', *Structural and Multidisciplinary Optimization* **21**(5), 361–371.

[7] Cooper, L., Molle, T. and Kleywegt, J. [2012], 'Learning and pricing with models that do not explicitly incorporate competition', *http ://www.menet.umn.edu/ billcoop/-competitive2012.pdf. Technical report, Working paper, University of Minnesota* .

[8] Fampa, M., Barroso, L., Candal, D. and Simonetti, L. [2008], 'Bilevel optimization applied to strategic pricing in competitive electricity markets', *Computational Optimization and Applications* **39**(2), 121–142.

[9] Holland, J. [1975], 'Adaptation in natural and artificial systems', *Univerisity of Michigan press, Ann Anbour* .

[10] Kalashnikov, V., Alexandrov, V. and Kalashnykova, N. [2016], 'A stochastic approach to solving bilevel natural gas cash-out problems', *Elsevier* **80**, 1875–1886.

[11] Kennedy, J. and Eberhart, R. [1995], 'Particle swarm optimization', *in: Proc. of IEEE International Conference on Neural Networks, Piscataway, NJ* (1942–1948).

[12] Kennedy, J. and Eberhart, R. [2001], 'Swarm intelligence', *Academic Press* .

[13] Kim, S., Pasupathy, R. and Henderson, G. [2011], 'A guide to sample average approximation', *National University of Singapore* .

[14] Kosuch, S., Bodic, L., Leung, J. and Lisser, A. [2012], 'On a stochastic bilevel programming problem', *Networks* **59**(1), 107–116.

[15] Patriksson, M. [2008], 'On the applicability and solution of bilevel optimization models in transportation science: a study on the existance, stability and computation of optimal solutions to stochastic mathematical programs with equilabrem constraints.', *Transportation Research Part B* **42**(10), 843–860.

[16] Patriksson, M. and Wynter, L. [1999], 'Stochastic mathematical programs with equilabrium constraints', *Operation Research Letters* **25**(4), 159–167.

[17] Pramanik, S., Banerjee, D. and Giri, C. [2012], 'Chance constrained linear plus linear fractional bilevel programming problem', *International Journal of Computer Applications* **56**(16), 34–39.

[18] Robbins, H. and Monro, S. [1951], 'A stochastic approximation method', *The Annals of Mathematics Statistics* **22**(3), 400–407.

[19] Vicente, L. and Calamia, H. [1994], 'Bilevel and multilevel programming: A bibliography review', *J Global Optima* **5**(3), 291–306.

[20] Wang, Y., Jiao, Y. and Li, H. [2005], 'An evolutionary algorithm for solving nonlinear bilevel programming based on a new constraint-handling scheme', *IEEE TRANSACTIONS ON SYSTEMS, MAN, AND CYBERNETICS—PART C: APPLICATIONS AND REVIEWS* **35**(2), 221–232.

[21] Werner, S. [2004], 'Bilevel stochastic programming problems: analysis and application to telecommunications', *Thesis, Norwegian University of Science and Technology* pp. 1–181.

[22] Woldemariam, T. and Kassa, M. [2015], 'Systematic evolutionary algorithm for general multilevel stackelberg problems with bounded decision variables', *Springer* **229**(1), 771–790.

[23] Xin-She, Y. [2010], 'Natured inspired metaheuristic algorithms', *Luniver Press* .

BIUST Research and Innovation Symposium 2019 (RDAIS 2019)
Botswana International University of Science and Technology
Palapye, Botswana, 4 - 7 June 2019

ISSN: 2521-2292

Classification of E-commerce online auctions and prediction of seller reputation

[1*]B. Valarmathi
Department of Software and Systems Engineering
School of Information Technology and Engineering
Vellore Institute of Technology
Vellore, India
valargovindan@gmail.com

[2]A Kavish pandit
Department of Information Technology
School of Information Technology and Engineering
Vellore Institute of Technology
Vellore, India
kavish.pandit2017@vitstudent.ac.in

[3]Pyla charan kumar
Department of Information Technology
School of Information Technology and Engineering
Vellore Institute of Technology
Vellore, India
pyla.charankumar2017@vitstudent.ac.in

[4]T. Chellatamilan
Department of Information and Engineering
Vellore Institute of Technology
Vellore, India
chellatamilan@gmail.com

[5]Abid Yahya
Professor,
Electrical, Computer & Telecommunication Engineering Department
College of Engineering & Technology
Botswana International University of Science & Technology
Palapye, Botswana
yahyabid@gmail.com

Abstract— Seller reputation plays a vital role in the E commerce market. The significant profit and analysis of the overall giant venture which provides both observable and heterogeneous reputation for the online community sellers. Greater validation and performance outcomes to be provided in the optimal algorithm preferred. The methodology that makes the outcome of a multinominal naïve bayes highly efficient, accurate and also enhances a better understanding in reference to E-commerce market and reputation by using singular value decomposition (SVD) algorithm. Online experiments and empirical studies on the data from an online auction market to show that reputation can generate cut-offs for sellers and to generate the detailed analysis of the reputation systems giving a proper boost to the online e-commerce community.

Keywords— Auction, Multinomial Naive Bayes, SVD, E-commerce, Reputation system.

I. INTRODUCTION

E-commerce website system heavily relies on the two major factor which includes trust and reputation. Reputation enhances not only the seller end but it generates the customer perspective regarding the online community base. Trust is used by an individual to assess the performance of another individual by his actions. Thus it becomes necessary to incentivize the sellers to be honest. Reputed online commerce websites such as Alibaba, Amazon, eBay generate tremendous economic value with huge transaction volume.

E-commerce systems serve as online shopping markets, where buyers can purchase products from online stores, each of which is operated by a seller. Further, it becomes very important to enhance the user interaction for the success of the E-commerce .Including a multi-dimensional approach in order to obtain a fine grained trusted computation. It is critical for the buyers to enhance the summarization and opinion extraction. It is critical for the buyers to enhance the summarization and opinion extraction.

Digging further into the concept of the performance outcomes to be provided, there is a need to apply the optimal algorithm .Hence there is a need to conduct experiments and figure out the appropriate classification techniques on the global dataset and generate the required outcomes.

Reputation models on the other hand provides the reputation and trust scores for further implementation of the trust metric. The paper involves the matrix factorization using the singular value decomposition for splitting the matrix into the set of factors as well.

ISSN: 2521-2292

Collaborative filtering and multi-dimensional trust models comes under the known application of the SVD algorithm and it considers the correlation between different data item sets.

Thus this article focuses on the best framework for the e-commerce reputation and defining the optimal classification techniques on the auction dataset with number of auction days as the class labels.

II. LITERATURE SURVEY

Techniques used for existing systems are mentioned below:

A. Ecommerce online auctions
B. Seller Reputation
C. Optimization Algorithm
D. Matrix Factorization technique applications.

A. Ecommerece online auctions

Hong xie et. al. [1] proposed the online Auction System is a practice followed by the Ecommerce sites which takes place between auctioneers and bidders. This enhances the growth from seller's side in terms of popularity, brand value with low term profits. All the transactions made during the auction are categorized into a dataset for further analysis. Different machine learning techniques are then applied on categorized data for performance outcomes. Both Auctioneers and bidders get simultaneous benefits as a seller reputation enhances with bidder requirement satisfaction. Ramanthan Guha et al. [9] proposed a model for a web of trust, a user can prepare and view of some other user without prior communication.

B. Seller Reputation

Daniel Houser and John Wooders [2] suggested the various sellers involved in the online auction to enhance their respective fields of reputation. Each seller have their own reputation, but in hierarchical manner when grouped together. This hierarchical manner can be visualized and analyzed by a technique named "Matrix Factorization technique applications". Concept related to linear algebra (Singular value decomposition) to be used for indexing and prioritizing the reputation scores of sellers. Vector representation is used to represent the user and product interactions. For effective prediction of ratings in collaborative filtering, standard SVD is used. [7] fortune ranking data are retrieved from fortune 500.
Ginger Zhe Jin et al. [10] mentioned that the online seller reputation is active for finding worthy sellers. In any case, restrictive on completed auctions, trustworthy venders don't give better quality. Stuart Landon et. al. [11] idea was taken which initialized the concept of quality expectations in ecommerece auction markets through the sellers reputation and prices.

C. Optimaztion Algorithm

Machine learning has enjoyed tremendous success and this success can be attributed to the data driven philosophy that underpins it. Machine learning algorithms are widely used in numerous datasets but there is a constant need to provide the accurate results. This brings the concept of optimization and relies on some selective algorithm.

Our paper deals with numerous attributes but we selectively focus on the auction type to classify the data. We arrive at the conclusion by applying the Multinomial naïve bayes classification and get the enhanced seller results. Thus the seller reputation is analyzed by classifying the data and comparing it with the previous bidder's rates. This further improves the ranking and increases the clear visibility for the preferred outputs. And making use of the basic ranking criteria also it arrives on the ecommerce reputation as well

D. Matrix Factorization technique applications.

Sulin Ba et al. [4] used the singular value decomposition (SVD). It is an one of the matrix factorization techniques and a unsupervised algorithm that to be applied on seller reputations to arrange the positions of popularity in a hierarchical manner. The seller at top of the hierarchical order is more reputed and recognized as the highly socialized seller among all the online community sellers.

The working mechanism of the Singular Value Decomposition follow as: Reputation scores or values are considered as the numerical entries and represented in a matrix. This matrix is further factorized into 3 matrices. U, Sigma ,V transpose are three matrices that are splitted matrices obtained by the singular value decomposition. Values in the column of the matrix U, gives the preferences or hierarchies over all the respective reputation scores. This is the concept which flows in the background to visualize and recognize the seller's popularity. John Gittins et al. [8] proposed the bandit process and described the dynamic allocation indices which was used as a reference for allocation of dynamic numeric indices for obtaining the rank and reputation.

III. BACKGROUND KNOWLEDGE

Enhancing the reputation systems by providing a pertinent solution and removing the fraudulent behaviour gives the E-commerce website a secure online base. This gives a better narrative to the upcoming research for our paper and hence enhance the decision making for the bidder. For instance a bidder will place a bid only if his/her value for the item would exceed the higher bid at the time and he/she first would consider viewing the auction. Also the count of bidders is mostly larger than the overall bidding done.

Moreover the best measure for the count of bidders might be the number of users who can click on the link to the auction's main page. Thus the link not only displays the current price, it would be focusing in undercounting the number of bidders. The best measure of the number of bidders might be the

ISSN: 2521-2292

number of users who click on the link to the auction's main page. The link provides the seller's reputation which defines in the way but provides it in the count of bidders affected by the seller's reputation.

Peter Auer et. al. [3] suggested the seller may choose an auction length of 1, 3, 5, 7 days when selecting an item. For example, consider an online reputed sire eBay which includes the largest concurrent auctions are conducted at one go among 40 million buyers by the auctioneers and seller behind the scenes expecting the reputation.

If eBay is taken as reference for the above case, it doesn't provide any warranty for auctions, it acts as a listing service. Buyers in this case, find that there is some risk correlated with it. Even fraudulent transactions are expected.

We as a team performed a task of finding out the optimal algorithm for the given dataset and to feature our results by finding out the relation between auction and the seller reputation. India online ecommerce base is plagued by several problems, and they are easily facilitated by the different fraudulent behaviours alongside.

Certain situations, there may be one way to find out an compare the raters reports to find out the referred peer reports and thus generate reward agreement. However, if the rewards are made part of the process, there may be certain chances of the danger. So, if there is a certain outcome which is most likely to occur, such as the positive experience with a seller at eBay who has a stellar feedback past experience, then there is a rater who has a bad experience which also expects that the next rater is likely to have a good experience.

Chrysanthos Dellarocas [5] suggested many online systems, however, raters seem to be quite motivated by prestige or privileges within the system. To the best of our knowledge, this was the first time that has corrected for this difference. And no previous study has corrected for this difference. This is because of measure mentor or in reputation variables, previous estimates of seller reputation effects are highly inconsistent and biased as well.

[6] According to the eBay website and it's analysed research, the auction contract develops the relation between the seller and the bidder which is both binding and have the utmost importance.

Henceforth, according to eBay without paying the item bid on Neither eBay nor the other main consumer-to-consumer auction sites provide away for bidders to post a depositor payment penalty in the event of default. We did emphasize on the seller reputation (but not bidder reputation) which significantly determines the auction prices.

Reputation recognized as a significant evolutionary part in online community auctions positive feedback from a user or buyer enhances the reputation of a seller community. Seller looks forward for emphasizing on this areas to build up his side from user perspective. This make sellers to take incentives for greater performances in their respective auctions conducted.

A deep study of how the process of reputation is going to build incentives for better performance in contracts is a key area for future researchers.

IV. EXPERIMENTS AND SYSTEM DEVELOPED

Fig. 1 emphasizes the various kinds of exploration done by us to obtain a optimized classification techniques among the all others applied up to know. This flow has a simultaneous techniques applied to focus on enhancing the seller reputation and ranking in an optimized fashion.

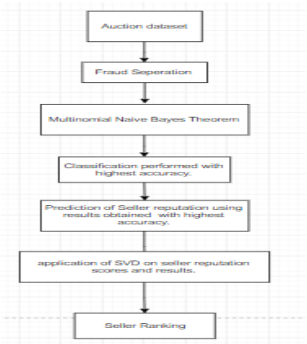


Fig. 1. The flow chart of proposed work

Auction data set is the most compatible for analysis of bid and bidder statistics which play a major role for detecting the seller reputation through online seller community auctions. 'Auction type' attribute from the dataset is taken as a class label to detect Auction day type.

Further the ranking generated is formulated through the SV algorithm and thus helps in clear division of the seller reputation in the online base. The classification performed also requires the highest accuracy. We can explain the concept by starting with the seller base which gets the direct benefit of the online auctions.

E-commerce websites have trusted sellers across the platforms who are an active member of the online community. Their reputation on the other hand increases by the help of the online auctions and this eventually helps in the transactional volume on the website as well. Further after the increase in the seller reputation we arrive to the increase in the popularity of the

ISSN: 2521-2292

online sites as well. Thus not only auctions help in increasing the reputation of the seller but it generates the required popularity for the e-commerce website a well. Auction data thus plays a 'major' role in the whole scenario and provides a efficient online environment for the sellers and the bidder as a whole.

Multinomial naive bayes theorem and methodology is applied on the online auction dataset. Table 1 shows results obtained from total number of instances [10681] for the accuracy of multinominal naïve bayes classifier.

TABLE 1: ACCURACY OF MULTINOMINAL NAÏVE BAYES CLASSIFIER

Description	Rows	Accuracy
Correctly Classified Instances	**10632**	**99.5412 %**
Incorrectly Classified Instances	49	0.4588 %

Through the performance outcomes of the classification technique applied, 10632 instances are correctly classified out of 10681 with an accuracy of **99.5412 %**. Naïve bayes multinomial theorem would be most efficient, preferable and optimized algorithm for classifying auction dataset and attributes. It would be recommended as a major task for analyzing online community auctions and result in best performance outcomes for further analysis of reputation and rankings of seller's community alongside.

V. DATASET DESCRIPTION

The dataset contains 10682 rows and it consists of 9 basic attributes as mention in the columns.

All the features in Auction dataset are described below.

a) Auction id: Each Auction has a unique identity represented by a identifier
b) Bid: the primary bid placed by a bidder in an auction.
c) Bid time: The time taken in days for a bid to get placed, from the start of the auction.
d) Bidder: Bidders eBay username.
e) Bidder rate: eBay provides a feedback option for bidders rating.
f) Open bid: It represents the open bid set by the respective seller
g) Price: The final price to which the item is sold. (Refers to the second highest bid+ a gradual increment.)
h) Item: auction item
i) Auction type: Representing the days of auction.

Fig..2 shows the graphical analysis between Bid value (Highest price) **a** buyer of a stock is willing to pay in x-axis and Bidder rate (Base currency) in y-axis

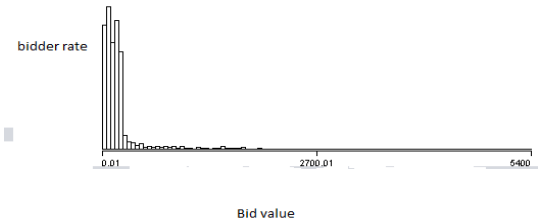


Fig. 2. Bid value versus Bidder rate

Fig. 3 shows the graphical analysis between Bidder time (Time taken for receiving the bid request and serving) in x-axis and Bidder rate (Base currency) in y-axis

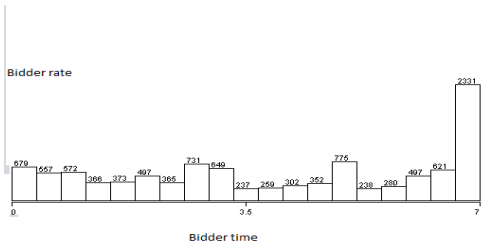


Fig. 3. Bidder time versus Bidder rate

Fig. 4 shows the graphical analysis between Items Available in Auction representing x-axis and y axis represents the count of bidder's participation in auction.

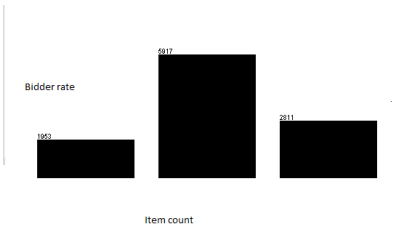


Fig. 4. Bidder count versus Item count

Fig. 5 shows the graphical Analysis of day type's (3 day, 5 day, 7 day) in x-axis and y-axis represents count of bidders participated in a particular day.

ISSN: 2521-2292

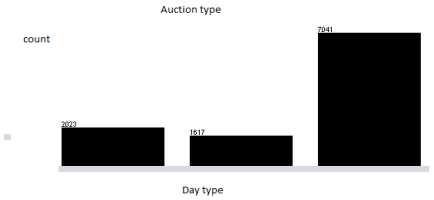


Fig. 5. Day type versus Count

V. PROPOSED WORK

Our research deals with the bidder seller relationship in the online world and shows the various possibilities that occur. This expands the further proposed work and relates it to the derived content as follows. Thus it includes various functionalities which are to be involved and mentioned below.

Steps involved in application of Multinomial Bayes Algorithm.

1. Read the auction dataset.
2. Formulate the mean and standard deviation of the predictor variable in different class of the auction dataset.
3. Repeat the following steps:

Formulate the probability of f, using the Gaussian density equation in each class. Until the probability of all predictor varaibles (f1,f2….fn) has been calculated and the likelihood for each class.

TABLE 2: COMPARISON OF DIFFERENT CLASSIFICATION ALGORITHMS

S.No.	Classification Technique	Accuracy obtained	Number of Instances classified
1.	Zero R	65.92%	7041
2.	Input Mapped Classifier	65.84%	7041
3.	Multinomial naïve Bayes Theorem	99.54%	10632

The different classification algorithms is applied on auction dataset such as Zero R, Input Mapped Classifier and Multinomial naïve Bayes Theorem. Table 2 shows the comparison of the accuracy results generated from the code of corresponding algorithm applied. Our research paper thus gives the highest accuracy for the multinominal naïve bayes and generates it for the 10,000+ instances alongside.

VII. FUTURE WORK

Any further advances in present paper concepts can be encouraged and those advances are kept remained for future due to less sufficiency of time, which is therefore linked with actual data and a time consuming process. This involves in deeper analysis of present concepts. It builds a new curiosity and ideas of evolution for further advances of present concepts when deep analysis is performed among the presented concepts in this paper.
Results obtained through experiments in this paper are quite satisfactory. Even further study and application of techniques is required in order to understand the functionalities to be developed or improved.

VI. CONCLUSION

Our results provide a simple and a generic framework that gives a detailed analysis on the effect of reputation and auction data. Further the use of the optimized algorithm by applying the multinomial naïve bayes algorithm gets the highest preferred outcome .The implications are being put on the best possible way.

Apart from the classification algorithm this paper addresses matrix representation technique in the form of singular value decomposition. The generated results have an accuracy of about 99.54% .We built all the histograms on the optimal attributes and scanned with the feedback system which thus provides incentives for good performance.

On the other hand, our paper provides clear knowledge on the relationship between the auction type and the seller reputation. To build trust between any two people in the system with higher accuracy, we show the distrust rounding and other types of phenomenon which will further have significant effects on how trust is propagated as well.

VIII REFERENCES

[1] Hong xie and Richard T. B.MA, John c. s. Lui, “Enhancing Reputation via Price Discounts in E-Commerce Systems: A Data-Driven Approach”, 2018.

[2] Daniel Houser and John Wooders, “Reputation in Auctions: Theory,and Evidence from eBay.2000. Journal of Economics & Management Strategy”, Vol. 15, pp. 353–369, 2006.

[3] Peter Auer, Nicolo Cesa-Bianchi, and Paul Fischer, “Finite-time analysis of the multiarmed bandit problem”, Journal of Machine Learning, Vol. 47, pp. 235–256, 2002.

[4] Sulin Ba and Paul A. Pavlou, “Evidence of the effect of trust building technology in electronic markets: Price premiums and buyer behaviour”, vol. 26, pp. 243–268, 2002.

[5] Chrysanthos Dellarocas,. “Analyzing the economic efficiency of eBay-like online reputation reporting mechanisms”, In Proc. of ACM EC, 2001.

[6] eBay. 1995. Homepage. Retrieved from http://www.ebay.com/.

[7] Fortune 500. 2015. Fortune Ranking. Retrieved from http://fortune.com/fortune500/.

[8] John Gittins, Kevin Glazebrook, and Richard Weber. 2011. Multi-armed Bandit Allocation Indices. John Wiley & Sons.

[9] Ramanthan Guha, Ravi Kumar, Prabhakar Raghavan, and Andrew Tomkins. 2004. Propagation of trust and distrust. In Proc. of WWW. 403–412.

[10] Ginger Zhe Jin and Andrew Kato, “Price, quality, and reputation: Evidence from an online field experiment” , The RAND Journal of Economics vol. 37, pp. 983–1005, 2006.

ISSN: 2521-2292

[11] Stuart Landon and Constance E. Smith, "Quality expectations, reputation, and price", Southern Economic Journal, vol. 64, pp.628–647, 1998.

BIUST Research and Innovation Symposium 2019 (RDAIS 2019)
Botswana International University of Science and Technology
Palapye, Botswana, 4 - 7 June 2019
ISSN: 2521-2292

Classification of Patients Data to Predict Signs of Diabetic Retinopathy

[1]Utsav Gupta
B.Tech.(Information Technology) Student,
Department of Information Technology,
School of Information Technology and Engineering,
Vellore Institute of Technology, Vellore, India
utsav.gupta2016@vitstudent.ac.in

[2*]B.Valarmathi
Associate Professor,
Department of Software and Systems Engineering,
School of Information Technology and Engineering,
Vellore Institute of Technology,
valargovindan@gmail.com

[3]K.Santhi
Associate Professor, Department of Analytics,
School of Computer Science & Engineering
Vellore Institute of Technology, Vellore, India
santhikrishnan@gmail.com

[4]Abid Yahya
Professor,
Electrical, Computer & Telecommunication
Engineering Department,
College of Engineering & Technology
Botswana International University of Science &
Technology, Palapye, Botswana
yahyabid@gmail.com

Abstract:

In healthcare, data mining is fetching increasingly common, if not gradually essential. Data mining submissions can greatly profit all parties involved in the healthcare commerce. For instance, data mining can help healthcare guarantors notice fraud and exploitation, healthcare officialdoms make purchaser connection administration decisions, doctors recognise effective conducts and best performs, and patients take better and more affordable healthcare amenities. So using the data mining tools only we are here going to predict the efficient algorithms for detecting the certainty of Diabetic Retinopathy on the basis of various vector form of the data from patients images. Diabetic Retinopathy is one of the major causes of blindness in the people at younger age. The support vector machine algorithm (SVM) algorithm is the most efficient classifier for dataset contains features extracted from the Messidor image set, since it produces the highest accuracy value of 71.38% than Decision Tree and Random Forest algorithms.

Keywords: Data Mining, healthcare, Diabetic Retinopathy, blindness, Random Forest, Decision Tree, SVM.

I. INTRODUCTION

Usage of data mining in the field of medical science has been increased significantly on data in the form of required medical data type, to identify the hidden patterns and classify data further. It is difficult for all medical practitioners to analyse the medical data and deduce the diseases since it is a complex task and requires maximum experience and expertise.

Data mining concepts, commonly characterized by volume, variety, velocity, and veracity includes data analysis, such as hypothesis-generation, apart from hypothesis-testing. It focus on data association stability, not on causal relationship, whereas probability distribution measures are essentially not required.

Medicinal facts as factual to be examined has numerous structures not just different from large data of other rectifications, but also dissimilar from outdated proven epidemiology.

Classification, a data mining system, is widely used in healthcare area and it advances the excellence of forecast, and analysis. The area of this project is to converse the part of Diabetic Retinopathy. In United States the carelessness about the health is the main reason of this disease affecting people of the age between 25-74. The careful machine by that polygenic disorder grounds retinopathy-vestiges blurred, however some ideas are hypothesised to elucidate the distinctive course and past of the malady.

The health problem will be analysed by fluoresceine X-ray photography and perception for the next features are given below:

Microaneurysms: The initial medical image of diabetic retinopathy; these happen secondary to vessel wall out pouching because of pericyte loss; they seem as little, red dots within the superficial tissue layerl layers Dot and blot haemorrhages: seem like smallaneurysms if they're minor; they occur as micro aneurysms separation within the

ISSN: 2521-2292

deeper sheets of the retina, like the within atomic and outer layers.
Flame-shaped haemorrhages: Splinter haemorrhages that occur within the a lot of superficial fibre layer Retinal hydrops and arduous exudates: Caused by the breakdown of the blood-retina barrier, permitting outpouring of bodily fluid proteins, lipids, and supermolecule from the vessels.
Macular exudates: Leading cause of visual impairment in patients with diabetes.

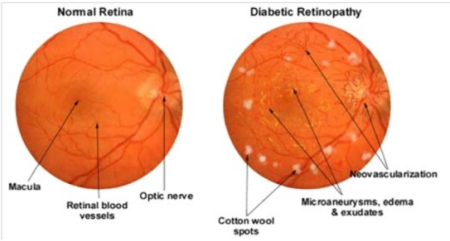


Fig.1 Eyeball Comparison

Fig.1 show the comparison of the eye of an normal individual with the eye of the diabetic retinopathy patient. The eyes of the retinopathy patient contains some cotton wool like structures in their eyes that is the main cause of defective sight.



Fig.2 Vision Comparison

The contrast between the visions of the normal person is shown with that of the diabetic patient and it is shown in the Fig.2
So, if we can predict beforehand the possibilities of emergence of such a disease, it will prove to be extremely helpful to counter this disease, and can thus be prevented. Hence, we will try and analyse the patient retina as being diabetic or not diabetic taking into consideration the available features, by using certain techniques lke classification, clustering and etc.
Classification is a pre-specified set of classes**.** Clustering is unsupervised learning used to find groupings in the data using distance metrics. Regression quantifies the relationships between dependent and independent variables.

Thus, with the analysis results obtained by the mentioned techniques, we will try and attain the best possible outcome from the insights of this data.

II. LITERATURE SURVEY

Kotsiliti et al.[1] have given the model that consists of two phase of analysis, first of which is the Retinal fundus preprocessing and the second one is to classify data for detection of this chronic deisease DR.. First one is used to reduce the non-uniform illumination of pictures.
Verma et al.[2] has proposed the most appropriate formula to remove blood vessel which is considered to be the next version of harmonised mesh. He has also given an advanced approach of identifying the depletion.
Kamaladevi et al.[3] for the given journal staed that the new method of MA approach of detection based upon multifeature fused dictionary have been generated. Multifeature dictionary takes two things, first one is the semantic relationship between different features of the images and secondly t takes the content of the pictures.
Ananthpadmanabhan et al.[4] suggested that in the exixting approach, at primary stage, we are required to do the preprocessingfor removing uneven illumination, bad visual features such as brightness and contras filters.. Furthermore, MSCF is every day to recognize all thinkable MA contenders from the fundus similes. Formerly, MA image areas and non-MA image coverings can be mined from these entrants.
Faust et al.[5] stated that the classifications efficiency of different DR systems is discussed. Maximum of the testified structures are extremely augmented with esteem to the examined fundus pictures, so a simplification of distinct outcomes is hard.
Ramani et al.[6] has explained clearly about the changes and damages that can be cuased to eye of the patient suffering from diabetic retinopathy.
And furthermore he has also thrown light on how to detect Dr on the image by applying various image processing techniques such as pre-processing, acquisition, feature extraction.
And after the features are extracted we can apply different data mining techniques to identify patterns using classifications;
Fraser et al.[7]for the section-II of the paper he has given the brief discusiion on blood vessel algorithms, haemorrhage identification algorithm and the last one is SVM classification.
Roychowdhary et al.[8] has given the clear insight of the various distinguished classification algorithms of data mining techniques. Different classifiers of data-mining tools are like GMM, KNN, SVM and Adaboost. Can be used effectively to work it out for non-lesions. He has

ISSN: 2521-2292

also identified that GMM and KNN are the best regarding this scope.
Akram et al.[9] suggested that if the eye-disorder patients are taking eye check-up on the regular basis, then there are chances that the DR can be eliminated or detctected frequently by 50%. In such circumstances, mechanical selection plans using fundus pictures prior to physical classifying can be tremendously cost-effective and useful.

III. DATASET DESCRIPTION

Our dataset contains the information which is mined from the recognised Messidor dataset, with the last parameter stating the presence or absence of the disease.

TABLE 1: DATASET CHARACTERISTICS

Data Set Characteristics	Multivariate	**No. Of Instances**	1151	**Area**	Life
Attribute Characteristics	Integer, Real	**No. of Attributes**	20	**Date Donated**	2014-11-03
Associated Tasks	Classification	**Missing Values**	N/A	**No. Of Web Hits**	53271

Table 1 shows all the valid information of the dataset release and its further usage in the industry with over 53271 web hits.

There are total 20 attributes in the dataset which are as follows:
0) Quality assessment. 0 = bad quality 1 = sufficient quality.
1) Classification, where 1 specifies severe retinal anomaly and 0 its absence.
2-7) The outcomes of MA finding. Feature value is equals to number of Mas found.
8-15) comprise the similar evidence as 2-7 for exudates. However, as exudates are symbolised by a set of points rather than pixels creating the lesions, these structures are standardised by distributing the number of scratches with the length of the ROI to reimburse dissimilar image dimensions.
16) The Euclidean distance of the centre of the macula and the centre of the optic disc to provide important information regarding the patient's condition.
17) The diameter of the optic disc.
18) The binary result of the AM/FM-based classification.
19) Class label. 1 = marks of DR (Accumulative label for the Messidor classes 1, 2, 3), 0 = no signs of DR.
The sample dataset is shown in Fig. 3.

IV. EXISTING SYSTEM

Diabetes Type-I is a enduring disease that leads to macro and micro vascular complications, such as retinopathy, nephropathy and neuropathy. This disease is the main reason of blindness in the world of economics. Collective occurrence of Type-I Diabetes and elderly people age is the reason behind occurance of diabetic related diseases. Poor glycaemic control and diabetic-tenure are thw risk factors contributing to this retinopathy problem. The Diabetes Control and Complications Trial/Epidemiology of Diabetes Intervention and Complications (DCCT/EDIC) have confirmed that exhaustive conduct of hyperglycaemia efficiently suspensions the onset and slows the progression of complications in T1D, including DR. Nephropathy, hypertension and dyslipidemia are the other danger factors included in this disease.

Ghamdi et al.[10] has given the advice through his journal that the patients who are suffering from DR should have to go to ophthalmologist for their direct checkup using ophthalmoscope. It can be used to detect random blood glucose which can be further used to analyse the disease.

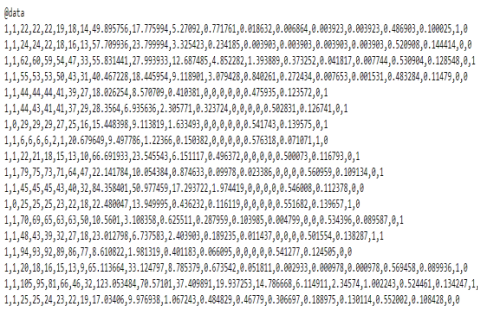


Fig.3 Dataset Snapshot

V. GAP IDENTIFIED

From the existing system, we came to know that Vision Threatening DR is the most critical consequence of Type-I Diabetes. And the above system do not come up with exact solution to detect whether the patient will going to have the Diabetic Retinopathy or not. So to resolve that issue came up with the different data mining techniques to predict the same. Then we will observe which technique will give the most optimum result. So that it can be used to predict the DR in patients having Diabetes Type-I.

VI. PROPOSED METHOD

The motivation for this project came from the fact that the highlighted disease is an important disease to address while considering counter measures for any situation. This disease is growing rapidly amongst our society and needs to be immediately countered. This is only possible when sufficient analysis is done on the data that is available from

ISSN: 2521-2292

the sources. Thus, we took this as the topic of our project.

Further, even on obtaining the data simply doesn't bring about a change on its own. We must then commence the process of analysis. To bring about the correct results which are apt and reveal information on the concept being tested, we must prepare the model very carefully and precisely. So, we took this challenge upon ourselves so as to learn through this process the depths of knowledge within this field.

In this project we are comparing the accuracy of classification by three different models.

For the analysis to be performed, we are choosing a three classification techniques and they are given below:

a) Decision Tree Algorithm
b) Random Forest Algorithm
c) Support Vector Machine Algorithm

Using these three tree-based classifier methods, we will try and find out which method is best suited for in this scenario, for this dataset. This can be found out by using certain comparison parameters like the accuracy of the prediction of the model.

VII. RESULTS AND DISCUSSIONS

a) Simple Decision Tree

Also, from the below graph, we can clearly see that as the critical performance (cp) value decreases, the size of tree increases, and the relative error in the X-val decreases, thus improving the performance of the Decision Tree classifier. In this classifier Gini Index is used and it gives the accuracy of 59.83%

TABLE 2. DECISION TREE (GINI) CLASSIFICATION REPORT

Average statics	precision	recall	f1-score	support
0.0	0.54	0.77	0.63	156
1.0	0.71	0.46	0.56	190
avg(micro)	060	0.60	0.60	346
avg(macro)	0.62	0.61	0.59	346
avg(weighted)	0.63	0.60	0.59	346

Table 2 shows the performance and accuracy measure of the Decision Tree Algorithm using Gini Index.

TABLE 3. DECISION TREE (ENTROPY) CLASSIFICATION REPORT

Average statics	precision	recall	f1-score	support
0.0	0.55	0.76	0.64	156
1.0	0.71	0.49	0.58	190
avg(micro)	0.61	0.61	0.61	346
avg(macro)	0.63	0.62	0.61	346
avg(weighted)	0.64	0.61	0.60	346

Table 3 shows the performance and accuracy measure of the Decision Tree Algorithm using Entropy and it gives the accuracy of 60.98%

.

b) Random Forest

Table 4 shows the performance and accuracy measure of the Random Forest Algorithm and it gives the accuracy of 67.91%

TABLE 4. RANDOM FOREST CLASSIFICATION REPORT

Average statics	precision	recall	f1-score	support
0.0	0.63	0.71	0.66	156
1.0	0.73	0.66	0.69	190
avg(micro)	0.68	0.68	0.68	346
avg(macro)	0.68	0.68	0.68	346
avg(weighted)	0.68	0.68	0.68	346

c) Support Vector Machine

Table 5 shows the performance and accuracy measure of the Support Vector Machine Algorithm and Table 4 shows the performance and accuracy measure of the Random Forest Algorithm and it gives the accuracy of 71.39%

TABLE 5.SUPPORT VECTOR MACHINE CLASSIFICATION REPORT

Average statics	precision	recall	f1-score	support
0.0	0.63	0.88	0.73	156
1.0	0.85	0.58	0.69	190
avg(micro)	0.71	0.71	0.71	346
avg(macro)	0.74	0.73	0.71	346
avg(weighted)	0.75	0.71	0.71	346

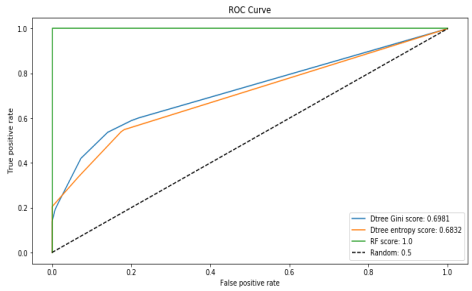


Fig.4 Receiver Operating Characteristic (ROC) curve

As per Fig.4, We can see that the area under the curve decides the efficiency of the algorithm in Receiver Operating Characteristic (ROC) curve. Hence we can see that the area under the SVM curve is maximum with the accuracy of 71.38%. Hence through this we can ensure that the SVM is the most efficient algorithm that can be used to predict the Diabetic Retinopathy in through this dataset.

As we have already discussed about our Messidor dataset which consists of 19 features and two classes where 1 represents the presence of retinal diabetic retinopathy and 0 represents its absence. As SVM uses only classification not regression it is

ISSN: 2521-2292

the best algorithm that we can use for the dataset. And it is the one among many of the classification algorithm that can easily take many features and work ont them smoothly to classify data. We have used Decision Tree, Random Forest and SVM algorithms for the dataset, For SVM we are getting 71.38% of accuracy, 59.83% of accuracy for Decision Tree and 67.91% of accuracy for Random Forest respectively. Even SVM can perform better if we increase the features considerably but the features should have to be sparse and classes should be two for the most effective results.

Hence, earlier in all our references we have noticed that SVM is not yet used for comparision and classification of the Messidor Diabetic Retinopathy data. So, by using SVM we have seen a great impact in the accuracy of the system.

VIII. CONCLUSION AND FUTURE WORK

Thus, we have found out that SVM was the most efficient classifier for this particular dataset taken, since it produced the highest accuracy value of 71.38%. This tells us that within the constraints of the given scenario and the techniques on hand, the most useful for analytics was proved to be the SVM classifier.

However, it must always be kept in mind that this conclusion can be only true for this particular scenario, and may vary for different cases. Thus, we must not conclusively establish this result as the benchmark result, for a much larger extent of analytics is required on a much larger scale to actually bring about certain defining characteristics, based on which we may then draw conclusions. In our future work, we are going to use the deep learning concepts for the larger dataset.

REFERENCES

[1] Kotsiliti, E., Al-Diri, B., & Hunter, A, "A classification model for predicting diabetic retinopathy based on patient characteristics and biochemical measures. *Journal for Modeling in Ophthalmology*, Vol. 1, pp. 69-85, 2017.

[2] Verma, K., Deep, P., & Ramakrishnan, A. G., "Detection and classification of diabetic retinopathy using retinal images", In *India Conference (INDICON), 2016 Annual IEEE,* pp. 1-6, 2016.

[3] Kamaladevi, M., SnehaRupa, S., & Sowmya, T., "Automatic Detection of Diabetic Retinopathy in Large Scale Retinal images", *International Journal of Pure and Applied Mathematics*, Vol. *119*, pp. 14181-14189, 2018..

[4] Ananthapadmanabhan, K. R., & Parthiban, G., "Prediction of chances-diabetic retinopathy using data mining classification techniques", *Indian Journal of Science and Technology,* vol.7, pp. 1498-1503, 2014.

[5] Faust, O., Acharya, R., Ng, E. Y. K., Ng, K. H., & Suri, J. S., "Algorithms for the automated detection of diabetic retinopathy using digital fundus images: a review", *Journal of medical systems*, vol. *36*, pp. 145-157, 2016..

[6] Ramani, R. G., Balasubramanian, L., & Jacob, S. G., "Automatic prediction of Diabetic Retinopathy and Glaucoma through retinal image analysis and data mining techniques", In *Machine Vision and Image Processing (MVIP), International Conference* IEEE, pp. 149-152, 2012.

[7] Fraser, C., DAmico, D., & Trobe, J., "Diabetic retinopathy: Classification and clinical features", *Netherlands: Wolters Kluwer*, 2015.

[8] Roychowdhury, S., Koozekanani, D. D., & Parhi, K. K., "DREAM: diabetic retinopathy analysis using machine learning", *IEEE journal of biomedical and health informatics*, vol. 18, pp.1717-1728, 2014.

[9] Akram, M. U., Khalid, S., & Khan, S. A., "Identification and classification of microaneurysms for early detection of diabetic retinopathy", *Pattern Recognition*, vol. 46, pp.107-116, 2013.

[10] Al Ghamdi, A. H., Rabiu, M., Hajar, S., Yorston, D., Kuper, H., & Polack, S., "Rapid assessment of avoidable blindness and diabetic retinopathy in Taif", Saudi Arabia. *British Journal of Ophthalmology*, vol. 96, pp.1168-1172, 2012.

BIUST Research and Innovation Symposium 2019 (RDAIS 2019)
Botswana International University of Science and Technology
Palapye, Botswana, 4 - 7 June 2019

ISSN: 2521-2292

Optimizing Cognitive Radio Deployment in Cooperative Sensing for Interference Mitigation

Temitope Fajemilehin
Department of Electrical Engineering
Pan African University Institute of Basic Sciences, Technology and Innovation
Nairobi, Kenya
fajemilehintope@yahoo.com

Kibet Langat
Department of Telecommunication and Information Engineering
Jomo Kenyatta University of Agriculture and Technology
Juja, Kenya
kibetlp@jkuat.ac.ke

Abid Yahya
Department of Computer, Electrical and Telecommunication Engineering
Botswana International University of Science and Technology
Palapye, Botswana
yahyabid@gmail.com

Jayeola Opadiji
Department of Computer Engineering
University of Ilorin
Ilorin, Nigeria
jopadiji@unilorin.edu.ng

***Abstract*— Cognitive radio system is one of the viable solutions for effective spectrum management. Cooperative spectrum sensing is very often used to mitigate the challenge of interference encountered in single sensing systems. This paper is aimed at developing a model to determine the required number of cognitive radios that would optimize the performance of a communication network with respect to energy utilization and bandwidth requirement. Energy detection was used as the cognitive radio sensing technique due to the limited energy, computational and communication resources required. The noise variance of the channel was set to -25dB. Spectrum sensing was carried out at a frequency of 936MHZ and a bandwidth of 200kHz. Enhancement in specificity of the detection was also explored using machine learning in order to minimize interference. Genetic Algorithm (GA) was used to optimize the number of cognitive radios putting into consideration all constraints in the network. The optimization produced an overall reduction of 59.26% in energy conserved without compromising the detection accuracy.**

Keywords—cognitive radio; energy detection; genetic algorithm; cooperative spectrum sensing

I. INTRODUCTION

Several portions of the radio spectrum (3GHz – 300GHz region) are under-utilized while some portions are overcrowded due to the emergence of more telecommunication applications and services [1]. Spectrum spaces between 30MHz and 3GHz that are not as crowded can therefore be effectively utilized for telecommunication services [2]. If this is not effectively carried out, more of the limited electromagnetic resources required for the increasing wireless devices and services depletes faster [3].

The Radio Communication Sector of International Telecommunications Union (ITU-R) put in place regulations to ensure that the radio spectrum is efficiently allocated to needing sectors. This also helps to avoid interference among various subscribers particularly in the era of increasing bandwidth demanding wireless technologies. In Africa alone, mobile broadband is expected to constitute about 87% of total connections across 690 million smartphones by 2025. The world-wide population of mobile phone subscriptions is already over 7.5 billion with each subscriber individually contributing an average data usage of 2.1GB to worldwide 8.8EB total mobile data traffic [2], [4]. More than 1 million mobile phone subscribers is anticipated to be added to the annual mobile device subscription database by 2022 which would increase the mobile subscribers worldwide to 9 billion [2]. This increases the demand for more telecommunications resources such as bandwidth, power and communicating frequency slots. New radio access technologies are therefore limited by the shortage of the useable available radio spectrum. This limitation is due to fixed radio functions, static spectrum allocation and limited network coordination which still exists in the present spectrum allocation scheme [5]. Improvement is urgently required in form of dynamic spectrum management applications which can accommodate the increased demand for telecommunication resources [6].

Cognitive radio system (CRS) is a dynamic spectrum management technique which is applicable in the GSM white space utilization effort. CRS is a software defined radio which can manage the spectrum by exploiting spectrum holes and permitting the deployment of multiple wireless systems [6]–[8]. It can sense the status of the transmitting channels to determine the occupancy status of such channels. It can tune the usage of the spectrum dynamically based on certain network and environmental related factors such as type of radios in the network, bandwidth required allocation, location of the radios, time of the day etc. [9].

The spectrum sensing function in cognitive radio is required to check if a particular channel is in use by a licensed user a

This research is supported by the African Union through the Pan African University Scholarship.

ISSN: 2521-2292

specific point in time [10]. It is crucial to avoid interference and channel misallocation. One of the commonly used spectrum sensing techniques is Energy detection-based sensing. It requires minimal resources to detect the occupancy status of the channel and is not as computationally demanding as the other techniques [11], [12]. But it has several limitations such as multipath fading, shadowing and consequently, the hidden terminal problem. It also cannot discriminate between the type of user occupying the channel (i.e. differentiating between Primary User (PU), Secondary User (SU) or Interfering User (IU)).

Cooperative sensing is often utilized to overcome several of the shortfalls. But it increases the communication overhead of the network and is usually also not able to determine the type of user occupying the channel particularly if the cooperating cognitive radios are sensing through energy detection technique.

Researchers have worked on improving detection sensitivity of energy detection-based spectrum sensing using several techniques using the concept of an adaptive threshold[13]. Several combining techniques for the cognitive radio users in cooperative spectrum sensing were considered while utilizing different modulation schemes. Significant improvements were recorded but the technique was not fully predictable in noisy channels.

Authors in [14], also proposed a method of improvement that enhanced the classical energy detection scheme and maintained a similar level of computational complexity and cost. Detection time was also reduced in comparison to other more sophisticated methods of sensing. But it could not differentiate between the type of users in the network. [15] used an augmented spectrum sensing algorithm where the energy detector's detection is augmented by cyclostationary detection. However, the technique requires information about the primary users' transmission characteristics which is not always available.

Multiple antenna techniques to improve the performance of energy detection and cyclostationary feature detection-based was used in [13]. This was implemented in a cooperative spectrum sensing scheme using Equal Gain Combining (EGC). It improved the detection sensitivity but was not focused on interference mitigation.

Authors in [16], used different channels without any information about the environment to improve on the usage of idle spectrum with due consideration for fairness in channel selection. This was improved upon by authors in [17] with the aid of a p-norm energy detector. The performance of the cooperative spectrum sensing was improved alongside improved gain in κ-μ fading channels. These improvements are the foundations on which the current paper is building on to increase the capacity of the cognitive radio identify the user occupying the channel.

More recently, [18] proposed a two-stage reinforcement learning approach to improve the performance of the cooperative sensing. The method minimized the number of sensing operations and reduced the energy required in the sensing operation. The channel sensing and allocation was improved, but demanded computational resources and learning time.

[19] further explored optimal threshold selection at low SNR to improve sensing performance. Better sensing performance was obtained compared to previous approaches which used constant false-alarm rate and constant detection rate threshold selection. However, there was no provision made for instantaneous SNR drop which sometimes occur.

[20] used an adaptive simulated annealing particle swarm optimization (ASASPSO) to improve cognitive radio power allocation. Parameters considered were the interference power threshold of the primary user, transmission rate limitation of secondary users and the signal to interference and noise ratio (SINR). Thus, the power consumed was reduced was reduced and an improved SINR and transmission rate was achieved.

The addition of more cognitive radios in the cooperative sensing scheme increases energy consumption and general communication overhead. What would therefore be the optimum number of cognitive radios in a communication network to ensure high quality performance in terms of interference mitigation and resource conservation? This paper seeks to find a solution to this salient question by developing a model to identify the required number of cognitive radios that would fulfil the objective of optimum performance.

II. SYSTEM MODEL

A. *Theoretical Background*

Energy detection is a non-coherent detection method which detects the operation of a licensed user within a particular communication channel [21]. In energy detection, the energy detected in the channel being sensed is measured and compared with a predefined threshold to determine the presence or absence of the primary user (PU) signal [7]. Energy detector is largely employed in ultra-wideband communication to utilize an idle channel when not in use by a licensed user.

In the implementation of the energy detector, the received signal $x(t)$ is filtered by a band pass filter (BPF) in line with the bounds of the frequency channel being sensed. This signal detected is then squared with a square law device. The band pass filter serves to reduce the noise bandwidth. Hence, noise at the input to the squaring device has a band-limited flat spectral density. The output of the integrator is the energy of the input to the squaring device over the time interval T. Afterwards, the output signal from the integrator (the decision statistic), Y, is compared with a threshold to decide whether a primary (licensed) user is present or not. Decision regarding the usage of the band will be made by comparing the detection statistic to a threshold [22].

The mathematical model for energy detection is given by the following two hypotheses [8]:

H_0: PU absent

$$y(n) = u(n) \quad n = 1,2, \dots N \tag{1}$$

H_1: PU present

ISSN: 2521-2292

$$y(n) = s(n) + u(n) \quad n = 1,2,\dots N \tag{2}$$

where $u(n)$ is noise and $s(n)$ is the PU's signal

Energy detector performs optimally in spectrum sensing if the noise variance is known. This is required to define the threshold which helps in deciding spectrum is occupied or not [23]. The challenge with the spectrum sensing of the energy detector is that it is unable to accurately detect the PU when the signal is weak i.e. at low SNR. The detection accuracy further deteriorates when the noise characteristics cannot be defined due to varying noise uncertainties [24], [25].

This study is aimed at managing interference which may occur in energy-detection based cognitive radio by introducing supervised machine learning. This is expected to help the cognitive radio system (CRS) learn the patterns in the unknown noise characteristics through a clustering algorithm. The specific properties of the PU were used as training data in a supervised learning technique to serve a feature detection algorithm in the CRS. This scheme intends to improve the detection accuracy of the energy detector in scenarios when the SNR falls to the SNR wall level.

Equation (3) shows the normalized test (decision) statistic for the detector and this was developed based on [26] as:

$$T' = \left(\frac{1}{N_{02}}\right)\int_0^T y^2(t)dt \tag{3}$$

where:

T'= test statistic in during sensing session

y = received signal input

T = sampling instant

N_{02} = two-sided noise power density spectrum

If the test statistics exceeds a fixed decision threshold then it results in H_1 hypothesis. However, when the test statistics is less than the decision threshold then H_0 hypothesis occurs.

As shown in [14], λ is the decision threshold which in the number of samples $N \gg 1$, can be expressed as a Gaussian distribution:

$$\lambda = \sqrt{\frac{2}{NQ^{-1}}}(P_{fa}^{CED} + 1) \tag{4}$$

where:

$$P_{fa}^{CED} = Q\left(\frac{\lambda - 1}{\sqrt{\frac{2}{N}}}\right) \tag{5}$$

$$P_d^{CED} = Q\left(\frac{\lambda - (1+\gamma)}{\sqrt{\left(\frac{2}{N}\right)(1+\gamma)^2}}\right) \tag{6}$$

$$\gamma = \frac{\sigma_s^2}{\sigma_w^2} \tag{7}$$

σ_s^2 is the received average primary signal power

σ_w^2 is the noise variance.

B. Optimization Model

The operating characteristics in the network can be assessed in frames (N). Energy test statistic ($Y^{\alpha}_{p|s|x,i}$) at the i^{th}frame of the user's transmission operations can be extracted as input data. Similarly, $Y^{\beta}_{p|s|x,i}$ and $Y^{\gamma}_{p|s|x,i}$can be extracted at specific points in the channel and receiver respectively.

Energy test statistics for the primary user ($Y_{p,i}$) is represented as:

$$Y_{p,i} \in (Y^{\alpha}_{p,i}, Y^{\beta}_{p,i}, Y^{\gamma}_{p,i}) \tag{8}$$

Energy test statistics for a secondary user ($Y_{s,i}$) is represented as:

$$Y_{s,i} \in (Y^{\alpha}_{s,i}, Y^{\beta}_{s,i}, Y^{\gamma}_{s,i}) \tag{9}$$

Energy test statistics for an interfering user ($Y_{x,i}$) is represented as:

$$Y_{x,i} \in (Y^{\alpha}_{x,i}, Y^{\beta}_{x,i}, Y^{\gamma}_{x,i}) \tag{10}$$

The labels identifying these input data in specific frames as primary user (U_p), secondary user (U_s) or interfering user (U_x) based on their respective energy test statistics can be represented as decisions (d_i).

Genetic Algorithm (GA) was selected as a suitable tool to optimize the number of cognitive radios putting into consideration constraints such as the spatial distribution of the cognitive radios, sensing time and noise characteristics. These are crucial to identify the optimal number of cognitive radios that would minimize resource consumption while ensuring interference mitigation in the system. This objective is achieved by the following function:

$$\min_n Y(n) = n_1 Y^{\alpha}_{p,i} + n_2 Y^{\beta}_{p,i} + n_3 Y^{\gamma}_{p,i} + n_4 Y^{\alpha}_{s,i} + \cdots$$
$$n_5 Y^{\beta}_{s,i} + n_6 Y^{\gamma}_{s,i} + n_7 Y^{\alpha}_{x,i} + n_8 Y^{\beta}_{x,i} + n_9 Y^{\gamma}_{x,i} \tag{11}$$

Subject to

$$n_1, n_2, n_3, n_4, n_5, n_6, n_7, n_8, n_9 \geq 0 \tag{12}$$
$$n_1 + n_2 + n_3 \geq 3 \tag{13}$$
$$n_4 + n_5 + n_6 \leq 3 \tag{14}$$
$$n_7 + n_8 + n_9 \leq 3 \tag{15}$$

Based on previous studies [27], cooperative sensing aids more accurate detection. The first constraint in (12) is therefore essential to ensure that sufficient cognitive radios operate cooperatively to minimize missed detections and false alarms.

ISSN: 2521-2292

The critical nature of primary user detection makes it imperative to include not less than 3 cognitive radios to cover every zone of operation. This is represented in the second constraint in (13).

An assumption made is that 3 cognitive radios are sufficient to monitor operations of potential secondary users and interfering users. This is based on previous studies [28] where the provision of an extra cognitive radio for monitoring other non-PU operations produces a more accurate sensing outcome.

C. Simulation Setup

The model implemented with MATLAB Simulink on MATLAB 2017a software. The model consisted of transmitters with an energy detector based cognitive radio through an additive white gaussian noise (AWGN) channel. The noise variance of the channel was set to -25dB. The sensing technique was employed using a frequency of 936MHZ and a bandwidth of 200 kHz and the threshold set to 0.2. Setting up the cognitive radio spectrum sensor (energy detector) in Simulink. Details of the simulation parameters are presented in **Error! Reference source not found.**.

TABLE I. SIMULATION PARAMETERS

Parameters	**Value**
SNR	-25dB
Pf	0.05
Operating frequency	936 MHz
Observation time	2 x 10^{-4}
Variance of the noise (σ^2n)	1 x 10^{-12}
Threshold	0.2
Operating power	40 mW
Bandwidth	200 kHz
Population type	Double vector
Population size	200
Scaling function	Rank
Selection function	Stochastic uniform
Crossover fraction	0.8
Crossover function	Constraint dependent
Generations	900

The sensitivity of the cognitive radio system was first improved using ML to ensure that the sensing accuracy is not compromised as the optimization is done. Tree algorithms and KNN were selected based on a previous study [29] which revealed that the algorithms performed reliably. After ensuring the accuracy of the CRS through ML, GA was then utilized to obtain the optimum number of cognitive radios that would minimize the energy consumption.

III. RESULTS AND DISCUSSION

The quick-to-train classification algorithms used to train the data were Complex Tree, Fine KNN, Weighted KNN, Cubic KNN and Medium KNN. Table 2 shows the accuracy for the different classifiers considered at -25dB. The receiver operating characteristics (ROC) for the CRS at -25dB to compare the accuracy of the ML-improved cognitive radio to the conventional version is presented in Fig. 1.

TABLE II. ACCURACY OF CLASSIFIERS AT -25DB

	PU		**SU**		**IU**		
CM	TPR (%)	FNR (%)	TPR (%)	FNR (%)	FNR (%)	TPR (%)	OA[1] (%)
WKNN	93	7	89	11	91	9	91.1
FKNN	91	9	89	11	92	8	90.8
MKNN	95	5	88	12	89	11	90.7
CKNN	95	5	88	12	89	11	90.4
CTree	>99	<1	85	15	87	13	90.5

OA[1]: Overall accuracy
CM: Classification methods
WKNN: weighted KNN
FKNN: fine KNN
MKNN: medium KNN
CKNN: cubic KNN
CTree: Complex tree
TPR: True positive rate
FNR: False negative rate

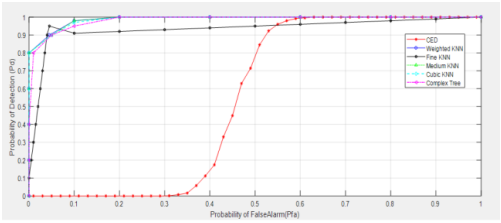


Fig. 1:ROC curve comparing five classifiers at -25dB

The results reveal the ML-improved cognitive radio operated at a higher accuracy level than the conventional cognitive radio. Using complex tree, as one of the most accurate algorithms in this context, accurate detection of PU was >99%. The detection accuracy for the SU and IU were 85% and 87% respectively with an overall detection accuracy of 90.5%. These results were obtained with the assumption that 9 cognitive radios monitoring each category of users (PU, SU, IU) would give more accurate results.

The result presenting the minimization of the number of cognitive radios using GA is presented in Fig.2. The results revealed that with 6 cognitive radios at various locations monitoring the PU, less resources would be incurred without compromising the detection accuracy. The results also show that 5 cognitive radios are sufficient to sensing the activities of the SU and the IU. Using this number, the detection accuracy would be optimum, with resource utilization minimized. The overall reduction in energy conserved based on the minimization of the cognitive radios is 59.26%.

ISSN: 2521-2292

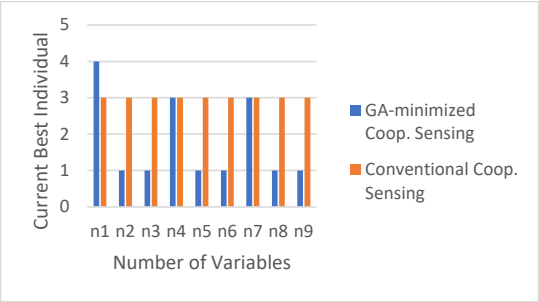


Fig. 2:Best Individual versus Number of Variables

IV. CONCLUSION

The results presented reveal that the use of GA optimized the number of cognitive radios used per sensing period. The ML introduced before the optimization helped in the reduction of the probabilities of false alarm and misdetections. Thus, enhancing the overall sensing outcomes of cooperative spectrum sensing in cognitive radio systems and conserving resources.

ACKNOWLEDGMENT

This research is supported by the African Union through the Pan African University Scholarship. Temitope Fajemilehin thanks Samuel Olatunji for his help, review and invaluable comments to help this paper better.

REFERENCES

[1] T. Chiwewe and G. Hancke, "A look at spectrum management policies for radio spectrum," *EngineerIT*, no. March, 2015.

[2] Ericsson, "Mobility Report," *White Paper*, no. May, pp. 7–8, 2016.

[3] S. Chaudari, *Spectrum Sensing for Cognitive Radios: Algorithms, Performance, and Limitations*, Aalto Univ. School of Electrical Engineering, Department of Signal Processing and Acoustics, 2012.

[4] S. Kemp, "Digital in 2017 Southeast Asia : A Study of Internet, Social Media, and Mobile Use Throughout the Region," *We Are Social*, p. 197, 2017.

[5] S. Haykin, D. J. Thomson, and J. H. Reed, "Spectrum sensing for cognitive radio," *Proceedings of the IEEE*, vol. 97, no. 5, pp. 849–877, 2009.

[6] G. S. A. K. Reddy, U. G. Raju, P. Aravind, and D. Sushma, "Intelligent Wireless Communication System of Cognitive Radio," no. 5, pp. 78–82, 2013.

[7] C. Mmary, "Cognitive Radio for Broadband Access in Rural Africa and other Developing Countries," *MSc. Thesis, University of York, UK*, no. December, 2011.

[8] S. Sudeep and K. Nirajan, "Energy detection based techniques for Spectrum sensing in Cognitive Radio over different fading Channels," *Journal of Selected Areas in Telecommunications*, vol. 4, no. 2, pp. 15–22, 2014.

[9] M. Marcus, J. Burtle, N. Mcneil, A. Lahjouji, and N. McNeil, "Report of the Unlicensed Devices and Experimental Licenses Working Group," *FCC, Spectrum Policy Task Force*, pp. 1–24, 2002.

[10] R. Mittal and E. D. Garg, "A Review on : Spectrum Sensing Techniques," *International Journal of Advanced Research in Computer Science and Software Engineering*, vol. 5, no. 5, pp. 1187–1192, 2015.

[11] M. Lakshmi, R. Saravanan, and R. Muthaiah, "Energy Detection Based Spectrum Sensing for Cognitive," *International Journal of Engineering and Technology (IJET)*, vol. 5, no. 2, pp. 963–967, 2013.

[12] P. Kumar Verma, S. Taluja, and R. Lal Dua, "Performance analysis of Energy detection, Matched filter detection & Cyclostationary feature detection Spectrum Sensing Techniques," *International Journal Of Computational Engineering Research (ijceronline.com)*, vol. 2, no. 5, pp. 2250–3005, 2012.

[13] R. F. Ustok, "Spectrum Sensing Techniques for Cognitive Radio Systems With Multiple Antennas," Izmir Institute of Technology, 2010.

[14] M. López-Benítez and F. Casadevall, "Improved energy detection spectrum sensing for cognitive radio," *IET Communications*, vol. 6, no. 8, p. 785, 2012.

[15] M. Kanti, D. Barma, H. Singh, S. Roy, and S. K. Sen, "Augmented Spectrum Sensing in Cognitive Radio Networks," *IJCSN International Journal of Computer Science and Network*, vol. 4, no. 6, 2015.

[16] J. Zhu, Y. Song, D. Jiang, and H. Song, "Multi-armed bandit channel access scheme with cognitive radio technology in wireless sensor networks for the Internet of Things," *IEEE Access*, vol. 4, pp. 4609–4617, 2016.

[17] M. Jain, V. Kumar, R. Gangopadhyay, and S. Debnath, "Cognitive Radio Oriented Wireless Networks," in *CROWNCOM 2015*, 2015, vol. LNICST 156, pp. 225–234.

[18] V. Raj, I. Dias, T. Tholeti, and S. Kalyani, "Spectrum Access in Cognitive Radio Using a Two-Stage Reinforcement Learning Approach," *IEEE Journal on Selected Topics in Signal Processing*, vol. 12, no. 1, pp. 20–34, 2018.

[19] A. Kumar, P. Thakur, S. Pandit, and G. Singh, "Analysis of optimal threshold selection for spectrum sensing in a cognitive radio network: an energy detection approach," *Wireless Networks*, vol. 0123456789, no. 1, 2019.

[20] H. Wang, F. Jiang, and M. Zhou, "Cognitive radio power allocation algorithm based on improved particle swarm optimization," in *IEEE International Conference on Communication Systems (ICCS)*, 2018, pp. 354–359.

[21] E. Union, "West African Common Market Project : Harmonization of Policies," 2008.

[22] K. Nirajan, S. Sudeep, S. Suman, and B. Lamichhane, "Performance Comparison of Energy Detection Based Spectrum Sensing for Cognitive Radio Networks," *International Refereed Journal of Engineering and Science (IRJES) ISSN*, vol. 4, no. 8, pp. 2319–183, 2015.

[23] E. Axell, G. Leus, E. G. Larsson, and H. V. Poor, "Spectrum sensing for cognitive radio : State-of-the-art and recent advances," *IEEE Signal Processing Magazine*, vol. 29, no. 3, pp. 101–116,

ISSN: 2521-2292

2012.

[24] N. Hoven, R. Tandra, and A. Sahai, "Some fundamental limits on cognitive radio," *Wireless Foundations EECS, University of California at Berkeley*, 2005.

[25] E. Axell and E. G. Larsson, "Optimal and Sub-Optimal Spectrum Sensing of OFDM Signals in Known and Unknown Noise Variance Optimal and Sub-Optimal Spectrum Sensing of OFDM Signals in Known and Unknown Noise Variance," *IEEE JOURNAL ON SELECTED AREAS IN COMMUNICATIONS*, vol. 29, no. 2, pp. 290–304, 2011.

[26] H. Urkowitz, "Energy Detection of Unknown Deterministic Signals," *Proceedings of the IEEE*, vol. 55, no. 4, pp. 523–531, 1967.

[27] T. O. Fajemilehin, S. A. Olatunji, and J. F. Opadiji, "Improved Energy Detection Algorithm for Cognitive Radios in Cooperative Spectrum Sensing," *International Journal of Information Processing and Communication (IJIPC)*, vol. 7, no. 1, pp. 148–163, 2019.

[28] J. F. Opadiji, S. A. Olatunji, and T. O. Fajemilehin, "On Energy Detection of Cognitive Radios in Cooperative Spectrum Sensing," in *URSI-NG Conference Proceedings*, 2015, pp. 29–36.

[29] A. M. Mikaeil, *Machine Learning Approaches for Spectrum Management in Cognitive Radio Networks*. Rijeka: IntechOpen, 2018.

BIUST Research and Innovation Symposium 2019 (RDAIS 2019)
Botswana International University of Science and Technology
Palapye, Botswana, 4 - 7 June 2019

ISSN: 2521-2292

Airblast Prediction in a Blasting Operation Using Artificial Intelligence

Kesalopa Gaopale[a]
Department of Mining and Geological Engineering
BIUST, Palapye, Botswana
gaokesa@gmail.com

Jamisola S. Rodrigo Jr[b]
Department Mechanical, Energy and Industrial Engineering
BIUST, Palapye, Botswana
jamisolar@biust.ac.bw

Itumeleng Seitshiro[b]
Debswana
Jwaneng, Botswana
ITSeitshiro@debswana.bw

***Abstract*—This paper presents the use of artificial neural network (ANN) to predict airblast that is induced by blasting in a diamond mine. A total of 94 blasting datasets were used to develop and train the ANN models using Levenberg–Marquardt algorithm. The input parameters were: burden, spacing, blasthole depth, blasthole diameter, stemming length, distance from the blast face, powder factor, and maximum charge. Airblast was the output parameter. Its values were predicted after the model was built. The ANN model with 8-12-1 architecture proved to have a better performance when compared to other ANN models. Comparisons were based on coefficient of determinant (R^2) and root mean square error (RMSE). The processes of building and characterization of the machine learning model are shown together with results on prediction accuracy. Each result is compared against different ANN architecture, transfer functions, and number of hidden neurons**

Keywords*— *Airblast, artificial neural network, blasting

I. Introduction

Blasting is the most common technique used in mining and civil engineering for rock fragmentation. Airblast or air overpressure is the one of the most hazardous effects of blasting operation on the environment. The noise generated during the blast can result in complaints from nearby local inhabitants and impact the personnel negatively psychologically. Also, more than 80% of the energy released during blasting results in adverse environmental effects such as airblast, ground vibration and flyrocks etc [1-3], as illustrated in Figure 1.

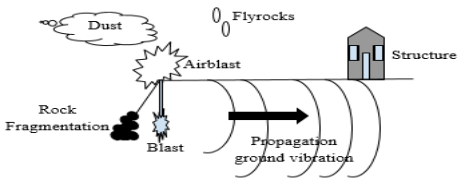


Figure 1. Environmental effects of blasting

Therefore, it is vital to predict blast-induced airblast to insure safe blasting operation. During blasting, airblast is generated when explosive gases get released into the atmosphere and create air pressure waves [4]. In blasting operation, airblast or air-overpressure is mainly a resultant of the following [5-7]

- Air pressure pulse (APP): displacement of the rock at bench faces as the blast progresses.
- Stemming release pulse (SRP): escape of gases from the blasthole when the stemming is ejected.
- Gas release pulse (GRP): escape of gases through rock fractures.
- Rock pressure pulse (RPP): induced by ground vibration.

Moreover, airblast is influenced by many factors which are divided into controllable and uncontrollable factors as shown in studies [8-12]. Controllable factors include blast design parameters such as burden and spacing, charge depth, stemming, maximum charge per delay, detonator accuracy and direction of initiation. However, uncontrollable factors include atmospheric conditions, weak strata, overcharging and conditions caused by secondary blasting. Various researchers has shown the predictive ability of the artificial intelligence methods across different fields of studies. Khandelwal and Kankar [9] predicted airblast using empirical models and support vector machine (SVM).They developed the models using 75 datasets. The results showed that SVM had high prediction accuracy as compared to empirical formulas. Armaghani et al [10] used a hybrid Al-based predictive model to predict blast induced air overpressure (AOp) at granite quarry site in Malaysia. The hybrid Al-based predictive model results were highly accurate as compared to conventional predictors.

ANN is the widely used soft computing method for prediction and this the first time ANN is applied to predict blast-induced airblast in a diamond mine according to the authors knowledge. The Orapa mine is located Orapa mine is located in Botswana, Southern Africa. It is situated 240 km west of Francistown in the Central District of Botswana as shown in Figure 1.1. It is positioned between the latitude and longitude of 21° 18′ 30″ S and 25° 22′ 10″ E respectively.

ISSN: 2521-2292



Figure 1.1 Map of Botswana showing the location of Orapa Diamond Mine

Orapa mine is a conventional open pit mine as demonstrated in Figure 1.2. The mine operates a four-shift system with 8 hours per shift. The mine operations start with drilling of the blastholes, charging blastholes with explosives and detonating blastholes. The resulting rock fragments from the blasting are loaded into dump trucks using hydraulic excavators. The waste material is hauled to waste dumps while the ore is transported directly to the crusher or to the stockpile. Dewatering is one of the processes that is also done as mining progresses to control water inflows thus creating workable dry conditions and reducing pore water pressure which affects slopes significantly.



Figure 1.2. Ariel view of Orapa open pit mine

Airblast or air overpressure is the one of the most hazardous effects of blasting operation on the environment. During blasting, airblast is generated when explosive gases get released into the atmosphere and create air pressure waves. These generated explosive gases have energy that leads to the rise of air pressure level above the normal atmospheric pressure. Atmospheric pressure wave can be subcategorized into two: audible and sub-audible [11].Audible pressure waves are those with high frequency sound while sub-audible pressure waves have low frequency sound. Blast induced airblast is a shock wave which is refracted horizontally by density variations in the atmosphere and gradually dies out with distance and time. The minimum frequency of sound that a human being can hear is 20 Hz and below that it cannot be heard. Airblast is measured in terms of Pascal (Pa) and Decibels (dB) [12]. Air blast results in inhabitants' annoyances and potential structural damage when air overpressure wave's energy is higher than the atmospheric pressure. Table I below shows the types of impacts that different levels of airblast can cause [13].

Table I. Airblast levels and their impacts

Airblast level	**Impacts**
<110 dB	Non
110-130 dB	Window Vibration
130-150 dB	Glass Break
180 dB	Structural damage

II. METHODS AND MATERIALS

A. Artificial Neural Network

Artificial neural network is one of the artificial intelligence method what mimics how the human brain works introduced in the early 1980s. ANN is defined by four stages which are choosing the network architecture, training, testing and validating datasets [14]. ANN is applicable in situations whereby the relationship between the inputs and outputs datasets is complex and nonlinear [15]. The most common used ANN type is the multilayer feed forward and has three layers that are interconnected to each other by neurons [16]. This three layers are input layer, hidden layer and the output layer. A typical ANN model is shown in Figure 2. The input layer receives the raw data (n) and then transmit it through neurons to the hidden layers via connection weights. The output of each hidden neurons is produced after transfer function such as the sigmoidal function to the hidden neurons net input. The process continues until the desired output is produced.

ISSN: 2521-2292

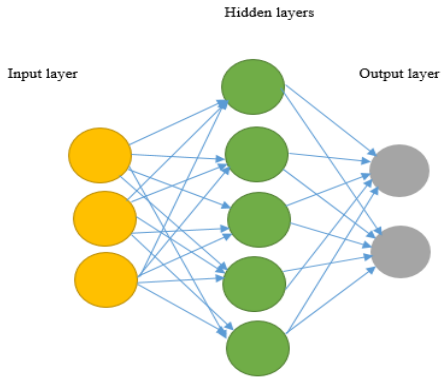


Figure 2. Typical ANN model

B. Training of the neural network

Firstly, neural network can be trained with back-propagation algorithm before new datasets are imported. There many algorithms used for training the neural network but for solving the predicting problems back-propagation algorithm is mostly used [17].The training of the network by back-propagation involves the following four steps (14)

1) Initialization of weights,
(2) feed-forward,
(3) back-propagation of errors, and
4) Updating of weights and biases.

Also, Levenberg–Marquardt algorithm can used for training the network as it fastest method with high accuracy. It is a built in function on MATLAB software [18]. Therefore, in this study it is used to train the network. The ANN behavior mostly depend on weights and transfer function. The transfer function output is multiplied weights connecting the hidden layer and the output layer to generate the network output. The commonly used transfer functions are tan-sigmoid, log-sigmoid and linear transfer function in back-propagation as shown in Figure 2.2, 2.3 and 2.4 respectively.

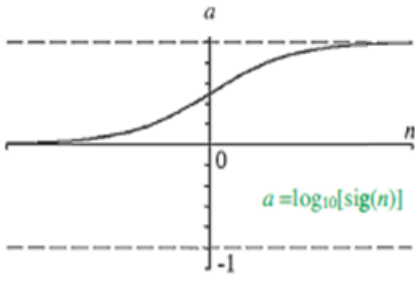


Figure 2.2. log-sigmoid function used for hidden layers [19]

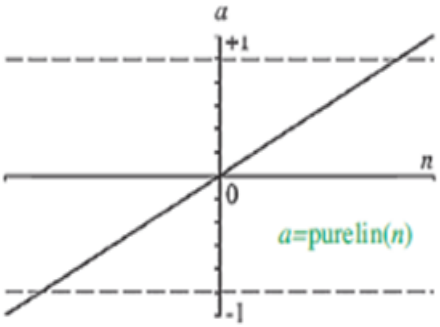


Figure 2.4.Liner transfer functions used for the output layer [19]

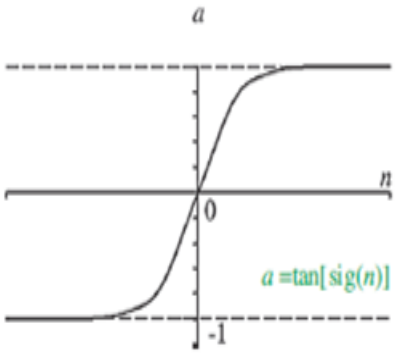


Figure 2.3. tan-sigmoid function used for hidden layers [19]

C. Datasets

Orapa diamond mine provided a total of 104 blasting datasets. A total of 94 datasets was used for development, training and testing the ANN model whereas 10 datasets was used for validating the ANN model. Eight input parameters and one output parameter were used to build the feed forward back propagation ANN system. Input parameters were blasthole depth, blasthole diameter, stemming length, spacing, burden, and distance from the blast face, powder factor and maximum charge per delay. On the other hand airblast was regarded as the output parameter. The optimum prediction model was established by feeding input and output parameters on a MATLAB-based ANN system. The range of input and output parameters are shown in Table II.

ISSN: 2521-2292

Table II. Range of Input and output parameters

Type of data	**Parameters**	**Range**
Input	Hole depth (m)	6.54 -18.43
	Hole diameter (mm)	150 – 250
	Spacing (m)	4-7
	Burden (m)	4-8
	Stemming length (m)	4-8
	Distance (m)	438 - 1500
	Powder factor (kg/m^3)	0.3 - 61.4
	Maximum charge per delay (kg)	27- 61.4
Output	Airblast (dBL)	91.5 – 126.7

Table III. Different ANN models

Model	**Transfer function**	**Network architecture**	**(R^2)**	**(RMSE)**
1	TRANSIG	8-10-1	0.935	0.385
2	TRANSIG	8-14-1	0.926	0.421
3	TRANSIG	8-12-1	0.983	0.149
4	LOGSIG	8-11-1	0.849	0.752

III. RESULTS AND DISCUSION

Optimum ANN model was selected from the models developed as shown in Table III. The selection was based on the evaluation performance using coefficient (R^2) and the root mean square error (RMSE). The ANN model 2 was chosen as then optimum model as it has R^2 an RMSE of 0.983 and 0.149 respectively. The indices shows the excellent predictive ability of the chosen model. The optimum ANN model had network architecture of 8-12-1 (8 inputs parameters, 12 hidden neurons and 1 output parameter with a transfer function of transig as illustrated in table III. Also the optimum ANN model is shown in Figure 3. Figure 3.1 demonstrates the graph between the measured airblast and predicted airblast by the optimum model on a 1:1 slope line. All the predicted data points are very close to 1:1 slope line. This shows the predictive ability of ANN to predict blasting effects such as airblast.

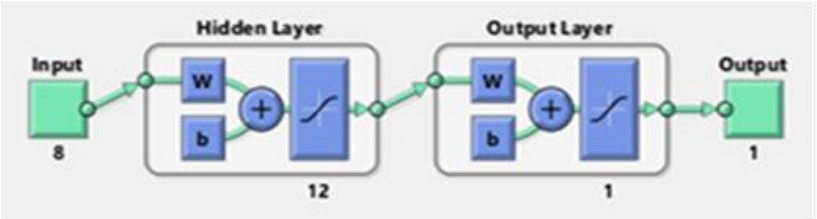


Figure 3. Optimum model network architecture

ISSN: 2521-2292

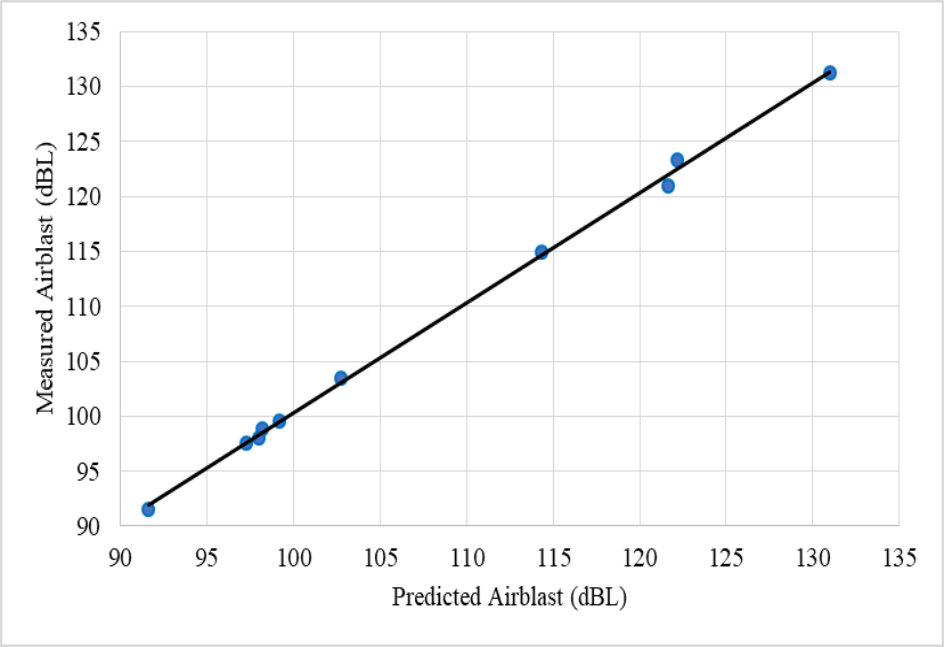


Figure 3.1. The relation between measured and predicted Airblast values by ANN model

IV. CONCLUSION

The neural network with two hidden layer, twelve hidden neurons and tran-sigmod transfer function has been found as the optimum model. Also, the predicted airblast values by the optimum ANN model shows the high degree accuracy of predictive capability of ANN when compared with the measured airblast values. Therefore, it can be concluded that ANN is an applicable tool to predict blast-induced airblast.

ACKNOWLEDGMENT

The authors wish to extend their appreciation to the Debswana Diamond Company especially Mr Eddie Mosware and Mr Moses Serojane for sharing blasting datasets with us to conduct airblast prediction using ANN.

REFERENCES

[1] Dindarloo SR (2015) Prediction of blast-induced ground vibrations via genetic programming. Int J Min Sci Technol 25:1011–1015

[2] Khandelwal M, Singh TN (2007) Evaluation of blast-induced ground vibration predictors. Soil Dyn Earthq Eng 27:116–125

[3] Shirani Faradonbeh R, Jahed Armaghani D, Abd Majid MZ, Tahir MMD, Ramesh Murlidhar B, Monjezi M, Wong HM (2016) Prediction of ground vibration due to quarry blasting based on gene expression programming: a new model for peak particle velocity prediction. Int J Environ Sci Technol. doi:10. 1007/s13762-016-0979-2

[4] Singh PK, Sinha A (2013) Rock fragmentation by blasting, Fragblast 10. Taylor & Francis Group, London, p 427

[5] Morhard RC, editor. Explosives and rock blasting. Atlas Powder Company; 1987

[6] Siskind DE, Stachura VJ, Stagg MS, Koop JW. In: Siskind DE, editor. Structure response and damage produced by airblast from surface mining. United States Bureau of Mines; 1980

[7] Wiss JF, Linehan PW. Control of vibration and blast noise from surface coal mining. Northbrook, IL (USA): Wiss, Janney, Elstner and Associates Inc; 1978

[8] Bhandari S. Engineering rock blasting operations. Netherlands: A.A. Balkema;1997

ISSN: 2521-2292

[9] Kuzu C, Fisne A, Ercelebi SG. Operational and geological parameters in the assessing blast induced airblast-overpressure in quarries. Appl Acoust 2009;70:404–11

[10] Dowding CH. Construction vibrations. In: Dowding, editor; 2000. p. 204–207

[11] Khandelwal M, Kankar PK (2011) Prediction of blast-induced air overpressure using support vector machine. Arab J Geosci 4:427–433

[12] Bhandari S. Engineering rock blasting operations. Netherlands: A.A. Balkema;1997

[13] Simpson P (1990) Artificial neural system: foundation, paradigms,applications and implementations. Pergamon, New York

[14] Rodríguez R, Lombardía C, Torno S. Prediction of the air wave due to blasting inside tunnels: approximation to a 'phonometric curve'. Tunn Undergr Sp Technol 2010;25:483–9

[15] Kuzu C, Fisne A, Ercelebi SG. Operational and geological parameters in the assessing blast induced airblast-overpressure in quarries. Appl Acoust 2009;70:404–11

[16] Rodríguez R, Lombardía C, Torno S. Prediction of the air wave due to blasting inside tunnels: approximation to a 'phonometric curve'. Tunn Undergr Sp Technol 2010;25:483–9

[17] Dreyfus G (2005) Neural networks: methodology and application.Springer, Berlin

[18] Rogers SJ, Chen HC, Kopaska-Merkel DC, Fang JH (1995) Predicting permeability from porosity using artificial neural networks.AAPG 79:1786–1797

[19] MathWorks Inc. Neural networks toolbox for use with MATLAB, User's Guide Version 9.2. MA, USA: The MathWorks Inc; 2017.

BIUST Research and Innovation Symposium 2019 (RDAIS 2019)
Botswana International University of Science and Technology
Palapye, Botswana, 4 - 7 June 2019

ISSN: 2521-2292

Application of Artificial Neural Networks to Predict Blast-Induced Ground Vibration in a Diamond Mine

Kesalopa Gaopale[a]
Department of Mining and Geological Engineering
BIUST, Palapye, Botswana
gaokesa@gmail.com

Jamisola S. Rodrigo Jr[b]
Department Mechanical, Energy and Industrial Engineering
BIUST, Palapye, Botswana
jamisolar@biust.ac.bw

Itumeleng Seitshiro[b]
Debswana
Jwaneng, Botswana
ITSeitshiro@debswana.bw

***Abstract*— In this paper, ground vibration that is induced by blasting was predicted using data gathered from a diamond mine. Artificial neural network (ANN) is used to train the model from the 94 blast dataset using Levenberg–Marquardt algorithm, and we tested and verified the built model. Different ANN models were compared using Root mean square error (RMSE) and coefficient of determinant (R^2), and the optimum ANN model was selected. Blasthole depth, blasthole diameter, burden, spacing, stemming length, powder factor, maximum charge and distance from the blast face to the monitoring point were used as input parameters. Ground vibration was the output parameter that was predicted using the built model. Processes in building the machine learning model are presented, together with prediction results and are compared against each other.**

Keywords*— *Artificial neural network, blasting, ground vibration

I. Introduction

Drilling and blasting is the most common economical viable method of rock fragmentation in mining, quarrying and civil engineering projects like road or dam construction and tunneling. During blasting, about 20-30 % of explosive energy generated is the on that actual breaks the rocks whereas the rest result in adverse environmental impacts such as ground vibration, backbreak, airblast, flyrock etc [1-3].Excessive generation of ground vibration due to blasting can result in harmful effects on nearby habitants and even damage to structures [4-10]. Hence the prediction of blast-induced ground vibration is vital way of controlling and prevent undesirable effects of blasting. Ground vibrations are measured in terms of peak particle velocity (PPV) in millimeters per second (mm/s) at a certain ground locations. Ground vibrations are influenced by controllable parameters and uncontrollable parameters. Controllable parameters are those that are man-made, mostly associated with explosive characteristics and blast design parameters such as explosive energy, charge per delay, blasthole diameter, blasthole depth, stemming etc. Uncontrollable parameters are those that are naturally occurring such as rock characteristics and geological conditions. The magnitude of the ground vibration at any locations is influenced by the following;

- Frequency: is the number of oscillations per second the wave undergoes. (measured in(Hz)
- Wave displacement : The distance a wave moves before returning to its
- original position (measured in mm)
- Wave velocity: the rate of change of displacement (measured in mm/s).
- Wave acceleration: This is the rate of change of velocity (measured in mm/s^2)

Several researchers has developed empirical formulas to predict induced ground vibrations however this empirical formulas do not include many factors that affect the blasting outcomes. Hence, the need to use more robust techniques that will incorporate many factors that affect the blasting outcome such as artificial neural network (ANN). Artificial neural network is a machine learning technique that was introduced in the 1980s. This technique is capable of developing the relationship between the inputs and outputs parameters without prior physics about them.

In this paper, a new ANN model is developed to predict blast-induced ground vibration in Orapa diamond mine. Also, different developed ANN models were compared with each other to determine the optimum ANN model.

A. The study area

Orapa mine is open mine and expected to reach the depth of 450m by 2026. The mine is situated in Botswana in Southern Africa as shown in Figure 1. It is about 240 km west of Francistown and was discovered by De Beers geologists in 1967 led by Manfred Marx. Also, it was official opened by the first the first President of Botswana, His Excellency Sir Seretse Khama in July 1971. The mine lies on igneous rocks known as kimberlite which bears diamonds and it was intruded about 92 million years ago. The Orapa kimberlite has two coalescing diatremes with preserved crater sedimentary facies named southern and northern lobes which lie on a 1.18 square kilometres at ground level.

ISSN: 2521-2292



Figure 1. Location of Orapa Diamond Mine in Botswana, Southern Africa

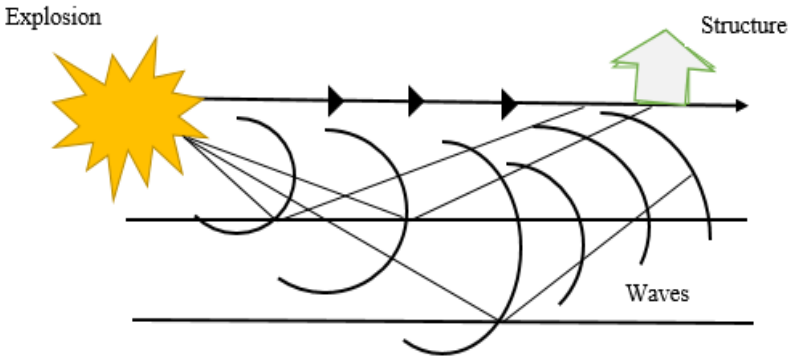


Figure 1.1. Ground vibration caused by blasting

B. Mechanism of ground vibration

When an explosive detonates within a blasthole, a large amount of chemical energy is released at high pressure thereby forming a hot gas [11]. After detonation, two forms of energy are generated; gas pressure energy and shock wave energy [12]. The shock wave energy greatly affects the walls of the blasthole and crushes it up. The damaged area surrounding the blasthole is called the crushed zone. Fracturing will result beyond the crushed zone caused by elastic and plastic waves and form what is called nonlinear zone [13]. Elastic waves propagate beyond this zone as shown in (Figure 1.1) while plastic waves lessen in this zone. As the elastic wave propagates beyond the nonlinear zone, this motion is referred to as peak particle velocity. Although, the intensity of ground vibration diminishes with distance, large amount usage of explosive can still cause damage to the nearby natural and man-made structure as result of dynamic stress being more that the material strength [14].

ISSN: 2521-2292

II. METHODS AND MATERIALS

A. Artificial Neural Network

The prediction ability of ANN is based on preceding learning [15]. Once the network has been developed and trained, any similarities in the new datasets presented, the pattern will be detected and new predictions will be made. Therefore, ANN has being used successfully across many different displaces and research as well. Eren et al. [16] applied the ANN system to predict densities and particle size distributions in mineral processing industry. The ANN system was used to predict ground subsidence in a metal mine by Zhao and Chen [17]. They found out that ANN model prediction results were highly accurate and consistent with the measured values. Therefore, ANN system proved it can used to monitor mine ground subsidence. Lal and Tripathy [18] predicted dust concentration using artificial neural network in an open cast coal mine in Jharkhand, India. ANN technique have also being used by many researchers for prediction of wide range of parameters from simple to complex [19, 20].

The neural network must be trained before the new datasets can be interpreted. There are many algorithms that are used to train the neural networks, however the most used algorithm is back-propagation which is robust, versatile plus it provides effective learning for multiple layer neural networks. The back-propagation neural networks are made up of three layers which are: input layer, hidden layer and output layer. Each layer consists of basic processing units called neurons. These neurons connects to next layer via approximate weights, i.e. the output of the neurons in the input layer serves as the input for the hidden layer neurons and similar with the connection between the hidden layers and the output layers. The number of input neurons is the equal with the number input variables and it is the same as number of output neurons and the output variables. However, the problem to be solved determines the number of hidden layers and neutrons in them. A typical structure of neural network is shown below in Figure 2.

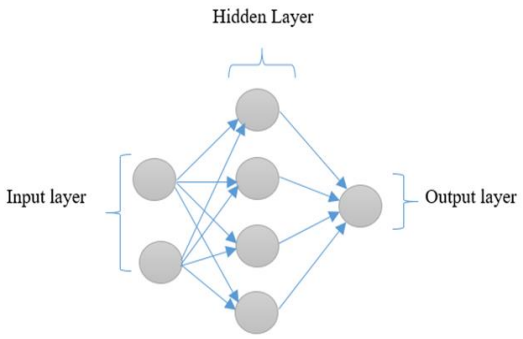


Figure 2. A typical structure of neural network

In this study a back propagation neural network is used with 'Levenberg-Marquardt' algorithm and different transfer functions to determine the optimum predictive model. Transfer functions include tan-sigmoid and log-sigmoid.

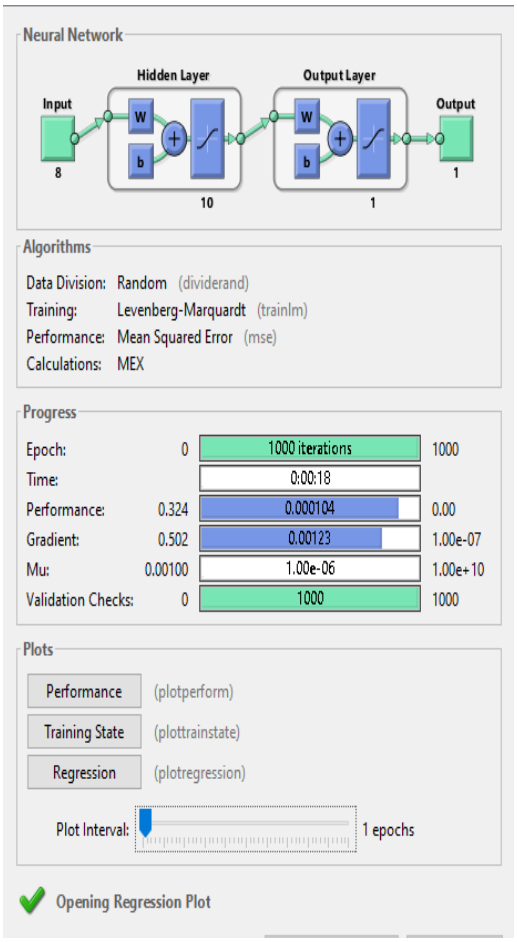


Figure 2. Training of back-propagation the neural network

B. Datasets

A total of 104 blasting datasets was provided by Orapa Diamond mine. For development of the ANN model, training and testing, 94 datasets was used while 10 datasets was used for checking the prediction accuracy of the developed ANN model. The ANN model was built with eight input parameters and one output parameter as shown in Table 1.The neural network architecture is shown in Figure 2.

ISSN: 2521-2292

Table 1. The range of parameter

Type of data		Parameters	Range
Input	1	Burden (m)	4-8
	2	Stemming length (m)	4-8
	3	Spacing (m)	4-7
	4	Hole depth (m)	6.54 -18.43
	5	Hole diameter (mm)	150 – 250
	6	Distance (m)	438 - 1500
	7	Maximum charge per delay (kg)	27- 61.4
	8	Powder factor (kg/m^3)	0.3 - 61.4
Output	1	Ground vibration (PPV), mm/s	91.5 – 126.7

III. RESULTS AND DISCUSSION

An ANN model 6 of 8-10-1 network architecture of transfer function of TRANSIG was found to be the optimum model as illustrated in Table 2. A pictorial representation of the optimum neural network architecture is shown in Figure 3. The coefficient of determination (R^2) of the optimum model is 0.945. This index is closer to 1 and this means it has the higher the prediction accuracy compared to other models. Ground vibrations was predicted by optimum artificial neural network using 10 new datasets that have not being used before. The predicted ground vibrations were compared with the measured ones as shown in Figure 4. It evidently shows by the R^2 that the predicted values by the optimum ANN model are closer to the measured values as shown in Figure 3.1 and it was 0.9849.This index shows that the chosen ANN model has an excellent prediction capabilities. Also, the root mean square error (RMSE) between the measured values and the optimum ANN predicted values was at the lowest with 0.24 and close to zero, thus providing to be a great predictive model.

Table 2. Different ANN models

Model	Transfer function	Network architecture	(R^2)
1	TRANSIG	8-20-1	0.935
2	TRANSIG	8-13-1	0.889
3	LOGSIG	8-10-1	0.860
4	LOGSIG	8-12-1	0.939
5	LOGSIG	8-16-1	0.848
6	TRANSIG	8-10-1	0.945

ISSN: 2521-2292

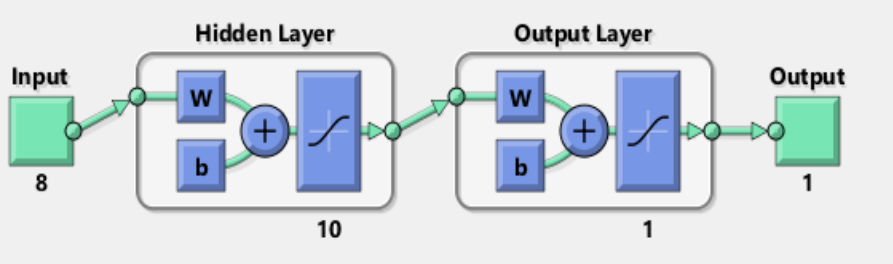


Figure 3. The optimum neural network achitecturure

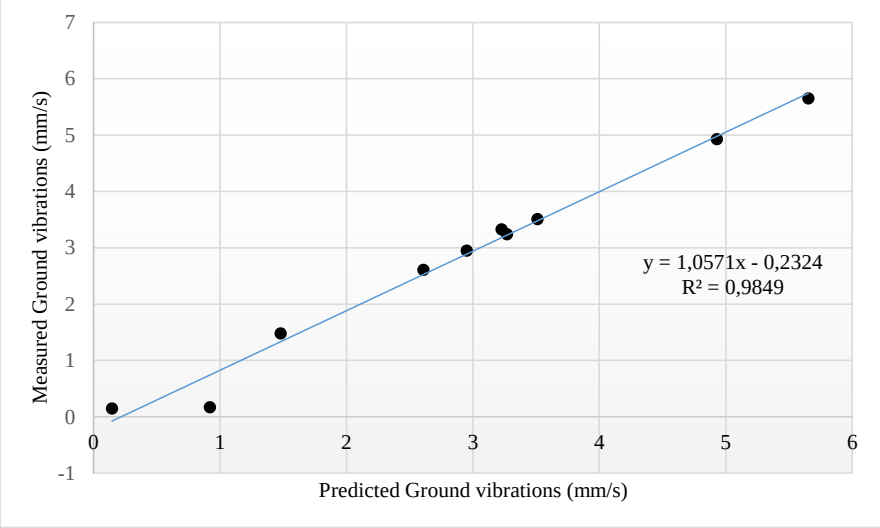


Figure 3.1. The relation between the measured and the predicted ground vibrations by ANN

IV. CONCLUSION

Based on the study, it shows that ANN model with network architecture of 8-10-1 with two hidden layer and transfer function of tran-sigmod has been found to be the excellent predictive model by merging back-propagation neural network with 'Levenberg-Marquardt' algorithm. Also, the optimum ANN model proved to be the best because of its highest coefficient of determination.

ACKNOWLEDGMENT

The blasting datasets was provided by Orapa Diamond Mine owned by Debswana, is thankfully acknowledged. The thanks are also due to the mine employees, Mr Eddie Mosware and Mr Moses Serojwane for providing assistance during mine visit.

REFERENCES

[1] Cheng, G., Huang, S.L., 2000. Analysis of ground vibration caused by open pit production blast. In: Holmberg (Ed.), Explosive and Blasting Technique, Balkema, pp. 63–70

[2] Monjezi, M, Bahrami, A., Yazdian, A., Sayadi, A.R., 2009. Prediction and controlling of flyrock in blasting operation using artificial neural network. Arab. J. Geosci. doi:10.1007/s12517-009-0091-8

[3] Hakan, A.K., Konuk, A., 2008. The effect of discontinuity frequency on ground vibrations produced from bench blasting: a case study. Soil Dyn. Earthq. Eng. 28, 686–694

[4] Nateghi R, Kiany M, Gholipouri O. Control negative effects of blasting waves on concrete of the structures by analyzing of parameters of ground vibration.Tunn Undergr Space Technol 2009;24(6):608–16.

[5] Toraño J, Ramírez-Oyanguren P, Rodríguez R, Diego I. Analysis of the environmental effects of ground vibrations produced by blasting in quarries.Int J Min Reclam Environ 2006;20(4):249–66.

ISSN: 2521-2292

[6] Kahriman A. Prediction of particle velocity caused by blasting for an infrastructure excavation covering granite bedrock. Miner Resources Eng 2001;10(2):205–18.

[7] Singh PK, Vogt W, Singh RB, Singh MM, Singh DP. Response of surface structures to rock blasting. Miner Resources Eng 1997;6(4):185–94.

[8] Faramarzi F, Ebrahimi Farsangi MA, Mansouri H. Simultaneous investigation of blast induced ground vibration and airblast effects on safety level of structures and human in surface blasting. Int J Min Sci Technol 2014;24 (5):663–9.

[9] Khandelwal M, Singh TN. Prediction of blast-induced ground vibration using artificial neural network. Int J Rock Mech Min Sci 2009;46(7):1214–22.

[10] Yi CP, Lu WB. Research on influence of blasting vibration on grouted rockbolt.Yantu Lixue/Rock Soil Mech 2006;27(8):1312–6.

[11] Hopler, R.B. (Ed.) (1998) Blasters' Handbook, 17th ed., International Society of Explosives Engineers, Cleveland, OH.

[12] Djordjevic, N.M. (1995) A Study on the Blast Induced Ground Vibrations and their Effects on Structures, PhD Thesis, Julius Kruttschnitt Mineral Research Centre, The University of Queensland, Brisbane, Australia

[13] Mortazavi, A. (1999) Modelling of Rock Blasting in Jointed Media using Discontinuous Deformation Analysis, PhD Thesis, Mining Engineering department, Queen's University, Canada

[14] Siskind DE, Stagg MS, Kopp JW, Dowding CH. Structure response and damage produced by ground vibration from surface mine blasting, vol. 8507. US Bureau of Mines, RI; 1980. p. 74.

[15] Simpson PK. Artificial neural system—foundation, paradigm, application and implementations. New York: Pergamon Press; 1990.

[16] Eren H., Fung, CC.,Wong, KW., (1997). An application of Artificial Neural Network for prediction of densities and particle size distributions in mineral processing industry. IEEE Instrumentation and Measurement. Technical Conference. Ottawa, Canada

[17] Zhao, K and Chen, S (2011). Study on artificial neural network method for ground subsidence prediction of metal mine. Science Direct. Volume 2. pp 177-182

[18] Lal, B and Tripathy, S. (2012) Prediction of dust concentration in open cast coal mine using artificial neural network. Atmos Pollut Res , Volume 3, Pp 211–218.

[19] Maulenkamp F, Grima MA. Application of neural networks for the prediction of the unconfined compressive strength (UCS) from equotip hardness. Int J Rock Mech Min Sci 1999;36:29–39.

[20] Kosko B. Neural networks and fuzzy systems: a dynamical systems approach to machine intelligence. New Delhi: Prentice Hall of India; 1994. p. 12–17.

BIUST Research and Innovation Symposium 2019 (RDAIS 2019)
Botswana International University of Science and Technology
Palapye, Botswana, 4 - 7 June 2019
ISSN: 2521-2292

Design of a Solar Charge Controller For DC Load Output

[1]Patrick Kandjise, [1]Pelonomi Tito, [1]Kesego Petso. [1]Bokani Mtengi
[1]Department of Electrical, Computer and Telecommunications Engineering
Botswana International University of Science and Technology
Palapye, Botswana
Email: patrick.kandjise@studentmail.biust.ac.bw

***Abstract*- One of several ways to provide power to off grid locations is through stored electrical energy devices such as batteries. This paper presents the design of an economical solar charge controller to be used in a stand-alone solar home system for providing power and increase lifespan of the battery. The designed system uses a direct current DC/DC converter and a microcontroller which implements the Perturb and Observe, algorithm of the maximum power point tracker (MPPT). The prototype is tested with 100 W photovoltaic panel and a 12 Volt lead acid battery.**

Keywords; Charge controller, Perturb and Observe, Microcontroller, Photovoltaic System, DC/DC converter.

I. INTRODUCTION

Sustainable development goals must be reliable, affordable, economically viable and socially acceptable and environmentally sound. To foster sustainable energy development sector, Botswana must innovate technology that reduces reliance on the finite resources to generate electricity. Unreliable electricity access is a detriment to economic growth. Researchers and policy makers have since made efforts to use the renewables or natural sources of energy such as solar which can be harnessed to generate electricity that can be supplied to remote areas. To take advantage of solar energy, there must be a way to store the generated solar energy for later use when the sun sets. One system that can supply solar generated stored energy is a solar home system. A Solar Home System (SHS) is a small-scale electricity supply system for households that are off the main power grid or have unreliable access to electricity supply. It harvests the sunshine and generates electricity which is then stored in a battery to provide power at night and during cloudy days when photovoltaic panels do not produce enough energy [1]. Solar Home Systems generate direct current that can be used for a range of applications including powering electrical appliances, lighting and powering electronic devices. Solar energy provides sustainable environmental and health benefits. By replacing fossil energy sources with renewable ones such as solar, wind, biomass, the move addresses emission issues caused by burning coal and reduces reliance on finite energy resources.

A solar home system typically includes one or more photovoltaic modules consisting of solar cells, a charge controller which distributes power and protects the batteries and appliances from damage and at least one battery to store energy for use during the hours when the sun is down. For many people, living in locations away from the main power grid, a custom-made solar home system is a way of connecting dc voltage to their homes to be used in dc machines. A standard 12-volt solar panel which can be used to recharge a battery, could be putting out, much more voltage than the battery needs. This difference in voltage between the required 12 volts need for the battery and actual volts being generated by the solar panel translates into a greater current flow into the battery. The result is that too much unregulated solar current will overcharge the battery causing the electrolyte solution within the batteries to overheat, resulting in a shortened battery life and ultimately, complete failure of the battery. The quality of the charge will directly affect the lifespan of any connected battery, so it is extremely important to protect batteries of a solar charging system from being overcharged, or even undercharged, and we can do just that using a battery charge regulation device called a charge controller [2]. A charge controller or alternatively a charge regulator is basically a voltage and/or current regulator, to keep batteries from overcharging. It regulates the voltage and current coming from the solar panels and going to the battery. Most 12-volt panels produce about 16 to 20 volts, so if there is no regulation, the batteries will be damaged from overcharging There are two known types of charge controllers; pulse width modulation (PWM) and maximum power point tracking (MPPT) which operate by adjusting charging rates of batteries depending on the maximum capacity and also monitor the battery temperature to prevent overheating [3] .This work proposes the design an affordable, reliable solar home system charge controller that uses locally sourced components for monitoring the charging status of a battery. The prototype will be used in homes that are located remotely from the main power grid for supply of electrical energy. This system will provide users

ISSN: 2521-2292

will the ability to monitor their energy consumption, making it cost effective.



Fig 1: Direct connection of a battery to a solar panel.

A. *Related Work*

Most works in the literature have studied and designed charge controllers as discussed in [5, 6, 7]. These works Jim Drew on his article about designing a solar cell battery charger deduced that all solar powered devices feature researchable batteries and the objective is to extract much power as could be reasonably be expected to charge the batteries rapidly and maintain the charge. He also stated that solar based cells are intrinsically inefficient devices but they do have a point of most extreme power yield

(Maximum power output) and operating at that point is a great desire. Figure 2 above shows, sun powered cell produces current in extent to the measure of daylight falling on it, while the cell's open-circuit voltage remains generally steady. Greatest power yield happens at the knee of each bend, where the cell transitions from a consistent voltage.

An article [4] proofed an idea for optimized and safe battery charging system for home, using solar charge controller by connecting the solar panel and the battery. This helps utilise solar in proficient way and expand the lifetime of battery too. Because of this, it very well may be comprehended that the condition of charge of battery is improved. They also compared the modelling of a charge controller and can be classified as single stage and multi stage regulators which are constant current and constant voltage regulators, series charge controller, shunt charge controller and combined series shunt charge controller.

From [5] article PWM and MPPT are the two distinct sorts of charging strategies sun oriented charge controllers can use to charge batteries from a sunlight based panel. The two advances are broadly utilized in the off-grid solar industry and are both extraordinary alternatives for effectively charging the battery. Pulse with modulation become an integral factor when the battery bank if full, it plays a big role on switching between connecting the battery which regulates the battery voltage keeping it constant.

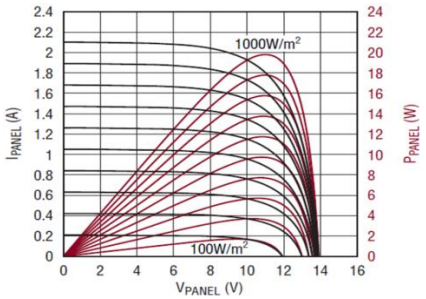


Fig 2: V-I graph for the solar panel

II. SOLAR HOME SYSTEM COMPONENTS

A. *Solar Panel*

A solar panel is a package connected assembly of photovoltaic cells. It can be used as a component of a larger photovoltaic system to generate and supply electricity in commercial and residential applications. Every solar panel has an I-V curve or I-V characteristics associated with it.in our case we are trying to extract as much as possible from the I-V curve.

B. *Lead Acid Battery*

Lead acid battery is an electrical storage device that uses a reversible chemical reaction to store energy. It uses a combination lead plates or grids and an electrolyte consisting of a diluted sulphuric acid to convert electrical energy into potential chemical energy and back again**Invalid source specified.**.All batteries tend to experience several phenomena, which affect their performance. Some of these conditions are named below, with proper charge design the following can be avoided increasing the lifespan of the battery.

- Self-discharge.
- Gassing
- Sulfation
- Freezing
- Dehydration

C. *Charge Unit*

There are basically different charging methods that all have different effects ad complications when designing. The main aim of the charging unit is to cut the supply when the battery is full and to start charging when low.

ISSN: 2521-2292

III. MAXIMUM POWER POINT TRACKING ALGORITHM

Maximum power point tracking (MPPT) algorithms are very important when it comes to maximising the power output at any moment.in many applications, the load can demand more power than the PV system can deliver. Therefore, there are many different approaches to maximising the power from a PV system, this range from using simple voltage relationship to move complexes multiple sample based analysis. The following are some of the conventional Maximum power point tracking methods;

- Constant voltage method
- Open circuit voltage method
- Short circuit current method
- Perturb and observe method
- Incremental conductance method

The algorithm is implemented in the microcontroller which will be controlling the DC-DC converter.

IV. SYSTEM DESIGN

In all, our project is to design solar charge controller with LCD display for voltages and use the MPPT method with "Perturb and Observe" algorithm to obtain the maximum power with the help of the pic controller. To save power loss the solar charge controller uses less switch.

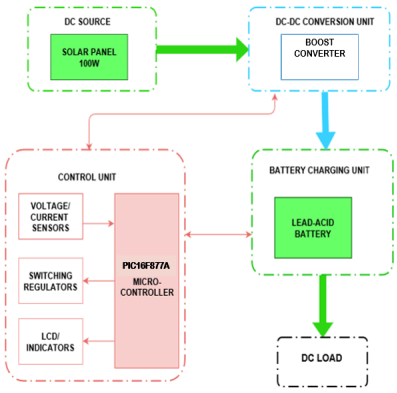


Fig 3: System flow chart

A. Sizing

The size of the solar panel depend on the overall output power of the load. Suppose we were to design three LED lights that operate at 15 W for 5hours per day has been selected and 4 smartphone chargers each operating at 5W for a period of 4 hours per day. Using a 5 Sun Peak hours which is common in Botswana;

$$Total\ power = \frac{305Wh}{5hrs} = 61\ W \qquad (1)$$

TABLE 1: TOTAL POWER OF LOAD

Description Iterm	Rating	Quantity	Number of Hours	Total Power
Smartphone charger	5 W	4	4	80 Wh
LED lights	15 W	3	5	225 Wh
Total Power				305 Wh

Using a factor of 1.4 to cater for diturbances

$$Total\ power = \frac{305Wh}{5hrs} * 1.4 = 85.4\ W \qquad (2)$$

Going for a panel that produces a minimum of 85.4 W is used but for standard rate,a solar panel of 100 W was selected.

B. DC-DC converter

In a boost converter, the output voltage is greater than the input voltage –hence the name "boost". A boost converter using a power MOSFET.

Why boost converter

- The inductor current is continuous.
- The circuit is operating in the steady state.
- The capacitor is large enough to assume a constant output voltage.

a. Design Assumptions

The output voltage is achieved by fast switching the device. The output voltage depends on the switching frequency applied to the device and it depends on the duty cycle of the frequency

The voltage and current ripple must be less than 0.5%. The switching Frequency is assumed 25 KHz. The Inductor current is assumed continuous100% efficient.

$$output\ current = Io = \frac{Po}{Vo} = \frac{100}{30} = 3.33A$$

$$The\ Duty\ ratio,\ \frac{Vo}{Vin} = \frac{1}{(1-\propto)}$$

$$\propto = \frac{(Vo - Vin)}{Vo} = \frac{30-12}{30} = 0.6$$

$$Load\ resistace = \frac{Vo}{Io} = \frac{30}{3.333} = 9.0\ \Omega \approx$$

ISSN: 2521-2292

$$Lmin = \frac{R \propto (1-\propto)^2}{2f} = \frac{9 \times 0.6(1-0.6)^2}{2 \times 25000}$$
$$= 69\ uH$$

L must be greater than Lmin so

$$L = 81\%\ of\ lmin = 0.81 \times 69\ uH = 55.99\mu H$$

Capacitor value

$$C \geq \frac{\propto}{R * \left(\frac{dv}{v}\right) * f} = \frac{0.6}{9 \times 0.005 \times 25000}$$
$$= 0.000533\ F \approx 540\mu F$$

Taking a capacity or of 560F at most which is commonly available.

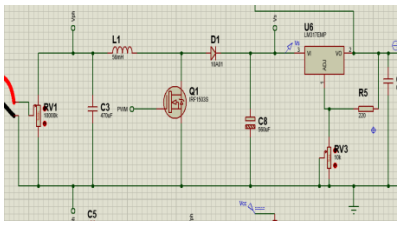


Fig 4: Boost converter

C. Power supply unit

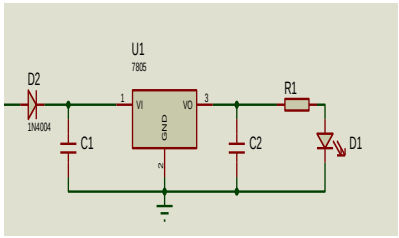


Fig 5: Power supply

For the microcontroller and sensors (voltage and current) they operate at lower voltage, a stable power supply was designed using LM7805 voltage regulator. Another reason for embedding the circuit in the system is because it produces a fixed output voltage.

In the data sheet it shows that the input voltage should be in range of 7 to 25 volts and our panel minimum voltage is around 11 volts and 18 Volts' maximum making it suitable for application. Input voltage will be applied across the first and second pin of 7805, Second pin is common to both input and output. It is connected to ground. Output voltage is taken across the third and second pin. Output voltage is fixed and will be 5V.

The Diode D2 is responsible for allowing current in one direction.

The capacitor C1 is present in the circuit in case there is an AC signal since it is a DC device like most amplifiers, it can become unstable if variations in supply voltage cause a change in output voltage. Capacitor C2 near the output, it helps in the transient response.

According to the Manufactures specification the values are not restricted, for 0.33µF and 0.1µF were chosen for C1 and C2 respectively. The fixed voltage regulator has a regulated output voltage of 5V is a current limiting resistor connected in series with an LED (power indicator) that indicates that the circuit is on.

$$R1 = \frac{Vs - V_D}{I_D} = \frac{5-2}{0.01} = 300\Omega \qquad (3)$$

Vs = 12V

Vd =2V

Id = (10mA-20mA)

D. Voltage regulator

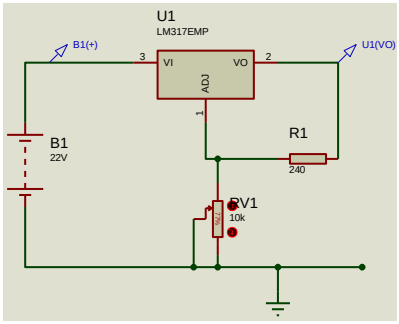


Fig 6: Voltage regulator

LM317 is an adjustable voltage regulator which takes an input voltage of 3- 40V DC and provides a fixed output voltage of 1.25V to 37V DC. It requires two external resistors to adjust the output voltage.in our case the DC-DC converter will boost the voltage and not provide a fixed voltage.The boost output is varying between 0- 29 volts ,the regulator will provide a fixed Voltage for charging the battery.

The required voltage for charging = 13.6V

Output Voltage= 13.6V+0.6=14.3V (0.6 voltage drop of the diode that is blocking the current from the battery). The Output Voltage of the regulator is dependent on external resistor values R1 and RV1 the variable resistor which can be fixed to get the fixed voltage but for our case it will be left to vary in case of charging different batteries.

$$Vout = 1.25 \times \left(1 + \frac{RV1}{RV1}\right) \qquad (4)$$

ISSN: 2521-2292

The above equation is used to calculate resistors. The recommended value for R1 is 240Ω but it can also be some other value between 100Ω to 1000Ω.

For example if the target output voltage is 16V then the R2 value is calculated as following:

$16 = 1.25x\ (1 + R2/240) \Rightarrow R2 = 2832\Omega.$

E. Voltage Sensor

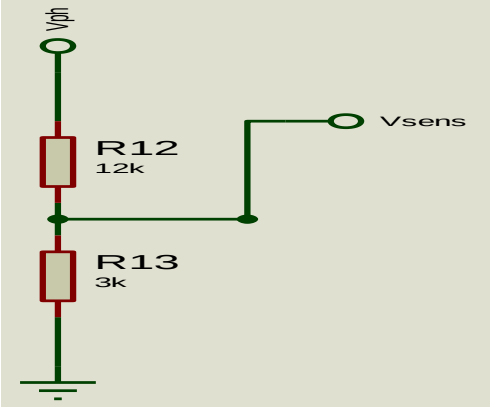


Fig 7: Voltage Sensor

Voltage divider network is used as voltage sensor for the microcontroller. The resistance values chosen are 12kΩ and 3kΩ. This gives the resistance ratio of 8.2KΩ/ (32KΩ+8.2KΩ) = 0.20 and therefore gives the maximum input voltage to the A/D conversion channel is 0.20×25=5

F. Current sensor

In the circuit diagram, maximum output of 17-volt DC source is applied to a 33 Ohm load. Current passing through this is measured with help of shunt resistor and a PIC16F877A microcontroller. The microcontroller cannot read current directly since they can only sense voltage. Therefore, this is why the current need to be converted into voltage form to be able to be read by the microcontroller. A 0.5 Ohm shunt resistor is used by connecting two 1 Ohm resistors in parallel. When current passes through shunt resistor, voltage appears across shunt resistor. This voltage can be easily measured with the help of analogue to digital converter channel of PIC16F877A microcontroller. This measured voltage value can be converted back into current in programming using ohm's law formula:

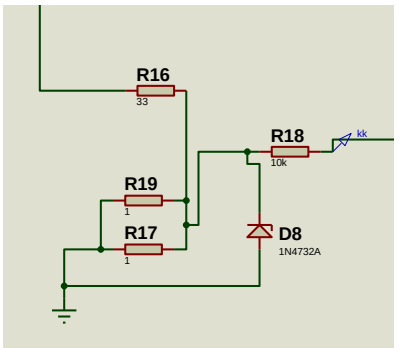


Fig 8: Current sensor

G. Protection

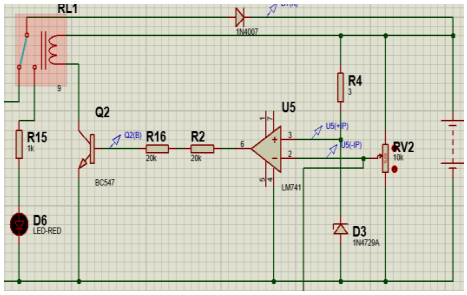


Fig 9: Protection Unit

Operational amplifier it's used to compare the reference value set from the battery with the varying voltage to the load. The output of the Operational amplifier is used to switch the MOSFET, based on the output voltage, so that the relay can be energized and de-energized, changing state to protect the battery.

H. Microcontroller

The microcontroller works with 5V from the supply, we have proposed a scheme as based on the use of conventional DC-DC converter, where combination of voltage and power feedback control system is implemented with the use of artificial intelligence Algorithm, which results in tracking strategy that makes output response faster, maximizes the power extracted from the solar module, and maintains the power delivered to the load. Maximum power point tracking is assured by varying duty cycle of the PWM signal to control MOSFET switch applied to a boost converter. The control logic is implemented to a microcontroller.

The chosen microcontroller to be the heart of our project is PIC16F877A, its duty will be based on displaying the measured voltage on LCD and producing the pulse for the MOSFET switch together with MPPT algorithm. The PIC16F877A micro controller is commonly used because it's to use and it has many internal peripherals. ADC interface and parallel slave port interface and its large programming memory. The external clock has been used which results in faster operation since you can select a 20MHz instead of 8MHz oscillator. External clock has been used which results in faster operation since you can select a 20MHz instead of 8MHz oscillator.

ISSN: 2521-2292

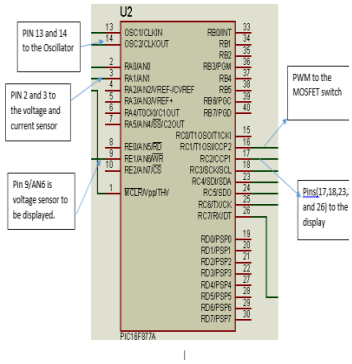


Fig 10: Microcontroller Pin layout

a. writing a code in MIKRO-c

Writing a code or programming on pic can be done in several languages such as assembler, C, BASIC &FLOW CODE etc. These are the most common ones and widely used languages, assembler is a mid-level language but are usually programmed very slowly and take up very least amount of space in the memory and giving the best result with execution. On the other hand, Programme on C language are very easy to learn and the instructions are really easy to understand. The disadvantage with it is that it is slower than Assembler. In this project C programming language is used using the software MIKRO C Pro for PIC. After writing the code it is compiled to hex file using ANSI C compiler

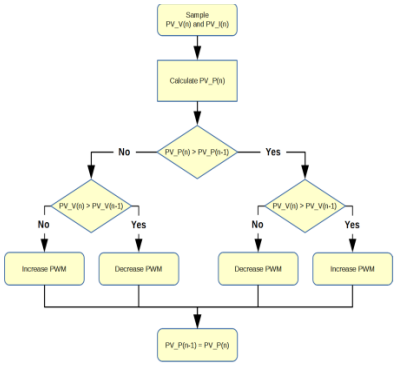


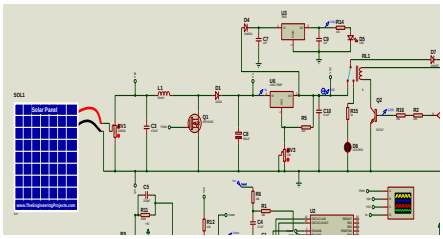
Figure 11: MPPT-P&O algorithm

```
void MPPT(void)
{
ADCON0= 0;
measuredvoltage = ADC_Read(0);                    /*
Read the voltage input from ADC channel 0 */
ADCON1= 1;                          /* select RA1 */
measuredcurrent = ADC_Read(1);   /* Read the
current input from ADC channel 1 */
power =(measuredvoltage*measuredcurrent);

    if (power>powerold)
    {   if (measuredvoltage >voltageold)
        {
          pwm++;
        }
        else
         {
           Pwm--;
         }
    }
      else
     {   if (measuredvoltage >voltageold)
         {
            pwm--;
         }
         else
         {
            pwm++;
         }
     }
         measuredvoltage=voltageold;
        power=powerold;
         PWM2_Set_Duty(pwm);

     }
```

V. RESULTS AND ANALYSIS



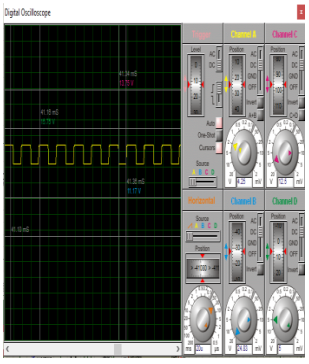


Fig 13: 50 % Pulse

ISSN: 2521-2292

The duty cycle is 50 % from Fig 13, the regulated voltage from channel C is 14.38 V. the boosted voltage is 29.50 V and the input is 11.17V

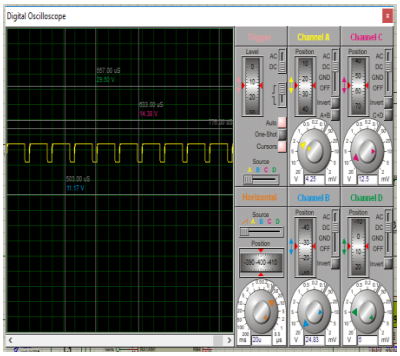


Fig 14: 60 % Pulse

The duty cycle is 60 % from Fig 14 the regulated voltage from channel C is 14.38 V. the boosted voltage is 29.50 V and the input is 11.17V.

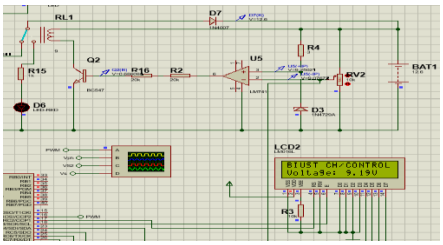


Fig 15: charging circuit

When the voltage of the battery to be charges is less than 9.20V the relay change state and connect the battery to be charging system as indicated in Fig 15

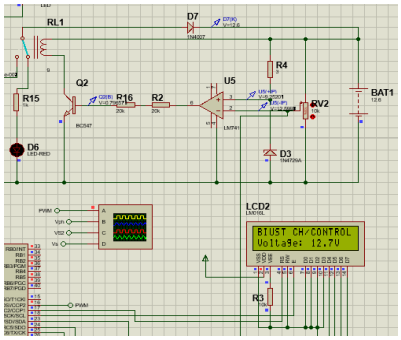


Fig 16: disconnect from solar panel

When the voltage of the battery to be charges is more than 12.6 V the relay change state and disconnect the battery from the charging system as indicated in Fig16

DISCUSSION

From the results we obtained, it showed that the voltage from the panel will always vary depending on the sun intensity hence this affects the voltage to the charger. This agrees with what we have found out in the literature review, a boost converter can be used to boost the voltage from the panel to make it suitable for charging with the help of MPPT algorithm to extract maximum power from the solar panel by varying the duty cycle to switch the MOSFET on or off. The microcontroller played a big role as it generates the PWM and displayed the output voltage on the LCD. The LED indicators are used for monitoring the state of the charger as it protects the battery from overcharging and discharging. Our results answer the objectives we set in the beginning.

CONCLUSION

In this project analysis of a solar charge controller with DC output has been carried out. To extract out maximum power boost converter is used, the energy then goes through the charge controller that monitors overcharging by the help of the relay and storing the energy in the battery. The battery is monitored by another circuit to protect it from over-discharging when is used by the load. Therefore, our motto has been achieved to make a solar charge controller as batteries will be monitored and kept safe increasing their lifespan and productivity.

RECOMMENDATIONS

Even though a boost can do, we will recommend a further study on a buck-boost charge controller as it maintains the constant voltage. Also we will recommend a further study on interfacing the microcontroller with the charge controller so that the microcontroller can control the flow of current into the battery until it gets full.

REFERENCES

[1] C.A. Osaretin, F.O. Edeko, “Design and implementation of a solar charge controller with variable output,” Journal of Electrical and Electronic Engineering, vol. 12(2), pp.40-50, November 2015.

[2] M. Ashiquzzaman, N. Afroze, J.M. Hossain, U.Zobayer, M.M. Hossain, “Cost effective solar charge controller using microcontroller,” Canadian Jouranl on Electrical and Electronics Engineering, vol.2(12), pp.2, December 2011.

[3] C.U.Ikeh, C.E.Uzor, “Design of a pulse width modulation (PWM) or standard charge controller for a photovoltaic system in Awka, Nigeria,” European Journal of Engineering and Technology, vol. 5(2), pp.44-47, 2017.

BIUST Research and Innovation Symposium 2019 (RDAIS 2019)
Botswana International University of Science and Technology
Palapye, Botswana, 4 - 7 June 2019

ISSN: 2521-2292

Energy requirement analysis for the design of solar photovoltaic micro-grids in Botswana

A study of Jamataka village

Kealeboga P. Motladiile and Tobias Bader
Department of Mechanical, Energy & Industrial Engineering
Botswana International University of Science & Technology
Palapye, Botswana
kealeboga.motladiile@studentmail.biust.ac.bw

Adrian Pugsley, Mervyn Smyth and Jayanta Mondol
Belfast School of Architecture and the Built Environment
University of Ulster, Jordanstown Campus
Newtownabbey, Northern Island
a.pugsley@ulster.ac.uk

Abstract

Substantial proportions of the world's poor live in remote areas that are geographically isolated and are often sparsely populated or have a comparably low electricity demand to justify the extension of the main electricity grid. Botswana with an average national electrification rate of 65.4% and 58.6% in rural areas as per December 2018 is no exception. Against this background, renewable energy is identified as a key enabler for increasing physical access to electricity to off-grid communities. The government of Botswana through its Sustainable Energy for All (SE4All) action and its Vision 2036 intends to increase the use of renewable energy sources for electrification purposes in Botswana with a mainstream to solar energy.

The core of a solar energy project for rural electrification is an energy requirement analysis which is critical for purposes of site selection, sizing and scaling of a solar-photovoltaic (PV) system. This paper conducts an energy requirement analysis of the un-electrified off-grid village called in the Central District of Botswana. The gained knowledge forms a basis to accommodate the load demands of the village I the course of the development of a PV micro-grid. The analysis at hand is based on the estimated daily load demand of government premises, commercial premises and residential buildings. Residential buildings were categorised into low-income, middle-income and high-income household as the amount of energy consumption is assumed to correlate with the disposable income. The user's basic energy need and their daily energy usage was obtained through a preliminary in-situ energy demand survey characterised by questionnaires, verbal interviews and on-site visits to the village. An aggregate load requirement profile for the community is derived from daily load profiles of the individual users. Hence, the total electricity demand of the community has been established to be 174kWh with a peak load and average demand of 16kW and 8kW respectively.

Keywords—Energy requirement analysis; rural electrification; solar-photovoltaic micro-grid; end-use model; energy load profile

I. INTRODUCTION

Substantial proportions of the world's poor live in remote areas that are geographically isolated and are often too sparsely populated or have a very low electricity demand to justify the extension of the main grid [1]. Botswana as a developing country is no exception with an average national electrification rate of 65.4% and 58.6% in rural areas in December 2018 [2]. Renewable energy is identified as a key enabler for increasing physical access to off-grid communities. Aside from physical access, the availability, reliability and affordability of supply are also central policy objectives for enabling energy access. A lack of domestic generation capacity and reliance on non-firm imports until recently resulted in substantial load shedding [3]. The government of Botswana through its Sustainable Energy for All (SE4All) action and the vision 2036 intends to increase the use of renewable energy sources for electrification purposes in Botswana with a mainstream to solar energy [4] [5].

This paper reviews existing literature on energy requirement analysis and reflects on the general principles of power requirement analyses including guidelines, recommendations and experiences regarding energy requirement planning for the design of solar PV micro-grids for electrification. Based on this thorough review, the paper gives an overview on the Solarfin2Go project by which the partners-Ulster University (UK) and Botswana International University of Science and Technology (BIUST) are aiming at the electrification of Jamataka village, Botswana. The core of this paper presents the energy requirement analysis carried out for Jamataka and the employed methodological approach. The results of the energy requirements analysis are discussed, and the electricity consumption profiles derived. The significance of the generated knowledge for the effective planning of the solar-PV micro-grid, systematically taking into consideration the demands of the village in the early planning stages, is shown. The paper concludes with an outlook on the current project funded by InnovateUK.

The SolarFin2Go project is a formed by a collaboration of international companies spearheaded by Ulster University in partnership with BIUST. The project conducts a pilot project of an innovative stand-alone PV-system developed by Ulster University's Centre for Sustainable Technology. SolaFin2Go stand-alone solar-storage systems designed are designed to provide affordable access to both electricity and hot water for off-grid households, businesses and community facilities through improved pay-as-you-go business models enabled by an innovative FinTech platform delivered through mobile, cloud and blockchain [6]. The smart connection of the individual

ISSN: 2521-2292

stand-alone PV-systems to provide a PV-micro-grid is an objective of the follow-up SolaNetwork project. The study at hand was carried out to professionally consider the village energy requirement in the planning process.

II. LITERATURE REVIEW

An essential component of the engineering planning and design of a solar energy system is to determine the net energy production required off the plant and hence its required net power supply [7], which matches the expected energy demand and load. This type of studies are forecasting the eventual energy requirement based on a load assessment. Energy demand refers to the required energy over whereby load relates to the instantaneous power. Demand analysis is a disaggregated, end-use based approach for modelling the requirements for final energy consumption in an area [8]. This process improves the quality and accuracy of the anticipated energy requirement since the diverse data required to conduct an energy requirement analysis is clustered into manageable divisions. The energy can be estimated at different levels depending on the intended application and its magnitude. Generally, grid-tied systems are flexible to solar intermittence compared to stand-alone PV-systems or micro-grids where energy is supplied instantaneously to the loads without grid backup. For this study, a candid energy consumption is of paramount importance since the nature of the energy service provided is a solution off the national electricity grid.

Energy requirement analysis is data intensive and based on the evaluation of diverse parameters [9]. Projecting energy requirements that reflects reality is rather complex, especially for prospective consumers with no record of prior energy and power use [10] as is the case for Jamataka village. In an ideal situation where a record of energy consumption such as electricity bills is available for a considerable timeframe (usually 1 year), a planner is able to compute average monthly consumption and total annual energy consumption. In the absence of such data, it is requisite for the designer to deduce an estimation of the total annual energy consumption based on the energy loads of the target group. This is referred to as a load analysis [9]. There are various guidelines and principles available on conducting power requirement analysis. In general, the procedure for carrying out an energy load analysis for a renewable energy project is dependent on numerous factors such as seasonal data, climate parameters, demographics, topology and economical boundary conditions [11]. Furthermore, seasonal factors, vacation and holidays have a significant impact and influence on the energy consumption. Last but not least the heat and power demand is influenced by the operational parameters of enterprises with large energy demand and by the consumer's behavior. Additionally the power and heat demand follow a daily cycle with low periods during the night hours and with peaks at different hours of the day.

Numerous codes and standards governing solar energy projects from a pool of different internationally recognised bodies are documented in literature. Akinyele extensively employs the Institute of Electrical Engineering and Electronics (IEEE) and International Electrotechnical Commiss ion (IEC) guidelines and standards in his research. The IEC standards are proposed for this research since they explicitly reflect on energy requirement analysis.

IEC standards

IEC/TS 62257-9-1: mainly provides technical specifications and recommendations for micro-power systems for isolated communities and gives insights with regard to selection an appropriate system for a particular area and discusses possible scenarios [12].

IEC/TS 62257-9-2: gives recommendations for small renewable energy systems for rural electrification with regard to developing electrical systems from energy demand requirements [13]. In this context, the standard presents methodologies for evaluating the socio-economic aspect of decentralised energy projects [14].

IEC/TS 62257-4: presents technical specifications and recommendations on the assessment of user needs and addresses different electrical power topologies for the specified needs [15].

In addition to the IEC standards, numerous methods exist for energy estimation and forecasting. These methods are classified into three groups; short, medium and long term and implore analytical concepts based on statistics, artificial intelligence (AI), knowledge based expert systems and hybrid techniques [16]. A wide variety of tools are available for computational analysis of energy needs based on available data requisite. Tools for energy demand forecasting specifically for Africa arguing that existing modelling tools are biased since they are developed for developed countries and extrapolated to low-income countries are discussed by Ouedraogo, [17]. Ouedraogo uses the Long-range Energy Alternatives Planning (LEAP) modelling system which is also used by Randall et al. [18] in the bottom-up demand analysis of long term electricity supply in the Southern African power pool. This modelling type is suitable for modelling energy forcast at a large scale however not suitalbe for small scale application due to its reliance on empirical data. In their study on energy supply, consumption and access dynamics in Botswana, Essah and Ofetotse [19], use questionnaire surveys combined with empirical study. They implore the end-use model as described by Alkhathami, [20] on their target group. The end use model fundamentally sources raw data from end user's by exploring data collection methods such as questionnaire surveys. The data collated is then aggregated to deduce energy demand profiles reflective of the end-users needs. End-use modelling is now a well-accepted energy forecasting approach of electricity usage and peak demands at national and utility level [21]. End-use modelling is adopted for this study based on the lack of empirical data for off-grid communities in Botswana and to ascertain accuracy in energy demand estimations. In-situ site surveys are conducted to collect first-hand data and access the behavioural patterns of end users.

III. METHODOLOGY

As described above, the load forecasting method employed in this power assessment analysis is referred to as the end-use model which is categorized as a bottom-up approach model. It estimates the energy consumed by utilizing information obtained directly from end users. This information might be in terms of consumers' use, size of houses, age of consumers, and

ISSN: 2521-2292

applications, among many others. The technique relies on statistical information from consumers accompanied by changes, which form the basis of the forecast [20]. This implies that end-use models focus mainly on the various uses of electricity in commercial, government and residential sectors. Thus, this method is based on the concept that electricity demand will always depend on the end user demand for refrigeration, cooling, lighting, etc. [22].

Mathematically the end-use model is a set of equations designed to disaggregate end-user household's prospective total annual energy consumption generally through residential energy consumption survey (RECS) [20]. RECS's were conducted during in-situ site visits and the disaggregated data sets in combination with population estimates were taken into consideration to determine the total energy consumption of end users. A questionnaire survey with a sample size of 60 was administered in Jamataka covering the various sectors within the village. Given a return rate of 83%, 50 questionnaires formed the basis for empirical study. The accuracy of this model is based on its ability to express electricity demand as a function of its various applications. However, the effectiveness of the model is extremely dependent on the quality and quantity of information sourced from end users. This method permits for integration of econometric methods such as client behavior and thus provides a realistic representation of the energy consumption. Supplementary to data gathered from prospective users, an in-situ survey characterized by interviews of strategically end users was conducted. This supplementary survey targeted the government officials, business owners and residents of different economic statuses according to the categorization made. Households were categorized into three groups; low, medium and high-income houses based on the average disposable income, size and price of a house in an area [19].

The following assumptions were considered regarding the analysis of energy demand data of Jamataka community:

- constant loads for cold appliances. Fridges are assumed to run for 5hrs per day at nominal power.
- electric water heaters (geysers) are not considered as part of the loads as the SolarFin2Go technology under investigation is equipped with a solar catcher (innovative solar-thermal collector).
- based on the dependence of residents on wood fuel for hot water supply and space heating, the lack of electric water heaters and air conditioners, electricity demand is assumed to be constant for all seasons and therefore only holidays considered for variation in electricity demand.
- the daily load demand is considered to be a worst case scenario.

A systematic set of basic mathematical functions relating various parameters to energy are used to generate and power demand requirements of clients. MS-Excel based peak load calculator was utilized to compute and reconcile all gathered electricity demand data into final load profiles. Equation (1) illustrates the formula used to compute the load estimation in this study;

$$E = \frac{IPH_dN_w}{7} \quad (1)$$

where;

E: total energy in Watt-hr

I: quantity of appliances

P: rated power of an appliance

H_d*: number of operating hours per day*

N_w*: number of operating days per week*

Thereby, the total energy consumption for all end use electricity consuming institution in Jamataka village was calculated. The procedure was applied to both AC and DC appliances and aggregated to derive the final energy consumption estimate for the community sampling only 50 residential households. The power ratings were gathered from available appliances during the conducted in-situ site surveys and from empirical data sets for estimation of appliances without power ratings and variant energy usage patterns over a day such as fridges, printers and desktop computers.

A. Site selection

Jamakata village is located in the Central District of Botswana 40 km west of Francistown. The coordinates of the village are -21.08 °N and 27.14 °E. The location of Jamataka is shown on the map below.

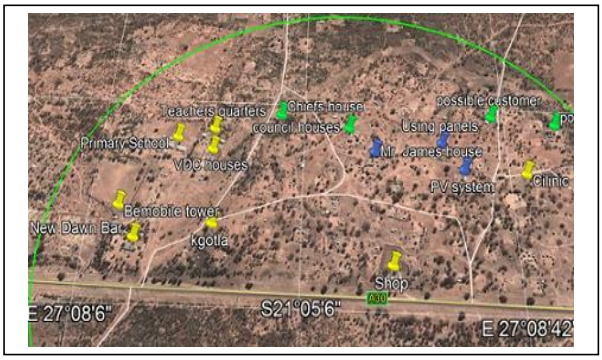


Fig. 1. Picture of Jamataka village with energy consuming institutions located [23]

According to the national statistics census conducted in 2011, the population of Jamataka was enumerated 650 inhabitants at an estimated annual expected growth rate of 1.9%

ISSN: 2521-2292

[24]. This trend in population growth has to be considered in designing the micro-grid flexible for expansion to accommodate the increasing population.

The current energy mix in the village was determined from literature and questionnaires distributed during an in-situ site survey of the village. The main source of energy is firewood which is extensively used for cooking and heating water. This has raised concern with the village leadership as it is reported that the harvesting of firewood has vastly grown as a means of gaining profit from selling it and thus has a negative environmental impact. The primary school also depends firewood purchase for the school kitchen. This is a direct result of the in-situ survey and verified by the findings of Statistics Botswana [24] which indicate that the use of wood for cooking and heating in the Central District is estimated at 71.9%

Other sources of energy include diesel for the operation generators to provide electrical energy for AC loads mainly at the school, the shopping facilities and a few high-income households. Otherwise candles are widely used for illumination whilst paraffin is the least used fuel in the entire village.

B. Solar Potential Assessment

The annual sum of direct normal irradiation (DNI) and GHI ranges around 2,000 $kWhm^{-2}a^{-1}$ (~5, 5 $kWhm^{-2}d^{-1}$). The annual daily sums of the global horizontal irradiation (GHI) in Botswana for the years 1996-2009 are within average ~ 5.6 – 6.5 $kWhm^{-2}d^{-1}$ (~2,050 – 2,400 $kWhm^{-2}a^{-1}$). The country-wide average is 6.17 $kWhm^{-2}d^{-1}$ which is (2,254 $kWhm^{-2}a^{-1}$ [3]. The solar resource map in Figure 2. shows that the geographical location of Jamataka village has the potential to yield 1889kWh of electricity per installed 1kW annually which results in an average 5.19kWhkWp^{-1}. The average GHI of Jamataka village over 10 year is shown on Figure 3.

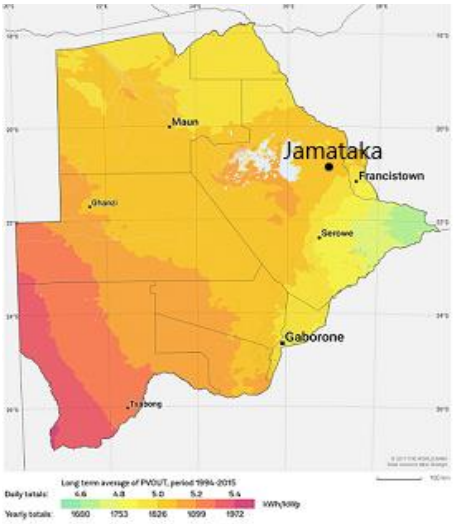


Fig. 2. Solar resource potenetial of Botswaha [25]

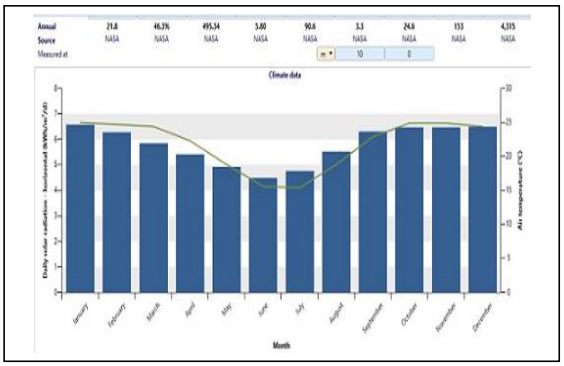


Fig. 3. The GHI of Jamataka village from 1995-2005 [26]

C. Energy Requirement Analysis

The load profile is a client's electric energy consumption pattern as a function of time. It is typically the energy demand over a period of 24hrs and regarded as the daily load curve [27]. The curve represents a composite of energy demands by the category of users in the community. The operation of loads varies with time (e.g. hourly, daily, weekly, seasonal, etc.), also depending on the users' lifestyles [28]. This data is used to determine the critical parameters in the design of the renewable energy system for both thermal and electric requirements: These include peak load and annual energy demand. In addition, six daily cycles are determined for workday, Saturday and Sunday, each for at least two typical seasons (summer and winter) including hourly averages and an annual load curve [7].

IV. RESULTS AND DISCUSSION

The result of power requirement analysis of the primary consumers in Jamataka village is shown in Table 1. The community's load profile as aggregate energy demand by the individual entities is illustrated in Figure 5. The residential sector is constituted by 50 households ranging from low, middle and high-income families and are split into a 15:10:5 ratio. The total daily residential energy demands according to the aforementioned categorization is 21kWh, 29kWh and 25kWh respectively. Altogether, residential consumers form 43% of the total daily consumption of the community which amounts to 174kWh with a peak load of 16kW and average demand of 7kW respectively. The estimates of daily energy consumption of the various groups of consumers' in village are shown in Figure 3. They were used to project the annual estimated energy consumption represented in Figure 4. The load profile depicts that energy consumption increases in the morning between 5am and 6am due to users preparing for work which reveals the significant number of government employees being analyzed. The curve further illustrates a reduction in consumption during day hours with hikes at 10am and 1pm. These hikes can be interpreted as tea and lunch breaks where e.g. teachers use electric appliances at their households. The peak load is projected for 8pm when the majority of users is predicted to be

ISSN: 2521-2292

home utilizing electricity consuming appliances such as television, lights, radio, cell phone chargers, etc. Furthermore, the ordinary residents are mainly farmers and spend their daytime in farms and communal grazing sites whilst some go to work in the city only to return in the evening. The shape depicted by the demand profile therefore reflects on the lifestyle of the residents of Jamataka.

TABLE I. TABLE OF AGGREGATE ENERGY DEMAND PER DAY, WEEK, MONTH AND YEAR FOR JAMATAKA

Facility	***Estimated Energy Demand in kWh***			
	Day	***Week***	***Month***	***Year***
School	25.90	181.33	725.32	9455.12
Staff housing	43.79	306.54	1226.18	15984.08
Clinic	9.15	64.07	256.29	3340.95
Kgotla	1.40	9.83	39.31	512.46
Bar	13.52	94.64	378.56	4934.80
High income	25.25	176.75	707.00	9216.25
Middle income	29.22	204.54	818.16	10665.30
Low income	20.70	144.90	579.60	7555.50
Kitsong centre	4.73	33.14	132.56	1728.01
Total in kWh	**174**	**1216**	**4863**	**63393**

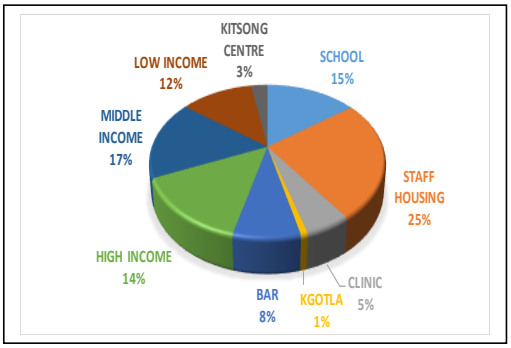


Fig. 4. Estimated relative proportion of the users and institutions to the energy demand in Jamataka village

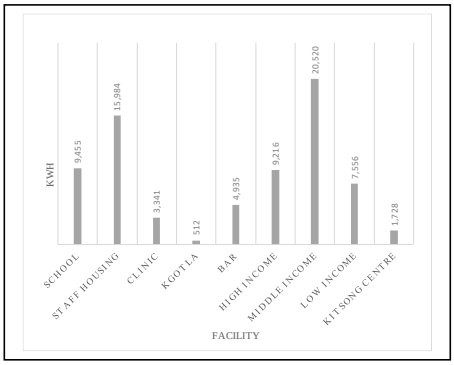


Fig. 5. Estimated annual energy demand of primary institutions in Jamataka

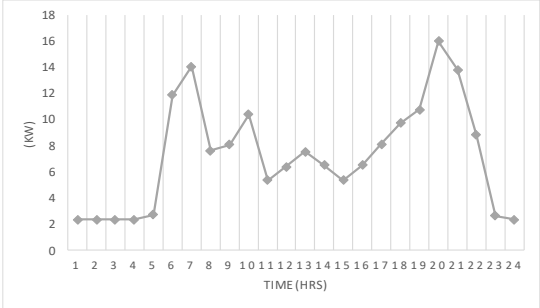


Fig. 6. Estimated daily energy demand profile of Jamataka village

V. CONLUSION

The analysis of energy requirement is essentially a critical aspect to the planning and development of renewable energy projects and associate technologies. This paper utilizes a systematic approach of analyzing disaggregated data following power requirement principles, guidelines, codes and standards. The end-use model is employed and a peak calculator used to generate a daily community load profile which is constitute of aggregated energy consumption profiles of institutions in Jamataka village. Non-numerical factors affecting energy consumption such as consumer preferences and behavior have been integrated into the model hence the load profiles generated are realistic representations of scenario of the community. The total energy demand of the community has been established to be 174kWh with a peak load, and average demand of 16kW and 7kW respectively. This energy demand accounts for all institutions together with a residential sector of a sample of 50 households which constitutes 43% of the total demand of the village. The commercial institutions represented by two shopping facilities constitute 8% of the total village consumption. The pattern expressed by the demand curve correlates with the lifestyle of the residents of Jamataka since most are day workers in government institutions who work regular 8 hours and constitute 46% of the electricity consumption.

ISSN: 2521-2292

The applicable codes and standards considered in this analysis are the International Electrotechnical Commission (IEC) relating to estimation of energy demand and consumption forecasting. Furtherance to that, they are other codes to be considered though they are not solar specific. Such codes are related to buildings and fire and are described by international bodies such as the ICC, IRC, IBC and IGCC. Local standards relating to solar are BOS 68-1:2005, BOS 13-1:2000 and BOS 13-2:2000 documented in the Botswana Bureau of Standards (BOBS).

The findings of this analysis are to be used in the expansion of the SolarFin2Go which is stand-alone technology catering for electrical and hot water supply.

VI. REFERENCES

[1] R. P. S. a. M. S. Kanase-Patil A. B., "Integrated renewable energy systems for off grid rural electrification of remote area," *Renewable Energy*, pp. 1342-1349, 2010.

[2] T. Bader, "Status of Renewable Energy in Botswana-Framework, Trends & Potential," in *Renewable Energy Conference-Decentral Power Supply in Botswana*, Germany, 2019.

[3] Economic Consulting Associates Ltd (ECA), 3E, DLR, "Renewable energy resource assessments," Department of Energy Affairs (DOE), Gaborone, 2016.

[4] Government of Botswana, "GOVERNMENT OF BOTSWANA SE4All Action Agenda," GOB, Gaborone, 2017.

[5] Vision 2016, "VISION 2036 - Achieving Prosperity for All," Lentswe La Lesedi (PTY) LTD, Gaborone, 2016.

[6] A. Z. M. S. D. M. J. M. Adrian Pugsley, "SolaFin2Go field trials in Sub-Saharan Africa: Off-grid village electrification and hot water supply," in *PV-SAT15*, Warwich, 2019.

[7] A. Wiese, "Energy demand and load analysis," in *RENEWABLE ENERGY:Lessons from the German Experience of the Energy Transition A Guide for Engineers, Policymakers and Administrators*, RENAC, Ed., Berlin, Germany, German Association of Consulting Engineers , 2019, p. 164.

[8] LEAP, "Demand Analysis," 2019. [Online]. Available: https://www.energycommunity.org/Help/index.htm#t=Demand%2FDemand.htm. [Accessed 16 May 2019].

[9] M. A. Chaaban, "Commercial Solar Electric Systems," 2018. [Online]. Available: https://www.e-education.psu.edu/ae868/node/922. [Accessed 13 May 2019].

[10] Z. M. a. R. Ramakumar, "Smart Integrated Renewable Energy Systems (SIRES): A Novel Approach for Sustainable Development," *Energies*, vol. 10, no. 8, 2017.

[11] W. Schellong, "Energy Management Systems: Energy Demand Analysis and Forecast," 1 August 2011. [Online]. Available: https://www.intechopen.com/books/energy-management-systems/energy-demand-analysis-and-forecast. [Accessed 7 May 2019].

[12] IEC, "Recommendations for small renewable energy and hybrid systems for rural electrification (Part 9-1: Micropower systems). IEC/TS 62257-9-1 standards," International Energy Council, 2008.

[13] IEC, " Recommendations for small renewable energy and hybrid systems for rural electrification (Part 2: From requirements to a range of electrification systems). IEC/TS 62257-2 standards," International Energy Council, 2004.

[14] D. O. Akinyele, "Techno-economic and life-cycle impact analysis of solar photovoltaic microgrid systems for off-grid communities," Victoria University of Wellington , Wellington, 2016.

[15] IEC, "Recommendations for small renewable energy and hybrid systems for rural electrification (Part 4: System selection and design). IEC/TS 62257-4 standards," International Energy Council, 2005.

[16] A. S. P. D. S. Srivastava A. K., "Short-Term Load Forecasting Methods: A Review," 2016.

[17] N. S. Ouedraogo, "Modelling sustainable long-term electricity supply demand in Africa," *Applied Energy*, vol. 190, pp. 1047-1067, 2017.

[18] e. a. Randall. Spalding-Fechera, "Electricity supply and demand scenarios for the Southern African power pool," *Energy Policy-Elsevier*, vol. 101, pp. 403-414, 2017.

[19] I. O. Emmanuel A. Essah, "Energy supply, consumption and access dynamics in Botswana," *Sustainable Cities and Society*, vol. 12, pp. 76-84, 2014.

[20] M. Alkhathami, "Introduction to Electric Load Forecasting Methods," *Journal of Advanced Electrical and Computer Engineering* , vol. 2, no. 1, pp. 1-12, 2015.

[21] H. Emmrich, "Demand forecasting & economic forecast development with the end use models," San Diego, 2008.

[22] G. D. Feinberg E. A., "Load Forcasting," in *Applied Mathematics for Restructured Electric Power Systems*, New York, Springer Science & Business Media, 2005, pp. 269-285.

[23] Google Maps Pro, 2016.

[24] Statistics Botswana, "Population &Housing Census Selected Indicators 2011 - Tutume Sub-district," Statistics Botswana, Gaborone, 2015.

[25] World Bank Group, "Global Solar Atlas," 2016. [Online]. Available: https//globalsolaratlas.info/downloads/botswana. [Accessed 3 May 2019].

[26] RETScreen, 2016.

[27] H. Saadat, Power system analysis, 2nd, p. 8-13 ed., McGraw-Hill, 2002.

[28] B. A. S. P. D. C. T. O. O. a. A. M. A.-M. Aderemi, "Techno-Economic Feasibility of Hybrid Solar Photovoltaic and Battery Energy Storage Power System for a Mobile Cellular Base Station in Soshanguve, South Africa," *Energies*, vol. 11, no. 1572, pp. 1-26, 2018.

BIUST Research and Innovation Symposium 2019 (RDAIS 2019)
Botswana International University of Science and Technology
Palapye, Botswana, 4 - 7 June 2019
ISSN: 2521-2292

Lamellipodial Motility of a squared shaped cell - mathematical model

Matlhogonolo Rakakae[1] and Sachin Shaw[1]
[1]Department of Mathematics and Statistical Sciences,
Botswana International University of Science and Technology, Private Bag 16, Palapye, Botswana

Abstract

Cell motility is an important biological action in the creation, operation and maintenance of our bodies. One of the best studied types of motility is the lamellipodial motility on flat, hard and sticky surface. To advance our understanding of this essential biological process, it is necessary to develop a mathematical model explaining cell motility. We have considered the turning behavior and dependence of the motile behavior on the model parameters and boundary conditions of 2D square shaped cells. The model consists of force-balance and myosin transport equations which solved numerically by using finite difference method in MATLAB after nondimensionalized the governing equations along with initial and boundary conditions. The model analysis shows that initiation of motility critically depends on four dimensionless parameter combinations which represent the myosin contractility, characteristic viscosity-adhesion length, effective velocity and local boundary velocity. By simulating numerically a minimal free-boundary model we observed that cells are stationary when contractility is weak and motile behavior of a cell is sensitive to conditions of force balance at the cell boundary.

1 INTRODUCTION

Biofluid mechanics is the study of certain class of biological problems from fluid mechanics point of view [1]. In this article we will be focussing on the shape and movements of a motile cell undergoing lamellipodial motility. Cellular motility is the spontaneous movement of a cell from one location to another by consumption of energy. It encompasses several types of motion, including swimming, crawling, gliding and swarming. It is a fundamental biological phenomenon that underlies many physiological processes in health and disease, including wound healing, embryo genesis, immune response and metastatic spread of cancer cells, to name a few [2].

Many important physiological processes during development, such as cell migration during gastrulation, axon guidance, tissue regeneration and embryological development require Cell motility to happen. Unregulated cell migration can be the cause for progression of cancer, for example during metastasis.

Cell migration can have a more sinister role which is secondary tumour growth that is caused by a cancer cellâAZs ability to migrate from a primary tumour into the lymphatic system (plays a key role in the immune system, fluid balance, and absorption of fats and fat-soluble nutrients), eventually taking up residence at an alternate location. Deficiencies in the proteins associated with cell motility during foetal development have also been implicated in diseases such as spinabifida (malformed vertebrae). Obviously, a strong understanding is needed of cell motility and the constituents, which control this process [3].

Cell motility is an important biological action in the creation, operation and maintenance of our bodies. To advance our understanding of

ISSN: 2521-2292

this essential biological process, mathematical models explaining cell motility have to be developed [4]. With accurate models it is possible to explore many permutations of the same event and concisely investigate their outcome [5].

One of the best studied types of motility is the lamellipodial motility on flat, hard and sticky surface. Lamellipodia are ribbon-like flat cellular protrusions that are formed at the boundary (outer edge) of a moving or spreading cell. Lamellipodia are enriched with a bidimensional nerve fibre array of a branched network of actin filament [4].

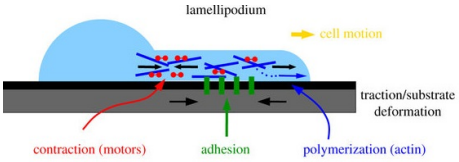


Figure 1: Illustration of the main physical mechanisms responsible for substrate-based cellular motion: actin polymerisation, substrate adhesion and contraction by molecular motors [4]

In Figure1, a thin sheet of actin filaments that stretches out to the cell's boundary, lamellipodia generate pushing forces that drive the cell forward. Micro-tubules can barely penetrate this actin network, but they direct cell motility in other ways, such as controlling cell adhesion and acting as the cell's internal compass. Adhesion exerts a powerful influence on a cell's behavior, controlling not only motility and structure but also growth and survival [6]. The following Figure 2 shows in detail how a cell moves with its lamellipodium.

Figure 2 explains the mechanisms involved in cell movement. There are three principal mechanisms that enable the keratocyte motility (keratocyte are erythrocytes with one or two projections that may form as a result of rupture of a vacuole or hole within an erythrocyte).
First, after determining its direction of motion, the cell extends a protrusion in this direction by actin polymerization at the leading edge. Secondly, it then attaches its leading edge to the surface on which it is moving and detaches at the cell body and rear. Finally, it pulls the whole cell body forward by contractile forces generated at the cell body and rear of the cell. Optimal adhesion strength for fast cell migration has been shown to depend on the level of myosin contraction [5].

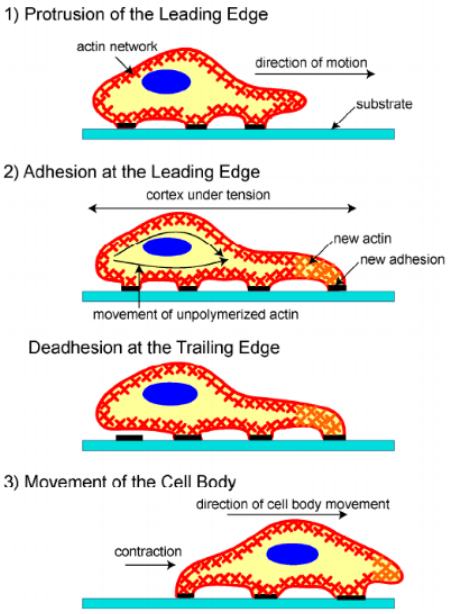


Figure 2: A schematic of the three stages of cell movement[6].

The corneal keratocytes (found on the surface of the cornea) shown in Figure 3 adopt distinct shapes dictated by adhesion onto surfaces coated with fibronectin (an extracellular matrix protein that anchors cells by binding adhesion receptors) [8]. These Keratocytes are composed of a highly elaborate polymer network, primarily actin filaments, which contract by the precise

ISSN: 2521-2292

alignment and binding of molecular motors. This type of contraction underlies the mechanical function of the cornea, but also the crawling and migration of other cells [9]. In this project we will be focused on the square shaped cell, bottom left.

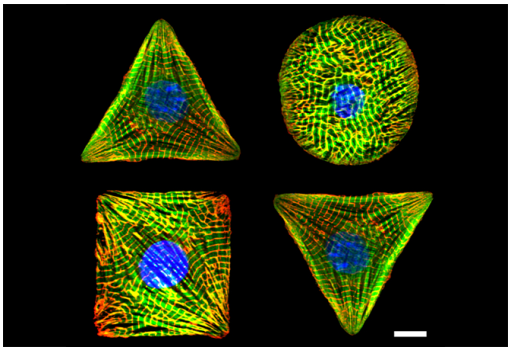


Figure 3: corneal keratocytes derived from embryonic stem cells[7]

The model in this project will predict the turning behavior and dependence of the motile behavior on the model parameters and boundary conditions of 2D rectangular shaped cells. We do this by simulating numerically a minimal free-boundary model by finding that
1) cells are stationary when contractility is weak
2) motile behavior of a cell is sensitive to conditions of force balance at the cell boundary [10].

2 MODELS AND METHODS

As stated previously Mechanics plays a dominant role in keratocyte motility. We concentrate on the second and last principal mechanism that enables keratocyte motility. The model consists of force-balance and myosin transport equations,

$$\eta \frac{\partial^2 U}{\partial X} + \sigma \frac{\partial M}{\partial X} - \xi U = 0\,, \qquad (1)$$

$$\frac{\partial M}{\partial T} = \frac{\partial}{\partial X}\left(D_{eff} \cdot \frac{\partial M}{\partial X} - U_{eff} M \right) \qquad (2)$$

For the velocity of actin flow **U**(X,t) and myosin concentration **M**(X,t) defined locally for $X \in \Psi(t)$, where $\Psi(t)$ is a moving 2D domain representing cell geometry. For the Force balance equation, equation (1);
• The first term describes the force due to passive viscous stresses in the deforming actin network where $\boldsymbol{\eta}$ is the effective actin viscosity [8]. We assume that the actin polymer mesh is compressible, so there is no incompressible condition.
• The second term describes the divergence of the myosin contractile stress. We assume the stress to be isotropic (exhibiting properties with the same values when measured along axes in all directions) and proportional to the myosin density, with $\boldsymbol{s}$ denoting the force per unit of myosin density.
• The third term describes the effective viscous drag arising from creeping movement of Filamentous actin (Factin;essential part of the cytoskeleton and build up many higher order structures in cells e.g. lamellipodia) relative to a substrate and characterized by the viscous drag coefficient $\boldsymbol{\xi}$ [10].
For the myosin transport,equation (2);
Kinetics of myosin can be interpreted in terms of transitions between two states:
• state of free myosin diffusing in the cytoplasm
• state in which myosin is bound to the actin network [11].

Clusters of the bound myosin contract the actin network and move with it. For low viscosity and slow diffusion, however, using U as an advection (movement of some material by the velocity of the fluid) velocity and constant diffusion coefficient (D) results in singular solutions, in which M and U develop Dirac-delta singularities [8]. The singular solutions are obviously unrealistic, given that myosin molecules have a finite size [12].

ISSN: 2521-2292

By introducing effective velocities which approach zero as $M \to M_{max}$ then the excluded volume effect can be taken into account [13] $\mathbf{U}_{eff} = \mathbf{U}(1 - M / M_{max,u})$.

Normally, in a free boundary problem, the actual maximum of myosin concentrations may significantly exceed the $M_{max,u.}$ This is because myosin accumulates at the rear of the cell where it is swept forward by a moving boundary and it only happens in motile solutions. This effect originates from the Rankine-Hugoniot boundary condition which describes the relationship between the states on both sides of a shock wave or a combustion wave (detonation) in a one-dimensional flow in fluids [9]. Hence, the effect of molecular crowding on myosin velocity should generally be written as;

$$\mathbf{U} = \begin{cases} \mathbf{U}(1 - M / M_{max,u}), & \text{if} \quad M < M_{max,u}, \\ 0 & \text{, Otherwise.} \end{cases}$$

As diffusion is also affected by crowding, then we have the effective diffusion which is given by $\mathbf{D}_{eff} = \mathbf{D}(1 - M/M_{max,d})$ with a value of the cut-off $M_{max,d}$ that exceeds the actual maximal densities of myosin [10].

2.1 Boundary Conditions

$$\mathbf{n}\cdot(\alpha\nabla\mathbf{u} + \beta m\mathbf{I})_{|\partial\omega(t)} = 0, \quad (3)$$

$$\mathbf{n}\cdot(-D_{eff}\nabla_x M + (\mathbf{U}_{eff} - \mathbf{V}_f)M)|_{\partial\omega(t)} = 0, \quad (4)$$

Equation (7), a diffusion-advection equation for myosin, is subject to the mass-on serving zero flux boundary equation (3), producing an additional dimensionless parameter,

$$\mu_{tot} = \int\int_{\omega(t)} m \cdot d\,|\omega|.$$

Also, for equation (8) its dimensionless boundary conditions are $\mathbf{u}|_{\partial\omega(t)} = 0$ and equation (4) Note that the varying parameter $k = KL^3D^{-1}$ is equivalent to re-scaling the actin polymerization constant. In addition, because the myosin contractility constant ß enters equation (8) with m, varying ß is similar to re-scaling μ_{tot} [10].

Cell becomes motile when myosin contractility is high [8] therefore we focus on the role played by four essential independent model parameters; v_f, μ_{tot}, α and u_{eff}.

2.2 Initial Conditions

$$u(x,0) = 0, \quad (5)$$

$$m(x,0) = (\mu_{tot}/|w|)(1 - gx), \quad (6)$$

By solving Equations (7) and (8) in domains with free boundaries steady dynamics of a motile cell were explored. Even though the force-balance equation does not involve time derivatives, the coupled system (7) and (8) constitutes an initial-value problem and one must specify initial conditions for both variables and the domain, ***m*(x,** 0), **u(x,** 0), and ***ω***(0) [10]. Initial conditions based on a stationary steady state in a rectangular geometry were used to clarify Equations (7) and (8) in domains with free boundaries.

2.3 Non-Dimensionalization

To nondimensionalize the model, we use the following set of units. The length unit L is defined as a characteristic linear size of the cell with a target area,

$$L = \sqrt{A_0/\pi}$$

Then the dimensionless variables, differential operator, and current and target cell areas are, respectively, $t = TD/L$.

$$t = TD/L, x = X/L, u = UL/D, m = M/M_0,$$

$$|\omega| = \frac{\Psi}{L^2}, a_0 = \frac{A_0}{L^2}$$

By using the above non dimensionalized parameter equation (1) and equation (2) reduces to:

$$\frac{\partial m}{\partial t} = \frac{\partial}{\partial x}\left(d_{eff}\frac{\partial m}{\partial x} - u_{eff}\,m\right), \quad (7)$$

$$0 = \alpha\frac{\partial^2 u}{\partial x^2} + \beta\frac{\partial m}{\partial x} - u, \quad (8)$$

where $u_{eff} = u(1 - m/m_{max,u})$, if $m < m_{max,u}$, and zero otherwise, and $d_{eff} = 1 -$

ISSN: 2521-2292

$m/m_{max,d}$. Equation (8) include two dimensionless parameters:

• the dimensionless viscosity-adhesion length parameter $a = n/L^2\xi$,

• the myosin contractility constant $\beta = \sigma M_0 / D\xi$.

The viscosity-adhesion parameter $\boldsymbol{a}$ is the ratio of the length scale of the mechanical action of the cell size, since the mechanical effect of localised myosin contraction spreads on the length scale $\sqrt{\eta/\xi}$ [10].

2.4 Numerical Techniques

From our equations (7) and (8) we simplify them using the finite difference method;

$$\alpha\Delta u_{n+1}^{k+1} + \beta\nabla m_n^{k+1} - u_{n+1}^{k+1} = 0,$$

(9)

$$\alpha\left(\frac{u_{j+1} - 2u_j + u_{j-1}}{(\Delta x)^2}\right) + \beta\left(\frac{m_{j+1} - m_{j-1}}{2\Delta x}\right) - \frac{1}{2}\left(u_{j+1} + u_{j-1}\right) = 0,$$

(10)

and

$$\partial_t m = \nabla\cdot(d_{eff}\nabla m - u_{eff} m) = d_{eff}\Delta m - u_{eff}\nabla m,$$

(11)

$$\frac{m_{j+1} - m_{j-1}}{2\Delta t} = d_{eff}\left(\frac{m_{j+1} - 2m_j + m_{j-1}}{(\Delta x)^2}\right) - u_{eff}\left(\frac{m_{j+1} - m_{j-1}}{2\Delta x}\right),$$

(12)

thus the following Thomas algorithm values are obtained; for equation (7) we get;

$$u_{diag} = \left(\frac{d_{eff}}{(\Delta x)^2} - \frac{u_{eff}}{\Delta x} - \frac{1}{2\Delta t}\right),$$

$$\text{diag} = \left(\frac{-2}{(\Delta x)^2}\right),$$

$$l_{diag} = \left(\frac{d_{eff}}{(\Delta x)^2} - \frac{u_{eff}}{\Delta x} + \frac{1}{2\Delta t}\right),$$

rhs = 0.

for equation (8) we get;

$$u_{diag} = \left(\frac{\alpha}{(\Delta x)^2} - \frac{1}{2}\right),$$

$$\text{diag} = \left(\frac{-2\alpha}{(\Delta x)^2}\right),$$

$$l_{diag} = \left(\frac{\alpha}{(\Delta x)^2} - \frac{1}{2}\right),$$

$$rhs = \frac{\beta}{2\Delta x}\left(m_{j+1}^k - m_{j-1}^k\right).$$

Second, the system equations (7) and (8), consists of the parabolic and linear equations, since were are dealing with a rectangular cell. The equations are coupled via the advection term of the parabolic equation and myosin dependent stress term in the linear equation, as well as through the boundary conditions at the moving boundary; also, the effective transport parameters are functions of the myosin concentration. To solve the system, we implemented a segregated solution strategy i.e (used the finite difference method in matlab), in which equations are solved one at a time and nonlinear terms are treated by fixed point iterations. One advantage of the segregated solver is that it prevents the matrix of a linearized system from becoming very large even with very fine computational grids [1]. The algorithm is illustrated below for one time step by the mathematical pseudo-code. In simple terms, Matlab was used to obtain the result.

- initial conditions
- boundary conditions
- set $m_1^{k+1} = m^k$ and $u_1^{k+1} = u^k$

for $n = 1: MaxNumIters$

- solve $\alpha\Delta u_{n+1}^{k+1} + \beta\nabla m_n^{k+1} - u_{n+1}^{k+1} = 0$ to get u_1^{k+1}
- evaluate u_{eff} and d_{eff} using $u_1^{k+1} = u^k$ and $m_1^{k+1} = m^k$.

-solve $\left(m_{n+1}^{k+1} - m^k\right)/\Delta t = \nabla\cdot\left(d_{eff}\nabla m_{n+1}^{k+1} - u_{eff} m_{n+1}^{k+1}\right)$ to get m_{n+1}^{k+1}.

ISSN: 2521-2292

-calculate absolute errors

$\| u_{n+1}^{k+1} - u_n^{k+1} \|_\infty$ and $\| m_{n+1}^{k+1} - m_n^{k+1} \|_\infty$.

- if solution converged, break the loop, else $m_n^{k+1} = m_{n+1}^{k+1}$, $u_n^{k+1} = u_{n+1}^{k+1}$ end of segregated loop.

If $n = 1 : MaxNumIters$ $m_n^{k+1} = m_{n+1}^{k+1}$, $u_n^{k+1} = u_{n+1}^{k+1}$, else iterations are stagnant.

Where MaxNumIters is the maximum allowed number of iterations. [10]

3 RESULTS AND DISCUSSION

3.1 Difference of myosin concentration and velocity with respect to varied effective velocity

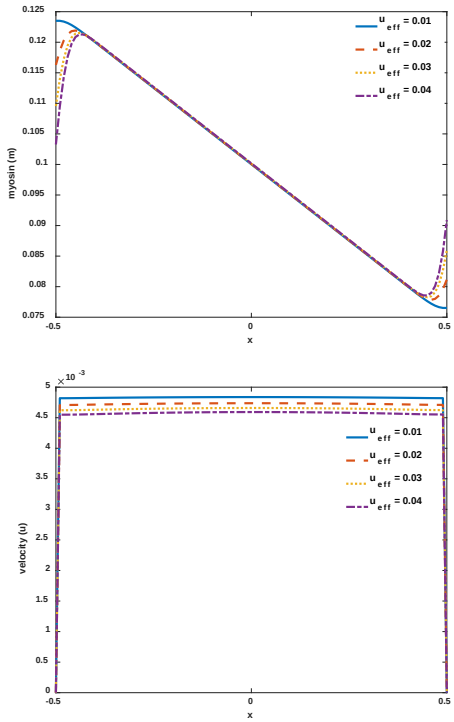


Figure 4: describes how the myosin concentration and velocity changes when the effective velocity is varied.

The myosin concentration model generally predicts significantly higher cell speeds compared to those in the velocity model (Figure 4). This is because in the myosin concentration model, the fast linear flows of cells generated by myosin at the rear boundary tend to decrease the cell area, leading to fast effective protrusion at the front [8]. As a result, as the cell area decreases with total myosin the cell speed increases. Interestingly, the cell speed in the velocity model decreases slightly as the effective velocity increases, which can be understood by noting that the cell area in this model increases with effective velocity, thus weakening the effect of myosin.

3.2 Difference of myosin concentration and velocity with respect to varied local boundary velocity

For figure 5, as the local boundary velocity is increases the myosin concentration model decreases steadily and the velocity increases as x increases. This means that as myosin relocates to the boundary, because of the zero actin velocities at the boundary. An initially small, local maximum of myosin (m) that appears at the boundary point closest the main maximum (*m*) due to slightly faster diffusion. Thus, the competition between the two maxima lowers the myosin gradients on one side of the cell, resulting in a net force acting on it in that direction [10]. Hence, resulting in the relocation of myosin. In the cell with a free boundary, the re-distribution of myosin is conferred to boundary velocity, resulting in slower outward and eventually inward movements of the part of the boundary that becomes the cell rear. The cell movement further skews the myosin towards the rear resulting in movement [10].

ISSN: 2521-2292

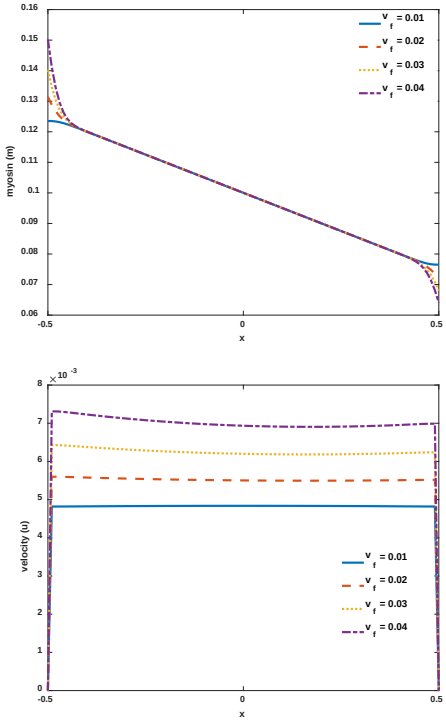


Figure 5: describes how the myosin concentration and velocity changes when the local boundary velocity is varied.

3.3 Difference of myosin concentration and velocity with respect to varied contractility parameter

As the myosin concentration and the velocity increases as shown in Figure6, the contractility also increases. That is, the contractile forces generating linear flow of myosin, are proportional to the myosin gradients which in turn, are reinforced by advection of myosin. Initiation of motility in the free-boundary models is driven by competition between the myosin contractile stress and dissipative processes (a process in which energy e.g. internal, bulk flow kinetic, or system potential, is transformed from some initial form to some final form) [10]. Motility occurs when the contractility prevails over the dissipation (a process in which energy is used or lost without accomplishing useful work) [8]. In the limit of large values of ***a***, the actin network is effectively stiff and thus does not allow for significant actin flows, thus making the cell less motile and slower. This is why the velocity goes to zero as the cell becomes less motile.

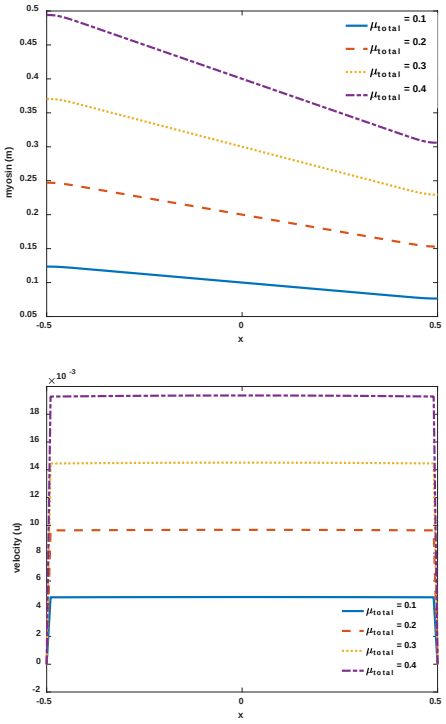


Figure 6: describes how the myosin concentration and velocity changes when the contractility parameter is varied.

3.4 Difference of myosin concentration and velocity with respect to varied cell viscosity-adhesion length

An increase in the cell viscosity-adhesion length (***a***) results in a significant in the myosin model, whereas the velocity model increases drastically. This is because for the large viscosity-adhesion length, the actin

ISSN: 2521-2292

network becomes very flexible at first and eventually becomes stiff after some time.

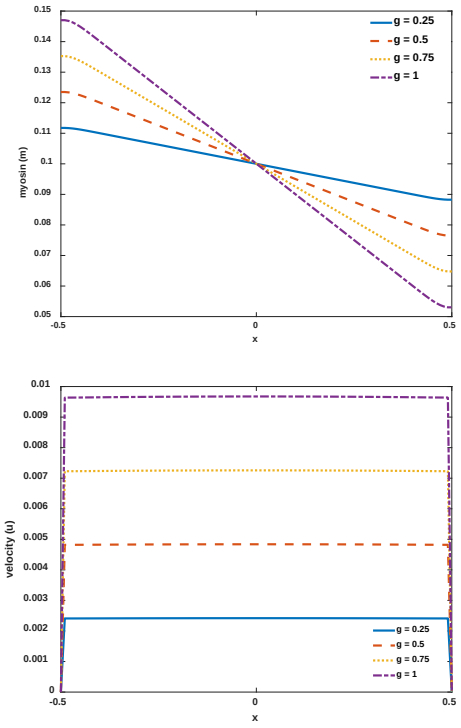


Figure 7: describes how the myosin concentration and velocity changes when the cell length is varied.

Thus, does not allow for significant actin flows, which makes the cell more symmetric and as a consequence less motile and slower, this is why the velocity model graphs approach zero eventually. So in the limit of very large values of viscosity- adhesion lengths, the cell is stationary, the same argument has been enforced by Etienne et al., [14]. In case of short viscosity-adhesion lengths, myosin forms a very small high-density aggregate, which affects the actin network only locally [10]. In this case, the steady motility is impossible and the cell starts to turn.

4 CONCLUSION

In this project, we explored the ability of a minimal actin-myosin contractility model [15] to reproduce observed mechanical states of the simplest motile cell. The model analysis has shown that the mechanical state of the cell critically depends on just four dimensionless parameters representing the myosin contractility, characteristic viscosity adhesion length, effective velocity and local boundary velocity. For the large viscosity-adhesion length, the actin network eventually becomes stiff and does not allow for significant actin flows, which makes the cell less motile and slower, and as a consequence the cell is becomes stationary. For short viscosity-adhesion lengths, steady motility is impossible, and the cell starts to turn. In conclusion, it can be said that for a cell to move straight and steadily, it has to keep the viscosity adhesion length on the order [14]. Intuitively, if myosin contractility is weak, the myosin spreads uniformly and the cell remains stationary and symmetric. The mode of motility depends on the boundary conditions [8]. For the zero actin velocity at the boundary and the sufficiently small actin growth constant and cell speed. The main finding of my study is that the contractile mechanism of motility results in a very strong turning behavior of the cell. Similarly, the model predicts that the lamellipodial area increases at lower myosin contractility, and that the cell speed increases with myosin contractility. Lastly, higher myosin contractility are predicted to promote the cell polarization and motility initiation [10]. Keratocyte motility and steady shape of the moving cell inspired a great deal of free boundary modeling in the past decade [15]. So in conclusion, mechanical force balance determines cell shape and movements.

References

[1] Jagan N. Mazumdar. Biofluid Mechanics. World Scientific Publishing

ISSN: 2521-2292

Co Pte Ltd, South Australia, 1992.
[2] Burridge K Firtel RA Ginsberg MH Borisy G Ridley AJ, Schwartz MA. Cell migration:. integrating signals from front to back, 302:1704–1709, 2003.
[3]P.E. McHugh Brendan Flaherty, J.P. McGarry. Cell biochemistry and biophysics. Mathematical models in cell motility, 49:14–28, 2007.
[4]Irina Kaverina Alissa M.Weaver Bong HwanSung, Xiaodong Zhu. Current biology, Cortactin Controls Cel l Motility and Lamellipodial Dynamics by Regulating ECM Secretion, 21:1460–1469, 2011.
[5] Alexander Mogilner Noa Ofer and Kinneret Keren. Plos biology,. Actin disassembly clock determines shape and speed of lamellipodial fragments,, 108:20394–20399, 2011.
[6] Revathi Ananthakrishnan and Allen Ehrlicher. International journal of biological sciences. The Forces Behind Cell Movement, 3(5):303–317, 2017.
[7] Yvonne S. Aratyn Kevin Kit Parker Francesco S. Pasqualini, Josue A Goss. I Heart Actin, 2009.
[8]Jacobson K Verkhovsky AB Mogilner A. Rubinstein B, Fournier MF. Biophys j. Actin-Myosin Viscoelastic Flow in the Keratocyte Lamellipod,, 101:545–553, 2011.
[9] Wazir Muhammad Ijaz Ali Peter Bastian Muhammad Sabir, Abdullah Shah. Computers and mathematics with applications. A mathematical model of tumor hypoxia targeting in cancer treatment and its numerical simulation, 74:3250–3259, 2017.
[10] Stephanie Pulford Aaron Rumack Jamie Brandon Boris M. Slepchenko Alex Mogilner Masoud Nickaeen, Igor L. Novak. Plos computational biology, A free-boundary model of a motile cell explains turning behavior,, 13, 2017,.
[11]S. Praetorius W. Marth and A. Voigt. Physica d. A mechanism for cell motility by active polar gels, 12(107), 2015.
[12]Yoshimi Takai Yoshiyuki Rikitake. International review of cell and molecular biology,. Directional cell migration regulation by small G proteins, nectinlike molecule-5 and afadin,, 287:97–143, 2011.
[13]Michal O. Nowicki E. Antonio Chiocca Avner Friedman Yangjin Kim, Sean Lawler. Journal of theoretical biology. A mathematical model for pattern formation of glioma cells outside the tumor spheroid core, 260:359–371, 2009.
[14]DÃlmosthÃlne Mitrossilis Nathalie Bufi Pauline Durand-Smet Jocelyn ÃLtienne, Jonathan Fouchard and Atef Asnacios. Pnas. Cells as liquid motors: Mechanosensitivity emerges from col-lective dynamics of actomyosin cortex, 112(9):2740–2745, 2015.
[15]Allen G.M. Theriot J.A. Mogliner A. Barnhart EL, Lee KC. Proc natl acad sci. Balance between cell-substrate adhesion and myosin contraction determines the frequency of motility initiation in fish keratocytes, 112(16):5045–5050, 2015.

BIUST Research and Innovation Symposium 2019 (RDAIS 2019)
Botswana International University of Science and Technology
Palapye, Botswana, 4 - 7 June 2019

ISSN: 2521-2292

A Smart Borehole Water Pumping System

Mpho David
Department of Electrical Computer and Telecommunications
College of Engineering and Technology
Botswana International University of Science and Technology
Palapye, Botswana
mpho.david@studentmail.biust.ac.bw

Dr Mmoloki Mangwala
Department of Electrical Computer and Telecommunication
College of Engineering and Technology
Botswana International University of Science and Technology
Palapye, Botswana
mangwalam@biust.ac.bw

Abstract—Sufficient water supply is one of the main success determining factors in livestock farming, hence a farmer should have a water borehole which can supply enough water for his animals. However, boreholes only hold a certain amount of water at their static levels and this water may not be enough for a farmer's use. Hence farmers pump water into a reservoir and wait for the borehole to recharge then pump again later. Since boreholes have limited yield, farmers may not obtain enough water for their livestock at the first instance of pumping. If water is continuously pumped until a borehole is empty (dry running), air is sucked in instead and this leads to the borehole collapsing or damaging the pumping system. To remedy this, a water pumping system is developed consisting of a microcontroller, level sensors, a liquid crystal display, piezo buzzer and a pump. The system detects water level in the borehole and reservoir and operates the pump based on the sensed levels, it also calculates the yield of the borehole in realtime.

Index Terms—Water pumping system; ultrasonic sensor; borehole yield

1 Introduction

Ideally a borehole should hold sufficient water for all livestock availed to a farmer; however, a borehole may have a certain amount of water at its static level and this water may not be enough for the farmer's use. Hence the farmer may have to pump the water out into a reservoir and wait for the borehole to recharge several time before he/she could reach enough water volume for usage. The reason is that a borehole has a limited yield hence a farmer may not obtain enough water for his livestock at the first instance of pumping. If a farmer continuously attempts to pump out water when the borehole is empty, he ends up sucking up air which leads to the borehole collapsing. This then makes it necessary to have a smart borehole water pumping system. In the last couple of decades, a lot of monitoring systems have been developed and accepted[1][2]. An automated system is a system that can turn a device on and off without human intervention. Unfortunately, these systems focused largely on monitoring the catchment tank water level and stopping the feeder pump once the maximum water level has been reached in the tank[3]. This results to a system which is not optimal, thus energy would be lost pumping an empty borehole and also resulting in damage to the borehole walls. A controlling system should take all aspects into consideration and should provide indications or audio-visual alarms at desired water levels. To optimize the system, proper monitoring is needed with distribution linked to sensing and automation. As such, automatic control of pumps based on the user's requirements should be included in water management systems[3]. The most ideal and cost effective way to automate these systems is to use microcontrollers for water level sensing, monitoring and controlling.

The goal of this paper is to present the design and simulation of a smart borehole water pumping system. This system controls the water pump that pumps water from a borehole to a reservoir. A microcontroller is used to determine the water levels in the borehole and reservoir and compares them to the set thresholds. The pump is switched on if there is insufficient water in the reservoir and sufficient water in the borehole. The system then calculates the yield of the borehole. Once the borehole has insufficient water, or when the reservoir is full, then the water pump will not be switched on. This system attempts to find a simple solution to a complex system. The organization of this paper is as follows. Chapter two discusses works related to the proposed systems. In chapter three we describe the materials used to construct this system along with the methods used in designing the system. The results and discussions follow in chapter four. Chapter five concludes this paper.

ISSN: 2521-2292

1.1 Related Works

There are several pumping systems that have been developed over the years. Knights energy designed a water pumping system that extracts water from lakes, boreholes and rivers based on a photovoltaic solar system which they used to extract the water [4]. Similar systems to the one developed by Knight Energy were developed by [5][6]. Their system differs from the system in question in the sense that they are only concerned with extracting water from underground without taking into consideration the level of the water underground and the level of the water in their catchment tanks. If the catchment tank is full the system does not know this and will keep pumping water which will in-turn spill over thus leading to water wastage.With the technological advances of mobile devices as a motivation Khaled Reza el al [3],based on the electrical conductivity of water proposed a water level monitoring and sensing system based on microcontrollers in a wireless and wired situation. The research result was a flexible, economical and easy configurable system designed on a low cost PIC16F84A microcontroller and finally, proposed a web and cellular based monitoring service protocol to determine and senses water level globally. However, this system only focused on the catchment tank and not the source of the water. Using moisture content in the soil [7][8][9], developed an irrigation water pumping system. Ejiofor Virginia Ebere and company[10] designed a system in which they were monitoring water being pumped into an over-head tank and switching off the pump once the over-head tank was full. They achieved this by embedding control system into an automatic water pump, they also used DC power instead of AC power to reduce the risk of electrocution. Ejiofor Virginia Ebere's system varies from the system being presented in this paper as it does not take into account the source of the water. Several automated water pumping systems driven by embedded microcontrollers have been developed [11][12][13], but, all these systems do not consider the source(wells,boreholes,rivers,lakes) into consideration, they only focus on the catchment tank and its capacity. These systems also do not consider the yield of their respective sources.

1.2 Materials and methods

1.2.1 smart borehole water pumping system

The smart borehole water pumping system consists of four subsystems all linked to the microcontroller. The microcontroller determines whether to turn on the pump based on the information provided by the sensors and preprogramed information. Additionally, yield of the borehole is calculated in the microcontroller. System status is displayed to the farmer via an LCD display, the microcontroller controls what is displayed to the farmer. More to this, the borehole water pumping system consists of the pump which pumps water from the borehole into the reservoir. A motor operated by a microcontroller will control the pump. Furthermore, the sensing system consists of sensors in the reservoir and borehole. These sensors obtain the levels of water in the borehole as well as reservoir and sends their readings to the microcontroller for further processing. An example of a use case is if water is being pumped into the reservoir and either the borehole runs out of water or the reservoir reaches maximum capacity, the farmer needs to be alerted to any of these changes so as to take appropriate actions to remedy the situation, and this is achieved through the use of a piezo buzzer which makes up the warning system. An LCD screen is used to display information to the farmer. figure 1.2.1 depicts the subsystems of the system. The system consists of a PIC18F2550 microcontroller, 16x2 LCD display, two ultrasonic sensors, a simple dc motor, a piezo buzzer, two transistors, three variable resistors and three resistors. The materials used for this system are shown in Table 1 below.

Name of component	Description
PIC18f2550	microcontroller
ultrasonic sensor	Hc-sr04 ultrasonic sensor *2
buzzer	piezo buzzer
motor	12v simple dc motor
LCD display	LM016L 16*2 LCD display
Transistors	2N3903 NPN transistor *2
variable resistor	1kΩ*3
Resistor	1kΩ*3

TABLE 1
Material list

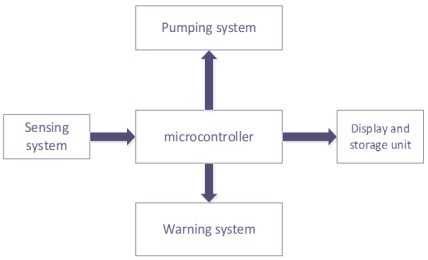


Fig. 1. system block diagram

There are two sensors in the reservoir and the borehole, these sensors obtain water levels in both the borehole and reservoir and sends their readings to the microcontroller for processing. Once data is received, the microcontroller compares the reservoir water level with the preprogramed maximum level to determine if the reservoir should be replenished. Furthermore the microcontroller also compares the borehole water level with the preprogramed minimum level. If water in the borehole is above the minimum required level, then the pump is turned on and the reservoir is replenished. Once the pump is turned on the borehole water level is stored. During the pumping process, the system keeps checking the borehole water level to ensure that the minimum set level is not exceeded. Once the minimum level is reached, the system automatically shuts down the pump. The system also keeps checking if the maximum level of the reservoir is not reached, once reached the system automatically shuts down the pump. When the pump is switched off the buzzer sounds to inform the farmer that the pump is no longer on. Once the pump is switched off

ISSN: 2521-2292

the current water level in the borehole is stored. Borehole level is stored after a predetermined time, this time allows the borehole to recharge its power source. The yield of the borehole is then calculated using the following formula obtained from[14]

$$k = \frac{2.303 \cdot A}{T} \cdot log_10\frac{H1}{H2}$$

- K is specific yield of a well in m3/hr
- A is the surface area of the borehole in m2.
- T is the time taken by the water to rise from H1 to H2
- H1 is the difference in water levels from the beginning of pumping and stopping.
- H2 is the difference of maximum water and current water level after a certain amount of time

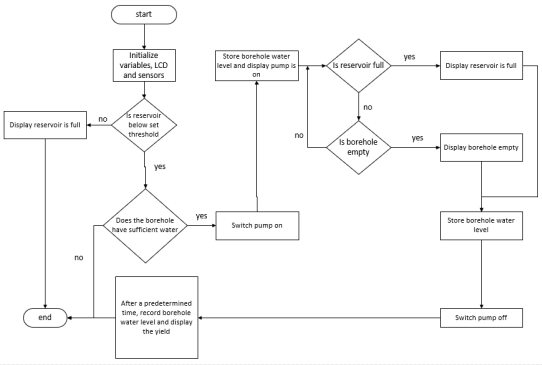


Fig. 2. system flow chart

The schematic of the system is shown in figure 1.2.1 below. The reservoir sensor has a maximum range of 800cm. Reservoirs are around 4m in height so 1cm is equated to be 0.005m meaning that 800cm is now 4m. This sensor is placed at the top of the reservoir. The reservoir is full at 3.8m that is to say a threshold of 40cm is set for the reservoir. If 40cm or anything less than that is sensed by the sensor then the reservoir is full. If the distance sensed exceeds the 40cm threshold, or the reservoir has less than 3.8m amount of water, then the reservoir can be replenished. The sensor placed on the borehole has a range of 500cm. Here 1cm is equated to 0.01m. Since our objective is to ensure that the borehole does not collapse in on its self-due to pumping when there is insufficient water in the borehole, the borehole should always have a minimum of 2m worth of water. If the distance sensed is 300cm or greater, then the system should not pump water into the reservoir. If water was already being pumped into the reservoir before the water reached the 300cm level or 2m capacity, then the system should stop pumping water into the reservoir. Initially, the water level in the reservoir is sensed and the distance sensed is fed into the microcontroller. If the pre-defined conditions set for the reservoir are satisfied then the water level in the borehole is sensed and the distanced fed into the microcontroller. If the pre-conditions set for the borehole are satisfied then the microcontroller switches on the motor which is in turn used to drive the pump and the reservoir is replenished from the borehole. The water levels in both the reservoir and the borehole are closely monitored to ensure that the conditions associated with either of them is not violated. When either the reservoir is full or the borehole level falls below the acceptable level, then the pump is turned off and the buzzer sounds to alert the farmer that water is no longer being pumped into the reservoir. The yield of the borehole is then calculated

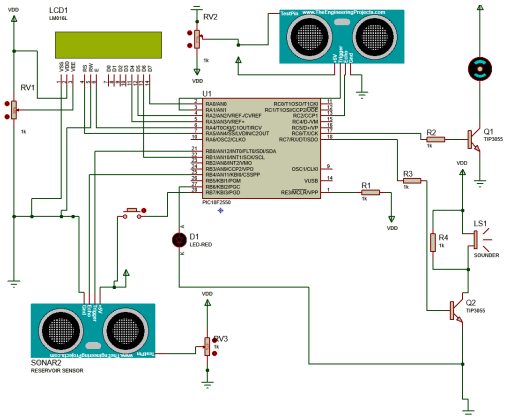


Fig. 3. circuit diagram of a smart borehole water pumping system

1.2.2 Pumping system

Dc motors cannot be driven from a microcontroller directly as a motor requires high current and high voltages that cannot be provided by a microcontroller. Pic18f2550 operates at 3.3V-5V and its input/output pins can provide 25mA of current which is not enough to drive the motor of the pump. Simple dc motors requires 12V and a minimum of 250mA current. Power supply independent from the microcontroller will be used to power the motor. A transistor will be used to act as a switch to provide power to the motor, the transistor will be controlled by the microcontroller.An NPN transistor will be used as a switch to control the motor.

Current flowing from the collector to the emitter is controlled by the current being pumped into through the base. A small amount of current through the base can control a large current flowing from the collector to the emitter. There is a voltage drop of 0.7V between the base and the emitter, meaning the transistor requires a minimum of 0.7V for it to run. The motor will be provided with a 12V power supply. The current flowing through the transistor should be greater than the minimum current needed to drive the motor. That is the collector current should be greater than 250mA.Since the transistor has a gain ratio of 1:100 the minimum current required from the base of the transistor is 2.5mA. the pic microcontroller can provide up

ISSN: 2521-2292

to 25mA of current.

$$I_B = \frac{V_B - V_{BE}}{R_1}$$

$$R_1 = \frac{V_B - V_{BE}}{I_B}$$

$$R_1 = \frac{5 - 0.7}{0.0025} = 1.72K\Omega$$

The base resistor should be less than 1.72KΩ. If a resistor greater than 1.72K is used then insufficient current will flow through the transistor and the motor will not operate.

1.2.3 Warning system

A buzzer is used to alert the farmer to any unexpected change in the system initiated by the system itself. When the reservoir is being replenished and water in the reservoir falls beneath the set threshold or the reservoir reaches maximum capacity, the pump is turned off and the buzzer sounds to alert the farmer to the change. The transistor operates as in the explanation given in the pumping system above.

As already calculated in the pumping system resistor R1 needs to be less than 1.72KΩ. since the buzzer has magnetic properties when the buzzer is disconnected; the magnetic field collapses and this causes a voltage spike which could damage the transistor. To avoid this, we include a resistor to discharge its capacitance. A 1kΩ resistor is used to protect the transistor.

1.2.4 Sensing system

Ultrasonic sensor will be used to obtain water level in both the borehole and the reservoir. The sensor requires 5V power supply to operate, this module includes ultrasonic transmitter which transmits high frequency sound pulses which travel at the speed of sound until they reach their target. An ultrasonic receiver which waits for the transmitted pulses and receives them as an echo signal. A control circuit which computes the distance based on the time difference between emitting the signal and receiving the echo.

Using I/O trigger for at least 10us high level signal(5V), the sensor sends bursts of 40KHZ this is to determine if there is an obstacle in front. If an obstacle is detected the bursts are reflected back. Echo goes high once the bursts are transmitted from the sensor and goes low once the signal is received back. Since the signal takes time to reach the obstacle and takes the same amount of time to return to the sensor, the distance has to be divided by 2 to obtain time taken to reach the obstacle. To calculate the time, we have to consider the medium in which the bursts travel, which is air. The speed of Air is 34000cm/sec. thus distance becomes

$$d = \frac{34000 \cdot time}{2}$$

To obtain the time it takes for the signal to return to the sensor we need to be able to tell how long the echo was high and this is achieved through the use of a timer specifically the timer1 module. Timer1 module includes two 8-bit registers TMR1H and TMR1L which are readable and writeable and increment from 0000H to FFFFH. These registers will be used to determine the duration of the signal. An internal clock (Fosc/4) is used with a prescaler of 2 that divides the internal clock. An oscillating frequency of 8MHZ is employed.

$$Time = TMR1H : TMR1L \cdot \frac{1}{InternalClock} \cdot Prescaler$$

$$Internalclock = \frac{fosc}{4} = \frac{8}{4} = 2MHZ$$

$$Time = TMR1H : TMR1L \cdot \frac{2}{2000000}$$

$$Time = TMR1H : TMR1L \cdot \frac{1}{1000000}$$

SINCE

$$d = \frac{34000 \cdot time}{2}$$

Then

$$d = \frac{TMR1H : TMR1L}{58.82cm}$$

1.2.5 Display

Once the sensors obtain the water level in both the borehole and the reservoir the farmer has to be notified the values sensed by both sensors and also has to be informed of the status of the pump, this is achieved by the use of a liquid crystal display (lcd) screen to display all information the farmer needs to know. The lcd is connected to the microcontroller and the displays read-write pin has to be grounded as information will be displayed on the lcd and nothing will be read from the lcd.

2 Results and Discussion

Testing was carried out using proteus-8 simulation software after designing the smart borehole water pumping system. Initially the system checks the water level in the reservoir to determine if the reservoir is at maximum capacity or if the reservoir needs to be replenished. Remember a threshold of 3.8m is set for the reservoir,so if the capacity of the reservoir is below 3.8m then the reservoir is believed to have insufficient water and can be replenished. if the capacity of the reservoir is greater than 3.8m then the reservoir is full and cannot be replenished. Figure 4 shows the results obtained after the system checked capacity of the reservoir.

ISSN: 2521-2292

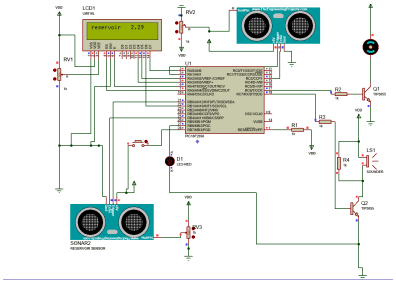


Fig. 4. detected reservoir water level

Since the reservoir is not at maximum capacity it can be replenished but the amount of water in the borehole needs to be checked to ensure that it contains sufficient water. Figure 5 shows the results after the capacity of the borehole was checked. The borehole is assumed to have

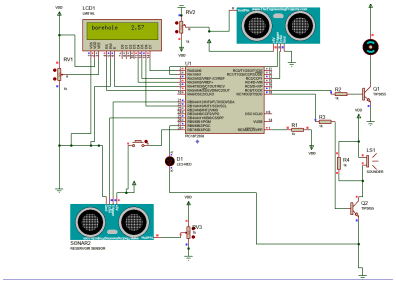


Fig. 5. detected borehole water level

insufficient water if its below 2m capacity. The borehole has sufficient water so the reservoir can be replenished. The pump is turned on and this is depicted by the turning of the motor, the status of the pump is then displayed on the lcd as shown in figure 6. While water is being pumped into the

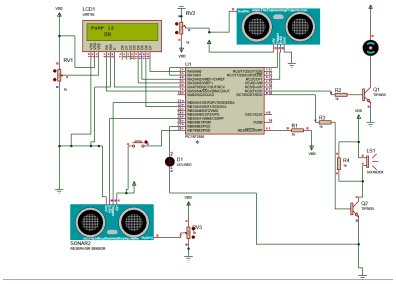


Fig. 6. pump status

reservoir the water levels in both the reservoir and borehole are periodically checked to ensure that their thresholds are not reached. Once either threshold is reached the pump is switched off and its status displayed on the lcd screen. Along with the status of either the reservoir or the borehole, which ever one reached its threshold as displayed on figure 7 and 8 respectively.

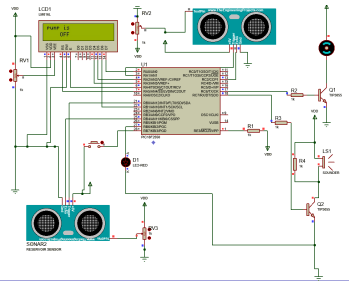


Fig. 7. pump status

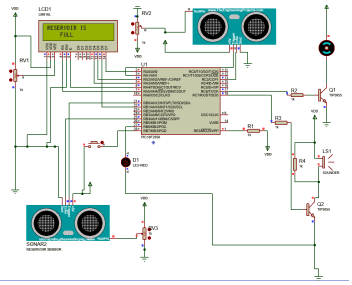


Fig. 8. results of either borehole or reservoir depending on which threshold was reached

After a determined time, the water level in the borehole is detected. This time allows the borehole to recharge itself and the depression heads are calculated as depicted by figure 9 and 10 respectively. The calculated depression heads are then used to compute the yield of the borehole which is displayed on the lcd screen.

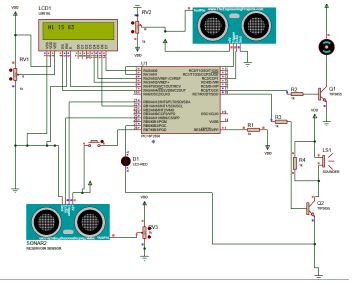


Fig. 9. first depression head

3 Conclusion

This paper presents the design and simulation of a smart borehole water pumping system. Ultrasonic sensors were

ISSN: 2521-2292

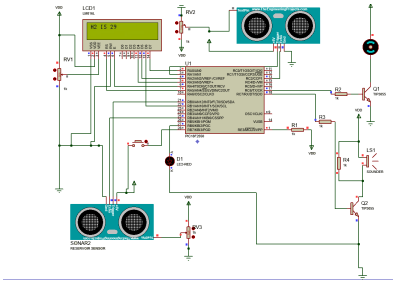


Fig. 10. second depression head

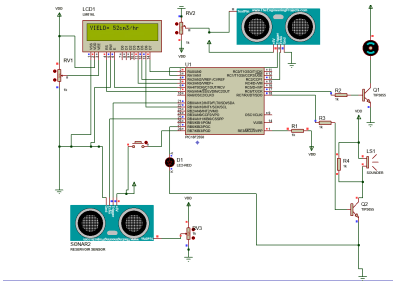


Fig. 11. the calculated yield

used to determine the capacity of the borehole and reservoir. A PIC18F2550 microcontroller was used for processing and controlling the entire system. The system is helpful to farmers as it prevents the farmer from pumping water from the borehole when it is at low levels hence prevents boreholes collapsing in on themselves. Knowing the yield of the borehole throughout the year, farmers are in a better position to find alternative ways to water their livestock around those times when the borehole has poor yields. The system automatically shuts down when the reservoir is at capacity, therefore limiting human interaction. This system was designed and simulated in Proteus simulation software and coded using Mikroc for pic of which is a C compiler for Microchip microcontrollers.In future the system could be equipped with a GSM module so that it can send the daily yield to the farmer's phone for a more detailed record. The system could use a wifi module, more specifically an ESP8266 module and store its daily yields in a cloud account. This will allow the farmer to visit this data at their own convenience and act accordingly based on these records. The system could be interfaced with a dial pad so that the farmer could obtain either the borehole water level and reservoir water level or obtain the previously calculated yield all from the press of a button.

References

[1] Q. Bin, W. Longshuang, Z. Wenliang, Z. Huiting, and W. Xin, "Design and Implement of Real-time Monitoring System of Urban Water Supply," in *2013 Third International Conference on Intelligent System Design and Engineering Applications*, Jan. 2013, pp. 536–539.

[2] Department of Electrical and Electronics Engineering, AmbroseAlli University, P.M.B 14, Ekpoma, Edo State, Nigeria., E. J. Band, and A. F. I, "Design of an Automatic Water Level Controller Using Mercury Float Switch," *IOSR Journal of Electronics and Communication Engineering*, vol. 9, no. 2, pp. 16–21, 2014. [Online]. Available: http://www.iosrjournals.org/iosr-jece/papers/Vol9-Issue2/Version-2/C09221621.pdf

[3] S. A. M. T. S. M. R. S. M. K. Reza, *Microcontroller Based Automated Water Level Sensing and Controlling: Design and Implementation Issue*, 2010.

[4] M. Dean, *Solar Power Water Pumping System | Knights Energy*. [Online]. Available: http://knightsenergy.co.ke/solar-water-pumping-system/

[5] *Solar Water Pumps - Submersible Borehole & Well Pumping Systems - UK*, 2017. [Online]. Available: http://www.solar-wind.co.uk/solar-water-pumps-borehole-well-pumping-irrigation.html

[6] M. Bansal, T. Bhatia, S. Srivastava, S. Gupta, and T. Goyal, "Automatic Solar Powered Water Pumping Using Zigbee Technology," vol. 4, no. 4, pp. 812–816, 2014. [Online]. Available: http://citeseerx.ist.psu.edu/viewdoc/download?doi=10.1.1.636.5748rep=rep1type=pdf

[7] K. Bhole and D. Chaudhari, "Soil Moisture Sensor Base Automatic Irrigation System Powered By Solar Energy," pp. 437–442, 2016.

[8] M. R. R. MR. PRATHAP NAIK T, MR. SHOBITH SR, "SOLAR POWERED AUTOMATED WATER PUMP PROJECT," pp. 5–6, 1986.

[9] S. Pathan, P. Kumar, S. Tendolkar, V. Patil, S. Lucas, and A. Daithankar, "Automatic control of a pump system for water level using Microcontroller and LabVIEW TM," *International Research Journal of Engineering and Technology*, pp. 2395–56, 2016. [Online]. Available: https://www.irjet.net/archives/V3/i5/IRJET-V3I5553.pdf

[10] E. V. Ebere and O. O. Francisca, "Microcontroller based Automatic Water level Control System," *International Journal of Innovative Research in Computer and Communication Engineering*, vol. 1, no. 6, pp. 1390–1396, 2013.

[11] H. Yelgudkar, S. Waghmare, and P. Parmar, "Design and Implementation of Microcontroller Based Self- Switching Control and Protection System for Twin Pumps," vol. 6, no. 7, pp. 34–37, 2016.

[12] J. Okhaifoh, C. Igbinoba, and K. Eriaganoma, "Microcontroller Based Automatic Control for Water Pumping Machine With Water Level Indicators Using Ultrasonic Sensor," *Nigerian Journal of Technology*, vol. 35, no. 3, p. 579, 2016. [Online]. Available: http://www.ajol.info/index.php/njt/article/view/140655

[13] O. O. Bamigboye, F. O. Ehiagwina, E. O. Seluwa, and K. O. Gbadamosi, "Development of microcontroller based water pump controller," *8th International Conference of School of Engineering and Environmental*, no. July, 2016.

[14] N. N. Basak, "Environmental Engineering," in *Environmental Engineering*, first edit ed. Tata McGraw-Hill, 2003, pp. 30–35. [Online]. Available: https://books.google.co.bw/books?hl=enlr=id=yq$_P$lo8v0KUCoi$=fndpg=PA1dq=environmental+engineeringby+N.N+Basakots=OVgK$_1$p9XQsig=sSy6-UZf0lp51BqDC-4moWaAp5wredir$_e$sc$=yv=onepageq=environmentalengineeringbyN.NBasakf=false$

BIUST Research and Innovation Symposium 2019 (RDAIS 2019)
Botswana International University of Science and Technology
Palapye, Botswana, 4 - 7 June 2019

ISSN: 2521-2292

Regulated Photovoltaic Panel with Maximum Power Point Tracking for Remote Area Electrification

Gosatla K. Ramontsho
UG Scholar, ECT
BIUST
Botswana

Kennedy Motswedi
UG Scholar, ECT
BIUST
Botswana

Otsile J. Mabutho
UG Scholar, ECT
BIUST
Botswana

Samikannu Ravi
Faculty of ECT
BIUST
Botswana

Abstract— **Solar PV system has an important place in the context of rural electrification where extension of distribution grid is not economically viable due to low population and low levels of income. The proposed system enables off grid electrification by using photovoltaic panel to satisfy electrical needs of people in rural areas. This project consists of a boost converter connected to the output of a solar panel. The output of the low power-rating converter is connected to a battery. MPPT is implemented between the boost converter and the solar panel at all times then feed the converter. The report proposes a P&Q algorithm based analogue MPPT controller, which uses low complexity circuit components to realize memory elements and does not require any signal multiplier for power calculation. The algorithm performs iteration until maximum power point is reached on the panel. Modelling and controlling of the PV connected converters are presented in this report. The simulation and research validate the operation of the system under real life input and loading conditions. The simulation is tested with PV modules. The PV system converts sunlight directly into ac voltage and stepped up to 240 volts to supply local loads in the rural area. The system is cost effective, reliable and user friendly.**

Keywords— Electrification, Maximum Power Point Tracking (MPPT), Perturb & Observe, DC-DC Boost Converter, Simulink, Photovoltaic.

I. INTRODUCTION

Energy is a driving force to foster economic, social and health condition. Renewable energy will be used to achieve this objective and it would be used in a decentralized manner where conventional grid connectivity is not possible. Botswana's rural electrification currently stands at 80 percent and the Government of Botswana aims to electrify the remaining 20 percent by 2020, this was revealed by Minister of Energy in 2012. Most remote areas, which have not yet been electrified, have some common characteristics such as [1].

- Being located in areas with difficult terrain such as hills, forests, deserts and islands.
- Being part of a protected forest area could isolate the village and prevent live conductors from being drawn through it.
- Being located far from the nearest existing grid
- Very low population and low number of households
- Low power demand, probably even in the near future, as the loads are mostly lighting
- Minimal transport and communication facilities
- Low income level and low affordability
- Poor literacy levels and technical skills



Fig.1. View of Remote Area

Currently there are 70+ proposed village electrification and network extension for 2018/19 and it will take time for electricity to be evenly distributed in Botswana. The proposition to light the remaining 20 percent of rural areas does not include remote areas due to the above mentioned characteristics. This gives a clear indication that isolated remote areas are not taken into consideration because high cost will be involved and there is a need for urgent solution for an alternative source of energy to meet the needs of modern day.

There is a significant solar potential because Botswana is a semi-arid climate which is the best weather for condition for optimal solar energy. On-site generation/distributed generation (DG) based on renewable sources would be an economic option to enable faster electrification of villages as compared to extension of a central grid [2]. Advantages of distributed generation-based rural electrification include energy loss reduction, reliability of supply, and reduction of indoor pollution arising from use of conventional fuel (wood or kerosene) for lighting [3].

ISSN: 2521-2292

The conversion of sunlight energy to electricity is relatively low and this leads to an inefficient solar system. This is caused by dynamic of irradiance and temperature. Therefore, a Maximum Power Point Tracking (MPPT) algorithm is used for efficient conversion of solar energy. The main problem solved by the MPPT algorithms is to automatically find the panel operating voltage that allows maximum power output. The popular MPPT algorithms techniques are Perturb and Observe (hill climbing method), Incremental Conductance method and Constant Voltage Method.

II. Literature Review

To gain a greater level of knowledge about the subject of solar power applications and MPPT, a major research making took place. Reading journals and websites provided a greater insight into the purpose of the project and answered many questions which arose on first glance of this project. The journals and papers which were chosen to review were obtained from the ecademia.edu website. The literature review gave a clear theoretical framework about the subject in which this project is based.

The concept of solar photovoltaics' electrification has been the cause for major discussion since its inception in the early 1800's [4]. Today the photovoltaic principle has evolved into a global leader for the provision of clean energy. To briefly describe a PV system, one can say that such a system converts light energy quanta in the form of photons into usable electricity by means of the Photoelectric Effect [4]. PV systems have evolved at a tremendous rate up until today with a continuous increase in efficiency and a systematic reduction in cost. Modern PV modules are built according to power and/or voltage specification by using a specific amount of basis-unit PV cells. These individual cells have characteristics coherent with the type of material it consists of [5].

Photovoltaic solar system gives an alternative way in which people can enjoy electricity they cannot get from the national grid due to the distance available and prices involved in it. Studies shows that solar electricity is important in bringing about development in the disregarded areas particularly the rural areas. It plays a more substantial role in supporting the use of electric light for evening studies, electrical appliances usage such as TVs, radios, and cellular phone charging, and most of all it supports income generating activities.

Photovoltaics (PV) system converts sunlight directly to produce DC output by means of PV cells. One of the best solar manufacturers in 2019 were ranked based on the efficiency of the solar panel as stated below [6];

- SunPower (22.2 %)
- LG (21.1 %)
- Solartech Universal (20.2 %)
- Silfab (20.0 %)

Solaria (19.4 %)

Studies shows that the majority of the solar panel range from 15% to 25% efficiency rating. The conversion of sunlight to electricity is low and researchers shows that a Maximum Power Point Tracking algorithm is necessary to increase the efficiency of the solar panel and boost converter is also used to stabilize the DC output.

To allow the PV system to produce the maximum possible power, many maximum power tracking techniques and algorithms have been developed. MPPT method ensures that maximum voltage and maximum current is reached as much as possible to make maximum utilization of PV modules and minimize the power with reference to environmental conditions [7]. The different types of MPPT algorithm include Perturb and Observe (hill climbing method), Incremental conductance, Fractional Short Circuit Current, Fractional Open Circuit Voltage, Fuzzy Control, Neural Network Control [8].

In this paper, Perturb and Observe algorithm is implemented. The algorithm is carried out by observing the array output power and determining the next action either to increase or decrease the array operating voltage. Iterations are carried out on the array until maximum power point is located. A DC-DC boost converter is introduced in the system. This converter is also useful for PV maximum power tracking purposes where the objective is to draw maximum possible power from the solar panels at all times and all conditions irrespective of the load. An inverter is another component of importance in any independent solar panel and battery power back-up system that requires AC power. Inverters are electronic devices that serve the purpose of changing direct current to alternating current to run electrical appliances. This system is thus feasible and will benefit people in rural in terms of convenience and cost.

III. Proposed System

This project is about electrification of remote areas to improve the socio-economic positons of rural people. The conversion of sunlight energy to electricity is relatively low and this lead to an inefficient solar system. This is caused by dynamic of irradiance and temperature. This main problem solved by the MPPT algorithms is to automatically find the panel operating voltage that allows maximum power output. Therefore, a proposed idea is to build a system using Maximum Power Point Tracking algorithm namely, Perturb and Observe method for efficient conversion of solar energy. The following Fig.2 shows a proposed MPPT system block diagram which consists of the solar panel, microcontroller, DC-DC converter and DC output. The Fig.3 shows block diagram of the proposed distribution of DC supply.

ISSN: 2521-2292

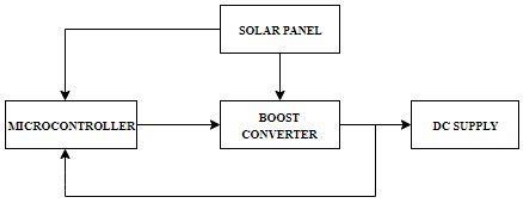


Fig.2. MPPT System Block Diagram

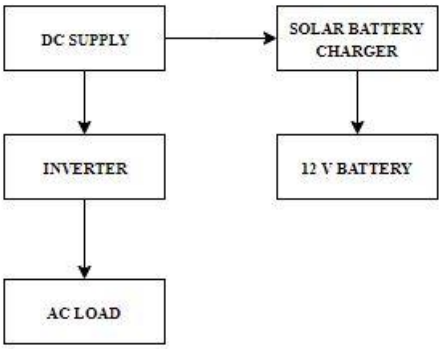


Fig.3. Distribution of DC Block Diagram

The solar panel produces a DC output, which is connected to the boost converter to charge the storage battery at a constant voltage and to power the inverter. The solar and the battery provide power supply to the inverter to be stepped up from D.C source to AC source. The solar also charges the battery during the day for night use. DC-DC boost converter is used to boost voltage.

A square pulse signal from the microcontroller is act as an oscillator to drive the boost converter by switching a transistor in an ON and OFF mode continuously at an operating frequency of 10 kHz. A PIC16F876A is used to work a PMW controller of the system, which takes analogue input as voltage and current from the photovoltaic module and changes its module according to the input.

A 2N222 NPN Transistor is driven by a square pulse of 10 kHz from the microcontroller for switching the transistor ON and OF continuously. It gives an output voltage magnitude that greater than the input voltage magnitude. The duty cycle is customized through feedback path B which receives the input from the battery. The duty cycle of the generated pulse from the microcontroller is customized such that the off-grid home solar powered battery system extracts maximum power from the photovoltaic panel to the battery or to the load. The Fig.4 shows the proposed MPPT circuit diagram. The Fig.5 shows the DC supply distribution circuit diagram.

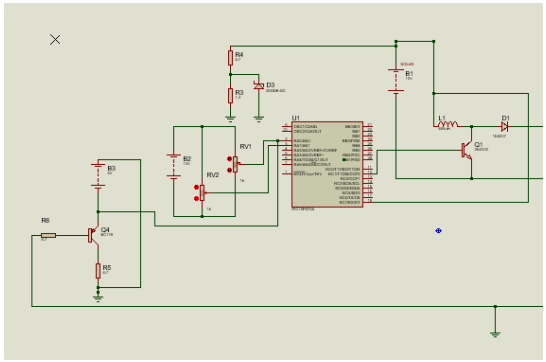


Fig.4. MPPT System Circuit Diagram

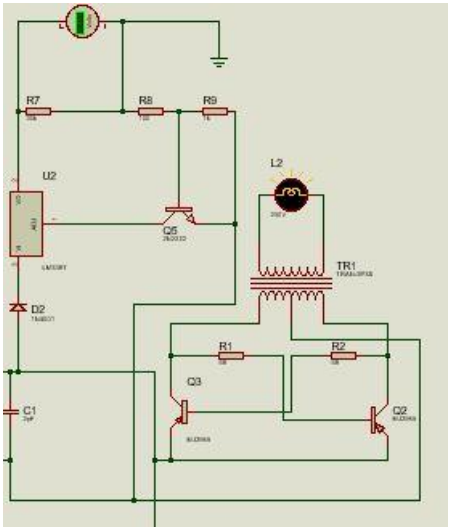


Fig.5. Distribution of DC Circuit Diagram

IV. RESULTS

In developing this system, the Perturb and Observe algorithm is developed through MATLAB code and mikroC code. The MikroC code is loaded on the microcontroller chip and the results are displayed by the oscilloscope connected. This maximum power tracking technique uses iteration process or perturbation to meet the objective of extracting maximum power from the PV panel. Respecting the results achieved it is possible to conclude that, the PV simulation ensures that the theoretical digits, namely the voltage factor assumed, is a very approximate value of what can be expected in real implementation of the solar panel. There are several different topologies of converter circuits and MPPT algorithms. Algorithms can always be improved by the cost of complexity, computer power and cost. Topologies can be combined to extract the best from each other carrying their

ISSN: 2521-2292

particular drawbacks and advantages. MPPT algorithms can work on several different information sources such as light and temperature, voltage and current and also from pilot cells. There is always the cost factor and reliability when trying to produce the most efficient system.

V. Conclusion

The proposed system includes MPPT solar system, which is designed to adjust solar voltage to utilize the maximum power output of the solar array to achieve maximum efficiency. An MPPT solar system allows the maximum power to be harvested and it provide substantially more power when the temperature is below 30 degrees Celsius and when the irradiance is very low. This project provides power or electricity using solar panel as it is efficient and an economic option that enables faster electrification of villages to people at remote areas. Solar was chosen to be the best alternative for rural electrification because is cheap and more efficient than biogas. This system remains the perfect option for villager because it is cheap and does not require much attention.

References

[1] A. S.mekhilef, "Incremental Conductance MPPT Method for PV system," *IEE CCECE*, pp. 345 - 347, 2011.

[2] E.V.R Sastry, "Village electrication programme in India," in In Proceedings of the 3rd World Conference on Photovoltaic Energy Conversion, Osaka, Japan, 11-18 May 2003.

[3] A. U. T. Hubble, "Composition, placement and economics of rural microgrids for ensuring sustainable development," 2018

[4] W. L. J. Theo, "Review of distributed generation system planning and optimisation technique," 2017

[5] S. Feron, "Sustainability of Off-Grid Photovoltaic Systems for Rural Electrification in Developing Countries," Sustainability, 19 December 2016.

[6] Best Solar Panels by Efficiency: https://news.energysage.com

[7] W. L Theo, J. S Lim “Review of Distributed Generation System Planning and Optimisation Technique,” Review and Sustainable Energy Reviews, vol. Volume 67, no. Issue 8, p. Pg 531 to 573, January 2017.

[8] Liu, S. and R.A. Dougal, “Dynamic Multiphysics Model for Solar Array,” IEEE Transactions on Energy Conversion, vol. Volume 17 17, no. Issue 2,p. Pg 285 to 294, June 2002.

BIUST Research and Innovation Symposium 2019 (RDAIS 2019)
Botswana International University of Science and Technology
Palapye, Botswana, 4 - 7 June 2019

ISSN: 2521-2292

Machine learning for maximum and minimum temperature analytics and prediction at local level

Tsaone Swaabow Thapelo and Rodrigo S. Jamisola, Jr.
Simulation, Machine Learning, Robotics and Technopreneurship Laboratory (SMaRT Lab)
Department of Mechanical, Energy and Industrial Engineering
Botswana International University of Science and Technology
Palapye, Botswana

***Abstract*— Despite the fact that machine learning approaches have demonstrated to efficaciously model the perturbations tangled within the weather patterns, they are still under deployed in under represented countries. This proves the existence of gaps between the weather service providers and institutions that advocate for the data driven approaches of modelling stochastic systems like weather. For instance, the Botswana Department of Meteorological Services is currently looking for new avenues that can be deployed to compliment the conventional weather models; particularly for one-to-three months step-ahead of localised minimum and maximum temperature forecasts. Thereto, this work applies predictive analytics on local climatological data harvested, using Perl, from the Shakawe automated weather station starting from 01 July 2014 to 28 February 2019. First, statistical metrics such as scatter plots, box-plots, and correlation coefficients are used to infer patterns and relationships hidden within the collected numerical data. The same process, coupled with Random Forests, is deployed to reduce dimensions of the collected data, hence redundant variables are discarded. In the first phase, the models (Multi-Layer-Perceptron (MLP), k-Nearest neighbourhood, Random Forests) are built using the available data. In the second phase, the selected variables (average air temperature, diurnal temperature range, average wind speed, humidity, minimum temperature and barometer pressure) are used to build and compare the proposed models. The models were fit to 70 % of the training data, and validated on 30 % testing data. The results show that MLP outperforms other models based on the correlation coefficient, Root Mean Squared Error and Minimum Absolute Error.**

***Index Terms*— Machine learning models, data analytics, prediction, automated weather stations, climatological data**

I. Introduction

Weather systems are simulated using sophisticated physical based computations. Such models are imperfect for regional and local weather forecasts due to coherent biases in both spatial and temporal model resolution. As a result, these models have limited information about extremely local terrain conditions. Local phenomena like maximum and minimum temperatures in winter seasons are intricate to replicate by global models [1]. These variables are less handled by the size of the grids of the numerical models since they can occur as a result of small perturbations at a local level, or can be influenced by a large spatial event such as El-niño.

II. Background Information

This work is focused on the study of minimum and maximum air temperature trends and variations for the Shakawe Automated Weather Stations in Botswana. Botswana is a land-locked country in the southern part of Africa sharing borders with Namibia to the west, South Africa to the south, Zimbabwe to the north east and Zambia to the north.

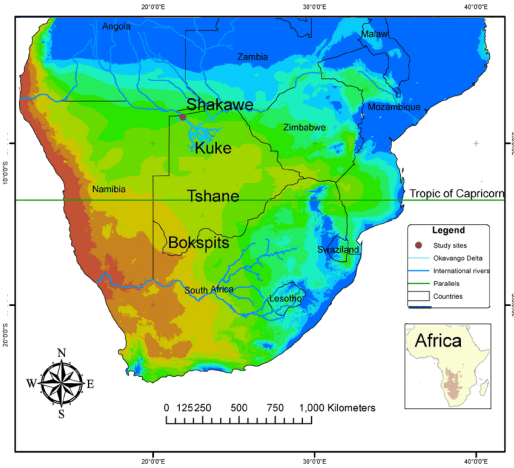


Fig. 1. Location of Shakawe in the northern west of Botswana

The country is characterised by a semi-arid climate, with great differences in day and night temperatures, low overall humidity and high pressure systems interacting with dry soils over the entire land [2], [3]. These have been reported to be associated with temperature trends, particularly high temperatures [4]. Botswana's mean monthly maximum temperatures range from 32 $^{\circ}C$ to 35 $^{\circ}C$. Daily maximums can reach as high as approximately 43 $^{\circ}C$; particularly from October to March. The country is predicted to experience harsh climate variability with local warming and drying above the global warming average of 1.5 $^{\circ}C$ [5].

ISSN: 2521-2292

III. Significance of Study and Envisioned Products

Small geographic changes in minimum and maximum air temperature can have significant impacts on human health, society and the economy [4]. Some researchers linked air temperature with mortality [6] resulting from severe weather and climate variations such as heat waves [4]. Botswana as a semi-arid country is also expected to have approximately "40 more days of heat waves at 1.5°C global warming, and about 75 more heatwave days at 2.0°C global warming" [7]. The re-occurrence of heat waves at recent has led to a number of studies regarding the analysis of temperatures. For instance, daily maximum temperature observational data was used in the study [4] to investigate the heat waves characteristics in the context of climate change.

Various human activities including electricity load forecasting [8], [9], agriculture and water management [10] depend much on these environmental systems. This underlines the value of weather modelling in operational services such as health sciences.

All these invite resilient avenues like the data driven approaches to compliment the physically based ones. Meanwhile, Botswana's environmental data science is still under-exploited despite the fact that climatological data collection has been going on in the country for long [11]. As a result, powerful models go un-explored [12] and potential data remain virgin; while the weather and climate change impacts continue to perpetuate the livelihoods of people.

This project aims to make use of the available open-source resources to add value to existing weather models in Botswana and the SADC region. The knowledge extraction process is particularly important for local to regional weather and climate studies. It presents cheaper and competitive modeling approaches to complement the convectional environmental models that deploy enormous computing systems with lower resolution than desired at regional and local level. Part of this work includes the implementation of recipes to analyse, visualize and assimilate climatological data. The data assimilation process will assist in filling the missing values in weather data.

Thus, the data driven models can be used to benchmark the level of detail that current regional models should be aiming for. In fact, ensembles models can improve model accuracy, robustness, confidence, efficiency, efficacy, reliability, and reduced costs. Lastly, but not least, the developed recipes and model products can be scaled to cater for the Southern African Community and hence facilitating knowledge sharing: all towards the transformation from resource based economies to knowledge based ones.

IV. Literature Review

Chauhan and Thakur presented a review of Data Mining Techniques to forecast several weather phenomena such as temperature, thunderstorms, and rainfall [13]. They found that major techniques like decision trees, lazy learning, artificial neural networks, clustering and regression algorithms are suitable to predict weather phenomena. They concluded that decision trees yield good results for this weather forecasting, followed by the ANN. They also suggested that DM can be considered as an alternative to traditional meteorological approaches.

Olaiya and Adesesan [14] applied decision trees (C4.5, CART) and artificial neural networks in their studies of weather prediction and climate change. They used a 10 years dataset with 4 variables (temperature, rainfall, evaporation, and wind speed) and 36000 instances to acquire an 82 % of accuracy via the percentage split. Meanwhile, their results show that the accuracy varies highly with the training dataset size. They concluded that given enough training data, data mining techniques can be efficiently used for weather prediction and climate change studies.

Petre used decision trees to predict the temperature values around Hong Kong. A 4 years data set with 48 instances was used, comprised of pressure, clouds quantity, humidity, precipitation, and temperature. The accuracy obtained was of 83 % [15]. They reported the need to increase weather variables for input, as well as the increase of data instances. The work also required the transformation of data. Maqsood presented the applicability of ensemble models [16] based on neural networks for one-day-ahead weather forecasting of temperature, humidity, and wind speed for winter, spring, summer and fall. The developed ensemble models generalized better than conventional regression with higher accuracy.

Kumar and Jha [17] used an ANN to predict minimum and maximum temperatures. They used a 100 year data set composed of monthly average min and max temperatures using the percentage split with 60 % for training and the remaining 40 % for testing. Their results showed that ANN may be an important tool for temperature forecasting. Meanwhile, they used only two input variables to compute two target variables.

V. Contribution of this work

Most of these studies discussed so far do not mention the methods used for: data collection, data cleaning and dataset generation as well as the data mining platforms used, or they use commercial platforms like Matlab [17]. The feature extraction and dimensionality reduction is also not explicit [15], [17]. All these make it difficult for reproducibility of results. For that main reason, the applicability of data driven approaches is lagged behind in operational meteorological services. If the data is not available, or the data mining platforms are not accessible, then no models will be developed [12]. Motivated by these, this work deploys the whole processes of predictive analytics or just data science to bridge this gap.

ISSN: 2521-2292

VI. Methodology

VI-A. Data Collection

The data used for modelling was harvested from http://www.sasscalweathernet.org/. Data cleaning and formatting was done using Perl scripting to transform it into consumable formats for `Weka`, `R` and `RWeka`. This was achieved using the `Gnumeric` spreadsheet application which comes with a command line utility called `ssconvert` to convert between a variety of file formats (`.xls` to `.csv`) as shown below:

$$ssconvert \quad InputFile.xlsx \quad OutputFile.csv$$

The basics of file handling were done by associating a named internal Perl structure, a *filehandle*, with an external entity (a .xls file). A variety of operators and functions within Perl were used to read and update the data stored within the data stream associated with the filehandle. The following syntax was used:

open(DATA, "< file.xlsx") or die "Couldn't open file file.txt!";

The source files included unwanted texts values, requiring some additional data processing to get rid of them. The array data structure was used to contain the data input and several Perl operating functions (`shift`, `pop`, `split` and `join`) were applied to manipulate the input data. A complete script was coded to automate the process, adding the shebang line to the code to extract a stream of data from an excel to `csv`, then prepare an `.arff` and `.csv` data sets. The code can then be used to extract data from the any file from any SASSCAL website then generate datasets.

VI-B. Data Pre-processing

Since some machine learning algorithms make assumptions about the data, the data transformation was done to map each point in the input data set X to selected functional output of that point.

$$output_i = Transformer(X_i) \tag{1}$$

The `Transformer()` functions are discussed below:

- The `Min-Max` (Equation 2) transforms the data to a new range [0,1] of values which is guaranteed by the existence of bounded minimum and maximum values.

$$X_{new1} = \frac{X - min(X_i)}{max(X) - min(X)} \tag{2}$$

- The `Z-Score Standardisation` (Equation 3) transforms the data to have zero mean and unit variance with the assumption that the data distribution is normal. It indicates how many standard deviations the data X is from the mean. It is sensitive to outliers [12].

$$X_{new2} = \frac{X - \mu}{\sigma} \tag{3}$$

- The `Magnitude Scaling` (Equation 4) transforms the variable by its maximum magnitude to create a maximum value of -1 or +1 depending on whether the maximum magnitude is negative or positive but it is not guaranteed to fill the entire range from -1 to +1.

$$X_{new3} = \frac{X}{max|X|}, \ in\ the\ range\ [-1, 1] \tag{4}$$

Data transformations can also to make machine learning algorithms such as ANN to train faster, avoid saturation.

VII. Data Partitioning

The `percentage-split` [18, pg. 182] was used to partition the data into `training` (to build the model) and the `testing dataset` to test the model.

VIII. Machine Learning Models

Data modelling and visualisation was done using Weka, R [19] and RWeka by Kurt [20]. These are all open source platforms for statistical computing and graphics. The most important R and Weka packages used in this work include: "nnet"package [21], [21], [22], "kknn"package [23].

VIII-A. Artificial Neural Networks

Artificial Neural Networks (ANN) are non-linear universal function estimators inspired by the multi-tasking and parallel processing of the nervous system [12], [24]; which is supported by its massive amount of sensory data [25, pg. 197]. They are considered to be `distributional free` models that are also `robust` to handle `outliers` and `noisy` data [26]. The models consist of several neurons connected by weighted edges. The interconnections facilitate the exchange of data between neurons. Weka's `MLP` and `R`'s `nnet` and `neuralnet` packages were used in this work.

The learning process starts when the vector x_i is supplied to the `input layer`. The task involves the selection of connecting `weights` w_i between the neurons (depicted in circles). Each neuron has two components [12, pg. 242]: the `transfer function` (T_f) and the `activation function` (A_c). First, the `weights` are initialised, then a `transfer function` in Equation 5 is applied to extract linear combinations of w_i and x_i, coupled with some `bias` b.

$$T_f(x_i, w_i, b_i) = \sum_{i=1}^{n} w_i x_i + b_0 \approx \mathbf{x}^T \mathbf{w} \tag{5}$$

The weighted sum T_f is executed as an argument to $A_c()$ (see Equation 6) at each layer and then the function value of $A_c()$ is propagated to the next layer (another hidden layer or the output layer). There are various common choices for activation function $A_c()$.

$$A_c\big(T_f((x_i, w_i, b_i)\big) = A_c\big(\sum_{i=1}^{n} w_i x_i + b\big) \tag{6}$$

ISSN: 2521-2292

TABLE I
THE COMMON CHOICES FOR ACTIVATION FUNCTIONS

Squashing function	Formula	Range
`Sigmoid (logistic)`	$\phi_1(x) = \frac{1}{1+e^{-x}}$	0 to 1
`Hyperbolic tangent`	$\phi_2(x) = \frac{sinh(x)}{cosh(x)} = \frac{e^x - e^{-x}}{e^x + e^{-x}}$	-1 to 1

VIII-B. k-Nearest Neighbourhood

The k-nearest neighbours (`k-NN`) algorithm is an instance-based type of learning model where new data are classified based on stored labelled instances (observations from the training dataset ℶ) [27, pg. 33]. The algorithm measures the distance between the input instance query and a set of instances residing in ℶ) to form $\hat{Y}$.

$$\hat{Y} = \frac{1}{k} \sum_{x_i \in N_k(x)} y_i \tag{7}$$

where $N_k(x)$ is the neighbourhood of x defined by the k nearest points $x_i \in$ ℶ. The main work of the kNN happens during prediction time, where the prediction of a new test data instance is derived based on some similarity distance measure deployed to determine the distance between the stored data and the new instance. The commonly distance metric used are:

- `Minkowski distance function`

$$d(x, y) = (\sum_{i=1}^{n} |x_i - y_i|^r)^{\frac{1}{r}}, \tag{8}$$

  and when $r = 1$, the distance is referred to as Manhattan, while $r = 2$ gives the Euclidean distance.
- `Absolute distance measuring`

$$d_{ABS}(x, y) = \sum_{i=1}^{n} |x_i - y_i| \tag{9}$$

  The Euclidean distance is used to computed the distance among the numerical attributes in k-NN.

In all the cases, n is the number of dimensions equivalent to the number of attributes, and x_i and y_i are the i^{th} attributes of x and y. The k most similar training cases (i.e. neighbours) are used to obtain the prediction for the given test case. If k is too small, then the result can be sensitive to noise points, but it should not be too large, since the neighbourhood may include too many points from other classes. The value of k should also be odd to avoid discrepancy in determining the final class.

VIII-C. Ensembles

An ensemble can be seen as a set of multiple learning methods where a model decision is taken by averaging the results from various standalone models. Several models and their respective clones/configurations can be applied to a single data set (or several) to investigate their predictive capabilities. Bagging, Boosting and Random Forests are examples of ensembles [**?**], [12], [18]. This work deploys the Random forests for variable selection as well as modelling.

IX. RANDOM FOREST

Literature shows that this algorithm implements Breiman's FORTRAN random forest algorithm for classification and regression [**?**, pg. 17]; which adds some randomness to bagging by constructing each tree using a different bootstrap sample of the data. In standalone tree based models, each node is split using the best split among all variables; while in a random forest, each node is split using the best among a subset of predictors randomly chosen at that node.

This work deploys R's `randomForest` package to provide an interface for coding. The method function takes in as inputs: a formula interface, predictors - specified as data frame via the x argument, responses denoted as a vector via the y argument. The algorithm is very user-friendly, requiring only two parameters: the number of variables in the random subset at each node, and the number of trees in the forest). Here, the response for classification is a factor; and continuous for regressions.

X. EXPERIMENTAL SET UP

The methodology deployed is the percentage splitting, where the models are fit to some training data, then evaluated on some unseen testing data. various partition ratios are used in this work, and the best parameters are selected based on the errors in training and testing data.

X-A. Statistical metrics of model assessment

Marques de Sá defines a `statistic` is a function, t_n, of n samples values of x_i [28]. The central idea in statistics is to find the ünderlying law.ºf the data by averaging out measurements errors from each single experiment.
Thus, in each of statistical metrics deployed, one first computes the error of an estimate- the actual value minus the predicted estimate, and then computes the appropriate statistic based on those errors.

1. The `Mean Squared Error` provides a gross idea of the magnitude of error.

$$MSE = \frac{\sum_{i=1}^{n} (y_{predicted} - y_{actual})^2}{n} \tag{10}$$

2. The root-mean-square deviation (RMSD) was also used to measure the differences between values (sample or population values) predicted by a model and the values observed.
3. The correlation was also used. The correlation coefficient between X_1 and X_2 is the co-variance of the standardisation of X_1 and X_2; and it is defined by

$$Cor(X_1, X_2) = \rho = \frac{Cov(X_1, X_2)}{\sigma_{X_1}, \sigma_{X_2}} \tag{11}$$

   where $-1 \leq \rho \leq 1$. The parameter ρ measures the linear relationship between between variables. If the correlation is positive then when X_1 is large, X_2 will tend to be large as well. If the correlation is negative then when X_1 is large, X_2 will tend to be small.

ISSN: 2521-2292

XI. Summarising the Data via descriptive statistics

This sections articulates some descriptive statistics indices used to give a global picture regarding where and how the data is concentrated and as well as its shape of distribution. The following indices will be analysed for the purpose of summarising the SAWS dataset.

Measures of Location

The following measures of location are used in order to determine where the data distribution is concentrated.

1. The `arithmetic mean` of the data x is the sample estimate of the mean of the associated random variable [28] and is denoted by
$$\bar{x} = \frac{1}{n}\sum_{i=1}^{n} x_i \tag{12}$$
2. The `median` of a dataset is that value of the data below which lie 50 % of the cases. Other measures of location include the mode, and the quantiles (see [28, pg. 59]).

Measures of Spread

The measures of spread (or dispersion) give an indication of how concentrated a data distribution is. The most usual measures of spread are presented below.

1. The `range` of a dataset is the difference between its maximum and its minimum,
$$range = x_{max} - x_{min} \tag{13}$$
It has a draw back that it is dependent on the extreme cases of the dataset; and it also tends to increase with the sample size [28, pg. 62].
2. The `inter-quartile range` is defined as:
$$IQR = x_{0,75} - x_{0,52}. \tag{14}$$
It has the advantage that it is less influenced by outliers, extreme cases nor the sample size as compared to the `range`.
3. The variance of a dataset can be interpreted as the mean square deviation (or `mean square error`, MSE) of the sample values from their mean. $Var(x)$ (sample variance) is defined as:
$$Var(x) = \sum_{i=1}^{n} \frac{(x_i - \bar{x})^2}{n-1} \tag{15}$$
The variance has $df = n-1$ degrees of freedom; while the mean, on the other hand, has n degrees of freedom [28, pg. 62].
4. The `standard deviation` of a dataset is the root square of its variance. It is, therefore, a `root mean square error` (RMSE) defined as:
$$\sigma = \sqrt{Var(x)} = [\sum_{i=1}^{n} \frac{(x_i - \bar{x})^2}{n-1}]^{\frac{1}{2}} \tag{16}$$
The standard deviation is preferable than the variance as a measure of spread, since it is expressed in the same units as the original data.

Measures of Shape

- The coefficient of skewness was determinded, which is the asymmetry measure around the mean, defined as
$$\gamma = \frac{E[(X-\mu)^3]}{\sigma^3} \tag{17}$$
This measure uses the fact that any central moment of odd order is zero for symmetrical distributions around the mean. For asymmetrical distributions γ reflects the unbalance of the density or probability values around the mean.
- The work also determined the coefficient of excess, kurtosis, which is just the degree of flatness of a probability or density function near the center of the data distribution.
$$\kappa = \frac{E[(X-\mu)^4]}{\sigma^4} - 3 \tag{18}$$
The factor 3 is introduced in order that $\kappa = 0$ for the normal distribution. Distributions flatter than the normal distribution have $\kappa < 0$; distributions more peaked than the normal distribution have $\kappa > 0$. More on this can be found in [28, pg. 65]

Measures of Association for Continuous Variables

The `correlation coefficient` (Pearson correlation) is the most popular measure of association for continuous type data. For a dataset with two variables, $V1$ and $V2$ the sample estimate of the `correlation coefficient` ρ_{V1V2} is computed as
$$r = r_{V1V2} = \frac{S_{V1V2}}{S_{V1}S_{V2}}, \tag{19}$$
where
$$S_{V1V2} = \sum_{i=1}^{n} \frac{(x_i - \bar{x})(y_i - \bar{y})}{n-1} \tag{20}$$
This dimensionless measure of the degree of linear association of the two random variables has [-1,1] as the interval; with:

- -1 $\Longrightarrow$ Total linear association, with V1 and V2 varying in the opposite direction,
- 0 $\Longrightarrow$ No linear association; V1 and V2 are linearly uncorrelated,
- 1 $\Longrightarrow$ Total linear association, with V1 and V2 varying in the same direction.

ISSN: 2521-2292

	vars	n	mean	sd	median	trimmed	mad	min	max	range	skew	kurtosis	se
TimeStamp	1	1704	NaN	NA	NA	NaN	NA	Inf	-Inf	-Inf	NA	NA	NA
AVG.AT	2	1693	22.58	4.43	23.35	22.75	4.74	11.59	32.80	21.21	-0.35	-0.83	0.11
Min.AT	3	1693	14.29	5.98	15.80	14.67	6.57	-0.50	26.88	27.38	-0.45	-1.07	0.15
DTR	4	1693	17.34	5.42	17.84	17.50	6.15	0.09	30.76	30.67	-0.23	-0.70	0.13
AVG.ST	5	1693	24.93	4.01	26.27	24.76	3.63	17.72	33.94	16.22	0.04	-0.94	0.10
P	6	1693	1.41	6.26	0.00	0.09	0.00	0.00	80.60	80.60	7.69	72.78	0.15
Avg.WS	7	1693	1.38	0.62	1.31	1.35	0.61	0.05	3.70	3.65	0.48	0.11	0.01
AVG.WD	8	1693	126.70	69.72	130.59	121.18	43.76	0.10	359.85	359.75	1.06	2.25	1.69
Max.WS	9	1693	4.47	1.08	4.33	4.38	0.98	1.76	10.10	8.34	0.93	1.59	0.03
Max.WD	10	1693	125.37	72.44	116.70	116.75	58.27	0.00	358.50	358.50	1.09	1.15	1.76
H	11	1693	54.83	18.12	54.45	54.32	19.72	16.67	100.00	83.33	0.20	-0.75	0.44
BP	12	1693	903.06	3.42	902.40	902.90	3.71	895.40	912.60	17.20	0.38	-0.68	0.08
AVG.SR	13	1693	281.26	58.68	276.91	282.19	56.22	36.87	528.03	491.16	-0.12	0.30	1.43
Sum.SR	14	1693	24.21	5.05	23.89	24.34	4.82	0.07	34.69	34.62	-0.31	0.37	0.12
LW	15	1693	164.27	10.55	160.01	161.91	2.90	154.96	259.60	104.65	3.18	14.46	0.26
DP	16	1693	10.94	6.88	10.94	11.11	9.31	-7.39	22.46	29.85	-0.12	-1.21	0.17
WB	17	1693	15.65	4.55	16.01	15.85	6.14	5.02	22.86	17.84	-0.25	-1.25	0.11
SD	18	1691	537.34	163.08	604.48	559.44	112.53	0.00	741.83	741.83	-1.17	0.71	3.97
Max.AT	19	1693	31.63	4.17	31.37	31.64	4.77	19.79	41.50	21.71	0.01	-0.75	0.10

Fig. 2. Summary statistics of the SAWS dataset. The mean value for Precipitation (P) seem to be strange though; its maximum is 80,80 mm while the minimum is 0,0 mm, yet the mean is 1,41 mm larger than the median, 0 mm.

Data visualisation via correlation plots

A correlation analysis provides insights into the independence of the numeric input variables. In this work, the Pearson's product-moment correlation was used to measure the numerical relationship of one variable to another within a 95 % confidence interval. Variables with high correlations have values close to 1 for positive correlations, and close to -1 one for negative correlations. The Figure 3 presents the numerical plot articulated so far.

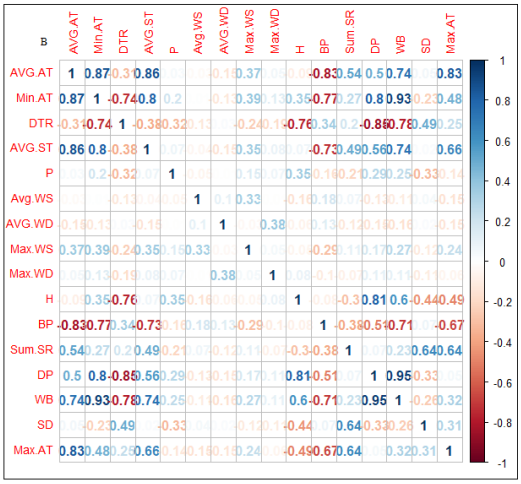


Fig. 3. The correlation coefficients for the SAWS dataset.

Visualisation via box-and-whiskers plots

A box-plot facilitated exploration of data distribution (centre and spread of a numeric variables). It uses the five-number statistics (Minimum, Q1 (first quartile), Q2 (median), Q3 (third quartile), and Maximum) of a vector. It visualises the range, outliers and skew of numerical variables, as well as the comparisons of such variables. This was used to diagnose the problems that are encountered within the data. Since the numerical variables in the dataset were from different instruments, they were normalised to allow a fair comparisons of the variables on the same scale. Figure 6 presents box-plots for our dataset. Only those variables selected via random forests are displayed. Among the variables with some outliers, Leaf Wetness and Precipitation had extreme outliers to the right; while Average Solar Radiation (AVG Solar R) had some outliers in both extremes. These values can be corrected to make the IQR box easier to visualise [29, pp. 62] .

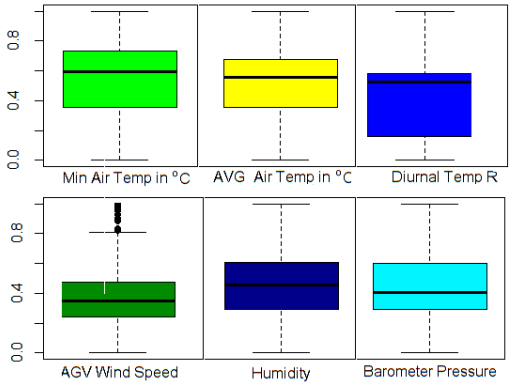


Fig. 4. Thw box-plots for the selected variables for maximum air temperature. We can note that the variable air temperature has some outliers above the extreme maximum whisker denoted by some dots

XI-A. Variable selection via Random Forest in R

Determining the influence measure of a variable is a time consuming and challenging task due to intricate interaction within the modelling variables. Fortunately, the `randomForest` package optionally provide access to two additional pieces (measures) of information: a measure of the importance of the predictor variables, and a measure of the internal structure of the data (the proximity of different data points to one another).

Thus, this work deploys a `randomForest` algorithm to estimate the importance of a variable regarding the target variables. The algorithm works by looking at how much prediction error increases when the modelling data for that variable is permuted. The necessary calculations are carried out tree by tree as the random forest is constructed.

To determine the importance of each variable, the measure is computed from permuting Out-Of-Bag (OOB) data. For each tree, the prediction error on the OOB portion of the data is recorded. For Regression, two metrics are used: the mean decrease in accuracy and the mean decrease in Mean Squared Error. In this work, the mean of squared residuals is computed as

$$MSE_{OOB} = n^{-1} \sum_{i=1}^{n} (y_i - \hat{y}_i)^2 \qquad (21)$$

ISSN: 2521-2292

where $\hat{y}_i$ is the average of the model predictions. The smaller the result value, the better the model; depending on the problem. It is good to compare to a reference model though.

```
Call:
 randomForest(formula = TMAX ~ ., data = SAWS, ntrees = 500, mtry = 13,
   importance = TRUE, keep.forest = TRUE, subset = train)
               Type of random forest: regression
                     Number of trees: 500
No. of variables tried at each split: 13

          Mean of squared residuals: 0.4703323
                    % Var explained: 97.27
```

Fig. 5. The random tree model with 500 trees, and 13 predictors tried at each tree split. It can noted that 97.27 % of the variation is .[ex]plained"by our model, and the mean of squared errors is ≈ 0.47; quite good.

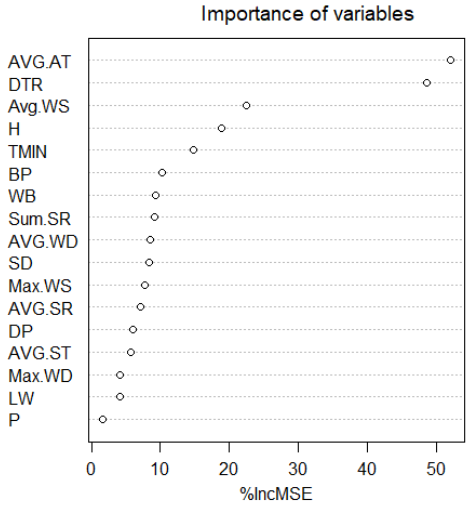


Fig. 6. Graph showing the importance of predictors on Maximum Air Temperature

We can see that the most contributing variables are average temperature (AVG.AT), Diurnal Temperature Range (DT), average wind speed (Avg.WS), and humidity (H).

XII. Results and Discussions

Different configurations were tested by varying the learning rate, momentum, number of iterations and the network structure as seen in Figure 8. Though MLP 2 gave better results during training compared to MLP 3, the later generalised well during the testing phase.

The k-NN was evaluated on the training (70 %) and testing (30 %) data. Different values of 'k' were experimented, and the model statistical results were recorded as shown in Table II It can be noted that the correlation coefficient reduces from 0.98 to 0.96 as more points are used as the number of neighbourhoods (k) increases; while other statistical metrics increases the training phase. Meanwhile, the opposite was observed during the testing phase where all the model replicas of k-NN showed some good performance on the

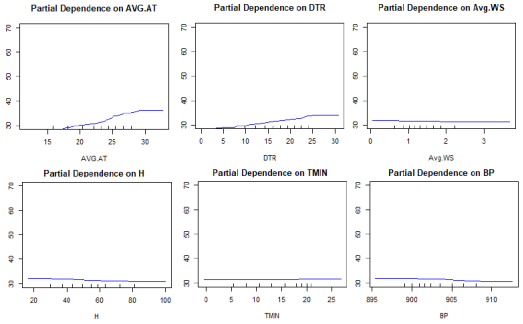


Fig. 7. Partial dependence of the first six elements selected based on random Forest. The first three elements shows some strong dependency with the Maximum air temperature

Training phase	Learning rate	Momentum	Iterations	Architecture	CC	MAE	RMSE
MLP 1	0.2	0.2	500	7,15,1	0.9998	0.0688	0.0904
MLP 2	0.4	0.2	500	7,15,1	0.9999	0.0438	0.06
MLP 3	0.8	0.6	700	7,15,1	0.9999	0.0678	0.0797
MLP 4	0.8	0.7	700	7,25,1	0.9986	0.5357	0.5765
MLP 5	0.8	0.4	700	7,15,1	0.9999	0.0951	0.112
Testing phase	**Learning rate**	**Momentum**	**Iterations**	**Architecture**	**CC**	**MAE**	**RMSE**
MLP 1	0.2	0.2	500	7,15,1	0.9998	0.0707	0.0917
MLP 2	0.4	0.2	700	7,15,1	0.9999	0.0868	0.1002
MLP 3	0.8	0.6	700	7,15,1	0.9999	0.0502	0.066
MLP 4	0.8	0.7	700	7,25,1	0.9979	0.5867	0.6517
MLP 5	0.8	0.4	700	7,25,1	0.9999	0.084	0.1039

Fig. 8. The MLP with a sigmoid activation function. We note that the MLP 3 is more stable for both training and testing phase as compared to the other configurations based on MAE and RMSE

testing data. A slight observation to the results from both the training and testing phase revealed that the model with 15 nearest neighbourhoods was more stable than the rest of the replicas; and with a MAE of 0:9 in the testing phase.

TABLE II
The k-Nearest neighbourhood with 75 % used for training

Training phase	**K = 2**	**K = 3**	**K = 4**	**K = 15**
Correlation coefficient	0.9841	0.9796	0.9769	0.9639
Mean absolute error	0.571	0.6407	0.6835	0.8783
Root mean squared error	0.7432	0.8432	0.899	1.1445
Time (seconds)	0.92	0.97	1.16	1.11
Testing phase	**K = 2**	**K = 3**	**K = 4**	**K = 15**
Correlation coefficient	0.9397	0.9502	0.9519	0.958
Mean absolute error	1.0956	0.986	0.9775	0.952
Root mean squared error	1.4153	1.2938	1.2777	1.2552

Lastly, the ANN model configurations and the Random Forest ensemble were selected to perform some final trends since they demonstrated better predictive capabilities compared to other models based on the proposed statistical metrics. The results are shown below.

XII-A. Base line model construction via Random Forest in R

In Figure 14, we can observe that the Red line is the Out of Bag Error Estimates and the Yellow Line is the Error calculated on Test Set. Both curves have a quite similar trend

ISSN: 2521-2292

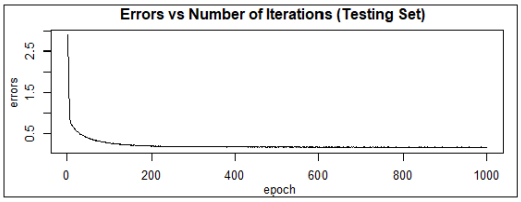


Fig. 9. The graph of the epoch versus error for minimum air temperature based on ANN. We note that the models converge at roughly 25 iterations

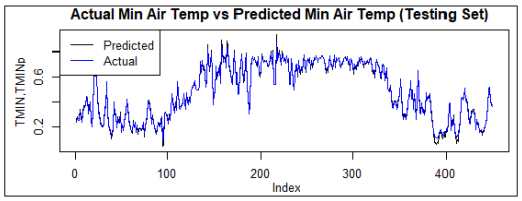


Fig. 10. The graph of the actual minimum air temperature vs predicted minimum air temperature based on ANN showing some perfect fit

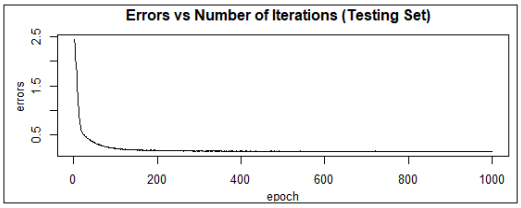


Fig. 11. The graph of the epoch versus error for maximum air temperature based on ANN

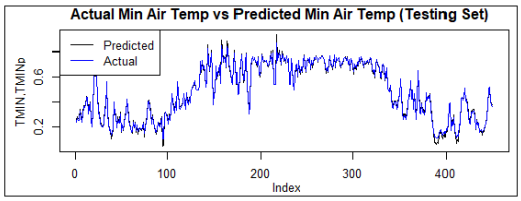


Fig. 12. The graph of ANN showing a perfect fit for the actual maximum air temperature vs predicted maximum air temperature

and the error estimates are somewhat correlated too. The Error Tends to be minimised at around $mtry = 6$. On the Extreme Right Hand Side of the above plot, we considered all possible 18 predictors at each Split which is only Bagging.

XIII. Conclusions

In this paper, we built predictive models for temperature analytics and modelling. Variable selection was done using Random forests and the modelling was done using ANN, kNN and Random forests for the Shakawe weather station. The results show that machine algorithms, can be add value to the convectional weather models. The patterns and trends were perfectly resembled by our models, with ANN outperforming the other two method though the difference was insignificant; all less than one in terms of Mean Squared Errors. Thus the overall errors are within the threshold used by the Botswana Department of Meteorological Services, which is plus or minus two for summers and plus or minus three for winters. Meanwhile, more weather stations should be tried to validate the experiments.

XIV. Future Work

To expand the research to cater for on-line real time machine learning and predictive analytics; and ultimately design a user friendly regional weather forecasting application based on the designed models.

References

[1] T. Tsaone, Swaabow, *Técnicas de aprendizaje automatizado para el pronóstico de temperaturas minímas en el Centro Meteorológico de Villa Clara, Santa Clara*. PhD thesis, Universidad Central "Marta Abreu"de Las Villas, 2014.

[2] T. Nkemelang, *Evaluating temperature and precipitation extremes under 1.5° C and 2.0° C warming above pre-industrial levels: Botswana case study*. PhD thesis, University of Cape Town, 2018.

[3] O. D. Kolawole, P. Wolski, B. Ngwenya, and G. Mmopelwa, "Ethno-meteorology and scientific weather forecasting: Small farmers and scientists' perspectives on climate variability in the okavango delta, botswana," *Climate Risk Management*, vol. 4-5, pp. 43 – 58, 2014.

[4] O. Moses, "Heat wave characteristics in the context of climate change over past 50 years in botswana," 2017.

[5] M. New, "What the latest assessment on global warming means for southern africa," *Quest*, vol. 14, no. 4, pp. 12–13, 2018.

[6] T. Li, R. M. Horton, D. A. Bader, F. Liu, Q. Sun, and P. L. Kinney, "Long-term projections of temperature-related mortality risks for ischemic stroke, hemorrhagic stroke, and acute ischemic heart disease under changing climate in beijing, china," *Environment International*, vol. 112, pp. 1 – 9, 2018.

[7] M. New, "What the latest assessment on global warming means for southern africa," *Quest*, vol. 14, no. 4, pp. 12–13, 2018.

[8] M. Dahl, A. Brun, and G. B. Andresen, "Using ensemble weather predictions in district heating operation and load forecasting," *Applied Energy*, vol. 193, pp. 455–465, 2017.

[9] T. Ahmad and H. Chen, "Short and medium-term forecasting of cooling and heating load demand in building environment with data-mining based approaches," *Energy and Buildings*, vol. 166, pp. 460 – 476, 2018.

[10] "Predictability of daily precipitation using data from newly established automated weather stations over notwane catchment in botswana," *Biodiversity & Ecology*, vol. 50-52, pp. 46–51, 2018. 12th WaterNet/WARFSA/GWP-SA Symposium: Harnessing the rivers of knowledge for socio-economic development, climate adaptation & environmental sustainability.

[11] G. Muche, S. Kruger, T. Hillmann, K. Josenhans, C. Ribeiro, M. Bazibi, M. Seely, E. Nkonde, W. de Clercq, B. Strohbach, K. Piet Kenabatho, R. Vogt, F. Kaspar, J. Helmschrot, and N. Jürgens, "Sasscal weathernet: present state, challenges, and achievements of the regional climatic observation network and database," *Biodiversity & Ecology*, vol. 6, 03 2018.

[12] D. Abbott, *Applied predictive analytics: Principles and techniques for the professional data analyst*. John Wiley & Sons, 2014.

[13] W. Boonsiritomachai, G. Michael McGrath, S. Burgess, and S. Liu, "Exploring business intelligence and its depth of maturity in thai smes," *Cogent Business & Management*, vol. 3, 08 2016.

[14] O. Folorunsho and A. Adeyemo, "Application of data mining techniques in weather prediction and climate change studies," vol. 4, 02 2012.

[15] E. G. Petre, "A decision tree for weather prediction," *PP*, vol. 77, p. 82, 2009.

ISSN: 2521-2292

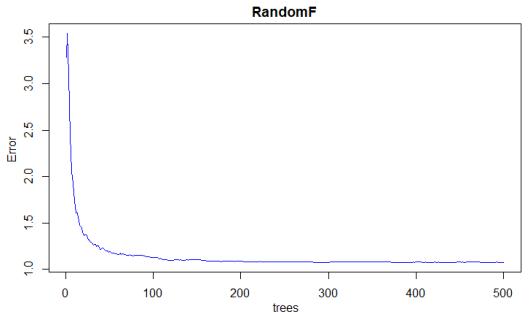


Fig. 13. The plot showing Error versus the Number of Trees. It can be noted that the Error drops gradually as the number of trees increases.

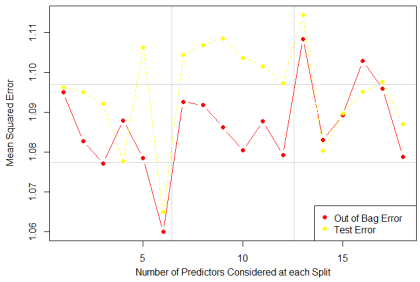


Fig. 14. Plot showing both Test Error and Out of Bag Error using random Forest. We can note that the overall pattern is well resembled, and the error is good, less than 1.2. Which is also less than the threshold for the convectional models of plus or minus two.

[16] I. Maqsood, M. R. Khan, and A. Abraham, "An ensemble of neural networks for weather forecasting," *Neural Computing & Applications*, vol. 13, no. 2, pp. 112–122, 2004.
[17] N. Kumar and G. K. Jha, "A time series ann approach for weather forecasting,"
[18] E. F. Ian H. Witten, *Data Mining: Practical Machine Learning Tools and Techniques*. Morgan Kaufmann Series in Data Management Systems, Morgan Kaufmann, 2 ed., 2005.
[19] R. Ihaka and R. Gentleman, "R: a language for data analysis and graphics," *Journal of computational and graphical statistics*, vol. 5, no. 3, pp. 299–314, 1996.
[20] K. Hornik, C. Buchta, T. Hothorn, A. Karatzoglou, D. Meyer, A. Zeileis, and M. K. Hornik, "Package 'rweka'," 2019.
[21] B. Ripley, W. Venables, and M. B. Ripley, "Package 'nnet'," *R package version*, vol. 7, pp. 3–12, 2016.
[22] S. Fritsch, F. Guenther, and M. F. Guenther, "Package 'neuralnet'," *Training of Neural Networks*, 2019.
[23] K. Schliep, K. Hechenbichler, and M. K. Schliep, "Package 'kknn'," 2016.
[24] C. Giuseppe and V. Balaji, *Neural Networks with R*. Springer Texts in Statistics, 2017.
[25] P. C. Edwin, K and Z. Stanislaw, H, *An Introduction to Optimization*. John Wiley & Sons, INC., fourth edition ed., 2013.
[26] K. Gibert, J. Izquierdo, M. Sànchez-Marrè, S. H. Hamilton, I. Rodríguez-Roda, and G. Holmes, "Which method to use? an assessment of data mining methods in environmental data science," *Environmental Modelling and Software*, 2018.
[27] H. Trevor, T. Robert, and F. Jerome, *The Elements of Statistical Learning*. Springer Series in Statistics, second edition ed., 2017.
[28] M. d. S. Joaquim, P, *Applied statistics using SPSS, STATISTICA,MATLAB and R*. Springer, 2007.
[29] J. Abbot and J. Marohasy, "Application of artificial neural networks to rainfall forecasting in queensland, australia," *Advances in Atmospheric Sciences*, vol. 29, pp. 717–730, Jul 2012.

BIUST Research and Innovation Symposium 2019 (RDAIS 2019)
Botswana International University of Science and Technology
Palapye, Botswana, 4 - 7 June 2019

ISSN: 2521-2292

Anti-poaching System using Wireless Sensors Network

Abid Yahya
yahyaa@biust.ac.bw

Karabo D Bogaisang
karabo.bogaisang@studentmail.biust.ac.bw

Odirile G Gamoshe
odirile.gamoshe@studentmail.biust.ac.bw

Dennis M Maina
dennis.maina@studentmail.biust.ac.bw

Abstract

Pertaining technology advancement, several innovations have been implemented in the wireless sensors networks field. This research seeks to facilitate innovation of a wireless network monitoring system that will be more efficient in gathering data from nodes of the wireless sensor network as it will be able to monitor from long range hence improving coverage. WSN will be employed to enhance LoRa data transmission from body-attached sensor nodes to a base station for analysis. The anti-poaching system will also have solar harvesting system for recharging batteries, hence this system is rendered non-intrusive.

Keywords— Wireless Sensor Network, Anti-poaching, Network coverage, Long Range Transmission

I Introduction

According to authors in [1], since the introduction of safari hunting tourism ban on rural livelihoods including elephants, the incidents of poaching has risen. Safari hunting tourism ban on rural livelihoods was one of the method used as a way of wildlife conservation, this paper focus on introducing a real time system for protecting one of the most endangered species in Botswana which is an attraction for tourism

Anti-poaching system is one of the most studied topic by researchers, in order to prevent or end poaching at all if possible. Various poaching detection technologies have been studied in relation to this topic. Poaching detection technologies is said to be classified into four domains by authors in [2]. The four domains are: perimeter based, ground based, aerial based and animal tagging based technologies.

This paper will be looking at animal tagging based technology where by a sensor node will be a part of WSN that will collect data from the target based on animal behavior. Animal behavior has been identified by researchers as a was of prevent poaching as animals have sensitive sensing as compared to humans [2].

The focus of this paper is to develop an anti-poaching wireless sensor network with a real time monitoring system, with improvements in network coverage employing probability algorithm schemes. Lastly analyze performance of various algorithm schemes.

II Literature Review

There is already a number of techniques and studies that have been implemented with an aim of combating poaching in Africa. Discussed below are some of the techniques;

In work [3] authors Mogomotsi and Madigela state that regardless of recent reductions in rhino poaching in Namibia and South Africa, it remains a worry. In their studies authors states that in response, the government of Botswana has implemented a (shoot-to-kill) policy, targeting poachers. The authors also goes further to say that the adoption of the green militarization in the form of a shoot-kill-policy has made a tension in northern Botswana where communities have complained of successive raids by the Botswana Defence force.

Nevertheless the study explains that militarized response effectively reduce poaching as the study went on say that Botswana had 1.12 percent of Africas rhinos in 2015, but accounted for only 0.1 percent of mortality's.In regard to analysis, this policy is intended to deter poachers by threat of death.(Shoot-to-kill) models are cheap to implement [4].

In a work [5] Mulero proposed utilizing drones as an anti-poaching strategies, authors mentioned that drones requires two fundamentals components which are the air frame and the ground station.Further the author stated that communication is facilitated between the air frame and the station,and that the aerial vehicles or drones use cameras and sensors in the gath-

ISSN: 2521-2292

ering of information. Mulero went on and state that he plane can operate at three various modes: autopilot, first person view mode and manually (radio control conventional mode/third person mode). An onboard first person view video camera, a GPS data logger with a barometric altitude sensor and an autopilot are equipped in the plane. The onboard screen board gives GPS data about the position, speed, course and height of the plane.The data is joined with the video from the camera is sent to the ground station.

In work [6] Mohan Rao and Sairam proposed that a communication system developed in wireless sensor networks should be able to achieve low power consumption for sensor using encoding of data at client nodes and decoding at the server node. The proposed system that use raspberry PI gadget to give web page and exchange the information onto web page so as to visualize the data from any location in this way accomplishing long distance transmission. The low power consumption is achieved based on encoding the data.

In a work [7] by Philip et al ,the authors strategy was based on dehorning the engaged species at Kruger National Pack, the authors put into thoughts that the horns will grow again. The authors states that according to statistics while dehorning was actualized then the country saw that there was 29.1 percent possibilities of survival of dehorned elephant as compared to horned rhinos. Dehorning technique is not viable as it is just a delaying strategy and also the execution cost is high, in addition poachers can retaliated by killing species or for the short stub that is left after dehorning.

In a work [4] the author state that DNA mapping is a one of strategies used to determine the precision location where the animal was killed. The authors went on to mention that a results of the implementation of the DNA mapping system was in 2002 by Singapore officials to trace back a container with 6.5 tons of ivory to Zambia, using a micro satellite a DNA is collected from the elephant dung and DNA was extracted from the tusks captured.However the method is ineffective because seizing the ivory does not save the elephants.

III Methodology

Based on the animal behavior of the animal, the parameter of interest was temperature. The sensor node interfaced with temperature sensor was used to detect difference in temperature from the elephant. The captured data was processed by the micro-controller. The processing function was to compare the detected temperature with already known data from studies.

From studies the normal temperature of an elephant is between 36.2 to 38.1. The processing was to check if the detected data is within this range if the data is not within this range.

Basically, since the WSN consists of 3 components: sensor nodes, gateway and observer. This network consists of similar components which are sensor node and gateway. The sensor nodes comprise of more individual components which are: power management circuit, temperature sensor , micro-controller and transceiver. While the gateway comprise of individual components like: transceiver, server and receiver station.

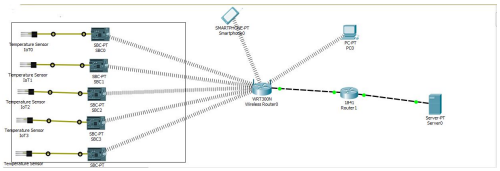


Figure 1: Network Diagram

The figure 1 shows the diagram of network arrangement from sensor node to the base station. The sensors are incorporated to the microprocessor to form a node.The temperature sensor captures analogue data of interest from the species and through microcontroller ,the data captured is processed and it is sent remotely to the wireless router.From the router a message will be sent to the base station through the antenna that is connected to the wireless transceiver. The obtained data is compared with known values. The authority in charge of the anti-poaching system will be notified of changes in the parameters of interest hence an alert will regarding the poaching activity.Therefore an action will be abruptly.

IV Results and Discussion

In the section regarding the outcomes, this is where the final stage of the network is encountered. The information received by the officers through the phone or computers at the receiving station. The officers will take relevant action based on the information they received.

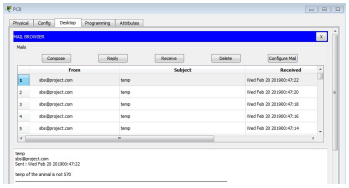


Figure 2: Results

Figure 2 shows readings are captured from the sensor, thereafter the data is being sent to the network through the wireless router. The data is meant for officers to see the situation of the animal and take relevant actions.

ISSN: 2521-2292

V Conclusion

The simulation was successful with the use of cisco packet tracer simulation tool. The simulation was based on wireless sensor network and data transmission where the sensor node temperature sensor was connected to the micro-controller for capturing and processing data. The micro-controller was also used to transmit the collected data to the base station where analysis was done and relevant action taken. In the future, Global positioning system will be incorporated in the system so as to enhance the tracking of endangered species.

References

[1] J. E. Mbaiwa, "Effects of the safari hunting tourism ban on rural livelihoods and wildlife conservation in Northern Botswana," *South African Geographical Journal*, vol. 100, no. 1, pp. 41–61, 2018.

[2] J. Kamminga, E. Ayele, N. Meratnia, and P. Havinga, "Poaching detection technologies-A survey," *Sensors (Switzerland)*, vol. 18, no. 5, 2018.

[3] G. Mogomotsi and P. Kefilwe, "Live by the gun, die by the gun. Botswana's "shoot and kill" policy as an anti-poaching strategy," *South African Crime Quarterly*, vol. 60, pp. 51–59, 2017.

[4] H. S. Koen and H. S. Koen, *Predictive Policing In An Endangered Species Context: Combating Rhino Poaching In The Kruger National Park*. PhD thesis, 2017.

[5] M. Mulero-Pázmány, R. Stolper, L. D. Van Essen, J. J. Negro, and T. Sassen, "Remotely piloted aircraft systems as a rhinoceros anti-poaching tool in Africa," *PLoS ONE*, vol. 9, no. 1, pp. 1–10, 2014.

[6] K. R. R. M. Rao and V. Sairam, "An Efficient Low Power Transmission Over Long Range in Wireless Sensor Networks for environmental studies," vol. 11, no. 2, pp. 657–665, 2016.

[7] M. A. Philip, C. H. How, H. S. Poh, Y. O. Lee, and H. Rishi, "Aerial Surveillance to Tackle Poaching,"

BIUST Research and Innovation Symposium 2019 (RDAIS 2019)
Botswana International University of Science and Technology
Palapye, Botswana, 4 - 7 June 2019

ISSN: 2521-2292

Numerical Fluid Mechanics Study of Effect of Rear Slant Length on the Drag of an Idealized Road Vehicle

Pako Pollard Mogotsi , Thato Phologolo
Dept of Mathematics & Statistical Sciences
Botswana International University of Science & Technology
Palapye, Botswana
Pako.mogotsi@studentmail.biust.ac.bw
Thato.phologolo@studentmail.biust.ac.bw

N.Subaschandar
Dept. of Mathematics and Statistical Sciences
Botswana International University of Science and Technology, Palapye, Botswana
raos@biust.ac.bw

***Abstract*— In all kinds of shapes and form road vehicles use up energy in the form of fuel. It is interesting to note that on the highway more than half of the useful energy output of the engine is used to accelerate and heat the surrounding air molecules. Aerodynamic drag is the aerodynamic force that opposes motion and accounts for a large fraction of transportation energy consumption. The main objective of this paper is to provide a solution to reduce the drag of an idealized road vehicle. This is achieved by modifying the design of vehicle by changing one parameter and then verifying mathematically whether the modification has any effect in reducing drag. Idealized vehicle geometry has been used. It has been known that the rear top slant angle of about 6 degs reduces the drag. In this research, a numerical fluid mechanics study has been carried out by keeping the rear slant angle constant, but changing the rear slant length from 50% to 10% of the rear half of the top surface. The computational part consists of numerical simulation of the flow around the body employing CFD (Computational Fluid Dynamics) techniques. Computations were carried out with and without ground effects. It was observed that drag coefficient reduced as the slant length is reduced from 50% to about 80% and then the drag coefficient starts increasing with rear slant length from about 80% to 90%.**

Keywords— ***Drag, turbulence, slant length, road vehicle***

I. INTRODUCTION

Studies show that a large fraction of goods worldwide are transported by road cargo transportation compared to other modes of transport. the excessive use of the road transport lead to numerous researches on how to increase the efficiency of the road cargo transportation. The industry of road vehicles is trying to develop various designs to reduce aerodynamic drag without constraints in the storage of the cargo. Also, the rapidly increasing fuel prices and the regulation of greenhouse gasses to control global warming give tremendous pressure on design engineers to enhance the current designs of the vehicle using the concepts of aerodynamics as to enhance the efficiency of vehicles.

Aerodynamic drag of a vehicle is directly related to the fuel consumption. In general, such vehicles are known to be aerodynamically inefficient compared to other ground vehicles due to their large frontal areas and bluff-body shapes. The inefficient aerodynamic shape results in excessive drag which leads to elevated fuel consumption rates. Contributions to heavy vehicle aerodynamic drag are mainly due to pressure drag, also known as form drag. It is estimated that the pressure drag on heavy vehicles accounts to more than 80% of the total aerodynamic drag [1], with frictional drag accounting for the remaining 20%. Any reduction in aerodynamics drag of a vehicle will help in reducing the fuel consumption thus helping in saving money and reducing the pollution caused by the burning of the fuel by the vehicles. With that motivation in mind, design engineers and manufacturers of vehicles, come up with different ways of reducing the aerodynamic drag of a vehicle. Retrofits for trucks aimed at improving aerodynamic performance and reducing the overall drag coefficient have recently shown great potential [2-4]. Examples of such drag-reducing devices include cab roof and side fairings, tractor and trailer side skirts, trailer-front fairings, vortex generators, and base-flaps. Studies for cab roof and side fairings show 9% to 17% drag reduction percentages on heavy vehicles [5-7]. Most of the studies carried out, as can be seen from the above references , are either experimental or real time empirical observations. Slant rear roof is one such technique used to reduce the drag of a road vehicle[1,3,6]. Most of the studies carried out, as can be seen from the above references, are either experimental or real time empirical observations. A numerical study presented in[8], estimated that a rear roof slant angle of 6^0 gave maximum reduction in drag of an idealized road vehicle. Also, their results showed that benefit occurred until the rear slant angle was about 12^0 and beyond that there was no benefit. However, the authors had fixed the rear roof slant length as 25% of the length of the vehicle. Since the flow over a three-dimensional road vehicle is very complex we consider an idealized configuration to represent the road vehicle. Also , because of the requirements of huge computing resources we

ISSN: 2521-2292

have modelled and carried out the research in a two dimensional space. The flow domain is assumed to be two dimensional and fluid is air. Steady, incompressible, constant viscosity and constant density assumptions have been made. Buoyancy and temperature effects have been neglected. The friction between the tires and the road, which happens in reality, has not been considered as this friction is common to all configurations and assumed to be uniform for all road vehicles. Also, drag due to the tractor in front of the trailer has not been considered as it is common to all configurations studied here. The two-dimensional CFD software Easy CFD has been used to carry out the computations and simulations and for data processing for all configurations[9].



Fig. 1 Picture of a road cargo transport vehicle without rear slant.

In the present study, the effect of the length of the rear slant length on the drag of an idealized road vehicle is presented. Fig. 1 shows the image of a road transport vehicle without rear slant. computational fluid dynamics(CFD) method has been used to carry out the research study. The computational fluid dynamics software EasyCFD has been used in this study. Easycfd is a computational fluid dynamics (CFD) software tool for the numerical simulation of two-dimensional and 3D axisymmetric fluid flow in a boundary fitted mesh[9].

II. COMPUTATIONAL DOMAIN

A two dimensional domain was used to study the effect of the rear slant length on the drag of an idealized road vehicle at a fixed angle of 6^0. The rear slant length started from the rear 50% of the vehicle and the slanted surface length decreased from 50% to 0% of the vehicle length, where 0% slant surface length represented a basic vehicle with any slant surface. For each configuration with different slant length the drag force acting on the truck was calculated and later used to calculate the drag coefficient which is defined by the Equation (1) bellow, where FD is the drag force, U_∞ is the airspeed, ρ is the air density, and A is the frontal area.

$$\mathbf{C_D} = \frac{\mathbf{FD}}{\mathbf{0.5 * \rho * U_\infty^2 A}} \quad \textbf{(1)}$$

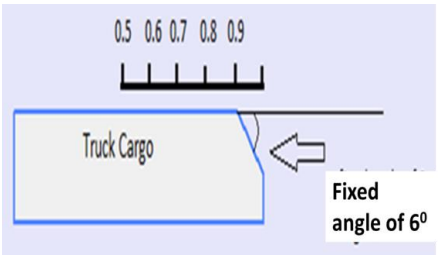


Fig 2: sketch of the geometry studied

III. MATHEMATICAL MODELLING

Governing Equations

1. Momentum Equations

- Horizontal Component

$$\frac{\partial(\rho u)}{\partial t} + \frac{\partial}{\partial x}(\rho u^2) + \frac{\partial}{\partial z}(\rho u w) = \frac{\partial}{\partial x}\left[\Gamma\left(2\frac{\partial}{\partial x} - \frac{2}{3}div\vec{V}\right)\right] + \frac{\partial}{\partial z}\left[\Gamma\left(\frac{\partial u}{\partial z} + \frac{\partial w}{\partial x}\right)\right] - \frac{\partial p}{\partial x}$$

- Vertical Component

$$\frac{\partial(p u)}{\partial t} + \frac{\partial}{\partial x}(\rho u w) + \frac{\partial}{\partial z}(\rho w^2) = \frac{\partial}{\partial z}\left[\Gamma\left(2\frac{\partial w}{\partial z} - \frac{2}{3}div\vec{V}\right)\right] + \frac{\partial}{\partial x}\left[\left(\frac{\partial u}{\partial z} + \frac{\partial w}{\partial x}\right)\right] - \frac{\partial p}{\partial z}$$

2. Continuity Equation

The conservation of mass law, or continuity equation, may be stated as:

$$\frac{\partial(\rho u)}{\partial t} + \frac{\partial}{\partial x}(\rho u) + \frac{\partial}{\partial z}(\rho w) = 0$$

ISSN: 2521-2292

3.The Standard k-ε Turbulence Model

The standard formulation of this turbulence model is described in [13].The turbulent viscosity is given by:

$$\mu_t = C_\mu \frac{\rho k^2}{\varepsilon}$$

The turbulence kinetic energy, k, as well as its dissipation rate, $\varepsilon [m^2/s^3]$, are computed with the following transport equations:

$$\frac{\partial(\rho k)}{\partial t} + \frac{\partial}{\partial x}(\rho u k) + \frac{\partial}{\partial z}(\rho w k) = \frac{\partial}{\partial x}\left[\left(\mu + \frac{\mu_t}{\sigma_k}\right)\frac{\partial}{\partial x}\right] + \frac{\partial}{\partial z}[(\mu + \frac{\mu_t}{\sigma_k})\frac{\partial k}{\partial z}] + P_k - \rho\varepsilon$$

$$\frac{\partial(\rho \varepsilon)}{\partial t} + \frac{\partial}{\partial x}(\rho u \varepsilon) + \frac{\partial}{\partial z}(\rho w \varepsilon) = \frac{\partial}{\partial x}\left[\left(\mu + \frac{\mu_t}{\sigma_\varepsilon}\right)\frac{\partial \varepsilon}{\partial x}\right] + \frac{\partial}{\partial z}\left[\left(\mu + \frac{\mu_t}{\sigma_\varepsilon}\right)\frac{\partial \varepsilon}{\partial z}\right] + \frac{\varepsilon}{k}(C_1 P_k - C_2 \rho \varepsilon)$$

The term P_1 represents the production rate of *k* as the results of the velocity gradients:

$$P_k = \mu_t[2\left(\frac{\partial u}{\partial x}\right)^2 + 2\left(\frac{\partial w}{\partial z}\right)^2 + (\frac{\partial u}{\partial z} + \frac{\partial w}{\partial x})^2]$$

The remaining constants are:

$$C_\mu = 0.09, \quad \sigma_{k=} = 1.0 \quad \sigma_\varepsilon = 1.3$$
$$C_1 = 1.44 \quad C_2 = 1.9$$

where K is known as the turbulent kinetic energy and ϵ is known the dissipation rate of the turbulent kinetic energy.

Boundary conditions for this computational study are given as follows :

Inlet Velocity=Inlet= 40 m/s

Outlet = Pressure outlet 1 atm.

Wall (truck-trailer) Stationary wall with no slip condition 0 m/s

Outer Walls = Walls = no slip condition

Numerical simulation to the road vehicle for both the basic and modified profiles was obtained by using EasyCFD software. Meshing to the geometrical model was done by opting 'body fit' mesh insert technique to vary the mesh element size in the computational domain.. The computational domain was meshed with fine mesh near the model and coarse mesh away from the model. The fluid was assumed to be incompressible air and its properties were constant. The flow is assumed to be two Dimensional and turbulent. Standard K-ϵ turbulence model has been used whose equations are given above. The Navier-Stokes equations selected for the conservation of mass and momentum have been were also given above.

IV. RESULTS AND DISCUSSION

In this section we present the results of the current research. The computations have been carried out taking ground effects into consideration and without taking ground effects into consideration. However only results for configurations without ground effects are presented here.

In computational fluid dynamics , final results should not be influenced by the number of grid elements in the computational domain(mesh size). To eliminate the influence of mesh size on the final result, a grid independence study was conducted. For this, flow past a two dimensional rectangle without rear slant surface was computed by changing the mesh size and for each case drag coefficient was calculated. Table 1 gives the values of the drag coefficient for various mesh sizes. From this we can see the drag coefficient value lies in the range of the values quoted in standard literature[10] and also the difference in the values of drag coefficient for the last two meshes is around 0.2%, which may be considered very small. Hence all subsequent computations were carried out by keeping the mesh size around 3000 elements.

Table 1 : Grid Independence study

Number of elements	Coefficient of drag(C_D)	Difference(%)
2560	1.4791	-
2754	1.5903	2.12
2910	1.6064	1.01
3040	1.6096	0.2

ISSN: 2521-2292

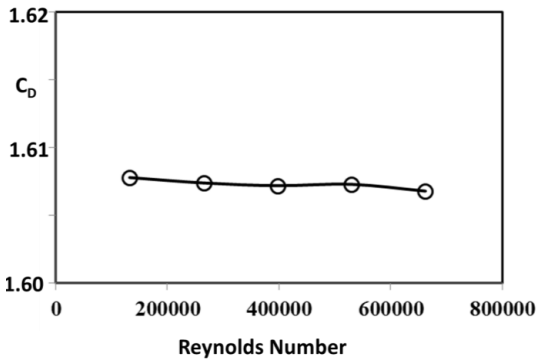


Fig. 3 : Variation of drag coefficient with Reynolds number

Figure 3 presents the variation of drag coefficient with Reynold number for the configuration without rear roof slant. Reynold number is defined as follows :

$$\text{Reynolds Number} = \frac{\mu U_\infty L}{\rho}$$

where L is the length of the vehicle , U_∞ , μ is the viscosity of air and ρ is the density of air. From the figure 3 we can see that at low speeds the drag coefficient for a configuration without rear roof slant does not vary with Reynolds Number and the average value of the drag coefficient is matching with the drag values quoted in literature[10]

Table 2 : Variation of drag coefficient with slant length

Configuration	Slant Wall Length(s/L)	C_D/C_{D0}	Reduction Drag(%)
no slant	0	1.000	
90% slant	0.1	1.003	-0.29
80% slant	0.2	0.942	5.78
70 % slant	0.3	0.925	7.75
60 % slant	0.4	0.923	7.77
50 % slant	0.5	0.929	7.09

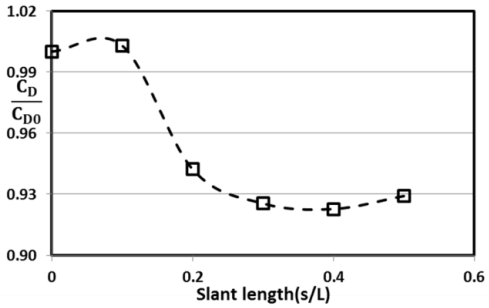


Fig. 4 Variation of drag coefficient with slant length

Table 2 and Figure 4 present the results of the current computations , namely , variation of drag coefficient with rear roof slant length. In Table 2 and Fig. 3, C_{D0} represents the drag coefficient when there no tailgate. From the table 3 and Figure 4 it can be seen that the drag coefficient initially increases and then starts decreasing as the rear roof slant length is increased reaching a minimum value of s/L = 0.4 which is equivalent to last 40 % of the vehicle length. After that it is increasing up to s/L=0.5 which is equivalent to the last 50% of the vehicle length upto which present computations were carried out.

V. CONCLUTIONS

The effect of rear roof length on the drag of an idealized road vehicle has been studied using computational fluid dynamics. The rear roof length was varied from s/L = 0 to 0.5. Effect of rear roof slant length on the drag coefficient with and without ground effect has been studied. Results on the effect of rear roof slant length on the drag coefficient without ground effect has been presented. It can be clearly seen from the results of this study that the rear roof slant length affects drag of an idealized road vehicle. The Drag coefficient initially increases with rear roof slant length and then starts decreasing recording a minimum value around s/L=0.4 which is equivalent to last 40% of the vehicle length. After that drag coefficient starts increasing reducing the benefit. The results show that a drag reduction upto 7.7 % can be achieved with a rear roof slant length of s/L=0.4. Studies with ground effect gave the same results.

REFERENCES

[1] Wood, R.M. Impact of Advanced Aerodynamic Technology on Transportation Energy Consumption. SAE Technical Paper 2004-01-1306, 2004, Washington.

[2] Wong H.Y., R.N. Cox, A. Rajan, Drag reduction of trailer-tractor configuration by aerodynamic means, Journal of Wind Engineering and Industrial Aerodynamics 1981, 9(1): p. 101–11.

[3] Hyams D.G., K. Sreenivas, R. Pankajakshan, D.S. Nichols, W.R. Briley and D.L. Whitfield. Computational simulation of model and full scale Class 8 trucks with drag reduction devices, Computers and Fluids 2011, 41(1): p. 27–40.

ISSN: 2521-2292

[4] Mohamed-Kassim Z and A. Filippone. Fuel savings on a heavy vehicle via aerodynamic
drag reduction, Transportation Research Part D 2010, 15(5): p. 275–284.

[5] Drollinger R.A. Heavy Duty Truck Aerodynamics. SAE Technical Paper 870001. 1986.
Washington, DC.

[6] Cooper K.R. Truck Aerodynamics Reborn-Lessons from the Past. SAE Technical Paper
2003-01-3376. 2003.

[7] Leuschen J., K.R. Cooper. Summary of full-scale wind tunnel tests of aerodynamic drag-

[8]. M.Mopipi, T.Phologolo and N. Subaschandar, "Numerical Fluid Mechanics study of effect of rear slant angle on the drag of an idealized road vehicle", Presented at the international Conference SAMSA2018, Southern African Mathematical Sciences Association, Palapye, Botswana, Nov 19-22, 2018.

[9]. http://www.easycfd.net/ , 2019, CFD software.

[10]. S.F. Hoerner, 1965, Fluid Dynamics Drag, Hoerner Publications, Bakersfield , CA , USA

BIUST Research and Innovation Symposium 2019 (RDAIS 2019)
Botswana International University of Science and Technology
Palapye, Botswana, 4 - 7 June 2019

ISSN: 2521-2292

STUDY OF EFFECTS OF TAILGATES ON THE DRAG OF AN IDEALISED ROAD VEHICLE USING NUMERICAL FLUID MECHANICS

Kenneth L. Bogatsu & Thato Phologolo
Dept of Mathematics and Statistical Sciences
Botswana International University of Science and Technology, Palapye, Botswana
kenneth.bogatsu@studentmail.biust.ac.bw
thato.phologolo@studentmail.biust.ac.bw

N Subaschandar
Dept of Mathematics and Statistical Sciences
Botswana International University of Science and Technology, Palapye, Botswana
raos@biust.ac.bw

Abstract:

In all kinds of shapes and form road vehicles use up energy in the form of fuel. It is interesting to note that on the highway more than half of the useful energy output of the engine is used to accelerate and heat the surrounding air molecules. Aerodynamic drag is the aerodynamic force that opposes motion and accounts for a large fraction of transportation energy consumption. The main objective of this paper is to provide a solution to reduce the aerodynamic drag of road vehicle. This is achieved by modifying the design of vehicle by attaching a tailgate to the end of the trailer and then verifying mathematically whether the modification has any effect in reducing drag. Idealized vehicle geometry has been used. In this study, a numerical fluid mechanics study has been carried out extending the tailgate on one side as well as on both sides. The angle of the tailgate is changed to study the influence of the tailgate angle on the drag of the trailer. Computations were carried out with and without ground effects. It was observed that drag coefficient reduced as tailgate angle is increased upto 25^0 and after that the drag starts increasing reducing the benefit.

I. INTRODUCTION

Road vehicles have been considered as one of the major causes of air pollution due to high fuel consumption caused by burning a lot of fuel to overcome drag. During the designs of all attributes of various vehicles, reduction of fuel economy is considered to be the most important thing. In the process of car design, the aerodynamics must be seriously considered. Therefore improving the fuel economy of trucks will have tremendous impact on energy security, emission of greenhouse gases and cost of fueling when fuel price rises. According to Wolf-Heinrich Hucho, road vehicles are bluff bodies in very close proximity to the ground and have an extremely complex detailed geometry. As is typical for bluff bodies, drag (which is a key issue for most road vehicles) is mainly pressure drag which is estimated to account for more than 90% of the total drag. Improving vehicle aerodynamics is one of the factors that play crucial role for getting better performance including the handling of the vehicle especially at high speeds Energy efficiency of vehicles can be improved by altering the exterior body shape to reduce the aerodynamic drag. It is estimated that the pressure drag on heavy vehicles accounts to more than 80% of the total aerodynamic drag[1], with frictional drag accounting for the remaining 20%. Any reduction in aerodynamics drag of a vehicle will help in reducing the fuel consumption thus helping in saving money and reducing the pollution caused by the burning of the fuel by the vehicles. With that motivation in mind, design engineers and manufacturers of vehicles, come up with different ways of reducing the aerodynamic drag of a vehicle. Retrofits for trucks aimed at improving aerodynamic performance and reducing the overall drag coefficient have recently shown great potential [2-4]. Examples of such drag-reducing devices include cab roof and side fairings, tractor and trailer side skirts, trailer-front fairings, vortex generators, and base-flaps. Studies for cab roof and side fairings show 9% to 17% drag reduction percentages on heavy vehicles [5-7]. Most of the studies carried out, as can be seen from the above references, are either experimental or real time empirical observations. In the current we study the effect of presence of the tailgate at the end of the trailer. We study the addition of a single tailgate at the end of the truck trailer. Closing the tailgate actually improves fuel efficiency because it creates a type of airflow called a separated bubble within the bed of the truck. As air flows over the moving truck, that bubble of slow-moving air deflects it over the raised tailgate. By guiding surrounding air over the top of a truck, that vortex effect prevents added drag. If air flow gets complex as in flows over a bluff body, the flow becomes turbulent and it is impossible to solve Navier-Stokes and continuity equations analytically. To come up with a solution to this problem Computational Fluid Dynamics methods and software are widely used in the very recent years. Since the flow over a three-dimensional road vehicle is very complex we consider an idealized configuration to represent the road vehicle. Also, because of the requirements of huge computing resources we have modelled and carried out the research in two dimensional space.

II. DESCRIPTION OF THE PROJECT

ISSN: 2521-2292

In this section we describe the research work that has been carried out in this project. The tailgate angle has been changed and for each configuration the flow field over the road vehicle has been simulated and drag coefficient has been calculated. We monitor the angle of one tailgate from the horizontal top of the truck trailer, the effect of increasing or varying the angle between the horizontal top of the truck trailer and the tailgate flap. This is computed and simulated using the Computational Fluid Dynamics method which is a numerical method along with appropriate conditions for the results.

The tailgate is mounted at end of the trailer and at the top of as an extension to the trailer. In reality, the tailgate is designed in such a way that access to the doors is not impeded, they sleep on the door surfaces, so opening doors will not be a problem. Tapering the back top end of a long vehicle will increase its base pressure by providing pressure recovery of the surrounding air flow before it leaves the sharp back top edge. The increase in base pressure provides a lowered overall pressure difference from the front to the back of the truck semi-trailer combination. The tailgate works by streamlining the trailer geometry. The air follows the flaps of the tailgate around the corner..

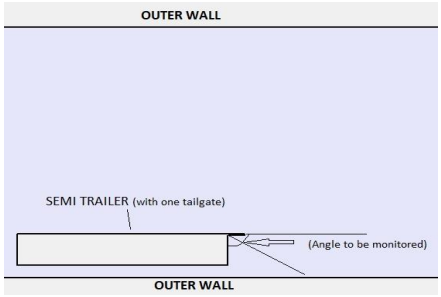


Fig 1: Sketch of the computational domain

Fig. 1 shows an idealized semi-trailer with a single tailgate aligned at the top of the horizontal part of the trailer, where the angle between the horizontal top of the trailer and the tail-gate flap is $\theta=0^{O}$. The computations have been simulated with and without ground effect, but the results have been presented with for configurations with ground effects because in reality road vehicles are very close to the ground. Hence ground effect plays a big role in aerodynamics of road vehicles. The inlet velocity is kept constant at 50m/s, which is about 180km/h.

The flow domain is assumed to be two dimensional and fluid is air. Steady, incompressible, constant viscosity and constant density assumptions have been made. Buoyancy and temperature effects have been neglected. The friction between the tires and the road, which happens in reality, has not been considered as this friction is common to all configurations and assumed to be uniform for all road vehicles. Also, drag due to the tractor in front of the trailer has not been considered as it is common to all configurations studied here. The two-dimensional CFD software Easy CFD has been used to carry out the computations and simulations and for data processing for all configurations[8].

III. MATHEMATICAL MODELLING

THE NAVIER-STOKE EQUATIONS :

Horizontal component;

$$\frac{\partial(\rho u)}{\partial t}+\frac{\partial}{\partial x}(\rho u^2)+\frac{\partial}{\partial z}(\rho uw) = \frac{\partial}{\partial x}\left[\Gamma\left(2\frac{\partial}{\partial x}-\frac{2}{3}div\vec{V}\right)\right] + \frac{\partial}{\partial z}\left[\Gamma\left(\frac{\partial u}{\partial z}+\frac{\partial w}{\partial x}\right)\right]-\frac{\partial p}{\partial x}$$

Vertical Component;

$$\frac{\partial(\rho u)}{\partial t}+\frac{\partial}{\partial x}(\rho uw)+\frac{\partial}{\partial z}(\rho w^2) = \frac{\partial}{\partial z}\left[\Gamma\left(2\frac{\partial w}{\partial z}-\frac{2}{3}div\vec{V}\right)\right] + \frac{\partial}{\partial x}\left[\left(\frac{\partial u}{\partial z}+\frac{\partial w}{\partial x}\right)\right]-\frac{\partial p}{\partial z}$$

Continuity Equation

$$\frac{\partial(\rho u)}{\partial t}+\frac{\partial}{\partial x}(\rho u)+\frac{\partial}{\partial z}(\rho w)=0$$

Turbulence Modelling Equations

$$\mu_t = C_\mu \frac{\rho k^2}{\varepsilon}$$

K-Equation

ISSN: 2521-2292

$$\frac{\partial(\rho k)}{\partial t}+\frac{\partial}{\partial x}(\rho uk)+\frac{\partial}{\partial z}(\rho wk)=\frac{\partial}{\partial x}\left[\left(\mu+\frac{\mu_t}{\sigma_k}\right)\frac{\partial}{\partial x}\right]+\frac{\partial}{\partial z}[(\mu+\frac{\mu_t}{\sigma_k})\frac{\partial k}{\partial z}]+P_k-\rho\varepsilon$$

ϵ- Equation

$$\frac{\partial(\rho\varepsilon)}{\partial t}+\frac{\partial}{\partial x}(\rho u\varepsilon)+\frac{\partial}{\partial z}(\rho w\varepsilon)=\frac{\partial}{\partial x}\left[\left(\mu+\frac{\mu_t}{\sigma_\varepsilon}\right)\frac{\partial\varepsilon}{\partial x}\right]+\frac{\partial}{\partial z}\left[\left(\mu+\frac{\mu_t}{\sigma_\varepsilon}\right)\frac{\partial\varepsilon}{\partial z}\right]+\frac{\varepsilon}{k}(C_1P_k-C_2\rho\varepsilon)$$

The modelling constants are :

$$C_\mu=0.09,\sigma_{k=}=1.0,\sigma_\varepsilon=1.3,\qquad C_1=1.44,\qquad C_2=1.9$$

where K is known as the turbulent kinetic energy and ϵ is known the dissipation rate of the turbulent kinetic energy.

Boundary conditions for this computational study are given as follows :

Inlet Velocity=Inlet= 40 m/s

Outlet = Pressure outlet 1 atm.

Wall (truck-trailer) Stationary wall with no slip condition 0 m/s

Outer Walls = Walls = no slip condition

Numerical simulation to the road vehicle for both the basic and modified profiles was obtained by using EasyCFD software. Meshing to the geometrical model was done by opting 'body fit' mesh insert technique to vary the mesh element size in the computational domain.. The computational domain was meshed with fine mesh near the model and coarse mesh away from the model. The fluid was assumed to be incompressible air and its properties were constant. The flow is assumed to be two Dimensional and turbulent. Standard K-ϵ turbulence model has been used whose equations are given above. The Navier-Stokes equations selected for the conservation of mass and momentum have been were also given above.

IV. RESULTS AND DISCUSSION

In this section we present the results of the current research. The computations have been carried out taking ground effects into consideration and without taking ground effects into consideration. However, only results for configurations without ground effects are presented here.

In computational fluid dynamics, final results should not be influenced by the number of grid elements in the computational domain(mesh size). To eliminate the influence of mesh size on the final result, a grid independence study was conducted. For this, flow past a two dimensional rectangle without tailgate was computed by changing the mesh size and for each case drag coefficient was calculated. Table 1 gives the values of the drag coefficient for various mesh sizes. From this we can see the drag coefficient value lies in the range of the values quoted in standard literature[10] and also the difference in the values of drag coefficient for the last two meshes is around 0.2%, which may be considered very small. Hence all subsequent computations were carried out by keeping the mesh size around 3000 elements.

Table 1 : Grid Independence study

Number of elements	Coefficient of drag(C_D)	Difference(%)
2560	1.4791	-
2754	1.5903	2.12
2910	1.6064	1.01
3040	1.6096	0.2

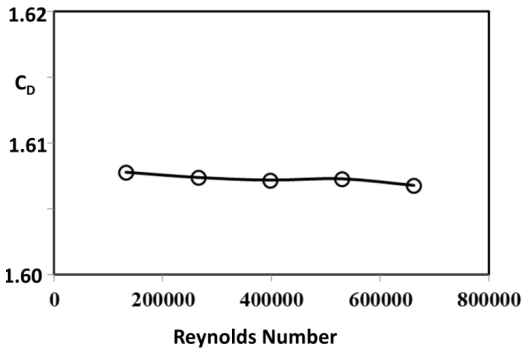


Fig. 2 : Variation of drag coefficient with Reynolds number

ISSN: 2521-2292

Figure 2 presents the variation of drag coefficient with Reynold number for the configuration without rear roof slant. Reynold number is defined as follows :

$$\text{Reynolds Number} = \frac{\mu U_\infty L}{\rho}$$

where L is the length of the vehicle , U_∞ , μ is the viscosity of air and ρ is the density of air. From the figure 3 we can see that at low speeds the drag coefficient for a configuration without rear roof slant does not vary with Reynolds Number and the average value of the drag coefficient is matching with the drag values quoted in standard literature [9]

Table 2: Showing drag coefficient at different angles

Tailgate Angle	C_D/C_{D0}
0	1.000
15	0.942
25	0.937
30	0.946
45	0.984

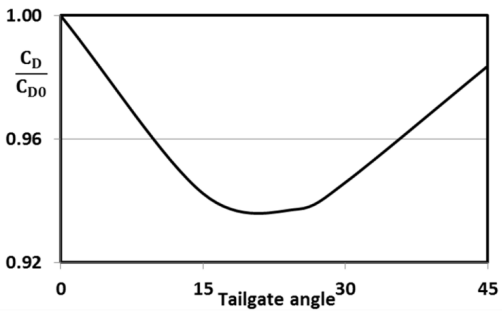


Fig 3: Drag coefficient variation with different angles of the tail-gate.

From Table 2 and Fig 3 we can notice that the drag coefficient was high at an angle of 0^0 and started decreasing as we increase the angle of the tail-gate with the horizontal top of the semi-trailer. In Table 2 and Fig. 3, C_{D0} represents the drag coefficient when there no tailgate. The drag coefficient kept decreasing up to an angle of about 25^0, then it started to increase with the increase of the angle of the boat-tails. At the tailgate angle of about 25^0 , the reduction in drag is about 6.3%. This reduction has been achieved for one tailgate. If we placed tailgates on all sides the resulting drag reduction will be more. However, in reality the flow is more complicated and the configurations are three-dimensional.

V. CONCLUSIONS

The effect of one tailgate on the drag of an idealized road vehicle has been studied using computational fluid dynamics. The tailgate angle was varied from 0^0 to 30^0. Effect of tailgate on the drag coefficient with and without ground effect has been studied. Results on the effect of tailgate on the drag coefficient with ground effect has been presented here. From all this simple modelling study we can see that tail-gating phenomenon is indeed possible and has a good impact on the drag coefficient an idealized road vehicles. It is shown that one tailgate mounted or placed at an angle of 25^0 will lower the amount of drag of an idealized road vehicle as much as by 6.3%. We can also conclude that the drag coefficient will be reduced further if tailgates are mounted on all sides at the end of the road vehicle.

REFERENCES

[1] Wood, R.M. Impact of Advanced Aerodynamic Technology on Transportation Energy Consumption. SAE Technical Paper 2004-01-1306, 2004, Washington.
[2] Wong H.Y., R.N. Cox, A. Rajan, Drag reduction of trailer-tractor configuration by aerodynamic means, Journal of Wind Engineering and Industrial Aerodynamics 1981, 9(1): p.101–11.
[3] Hyams D.G., K. Sreenivas, R. Pankajakshan, D.S. Nichols, W.R. Briley and D.L. Whitfield. Computational simulation of model and full scale Class 8 trucks with drag reduction devices, Computers and Fluids 2011, 41(1): p. 27–40.
[4] Mohamed-Kassim Z and A. Filippone. Fuel savings on a heavy vehicle via aerodynamic drag reduction, Transportation Research Part D 2010, 15(5): p. 275–284.
[5] Drollinger R.A. Heavy Duty Truck Aerodynamics. SAE Technical Paper 870001. 1986. Washington, DC.
[6] Cooper K.R. Truck Aerodynamics Reborn-Lessons from the Past. SAE Technical Paper 2003-01-3376. 2003.
[7] Leuschen J., K.R. Cooper. Summary of full-scale wind tunnel tests of aerodynamic drag-
[8]. http://www.easycfd.net/ , 2019, CFD software.
[9]. S.F. Hoerner, 1965, Fluid Dynamics Drag, Hoerner Publications, Bakersfield , CA , USA

BIUST Research and Innovation Symposium 2019 (RDAIS 2019)
Botswana International University of Science and Technology
Palapye, Botswana, 4 - 7 June 2019

ISSN: 2521-2292

Autonomous Trash Collector Robot with Wireless Charging System in a Campus Environment

Analene Montesines Nagayo[1], Bindu Puthentharayil Vikraman[2], Mazna S.H. Al Saidi [3], Ammar S. Al Hosni[4], Ali K. Al Kharusi[5]
Department of Engineering
Al Musanna College of Technology
Muladdah, Sultanate of Oman
[1]analene@act.edu.om, [2]bindu@act.edu.om,
[3]2J13302@act.edu.om, [4]52S12127@act.edu.om,
[5]52S1264@act.edu.om

Rodrigo S. Jamisola Jr.[6]
Mechanical, Energy and Industrial Engineering Department
Botswana International University of Science and Technology
Palapye, Botswana
[6]jamisolar@biust.ac.bw

***Abstract*— This work presents the design and implementation of an autonomous trash collector VEX Clawbot attached with a loading bin that is controlled by Arduino microcontroller. Features of the robot include GSM and GPS modules for localization and status update, as well as automatic wireless charging from solar power source. The robot prototype travelled an entire path of 3.5m, with an average time 30 sec, where a waste segregator is located at the end of the path. Average time to pick up each type of trash and place in backside loading bin is 20 seconds with an 80% accuracy.**

Keywords*— *Waste collection, VEX clawbot, Arduino microcontroller, GSM/GPS monitoring, wireless charging, solar power

I. Introduction

Manual waste collection and segregation of waste materials is still done in many countries like Oman, India and Philippines [1] - [5]. According to [4], human rag pickers and garbage collectors are still extensively employed in the gathering and disposing of solid waste. However, they are susceptible to to skin infections, allergic disorders, respiratory and gastrointestinal problems [5]. To contribute to the solution of waste collection with minimum human involvement, a self-driving trash collector robot was designed and implemented.

This research allows waste collection to be done with minimal health hazard and safety risk to humans using engineering technology. The robot is battery operated which can be charged wirelessly using a solar energy power source, making the system eco-friendly.

In this paper, Section II cites the recent developments in the design and implementation of autonomous trash collector robots. Section III describes the design, set-up and implementation of the autonomous trash collector robot with wireless charger, GSM and GPS monitoring system. In Section IV, the experimental data are presented to show the performance and response time of the designed robot in promoting a clean and green campus environment. Lastly, Section V concludes the paper and presents the future directives of the robotic system for extensive waste management program.

II. Recent Developments in the Design and Implementation of a Trash Collector Robot

Several researches are done about autonomous garbage collecting robot with one common goal which is to pick trash and deposit it to its appropriate recycle bin [6]-[17]. The design methods and implementation of these robots may vary depending on the application.

A study in [6] presented a line following mobile garbage collector that will gather wastes from three bins, then deposits the waste in an automatic sorter system. The system was implemented using PIC microcontroller interfaced with line following sensor, H-bridge motor drive and DC motors. The robot completed the task of collecting and delivering the trash in 4 minutes and 36 seconds [6]. Line following robots are simple to implement but have slow speed and instability with different line width or stiff angles [7].

Another PIC-based robot was developed for collecting the garbage at the beach [8]. Bluetooth and Adhoc wireless communication technologies were applied to the robot for remote controlled operation at an average speed of 0.5 m/s on the sand [8]. The trash collector robot can be easily controlled using push button switch or mobile phone using Bluetooth technology, but the user can only operate it at a limited distance [9].

An automatic garbage collector named AGATOR shown in [10] was developed to limit the accumulation of wastes in a river under weak or no water flow condition. The system uses ATMega16 as master robot controller, while ATMega8 read signal from ultrasonic sensor to determine the position of the garbage and communicate serially with the master controller for necessary trash collecting operation [10]. This system is not capable of tracking the location of AGATOR when working on the river, so the use RFID as a monitoring tool was recommended by the researchers.

Another design of trash collector robot is done in [11] using Arduino microcontroller interfaced with ultrasonic and infrared sensors. The sensors are used to detect and avoid obstacle in the robot's path using the combination of S-shaped and wall follow algorithms. A vacuum cleaning device was used for waste collection by means of suction [11]. To improve robot vision in

ISSN: 2521-2292

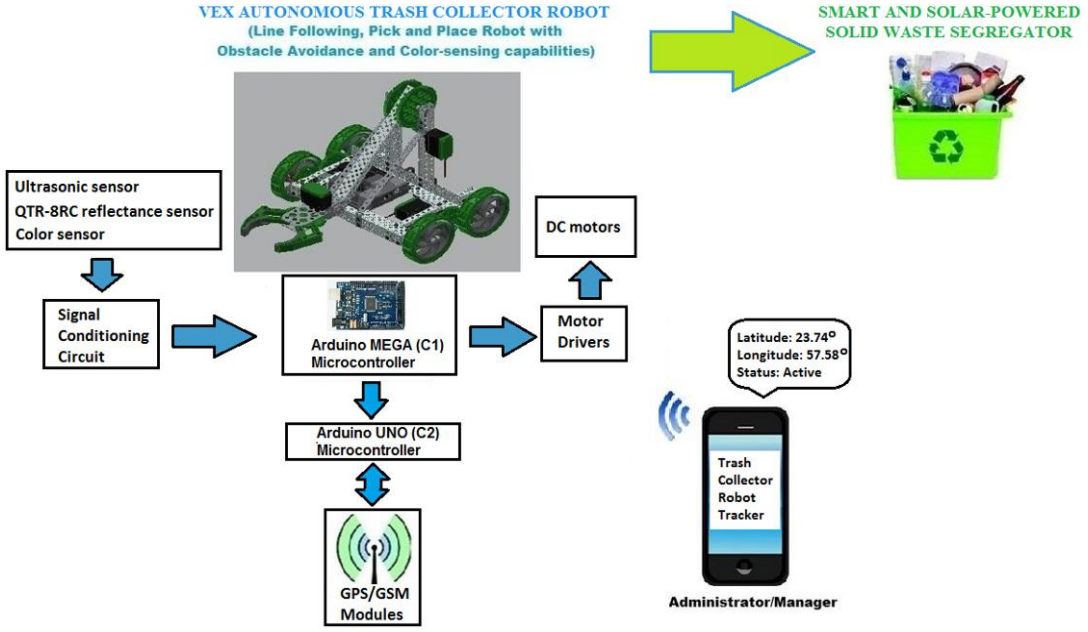


Fig.1. Block Diagram of the trash collector robot

detecting trash if it is biodegradable or not, image processing technique is employed by Ranganath et al. [12]. Raspberry Pi serves as the master controller where image processing program is executed, and the instructions are sent serially to Arduino which acts as a slave that will control the robot movement [12].

Robot localization, activity status update and motion planning of trash collecting robot may be implemented using Wi-Fi [13],[14], GPS [15] and GSM [15],[16] technologies. An access point or Wi-Fi Board must be installed to the robot in order to connect to a WLAN and a high speed internet connection is needed for real time transmission of status update and robot's location [9]. For robot absolute localization, GPS [15] or optical beacons [17] may be used. However, GPS signal is weak indoors and its accuracy is poor for small distances [18]. According to [16], GSM can be used in monitoring robots due to its established long range, secure, fast and reliable connection.

III. Autonomous Trash Collector Robot Control and Monitoring System Design Considerations

A. Block Diagram of the Trash Collector Robot

Referring to Fig.1, the trash collector robot (TCR) system is an autonomous line follower robot that utilizes color sensors, QTR reflectance sensors, ultrasonic sensors and DC motors to properly pick-up recyclable waste materials such as aluminum cans, plastic bottles, glass bottles and papers along its path, drop the trash in its backside loading bin then bring it to the receiving end of a Solid Waste Segregation System (SWSS). The wastes are dumped by the robot to the elevator conveyor which will transfer the trash to the horizontal belt conveyor for sorting. The Arduino MEGA (C1) is the master controller which reads and processes data from various sensors, and actuates the motors to perform a controlled robotic operation. The Arduino UNO (C2) is a slave microcontroller used for robot localization and status update. A GPS shield is connected to the microcontroller C2 for monitoring the location of the TCR. A GSM modem is interfaced with the microcontroller C2 that sends SMS message to the administrator about the latitude and longitude coordinates of the robot, status of the robot and if breakdown is detected in the TCR. Moreover, the robot is charged wirelessly from a solar power source as it parks at the docking bay.

B. Design Considerations for the Trash Collector Robot Mechanism

The wheels, body chassis and arms of the trash collector robot (TCR) were assembled using a VEX Clawbot kit [19] as presented in Fig. 2. At the back of the TCR, a loading bin constructed to carry aluminum cans, plastic bottles, papers and glass bottles towards the receiving end of a solid waste segregation system (SWSS).

A gravity actuated unloading design was adopted instead of a motor actuated to significantly reduce the overall weight of the robot by eliminating the motor and additional battery. The swinging door of the bin can be opened or closed by a small electromagnet which will be activated by the microcontroller. The loading bin for the trash collector robot is shown in Fig. 2.

ISSN: 2521-2292

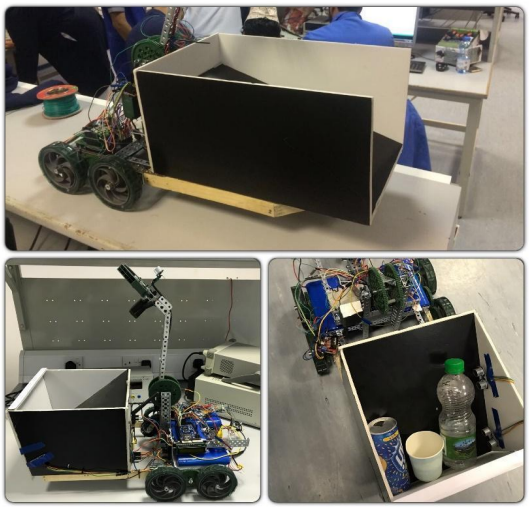


Fig. 2. Trash collector VEX Clawbot with backside loading bin

C. *Control System of Trash Collector Robot*

The line following, pick and place and obstacle avoidance tasks of the trash collector robot (TCR) are accomplished using the following sensors: (a) QTR-8RC reflectance sensor that detects black and white line in the robot's path; (b) color sensor that detects the unloading point at the SWSS area marked by red color, and (c) Ultrasonic sensor that detects objects along the robot's path and identifies if the trash bin is full or not.

The Arduino MEGA (C1) microcontroller was programmed to read and process data from various sensors that would determine the robot's path and movement. The robot consists of two motors activated by the Arduino microcontroller through the LN298 driver circuits based on the sensor readings. The program flowchart for the TCR is shown in Fig. 3.

Microcontroller C1 continuously reads all sensors connected to its input pins. When the color sensor output reaches a predefined value, the microcontroller sends sequence of control signal for unloading the trash. If the color sensor value is not in the range of detection, it checks the ultrasonic output. Ultrasonic sensor monitors the obstacles in front and if the distance is less than the cutoff value, microcontroller C1 sends signal to stop the robot. The control signals needed for pick and place the object is send by the microcontroller. The robot follows the assigned path based on the line tracking sensor output values. It continuously monitors the QTR output values and decisions on its left, right, forward and reverse movement is done.

The designed trash collector robot (TCR) can follow a path with a black line on a white surface using QTR 8A reflectance sensor array. The robot uses an array of 3 IR LED as emitter and phototransistor as receiver, which are facing the ground to sense the line. The output of the sensors is an analog signal which depends on the amount of light reflected. This analog signal is fed to the microcontroller input pin. The microcontroller C1 decides the next movement based on the program written and the input obtained from the line tracking sensors.

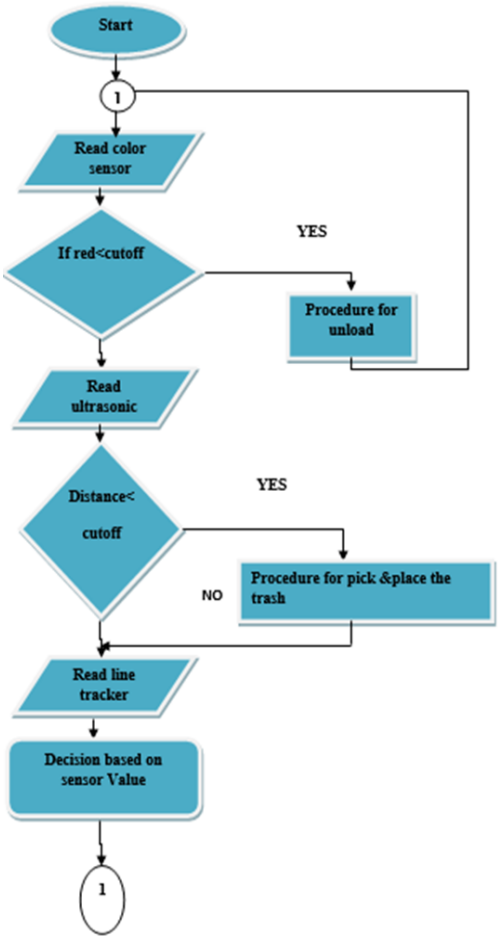


Fig. 3. Program flowchart for the trash collecting robot

For the pick and place task of TCR, two DC motors were utilized. One motor is used for the arm movement and the other one for the claw movement. These two motors are interfaced to the microcontroller using motor driver IC LN298. The PWM pins of microcontroller C1 is used for sending control signal for the arm and claw movements, as control of movement speed can be done through these pins. Normally, the arm will be in the down position with claw open. When the ultrasonic sensor identifies the trash, the microcontroller sends signal to grab and hold the trash. Consequently, the claw closes and control signal is given to move the arm up, until it reaches the back bin. The microcontroller C1 sends signals for opening the claw to keep the trash in the bin. After placing the trash in the bin, the arm is moved back to its original down position, with claw open.

For the overall control of the TCR, the three reflectance sensors connected to microcontroller C1 gives information about the path that the robot must follow. Depending on these sensor output values, the microcontroller sends signals for

ISSN: 2521-2292

forward, left and right movement of the TCR. The TCR movement is performed using a pair of motors, interfaced through the motor driver IC with the microcontroller C1. The ultrasonic sensor connected to the microcontroller gives information about the trash ahead in its path. When it identifies a trash, a sequence of control signals is sent to pick the trash on its path and for placing it in the robot backside bin. An ultrasonic sensor is connected to the microcontroller C1 for determining whether the backside loading bin of robot is empty or full of trash. If it is full the robot goes to the final destination marked with a red post. The color sensor interfaced with the microcontroller gives information about the final destination where the trash is transferred to the conveyor for segregation. When the TCR identifies the assigned color for destination, control signals are sent to keep the robot near to the conveyor belt. After reaching the conveyor belt, the microcontroller C1 sends signals to energize the relay, which in-turn deactivates the electromagnet and opens the back bin to drop the trash in the elevator conveyor. Microcontroller C1 generates digital output signals to indicate the status of the robot and backside loading bin.

For the power management of the TCR, microcontroller C1 reads the voltage level of the battery from one of its analog pins. If the voltage level is below 7.0 V, TCR is programmed to go to the starting point where a docking bay is installed for wireless charging.

D. Monitoring System of Trash Collector Robot

For monitoring purposes, A GSM modem SIM900 is interfaced with Arduino UNO (C2) microcontroller to send SMS message to the administrator about the status of the robot, its activity and if breakdown has occurred in the TCR. A GPS shield is also interfaced with microcontroller to monitor the location of the Trash Collector. To determine if robot is active, fault has occurred or the trash bin is full, the microcontroller C2 reads status signal sent by microcontroller C1. Fig. 4 shows the actual implementation of the TCR monitoring system.

E. Wireless Charging System of Trash Collector Robot

Referring to Fig. 5, the solar panel connected to charge controller charges the 12 V, 200 Ah deep cycle battery. A DC to DC converter is connected to solar power source to step down the voltage from 12 V DC to 5 V DC in order to meet the transmitter circuit requirement. The transmitter circuit converts the DC voltage into a high frequency alternating current then it is fed to the transmitting coil [25]. The high frequency AC signal flowing within the transmitter coil creates an alternating magnetic flux which extends to the receiver coil when the two coils are placed within a specified distance [26]. As the robot parks in the docking area, the magnetic flux is transmitted from the transmitter coil mounted in the floor to the receiver coil placed in the bottom of the robot by electromagnetic induction.

In the wireless receiver side, the receiver coil receives the energy as an induced alternating voltage in accordance to Faraday's Law of Induction [24]. Rectifier, filter and linear regulator are used to convert the induced AC voltage into a stable DC voltage required by the robot's battery [27]. The prototype for the Robot Wireless Charging System is shown in Fig. 6. The robot parks in the docking bay to charge its battery.

IV. Experimental Data and Analysis of Results for the Self-Driving Trash Collector Robot System

A. Experimental Set-up and Test Results of the Control and Monitoring System for the Autonomous Trash Collector Robot

Prior to the actual testing, the sensors attached to the microcontroller C1 of the trash collector robot (TCR) such as QTR sensor, color sensor and ultrasonic sensors were calibrated to perform task accurately. A 3.5-meter arena is set-up to test the performance of the TCR. Table I shows the performance and response time of the robot in completing the task of following the black path, identifying trash along its path, picking and placing the trash to its backside loading bin and identifying the final destination point going to the SWSS area for 5 test runs. Each test run is done with 5 trials.

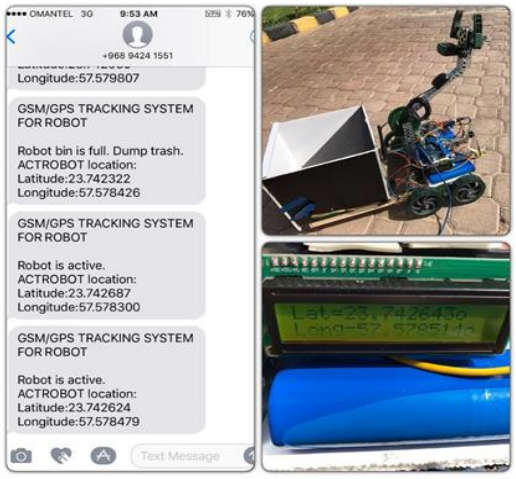


Fig. 4. Trash collector robot monitoring system

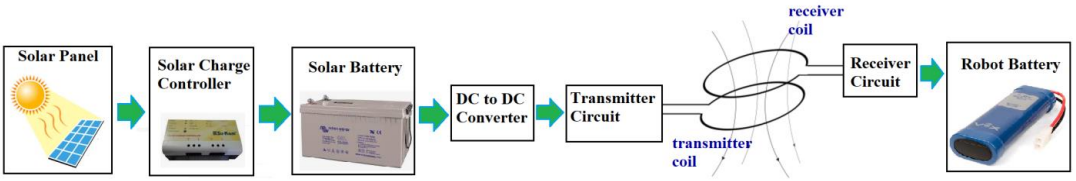


Fig. 5. Robot Wireless Charging System Block Diagram

ISSN: 2521-2292

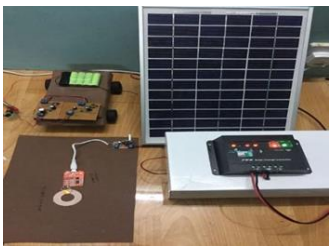


Fig. 6. Wireless charging system of the trash collector robot

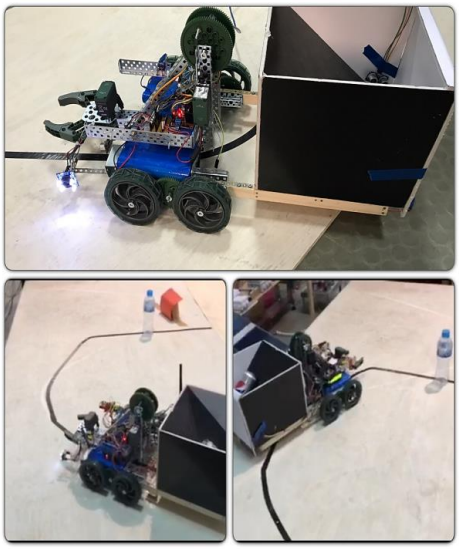


Fig. 7. Line following operation of the trash collecting robot

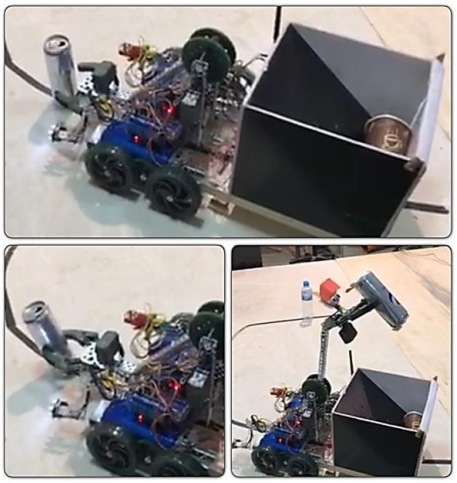


Fig. 8. Pick and place operation of the trash collector robot

Fig. 7 shows the line following operation of the TCR using QTR. The robot followed the path with black line with an 88% reliability as seen in Table I. The failure rate was due to the instability of the robot in following stiff curve.

Fig. 8 presents how the robot performs the pick and place task with a reliability of 80%. The ultrasonic sensor connected to the microcontroller gives information about the trash along the robot's path. When it identifies a trash, a sequence of control signals is sent to pick the trash on the path and place it in the backside loading bin of the robot. The failure rate in picking the trash is due to the position of the trash along the path.

As seen in Fig. 9, color sensor interfaced with the microcontroller gives information about the final destination where the trash is transferred to the conveyor for segregation. When the TCR identifies the red color for final destination, control signals are sent to make the robot move backwards going to the elevator conveyor. From Table I, the robot was able to detect the red colored post for the final destination with 80% reliability.

The monitoring system for the TCR was done using GSM and GPS shields interfaced with Arduino microcontroller. The sample SMS received by the administrator for monitoring the robot status, activity and location is shown in Fig. 4. Also, the location of the robot in terms of latitude and longitude are displayed in the LCD installed in the TCR.

TABLE I. PERFORMANCE AND RESPONSE TIME OF THE TRASH COLLECTOR ROBOT

Test Run	Robot task		Average time taken to complete the task in seconds	Reliability
1	Pick and place	Object1	Unsuccessful	33.33%
		Object2	Unsuccessful	
		Object3	24 sec	
	Following the path		19 sec	60%
	Identifying the destination by using color sensor		12 sec	60%
2	Pick and place	Object1	24 sec	66.67%
		Object2	Unsuccessful	
		Object3	13 sec	
	Following the path		22 sec	80%
	Identifying the destination by using color sensor		3 sec	60%
3	Pick and place	Object1	24 sec	100%
		Object2	23 sec	
		Object3	13 sec	
	Following the path		24 sec	100%
	Identifying the destination by using color sensor		5 sec	80%
4	Pick and place	Object1	13 sec	100%
		Object2	24 sec	
		Object3	25 sec	
	Following the path		24 sec	100%
	Identifying the destination by using color sensor		5 sec	100%
5	Pick and place	Object1	24 sec	100%
		Object2	23 sec	
		Object3	13 sec	
	Following the path		28 sec	100%
	Identifying the destination by using color sensor		5 sec	100%

ISSN: 2521-2292

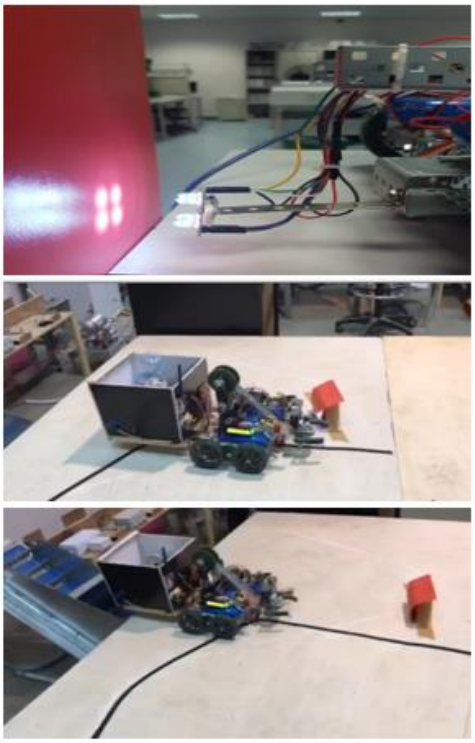


Fig. 9. Color sensing operation of the trash collector robot

B. *Experimental Set-up and Test Results of the Wireless Charger System for the Trash Collector Robot*

At the transmitter side of the wireless charger, the circuit was tested by taking its frequency and voltage readings. The transmitter was able to generate a high frequency AC signal as seen in Table II. The receiver circuit was able to charge the 7.2 V battery of the VEX robot in a time of 100 minutes. Fig.10 shows how the robot parks in the docking bay found at the starting point for wireless charging operation.

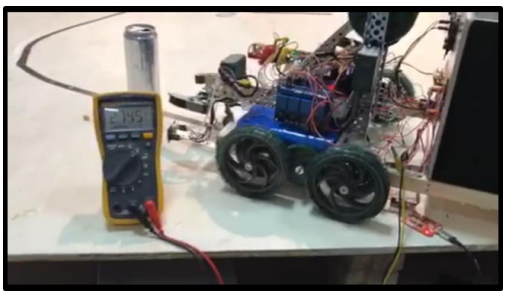


Fig 10. Robot parks in the docking bay for wireless charging operation

TABLE II. FREQUENCY AND VOLTAGE OUTPUT OF TRANSMITTER CIRCUIT

Frequency (KHz)	Voltage (V)
172	21
185	20.8
209	23
211	26

V. CONCLUSION

The recent researches in the design and implementation of a trash collector robot are presented in this paper with one mutual aim which is to gather waste materials and deposit them in their appropriate garbage bins with minimal health and safety risks. The design and implementation of an Autonomous Arduino-based Trash Collector Robot (TCR) was accomplished which allow solid wastes to be gathered and delivered for waste segregation. The line following, pick and place and obstacle avoidance tasks of the TCR are accomplished using QTR-8RC reflectance sensor, color sensor and ultrasonic sensor. In the pick and place operation, proper placement of trash in the lined path plays a crucial part in determining the accuracy of the TCR. Real-time monitoring of the robot's status and location were achieved using wireless communication technologies. A GPS shield is connected to the microcontroller for robot localization. GSM modem is connected to microcontroller to sends SMS message to the waste administrator about the status, location and any malfunction of the TCR. A wireless charging module powered from a solar source was successfully designed and implemented to charge the TCR batteries as needed when it parks in the docking bay.

Based on performance and response time testing of the TCR, this work recommends an improvement on its pick and place capability by using additional ultrasonic sensors and high-powered DC motors [6], as well as integration of camera and image processing techniques [12]. It is also recommended that for relative and indoor localization of TCR, on-board sensors such as gyroscope, accelerometer and encoders may be used [18].

ACKNOWLEDGMENT

Special thanks to Al Musanna College of Technology (ACT) for the full support given to this multi-disciplinary project, and The Research Council (TRC) of Oman for funding major part of this project. Thanks to SWSSTCR team members: Eugene Vega, Cesar Mendoza, Omar Rashid Al Maqbali, Ammar Yousuf Al Farsi, Tasnim Khasif Al Mughaizwi, Raja Muhammed Al Rawahi, Emanuel Rances, Jefferson Zason, Rolando Cabais, Jorge Ramos, Alex Boral, Ericson Recamata for all their support and cooperation.

REFERENCES

[1] T.M. Palanivel and H. Sulaiman, "Generation and Composition of Municipal Solid Waste (MSW) in Muscat, Sultanate of Oman," APCBEE Procedia, Vol. 10, Pages 96-102, 2014

[2] Zafar, S. (2015). Solid Waste Management in Oman. [Online] Available: http://www.ecomena.org/solid-waste-oman [Accessed: March 2, 2016]

[3] M. Joubert (2013). National Strategy for Waste Management. [Online] Available: http://omanobserver.om/national-strategy-for-waste-management [Accessed: March 2, 2016]

ISSN: 2521-2292

[4] V. K. Ojha, V. Tripathi and V. Krishna, “Role of rag pickers in solid waste management: a case study of Mirzapur, UP,” International Journal of Environmental Technology and Management, 17(2-4), 134-142, 2014.

[5] S. Dwivedi, M. Fernandes and R. D’souza, “A Review on PLC based Automatic Waste Segregator,” International Journal of Advanced Research in Computer Engineering & Technology (IJARCET), vol.5, no. 2, 280-285, 2016

[6] F. G. Ang, M.K.A. Gabriel, J. Sy, J. J. O. Tan and A. C. Abad, “An Automated Waste Sorter with Mobile Delivery Waste System,” presented at 2013 DLSU Research Congress. DLSU, Manila, 2013

[7] Line Follower Robot. [Online] Available: https://www.pantechsolutions.net/robotics-projects/line-follower-robot [Accessed: April 11, 2019]

[8] S. Wattanasophon, S. Ouitrakul, "Garbage Collection Robot on the Beach using Wireless Communications," Int. Proc. Chem. Biol. Environ. Eng., vol. 66, pp. 92-96, 2014.

[9] S. Kahar, R. Sulaiman, A. S. Prabuwono, N. A. Ahmad and M. A. Abu Hassan, "A Review of Wireless Technology Usage for Mobile Robot Controller," 2012 International Conference on System Engineering and Modeling (ICSEM 2012) IPCSIT vol. 34, pp. 7-12, 2012.

[10] O. Nurlansa, D. A. Istiqomah and M. A. S. Pawitra, “AGATOR (automatic garbage collector) as automatic garbage collector robot model,” International Journal of Future Computer and Communication, 3(5):367–371, 2014.

[11] G. Sivasankar, B. Durgalakshmi and K. Seyatha, “Autonomous Trash Collecting Robot,” International Journal of Engineering and Technology, 6(4):162-165, 2017.

[12] R. Ranganath, B. Sharma, P. AR, R. C. Jadhav, A. A., “Autonomous Garbage Collecting Robot Wall-E,” International Journal of Scientific Research and Development, 5(4):524-526,2017.

[13] V. T. Wilson, M. Venkatesh, S. Panicker, S. G. Bhat and R. Sanjeetha, "Smart waste Collecting Hopper (SWaCH): A service for all," 2015 Twelfth International Conference on Wireless and Optical Communications Networks (WOCN), Bangalore, 2015, pp. 1-4.

[14] Kisron, B. S. B. Dewantara and F. Ardilla, "Self-Monitoring, Failure-Detection and Decision-Making System to Support E-TrashBot (EEPIS Trash Bin Robot) Operations: Preliminary Report," 2018 10th International Conference on Information Technology and Electrical Engineering (ICITEE), Kuta, 2018, pp. 1-6.

[15] A.M. Nagayo, M. S. H. Al Saidi, O. R. Al Maqbali, A. Y. Al Farsi, A. K. Al Kharusi, A. S. Al Hosni, T. K. Al Mughaizwi, R. M. Al Rawahi, “A Smart Solar-powered Waste Segregation System with Integrated Self-driving Robot Collector towards Environmental Sustainability in School Campus,” presented at the National Research Forum, TRC, Sultanate of Oman, December 2017, unpublished.

[16] B. N. Binoy, T. Keerthana, P. R. Barani, A. Kaushik, A. Sathees and S. N. Aswathy, "A GSM-based versatile Unmanned Ground Vehicle," INTERACT-2010, Chennai, 2010, pp. 356-361.

[17] G. Ferri, A. Manzi, P. Salvini, B. Mazzolai, C. Laschi and P. Dario, "DustCart, an autonomous robot for door-to-door garbage collection: From DustBot project to the experimentation in the small town of Peccioli," 2011 IEEE International Conference on Robotics and Automation, Shanghai, 2011, pp. 655-660.

[18] P. Goel, S.I. Roumeliotis, and G.S. Sukhatme, “Robot Localization using Relative and Absolute Position Estimates,” in Proc IEEE Int. Conference on Robots and Systems, Kyongju, Korea, 1999.

[19] VEX Clawbot. [Online] Available: https://www.robotmesh.com/vex-clawbot-kit [Accessed: October 1, 2016].

[20] F. Kaiser, S. Islam, W. Imran, K. H. Khan and K. M. A. Islam, "Line follower robot: Fabrication and accuracy measurement by data acquisition," 2014 International Conference on Electrical Engineering and Information & Communication Technology, Dhaka, 2014, pp. 1-6.

[21] Yuta, S. I., Suzuki, S., & Iida, S, “Implementation of a small size experimental self-contained autonomous robot—sensors, vehicle control, and description of sensor-based behavior,” Experimental Robotics II, 344-358, 1993.

[22] T. Kotthauser and G. F. Mauer, "Vision-based autonomous robot control for pick and place operations," 2009 IEEE/ASME International Conference on Advanced Intelligent Mechatronics, Singapore, 2009, pp. 1851-1855.

[23] K. Bhagat, S. Deshmukh, S. Dhonde & S. Ghag, “Obstacle Avoidance Robot,” International Journal of Science, Engineering and Technology Research (IJSETR), 5(2), 439-442, 2016.

[24] Chin-Sheng Wu, "Obstacle avoidance of autonomous mobile robots," Proceedings IEEE 31st Annual 1997 International Carnahan Conference on Security Technology, Canberra, ACT, Australia, 1997, pp. 158-160.

[25] A. Parmar and S. Khurana. Wireless Charging. [Online] Available: https://medium.com/swlh/wireless-charging-c0a35351ffe8 [Accessed: October 1, 2016].

[26] Sam Sattel. Wireless Charging: How Qi Charging works. [Online] Available: https://www.autodesk.com/products/eagle/blog/wireless-charging-qi-charging-works/ [Accessed: April 11, 2019].

[27] Introduction to Wireless Battery Charging. [Online] Available: https://www.idt.com/products/power-management/wireless-power/introduction-to-wireless-battery-charging [Accessed: April 11, 2019].

BIUST Research and Innovation Symposium 2019 (RDAIS 2019)
Botswana International University of Science and Technology
Palapye, Botswana, 4 - 7 June 2019

ISSN: 2521-2292

A Smart and Solar-Powered Solid Waste Segregator with Cloud-Based Wireless Monitoring System in a School Campus

Analene Montesines Nagayo[1], Eugene Vega[2], Omar Rashid Al Maqbali[3], Ammar Yousuf Al Farsi[4]
Department of Engineering
Al Musanna College of Technology
Muladdah, Sultanate of Oman
[1]analene@act.edu.om, [2]eugene@act.edu.om,
[3]12S12331@act.edu.om, 452S12329@act.edu.om

Rodrigo S. Jamisola Jr.[5]
Mechanical, Energy and Industrial Engineering Department
Botswana International University of Science and Technology
Palapye, Botswana
[5]jamisolar@biust.ac.bw

***Abstract*— This work presents the design and implementation of a smart and solar-powered solid waste segregation system using Arduino microcontroller interfaced with sensors, actuators. and Particle Photon cloud for wireless monitoring. The materials segregated are metal and non-metal that includes plastic, paper, and glass. Metal detection is done using inductive proximity sensor. Plastic is detected using infrared sensor based on shape and size. Laser and light dependent resistor (LDR) pair is used to detect paper. And lastly, glass bottles are detected using capacitive sensor. The prototype has an average percentage accuracy of 90.67% for sorting 30 assorted waste samples.**

Keywords*— *Waste management, automation, control design, solar energy, cloud-based monitoring, electronic sensors

I. Introduction

Waste management is one of the concerns that countries needs to address at present due to the high waste generation rates and limited number of waste disposal sites [1]. According to the study conducted by Palanivel and Sulaiman [2], the daily solid waste generated in the municipalities of Oman is around 0.97 Kg /day/person by weight, 3.113 x 10-3 m3/day/person by volume with a density of 311.73 Kg/m3. Based on the data published by Zafar [3], municipalities in Oman generated about 1.6 million tons of solid waste in 2010 and continues to increase over the years. High percentages of these municipality solid wastes are biodegradable and recyclable materials [3]. In solving the problem of waste management and disposal, the initiative of recycling and segregation of waste should begin in homes, school campuses and offices [4].

Recycling is a resource recovery method which involves collection, sorting and reuse of waste materials such as glass bottles, plastic containers, tin cans and papers. One method of recycling is called single-stream recycling wherein all recyclable materials are placed in a single bin for collection, and the sorting is done at a central facility [5]. Recycling is done to reduce energy usage, limit filling up landfills, lessen air and water pollution, minimize greenhouse gas emissions and preserve natural resources for future generations [6],[7]. For these reasons, a solar-powered solid waste segregation system (SWSS) with cloud-based wireless monitoring was designed and implemented.

This research promotes the use of modern engineering technology in waste management to keep a clean and green campus environment. This project allows waste collection and segregation with minimum human intervention for sanitation and health safety. Furthermore, this eco-friendly system is powered up by a renewable energy source in form of solar energy.

In this paper, Section II cites the current developments in the design and implementation of solid waste segregation system. Section III describes the design, set-up and implementation of the solar-powered solid waste segregator with cloud-based wireless monitoring system. In Section IV, the experimental data are presented to show the performance of the designed system in promoting environmental sustainability in Al Musanna College of Technology (ACT) campus. Lastly, Section V concludes the paper and recommends the possible improvements in the designed system for large-scale waste management. A demo video of the system can be seen here: https://youtu.be/qgB_9oPyIiY.

II. Current Developments in the Waste Segregation Control and Monitoring System

The need to automatically control and constantly monitoring segregation system for environmental sustainability is extensively studied. Waste segregation process may be implemented using radio-frequency identification (RFID) [9]-[11], programmable logic controller (PLC) [12]-[14] and microcontroller [15]-[19].

Several RFID and sensor models were developed for smart waste management system, including automatic waste sorting, weight classification and stolen bin identification. [9]-[11]. In an RFID-based segregation system, each waste material has an RFID tag that stores the information about the object which travels on a conveyor belt [12]. Whenever waste comes near the RFID reader, it sends the vital information to the RFID reader. This information is conveyed to the microcontroller for sorting process and releasing the waste material in its proper bin. The drawbacks of this kind of system are as follows: (a) cost of using RFID tag in consumer products and (b) dissipation of toxic and/or valuable substance present in RFID tags [10].

ISSN: 2521-2292

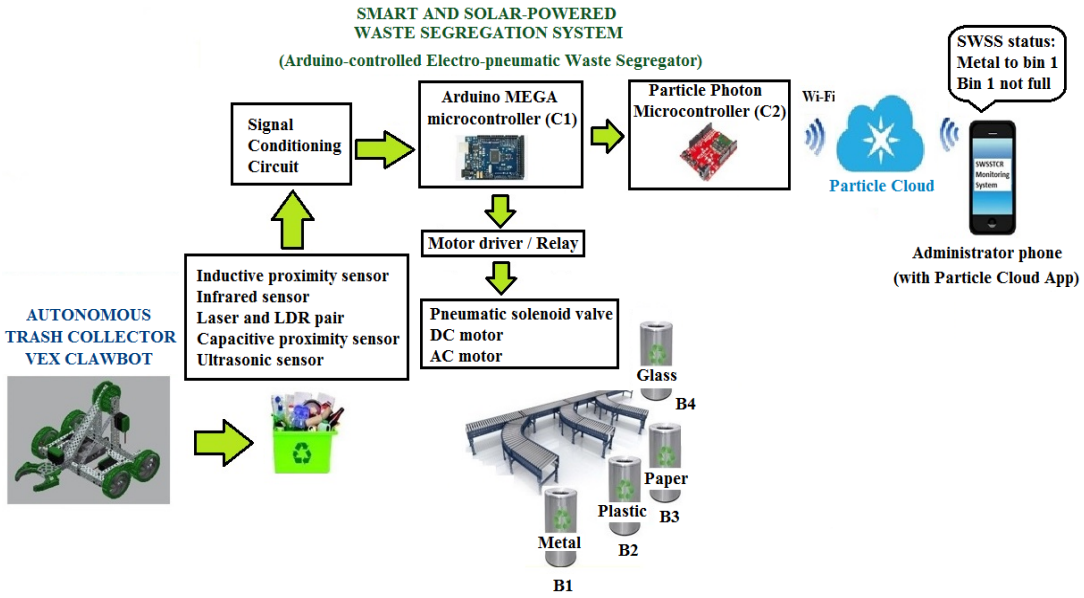


Fig. 1. Over-all block diagram of the solid waste segregation control and monitoring system

A higher level of automation such as industrial and commercial waste segregation process can be designed and implemented using programmable logic controllers (PLC) [12]-[14]. The PLC-based waste segregation system consists of the following: (a) controller which acquires the digital and analog data from an input module and produces an output based on the input conditions in real-time; (b) action performing component such as rotating conveyor belt and pneumatic cylinders which require the application of energy to drop the waste object into its correct bin; and (c) sensors which are used to detect the presence of the object on the conveyor belt, detect the type of object to be sorted, and signal the PLC to start the conveyor [12],[14]. PLC-based systems are reliable, rugged and tough to fit industrial environment. However, it is costly and requires higher power than microcontroller-based system.

In waste segregation system using microcontrollers such as PIC [15],[17], 8051 [16] and Arduino [18],[19], the operation and synchronization of all the subcomponents to sort the waste materials are controlled by the microcontroller [12]. It receives the signals from various sensors, actuates the solenoid valves connected to a door that opens, and distributes the waste to its correct recycle bin [15]-[19]. This type of system has smaller size, low cost and low power requirement.

Wireless monitoring of the sorting activities may be IoT-based [18]-[21], Zigbee-based [22] or GSM-based. Zigbee-based monitoring has limited area of coverage and less secured than IoT-based system. In reducing the cost of monitoring the waste segregation system performance and increasing the system's accessibility, Nagayo and Jamisola [23] recommended the use of Wi-Fi technology and cloud data storage instead of GSM technology.

III. Solar-Powered Waste Segregation Control and Monitoring System Design Considerations

A. *Block Diagram of the Solid Waste Segregation Control and Monitoring System*

Based on Fig.1, the solid wastes are dumped by a trash collecting robot to the elevator conveyor which will transfer the trash to the electro-pneumatic segregation system. Then, trashes are passed one by one through the sensor array via the horizontal belt conveyor. Inductive proximity sensor is used to identify empty aluminum cans, infrared proximity sensor is used to detect empty plastic bottles, laser-light dependent resistor (LDR) pair is used to detect papers, capacitive proximity sensor is used to detect clear glass bottles and unclassified wastes are dispensed at the end of conveyor belt by the process of elimination. Arduino microcontroller (C1) receives the signals from the sensors, activates the pneumatic solenoid valves connected to a flap door that opens, and dispenses the trash to its appropriate recycle bin. Particle Photon cloud-based wireless monitoring system is also designed to monitor events in the waste segregator. The whole system works on the concept of a renewable energy source which is solar energy.

B. *Design and Assembly of the Solid Waste Segregation System (SWSS) Mechanism*

The design of the solid waste segregation system is based on the process flowchart shown in Fig. 2. From the flowchart, the necessary components of the system were identified by the researchers.

ISSN: 2521-2292

1) Electro-pneumatic System

Electro-pneumatic systems combine pneumatic and electrical technologies into one system where the control medium is the electrical signal and the working medium is the compressed air [24]. In this system, relays and solenoid valves are used to interface electrical control with pneumatic action. The schematic diagram of the pneumatic system and its components are shown in Fig. 3 and Table I. The components of the pneumatic system are specified in Table I.

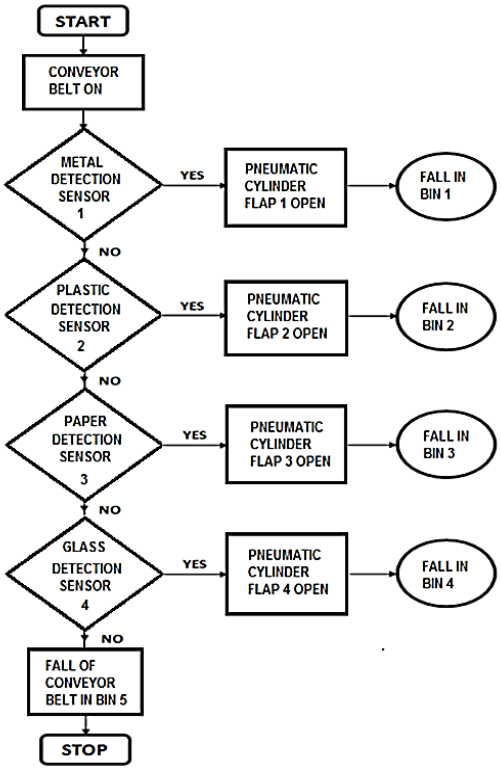


Fig. 2. Solid waste segregation system process flow

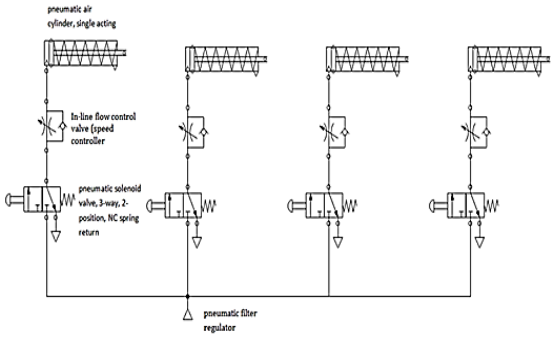


Fig. 3. Schematic diagram of the pneumatic system

TABLE I. COMPONENTS OF THE PNEUMATIC SYSTEM

air compressor	12 V DC, 120 psi with tank
pneumatic cylinder	Single acting spring return 15 mm bore x 75 mm stroke
directional control valves	Pneumatic solenoid 3/2 way, spring return, 24 V DC
working pressure	30 psi

TABLE II. HORIZONTAL BELT CONVEYOR SPECIFICATIONS

Length	1500 mm
Width	100 mm
Roller diameter	65 mm
Motor power	60 W
Speed	30-180 mm/s

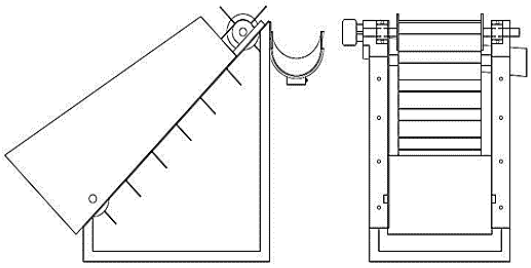


Fig. 4. Design of elevator conveyor with bins and vibrating chute

2) Horizontal Belt Conveyor

The horizontal belt conveyor, installed with swinging pneumatic doors was designed based on the following user requirements:

(a) It should carry all wastes with 1.0 kg maximum.

(b) It should able to convey common sizes of aluminum soda cans, plastic bottles, glass bottles and tea cups.

(c) It should have control speed.

The final horizontal belt conveyor specifications are shown in Table II.

3) Elevator Conveyor

The design of the elevator conveyor is shown in the Fig. 4. The width is 500 mm and the total length is 700 mm. The elevator is fitted with belts with ridges that runs over two pulleys. The ridges in the belt will serve to separate the waste one by one with each waste falling horizontally between the ridges. The angle of the belt is 45 degrees. Wastes which will not fall horizontally between the ridges falls back by gravity to the bottom of the bin where they are reoriented by the rotating belt. The pulleys are driven by a 40W low speed geared DC motor. Since the elevator cannot drop the waste directly into the horizontal conveyor and the problem posed by the metal sensor required to be in contact with the waste, a vibrating cylindrical chute is considered which will convey the waste from the elevator to the belt of the segregator.

ISSN: 2521-2292

C. Control System of the Solid Waste Segregator

Referring to Fig.1, the trash collecting robot dumps the wastes in the elevator conveyor which will transfer the trashes to the horizontal belt conveyor. Ultrasonic sensor is used to detect the presence of waste in the elevator conveyor. The signal from the sensor allows the Arduino microcontroller (C1) to synchronize the operation time of the conveyors. As the solid waste reaches the electro-pneumatic segregation system one at a time, it passes through various sensors for sorting.

The first sensor that the waste touches is the inductive proximity sensor which determines if the object is metal or not. If the output of the inductive proximity sensor is 0 V, metallic waste like aluminum can is detected. Door 1 (D1) will open and metal can will fall in garbage bin 1 (B1). If it is not a metal, the trash will be transferred by the conveyor belt to second sensor area wherein infrared (IR) sensor is used to detect if the object is a plastic bottle or not. Plastic bottles were detected by the IR sensor based on their size and shape. If IR sensor output ranges from 490 to 520, the trash detected is a plastic bottle. Door 2 (D2) will open and plastic bottle will fall in garbage bin 2 (B2); otherwise, the trash will go to third sensor zone which consists of laser and light dependent resistor (LDR) pair. The LDR will sense the intensity of the light produced by the laser. If the LDR reading is greater than or equal to 3 V, it means paper waste is detected. Consequently, door 3 (D3) will open and paper will fall in garbage bin 3 (B3). For glass waste detected by the capacitive sensor, it will fall in garbage bin 4 (B4). Any unsorted waste item goes to garbage bin 5 (B5) at the end of the conveyor.

The microcontroller C1 generates digital output signals to indicate the status of each door and which trash bin receives the waste. Ultrasonic sensor installed on top of each garbage bins is used to determine if the bin is full or not. If the reading of the ultrasonic sensor is less than 2cm, it means the trash bin is already full. The microcontroller C1 also produces digital output signals to indicate the status of each trash bins.

D. Monitoring System of the Solid Waste Segregator

Particle Photon cloud-based wireless monitoring system is designed to monitor events in the waste segregator and to monitor if the garbage bins are full or not. Particle Photon microcontroller (C2) reads the digital signals generated by Arduino microcontroller (C1) indicating the status of the doors and trash bins. The events in the SWSS are published on the Particle Cloud which the administrator can access using his mobile phone.

E. Solar Energy Conversion Station for the Solid Waste Segregation System (SWSS)

The SWSS is powered-up reliably for 8 hours daily. During its operation the horizontal belt conveyor, elevator conveyor, switch-mode power supply and air compressor are activated. With these conditions, the AC power requirement of the SWSS is computed as 402 Watts and the total energy requirement per day after correction factor is 3,344.64 Watt-hours. Considering the calculated solar energy needed daily, two (2) 300 W, 28 V PV panels and two (2) 12V, 200 Ah deep-cycle batteries are utilized, which are designed to be discharged at 25% to extend the battery life. A 30 A, 24 V PWM solar charge controller is used to match the ratings of the batteries. To provide a 220 Vrms AC output, a 1000 W inverter with 24 V DC input is utilized for the system. According to A.M. Nagayo and R. Jamisola [23], the inverter power rating should be 25% to 30% greater than total wattage of the load and its DC input voltage should match the voltage of the battery bank. The connection diagram for the solar energy conversion station of the SWSS is shown in Fig. 5.

IV. Experimental Data and Analysis of Results for the Solar-Powered Solid Waste Segregation System

A. Experimental Set-up and Test Results of the Control and Monitoring System for the Solid Waste Segregation System

Prior to the actual testing, the sensors attached to the microcontrollers of SWSS such as inductive proximity sensor, infrared sensor, LDR, capacitive proximity sensor and ultrasonic sensor were calibrated to perform task precisely. To determine the optimum speed of the horizontal belt conveyor, the response time and reliability of SWSS in sorting thirty (30) assorted waste materials were noted down in Table III for five (5) different speed settings (S1 to S5). Based on the results, the designed waste segregator has an average percentage accuracy of 90.67% for sorting 30 assorted waste samples. The optimal speed of the horizontal belt conveyor with minimal failure rate is S4.

The ability of the elevator conveyor to separate the wastes and feed into the SWSS one by one is tested by dumping the wastes together in the bin of the elevator and recording how many wastes are separated accordingly. The results are as shown in Table IV with a 100% success rate for separating metals, 89% success rates for separating plastic and paper wastes, and 78% success rate for separating glass bottles. The failure rates were due to the position of wastes as they are dumped into the bin, as well as the size and weight of the waste materials.

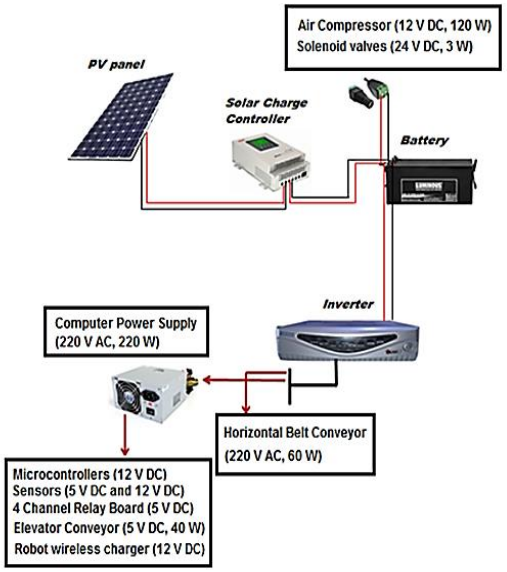


Fig. 5. Connection diagram of the solar energy conversion station of the solid waste segregation system

ISSN: 2521-2292

The reliability and response time of the SWSS in sorting the trash properly with the horizontal belt conveyor speed set at S4 are shown in Table V. The smart solid waste segregation system completed the task of sorting 30 assorted waste materials in a time of 1 minute and 45 seconds with a sorting success percentage of 96.67%. Based on the observations, the common causes of errors in the sorting process are as follows: (a) friction between the object and the conveyor belt, (b) the material is stuck at the door due to its size or position, (c) timing synchronization, and (d) glass wastes material is not a transparent glass which is one of the limitation of the system. The actual waste segregation system and its sorting process is shown in Fig. 6 and Fig. 7.

For monitoring purpose, the events or occurrences happening in the SWSS are published in the Particle Cloud. The administrator can access the data anytime using mobile phone by logging in to his/her Particle Cloud account. Fig. 8 shows a sample published events for SWSS in the Particle Cloud.

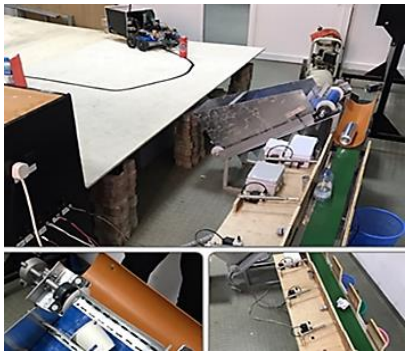


Fig. 6. Actual set-up of the solid waste segregation system

TABLE III. RESPONSE TIME AND RELIABILITY OF SWSS FOR FIVE (5) DIFFERENT SPEED SETTINGS

Speed setting	Total Number of Solid Waste Materials	Total Number of Items Sorted Successfully	Total Time to Complete the Segregation Process in seconds	Sorting Success Percentage
S1	30	25	2 min and 32 sec	83.33%
S2	30	26	2 min and 16 sec	86.67%
S3	30	28	1 min and 59 sec	93.33%
S4	30	29	1 min and 45 sec	96.67%
S5	30	28	1 min and 31 sec	93.33%

TABLE IV. DATA AND RESULTS FOR THE ELEVATOR CONVEYOR

Type of waste	Trial	No. of waste	Total Number of Items Separated Successfully	Success Rate %	Total success rate %
Plastic water bottle	1	3	2	67	89
	2	3	3	100	
	3	3	3	100	
Paper tea cup	1	3	3	100	89
	2	3	2	67	
	3	3	3	100	
Soda can	1	3	3	100	100
	2	3	3	100	
	3	3	3	100	
Glass bottle	1	3	2	67	78
	2	3	2	67	
	3	3	3	100	

TABLE V. DATA AND RESULTS FOR THE SWSS WITH HORIZONTAL BELT CONVEYOR SPEED SET AT S4

SN	Solid Waste Items	Total Number of Solid Waste Materials	Total Number of Items Sorted successfully
1	metal	7	7
2	plastic	9	9
3	paper	9	9
4	glass bottle	5	4



Fig. 7. Sorting process of the solid waste segregation system

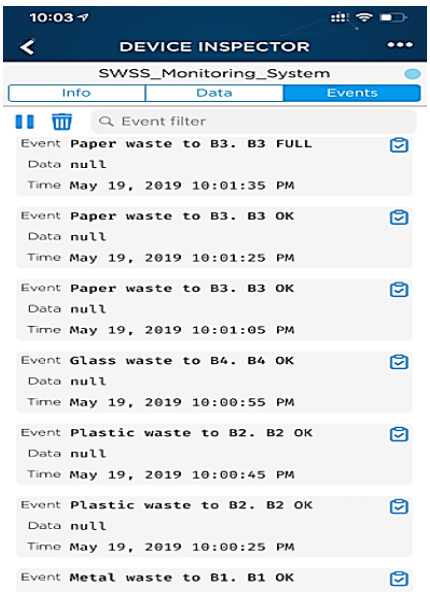


Fig. 8. Sample published events for SWSS in the Particle cloud

ISSN: 2521-2292

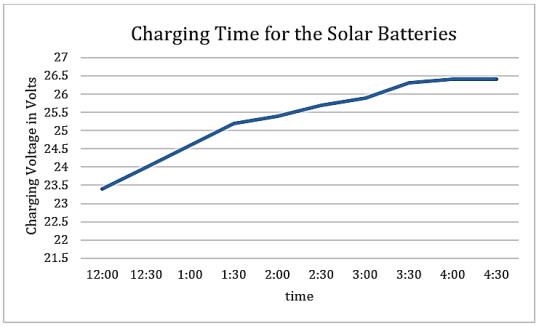


Fig. 9. Charging time of the deep-cycle batteries

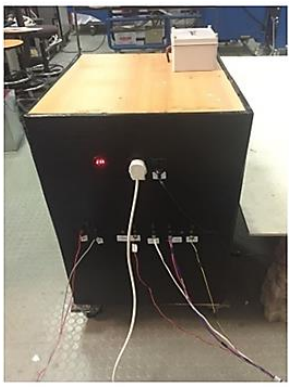


Fig. 10. Solar power conversion system for the solid waste segregator

B. *Experimental Set-up and Test Results of the Solar Energy Conversion Station*

For testing the deep-cycle batteries, the solar panel was connected to charge controller, then the charging time of the deep-cycle batteries were taken as seen in Fig. 9. The actual Solar Power Conversion System for the Solid Waste Segregator is shown in Fig. 10. With the solar energy conversion system design, the SWSS operates continuously for more than 8 hours daily.

V. Conclusion

The current developments in the design and implementation of waste segregation system are presented in this paper with one common goal which is to sort recyclable waste to its appropriate bins to achieve a clean and green campus environment with minimum human intervention. A smart and solar-powered solid waste segregation system (SWSS) was designed and implemented to sort out four (4) different types of solid waste materials, then distribute each trash to its proper recycle bin. With the sensor-based segregation method, the spacing, position and size of the wastes passing through the horizontal conveyor belt plays an important part in determining the accuracy of the system. With respect to the transferring of wastes from the elevator conveyor to the SWSS area, singulation of the waste materials plays a critical part in controlling the flow of waste to the sensor array. Based on the results, the maximum sorting percentage of the system is 96.67% with a time of 1 minute and 45 seconds to complete the task of sorting 30 assorted waste items. Internet of things (IoT) technology and cloud data storage are utilized instead of GSM to reduce the cost of monitoring of the SWSS and increase accessibility to the system's activities. The solar power conversion set-up supplies electricity to the SWSS within the specified operating hours even when all loads are turned on.

For a large-scale waste facility, the following may be done as future directives: (a) use of alternative sorting methods such as image processing or X-ray imaging as suggested by H. Jiu et al. [25]; (b) modifications in the design of elevator and horizontal conveyors, as well as additional sensors may be added as future directive for better timing synchronization, better singulation and faster sorting process while maintaining a high sorting percentage.; (c) integrate wet and food waste sorting using moisture sensor, methane sensor and other gas sensors [17]; and, (d) incorporate waste to electrical energy generation method in the system [17].

Acknowledgment

Special thanks to Al Musanna College of Technology (ACT) for the full support given to this multi-disciplinary project, and The Research Council (TRC) of Oman for funding major part of this project. Thanks to SWSSTCR team members: Cesar Mendoza, Bindu P.V., Mazna Said Hamdan Al Saidi, Ali Khamis Ali Al Kharusi, Ammar Said Al Hosni, Tasnim Khasif Al Mughaizwi, Raja Muhammed Al Rawahi, Emanuel Rances, Jefferson Zason, Rolando Cabais, Alex Boral, Jorge Ramos, Ericson Recamata for all their support and cooperation.

References

[1] L.A. Guerrero, G. Maas, W. Hogland, "Solid waste management challenges for cities in developing countries," *Journal of Waste Management*, 33(1), 220–232, 2013

[2] T.M. Palanivel and H. Sulaiman, "Generation and Composition of Municipal Solid Waste (MSW) in Muscat, Sultanate of Oman," *APCBEE Procedia*, Vol. 10, Pages 96-102, 2014

[3] Zafar, S. (2014). *Waste Management Scenario in Oman*. [Online] Available: http://www.bioenergyconsult.com/waste-oman [Accessed: March 2, 2016]

[4] Shammas, M. E. *The Report of the Sultanate of Oman on Solid Waste Management*. [Online] Available: http://www.unep.or.jp/ietc/Publications/TechPublications/TechPub-17/oman2.asp [Accessed: March 3, 2016]

[5] Lakhan, C., "A Comparison of Single and Multi-Stream Recycling Systems in Ontario, Canada," *Resources 2015*, 4(2), 384-397, 17 June 2015

[6] R.P.Bagozzi and P.A.Dabholkar, "Consumer recycling goals and their effect on decisions to recycle: A means-end chain analysis," *Psychology & Marketing*, 11(4), 313-340, 1994

[7] J. Heimbuch (2011). *Trash Sorting Robot Cold Reduce Waste Going to Landfill by 50%*. [Online] Available: http://www.treehugger.com/clean-technology/trash-sorting-robot-could-reduce-waste-going-to-landfill-by-50.html [Accessed: June 4, 2015]

ISSN: 2521-2292

[8] M. Joubert (2013). *National Strategy for Waste Management*. [Online] Available: http://omanobserver.om/national-strategy-for-waste-management [Accessed: March 2, 2016]

[9] M. Arebey, M. A. Hannan, H. Basri, R. A. Begum and H. Abdullah, "Solid waste monitoring system integration based on RFID, GPS and camera," *2010 International Conference on Intelligent and Advanced Systems*, Manila, 2010, pp. 1-5.

[10] S. Abdoli, "RFID Application in Municipal Solid Waste Management System," *International Journal of Environmental Research*, 3(3), 447-454, 2009

[11] B. Chowdhury and M. U. Chowdhury, "RFID-based real-time smart waste management system," *2007 Australasian Telecommunication Networks and Applications Conference*, Christchurch, 2007, pp. 175-180.

[12] S. Dwivedi, M. Fernandes and R. D'souza, "A Review on PLC based Automatic Waste Segregator," *International Journal of Advanced Research in Computer Engineering & Technology (IJARCET)*, vol.5, no. 2, 280-285, 2016

[13] P. Elamurugan, K. VinothBresnav, D. Abirami, K.G. Suhirdham, "Automatic Material Segregation Using PLC," *International Journal of Engineering and Technology*, 7(2.24), 376-380, 2018

[14] R. M. Kittali and A. Sutagundar, "Automation of Waste Segregation System using PLC," *International Journal on Emerging Technologies*, 7(2), 265-268, 2016

[15] F. G. Ang, M.K.A. Gabriel, J. Sy, J. J. O. Tan and A. C. Abad, "An Automated Waste Sorter with Mobile Delivery Waste System," presented at 2013 DLSU Research Congress. DLSU, Manila, 2013

[16] M. K. Pushpa, A. Gupta, S. M. Shaikh, S. Jha, S. V., "Microcontroller Based Automatic Waste Segregator," *International Journal of Innovative Research in Electrical, Electronics, Instrumentation and Control Engineering*, vol. 3, no. 5, 104-108, 2015

[17] R. Rajkamal, V. Anitha, P. G. Nayaki, K. Ramya and E. Kayalvizhi, "A novel approach for waste segregation at source level for effective generation of electricity — GREENBIN," *2014 International Conference on Science Engineering and Management Research (ICSEMR)*, Chennai, 2014, pp. 1-4.

[18] S. Suryawanshi, R. Bhuse, M. Gite and D. Hande, "Waste Management System Based on IoT," *International Research Journal of Engineering and Technology*, 5(3), 1835-1837, 2018

[19] A.M. Nagayo, M. S. H. Al Saidi, O. R. Al Maqbali, A. Y. Al Farsi, A. K. Al Kharusi, A. S. Al Hosni, T. K. Al Mughaizwi, R. M. Al Rawahi, "A Smart Solar-powered Waste Segregation System with Integrated Self-driving Robot Collector towards Environmental Sustainability in School Campus," presented at the National Research Forum, TRC, Sultanate of Oman, December 2017, unpublished.

[20] V, S., P, S., & S, H. J. R., "Smart Waste Segregation and Monitoring System using IoT," *International Research Journal of Multidisciplinary Technovation*, 1(3), 1-10, 2019

[21] I. Hong, S. Park, B. Lee, J. Lee, D. Jeong, and S. Park, "IoT-Based Smart Garbage System for Efficient Food Waste Management," *The Scientific World Journal*, vol. 2014, Article ID 646953, 13 pages, 2014

[22] V. M. Kantila and A. P. Lakhlani, "Zigbee based Wireless Monitoring and controlling of Automation System using PLC & SCADA," *International Journal of Advanced Research in Electrical, Electronics and Instrumentation Engineering*, 3(1), 6768-6775, 2014

[23] A. M. Nagayo & R. Jamisola, "Cloud-based Wireless Monitoring System and Control of a Smart Solar-Powered Aquaponics Greenhouse to Promote Sustainable Agriculture and Fishery in an Arid Region," *2017 BIUST Research & Innovation Symposium (RDAIS)*, Palapye, Botswana, 2017, pp. 144-151

[24] *Electro-Pneumatic System in Action*. [Online] Available: http://www.library.automationdirect.com [Accessed: October 1, 2016]

[25] J. Huang, T. Pretz and Z. Bian, "Intelligent solid waste processing using optical sensor based sorting technology," *2010 3rd International Congress on Image and Signal Processing*, Yantai, 2010, pp. 1657-1661A.

[26] B. R. S. Kumar, N. Varalakshmi, S. S. Lokeshwari, K. Rohit, Manjunath and D. N. Sahana, "Eco-friendly IOT based waste segregation and management," *2017 International Conference on Electrical, Electronics, Communication, Computer, and Optimization Techniques (ICEECCOT), Mysuru*, 2017, pp. 297-299.

BIUST Research and Innovation Symposium 2019 (RDAIS 2019)
Botswana International University of Science and Technology
Palapye, Botswana, 4 - 7 June 2019
ISSN: 2521-2292

Book of Abstracts

BIUST Research and Innovation Symposium 2019 (RDAIS 2019)
Botswana International University of Science and Technology
Palapye, Botswana, 4 - 7 June 2019
ISSN: 2521-2292

On a sphere bundle on complex Grassmannians

Oteng Maphane[1] **& Jean Baptiste Gatsinzi**[2]
[1]Botswana International University of Science and Technology
E-mail address: maphaneot@biust.ac.bw

[2]Botswna International University of Science and Technology
E-mail address: gatsinzij@biust.ac.bw

ABSTRACT

A continuous map $p : E \to B$ has the *homotopy lifting property* with respect to a pair of spaces $(X \times I, X \times \{0\})$ if for every commutative diagram of the form

$$\begin{array}{ccc} X \times \{0\} & \xrightarrow{g_0} & E \\ \downarrow & \overset{G}{\nearrow} & \downarrow p \\ X \times I & \xrightarrow[F]{} & B \end{array}$$

there is a continuous map $G : X \times I \to E$ such that $G(x, 0) = g_0(x)$ for $x \in X$ and $pG = F$, where I is the unit interval $[0, 1]$. A surjective continuous map $p : E \to B$ is a *Serre fibration* if p has the homotopy lifting property with respect to every space $(X \times I, X \times \{0\})$ for all CW-complexes X. Here E is the *total space* and B is the *base space* of the fibration p. Every fibre bundle is a Serre fibration [1]. A matrix $A \in M_n(\mathbb{C})$ is unitary, if $AA^* = I$, where $A^* = \bar{A}^T$, then the group consisting of all unitary matrices is a compact Lie group called the unitary group, and is denoted by $U(n)$. Let $G_{k,n}(\mathbb{C})$ denote the homogeneous space $U(n)/(U(k) \times U(n-k))$. The homogeneous space $G_{k,n}(\mathbb{C})$ is the complex Grassmann manifold of k-dimensional vector subspaces of $\mathbb{C}^n$. A simply connected space X is called formal if there is a quasi-isomorphism $(\wedge V, d) \to H^*(\wedge V, d)$, where $(\wedge V, d)$ is the Sullivan minimal model of X and V is a finite dimensional vector space. Formal spaces include spheres, projective complex spaces, homogeneous spaces G/H, where G and H are Lie groups of the same rank and Kähler manifolds. In this paper we study the formality of the total space of a sphere bundle on complex Grassmann manifolds.

Keywords: *Fibration, Complex Grassmann manifolds, Formal*

Category: **Mathematics**

References

[1] Y. Félix, S. Halperin, J. Thomas, *Rational Homotopy Theory*, Springer, New York, (2001).

BIUST Research and Innovation Symposium 2019 (RDAIS 2019)
Botswana International University of Science and Technology
Palapye, Botswana, 4 - 7 June 2019
ISSN: 2521-2292

Optimal Portfolio For An Investor Who Receives Stochastic Income

Kebareng I. Moalosi-Court[1] & Edward M. Lungu[2]
[1,2]Department of Mathematics and Statistical Sciences,
Botswana International University of Science and Technology,
Palapye, Botswana
kebareng.moalosi@studentmail.biust.ac.bw, lungue@biust.ac.bw

Abstract

In this paper we study and observe the optimal portfolio of an investor's total wealth with a stochastic income. In the first part of the study, we suggest an approach that quantifies a unique Markov stochastic income which optimizes the investor's total wealth, and yield a Merton kind of optimal portfolio.
In the second part of the study, we assume a stochastic income which is given in the form of an asset. Hence the optimal portfolio of the investor's wealth result is unique and depended on the Merton proportion. These proportions were also studied under exponential and logarithmic utilities over the terminal wealth using dynamic programming.

Keywords: *Stochastic income; Dynamic Programming; Exponential Utility; Logarithmic Utility*

BIUST Research and Innovation Symposium 2019 (RDAIS 2019)
Botswana International University of Science and Technology
Palapye, Botswana, 4 - 7 June 2019

ISSN: 2521-2292

Assessing the impact of wastewater irrigation on antibiotic resistance dynamics and bacterial species diversity using soil microcosm experiments

Onalenna Onthatile *, Rahube Teddie

Botswana International University of Science and Technology, Private Bag 16, Palapye, Botswana

**Corresponding author:* onthatile.onalenna@studentmail.biust.ac.bw

Abstract

Microcosm experiments are artificial, miniature ecosystems that are used to mimic the natural ecosystems under controlled conditions. Irrigation with wastewater effluent exposes soil and vegetable crops to antibiotic resistant bacteria (ARB) and antibiotic resistant genes (ARGs) which are consequently introduced to humans through the food chain. In this study the impact of wastewater irrigation on antibiotic resistance dynamics and diversity of bacterial species in soil was assessed. The study involved 4-month long microcosm experiments where Palapye wastewater treatment plant (PWWTP) effluent was used for irrigation of agricultural soil. Notwane farms where effluent from Gaborone wastewater treatment plant (GWWTP) is used for irrigation was also included to determine the long-term impact of wastewater irrigation on soil resistome and microbiome. In this paper we describe the use of culture-dependent methods; selective isolation and quantification of viable ARB and culture independent methods; real-time quantitative PCR and metagenomics as important tools to determine the occurrence, diversity and abundance of ARB and ARGs in wastewater irrigated soils. We also discuss preliminary results from the field and microcosm experiments. Bacterial species *Shigella, Enterobacter, Listeria, E. coli, Pseudomonas and Campylobacter* were found to be the predominant ARB in PWWTP effluent, where all the isolates were resistant to Penicillin, Erythromycin, Ampicillin and Meropenem antibiotics at clinical breakpoint concentrations. In the microcosm experiments, *Listeria, Campylobacter and Staphylococcus species* were isolated and quantifiable in the soil following irrigation with PWWTP effluent. All isolates from the microcosm experiments were resistant to Penicillin whereas only 14.3% were resistant to Erythromycin, Meropenem and Ampicillin. From the field study, all soil isolates were resistant to Penicillin, Erythromycin, Cephalosporin, Ampicillin, and only 40% isolates were resistant to Streptomycin and Tetracycline. The preliminary results suggest an increase in the occurrence, and abundance of viable ARB species in the soil following irrigation with wastewater effluent. More investigations using molecular methods will be employed to further support the hypothesis suggesting that long term use of effluent wastewater results in accumulation of antibiotic resistance determinants in the soil.

Keywords: Antibiotic resistant bacteria, antibiotics, wastewater effluent, microcosm, soil

BIUST Research and Innovation Symposium 2019 (RDAIS 2019)
Botswana International University of Science and Technology
Palapye, Botswana, 4 - 7 June 2019

ISSN: 2521-2292

RESEARCH & INNOVATION SYMPOSIUM AND STEM FESTIVAL 2019
June 3 - 7 , 2019.Botswana International University of Science & Technology (BIUST) Campus Palapye, Botswana

IMPACT OF THE STRESS JUMP AND SLIP CONDITIONS ON THE DISPERSION DURING NANOPARTICLES BASED DRUG DELIVERY - TWO PHASE MODEL

Annah Moitoi[1] **& Sachin Shaw**[2]
1Department of Mathematics and Statistical Sciences, Botswana International University of Science and Technology, Private Bag 16, Palapye, Botswana
E-mail address: annah.moitoi@studentmail.biust.ac.bw (A Moitoi), shaws@biust.ac.bw (S Shaw)

ABSTRACT

The study of the longitudinal dispersion of a drug delivered through a microvessel is irreversibly absorbed or undergoes an exchange process at the boundary and has many applications in the field of chemical engineering, environmental dynamics, biomedical engineering and physiological fluid dynamics. The dispersion of nanoparticles plays a vital role in medical science during drug delivery through a microvessel. The current problem deals with the dispersion characteristic of blood during drug delivery through a microvessel. The nature of the blood flow is considered as a two phase fluid model, where the clear region is considered as non-Newtonian Herschel-Bulkley fluid while the peripheral region is considered as Newtonian fluid. The governing equations are solved analytically in the form of bessel functions while others are solved in the form of numerical integration method. We analyze how the governing parameters such as pressure distribution, nanoparticle volume fraction, the permeability of the blood vessel, yield stress and the radius of the nanoparticle influence dispersion of nanoparticles during drug delivery.

Keywords: *Drug delivery,Dispersion, Herschel-Bulkley fluid, non-Newtonian fluid, two phase model,Newtonian fluid, nanoparticle*

Category: **Mathematical Biology**

References

[1] Shaw, S., Ganguly, S., Sibanda, P. and Chakraborty, S. (2014). *Dispersion characteristics of blood during nanoparticle assisted drug delivery process through a permeable microvessel*. Microvascular Research, 92.

[2] Srivastava, V. (1996). *Two-phase model of blood flow through stenosed tubes in the presence of a peripheral layer*: Applications. Journal of Biomechanics, 29(10).

BIUST Research and Innovation Symposium 2019 (RDAIS 2019)
Botswana International University of Science and Technology
Palapye, Botswana, 4 - 7 June 2019

ISSN: 2521-2292

The role of epidemic plasmids in antibiotic resistance dissemination across different environments

Juliet Eze*, Teddie Rahube

Department of Biological Sciences and Biotechnology

Botswana International University of Science and Technology,

Private Bag 16 Palapye, Botswana

juliet.eze@studentmail.biust.ac.bw

Abstract

Plasmids encoding resistance genes to different classes of clinically relevant antimicrobials are widely distributed across bacterial populations in different environments; soil, water, food and air. However, the ecology of epidemic antibiotic resistance plasmids (ARPs) remains poorly understood and relatively uncharacterized globally. The aim of this study is to use a 'one health' approach to characterize the epidemic ARPs from complex sources linked to humans, animals and the ecosystem. We have identified Palapye wastewater treatment facility (PWWTF) and the downstream effluent receiving pond as one of the ideal study sites within the one health framework because of its association with human and animal activities occurring in the downstream environment. In this paper, we discuss the use of culture-based, molecular and next generation DNA sequencing methods in determining the occurrence, diversity, mobility and antibiotic resistance patterns of plasmids in various sample sources. The preliminary results obtained through isolation and expression of plasmids in susceptible host bacteria reveal varying resistance patterns to common classes of antibiotics including tetracycline, beta-lactams, aminoglycosides and macrolides. The occurrence and diversity of the plasmids encoding these resistance phenotypes may suggest high possibilities of conjugation and rapid transfer of multiple resistance between closely or distantly related bacterial populations. This study further provides insights on the impact of self-transmissible ARPs that are potentially transferred from routinely discharged effluents from wastewater treatment facilities. It is therefore, very critical to determine the prevalence and self-mobilization of ARPs that are introduced into downstream environments that are associated with anthropogenic activities. Effluent contaminated water bodies are frequently linked to activities such as swimming, drinking and irrigation of farm crops. The high interaction between human and animals at the site may have a negative impact to public health if the conjugative ARPs are frequently transferred between environmental non-pathogenic and pathogenic bacterial communities.

Keywords: Antibiotics, antibiotic resistance plasmids, conjugation, wastewater effluent, public health.

BIUST Research and Innovation Symposium 2019 (RDAIS 2019)
Botswana International University of Science and Technology
Palapye, Botswana, 4 - 7 June 2019
ISSN: 2521-2292

Production of Biodiesel from *Scinzionphyton rautanenii* (Manketti) nut oil by a Heterogeneous catalyst.

KEENE C. MMUSI[1], SEBUSI ODISITSE[1],

[1]*Botswana International University of Science and Technology (Department of Chemistry and Forensic Sciences, Palapye, Botswana)*

Schinziophyton rautanenii (Manketti) is a multipurpose plant species in Southern Africa with an ecosystem that provides a variety of goods and services such as food security, employment and source of income to most people from rural communities in Southern Africa [1]. Manketti tree produces oil extracted from its nut which has potential to produce biodiesel. Biodiesel has been found to be a potential alternative fuel for diesel (fossil fuel) as it is eco-friendly and renewable, and it is produced by chemical reactions such transesterification in the presence of a catalyst [2]. Biodiesel has the potential to resolve the energy crisis depending on the availability of feedstock and catalyst. A heterogeneous catalyst, calcium oxide (CaO), was used in this study because it is highly active and is the commonly used solid catalyst for transesterification reaction. Calcium oxide nano-particles was prepared by reacting sodium hydroxide (NaOH) with calcium nitrate tetrahydrate ($Ca(NO_3)_2$) and the product was finally calcinated at temperature of 900°C. The other catalyst which was employed for transesterification reaction was eggshells which were also calcinated at a temperature of 800°C to form eggshell ash. In this study we do synthesize and characterize CaO nano-particles and compare the catalytic behavior with CaO from eggshell ash towards biodiesel production. We report the production of biodiesel from Manketti nut oil by transesterification reaction in the presence of a heterogeneous catalyst, calcinated eggshell ash and synthesized calcium oxide nano-particles (CaO-NPs). The catalysts were characterized for their physical and chemical properties by; Scanning Electron microscope- Energy Dispersive X-Ray Analyzer (SEM-EDS), X-ray Diffraction (XRD), X-Ray Fluorescent (XRF) and Fourier Transmission-Infrared (FTIR).

Keywords: biodiesel, transesterification, heterogeneous catalyst, renewable energy

[1] I. Vermaak, G. P. P. Kamatou, B. Komane-Mofokeng, A. M. Viljoen, and K. Beckett, "African seed oils of commercial importance - Cosmetic applications," South African J. Bot., vol. 77, no. 4, pp. 920–933, 2011.

[2] H. R. Harsha Hebbar, M. C. Math, and K. V. Yatish, "Optimization and kinetic study of CaO nano-particles catalyzed biodiesel production from Bombax ceiba oil," Energy., vol. 143, pp. 25–34, 2018.

BIUST Research and Innovation Symposium 2019 (RDAIS 2019)
Botswana International University of Science and Technology
Palapye, Botswana, 4 - 7 June 2019
ISSN: 2521-2292

Automatic Dog Feeder

[1]Obakeng Odumetse, [1]Seth Kurusa, [1]Justice A Kenyaditswe, [2]Mothusi Morapedi, [1]N.M.J. Ditshego
[1]Electrical, Computer and Telecommunications Engineering Department, FET,
Botswana International University of Science and Technology (BIUST), BIUST Research and Innovation Centre,
Private bag 16, Palapye, Botswana
[2]Mater Spei College Senior Secondary School,
P/Bag F12, Francistown
Email: obakeng.odumetse@studentmail.biust.ac.bw, seth.kurusa@studentmail.biust.ac.bw, aobakwe.kenyaditswe@studentmail.biust.ac.bw

Abstract
The aim of the project is to provide convenience for dog owners by helping them to feed their dogs easily and smartly. The project has a clock, three (3) alarms and GSM technology. The system allows feeding three (3) meals a day for seven days without the owner's intervention and the time of feeding is determined by the dog owner. The owner can also choose to feed the dog any other time remotely. The remote access is implemented through a global system for mobile communication (GSM). Direct current (DC) components are used to control alternating current (AC) loads. To isolate these components from each other, relays with a network of resistors and diodes are used. The project has a microcontroller (ATMEGA328p) which is used to store data and improve performance through 'C' programming language. In future, the food level in the food dispenser will be verified so as to check desired levels and if it is not then the owner is alerted through GSM module that the food levels are below threshold so that refill can be made. For it to be able to open the food container and dispense food into the dog plate motors, levers and pullers will be used.

Keywords: automatic dog feeder, global system for mobile communication (GSM), microcontroller (ATMEGA328p), 'C' programming language, clock, alarms, food dispenser

BIUST Research and Innovation Symposium 2019 (RDAIS 2019)
Botswana International University of Science and Technology
Palapye, Botswana, 4 - 7 June 2019
ISSN: 2521-2292

GC-ECNI-MS AND QUANTUM CHEMISTRY APPLICATION: EFFECTS OF SUBSTITUENTS ON THE STABILITY OF BENZOQUINONE

ABSTRACT

Mass spectrometry is one of the powerful analytical techniques used worldwide for both qualitative and quantitative techniques. With a suitable ionisation technique, a molecule can be fragmented to give charged fragments whose masses are determined after separation using the mass to charge ratio (m/z). With the use of electron capture negative ionisation technique (ECNI), benzoquinones can capture an electron to produce stable and unstable anions. The stability of substituted benzoquinone anions has never been studied but benzoquinones are extremely used in industry. In the study a combination of GC-ECNI-MS and quantum chemistry calculations was applied to understand and quantify the Electron Affinity (EA) of differently substituted PBQ molecules. Data on Electron Affinities is important, e.g. in theories of chemical reaction and intermediate species, for biochemistry (biological redox processes, radiation damage), to our understanding of chemical bonds and in theories of electronic devices (semiconductors, dielectrics). Neutral benzoquinones have high EA therefore they can capture thermal electrons under ECNI technique to form stable molecular anion (M^-) hence a strong M^- peak is produced on mass spectrum. Different substituents on PBQ affect EA of PBQ hence stability of M^-.

BIUST Research and Innovation Symposium 2019 (RDAIS 2019)
Botswana International University of Science and Technology
Palapye, Botswana, 4 - 7 June 2019
ISSN: 2521-2292

Chalcones: Towards the Synthesis of Bioactive Heterocyclic Compounds

Lesego L. Masutlha[1] and Ofentse Mazimba[2]
[1,2]Department of Chemical and Forensic Sciences,
Botswana International University of Science and Technology,
Palapye, Botswana.
lesego.masutlha@studentmail.biust.ac.bw, mazimbao@biust.ac.bw

Abstract

Chalcone (1, 3-diaryl-2-propen-1-one) is an aromatic ketone consisting of two aromatic rings containing unsaturated α,β-carbonyl three carbons system, belonging to a class of open chain flavonoids that is not only biosynthesized by plants but also can be chemically synthesized. Chalcones are an important constituent of many natural sources possessing a wide spectrum of pharmacological activities such as antioxidant, antimalarial, antimicrobial, anti-inflammatory, antifungal, antibacterial, antiprotozoal, anti-tubercular, anti-ulcerative, cytotoxic, anti-hyperglycemic, antiplatelet, immunomodulatory activities depending on their substitution pattern. The presence of the enone pharmacophore in their structure is found to be responsible for their biological activity. Their bi-electrophile character makes them more attractive to be used as synthon in the synthesis of heterocyclic compounds. Unsaturated ketones are not only important building blocks in organic synthesis, but are also applied in many fields including perfumery, agriculture, biochemistry, food chemistry, polymer, material science etc. Taking into account the above facts, development of high yielding methods for chalcone synthesis is of adamant importance. Chalcones have maintained a considerable amount of interest in both academic and industrial cycles particularly to synthetic drug development. In the present study a series of chalcone derivatives were synthesized by modified Claisen-Schimidt base catalyzed condensation of substituted aromatic ketones with salicylaldehyde in alcohol, stirred for 2 hours at 60 ^{o}C or by green solvent-less methods of grinding the components. The chalcones were prepared in 51-60% yields. The synthesized compounds were characterized on the basis of their melting points, elemental analysis, UV and FT-IR spectral data. These chalcones are precursors in a project aimed at the synthesis of flavonoids and 6H-benzo[c]chromen-6-ones heterocyclic. These heterocyclic compounds will be evaluated for their antioxidant, antimicrobial and anticancer properties.

Keywords: Chalcones, flavanoids, 6*H*-benzo(c)chromen-6-ones, claisen-schimidt condensation

BIUST Research and Innovation Symposium 2019 (RDAIS 2019)
Botswana International University of Science and Technology
Palapye, Botswana, 4 - 7 June 2019
ISSN: 2521-2292

Polyphenols and Antiparasitic Activity from Rangelands Plants

Author: O. Tibe[1], O. Madibela[2], B.G. Mathapa[1]

[1]*Botswana University of Agriculture and Natural Resources, Faculty of Sciences, Department of Basic Sciences, Private Bag 0027, Gaborone, Botswana*

[2]*Botswana University of Agriculture and Natural Resources, Faculty of Animal and Veterinary Sciences, Department of Animal Science and Production, Private Bag 0027, Gaborone, Botswana*

Correspondence e-mail: otibe@buan.ac.bw or olekilet@gmail.com

Abstract

Diseases associated with gastrointestinal nematodes (GIN) significantly reduce protein utilisation in ruminants, and animals can suffer from diarrhoea, anaemia, inappetance and consequent loss of body-weight leading to death. One of the widely employed control strategy for GIN is the use of anthelmintic drugs. However, the sustained use of these drugs results in anthelmintic resistance, public concern over chemical residues in meat and milk products, unavailability and unaffordability, as well as improper and inappropriate use of these chemicals, particularly in smallholder farm setting. This suggests that alternative strategies are urgently needed to address this problem. One such innovative approach may be to use forage plants containing plant secondary metabolites, particularly polyphenols (condensed tannins-CT and low molecular weight phenolics). Current state of the art has shown that administration of purified condensed tannins reduces faecal egg count and nematode burdens in parasitized livestock or immobilise free living *in vitro*. Therefore, the interaction between these forage sources with ruminants provides a knowledge resource base for the discovery of new bioactive compounds, or new activities and new uses for known compounds for nutraceutical and pharmaceutical products. The focus of this paper will be on the content, structure and antiparasitic activity of the crude and purified CT and low molecular weight phenolic extracts from rangelands plants.

Keywords: nematodes, rangeland plants, polyphenols, ruminants, antiparasitic

BIUST Research and Innovation Symposium 2019 (RDAIS 2019)
Botswana International University of Science and Technology
Palapye, Botswana, 4 - 7 June 2019
ISSN: 2521-2292

Total phenolic content and antioxidant activity of cowpea leaves (*Vigna unguiculata* (L) Walp) in Botswana

Author: O. Tibe[1], B.G. Mathapa[1], B. Tiro[1]

[1]*Botswana University of Agriculture and Natural Resources, Faculty of Sciences, Basic Sciences Department, Private Bag 0027, Gaborone, Botswana*

Correspondence e-mail: otibe@buan.ac.bw or olekilet@gmail.com

ABSTRACT

The leaves of cowpea (*Vigna unguiculata* (L) *walp*) are an important source of minerals, vitamins, proteins and antioxidants in Botswana. This study was carried out to determine the total phenolic content and antioxidant activity of fresh tender and traditionally processed leaves of cowpea (*Vigna unguiculata (L) walp*). Both unprocessed and processed (boiling and sun drying) fresh leaves were used. Total phenolic content of the cowpea leaf extracts was determined by the Folin-ciocalteau method. Unprocessed methanol leaf extract (UM) had the highest phenol concentration at 1204.33 mg/L GAE and followed by the processed ethyl acetate leaf extract (PEA) at 670 mg/L GAE. The total phenolic content of processed methanol leaf extract (PM), processed chloroform-hexane leaf extract (PCH), unprocessed chloroform-hexane leaf extract and unprocessed ethyl acetate leaf extract (UEA) was 571, 327, 136.83 & 93.5 mg/L GAE, respectively. Free radical scavenging was determined using the DPPH method. The free radical scavenging power of the unprocessed methanol extracts was higher than the processed methanol extracts across all concentrations (25, 50, 100 and 200 µg/mL), relative to the negative control. At 200 µg/mL, the free radical scavenging activity of the unprocessed methanol extract was 58% while for the processed methanol leaf extracts was 43%. The lowest free radical scavenging activity was at 25 µg/mL. As the concentration of the extracts increased, the free radical scavenging power also increased. This study will help in exploring the effect of processing on the total phenolic content and antioxidant activity of cowpeas, and beneficial health effects of leaves of cowpea as potential functional foods in Botswana.

Keywords: cowpea, unprocessed, processed, phenols, antioxidant, Botswana

BIUST Research and Innovation Symposium 2019 (RDAIS 2019)
Botswana International University of Science and Technology
Palapye, Botswana, 4 - 7 June 2019

ISSN: 2521-2292

Research and Innovation Symposium 2019 (RDAIS 2019)
June 3rd to 7th , 2019. Botswana International University of Science and Technology, Palapye, Botswana

Significance of contact and mating on the long term dynamics of Devil Facial Tumour Disease.

Morelyn Sigauke[1] **& H. J. B. Njagarah**[2]
[1]Botswana International University of Science and Technology
E-mail address: morelyn.sigauke@studentmail.biust.ac.bw

[2]Botswana International University of Science and Technology
E-mail address: njagarahh@biust.ac.bw

ABSTRACT

A mathematical model for transmission dynamics of Devil Facial Tumour Disease is developed and analysed. The model considers mainly two transmission pathways namely, via contact and mating. The relative transmission rates through mating from male devils to female devils and vise versa are assumed to be different. The positivity of solutions for the model was done and it was shown that all state variables are non negative. The model disease threshold evaluated and used to analyse the model properties including existence and stability of equilibrium of steady states. For values of the disease threshold greater than unit, the disease remain prevalent and negligible values are observed when the disease threshold is less than unit. Using LHS it is observed that contact rate and the proportion of newly devils into susceptible population are the parameters with the greatest potential of making the disease epidermic worse when they are increased. The long term dynamics of the infection is characterised by an explosive outbreak reaching peak values in about 60 days and then followed by a gentle decline in the number of infected devils as a result of self-regulation. The infection is observed to devastate more the female devil population. Our sensitivity results related contact and mating indicated that for both male and female devils, the higher the contact rate, the faster (and the higher) the peak values are reached. Our results show that the transmission rates from male to female and female to male was not significantly different.

Keywords: *Devil Facial Tumour Disease; Sensitivity Analysis; Latin Hypercube Sampling(LHS); Steady States; Reproduction Number*

Category: **Mathematical Biology**

References

[1] M. Beeton and H. McCallum. Models predict that culling is not a feasible strategy to prevent extinction of Tasmanian devils from facial tumour disease. *Journal of Applied Ecology*., 48:1315-1323, 2011.

[2] H. Rodrigo, B. Jim, J. Menna and M. Hamish Simulating Devil Facial Tumour Disease outbreaks across empirically derived contact networks. *Journal of Applied Ecology*., 49:447-456, 2012.

[3] P. van den Driessche and J. Watmough. Reproduction numbers and sub-threshold endemic equilibria for compartmental models of disease transmission. *Mathematical Biosciences*., 180:29–48, 2002.

BIUST Research and Innovation Symposium 2019 (RDAIS 2019)
Botswana International University of Science and Technology
Palapye, Botswana, 4 - 7 June 2019
ISSN: 2521-2292

Fermentative microbiota of *khadi*, a traditional wine of Botswana

Koketso Motlhanka*, Kebaneilwe Lebani and Nerve Zhou

Department of Biological Sciences and Biotechnology, Botswana International University of Science and Technology, Private Bag 16, Central District, Palapye, Botswana; lebanik@biust.ac.bw (K.M); zhoun@biust.ac.bw (N.Z)

**Correspondence: koketso.motlhanka@studentmail.biust.ac.bw (K.M); Tel.: +267-7632-5058/ +267-7427-659*

Abstract

Khadi is a popular traditional fermented alcoholic beverage in Botswana produced from the spontaneous fermentation of *Grewia flava* fruits supplemented with brown table sugar. Even though this beverage is popular, there is little information known about its fermentative microbes. To isolate and identify these microbes, dried *G. flava* fruits and *khadi* samples were collected from 18 traditional brewers from Central and Northern Botswana. The fruits predominantly harbored bacteria (77.8 %) and a lower percentage of yeasts (22.2 %). Interestingly, all isolates from *khadi*, were fermentative *Saccharomyces* and non-*Saccharomyces* yeasts, with no bacteria, producing a beverage with an average alcohol content of 5.27 ± 2.02 % (*v/v*) and an overall pH of 2.64. *Saccharomyces cerevisiae* isolates were the most predominant (50%) yeast species and the isolates were genetically identical to the commercial baker's yeast suggesting use of this yeast as a starter culture. The presence of non-*Saccharomyces* yeast in *khadi* further suggested that this beverage can be produced through spontaneous fermentation. These results also show that *khadi* is a product of a mixed consortia of yeasts with a potential be used as starter cultures for the production of a consistent quality *khadi*.

Keywords*:* *Grewia flava* fruits, *khadi*, spontaneous fermentation, microorganisms

BIUST Research and Innovation Symposium 2019 (RDAIS 2019)
Botswana International University of Science and Technology
Palapye, Botswana, 4 - 7 June 2019
ISSN: 2521-2292

A Dual - Arm Robotic Nurse(DARN) for Assistance in Healthcare Facilities

Tlamelo Makati, Dimpho Kgosiemang and Tagala Smarts

Department of Mechanical, Energy and Industrial Engineering

Botswana International University of Science and Technology: Contacts:
tlamelo.makati@studentmail.biust.ac.bw ; +26774339135

DARN is a dual - arm robotic nurse that is designed to lift or transfer bedridden or unconscious patients from a bed to a wheelchair/another bed and back. It uses the relative Jacobian matrix to control the movements of the arms and takes into consideration the Human - Robot Interaction (HRI) by incorporating series - elastic actuators for a more softer robot to ensure human safety when interacting with the robot. The robot is designed on the SolidWorks platform and has six main Degrees of Freedom(DOF) that will allow the robot to bend forward and backward, move arms forward and sideways, move forearms upward and downward and move the wrists up and down. The design of the robot will be 3D printed to test these DOF. The robots trajectory is implemented using forward and inverse kinematics. The manipulator forward kinematics uses the initial vector of joint angles to find the vector of end effector positions. The manipulator inverse kinematics involve using the end effector positions to find the joint angles. Our initial simulation was carried out using GAZEBO which allowed us to see the initial model of the dual arm and also how the relative jacobian matrix maps out the dual arm movements. This research project's main aim is to fill the gaps of assistive robots in the medical field as there are currently no autonomous robots that deal with patients in hospitals. Those existing require a nurse or doctor to assist in lifting and carrying patients from one bed to another. They are not able to carry humans from wheelchairs or place them on one when necessary. The research tries does this by looking at the design, simulation and safety of the human - robot interaction and how these three concepts can be combined and optimized to create the ultimate autonomous Dual - Arm Robotic Nurse to assist in healthcare facilities.
Keywords: *DARN, Design, Simulation, HRI, Safety*

BIUST Research and Innovation Symposium 2019 (RDAIS 2019)
Botswana International University of Science and Technology
Palapye, Botswana, 4 - 7 June 2019
ISSN: 2521-2292

Integrated Solar and Wind Hybrid System with Remote Monitoring

Jeet Parikh, Tariku Alemayehu, Janardan Yadav, Ravi. Samikannu

Faculty of Engineering, Department of Electrical, Computer and Telecommunication Engineering
Botswana International University of Science & Technology, Palapye, Botswana

Abstract
Clean and Green Energy is now a need for all human beings for a healthy lifestyle and a non-polluting environment. The best and clean way to generate power is by using renewable source of energy as it is clean and keeps the environment clean. The aim of this paper is to investigate and design a power source made using Wind and Solar as the renewable sources. The solar energy is harnessed with a solar panel and the wind is harnessed with a wind turbine. Furth more a remote monitoring system is added so as to easily and remotely monitor the outputs from the sources and the battery voltage. This paper reviews the system under different conditions to see the efficiency of the system. Wind speeds are average throughout the whole year in Botswana and due to that we have designed a vertical axis wind turbine using a light material which can rotate easily and generate power. This system is eligible for small electrical equipment such as Solar street lights, solar bikes. We further plan to develop this system on a large scale to make it work for a normal 2 bedroom house. The idea is to minimise the use of a battery due to its maintenance costs and relatively high temperatures in Botswana throughout the year. This project was designed and developed by students and lecturer of Botswana International University of Science and Technology (BIUST). A hardware prototype has been developed and tested using 12V DC lamp and remote monitoring part has been installed to constantly monitor solar and wind yields being produced. We are working on developing this prototype to an industrial design which we can start by using it and further expanding it at BIUST.
Keywords: Solar, Wind, Hybrid system, Remote Monitoring

BIUST Research and Innovation Symposium 2019 (RDAIS 2019)
Botswana International University of Science and Technology
Palapye, Botswana, 4 - 7 June 2019
ISSN: 2521-2292

Developing a Miniature Train to Deliver Medicines and Documents in Hospitals

Leaname Thaolang, Kebalebile Oteng Telekelo and Tapologo Chigocha
Department of Mechanical, Energy and Industrial Engineering
Botswana International University of Science and Technology
Emails: leaname.thaolang@studentmail.biust.ac.bw, kebalebile.telekelo@studentmail.biust.ac.bw, tapologo.chigocha@studentmail.biust.ac.bw

ABSTRACT

This work builds, simulates and controls a miniature train that will deliver medicines and documents in a hospital setting. There are three parts in the project: the physical design and fabrication, simulation, and control in both simulation and in physical simulation. The train will have its ground rail track passing through every designated point and utilise the principles of electric powered rails drive mechanism. The simulation will be performed under hospital environment conditions to validate the train motion and control. The train control, both in simulation and actual physical implementation, will allow the user to call the train for either pick up or delivery, with priority settings determined according to distance and urgency. A user interface and software manager will be developed that will be designed to coordinate the train motion and customer demand.

KEYWORDS: Fabrication, miniature train, hospital, delivery, interface, customer demand

BIUST Research and Innovation Symposium 2019 (RDAIS 2019)
Botswana International University of Science and Technology
Palapye, Botswana, 4 - 7 June 2019
ISSN: 2521-2292

PHYSICO-CHEMICAL PROPERTIES AND GEOCHEMICAL MASS BALANCE OF TWO WEATHERING SOIL PROFILES IN LETLHAKENG

Yvette Matshameko, Peter N Eze
Department of Earth & Environmental Science
Botswana International University of Science & Technology (BIUST)
Palapye, Botswana
yvette.matshameko@studentmail.biust.ac.bw, ezep@biust.ac.bw

ABSTRACT

There are quite a lot of understudied soils in Botswana, amongst those soils are the ones found in Letlhakeng which is situated on the sandveld at the confluence of three major fossil valleys. The local indigenous knowledge classifies the soil in Letlhakeng as clay which is mostly used for pottery making and traditional house decorations. The aim of this study is to determine the geochemical mass balance and physico-chemical properties of the weathering soil profiles from Letlhakeng. Two profile pits were sited following a reconnaissance survey of the depositional environment. Soil samples were collected from each genetic horizon of the profile pits and shipped to the laboratory for further analysis. Selected physico-chemical properties including bulk density, pH, electrical conductivity (EC), organic matter content, carbonates and soil porosity were determined using routine laboratory procedures. The total elemental analysis were done using the X-ray fluorescence (XRF) spectroscopy, geochemical mass balance was used to assess the elemental losses and gains across the soil profiles. To estimate the degree of chemical weathering; Index of compositional variability (ICV) values were calculated. From the Munsell color chart, both the wet and dry samples of these soils are reddish with readings of 10R 5/4 and 10R 5/3 hence their use for house painting and pottery. These samples have a pH (H_2O) ranging between 8.3 and 9.0 while pH (KCl) ranges between 7.0 and 7.5 which means that the samples are slightly alkaline. The low EC range of 110 to 750 µS/cm of the soil suggests that they are non-saline. The carbonate content in both profiles ranges between 7.1-10.2% and this can be attributed to the carbonate fragments that were found in the soil profiles. There is a fluctuation of bulk density down the soil profile A while in soil profile B, the bulk density increases with depth as the soil porosity decreases, this was also seen as there were less root penetrating down the soil profile pit. In both soil profiles, there is an enrichment of Al, Mg, Mn, Ca and Na while K and Fe are depleted with increase in depth. The two soil profiles have positive ICV values ranging between 1.74 to 4.32 in profile A and 1.74 to 2.77 in profile B which means that the soils in the study location are immature and young.

Keywords: Clays, index of chemical alteration, sandveld ecosystem, pedogenesis, weathering

BIUST Research and Innovation Symposium 2019 (RDAIS 2019)
Botswana International University of Science and Technology
Palapye, Botswana, 4 - 7 June 2019
ISSN: 2521-2292

ESTIMATING THE LS FACTOR OF THE RUSLE MODEL IN A GIS BASED ENVIRONMENT FOR TWO SEMI ARID WATERSHEDS.

Thatayaone Popego, Peter N. Eze

Department of Earth and Environmental Science

ABSTRACT: Soil erosion is a naturally occurring geomorphic process resulting from the detachment, transportation and deposition of soil particles on landscapes. Triggered by rainfall and wind, soil erosion represents one of the most pressing contemporary environmental issues, decreasing agricultural productivity and degrading crucial soil ecosystem functions. Botswana, like many places in the world, has witnessed varying severity of soil erosion. The objective of this study is to model the slope length and steepness factor in order to detect soil erosion prone areas in Botswana watersheds. Tshimoyapula, a dominantly agricultural watershed and Ntlhantlhe, a rangeland watershed were chosen for this study because of the glaring evidence of varying degrees of active rill and gully erosion found in the areas. Of the five components in the RUSLE the slope length and steepness (SL) combines the effect of slope length factor(L) and slope steepness factor(S).Slope length in most cases increases total erosion per unit area as a result of increase in flow accumulation down slope due to rainfall-runoff. Slope steepness contribute to velocity and increase in runoff erosivity. The LS factor of the watersheds was obtained in a GIS based environment through pixel-based computing to determine its contribution to soil loss. In this study the LS factor of Tshimoyapula agricultural watershed varies according to the slope steepness. This watershed LS factor is categorized into five classes which are 0-1, 1-4, 4-11, 11-29 and >29. The highest LS factor classes categorized as >29 are found in steeper slope of 5.57 with a mean value of 15.2 and in the western side of the agricultural watershed with a greater value of 29.43 and slope degree of 15.11.The watershed is dominated by the LS factor class 0-1 and 0-4 which has a slope steepness ranging from 0 to 0.65 respectively. These LS factor class covers an area of 81.65 km^2 and 21.05 km^2 of the watershed respectively which is 77% of the agricultural watershed with a mean value and standard deviation of 0.05 and 0.65 respectively. Ntlhantlhe rangeland watershed is also categorized into five LS factor classes which are 0-0.3, 0.3-1.10, 1.10-2.10, 2.10-3.60 and 3.60-7.70.The rangeland watershed is dominated by LS factor of class 0-0.3 which is 0 signifying that the landscape is flat.In most parts of the watershed the slope length and steepness of the class 0.3-1.10 have a slope degree of 4 which is evenly distributed across the entire watershed covering an area of 75% of the entire watershed. The LS factor of class 3.60-7.70 is scattered around the watershed with greater values ranging from3.27 to 7.65 respectively with a slope steepness of 6.5^0. These results would be used as inputs to calculate the estimate soil loss from erosion in the watersheds using RUSLE model.

Key Words: Revised Universal Soil Loss Equation (RUSLE), Remote Sensing, Ntlhantlhe ,Tshimoyapula, soil erosion

BIUST Research and Innovation Symposium 2019 (RDAIS 2019)
Botswana International University of Science and Technology
Palapye, Botswana, 4 - 7 June 2019
ISSN: 2521-2292

In silico evaluation of phytocannabinoids as peroxisome proliferator-activated receptor gamma (PPARγ) agonists for type 2 diabetes mellitus therapy.

Keagile Bati* and Tebogo E. Kwape, Ph.D
Department of Biological Sciences and Biotechnology
Botswana International University of Science and Technology
Palapye, Botswana
*Corresponding author email: bk18100101@studentmail.biust.ac.bw

Abstract

Diabetes mellitus is a metabolic disorder characterized by chronic hyperglycemia due to absolute or relative insulin deficiency and action. With the continued search for antidiabetic drugs, PPARγ agonists have gained attention as target for drug development. Peroxisome proliferator-activated receptor gamma (PPARγ) is a member of the nuclear receptor superfamily and regulate the gene expression of proteins involved in the regulation of glucose and lipid metabolism, inflammation and adipogenesis. PPARγ binds with natural and synthetic ligands to exert pharmacological effects. PPARγ agonists like Rosiglitazone of the Thiazolidinedione drugs modulate insulin sensitivity and glucose metabolism in type 2 diabetic and metabolic syndrome patients. Phytocannabinoids are naturally occurring compounds from cannabis species and have pharmacological value. Therefore, the current study evaluated the potential anti-diabetic effects of phytocannabinoids using virtual screening and molecular docking on PPARγ. Canonical smiles of different phytocannabinoids and Rosiglitazone were pulled from PubChem and transformed to 3D structures and prepared for docking by energy minimization using Chimera. A pdb file of the 3D structure of PPARγ was pulled from Protein data bank and prepared by removing water molecules and other unwanted molecules, addition of hydrogen's and charges using chimera. Docking was done by Autodock vina through PyRx software and visualized on PyMOL. The results indicated that cannabinoid compounds bind to PPARγ and the binding energies were ranging from -4.3 to -7.7 Kcal/mol. Cannabichromene had the lowest binding energy of -7.7 Kcal/mol which is comparable to the binding energy Rosiglitazone (-8.7 Kcal/mol). It was concluded that phytocannabinoids interact with PPARγ hence has the potential for development into as antidiabetic agents.

Keywords: Diabetes mellitus, peroxisome proliferator-activated receptors (PPARs), phytocannabinoids, virtual screening, molecular docking.

BIUST Research and Innovation Symposium 2019 (RDAIS 2019)
Botswana International University of Science and Technology
Palapye, Botswana, 4 - 7 June 2019
ISSN: 2521-2292

Design and Implementation of Electronic Variable Speed Number Counting Game for Young Learners using Pic 16f887 Microcontroller

Phalaneng Maphane
Department of Physics and Astronomy
Botswana International University of Science and Technology
Palapye, Botswana
maphanep@biust.ac.bw

Abstract
For innovation category, this work will present an electronic board game prototype, designed and implemented as an educational game tool for young kids who are learning to recognize numbers and correct sequence of counting numbers. The game tool is designed and implemented using PIC 16f887 microcontroller, which is programmed using PIC BASIC PRO (PBP3) language. The game is played by first setting speed of counting through a delay set push button, which allows longer delays to be set for beginners and progressively shorten delays as they gain confidence. The game tool consists of an interactive LCD screen where one can observe varying delay values during setting, scores of the game and congratulatory comments for good performance. The counting intervals are accompanied by beeps from a buzzer and a blinking amber LED. Every time a correct number is pressed within a set delay period a green LED is illuminated accompanied by corresponding unique buzzer sound else if the delay set period elapses, a time up unique buzzer sound and red LED illumination are activated together with a total score and comment on LCD screen. The presentation of this tool also acts as a catalyst for industrialisation, as it will motivate aspiring innovators locally and regionally to start building up of their ideas and turning them into tangible ideas, hence growing the needed industrialisation sector.

Keywords: Electronic board game, speed counting, pic microcontroller, pic basic pro, young kids

BIUST Research and Innovation Symposium 2019 (RDAIS 2019)
Botswana International University of Science and Technology
Palapye, Botswana, 4 - 7 June 2019

ISSN: 2521-2292

Surface water demand and supply of Gaborone City and surrounding areas: Response to climate change and population increase

Bosa Mosekiemang, and Gizaw Mengistu Tsidu

Department of Earth and Environmental Sciences,
Botswana International University of Science and Technology
Palapye, Botswana
bosa.mosekiemang@studentmail.biust.ac.bw & mengistug@biust.ac.bw

Abstract

Most governments have implemented laws and water management strategies. However, the adequate supply of the ever-increasing demand of fresh water continues to be a challenge. For example, many regions are facing formidable freshwater management challenges. The challenge has been aggravated due to increasing population and climate change. The anticipation for better lifestyles and improved water supply has resulted in an increase in migration from rural settlements leading to an increase in the populations of many cities globally. This study therefore investigates the variability and trends in the surface water demand and supply of the city of Gaborone and surrounding areas in response to population growth and climate change using the Water Evaluation and Planning (WEAP) model for historical and future scenarios. The study includes analysis of population trends, water production and consumption rates, hydrological information as well as historical and projected climate data at a high spatial resolution of 1 km^2. The current General Circulation (GCM) or Regional Climate (RCM) models are not able provide such data. Therefore, the climate data for existing GCMs is statistically downscaled using the high resolution Worldclim data to spatial resolution of 1 km^2 and bias corrected against Global Climatology Precipitation Centre (GPCC) precipitation and Climate Research Unit (CRU) minimum and maximum temperature. The GCM data for historical as well as mid-range Concentration Representative Pathways (RCP4.5) and high emission RCP 8.5 future scenarios of Coupled Model Inter-comparison Project Phase 5 (CMIP5) are employed in the study. The result shows that the projected population of Gaborone, Mogoditshane and Tlokweng using the high population growth rate of 3.4% will be about 4106670, 1029877, and 644092 respectively by the year 2100. Under both RCP4.5 and RCP8.5 scenarios, the reservoir inflow indicates that the level of reservoirs at Foresthill, Diremogolo, Gabane hill, Oodi hill and Mabutswe will be reduced during 2081-2097 period. The unmet water demand of the whole study area will be 261.17 million m^3 in 2074 as compared to 1389.78 million m^3 in 2100 under RCP 8.5 climate and high population growth scenarios. However, the unmet demand under RCP4.5 climate and high population growth scenarios will be 254.58 million m^3 in 2074 as compared to 1354.17 million m^3 in 2100. The climate under RCP8.5 emission scenario will be drier than that of the RCP4.5. On the other hand, the unmet water demand will be 62.73 million m^3 in 2074 as compared to 169.04 million m^3 in 2100 under the RCP4.5 climate with low population growth rate of 2.2% scenario. In contrast, the unmet demand is as high as 65.52 million m^3 in 2074 and 186.21 million m^3 in 2100 under the RCP 8.5 climate with low population growth rate. The unmet water demand in both high and low population growth and the dry climate of RCP8.5 climate scenario will lead to severe shortage of water in the city. The most effective water management options could be, encouragement of water re-use, tariff increments and rain water harvesting which could reduce the unmet water demand to some extent.

Keywords: Climate change, population, unmet water demand, WEAP

BIUST Research and Innovation Symposium 2019 (RDAIS 2019)
Botswana International University of Science and Technology
Palapye, Botswana, 4 - 7 June 2019
ISSN: 2521-2292

EXTRACTION AND CHARACTERIZATION OF *Croton gratissimus* LEAF ESSENTIAL OIL FROM BOTSWANA

Eniah Lemogang Serame, Tshepo Pheko-Ofitlhile, Wellington Masamba

Botswana International University of Science and Technology (BIUST), Private Bag 0016, Palapye, Botswana

phekot@biust.ac.bw, masambaw@biust.ac.bw, eniah.serame@studentmail.biust.ac.bw

ABSTRACT

Essential oils are of great commercial interest due to their wide applicability in many industries. *Croton gratissimus* plant is a widely distributed aromatic plant in Botswana and neighbouring countries which is commonly used as a traditional medicine for abdominal and respiratory tract disorders, cough, fever and skin inflammation. The extracts and essential oils of this plant have been reported to have considerable antimicrobial and antioxidant activities. Despite its wide distribution and availability, characterization of essential oils from *Croton gratissimus* found in Botswana has not been done. In this study, essential oils were extracted by hydrodistillation and ultrasonic pre-treatment followed by hydrodistillation from the leaves of *Croton gratissimus* plant found in Botswana. The essential oils obtained were characterized by gas chromatography mass spectrometry. The percentage yields of essential oils from *Croton gratissimus* ranged from 0.09 to 0.26 % for hydrodistillation and 0.13 to 0.27 for ultrasonic pre-treatment hydrodistillation, with highest oil yields (0.23- 0.27%) recorded for leaves harvested between 0940 hours to 1000 hours. Camphor was found to be the most dominant component of *Croton gratissimus* essential oil extracted by both hydrodistillation and ultrasonic pre-treatment hydrodistillation. Other major components identified in essential oils obtained by both methods include Ŭ-terpineol, bourbonene, Ŭ-cubebene, ɓ-cubebene, Ŭ-curcumene and ɔ-eudesmol.

Keywords: *Croton gratissimus, essential oil, hydrodistillation, camphor, ultrasonic pre-treatment*

BIUST Research and Innovation Symposium 2019 (RDAIS 2019)
Botswana International University of Science and Technology
Palapye, Botswana, 4 - 7 June 2019
ISSN: 2521-2292

DEVELOPMENT OF A CLEAN ENERGY DRIVEN AUTONOMOUS VEHICLE DESIGNED FOR ALL-TERRAIN DRIVE AND BEAUTY

Thabo Malete Maikano Vryburg Bakang Mokgethe and Kagiso Moilwa
Department of Mechanical, Energy and Industrial Engineering
Botswana International University of Science and Technology,
Palapye, Botswana

ABSTRACT

The project is focused on developing an autonomous electric automobile along with a solar charge solution with an emphasis on multiple terrain handling and visual appeal. The vehicle's autonomy was achieved by building a completely wire based low level control system and implementing both robotic modelling and machine learning to make driving decisions from sensor fusion of sonar, camera and radar sensor data. For the all-terrain mechanism passive, semi-omnidirectional legged wheels were chosen to navigate through various terrains. The wheels were developed as CAD models and tested through different environment simulations to determine their efficiency and maneuverability in any terrain. With the use of an evaluation criteria aimed at determining the high ground clearance, maneuverability and stability on uneven terrain for the different simulation environments we were able to categorize the initial designs with the passive, semi-omnidirectional wheels being the ideal choice. Taking advantage of the ample solar power to make the car independent of the grid power and environmentally friendly a solar powered charging station with solar panels and batteries will be implemented to charge the car and act as backup power to the household. From the data of BIUST as sample a charging station was simulated on PowerSim to demonstrate its viability. The power from the charging station will be used charge the onboard battery which is used to power the motor that drives the car and the control system. To quantify beauty, various design concepts are identified and weighted for each attribute. The average of all attributes is then selected and implemented into the final vehicle model. Each attribute implements the GESTALT principles (Closure, Proximity, Continuation, Similarity, Figure and Ground) as well as the Design Process to implement concepts of beauty onto the vehicle. Additionally, as an Aesthetic measure, Birkhoff's equation of beauty which is a function of Order divided by Complexity was utilized to quantify the overall beauty of the vehicle.

Keywords: Autonomous vehicle, all-terrain, aesthetics, renewable energy, energy efficiency, machine learning

BIUST Research and Innovation Symposium 2019 (RDAIS 2019)
Botswana International University of Science and Technology
Palapye, Botswana, 4 - 7 June 2019
ISSN: 2521-2292

Impact of stress jump condition and heterogeneous reaction on velocity, temperature and concentration during bio-fluid flow through a permeable microvessel

Godfrey Bashaga[1] **& Sachin Shaw**[2]
Department of Mathematics and Statistical Sciences, Botswana International University of Science and Technology, Private Bag 16, Palapye, Botswana
E-mail address: godfrey.bashaga@studentmail.biust.ac.bw (G Bashaga), shaws@biust.ac.bw (S Shaw)

Abstract

Understanding how fluid flow in human bodies is crucial in Biomedical Engineering. Studying blood rheology is crucial as it may help in detecting , if not designing a treatment for some blood related diseaseses or understanding them better . The aim of this paper is to study the heterogeneous reaction of blood flow velocity, temperature and diffusion through microvessel with the stress-jump condition at the interface of the clear and peripheral region and velocity slip condition at the wall of microvessel .We have considered a two phase model where the radius of the microvessel is divided into two parts. The flow nature at the clear region is defined by non-Newtonian Casson fluid and the flow at peripheral region is defined by Newtonian fluid. The wall of the microvessel is considered as permeable and the nature defined by Brinkman model.

Keywords: *Blood Flow, Two phase model, non-Newtonian fluid, stress-jump condition, heterogeneous reaction*

BIUST Research and Innovation Symposium 2019 (RDAIS 2019)
Botswana International University of Science and Technology
Palapye, Botswana, 4 - 7 June 2019

ISSN: 2521-2292

RDAIS 2019: BIUST Research and Innovation Symposium 2019
June 4 - 7, 2019. Botswana International University of Science and Technology, Palapye, Botswana

Modelling Substance Abuse in Botswana in Presence of Multiple Amelioration Stages and Outpatient Rehabilitation

T.L Gasebonno[1,2] **& J.B.H. Njagarah**[2]
[1]Botswana International University of Science and Technology
E-mail address: thatayaone.gasebonno@studentmail.biust.ac.bw
[2]Botswana International University of Science and Technology
E-mail address:njagarahh@biust.ac.bw

ABSTRACT

Substance abuse in Botswana is a growing problem with a variety of drugs being abused including cocaine, heroine, methamphetamine, marijuana and alcohol among others. At the forefront of trying to address the drug abuse problem is the Botswana Substance Abuse and Support Network (BoSASNet) which operates outpatient rehabilitation and support services that constitute its clinical programme. Due to criminalisation and stigma associated with drug use and dealing in drugs, the number of individuals who seek rehabilitation from BoSASNet is believed to be lower than the actual number of drug users who really need the service. We developed a mathematical model to analyse the dynamics of substance abuse in Botswana. The model is composed of eight compartments. All the drug users including those in rehabilitation are assumed to contribute to initiations into drug use since they are still in contact with potential drug users. The developed model has a globally asymptotically stable drug free equilibrium when the threshold is less than unit. Sensitivity analysis of the parameters to the model output was carried out using the Latin hypercube Sampling scheme. Our results show that the parameters with the highest positive partial rank correlation coefficients(PRCCs) are parameters related to contact between potential drug users and individuals using drugs. The parameters related to amelioration processes, quitting and rehabilitation were observed to have highest negative PRCCs. Therefore, if such processes are enhanced, it increases the likelihood of containing the drug epidemic. From our results, we recommend that preventive strategies should be directed toward reducing the contact rates, enhancing rehabilitation, accelerating quitting and preventing relapse. We recommend embarking on inpatient rehabilitation programmes as these may prevent contact between drug users in treatment and susceptible individuals thereby reducing initiations.

Keywords: *Substance Abuse; Amelioration; Rehabilitation; Sensitivity Analysis*

Category: **Life Sciences, Environment and Physics**

References

[1] *J.B.H. Njagarah and F. Nyabadza; Modeling the impact of rehabilitation, amelioration and relapse on the prevalence of drug epidemics, Journal of Biological Systems, Vol.**21**:No. 1 (2013) 1350001 (23 pages)*

[2] *J. Lasalle(Ed.); The Stability of Dynamical Systems, SIAM, Philadelphia: 1976*

[3] *L. P. Swiler and G. D. Wyss; A User's guide to Sandia's Latin Hypercube Sampling Software: LHS UNIX Library/Standalone Version, 2004*

ISSN: 2521-2292

***Corresponding author. tel.:74022641**
E-mail address:tshephang.kabelo@studentmail.biust.ac.bw

Title: Assessment of the Sensitivity of Primary Cells and Cell Lines to the Southern African Territories (SAT) Serotypes in the Diagnosis of Foot-and-Mouth Disease Virus

T. Kabelo[a], E. Fana[b] and K. Lebani[a]

a. *Department of Biological Sciences and Biotechnology, Faculty of Science, Botswana International University of Science and Technology, Palapye,Botswana*

b. *OIE FMD Regional Reference Laboratory for Sub-Saharan Africa, Botswana Vaccine Institute, Gaborone, Botswana*

Abstract

Foot and mouth disease (FMD) is a zoonic disease that is endemic to many countries in the Sub Saharan region including Botswana. In controlling an FMDV outbreak there is a need rapidly diagnose the disease so as to manufacture the relevant vaccines. A popular procedure used for FMD diagnosis is the virus isolation procedure. This procedure requires the use of FMDV sensitive cells, this allows for rapid and consistent diagnosis. Most FMDV diagnostic laboratories including the one in Botswana use primary cells for virus isolation procedures. However primary cells have varied sensitivity from one cell batch to another, giving rise to result inconsistencies. With this problem at hand there is a need to transition to the use of a different cell culture system. In this study we aimed to compare the sensitivity of the conventionally used primary lamb kidney cells (RM) to two cell lines, baby hamster kidney cells(BHK-21) and a derivative of female pig kidney cells(IR-P1), to the Southern African Territories (SAT) serotypes of FMDV.This was done by determining the virus concentration required to induce signs of infection on each cell type. The results from this study suggest RM and IR-P1 cells have a relatively similar sensitivity to FMDV($P<0.05$).BHK-21 however, demonstrated a low sensitivity to the FMDV strains used. Comparisons of two batches of each cell type were also done to establish the consistency of the sensitivity of these cells to FMDV infection.IR-P1 and BHK-21 cell batches gave consistent results while RM cells demonstrated a significant variation ($P<0.05$) between batches. The TCID 50/mL was also used as a measure of sensitivity. Both cell batches of IR-P1 cell linehad consistently higher TCID50/mL while RM cell batches displayed a variation in TCID50/mL values,with batch 1 having a higher TCID50/mL than batch 2.This work therefore showed the best FMDV diagnosis-favorable results with the IR-P1 cell line which could be considered for use in routine diagnosis in veterinary laboratories.

Keywords: FMD, Virus isolation, IR-P1 cell line, Sensitivity

BIUST Research and Innovation Symposium 2019 (RDAIS 2019)
Botswana International University of Science and Technology
Palapye, Botswana, 4 - 7 June 2019
ISSN: 2521-2292

Environmental biotechnology of extremophiles: application of alkaliphiles for the biological treatment of industrial effluents

Amare Gessesse

Department of Biological Sciences and Biotechnology
Botswana International University of Science and Technology
e-mail: gessessea@biust.ac.bw

Industrial production processes inevitably lead to the generation of substantial quantities of effluent that contain high concentrations of organic and inorganic chemicals. Releasing such effluents into the environment could cause severe environmental pollution. In many African countries gold mining, leather tanning, and textile processing are widely practiced. These industrial are also known to release huge quantities of toxic effluents that alkaline in nature. Environmental pollution caused by such factories affect tens of thousands of people living in the surrounding area. In some countries, such as Uganda and Ethiopia, complaint by people in the localities of the factories has resulted in the closure of factories. However, factory closure could also have serious consequences on the livelihood of workers and could have serious negative impacts on the economy. The best option could, therefore, be to treat the effluent before it is released into the environment. Although both physicochemical and biological treatment methods are available as options, because of its cost effectiveness and its efficiency, biological treatment process is often the most preferred method.

Effluent released by leather tanning, textile, and gold mining industries have high pH and high ionic strength. On the other hand, biological treatment process traditionally employed for the treatment of domestic wastewater are operated at neutral pH and in the presence of low salt concentration. This is because, a large majority of microorganisms involved in biological treatment processes optimally grow at neutral pH and in the presence of low salt concentration. On the other hand, different extremophiles that optimally grow at extremes of pH or in the presence of high salt concentration are known to exist in extreme environments in different parts of the world. In our laboratory the potential of alkaliphilic and haloalkaliphilic microorganisms for the biological treatment of alkaline effluents arising from textile, leather tanning, and gold mining industries was evaluated. Laboratory scale studies showed that for all the three effluent types, the use of alkaliphiles and haloalkaliphiles resulted in a 90 -100% removal of efficiency of the toxic components in the effluent. Because the organisms are naturally adapted to living at alkaline environments and in the presence of high salt concentration, there was no need for pH salt concentration adjustment making the treatment processes highly cost effective. In the case of gold mining effluents, because of the absence of organic carbon source, it will be necessary to supplement the effluent feed with a carbon and energy source. Scale up and optimization of these processes could, therefore, be expected to lead to the development of an efficient biological treatment process for treatment of difficult-to-treat industrial wastes.

BIUST Research and Innovation Symposium 2019 (RDAIS 2019)
Botswana International University of Science and Technology
Palapye, Botswana, 4 - 7 June 2019

ISSN: 2521-2292

RDAIS 2019: BIUST Research and Innovation Symposium 2019 Botswana International University of Science and Technology Palapye, Botswana, June 4-7, 2019

Viscosity type Douglas-Rachford Splitting methods for a Zero of the Sum of a finite family of maximally monotone mappings in Hilbert spaces

Getahun B. Wega, Habtu Zegeye & Oganeditse A. Boikanyo
Department of Mathematics and Statistical Sciences, Botswana International University of Science and Technology, Pvt Bag 16, Palapye, Botswana
getahunbekele2012@gmail.com, habtuzh@yahoo.com, boikanyoa@gmail.com

ABSTRACT

Let H be a real Hilbert space. Let $A_i : H \to 2^H$, for $i \in I = \{1, 2, ...N\}$ and $N \geq 2$, be maximally monotone mappings satisfying $\Omega := \{x \in H : 0 \in A_1x + A_2x + ... + A_Nx\} \neq \emptyset$. In this paper, we study the method of approximation for a zero of the sum of a finite family of maximally monotone mappings using Viscosity type Douglas-Rachford splitting algorithm and prove some strong convergence theorems of the proposed algorithm under suitable conditions. In addition, we give some applications to the minimization problems and a numerical example which supports our main result. Our theorems improve and unify most of the results that have been proved for this important class of nonlinear mappings.

Keywords: *Hilbert spaces; Monotone mapping; Strong convergence; Zero points.*

Category: **Nonlinear Analysis**

BIUST Research and Innovation Symposium 2019 (RDAIS 2019)
Botswana International University of Science and Technology
Palapye, Botswana, 4 - 7 June 2019

ISSN: 2521-2292

Spatio-temporal drought analysis under a changing climate over Botswana using Standardized Precipitation Evapotranspiration Index

Onneile Nomsa Keitumetse1 and Gizaw Mengistu Tsidu1

1. Department of Earth and Environmental Sciences
Botswana International University of Science and Technology
Palapye, Botswana

onneile.keitumetse@studentmail.biust.ac.bw

mengistug@biust.ac.bw

Abstract

Recently there has been an increased water scarcity around the world due to high water demand, which is worsened by the spatial and temporal variability of drought incidences along with the uncertainties associated with climate change. As a result, drought has been mostly studied in order to derive ways of minimising its adverse effects. Droughts are generally defined as a period of prolonged below normal precipitation over a specific area. They are mostly distinguished by various characteristics such as duration, severity and frequency. These parameters are important in drought monitoring and decision-making for reliable disaster early warning system, water resources planning and management. Semi-arid environments, of which Botswana is known for, exhibit high variability in climate leading to recurring droughts over the area. Hence there is a need to conduct a study in order to understand the spatio-temporal complexity of droughts over Botswana. The Standardized Precipitation Evapotranspiration Index (SPEI) was used for analysing drought based on gridded rain gauge data referred to as Climatic Research Unit (CRU) data covering a period of 1901-2015 at a time scale of 12 months. SPEI quantifies the occurrence of drought and analyses the severity of drought by indicating the dry and wet periods based on standardized 12-month aggregate rainfall and potential evapotranspiration (PET). SPEI was able to detect severe droughts of 1947, 1974, 1983, 1995 and most of the years that followed El-Niño events. The western and southern parts of the study area are mostly affected by the severe drought conditions while the northern, central and eastern parts registered mostly moderate drought conditions. SPEI was also able to detect the influence of temperature on drought variability with severe drought occurring during January, February and March over most parts of the study area. Moderate droughts had a high frequency of occurrence, severe droughts had a low frequency of occurrence while extreme drought was very low chance of occurrence. The conditional return period of drought of different categories were determined in a multivariate context by coupling duration, severity, inter-arrival time of drought based on copula distribution and cumulative density functions. The determined returned periods over the country can be useful in planning and management of water resources systems over the country.

Keywords: Drought, changing climate, copula distribution, Standardized Precipitation Evapotranspiration Index (SPEI), Spatio-temporal analysis

BIUST Research and Innovation Symposium 2019 (RDAIS 2019)
Botswana International University of Science and Technology
Palapye, Botswana, 4 - 7 June 2019
ISSN: 2521-2292

SYNTHESIS AND CHARACTERIZATION OF RUTHENIUM (II/III) POLYPYRIDYL COMPLEXES WITH ANTI-MICROBIAL PROPERTIES.

JAMES T.P. MATSHWELE[1], SEBUSI ODISITSE[1], FLORENCE NAREETSILE[2]

[1]Botswana International University of Science and Technology (Department of Chemistry and Forensic Sciences, Palapye, Botswana)
[2]University of Botswana (Department of Chemistry, Gaborone, Botswana)

Ruthenium polypyridyl complexes are widely studied in medicinal transition metal chemistry because they are continuously showing bio-activity, especially in all forms of diseases seen in the human body. This work describes the synthesis and characterization of novel ligands and their corresponding Ru(II)/(III) complexes. The ligands denoted as BUT and 2BUT were synthesized from their intermediates and successfully elucidated through proton NMR, ESI-MS and FTIR. These ligands were further coordinated to ruthenium to form Ru(II)/(III) complexes; $Li[Ru(Cl)_4(DPA)]$, $[Ru(BUT)(DMF)(DPA)](BH_4)_2$, $[Ru(BUT)(Cl)_3]$, $[Ru_2(2BUT)(DMF)_2(DPA)_2](BH_4)_4$ and $[Ru_2(2BUT)(Cl)_6]$. The prepared complexes were characterized by ESI-MS, FTIR (Group Theory included), UV/Vis and Magnetic Susceptibility. However, the larger complexes with the 2BUT ligand had diminished molecular ion peak in ESI-MS but were still characterized through investigation of their spectra. All these compounds were formed at satisfactory yields. The synthesized ligands and their corresponding ruthenium complexes were then tested for antibacterial activity on two species *Staphylococcus aureus* and *Klebsiella pneumoniae,* as well as their drug resistant strains *Methylene resistant Staphylococcus aureus* and *Multidrug resistant-Klebsiella pneumoniae.* All the compounds had activity against the non-resistant strains of bacteria *S. aureus* and *K. pneumoniae.* There was growth inhibition on *MRSA* only for the resistant strains. However, only one complex $[Ru_2(2BUT)(DMF)_2(DPA)_2](BH_4)_4$, together with the ligands, showed this activity, while all other complexes did not show any antibacterial activity towards *MRSA*. The ligand 2BUT did not have activity while the other ligands and the complex $[Ru_2(2BUT)(DMF)_2(DPA)_2](BH_4)_4$ of which it belongs to had activity towards *MRSA*. It was observed that gram-positive *S. aureus* and *MRSA* bacteria had more activity than the gram-negative *K. pneumoniae* bacteria. These compounds mode of action was assessed through gel electrophoresis. The mode of action after gel electrophoresis is assumed to be interaction with genomic material by DNA denaturing where the complexes showed complete DNA nuclease activity. More assays should however be done to assess if these compounds have one or multiple modes of action.

Keywords: Anti-microbial, MIC, ruthenium, bioinorganic chemistry

BIUST Research and Innovation Symposium 2019 (RDAIS 2019)
Botswana International University of Science and Technology
Palapye, Botswana, 4 - 7 June 2019
ISSN: 2521-2292

RU(II/III) COMPLEXES OF POLYPYRIDYL LIGANDS WITH ANTI-BACTERIAL PROPERTIES.

LEBOGANG G. JULIUS[1], DAPHNE MAPOLELO[1]and FLORENCE NAREETSILE[1]

[1] University of Botswana (Department of Chemistry, Gaborone, Botswana)

Keywords: (anti-microbial, MIC, ruthenium, bioinorganic chemistry)

Ruthenium-based complexes have become the interest of drug development research due to their properties that are well suited towards pharmacological applications. Herein we report the synthesis and characterization of a bidentate pyridyl ligand = [(2-PC)], and octahedral amino pyridyl based ruthenium complexes being [Ru(BBE)(2-PC)$(Cl)_2$] and [Ru(DPA)(2-PC)$(Cl)_2$]. The ruthenium complexes were synthesized from Li[Ru(BBE)$(Cl)_4$] and Li[Ru(DPA)$(Cl)_4$] intermediate complexes respectively. Spectroscopic characterization of the synthesized complexes was done by FTIR, GC/MS and UV-vis spectroscopy. The synthesized complexes were then tested against series of both gram-positive and gram-negative bacteria strains being *E. coli, P.aeroginosa, K.pneumoniae, Multi-Drug resistant-K.pneumoniae, S.aureus and Methicillin-resistant Staphylococcus aureus (MRSA).* Bacterial strains proved inhibited growth to the complexes [Ru(BBE)(2-PC) $(Cl)_2$] and [Ru(DPA)(2-PC)$(Cl)_2$] and intermediate complexes [Li[Ru(BBE)$(Cl)_4$] and [Li[Ru(DPA)$(Cl)_4$] and reported in this work are the Minimum Inhibition Concentrations (MIC) as determined by the Kirby disc diffusion assay.

BIUST Research and Innovation Symposium 2019 (RDAIS 2019)
Botswana International University of Science and Technology
Palapye, Botswana, 4 - 7 June 2019
ISSN: 2521-2292

Improving energy efficiency in Botswana's hotel sector – a systematic review of energy audit and management principles and previous findings

Thebe Kgare, Bao Motshwanaesi, Botsogo Kefalotse, Tsotlhe Leshetla and Tobias Bader
Department of Mechanical, Energy & Industrial Engineering,
Botswana International University of Science & Technology,
Private Bag 16, Palapye, Botswana

Abstract
The travel and tourism sector in Botswana significantly contribute to the national economy by around 10% and is predicted to further grow regarding the national efforts to diversify the economy. This forecasted growth will go along with an increased energy consumption of hotels and its related impact on emissions and energy costs. Beyond that background it is of importance to increase the energy efficiency of hotel buildings and its equipment. Energy consumption has increased due to competition of hotels and increased tourism in Botswana, mostly in the major cities like Gaborone, Francistown or Kasane. Therefore, hotel businesses are about to adopt energy saving measures reduce energy consumption, energy costs and related carbon emission. An annual increase in population of approximately 2%, raises the need for accommodation. Hence more hotels are built increasing the energy consuming capacity for ventilation, air-conditioning, lighting and other electrical appliances as they are common in a hotel. A study by (Burnett & Deng, 2000) shows that at least one-third of total energy in hotel buildings is used for air conditioning. Other factors that determine the energy consumption of a hotel include the age of the building, and the hotel type. Lack of capital and lack of knowledge on energy consumption patterns as well as on energy efficiency measures are the main barriers to the implementation of effective energy conservation measures.
Beyond this background, this paper discusses the hotel sector in Botswana and the main energy consuming equipment in hotel buildings. It further discusses national and international regulations and policies and standards on buildings energy efficiency and assesses the situation in Botswana. Energy audit and management standards are reviewed; relevant energy audit methodology and equipment is presented and evaluated. As a core, the paper sheds light onto previous findings on energy efficiency analyses and improvement through energy audits in hotels. The paper concludes with an overview on an ongoing hotel energy audit project in Botswana.

Keywords: Energy efficiency in hotels, energy audit of hotels, management principles in hotels

BIUST Research and Innovation Symposium 2019 (RDAIS 2019)
Botswana International University of Science and Technology
Palapye, Botswana, 4 - 7 June 2019
ISSN: 2521-2292

Review of solar cooling and air-conditioning

T. Motlhabane and T. Bader
Department of Mechanical, Energy & Industrial Engineering,
Botswana International University of Science & Technology,
Private Bag 16, Palapye, Botswana.
taboka.motlhabane@studentmail.biust.ac.bw
tbader@biust.ac.bw

Abstract
As the global population and the number of middle-income households around the world rise, the demand for goods customarily considered wants shifts to needs for majority of the world's population. Air-conditioning systems, once considered a luxurious investment, have become a necessity which is comparably low in cost and the use of these is expected to dramatically increase by the year 2030. By adding a strain of an ever-increasing load of air-conditioning units to national grids, increases the demand of energy, while the supply is not amassing at the level of the demand, leading to an overwhelmed grid. The use of air-conditioning units has a direct bearing on carbon emissions, as the primary source of electricity generation for the conventionally applied electrically-driven chiller remains fossil fuel based. Solar-driven air-conditioning systems purpose to address the foretold challenges of an increasing cooling demand. Both, solar-photovoltaic (PV) systems and solar-thermal systems can be utilized to drive cooling and air-conditioning processes for residential, non-residential and industrial purposes.
This paper provides a review of solar-driven cooling and air-conditioning with a focus on solar photovoltaic (PV) air-conditioning. The paper provides an overview on the working principles of solar cooling and air-conditioning technologies including, both, thermally and electrically driven processes. The review illustrates their key performance parameters such as coefficients of performance, cooling capacity and working temperatures and describes research experiences in the field and technological challenges. The study further focusses on solar PV driven air-conditioning and reviews advancements from most recent publications. Regarding the applied refrigerant the paper also reviews the climate-friendly refrigerants as recommended by UNFCC for future systems. The paper eventually derives recommendations and ideas for actual research work at BIUST.

Keywords: Solar Cooling & Air-conditioning, Solar PV driven air-conditioning, Climate-friendly refrigerants, Climate change, Renewable energy

BIUST Research and Innovation Symposium 2019 (RDAIS 2019)
Botswana International University of Science and Technology
Palapye, Botswana, 4 - 7 June 2019

ISSN: 2521-2292

A Review: DNA Recombination technology, its applications and different expression systems used in the production of recombinant proteins.

Keletso G. Masisi & Goabaone Gaobotse

Department of Biology and Biotechnology

Botswana International University of Science and Technology

Palapye, Botswana

mk18100061@studentmail.biust.ac.bw *&* ***gaobotseg@biust.ac.bw***

Abstract

Recombinant proteins are useful for medical, industrial and research purposes. It is essential to explore effective expression systems in order to make it easier and cheaper to obtain these proteins. This paper focuses on exploring different expression systems used in the production of recombinant proteins such as bacteria, yeasts, animal cells and plants. Current applications of DNA Recombination will also be reviewed. Diseases like HIV, diabetes and clotting disorders are examples of human diseases related to protein absence, presence or malfunction. Recombinant DNA technology provides a platform for research and the production of pharmaceuticals for disease treatment. It is therefore essential that different expression systems are explored in order to produce sustainable and easy to obtain proteins. Examples of expression systems are bacteria, yeasts, animal cells and plants. However bacteria are a standard way of producing recombinants followed by yeasts. Recently higher organisms like plants have gained recognition in recombinant protein production because they are easy to manage, cheap to sustain and they can produce large and properly folded proteins. This is why recently plants have been used for the production of vaccines and pharmaceuticals. Production entails the use of DNA recombination technology where a gene of the desired protein is analyzed, amplified, cloned into a vector and transferred to a production system of choice where the expression takes place. The protein is then purified and analyzed. It is important that a proper vector is used as it is necessary for verification of clones and transcription of the gene of interest in the production system. The paper will review different expression systems for recombinant proteins, DNA recombination and its current applications.

Key words: DNA recombination, cloning, genome editing & recombinant proteins

BIUST Research and Innovation Symposium 2019 (RDAIS 2019)
Botswana International University of Science and Technology
Palapye, Botswana, 4 - 7 June 2019
ISSN: 2521-2292

The Role of Nickel and Cobalt Nano-particles on Biogas Production from Abattoir Wastewater

Mpho Radipodi, Gofetamang Ditalelo

Department of Civil and Environmental Engineering
Botswana International University of Science and Technology
Private Bag 16, Palapye, Botswana

Email; rm18100163@studentmail.biust.ac.bw, ditalelog@biust.ac.bw

ABSTRACT

The need to develop sustainable energy sources is eminent due to the finite nature of fossil fuels. Anaerobic digestion of abattoir waste has positive environmental effects since it combines waste management, biogas and fertilizer production. Abattoir effluent has large amount of organic matter, suspended solids, and it is associated with repugnant odor. When improperly disposed, it pollutes the environment either directly or indirectly. Contamination of river bodies and land from abattoir wastes constitute a significant environmental and health hazard, hence it is paramount to find ways of its sustainable management. During anaerobic digestion of abattoir wastewater there are potential inhibitory compounds which can be formed during the degradation of the proteins and lipids. These can make the process sensitive and prone to failure therefore new approaches have to be developed, such as catalyzation of the process through supplementation of trace metal ions to the reactors.

Deficiencies of metals ions can lead to suboptimal digester performances and therefore an opportunity to catalyze anaerobic digestion process exists. Among the essential trace elements, nickel and cobalt are involved in multiple key enzymes necessary for efficient anaerobic digestion. This study will investigate the effect of individual and combined dosage of nickel and cobalt on biogas production from abattoir wastewater. Metal supplements will be dosed in the form of nanoparticles. The nanoparticles will be dosed at different concentrations so as to determine the concentration leading to optimal methane production. Serum bottles will be used for digestion. The gas produced will be measured on daily basis and the results will be statistically analyzed to determine the significance of micro nutrients dosage. The Boyle's stoichiometric equation and the ideal gas law will be used to predict the amount of theoretical methane and biogas that could be obtained from the conversion of the wastewater. The periodic biogas production data will be compared to theoretical values.

The focus of the research is to determine and evaluate the methane content generated from individual and combined dosage of Nickel and Cobalt nanoparticles. The paper aims to determine the energy potential generated and the possibility of the abattoir powering itself through the generated energy from combustion of methane in a Combined Heat and Power Plant.

Keywords: Anaerobic digestion; Abattoir waste water; Trace elements; Nickel; Cobalt; Biochemical Methane Potential

BIUST Research and Innovation Symposium 2019 (RDAIS 2019)
Botswana International University of Science and Technology
Palapye, Botswana, 4 - 7 June 2019
ISSN: 2521-2292

Feasibility study on the utilization of solar-photovoltaic technology for water pumping and electrification of an agro-pastoral farm.

G.Gaedupe, M. Matlapeng, K. Lesole, K. Keisang and T. Bader

Department of Mechanical, Energy & Industrial Engineering,

Botswana International University of Science & Technology, Private Bag 16, Palapye, Botswana

ABSTRACT

Kgare is a small farming land that has not been recognized as eligible to be developed as a village and thus solar technology has not been ventured into in the area. It however comprises of wide open land that could suit installations of PV systems to harness the energy of the abundant sun available in the area. Emphasis on utilization of clean fuel technologies continues to grow as countries push toward reducing the global greenhouse gas emissions from conventional power plants. Renewable energy i.e. solar power, wind energy, geothermal are quite useful in a wide range of off-grid remote rural area application. Some of the applications being village electrification, hot water preparation, water pumping and different industrial purposes .Activities in the agricultural industry require sufficient and reliable supply of water to be carried out. In most cases to meet this water demand, coal generated electricity, diesel or petrol are used to power water pumps. It is therefore evident that conventional water pumping causes carbon dioxide emissions thus contributing to global warming and depletion of fossil resources. Solar photovoltaic water pumping (PVWP) is a potential solution to that problem. This paper focuses on supply of water with solar PVWP for agricultural purposes, specifically for livestock (cattle) at the Maphakwane farm in Kgare Kweneng District in Botswana that has 250 cattle. In this context the paper presents the concept of a feasibility study on the utilization of solar-PV technology for water pumping and electrification project in agro-pastoral farming. The farm under investigation is introduced with the needed outlined data for a solar PVWP project. An in-depth literature review on the planning and simulation of solar PVWP systems is carried out, focusing on project experiences, energy requirement analysis, system design, guidelines and available standards. Based on this review a comprehensive energy requirement analysis is carried out at the Maphakwane farm for planning purposes. The utilization of the data for a subsequent simulation study is described. Furthermore details on comparison of different PVWP systems for the farm are provided and available state of the art simulation software and the implemented models for the simulation of the PVWP systems are assessed. The following is a classification of PVWP systems mentioned in the paper which depends on the components of the system: basis of battery storage (battery coupled, direct driven), basis of electric power input, (DC, AC), basis of pump types (surface mounted pumps, deep well pump set), basis of tracking power source (fixed SPV panels/arrays, tracking SPV panels/ arrays).

Keywords; Off-Grid, Photovoltaic, Solar Photovoltaic water pumping system (SPVWP), irrigation, commercial beef farming, Agro-farming.

BIUST Research and Innovation Symposium 2019 (RDAIS 2019)
Botswana International University of Science and Technology
Palapye, Botswana, 4 - 7 June 2019
ISSN: 2521-2292

AUTISM MELTDOWN DETECTION DEVICE

*Pearl Nthusang and Tshiamo Tsheole

Department of Electrical, Computer and Telecommunication Engineering

Botswana International University of Science and Technology

Private Bag 16, Palapye, Botswana

*tshiamo.tsheole@studentmail.biust.ac.bw; pearl.nthusang@studentmail.biust.ac.bw

ABSTRACT

Autism spectral disorder is a child predominant neurodevelopmental deficit that can be detected in children as early as 2 years old and affects mostly the child's social skills and their ability to communicate and express themselves. It is accompanied by sudden random meltdowns that can leave the patient exhausted and sometimes with injuries. The central problem met by caregivers and patients is uncertainty of the next meltdown; not knowing when it will happen. Research shows that a buildup of stress ultimately leads to a meltdown. Heart rate variability (HRV), a measure of the difference between consecutive heart beats is a measure directly linked to the autonomic nervous system. Galvanic skin response and HRV are measures linked to mental stress. This project uses automated machine learning techniques through TPOT, Auto-Sklearn to create a model that detects mental stress through bio impedance sensors and raspberry pi. The problem is taken to be a binary classification problem with integers 1 and 0 representing stressed and not stressed respectively. Using a supervised learning approach a threshold is detected prior to physiological data that is fed into the system. Anything below the threshold represents stressed and anything above the threshold represents not stressed. Upon detection of a meltdown, a notification is sent to the caregiver's or the patient's phone to provide calming down measures on time with the purpose of preventing the meltdown from occurring.

Keywords: Autism, monitoring, Heart Rate Variability, Galvanic Skin Response, automated machine learning, TPOT, Auto-Sklearn, bio impedance sensors, raspberry pi, binary classification, supervised learning, threshold, impending meltdown.

BIUST Research and Innovation Symposium 2019 (RDAIS 2019)
Botswana International University of Science and Technology
Palapye, Botswana, 4 - 7 June 2019
ISSN: 2521-2292

Review on performance and processing of natural fibers for thermal insulation purposes

Nametso Linda Moumakwa, Eyitayo Olatunde Olakanmi, Tobias Bader
Department of Mechanical, Energy and Industrial Engineering
Botswana International University of Science and Technology
Palapye, Botswana
nametso.moumakwa@studentmail.biust.ac.bw

Abstract
This contribution aims to explore the reasons leading to the increased interest in natural fibers in research and the industry at large. The paper presents a review of relevant literature on natural fibers, its surface modification and challenges associated with its processing. Also explored is the definition of natural fibers, its classification, structures and properties as they affect their performance as thermal insulators when incorporated into natural fibers reinforced polymer composites (NFRPCs). Furthermore, the nature of the surfaces of natural fibers is elucidated to understand how various surface modification treatments influence its microstructure, surface morphology, chemical, mechanical and physical properties. This paper also dwells on how various surface modification methods and treatment parameters influence the physical, chemical, microstructural and thermal quality characteristics of natural fibers. The principles of fiber characterization regarding chemical functional group, microstructure and surface morphology, crystallinity index and thermal stability using Fourier Transform Infra-red Spectroscopy (FTIR), Scanning Electron Microscopy (SEM), X-ray Diffraction (XRD) and Thermal gravimetric (TG/DTG) analysis respectively are also discussed. The outcomes of this study reveal that alkali treatment of fibers results in clean and rough fibers as a result of part elimination of lignin, hemicellulose and other impurities. Fibrillation and removal of impurities on the surface intensifies the surface area necessary for matrix and fiber mechanical interlocking, therefore improving the interfacial bonding.

Keywords: Hyphaene Petersiana, Phragmites Australis, Natural Fibers, Surface Treatments, Thermal Properties

BIUST Research and Innovation Symposium 2019 (RDAIS 2019)
Botswana International University of Science and Technology
Palapye, Botswana, 4 - 7 June 2019
ISSN: 2521-2292

A study of Energy Performance of Hotel Buildings in Palapye

Segolame Phegelo, Mushabi Pule and Tobias Bader
Department of Mechanical, Energy and Industrial
Botswana International University of Science and Technology
Palapye, Botswana
mushabi.pule@studentmail.biust.ac.bw

Abstract
Global warming has become one of the fore most issues of the world. In efforts to achieve sustainable development hence reduction in global warming, energy efficiency has become a core objective. Buildings use up to 39% of the energy resources available to the world making them ideal to carry energy performance study to identify possible energy saving opportunities ultimately leading to energy efficiency. The study focuses on two hotels in the Palapye area. The breakdown of energy use showed that electricity dominated total energy consumption with 84% on average. The bulk of the installed electric capacity is for air-conditioning equipment (avg. 34%). Gas is used in both hotels (avg. 12%) to facilitate cooking, whereby diesel (avg. 4%) is used to power a standby generator. Both hotels are not involved with any renewable energy which is identified as a possible recommendation to achieve energy efficiency. The relationship between the monthly energy consumption and total monthly bookings generated suggest bookings will not necessarily affect the energy consumption in the hotels. Based on a preliminary analysis, the main audit was conducted, including a detailed thermographic analysis to identify heat or cold losses of the building envelope, equipment and hot-water pipes. A simulation with 3E Plus demonstrated, that the application of a glass wool insulation at the pipes at a thickness of 40 mm, as recommended by ASHRAE for process temperatures up to 90°C, could reduce the losses of the pipes by 93%.

This paper documents the described energy audits. Based on a literature review on audits in hotel buildings, the applied audit methodology is introduced. The results of the preliminary analysis and the main audit are described and recommendations for the hotel operators are derived.

Keywords: Energy Audit, Energy Efficiency, Renewable Energy, Hotel Building, Insulation, ASHRAE

BIUST Research and Innovation Symposium 2019 (RDAIS 2019)
Botswana International University of Science and Technology
Palapye, Botswana, 4 - 7 June 2019

ISSN: 2521-2292

Preservation methods for herbarium specimens in Botswana

J. Michael*, T. Bader** and T. Schrag*
Institute for new Energy Systems, Technische Hochschule Ingolstadt,
Esplanade 10, 85049 Ingolstadt

Department of Mechanical, Energy & Industrial Engineering, Botswana International University of Science & Technology, Private Bag 16, Palapye, Botswana

Abstract

The Okavango Research Institute (ORI) in Maun, Botswana, operates the Peter Smith University of Botswana Herbarium (PSUB). With approximately 30,000 specimens and an estimated variety of more than 16,000 species, the PSUB houses collections from all of Botswana, with over 80% of specimens collected from the Okavango Delta. This inland delta system is unique. With an almost intact wetland system, it is inscribed as an UNESCO World Heritage Site. Although new species are constantly discovered from the collection, a considerable number of species are no longer found at their documented coordinates and are threatened by extinction. The current herbarium facility in a pre-fab building of an approximate room volume of 120 m^3 does not allow a proper conservation of the collection. However, is the best possible solution in the present circumstances. The storage facility is merged with a meeting room with human traffic and the installed chiller is operated at a constant supply temperature of T_{sup} =17° C. Though, the actual herbarium room temperature and the humidity cannot be controlled. The historical botanical specimens are threatened by insect and rodent infestation due to inappropriate conservation methods and adverse climate conditions. Yet, using adequate conservation measures and climate settings, it is possible to eliminate insect propagation. This paper carries out a thorough literature review on conservation methods and various herbarium indoor temperature settings. Based on a selected indoor climate requirement, a basic solar-photovoltaic (PV) configuration is suggested to suit the energy consumption of the cooling system. A simulated model is created using MATLAB to quantify the energy consumption for these identified temperature settings. A market research on current herbarium installations shows that climate-controlled settings are prevalent in most large herbariums to decrease the rate of sample deterioration. Based on the evaluation of annual energy consumption of various indoor temperature settings, an appropriate solar-PV system is determined by simulation and a cost-analysis is conducted. As a result, it can be concluded that a controlled herbarium temperature below 15° C can eliminate specimen deterioration and the conditions are possible to be primarily powered using solar PV technology.

Keywords: Herbarium, Solar cooling, Decay prevention, Climate control

BIUST Research and Innovation Symposium 2019 (RDAIS 2019)
Botswana International University of Science and Technology
Palapye, Botswana, 4 - 7 June 2019

ISSN: 2521-2292

Bat guano and the risk of contracting histoplasmosis on BIUST campus

Lefang Leo Chobolo, Monamodi Kesemang, Modise Goodwell, Emmanuel Kefilwe Sekopo, Leungo Daddie Mukoka, Galaletsang Makgarebe Dintwe, Naledi Troy Gonnye, Precious Mpofu, Riach Chifatso Masamba, Nerve Zhou and *Tharina Louise Bird

Department of Biological Sciences and Biotechnology
Botswana International University of Science and Technology (BIUST)
Palapye, Botswana
**Corresponding author: tharinab@gmail.com*

Abstract

Histoplasmosis, or 'cave disease', is a mycosis that is usually asymptotic or benign, but which can be fatal in rare cases. Histoplasmosis is contracted when spores of the thermally dimorphic fungus *Histoplasma capsulatum* is inhaled. *Histoplasma* is often associated with accumulated bat fecal pellets. Given that many Midas free-tailed bats (*Mops midas*) and African yellow house bats (*Scotophilus dinganii*) roost in buildings on the campus of Botswana International University of Science and Technology (BIUST), there is a concern that the accumulation of bat guano at these roosting sites expose people to *Histoplasma* infections. Whether *H. capsulatum* is present in bat guano has, however, never been investigated in Botswana. To determine whether the fungus is present in bat guano on BIUST campus, we did a survey of fungi based on nine bat guano samples taken from roosting sites across campus (approximately 40% of the total number of campus buildings known to serve as bat roosting sites). We cultured all fungi in the guano samples, and extracted, amplified (PCR) and sequenced the fungal DNA from each cultured colony. For species identification, we used the Basic Local Alignment Search Tool (BLAST) to compare sequences with different online fungal databases. We recorded 26 species of fungi, belonging to 12 genera. Most of the species belong to the genus *Aspergillus*, for which we recorded 14 species. The rest of the species belong to 11 genera (*Chaetomium*, *Clavispora*, *Fusarium*, *Hyphopichia*, *Mucor*, *Ovatospora*, *Phialocephala*, *Rhizoctonia*, *Rhizopus*, *Saccharomycopsis*, *Thielavia*, *Glomus*) each represented by a single species. Four species could not be identified to species level, and might be new to science. We found no match for *Histoplasma*. We conclude that there is no indication that the bats that roost on BIUST campus bear any risk of *Histoplasma* infection, or of contracting histoplasmosis.

Keywords: Bat guano, Botswana, fungal diversity, *Histoplasma*

BIUST Research and Innovation Symposium 2019 (RDAIS 2019)
Botswana International University of Science and Technology
Palapye, Botswana, 4 - 7 June 2019
ISSN: 2521-2292

OPTIMIZATION OF ULTRASOUND ASSISTED EXTRACTION METHOD FOR HPLC-DAD UV/VIS DETERMINATION OF FLAVONOIDS IN MEDICINAL PLANTS AND EVALUATION OF ACE INHIBITION ACTIVITY

KATSO BINANG[1] AND DAVID T. TAKUWA[2]
University of Botswana, Department of Chemistry, P/Bag UB 00704, Gaborone, Botswana
[1]Katso Binang e-mail: binangkatso@gmail.com

The world today is faced with this global problematic disease hypertension, which is life threatening and add more burden to economic growth. Medicinal measures that are available are not offering 100% treatment, though we have traditional medicinal plants in our native countries that are rich in flavonoids which serves as successful therapeutic compounds to hypertension and other cardiovascular diseases, provided that an efficient extraction and analysis method is developed that will be applicable to pharmaceutical industries for drug discovery. It is essential to develop and share best applicable methods that determine anti-hypertensive compounds for affordable and effective pharmaceutical processes in treatment of hypertension. Hence the aim of this investigation is to optimize Ultrasound assisted extraction (UAE) method and develop chromatographic analysis method for flavonoids in traditional medicinal plants. This research also seeks to provide a minimal single step method where many known compounds with anti-hypertensive properties can be determined within a short time. To determine the optimum parameters Central Composite Design (CCD) will be used. A comprehensive study on ACE (Angiotensin Converting enzyme) inhibition activity, DPPH (2,2-diphenyl-1-picrylhydrazyl) radical scavenging activity of the plant extracts will also be evaluated. At the end of this investigation the appropriate quick screener method of anti-hypertensive compounds will be determined and flavonoids and other additional phenolics in the selected traditional medicinal plants will be separated, identified and their effect against hypertension activity used as a recommendation for proposal of new anti-hypertensive drugs.

Key words: hypertension, medicinal plants, flavonoids, ultrasound assisted extraction, angiotensin converting enzyme

BIUST Research and Innovation Symposium 2019 (RDAIS 2019)
Botswana International University of Science and Technology
Palapye, Botswana, 4 - 7 June 2019
ISSN: 2521-2292

Quality of Water With Respect To Carbonyl Compounds in Selected Water Bodies in Botswana

T. Mogatsaseno[1*], K. Sichilongo[1]

[1]*Department of Chemistry, University of Botswana, Botswana*
*Author for correspondence e-mail: nakakashwe.mogatsa@gmail.com

Carbonyl compounds make up most part of the environment as well as the atmosphere of developed and developing countries. Some carbonyls are associated with adverse health impacts and most of them are precursors for radical and photo-oxidant formation in the atmosphere [1] Carbonyl compounds should be detected early to avoid their adverse side effects on all life. We present in this study, results of carbonyl compounds mapping in selected water bodies in Botswana using gas chromatography-mass spectrometry (GC-MS) and liquid chromatography-mass spectrometry (LC-MS). The selected water bodies lie between Kanye and Francistown. This study incorporates some fundamental analytical techniques such as a comparison of liquid liquid extraction (LLE) with dispersive liquid liquid microextraction (DLLME) in sample preparation.

Preliminary experiments indicate that the GC-MS detection of of low molecular weight carbonyl compounds such as cyclohexanone is feasible without necessarily subjecting the samples to rigrous and laborious derivatization procedures. Figure 1 shows a total ion chromatogram and mass spectrum of cyclohexanone obtained using the Agilent Technologies 5975C Series GC-MS system using a 30 m HP5-MS column also by Agilent Technologies and helium as a carrier gas. It is anticipated that 12 carbonyl compounds spanning from low to high molecular weight, will be determined in the water bodies.

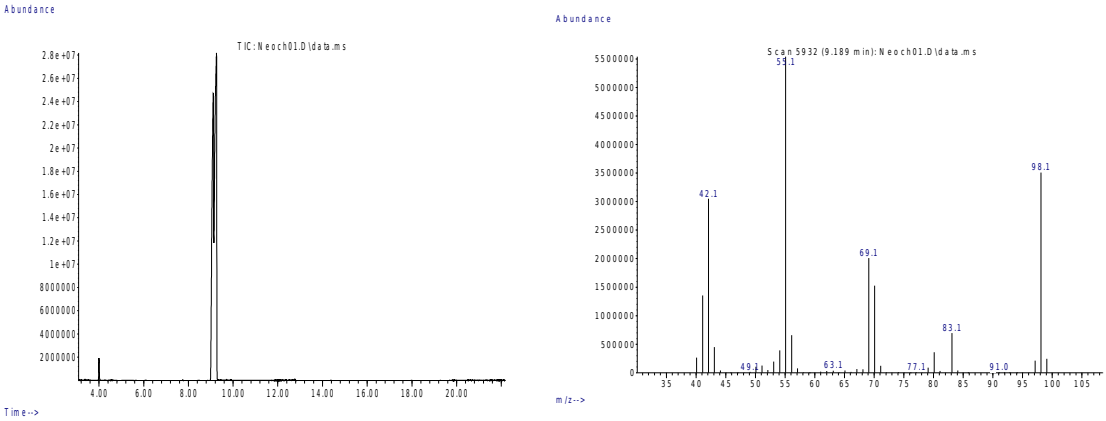


Figure 1: Cyclohexane chromatogram and mass spectrum

References

1. F. W. Lurmann, A. S. Wexler, S. N. Pandis, S. Musarra, N. Kumar, and J. H. Seinfeld, Atmospheric Environment, 31 (17), (1997), 2695.

BIUST Research and Innovation Symposium 2019 (RDAIS 2019)
Botswana International University of Science and Technology
Palapye, Botswana, 4 - 7 June 2019
ISSN: 2521-2292

Making Silver Incarcerated Microporous Ceramic Membranes For Water Purification

Bogadi Pako Letsile, Gorata Pearl Morake, Rachel Utlwang Bikimane

Botswana International University of Science and Technology

Chemistry Department

Over the centuries chlorine has been used as a disinfectant in water treatment in Botswana. Though it has been effective, it does not extensively kill protozoa and has low disinfection in turbid waters. However the ceramic membranes has proven to be more lucrative. Ceramic membranes are a type of artificial membranes made from inorganic materials. Inorganic membranes have the advantage of resistance against aggressive chemicals, high temperature, high and constant flux and have a long service life. The incarceration of colloidal silver nanoparticles into alpha aluminum ceramic membrane is used to purify the water. The incarceration of silver nanoparticles services to destroy bacteria, algae and protozoa. The four main type of membranes are Nano-filtrations (NF), Microfiltration (MF), Ultrafiltration (UF) and Reverse Osmosis (RO) but this paper mainly focuses on MF.

Keywords: Incarcerated, microporous, purification, and ceramic membranes

BIUST Research and Innovation Symposium 2019 (RDAIS 2019)
Botswana International University of Science and Technology
Palapye, Botswana, 4 - 7 June 2019
ISSN: 2521-2292

Wireless Sensor Networks Based Localization and Tracking: Roadside Livestock Monitoring System

Lone Kolobe
Department of Electrical, Computer and Telecommunication Engineering
Botswana International University of Science and Technology
Palapye, Botswana
lone.kolobe@studentmail.biust.ac.bw

Adamu Murtala Zungeru
Department of Electrical, Computer and Telecommunication Engineering
Botswana International University of Science and Technology
Palapye, Botswana
zungerum@biust.ac.bw

Joseph Chuma
Department of Electrical, Computer and Telecommunication Engineering
Botswana International University of Science and Technology
Palapye, Botswana
chumaj@biust.ac.bw

Abstract

Wireless Sensor Network (WSN) based technology is ideal for deployment in areas with infrequent or reduced access to energy, network, processing power, and other resources. They enable researchers and organizations to use remote sensing technologies at a fraction of the cost associated with repeatedly deploying labor and sensors to monitor a given parameter. However, the robustness of the technology has allowed it to be deployable in the most inhospitable areas with little to no human intervention. This work assesses the suitability of WSN based technology for a roadside livestock detection system based on existing WSN technology mainly the Libelium WaspMotes sensors. Besides, the work provides proof of concept through a literature review, a simulated model and prototype. The system is based on the ATmega 1281 Libelium Waspmote with an event board, SIM5215 GSM module for communication, PIR, flexible solar panel, rechargeable battery pack with a supply voltage of 3.7V and 1150mAh. Also, the work identifies areas which could benefit from the systems' deployment such as game reserves, busy inter-district roadways (A1, A10) using quantitative data as justification and guidance for possible implementation in Botswana while also discussing the success of similar systems in developed countries. More to this, the proposed solution achieves this in part by visually warning drivers using bright, low-frequency strobe lights. Lastly, animal migration towards the road is discouraged by inducing neophobic responses and alerting animal patrol of the movement using GSM and Long Range (LoRa) communication network.

Keywords: **Wireless Sensor Network; Animal monitoring; roadside monitoring; localization and tracking; livestock; long range (LoRa)**

BIUST Research and Innovation Symposium 2019 (RDAIS 2019)
Botswana International University of Science and Technology
Palapye, Botswana, 4 - 7 June 2019
ISSN: 2521-2292

A biopsy needle detection tool for 3D ultrasound imaging

Nayna Ann Moni[1], Bakary Diarra[2], Boyce Sigweni[1]

[1]Electrical, Electronics, Computer & Telecommunication Engineering Department, Botswana International University of Science & Technology (BIUST), Palapye, Botswana,

[2]Electrical Engineering Department, Institute of Applied Sciences, University of Sciences, Techniques and Technologies of Bamako (USTTB), Bamako, Mali

In medical surgeries, flexible needles are inserted into the tissue to extract samples for more advanced investigations. Such procedures rely on the experience of the medical practitioner. The accuracy and the position of the needle are very important in biopsy because several attempts before the collection of the right sample can harm healthy tissues during the procedures. Current limitations are the low quality of images and the reduction of needle visibility due to image clutters as some tissues like fat and bones have similar intensity to metallic tools making real-time tracking of the needle difficult. Many non-image based solutions, like passive markers at the tip of the needle, are applied to enhance the needle visibility in the ultrasound images.
The aim of this work is to create a tool to automatically detect the biopsy needle position in 3D medical images with an improved contrast in real-time. This research will investigate various needle detection methods and algorithms, so as to determine the best algorithm for automatic detection of a biopsy needle. A graphical user interface will be designed for the tool and the algorithm tested. Ultimately, the comparative advantages of the tool against existing methods will be evaluated.

BIUST Research and Innovation Symposium 2019 (RDAIS 2019)
Botswana International University of Science and Technology
Palapye, Botswana, 4 - 7 June 2019
ISSN: 2521-2292

Development of Analytical Methods for the Determination of Efavirenz Using GC-MS and HPLC for Applications in Forensic, Clinical and Environmental Analysis

W. Masenga[1*], K. Sichilongo[1] and G. M. Paganotti[2]

[1]*Department of Chemistry, University of Botswana, Botswana*
[2]*Department of Medicine, University of Botswana – University of Pensylvania Partnership, Botswana*
*Author for correspondence e-mail: masengawangu@gmail.com

Efavirenz (EFZ) is antiretroviral (anti-HIV) drugs that is part of the non-nucleoside reverse transcriptase inhibitor (NNRTIs) and has been used in combination therapy despite its suspected teratogenicity. EFZ has also been reportedly abused for recreational purposes in some African countries where it is crushed and mixed with illicit drugs like marijuana and smoked. Medical use thus places a need for therapeutic drug monitoring (TDM) while abuse raises the need for forensic detection using simple detection tools such as point of care testing devices (POCT). Additionally, forensic detection would entail the screening of communities by mining for illicit drugs in environmental samples. In this study, we aim to develop GC-MS and LC-MS methods that can detect EFZ in non-invasive such as saliva and urine for forensic detection, for TDM and environmental samples. Detection of EFZ in non-invasive samples will eventually lead to simple easy use in forensic point of care testing (POCT) gadgets for on-site use by clinicians and law enforcement agencies. TDM would eventually be realised from the methods where EFZ is still in use and in historical samples where it has been substituted with other drugs of the same class. Preliminary results from simple GC-MS runs of neat 5 ppm (w/v) EFZ standards using metronidazole (MNZ) and nevirapine (NVP) at 5 ppm (w/v) each as internal and surrogate standards respectively on an Agilent 5975C Series system with an HP5-MS column, gave excellent chromatograms seen in Figure 1. This was obtained using helium at a flow rate of 1 µL/min and pulsed spilt less mode of injection. We envisage a full study of the drug on the GC-MS and LC-MS method and whose results will be presented in this report.

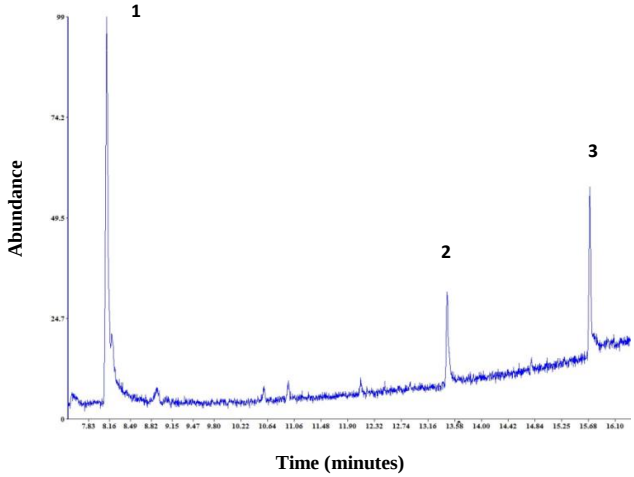


Figure 1: Total ion chromatogram (TIC) of a mixture of (1) MNZ, (2) EFZ and (3) NVP

BIUST Research and Innovation Symposium 2019 (RDAIS 2019)
Botswana International University of Science and Technology
Palapye, Botswana, 4 - 7 June 2019

ISSN: 2521-2292

Dunaliella salina microalgae medium optimization for lipid production using response surface methodology

Kevin Nyoni[1], Leungo Kelebopile[1] & Lesedi Lebogang[2]
[1]*Department of Mechanical, Energy & Industrial Engineering,*
[2]*Department of Biological sciences and Biotechnology,*
Botswana International University of Science and Technology, Palapye, Botswana
Kevin.nyoni@studentmail.biust.ac.bw

Abstract

Biodiesel production from microalgae has received a worldwide recognition as an alternative source of fuel to conventional petroleum diesel. However, the cost of production of biodiesel has limited its development, and the culturing stage of the microalgae to enhance its lipid production contributes significantly to the costs. Lipid production is an important indicator on the microalgal species for biodiesel production. Micronutrients and macronutrients are a source of energy to the microalgae, which enhances the growth of biomass and induction of lipids. In this study, Plackett-Burman design and Box-Behnken design of response surface method (RSM) were used to screen and optimize medium nutrient concentrations. In the first stage of the design, Plackett-Burman method identified $NaHCO_3$, $NaH_2PO_4.2H_2O$ and $NaNO_3$ nutrients as factors that were significantly influencing the lipid production. In the second stage, the significant nutrients from the first stage were further optimized and a predicted model was generated with a regression coefficient (R^2) of 0.9575. Thin layer chromatography was used to analyze for the presence of the lipids. The optimum medium comprised of 1302.42 mg/L $NaHCO_3$, 22.46 mg/L, $NaH_2PO_4.2H_2O$, 181.10 mg/L, $NaNO_3$, 44.72 mg/L $CaCl_2$, 2355 mg/L $MgSO_4.7H_2O$, 5.6 ml/L of micronutrient solution, which produced a maximum lipid production of 181mg/L with a total of 41% of lipids content. The optimized medium improved the lipids content by 12% from 127mg/L of produced lipids with reference to the original culture medium concentration (P-value =0.0005). The interaction between $NaHCO_3$ and $NaH_2PO_4.2H_2O$ has significant effect (P-value =0.0202) on lipid production. In addition, the interaction between $NaNO_3$ and $NaH_2PO_4.2H_2O$ had a significant effect (P-value = 0.029) on lipid production. An increase in these nutrients interaction concentrations resulted in increase on lipids. Lipid analysis identified linoleic acid, oleic acid and other unidentified triacylglycerides as the lipids in *D. salina* microalgae. In conclusion, RSM could be an effective method to determine optimum nutrients that give a maximum lipid output on *D.salina*.

Keywords: biodiesel; lipid production; *Dunaliella salina*; media optimization; response surface methodology.

BIUST Research and Innovation Symposium 2019 (RDAIS 2019)
Botswana International University of Science and Technology
Palapye, Botswana, 4 - 7 June 2019
ISSN: 2521-2292

Characterization of Selected Honey from Different Floral and Geographical Origins including Botswana

T. Padiso[1*] and K. Sichilongo[1]

[1]*Department of Chemistry, University of Botswana, Botswana*

*Author for correspondence e-mail: tumelopadiso5@yahoo.com

Bee honey production is blossoming in Botswana. Honey production is beneficial in terms of health, economic and environmental aspects. If well nurtured, honey can reap five times more profit than crude oil. Bee keepers are often compelled to grow plants for nectar and bees play a key role in cross pollination which is useful in food production. Planting trees for nectar is reforestation and good for the environment. Apart from GDP enhancement, countries that have ventured into honey production have reaped the benefits above. There have been however, numerous cases of fraud in honey trade due to mislabeling of honey products to imitate those that sell at higher prices as well as adulteration with syrups to increase the volume of sales. GC-MS, LC-MS and classical analysis have been used to classify botanical origins and as well as detect adulteration to forestall these fraudulent activities. This project is premised on employing these methods to characterize honey from selected areas including Botswana according to botanical/flora origin as well as establish physicochemical characteristics. Results were obtained using three commercial honeys, two from Zambia (ZAM1 and ZAM2) and one from Botswana (BOT). In addition, three real honey samples from Botswana were characterized. Their physicochemical properties of moisture content and electrical conductivity were determined. Values for two samples are shown in Tables 1 and 2, the RSD_R% values less than 10 % indicated good precision.

Table 1. Moisture content g/100g of the honeys.

Sample Name	Moisture content g/100g (mean value)	RSD_R%(n=5)
ZAM2	17.66	8.086
ZAM1	18.06	10.54
BOT	19.65	5.272

Table 2. Electrical conductivities for the honeys.

Sample Name	Electrical Conductivity (mS/cm) (mean value)	RSD_R%(n=5)
ZAM2	0.645	3.04
ZAM1	0.726	3.86
BOT	0.834	9.94

In this study, results from physicochemical characterization of samples above and additional ones from Bee Keepers before processing will be presented. Some volatile characteristics of the honeys using SPME GC-MS will be presented.

BIUST Research and Innovation Symposium 2019 (RDAIS 2019)
Botswana International University of Science and Technology
Palapye, Botswana, 4 - 7 June 2019
ISSN: 2521-2292

Drone Forensics:

How the growing use of Drone creates new challenges for Digital Forensics Investigation

Peter Holowala Gblorso
Department of Information Systems, College of Information and Communications Technology
Botswana International University of Science and Technology
Palapye, Botswana
gp18100134@studuentmail.biust.ac.bw

Abstract

The recent years of technological growth have seen a rapid adoption and diffusion of drones in the public and private sectors. Reduction of production costs for unmanned aerial vehicles (UAVs) their sensors, and actuators, along with the recent technological improvements, made UAVs easily accessible for industrial and private purposes. Unmanned aerial vehicles are transforming our way of thinking about flight operations and services that can be provided by them. Potential use of this technology ranges from recreational purposes, educational purposes, commercial, leisure, civil security, search and seizure, and are also intensively used in agricultural and aerial photography. In addition to the numerous beneficial uses, drones have also been used illegally most times to facilitate criminal activities. Organizations, individual, public safety and national security are greatly threatened by the misused of this technology at such the need for forensics practitioners to analysis these devices is keen. However, there are numerous challenges associated with a thorough forensic investigation of drones to uncover evidence for admissibility in court. Despite its increased importance, “drone forensics” remains a relatively unexplored research topic. This work examines the technological challenges faced by digital forensic investigation on drones and provides possible solutions to some of those challenges.

BIUST Research and Innovation Symposium 2019 (RDAIS 2019)
Botswana International University of Science and Technology
Palapye, Botswana, 4 - 7 June 2019
ISSN: 2521-2292

Structural and optical properties of Ce-doped CuO nanoparticles prepared by hydrothermal synthesis.

Romang Bosigo , Lucia Lepodise, and Cosmas Muiva
Department of Physics and Astronomy,
Botswana International University of Science and Technology, P/Bag 16 Palapye, Botswana.

Abstract

Metal oxide nanoparticles have been gaining a lot of attention in recent years due to their various applications ranging from domestic to industrial environments. Different metal oxides such as ZnO, TiO2, CuO, MgO, CeO2, SnO2, In2O3, WO3, V2O5, and SiO2 are being investigated by numerous research groups. In work presented here, a simple hydrothermal method was used for the synthesis of the cerium doped copper oxide with doping concentrations of 0%, 3% and 6%. This method was selected because it is of low cost, fast, environmentally friendly and produces high-quality CuO nanoparticles. The synthesized powders were characterized by X-ray diffraction analysis (XRD), thermal gravimetry (TGA), Fourier transform infrared spectroscopy (FTIR), UV-Vis spectrophotometer and field-emission scanning electron microscopy (FE-SEM) equipped with energy dispersive X-ray spectroscopy (EDS). The XRD plots showed pure highly crystalline single phase monoclinic CuO for the undoped and 2 % Ce-doped CuO and additional cubic CeO2 structures for the 6% Ce-doped CuO. TGA analysis showed a single step of weight loss attributed to escape of impurities which confirms formation of pure nano-crystalline products as observed under XRD. FE-SEM images depicted formation of agglomerated nanospheres for the undoped CuO and a nanospheres/nanorods mixture for 3% and 6% Ce-doped CuO. The dopant concentration percentage was confirmed by calculations from the EDS spectra and the elemental mapping confirms the homogeneous dispersion of the elements in the samples. The optical band gap was obtained from Tauc's plot method and the result showed that the band gap values increased monotonously with Ce doping. The functional group analysis carried out by FTIR confirmed the formation of CeO2/CuO indicated by the characteristic stretching vibrations of Cu-O and Ce-O identified in the samples. These changes in the properties of CuO induced by incorporation of Ce into CuO could present novel strategies leading to tailored metal oxide nanoparticles for various desired applications

Keywords: Metal oxide, cerium, copper oxide, nanoparticles, hydrothermal synthesis, doping

BIUST Research and Innovation Symposium 2019 (RDAIS 2019)
Botswana International University of Science and Technology
Palapye, Botswana, 4 - 7 June 2019

ISSN: 2521-2292

Design and Simulation of a Lower-Limb Exoskeleton using Relative Jacobians for Mobility Enhancement and Rehabilitation

Authors:Olebogeng Mbedzi & Zimele Gwebu

Botswana International University Of Science and Technology
Department Of Mechanical And Energy Engineering

Abstract

This work presents development, fabrication and simulation of a human lower-limb exoskeleton for enhanced mobility and gait rehabilitation implemented using a modular relative jacobian. The design consists of two limbs each consisting of three degrees of freedom driven by electric motors and controlled using relative motion between the two feet and posture of the two legs.

It presents a model replicated and benchmarked from existing lower-limb exoskeletons, which consist of a single active degree of freedom on the hip,knee and ankle. The two legs are equivalent to the two arms of the dual-arm,while the two feet are equivalent to the two end-effectors of the dual-arm. Two legs, each with three degrees-of-freedom (3-DOFs), are combined to form a 6-DOFs bipedal robot. Then the 3-DOFs relative position between the two feet of the bipedal robot are controlled as the relative end-effectors of the relative Jacobian, while the remaining 3-DOFs are used to control the robot posture. As in a robot manipulator control, the first priority is the relative feet motion, while the second priority is bipedal robot posture in the null space. It is noted that if individual leg control for each foot was used, with 3-DOFs control on each foot, there will be no more DOFs to control the biped robot posture. The control uses dynamics information on inertia, gravitational torques, and dynamically consistent relative Jacobian inverse. Bipedal walking simulation is shown in Gazebo.

Keywords: Relative Jacobians, Exoskeleton, Simulation, Design, Rehabilitation

BIUST Research and Innovation Symposium 2019 (RDAIS 2019)
Botswana International University of Science and Technology
Palapye, Botswana, 4 - 7 June 2019

ISSN: 2521-2292

SolaNetwork: Integrated and affordable solar energy access solutions for socioeconomically diverse rural communities in Botswana

Mervyn Smyth[1], Adrian Pugsley[1], Jayanta Mondol[1], Jeet Parikh[2], Kealeboga Motladiile[2], Ravi. Samikannu[2], Tunde Oladiran[2] and Tobias Bader[2]

** Centre for Sustainable Technologies*
Ulster University, Jordanstown Campus, Shore Road, Newtownabbey, BT37 0QB

[2]Faculty of Engineering, Energy Research Group
Botswana International University of Science & Technology, Palapye, Botswana
badert@biust.ac.bw

Abstract

More than 80% of Africa's electricity is fossil fuel generated leading to climate change effects which disproportionately affect the sub-Saharan region where 588 million people live without modern energy access. In Botswana, 42% of the rural population has no access to electricity. Lack of basic services such as lighting or communication compounds poverty by limiting educational opportunity, constraining the ability to generate income and leaving populations vulnerable to crime at night. Low-income households in rural areas burn wood, charcoal, or animal dung for cooking and boiling water, leading to deforestation, soil degradation and air pollution as well as adverse health effects which disproportionately affect women. The vast amount of available solar irradiation throughout the year of 2,300 kWh $m^{-2}a^{-1}$ in average remains widely unused in Botswana. SolaFin2Go systems provide affordable access to both electricity and hot water for off-grid application. Jamataka village was selected for a field trial of the SolaFin2Go approach as it is regarded as ideal environment for developing new off-grid energy access infrastructure approaches. In a first phase of the project, four SolaFin2Go-systems were installed in Jamataka in the primary school and teacher's staff houses. The project team consisting of Ulster University and BIUST as well as industry partners has been granted funding for the subsequent SolaNetwork project. SolaNetwork builds upon the successful demonstration of the energy access technology and intends to implement scaled-up deployments of the technology interconnected to form physical and virtual node-to-node networks that facilitate energy service delivery and provide essential business intelligence. A not-for-profit distributed energy service company (DESCO) will operate and maintain the stand-alone units and grid network; manage electricity trading between community prosumers; and deliver targeted training to promote off-grid solutions and develop local capacity in the sector.

Keywords: Rural energy access, solar off-grid, node-to-node network, DESCO energy service

BIUST Research and Innovation Symposium 2019 (RDAIS 2019)
Botswana International University of Science and Technology
Palapye, Botswana, 4 - 7 June 2019
ISSN: 2521-2292

Enhanced peroxidase-like activity of silver nanoparticles doped magnetic nanoparticles for sensitive detection of L-cysteine

Micode Mazhani, Melisew Tadele Alula*, and Davison Murape
College of Science; Botswana International University of Science and Technology; Plot 10071, Private Bag 16, Palapye, Botswana, Email: alulam@biust.ac.bw

Abstract

Magnetic nanoparticles, particularly magnetite, has proven to possess intrinsic enzyme mimicking capabilities as discovered by Gao et al in 2007. Since then, a series of nanomaterials, in an effort to enhance their enzymatic have been investigated. In this work, a facile one step solvo-thermal procedure has been employed in generating magnetite-silver core shell nanocomposites (Fe_3O_4@AgNPs) with enhanced peroxidase-like catalytic property. The composites were characterized using different techniques such as transmission electron microscopy, scanning electron microscopy, X-ray diffraction, and surface-enhanced infrared absorption spectroscopy. In the presence of hydrogen peroxide, the synthesized composites were able to oxidize the colorless o-phenylenediamine to a yellow color 2, 3-diaminophenazine with a better peroxidase-like activity than Fe_3O_4 alone.Based on the peroxidase-like catalytic property, a sensor was developed for detection of cysteine with high sensitivity. The sensor also exhibited excellent selectivity against potentially interfering molecules that makes the sensor promising for clinical diagnosis, environmental analysis and pharmaceutical analysis.

Keywords: cysteine; peroxidase-like activity; silver nanoparticles; magnetic nanoparticles.

References:

1. Lizeng Gao, Jie Zhuang, Leng Nie, Jinbin Zhang, Yu Zhang, Ning Gu, Taihong Wang, Jing Feng, Dongling Yang, Sarah Perrett & Xiyun Yan, Intrinsic peroxidase-like activity of ferromagnetic nanoparticles, Nat. Nanotechnol. 2007, 2, 577–583
2. Zili Huang, Yufang Yang, Yijuan Long and Huzhi Zheng, A colorimetric method for cysteine determination based on the peroxidase-like activity of ficin, Anal. Methods, 2018,10, 2676-2680

BIUST Research and Innovation Symposium 2019 (RDAIS 2019)
Botswana International University of Science and Technology
Palapye, Botswana, 4 - 7 June 2019
ISSN: 2521-2292

Comparison of Measured to Estimated Global Solar Radiation Using the Liu and Jordan Method for Gaborone, Botswana

Bashi Thipe

Botswana International University of Science & Technology

Department of Physics & Astronomy

Gaborone, Botswana

thipeba@biust.ac.bw

ABSTRACT

The design of sustainable energy systems require a basic understanding of solar radiation measurements. Solar radiation measurements are obtained directly by measuring using relevant instrumentation or by estimation using tested methods. However, the use of instrumentation in acquiring data is a costly complex process that requires sophisticated devices designed and installed for that particular purpose. In this paper, the Liu and Jordan method of estimating global solar radiation was tested for compatibility for Gaborone and surrounding areas. Estimated global solar radiation data using the method was generated and graphed alongside measured data. Variations of measured data to estimated data were calculated and it was observed that, for clear skies, the method estimated daily global solar radiation with an average uncertainty of 0.4% for the hours before noon and 1.3% for the hours after noon. Much higher percentages were observed in terms of daily averaged cumulative errors with a recorded max of 7.6% for March. The method yields very good estimates for Gaborone and surrounding areas, Furthermore, both experimental and measured data are in agreement with minimal variations that could be attributed to the transmittance constant. Further research is needed on improving the transmittance coefficient to be a function dependant on multiple weather parameters. With reasonable estimates observed, the method could be further checked for compatibility for other local areas and used to generate data that could be used in solar radiation forecasts.

BIUST Research and Innovation Symposium 2019 (RDAIS 2019)
Botswana International University of Science and Technology
Palapye, Botswana, 4 - 7 June 2019
ISSN: 2521-2292

Leveraging Indigenous Knowledge in Rural Botswana through Grassroots Innovation

Thabiso Mashaba

These Hands GSSE (PTY) LTD

Gaborone, Botswana

thabisoblak@these-hands.org

Abstract:

International Development sector has historically followed a top-down approach to development and technology intervention. This lack of coordination between development experts and the people they serve has led to many challenges including the failure of projects. Botswana has managed to attain higher middle-income country status, but many are still left behind. There are 400, 000 people living in urban Botswana compared to 850, 000 people living in rural Botswana. Over 40 percent of the latter live in abject poverty. These Hands, a local for profit Social Enterprise has pioneered a bottom-up approach which focuses on community-led developmental interventions by working with local communities to help them create technological solutions to their livelihood challenges and generate income by participating in the creative industries sector (industries based on art, design, and technological innovation).Their co-creative design process approach to technology-based development has helped to provide the communities of Dkar, Dutlwe, Rakops, Kaputura, Lesoma, Sekandoko, Mosu and Seronga with the necessary resources to engage in the creative industries sector. With the support of These Hands, these communities have produced several prototypes of technological inventions that help address their local community development needs, including a dough mixer, a human-powered bean thresher, a hydroponic fodder grower, and a wheelchair that can be used in deep-sand. Many of these prototypes have been refined and are ready to go to market, with some also ready to be explored for further research and development and filing as Utility Model Patents. These Hands anticipates assisting to get most of these technologies to market and attracting impact investors to help them scale, which will provide these communities with sustainable development opportunities and jobs based on their indigenous knowledge.

Keywords: Co-creative Design Process, Grassroots Innovation, Indigenous Knowledge Systems, Rural Communities, Intellectual Property, Creative Industries.

BIUST Research and Innovation Symposium 2019 (RDAIS 2019)
Botswana International University of Science and Technology
Palapye, Botswana, 4 - 7 June 2019
ISSN: 2521-2292

ANALYSIS OF THE IMPACTS OF LIVESTOCK SEDENTARISM ON SOIL CARBON FLUXES IN THE KALAHARI ECOSYSTEM.

M. Bitsang[1], O. Dikinya[1], B. G. Moganane[1] and B. Mosetlhi[1]
[1]Department of Environmental Science, University of Botswana.
Private bag 00704, Gaborone, Botswana.

Corresponding author email: (mkbitsang@yahoo.com)

ABSTRACT

Livestock sedentarism enhances GHGs emissions due to the presence of active "hotspots" that boosts continuous supply of animal dung and urine. These "hotspots" represent high local additions of readily available carbon resulting in increased surface CO_2 emissions. The south western Kalahari ecosystem of Botswana, is inundated with established ranches and artificial water sources in the form of drilled boreholes that has sedentarized cattle production. This has resulted in localised cow dung and urine accummulation and soil degradation. Data on how this phenomena affect carbon dioxide fluxes in rangelands is lacking. Therefore, a study was conducted to analyse the impact of livestock sedentarism on soil carbon fluxes and other soil characteristics in Kgalagadi District, south west Botswana. Following the piosphere principle, the study analysed how carbon fluxes change with distance from the hotspots. A total of 90 soil samples from top and subsurface soil layers were collected from 6 livestock watering points, wildlife management areas (WMA) and from the National Park which was treated as a control. 40 composite soil samples were made for laboratory analysis. CO_2 fluxes with 3 replicates were measured using the LI-8100A equipment at each soil sampling site. Soil degradation was observed to be concentrated in close vicinity to watering sites gradually exerting changes on soil properties. The soil pH decreased (8.0 to 4.5) with distance from the watering point. Similarly other soil propertis such as nitrogen, phosphorus, EC and organic carbon indicated the same pattern. Soil carbon fluxes measurements showed a significant decrease ($p<0.05$) with distance from within a 10m radius of the livestock watering site loaction to 100m and thereafter remained almost constant. The CO_2 fluxes decreased from 7.41µmol/m^2/s to 0.34µmol/m^2/s at livestock watering sites to a distance of 2.5km respectively, and in WMAs and the control it remained similar at 0.32µmol/m^2/s. These results suggest that livestock sedentarism could be a major factor in enhancing soil carbon fluxes processes in the Kalahari region.

Keywords: ***CO_2 fluxes, livestock concentration areas, piosphere, land use, sedentarism***

BIUST Research and Innovation Symposium 2019 (RDAIS 2019)
Botswana International University of Science and Technology
Palapye, Botswana, 4 - 7 June 2019
ISSN: 2521-2292

Density Based Traffic Light Control System

Kaloso M. Tlotleng, Lame K. Mosoboloko, Otlaatla Marumo, Moses Mosate and Oduetse Matsebe(Supervisor)

BOTSWANA INTERNATIONAL UNIVERSITY OF SCIENCE AND TECHNOLOGY

MECHANICAL, ENERGY AND INDUSTRIAL ENGINEERING

Contacts: mpho.tlotleng@studentmail.biust.ac.bw

In almost every country in the world, including Botswana, the need to control traffic was found to be essential hence why traffic lights are used to control this congestion. The idea is to allow every vehicle from any direction to have a chance to proceed through and most of these systems are automated and use timers which follow a logical sequence to operate. Most of these signals fail to control traffic congestion effectively because they are programmed to be fair regardless of the status of the lane with respect to the number of motor vehicles. This will result in one lane having many cars while the other has less or zero cars but the signal has opened for the latter. This has provoked us to come up with an intelligent/smart traffic control system which uses sensors to detect traffic congestion by sending the signal to either a programmable logic controller(PLC) or microcontroller. To control the traffic density in Botswana, a system would be used whose main objective is to consider lanes with the highest traffic congestion and open for them first then, follow some predefined logic for one loop. For the second loop, a lane with the highest density of motor vehicles is opened first, then again open all other lanes logically until a loop is complete. Upon sensing the lane with the highest number of cars, that is the only signal which will be sent to the programmable logic controller hence allowing the PLC to open the traffic light on that lane. Once the time has elapsed, the traffic light system will follow the normal logic to allow traffic in other lanes to pass through. When the loop is complete, the PLC

BIUST Research and Innovation Symposium 2019 (RDAIS 2019)
Botswana International University of Science and Technology
Palapye, Botswana, 4 - 7 June 2019
ISSN: 2521-2292

A SECURED SMART HOME SWITCHING SYSTEM BASED ON WIRELESS SENSOR NETWORKS

* Jwaone Gaboitaolelwe, Adamu Murtala Zungeru, Nonofo Ditshego, and Joseph Chuma

Department of Electrical, Computer and Telecommunication Engineering
Botswana International University of Science and Technology
Private Bag 16, Palapye, Botswana

* jwaone.gaboitaolelwe@studentmail.biust.ac.bw; zungerum@biust.ac.bw; ditshegon@biust.ac.bw; chumaj@biust.ac.bw

Abstract

This innovative work presents the design and implementation of a secured smart home switching system based on wireless communications and self-energy harvesting. Traditional building switching systems (TBSS) used in buildings face many problems of which can be grouped into control, monitoring, energy management, security, and access control. These problems pose inconveniences for the residents of such buildings. Apart from the issues mentioned earlier, electricity prices are on the rise due to the world changing into a cleaner and more sustainable energy system. As a result, in both private and public buildings, there is a desire to reduce electricity usage, automate appliances, and move towards optimizing the electricity usage of buildings. The proposed secured smart home switching system is intended to integrate security (access control) of a building's electricity, renewable energy harvesting, and energy storage for the systems active electronic components. The work gives two major contributions to the design of smart home systems. Firstly a practical design and implementation of security (access control system) for a building's power supply which adds a locking feature such that only authorized personnel is capable of altering the power state of the smart sockets and smart switches in a building. Secondly, a model of energy harvesting and storage system for the active electronic components and wireless communication of the system is also presented. A prototype with results that demonstrate the feasibility of a secured smart home switching system produced, which is intended to add value to the research community.

Keywords

Wireless Sensor Network; Smart home; Smart switch; Smart socket; Energy harvesting; Wireless communication; Access control.

BIUST Research and Innovation Symposium 2019 (RDAIS 2019)
Botswana International University of Science and Technology
Palapye, Botswana, 4 - 7 June 2019
ISSN: 2521-2292

Analysis of energy consumption patterns in tourist lodges for improved energy efficiency – The case of Kwadiwa Lodge in Botswana

Katlego Seleofeng Rahube, Boitumelo Elizabeth Makatane, Tshepiso Mokoka, Tshepho Letshwenyo and Tobias Bader
Department of Mechanical, Energy & Industrial Engineering,
Botswana International University of Science & Technology,
Private Bag 16, Palapye, Botswana

Abstract
The tourism sector in Botswana significantly contributes to the national economy and thus significantly to the energy consumption in the country. Hotels are noteworthy in the commercial sector, where the demand for energy continues to grow. The travel and tourism sector add around 10% to the national GDP and is forecasted to continuously grow. This committed growth of the tourism business will go along with an increased energy consumption in the tourist destinations, leading to increasing energy costs. Given the fact, the predominant accommodation facilities besides hotels are remote tourist lodges, which are mostly located in naturally sensitive environments; it is of essence, that the mentioned growth of tourism is carried out or maintained sustainably. Hence, energy efficiency standards need to be introduced and monitored by means of energy management and energy audits. This can be a minimum basis for the successful implementation of renewable energy facilities and minimisation of carbon footprint as it will positively influence energy conservation and energy efficiency.

This paper introduces the energy audit project on Kwadiwa lodge in the described context and reflects on the importance of energy audits in the Botswana tourist sector. It gives an overview on reviewed energy audit standards, methodologies and procedures and energy management systems for lodges. The paper further recommends the required measurement equipment in form of an energy audit toolkit with specifications for auditing tourist lodges in Botswana.

Keywords: Energy audit, energy management, tourism, energy efficiency

BIUST Research and Innovation Symposium 2019 (RDAIS 2019)
Botswana International University of Science and Technology
Palapye, Botswana, 4 - 7 June 2019

ISSN: 2521-2292

Variations in Kinetics of Coal Pyrolysis at Different Size Ranges and Heating Rates Using a TGA

[1]Mmoloki Makoba, [2]Laszlo-Zsolt Szabo, [1]Paul Serban Agachi

[1]Department of Chemical, Metallurgical & Minerals Engineering
Botswana International University of Science and Technology
Palapye, Botswana
[2]Department of Chemical Engineering
University of Babeş-Bolyai, Romania

makobam@biust.ac.bw

Abstract

This study seeks to investigate Botswana coal at different heating rates using a thermogravimetric analyser (TGA). Kinetics of coal pyrolysis were acquired at different heating rates varying from 10 – 50 °C/min and varying particle size ranges from 0.85 – 10 mm. The aim of this experiment was to demonstrate that big particles have not only kinetic control but also more mass diffusion control. This study also identifies the stages of the pyrolysis (drying, slow pyrolysis and fast pyrolysis). The results show that there is a delay in time during the weight loss for big particles compared to small particles. This is caused by diffusion control which is added to the reaction kinetic control. In big particles the peak for heat loss appears later in time compared to the small particles, which means that the diffusion control is increasing.

Keywords: Kinetics, heating rate, pyrolysis, TGA

BIUST Research and Innovation Symposium 2019 (RDAIS 2019)
Botswana International University of Science and Technology
Palapye, Botswana, 4 - 7 June 2019
ISSN: 2521-2292

Survival, Growth and heavy metal accumulation of Vetiver in different mine-affected soils as influenced by fly ash and compost amendments

Oarabile Lefadola, Trust Manyiwa and Venecio U. Ultra. Jr. *

Department of Earth and Environmental Sciences, Faculty of Science, Botswana International University of Science and Technology, Palapye, Botswana

*Corresponding author: ultrav@biust.ac.bw

Abstract

A greenhouse study was conducted to monitor the metal tolerance, metal accumulation and growth rate of *Vetiveria zizanioides* in heavy metal contaminated soils with fly ash (FA) and compost amendments. Vetiver is tropical grass well-known for its soil erosion control properties and an aromatic oil in the roots which is used in the production of perfumes; and a potential for phytoremediation because of its ability to survive in toxic environments and in harsh climatic conditions. Vetiver was grown on three different soil sample, (A) surface runoff from the tailing dump from BCL mine, (B) sediments at the base of smelter sludge from BCL mine and (C) soil from the abandoned Monarch gold mine. Three treatments were applied for growing the grass for each soil type: (T1) mine tailing or soil alone, (T2) soil/mine tailing + compost and (T3) soil/mine tailing + fly ash. The results collected after a period of 4 months showed that the survival of the grass was much higher in the gold mine soil than in the soil samples from the copper-nickel mine. On average the dry matter of *Vetiveria zizanioides* produced from surface runoff soil of the tailing dump from BCL mine was higher than from the other two types of soil samples. In BCL surface soil, FA increased the concentration of As, Co, Cu, Mn, Ni and Pb while compost decreased the As concentration in shoots. FA decreased the As, Cu, Cr, Ni and Pb in the sediments of BCL smelter while compost amendments slightly decreased the As concentrations in green shoots. In Monarch Gold mine tailing, FA decreased the Co, Cr, Mn, Cu and Ni concentrations in green shoots while compost also decreased the Co and Ni in green shoots of Vetiver. Overall, fly ash and compost enhanced the survival and growth of Vetiver in the different heavy metal contaminated soil and mine tailing which could be attributed to the ability of fly ash and compost to modify the solubility of heavy metals and to supply essential nutrients for plant growth and development. This study would indicate that the potential of *Vetiveria zizanioides* to rehabilitate degraded mine sites could be enhanced by fly ash and compost amendments. Future investigations include pilot testing to assess the phytoremediation potential of vetiver to under field conditions and to develop and identify suitable post-harvest process of the harvested biomass.

Keywords: heavy metals accumulation, heavy metal availability, mine tailings, phytoremediation, soil amendments

BIUST Research and Innovation Symposium 2019 (RDAIS 2019)
Botswana International University of Science and Technology
Palapye, Botswana, 4 - 7 June 2019
ISSN: 2521-2292

Status of renewable energy in Botswana - part 1: conventional energy supply, solar potential & framework

Tobias Bader
Department of Mechanical, Energy and Industrial Engineering
Botswana International University of Science and Technology
Palapye, Botswana
badert@biust.ac.bw

Abstract
Most of Botswana's energy supply is based on coal, and thus on a non-renewable energy source. This massive consumption of fossil primary energy affects the depletion of natural resources. Furthermore, the use of non-renewable resources contributes to the global warming through CO2-emissions. In addition, this centrally organised power supply by thermal coal-fired power plants does not reach the country's population in the rural areas, where 42% of the population has still no access to electricity, even though Botswana is among the wealthiest countries in Sub-Saharan Africa regarding its GDP per capita. However, Botswana is on the one hand committed to the Paris Agreement (2015) to reduce its carbon emission by 15% until 2030. On the other hand, the country is determined to create sustainable access to energy for its rural population as envisioned in the Vision 2036 and planned through the National Development Plan NDP 11 (2017).
This presentation is divided into two parts. The first part of this presentation deals with the conventional energy supply in Botswana fed by the vast coal reserves in the country. The presentation sheds light onto the country's electricity grid, the current electricity demand and the energy access rate. The energy market and the electricity tariff structure are described. Based on the detailed description of the current energy market, the solar energy source and its potential for Botswana are discussed. The role of solar energy to cover energy requirements in rural villages is emphasised, and the opportunities of solar installations to mitigate power outages are presented. Having introduced the field of tension between centralised coal power and the opportunities of decentralised solar power in Botswana, the political background and framework are presented. This leads from the national commitment to the Paris Agreement 2015 towards the National Vision 2036 and the National Development Plan NDP 11 (2017). In this context it is mentioned, that the government has up to date not passed a renewable energy legislation and is rather relying on a Renewable Energy Strategy and an Energy Efficiency Strategy that has been developed in collaboration with the World Bank. A summary of the Botswana energy targets until 2030 eventually concludes part one "Status of renewable energy in Botswana" presentation.
Keywords: Renewable energy Botswana, status, solar potential, renewable energy policies

BIUST Research and Innovation Symposium 2019 (RDAIS 2019)
Botswana International University of Science and Technology
Palapye, Botswana, 4 - 7 June 2019
ISSN: 2521-2292

Status of renewable energy in Botswana – part 2: higher education, research and trends

Tobias Bader
Department of Mechanical, Energy and Industrial Engineering
Botswana International University of Science and Technology
Palapye, Botswana
badert@biust.ac.bw

Abstract
The Botswana energy targets until 2030, as described in part 1 of the presentation, consists of the pillars: energy access, energy efficiency and renewable energy. The renewable energy targets include inter alia, 15% of electricity (on-grid and off-grid) to be generated from renewable sources. Working towards its Vision 2036, the government is committed to support renewable sources throughout the energy sector including transport and heat fuels. The successful application of solar energy technologies will be significant to the access of hundred percent of households to electricity. This envisaged sustainable development urges the transformation towards a more sustainable society and hence drives ahead research and development of new, sustainable technologies in the energy sector. Linked to this development is the need for skilled personnel in the diverse fields of the renewable energy sector, associated with the expansion of related training and higher education in the relevant disciplines.
Having discussed the conventional energy supply, solar potential and the political framework in the first part of the presentation "Status of renewable energy in Botswana", part two covers the contents: higher education and research in renewable energy technologies in Botswana and illustrates current trends. The presentation concludes with renewable energy plans of Botswana's Department of Energy including, inter alia: the rollout of 145,000 off-grid products and packages; the implementation of solar mini-grids (65 MW); the connection of a 100 MW solar power plant and the launch of a rooftop solar deployment programme.

Keywords: Renewable energy Botswana, higher education, research, trends, transformation

BIUST Research and Innovation Symposium 2019 (RDAIS 2019)
Botswana International University of Science and Technology
Palapye, Botswana, 4 - 7 June 2019
ISSN: 2521-2292

USING DRONES FOR WAREHOUSE MANAGEMENT AND QUELEA BIRDS CONTROL

By: Oteng Sephiri, Kenaleone Sebikiri, Gaopalelwe Tsima and Bernum Masu

Department of Mechanical and Energy Engineering

Affiliation
Botswana International University of Science and Technology (BIUST)

ABSTRACT
This project focuses on the application of autonomous drones for warehouse management and quelea birds pest control to improve cereal crop production. Warehouse management drones use RFID technology for stock inventory, Object Detection System(ODS) and Indoor Positioning System(IPS) for navigation in the warehouse while for quelea birds pest control drones use computer vision for birds detection and predator sound to scare birds off. The main problem in most warehouse management systems is manual inventory check which leads to resource misusage. These include time wastage, labour costs and in large warehouses stock may go unnoticed due to poor stock taking approaches. The rise of e-commerce, higher customer demands of retail stores and skilled labour shortage have magnified the need for efficient warehouse operations. Leading companies like Eysee, pinc,Argon and Aerolion have developed warehouse drones. The downside of their developments is that they are not automated, they require human supervision at all times to perform tasks. These drones use barcode scanners which capture data one at a time therefore it is time consuming. To solve these problems we propose the use 21st century automated drones with better warehouse management capabilities. RFID chips and readers will be used for inventory counting because they can capture a lot of stock data at once as compared to barcode scanners. Object Detection System(ODS) and Indoor Positioning System(IPS) will be used for navigation in the warehouse.
On the other hand, Botswana is lacking behind on food self sufficiency and apart from unsuitable weather, one of the contributing factors is pests in farms. The most deadly pests are the quelea birds which attack cereal crops (millet and sorghum), the main source of food to Batswana. Over the years, farmers have adopted the use of some traditional methods of controlling these pests like using scarecrows, explosives and chemical repellents among others. The birds get used to these scarecrows with time and they end up not being effective, explosives harm other organisms which are beneficial to the ecosystem and chemicals take too long to get depleted which slows down production. However in large commercial farms the use of drones to control quelea birds has been adopted but unfortunately they have not really been effective because they are manually controlled. This project proposes to improve the use of drones for quelea birds control by introducing the quelea birds detection system and an autonomous self deploying drones.

Keywords: Drones, Warehouse Management, Quelea Birds, Autonomous, Detection, Stock Inventory.

BIUST Research and Innovation Symposium 2019 (RDAIS 2019)
Botswana International University of Science and Technology
Palapye, Botswana, 4 - 7 June 2019
ISSN: 2521-2292

Resistivity surveying in geothermal exploration at a hot spring in Kasane region, northwest of Botswana.

C. D. Ramotoroko[1], A. P. Thiede[2], E. M. Shemang[1], A. G. Junge[2]
[1]Botswana International University of Science & Technology, Department of Earth & Environmental Sciences
[2]Goethe University Frankfurt am Main, Institute of Geoscience

Corresponding author email: ramotorokoc@biust.ac.bw

Geothermal exploration involves geology, geochemistry and geophysics. In geophysical exploration, resistivity surveying plays the most important role in delineating the reservoir and heat source. The resistivity measurements are one of the most powerful surface exploration tools in geothermal prospecting as they give an indication of the sub-surface temperature, prior to drilling. The parameters that control the geothermal system show a strong response to electrical resistivity. The resistivity method that is currently used in geothermal exploration at Kasane hot spring region is magnetotellurics. The application of this method is discussed in this research together with its preliminary results.

Preliminary results are derived from two-dimensional (2D) inversion of magnetotelluric data acquired along two parallel profiles within Kasane hot spring region. 2D electrical resistivity models show significant lateral variation. The area is characterized by thin conductive cap on the outer margins underlain by higher resistive structure. The previous studies of resistivity in high temperature geothermal systems around the world have shown similar model.

Keywords: magnetotelluric, resistivity, geothermal, Kasane, Botswana

BIUST Research and Innovation Symposium 2019 (RDAIS 2019)
Botswana International University of Science and Technology
Palapye, Botswana, 4 - 7 June 2019
ISSN: 2521-2292

Survival and growth of vetiver (*Vetiver zizanioides*) in mine tailings amended with cow manure and mycorrhizal fungi

Kushatha P. July and Venecio U. Ultra. Jr.
Department of Earth and Environmental Sciences, Faculty of Science, Botswana International University of Science and Technology, Palapye, Botswana
ultrav@biust.ac.bw

Abstract

To enhance the phytoremediation potential of *V.zizanioides*, this study was conducted to assess the influence of cow manure amendments and mycorrhizal inoculation on the survival and growth of this heavy metal accumulating grass in the tailings of the BCL mine in Selebi-Phikwe, Botswana. A pot experiment was carried out for 20 weeks involving 10% amendment of cow manure and arbuscular mycorrhiza inoculants. The four treatment combinations are T1 (pure tailings), T2 (Tailings +10% cow manure), T3 (tailings + mycorrhiza) and T4 (Tailings +cow manure +mycorrhiza). The BCL tailings used in the experiments have a pH of 4.07, EC of 3.16 mS/cm, 2399.60 mg/kg Cu, 613.20 mg/kg Mn, 411.60 mg/kg Ni, 169.20 mg/kg Pb and 180 mg/kg Zn. The cow manure used had a pH of 9.0 and tailings mixed with cow manure had a pH of 7.5. Eleven weeks after planting, *V.zizanioides* had very low survival rate in treatments involving pure mine tailings. However, cow manure amendments had increased its survival to 100% regardless of the presence of mycorrhiza. Mycorrhiza inoculation alone slightly enhanced the survival of *V.zizanioides* in pure tailings. Based on the plant height of the grasses, *V.zizanioides* grown in pure tailings had a slower growth rate of 3.73 cm/week as compared to the growth rate of 8.04cm/week of *V.zizanioides* grown in tailings + cow manure. Mycorrhiza inoculation likewise enhanced the growth rate up to 8.58cm/week in treatments involving tailings + cow manure + mycorrhiza. The number of shoots was also significantly enhanced by cow manure amendments and mycorrhiza inoculation by more than 200%. The results reveal that tailings amended with cow manure and mycorrhiza yielded the best results for *V.zizanioides* growth and survival, followed by tailings amended with cow manure alone. Overall, the results indicated that cow manure amendment improved the potential of *V.zizanioides* as phytoremediation agent in BCL tailings and with mycorrhiza inoculation, together could further enhance the growth and survival of these grasses under this environment. It appeared that cow manure played a significant role by increasing soil pH and together with mycorrhiza, enhanced the nutrient supply essential for plant growth, hence better growth and survival of *V.zizanioides*.

Key Words: Cow manure, Cu-Ni mine tailings, growth rate, heavy metals, mycorrhiza,

BIUST Research and Innovation Symposium 2019 (RDAIS 2019)
Botswana International University of Science and Technology
Palapye, Botswana, 4 - 7 June 2019

ISSN: 2521-2292

Temporal dynamics of heavy metals from different mine tailings and contaminated soils as influenced by soil amendments based on lysimeter studies

Trust Manyiwa and Venecio U. Ultra. Jr. *
Department of Earth and Environmental Sciences, Faculty of Science, Botswana International University of Science and Technology, Palapye, Botswana
ultrav@biust.ac.bw

Abstract
The study was conducted to assess the influence of fly ash (FA) and compost on the heavy metal dynamics in the mine tailings from BCL mine (BCL), Mupane Gold mine (MuG) and Monarch gold (MoG) mine through a modified lysimeter. The modified lysimeters are made of 85cm and 100cm long HDPE pipes installed with micro-rhizon samplers at 15cm, 30cm and 60cm down the surface, filled-up with soils and the amendments were applied at the upper 20cm of the column at the rate of 10% FA or compost (by weight of the 20cm layer soil). Periodic sampling of soil solution (SS) at different depths were carried at two weeks interval for a period of four months for chemical characterization. Results showed that FA and compost had variable influence on several soil parameters depending of the soil type. In MuG, FA increased the pH of the SS from surface layer while compost have the opposite effect. The SS-pH decreased down the lower depth during the different sampling period. The SS- EC from MuG tailings was reduced due to FA and compost amendments as compared to the control. For the tailings from MoG, FA and compost amendments increased the SS-pH and the SS-EC at the surface while in BCL, the SS-pH acidified through time at different depths, but the acidification was slightly reduced by the FA and compost. The concentrations of As, Cu, Ni, Mn and Cr in the SS had increased down the profile during the experiments without amendments. Fly ash and compost increased the concentration of Cr, Mn, and Ni at initial stage of the experiment but reduced the concentration of As, Ni, Mn, and Cr after four months of sampling in MuG. For MGM tailings, FA increased the concentration of Cr. Cu and As while compost reduced the Mn, Ni and As in the soil solution extracted at the surface layer. Overall, these results had demonstrated that FA and compost amendments could influence the availability of different heavy metals not only at the surface where the amendments were applied but its influence could be manifested down the soil column.

Keywords: Compost amendments; fly ash amendment; heavy metal dynamics; heavy metal solubility; modified Lysimeter

BIUST Research and Innovation Symposium 2019 (RDAIS 2019)
Botswana International University of Science and Technology
Palapye, Botswana, 4 - 7 June 2019
ISSN: 2521-2292

Forensic Science Practice in Botswana: Prospects & Challenges.

Paul Ogbole Peter (Bmls,Aimls,Pdm)

Director: Labscroll medicals

Francistown, Botswana

ogbolepp@yahoo.com

Forensic science is an act where science and technology are combined and geared towards solving man's daily need. These important and growing scientific world with diverse application in sports, medicine, Judicial/legal system, Tourism, Food industry etc. have seen a tremendous growth in many parts of the world.

The place of YSTR chromosome as an adherent forensic procedure in the administration of justice, animal tracking system as an antipoaching tool, forensic toxicology etc. are current forensic tools that will assist the various sectors of our economy in Botswana.

However, Botswana a nation which has achieved an acrued peace profile from other nations of the world with visible stability in the economy, democracy , rule of law and growing population ranking high in the mining , tourism industry and sporting world pays little attention to these almighty problem-solving formulae called Forensic science thereby losing over 20 billion dollar annually in Various sectors of the economy.

The aim of the presentation is to X-ray the huge potentials and opportunities in the field of forensic science with particular focus to the Botswana Nation, present relevant data and high light some of the challenges with an utmost aim of steering a clear course of action for the future of Forensic science in Botswana.

BIUST Research and Innovation Symposium 2019 (RDAIS 2019)
Botswana International University of Science and Technology
Palapye, Botswana, 4 - 7 June 2019

ISSN: 2521-2292

Heavy metal speciation and availability in soils from the vicinity of BCL mines as influenced by fly ash and compost amendments

Boitshwarelo Setuwe, Serwalo Mercy Mokgosi and Venecio U. Ultra. Jr.
Department of Earth and Environmental Sciences, Faculty of Science, Botswana International University of Science and Technology, Palapye, Botswana
ultrav@biust.ac.bw

Abstract

Heavy metal availability in soils from mines poses a potential risk to human and ecosystems. Soil remediation amendment might be an option for reducing the degree of heavy metal speciation and availability in mining sites soils. The aim of this study was to evaluate the effect of fly ash and compost amendments on the heavy metal speciation and availability in soils from the vicinity of BCL mine, Botswana. Soil amended with 10% fly ash and 10% compost were mixed and incubated for 32 weeks before sequential extraction. The following extracting solutions were used for sequential extraction based on the method of Tessier (1979): F1- exchangeable using 1M NaOAC; F2-bound to carbonates (1M NaOAC at pH 5); F3-bound to iron and manganese oxides (0.04M NH_2OH-HCl in 25% (v/V) HOAc), F4-bound to organic matter (digested with 0.02M HNO_3 and 30% H_2O_2 heated at 85^{o}C); and F5-residual (HNO_3-H_2O_2 digestion). The heavy metals contents in the extract were quantified using ICP-MS. The soil has a pH of 3.6 and total concentrations of Cr (21475 ppm), Mn (362 ppm), Ni (1029 ppm), Cu (6864 ppm), As (16 ppm) and Pb (101 ppm). Initially, the Cr in soil was dominantly associated with Fe and Mn oxides, followed by those associated with carbonates and organic matter. Compost amendments increased the amount of organic bound Cr in soils. For Mn, compost and FA shifted the amount of Mn to Fe and Mn oxides and carbonates. Compost increased the proportion of Ni bound to Fe and Mn oxides while FA and compost shifted Cu to carbonate bound and OM bound fraction, respectively. FA and compost shifted the As into Fe and Mn oxide fraction from residuals and OM bound fraction. Lead are mostly associated with carbonates in soil. Based on the concentrations of different heavy metals in the exchangeable fractions, FA enhanced the availability of Cr, Mn, Ni and Cu while compost selectively enhanced the availability of Mn and reduced the exchangeable Cu, Ni, and Cr. Overall, the results of this study indicated that FA and compost could trigger changes in the speciation of heavy metal in soils that ultimately influence the availability of these metals to organisms and plants. The degree of influence of FA and compost are metal specific.

Keywords: Compost amendment, Fly ash amendment, Heavy metal speciation, Mine tailings

BIUST Research and Innovation Symposium 2019 (RDAIS 2019)
Botswana International University of Science and Technology
Palapye, Botswana, 4 - 7 June 2019
ISSN: 2521-2292

DESIGN OF A RECYCLING PLASTIC WASTE MINI PLANT

Thabo Mokomo, Emmanuel Kootswetse, Albert Ude
Department of Mechanical, Energy and Industrial Engineering
Botswana International University of Science and Technology,
Private Bag 16, Palapye, Botswana

ABSTRACT

Plastic is a widely used material that has proven indispensable in our lives, but at a heavy cost. Waste plastics, disposed carelessly in our environment are causing a number of health and environmental problems. The aim of this study is to proffer solution by designing a mini plant to convert waste plastic into usable products such as paving tiles as well as curbing its negative effects in our environments.
The mini recycling plant consist of three main machines: (1) the shredding machine, to reduce the waste plastic into workable pellet sizes, (2) the extrusion machine, this will be used to melt and extrude the plastic pellet and (3) compression molding machine, this will be used to shape the extruded recycled plastic into its final product, for this project a paving tiles. The mini plant has potential to reduce the amount of waste plastic that ends up in landfills, and also create job opportunities for Batswana. The results of this project will add to the available resources and for more advanced research where plastics wastes can be used as a resource and not just become waste after performing their primary function in Botswana.

Keywords; Recycling, design, reuse, plastic waste

BIUST Research and Innovation Symposium 2019 (RDAIS 2019)
Botswana International University of Science and Technology
Palapye, Botswana, 4 - 7 June 2019

ISSN: 2521-2292

Characterization of individual atmospheric particles in the Gaborone urban aerosol, using Scanning Electron Microscopy-Energy Dispersive X-ray Spectroscopy (SEM-EDX/EDS)

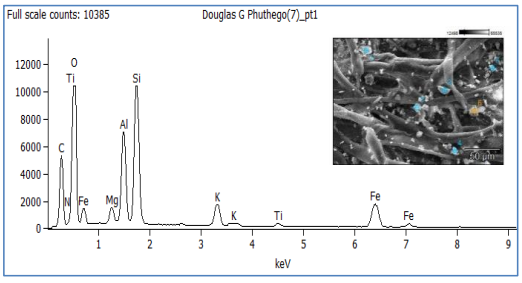
Douglas G. Phuthego[1,*] and Baagi T. Mmereki[1]

[1]*Department of Chemistry, University of Botswana, Botswana*

*Author for correspondence e-mail: dargie12@yahoo.com

***Keywords*:** Urban Air Pollution, Particulate Matter, Public Health, Scanning Electron Microscopy

Ambient air pollution in the urban atmosphere is well documented and is highlighted by air pollution episodes such as The Great London Smog Disaster of December 1952, which was a severe air pollution event mainly caused by the use of coal as fuel, The Donora Pennsylvania Incident of 1948 occurred in Donora in a river valley which was heavily industrialized with a variety of air pollution sources. Atmospheric particulate matter (PM) is linked to a wide range of human diseases and excess deaths due to respiratory and cardiovascular health problems. PM emissions from road traffic have also attracted public attention due to the traffic's high population densities in the urban setting. Numerous studies on urban air pollution have been reported from other countries like US, Canada, Japan, China, UK, etc., and very little have comparatively been done in Botswana. Air pollution is already severe in some large African cities and can worsen due to rapid urban population growth and lack of emission controls. Adverse health effects are found at even lower levels of air pollution and air quality problems are growing in many developing countries. For this reason, research is also needed in Botswana to better understand the chemical and physical properties of complex air pollutant mixtures and identify the possible source sectors, to better quantify their elemental compositions, capturing effects and probably coming up with new mitigation strategies. The method of Scanning Electron Microscopy with Energy Dispersive X-ray spectroscopy (SEM-EDX) has been widely used in the past to characterize individual atmospheric particles. This project aims at employing this method to characterize ambient PM samples collected from the air of Gaborone city at the campus of University of Botswana (UB), from two sampling sites; an urban site (UB Rooftop) and a roadside site (UB Roadside) in order to decipher the influence of traffic to particle chemistry. Results obtained allowed the qualitative analysis (elemental composition) of the sites being studied, and the possible emission sources of these ambient particles can be predicted. The quantitative analysis of the sites studied was also done by Inductively Coupled Plasma-Optical Emission Spectrometry (ICP-OES).



																													TOTAL ELEMENTS
ALL Identified Elements	C	O	Be	Na	Mg	Al	Si	P	K	Ca	Ti	Cr	Mn	Fe	Cu	Zn	Ge	Mo	Pd	Ag	Sn	Ba	Pm	N	F	S	Cl		27
Empty Filter Paper (Control)	C	O																											2
Rooftop Site	C	O	Be	Na	Mg	Al	Si	P	K	Ca	Ti	Cr	Mn	Fe	Cu	Zn	Ge	Mo	Pd			Ba			F	S	Cl		23
Roadside Site	C	O	Be	Na	Mg	Al	Si	P	K	Ca	Ti	Cr	Mn	Fe	Cu	Zn		Mo		Ag	Sn		Pm	N	F	S	Cl		24

Figure 1: Energy Dispersive (X-ray) Spectrum (EDS Spectra) with SEM image (left) and a list of identified elements for the urban and the roadside sites (right) (Results obtained by SEM-EDX in BIUST).

BIUST Research and Innovation Symposium 2019 (RDAIS 2019)
Botswana International University of Science and Technology
Palapye, Botswana, 4 - 7 June 2019
ISSN: 2521-2292

DESIGN OF A GSM-BASED FINGERPRINT ACCESS CONTROL SYSTEM

*Keene B. Ntesang, Lefika Molebatsi, Mothusi Lebogang, and Adamu Murtala Zungeru

Department of Electrical, Computer and Telecommunication Engineering
Botswana International University of Science and Technology
Private Bag 16, Palapye, Botswana

*keene.ntesang@studentmail.biust.ac.bw; lefika.molebatsi@studentmail.biust.ac.bw;
mothusi.lebogang@studentmail.biust.ac.bw; zungerum@biust.ac.bw

Abstract

Security has become one of the essential human necessities, and with the dynamic culture of living that is heavily invested in technology, access control authorization is paramount. The current generation needs security measures that can quickly adapt to the developments with no hassle. This work provides a possible access control system that will provide versatility through the use of GSM technology and still satisfy the main objective of access control and monitoring. The system incorporates the concept of embedded systems (through the use of PIC microcontroller), biometric data technology (through the use of a fingerprint module) and GSM technology (through the use of a GSM module) to achieve its mandate. The added versatility trait entails providing a security administrator the ability to control and monitor access via a GSM technology remotely. The process is done by sending a short message service (SMS) notification to the administrator's mobile phone every time enrolled and non-enrolled users request and/or gain access to the restricted area, regardless of the security administrator being within or outside the vicinity of the restricted access area. For non-enrolled users whose fingerprints have not been stored in the security system, the administrator has an option of granting/denying the user access through an SMS request response in cases where the administrator is not within the vicinity of the restricted access area.

Keywords

Global System for Mobile Communication (GSM); Peripheral Interface Controller (PIC) microcontroller; Biometry; Access Control

BIUST Research and Innovation Symposium 2019 (RDAIS 2019)
Botswana International University of Science and Technology
Palapye, Botswana, 4 - 7 June 2019

ISSN: 2521-2292

PGEs in chromitite concentrated by exsolution?

Alexander Proyer
Department of Earth and Environmental Sciences
Botswana International University of Science and Technology
Palapye, Botswana
proyera@biust.ac.bw

Abstract

At least two interesting problems exist with regard to chromitites of different origin: One is exemplified by chromite-rich layers in layered intrusions which are also characterized by abundant sulfides and enrichment of platinum group elements (PGEs). The other problem concerns ophiolite-related chromitite pods, reported particularly from the Himalayan and the Ural mountain chains, where elaborate mineral separation efforts have led to the recovery of not only diamonds but also a great variety of highly reduced minerals like carbides, metals and alloys. Adding to existing models, an alternative view is presented here, which highlights the potential crucial role of chromite itself as a trigger of reduction reactions in its vicinity.

This model is based on the evidence of high-grade garnets exsolving rutile and ilmenite which requires an open system behavior of the mineral, i.e. diffusional ion exchange with the matrix in order to accomplish exsolution [1]. Importantly, the fastest exsolution reaction envisaged is a redox-reaction: Ti on the octahedral site is replaced by a Fe^{2+} from the dodecahedral site, which, in the process, oxidized to Fe^{3+}. The net result of the entire complex reaction is release of Fe^{0} (or Fe2+ + 2 e^{-}) from garnet, causing reduction in the environment. This mechanism is possible because Fe can occur in garnet in two possible structural positions demanding different valence states. The same holds true for the spinel group and thus for chromite.

For chromite, a mechanism can be envisaged, which also requires open system behaviour, perhaps in a slowly cooling environment: Lattice strain caused by reduced miscibility of ulvospinel causes Ti to diffuse out of the crystal, most likely in reduced form, while Fe is oxidized internally and a divalent ion from the matrix replaces Ti on its site: $TiFe_2^{2+}O_4 + Fe^{2+} = Fe_3O_4 + Ti^{3+} + e^{-}$.

A chromite-dominated rock could thus cause significant reduction in the rock matrix, which could result in PGEs precipitating, as well as available volatile species getting very reduced, thus potentially contributing to the formation of metals and elemental carbon, e.g. as diamond. The validity of this theory can be tested in several ways: The exsolved Ti should be found in some form in the vicinity, which is documented in the present study, and a significant difference in Ti-content and/or P-T history must exist between chromitites with and without reduced phases.

An entirely different alternative explanation is to assume the source of particular chromite occurrences and its PGEs or reduced minerals in the D‘‘ layer at the bottom of the mantle, entrained by an ascending plume and deposited where this plume material is inserted into the crust. This hypothesis assumes that the D‘‘ layer is largely a product of the differentiation of the metallic outer core and its interaction with the lowermost mantle.

Keywords: Platinum, PGE, chromitite, exsolution, redox reactions, ultra-reduced minerals

BIUST Research and Innovation Symposium 2019 (RDAIS 2019)
Botswana International University of Science and Technology
Palapye, Botswana, 4 - 7 June 2019
ISSN: 2521-2292

Gem diamond growth caused by exsolution?

Alexander Proyer
Department of Earth and Environmental Sciences
Botswana International University of Science and Technology
Palapye, Botswana
proyera@biust.ac.bw

Abstract

Exsolution is a common phenomenon in solid solution minerals of crustal rocks that cooled from magmatic or high-grade metamorphic conditions, but corresponding textures are not preserved if the cooling history was too slow, as then exsolutions segregate to the rock matrix. Until recently, exsolution phenomena have not been linked to redox reactions, but Proyer et al. (2013) have shown that some types of exsolution, like that of rutile or ilmenite in garnet and some other rock-forming minerals requires additional (diffusional) exchange of ions with the rock matrix and that the fastest potential mechanism found to date is actually a redox mechanism. Ti on the octahedral site of garnet is replaced by a Fe^{2+} from the dodecahedral site, which, in the process, oxidized to Fe^{3+}. The net result of the entire complex reaction is the release of Fe^{0} (or Fe^{2+} + 2 e^{-}) from garnet, causing reduction in the environment. This is supported by observations that primary rutile inclusions in garnet and sometimes matrix rutiles obtain a bluish to purplish black colour, which is a sign of increasing amounts of Ti^{3+} in the structure. Other evidence might be in some cases the formation of nano-diamonds or graphite in CO_2-bearing fluid inclusions.

If we consider the above observations and their interpretation valid, we can envision on a broader scale that any unmixing of Ti from a high-grade Fe-bearing mineral where Ti^{4+} substitutes (mainly) for Al^{3+} might operate in a similar fashion, i.e. the energy of lattice strain generates a diffusional reducing current to the matrix. If matrix reduction is very localized as by the formation of a few nuclei of diamond from carbonate or CO_2-bearing pore fluid, a few larger crystals of diamond would buffer and accommodate the reduction reaction.

All minerals in an upwelling mantle current or convective flow would be subject to decompression, some cooling and an unknown degree of compositional adjustment. Exsolution phenomena can be expected in the uppermost asthenosphere where cooling starts to predominate over decompression effects. Material caught by deep and relatively cool cratonic roots might be a good example for that. Hence this could be a place where exsolution of Ti-minerals (rutile or ilmenite) could create a transient reducing environment in which diamond formation could be favoured if CO_2 or carbonates are present in some form. Ti-rich garnet is also generated within cool lithospheric roots by the infiltration of hot Ti-rich fluids or melts from a deeper mantle source ("mantle metasomatism"), and will later exsolve Ti again during cooling. Such Ti-enriched mineral compositions occur in "sheared peridotites" that have been sampled from these deep lithospheric roots by kimberlite magmas.

Keywords: Diamond, exsolution, redox reactions

BIUST Research and Innovation Symposium 2019 (RDAIS 2019)
Botswana International University of Science and Technology
Palapye, Botswana, 4 - 7 June 2019

ISSN: 2521-2292

From fundamental to applied sciences: A potential new type of batteries and sensors based on stress in crystal structures

Alexander Proyer
Department of Earth and Environmental Sciences
Botswana International University of Science and Technology
Palapye, Botswana
proyera@biust.ac.bw

Abstract

Prior research on a special type of metamorphic schist has revealed that the mineral garnet incorporates a considerable amount of titanium at elevated temperatures, which during subsequent cooling causes significant stress in the crystal structure of garnet that is finally released by exsolution of titanium as the mineral rutile (TiO_2).

This type of exsolution requires (a) a re-arrangement of other cations within the garnet structure so as to compensate for the loss of titanium, (b) a redox reaction that turns Fe^{2+} into Fe^{3+} which replaces Ti^{4+} in its crystallographic site and (c) the release of electrons from garnet which will cause reduction in the medium surrounding garnet.

Overall this corresponds to a series of battery reactions that create a battery effect to the degree that the oxidizing and reducing reaction sites occur at different locations that are kept separate by the crystal structure. The energy source of the battery is the physical stress building up in a solid solution mineral during cooling, which gets released by redox-reaction facilitated exsolution. These reactions are strongly temperature-dependent, hence the electrical current that develops can also be used as a temperature sensor within a limited temperature range.

Taking the very principle of a crystal-stress-driven battery or sensor and applying it to other types of crystals will allow a tailoring of application temperature, battery capacity etc. Such a battery or sensor is for one-time use only but could be "recharged" by re-homogenizing the solid solution crystal by annealing at high temperatures. The battery does not discharge at all at "low" temperatures and is activated only when ambient temperatures approach the diffusion threshold for the redox reactions.

Potential use for such garnet-based batteries or sensors could be found in high-temperature and/or high-pressure applications where regular batteries would not sustain the ambient conditions. If the principle is transferred to other silicates or non-silicates, a much wider range of operating conditions could be made available in a tailored fashion.

Keywords: garnet, battery-effect, sensor, stress-induced redox reactions

BIUST Research and Innovation Symposium 2019 (RDAIS 2019)
Botswana International University of Science and Technology
Palapye, Botswana, 4 - 7 June 2019

ISSN: 2521-2292

Diamond genesis: The ultimate challenge for a petrologist

Alexander Proyer
Department of Earth and Environmental Sciences
Botswana International University of Science and Technology
Palapye, Botswana
proyera@biust.ac.bw

Abstract

There are numerous reasons why diamond is a difficult research subject for a geologist/petrologist: (1) they are extremely rare, expensive and hard to get hold of as research objects, and one must not use destructive analytical techniques, particularly on the larger stones. (2) most diamonds are extremely old (billions of years) and their host rocks may have changed multiple times since their formation. (3) diamonds form at great depth, 10 times deeper that accessible by drilling, so they can never be sampled where they actually form – and their growth environment is not well known – only from fragments brought to the surface by deep (kimberlite) volcanism.

Focusing on the economically most relevant type of diamond occurrence – as xenocrysts in rare magmas sourced deep in the mantle – the paradigm for diamond exploration successful for many decades is ***Clifford's rule*** which states that diamondiferous kimberlites are restricted to old cratons. Such cratons have or had a deep lithospheric mantle root which can be diamondiferous below ca. 120 km depth.

Looking at the broader picture, diamond is thermodynamically stable down to pressure-temperature conditions of the Earth's core, so they could form even in the lower mantle and potentially in the outer core. As diamond is essentially pure carbon, the growth environment can only be derived by comparing inclusions of other minerals in diamond with known or postulated country rocks. Experiments conducted under the extreme pressures and temperatures of the Earth's mantle, down to the core-mantle boundary have revealed what new minerals to expect at these extreme depths in the mantle, and some of these minerals have in fact been found in diamonds, even though they seem to be rather rare. However, most diamonds do not contain any inclusions, so it is hard to adjudicate what quantity of diamonds may have formed in what rock at what depth. Even more recent finds of diamonds with inclusions of Fe-Ni-S-P alloy and reduced gases (H_2, CH_4) indicate a potentially much deeper environment, down to the outermost core. Efforts to correlate trace elements in diamond (like N, B etc.) or isotopic compositions (C, N) with environments or depths of formation have not yet resulted in any reasonable model.

The relatively recent finds of diamonds with sub-lithospheric inclusions tell us that diamond formation is not restricted to old cratons and their mantle roots and that other types of diamond deposits are possible, depending only on the quantity of diamond available at depth, suitable magmas as carriers and a sufficiently rapid penetration of the lithosphere to deposit diamonds in near-surface volcanic rocks.

Keywords: Diamond, paradigm change, superdeep diamond sources

BIUST Research and Innovation Symposium 2019 (RDAIS 2019)
Botswana International University of Science and Technology
Palapye, Botswana, 4 - 7 June 2019
ISSN: 2521-2292

Peridotite xenoliths from Lethlakane: a comparison of geothermobarometers

Alexander Proyer[1], Christoph Hauzenberger[2], Lukas Belohlavek[2]
1: Department of Earth and Environmental Sciences, BIUST, Palapye, Botswana
2: Nawi Graz Geocentre, University of Graz, Graz, Austria
proyera@biust.ac.bw

Abstract
The Letlhakane diamond mine in Botswana produces a great variety of crustal and mantle xenoliths. Major and trace element mineral chemical data were collected from five types of peridotites: spinel- and garnet-lherzolites and -harzburgites as well as spinel-dunites. Most samples display interaction with a melt, forming up to 0.1 mm wide veinlets, which are typically associated with newly grown calcite, phlogopite and clinopyroxene. Spinel-lherzolithe contains spinel up to 1 mm in size within a generally equigranular matrix consisting of olivine, clinopyroxene and orthopyroxene. Spinel-harzburgite is comparable in texture without clinopyroxene in the matrix but newly formed along the melt veinlets. The garnets in garnet lherzolite are up to 8 mm in size, with up to 0,5 mm wide kelyphitic rims. The matrix consists of equigranular olivine, hypidimorphic clinopyroxene and orthopyroxene. Garnet harzburgites are similar in texture but notably rare. Typical porphyroclastic peridotites display a fine-grained olivine matrix, sometimes with relict mm-sized olivine porphyroclasts, as well as clasts of orthopyroxene, clinopyroxene and garnet up to 2mm in size. In 4 Samples an intergrowth of spinel and garnet was found.
Four approaches were used to determine temperatures and pressures: (1) The Al in opx barometer in combination with either the Cpx-Opx thermometer (BREY & KOEHLER, 1990) and the Al and Cr in Ol thermometer (DE HOOG et al., 2010). (2) The cpx-based thermometer and barometer of Nimis & Taylor, 2000), (3) Where possible, samples were cross checked with the Ni in Garnet Thermometer (CANIL,1999). An average geotherm was constructed from these data and compared to the average geotherm for the Kapvaal craton (FULLEA et al., 2011). (4) The remaining samples for which only temperatures could be determined were plotted along these geotherms to increase the data set. Correlations of rock type with depth as well as Cr and rare earth element (REE) content of garnet with depth were investigated.
The highest temperatures were found in porphyroclastic garnet lherzolites with 1200 to 1350C. The pressure for the spinel and garnet bearing mantle xenoliths is around 2.3 GPa, when plotting the calculated temperatures on the the average geotherm for the Kapvaal craton (FULLEA et al., 2011). Pressures range from 3.7 GPa up to 6.1 GPa for garnet bearing xenoliths where the highest pressures occur in porphyroclastic samples.
The various geothermobarometers have different sensitivity to compositional variations (analytical uncertainty). This contribution compares them and shows that some of the most trusted ones are actually the least reliable.

Keywords: geothermobarometry, peridotite xenoliths, Letlhakane diamond mine

BIUST Research and Innovation Symposium 2019 (RDAIS 2019)
Botswana International University of Science and Technology
Palapye, Botswana, 4 - 7 June 2019
ISSN: 2521-2292

Generation of Artificial Waves Optimized for Surfing in a Water Pool

Tiro Gaogape, Lucky Mohutsiwa, Mmilili Thibedi, and Maemo Rathedi

Department of Mechanical, Energy and Industrial Engineering
Botswana International University of Science and Technology, Palapye, Botswana

This work presents how waves can be generated artificially in an inland water pool through motor control agitation of a hydrofoil and a specially designed pool floor. It aims to duplicate Kelly Slater waves by optimizing the wave parameters on a straight water pool. The project is inspired by the fact that today's generation is interested in exotic sports and activities but there is little or no access to naturally occuring waves at oceans since they are only available at certain geographical locations and climates. Its implementation is mostly anticipated for landlocked countries like Botswana, where surfing enthusiasts do not have access to waves at oceans. In order to achieve this project, parameters that characterize a perfect wave have been set as a datum point, these include a wave height of about 2.4 to 3 meters, a wave peel angle of 30°, a medium breaking intensity and a wave section length of 10 meters.The parameters will be simulated on ANSYS software therefore careful optimization will be performed on results in order to generate nearly perfect waves for surfing.

Keywords: Artificial Waves, Optimized Wave, Water pool, Wave Peel Angle, Breaking Intensity

BIUST Research and Innovation Symposium 2019 (RDAIS 2019)
Botswana International University of Science and Technology
Palapye, Botswana, 4 - 7 June 2019

ISSN: 2521-2292

Morphological Classification of Radio Galaxies Using Convolutional Neural Networks

Tselanngwe Seleka and Rodrigo Jamisola Jr

Mechanical, Energy and Industrial Engineering Department
Botswana International University of Science and Technology
Palapye, Botswana

tselanngwe.seleka@studentmail.biust.ac.bw and jamisolar@biust.ac.bw

Abstract

This work proposes a machine learning approach to automatically classify radio galaxies based on their morphology as seen from radio images, and grouped into the Fanaroff and Riley I and II (FRI and FRII) classes. Majority of the SKA's key science programs involve the study of radio galaxies, thus there will be large amounts of radio galaxy data that will need automatic classification by machine computation. We apply a deep learning machine learning technique, namely, the convolution neural network (CNN). To obtain the radio images, we use the FIRST catalog of FRI radio galaxies (FRICAT) and FIRST catalog of FRII radio galaxies (FRIICAT). For each class, we have a training sample size of around 200 images, which have been augmented by their rotated versions. The convolutional neural network has training accuracy of 96% and a validation accuracy of 97% with training losses of 0.12 and validation losses of 0.1. Testing image classification has a total accuracy of 89% for FRI and 90% for FRII.

Keywords: Radio galaxies, fanaroff and riley, morphology, machine learning, convolutional neural network

BIUST Research and Innovation Symposium 2019 (RDAIS 2019)
Botswana International University of Science and Technology
Palapye, Botswana, 4 - 7 June 2019

ISSN: 2521-2292

A FRAMEWORK FOR ENHANCING SECURITY FOR IOT ENABLED BANKING SERVICES

* Pendukeni Phalaagae, Adamu Murtala Zungeru, Boyce Sigweni, and Joseph Chuma

Department of Electrical, Computer and Telecommunication Engineering
Botswana International University of Science and Technology
Private Bag 16, Palapye, Botswana

**pendukeni.phalaagae@studentmail.biust.ac.bw; zungerum@biust.ac.bw;*
sigwenib@biust.ac.bw; chumaj@biust.ac.bw

Abstract

The advent of mobile and wireless communication has led to the emergence of an epitome termed the Internet of Things (IoT). IoT defines a pervasive universe of connected devices through wired and wireless communication for purposes of gathering information, processing and analyze it into meaningful information. IoT allows billions of smart devices to be connected, allowing for mass collection and exchange of information from sensors to objects and the cloud. When intelligent devices interact they transform lives, businesses, vast sectors of the economy and the entire world. The banking sector uses IoT technologies such as smartphones to give their customer's necessary bank to customer relationship and access to real-time, personalized and more engaging solutions to help customers make sound and smart financial solutions. The smart devices, however, have constraints such as limited physical resources short battery life, small memory, and limited computational power. Despite the tremendous benefits of IoT enabled banking systems, a major challenge in online banking systems is security against fraudulent behavior. Banks and other financial institutions have no control over devices used to access online banking systems leading to compromised nodes (devices) and compromised communication channels. Unsecured communication between user devices and banking systems leads to unauthorized access by intruders to customer's confidential financial data hence compromising the data confidentiality and integrity. Therefore, this work aims to do investigations by reviewing existing literature and comparing secure communication methods between IoT enabled banking user devices and banking systems and proposing a framework for enhancing security for IoT enabled banking services.

Keywords: IoT, online banking, fraud, confidentiality, Integrity

BIUST Research and Innovation Symposium 2019 (RDAIS 2019)
Botswana International University of Science and Technology
Palapye, Botswana, 4 - 7 June 2019

ISSN: 2521-2292

Software Defined Radio (SDR) Based Visible Light Communication (VLC) System

Naledi Maniki[1], **Lame Matsuokwane**[2], **Gaopalelwe Sefako**[3], and **Dr. B Basutli**[4]

Botswana International University of Science and Technology(BIUST
naledi.maniki@studentmail.biust.ac.bw
lame.matsuokwane@studentmail.biust.ac.bw
gaopalelwe.sefako@studentmail.biust.ac.bw
basutlib@biust.ac.bw

Abstract

Wireless communication has been used over the years since 1880s. This communication involves the transmission and reception of information between two or more devices without any physical channel. Wireless communication has been using mostly the radio frequency (RF) waves and they have frequency range from 3 kHz to 300GHz. Over the years RF band has been consumed, the 21th century brought along with many challenges to wireless communication. Due to the technological advancements, almost all mobile devices and applications uses wireless communication. There is a demand for high data rates. As the use of wireless devices continues to grow, security of the wireless networks becomes a challenge, and RF waves can penetrate through most of the objects which makes them uncontrollable. The base stations deployed for Rf wireless communications consumes a lot of power and often need cooling systems, this makes them inefficient. Moreover the RF band is experiencing spectrum crunch due to high bandwidth consumption. Research is being done to seek ways to complement RF wireless communication and visible light communication comes to be the best option so far for the following reasons;

- Due to its high bandwidth (10000 times more than RF band).
- Unlicensed spectrum.
- Many applications which are not possible with RF, e.g underwater communication, restricted RF areas like airplanes, vehicular to vehicular communication.
- Security and Efficiency of the system is high.

In our project we present the design and implementation of Software defined radio (SDR) based visible light communication (VLC) system for indoor environment. The visible light communication falls under optical wireless communication. Visible light is part of electromagnetic spectrum and has frequency range from 430THz to 750THz, with these frequencies, high data rates can be achieved. Light Emitting Diodes (LEDs) are used to transmit information and light sensors (photo-diode) are used to receive the information. The semi-conductor properties of an LED allows it to be modulated at very high speeds to transmit information. LEDs will be used for illumination and communication at the same time. The light sensor at the receiving end detects subtle changes in light from the LED and converts them into an small current signals which are then amplified and processed for final output. To achieve this kind of transmission and reception fast and cheap, software defined radio approach is used. In this approach, a general purpose processor (GPP) called Universal Software Radio Peripheral (USRP) is used along with a software called GNU Radio, which is responsible for most of the signal processing. Most of the components that would have been hardware are now software defined in GNU Radio.

Keywords: Software defined radio (SDR), GnuRadio, universal software Radio peripheral (USRP), visible light communication (VLC), Light Emitting Diode (LED), light sensors (photo-diode).

BIUST Research and Innovation Symposium 2019 (RDAIS 2019)
Botswana International University of Science and Technology
Palapye, Botswana, 4 - 7 June 2019
ISSN: 2521-2292

Nutritive value of silage from maize & sorghum inoculated with urea or *Saccharomyces cerevisiae*

Thuto, M.[1], Madibela, O. R.[1], Legodimo, M. D.[1], and Nermark, F.[1,2]
[1]Department of Animal Science and Production, Faculty of Animal & Veterinary Sciences, Botswana University of Agriculture and Natural Resources, P/Bag 0027, Gaborone, Botswana
[2]Botswana Institute for Technology Research and Innovation, P/Bag 0082, Gaborone, Botswana

Abstract

Silage making is one way of preserving forages with high moisture content. In suitable climates, maize is a crop of choice for making silage due to its high digestibility and high energy. However, in arid and semi-arid areas such as in Southern Africa, maize cultivation can be a challenge due to limited soil moisture as a results of erratic and unreliable rainfall. Due to the physiological superiority of sorghum over maize, such as moisture absorbing efficiency, a sorghum crop may overcome mid-season drought and perform better that maize. Therefore, research on silage making using sorghum is worth exploring. However, additives may be needed to ease fermentation in the silo.
This paper determined the quality and chemical composition of maize and sorghum silages inoculated with 0.5% of urea or yeast (*Saccharomyces cerevisiae*).
Maize and sorghum crops were planted at Botswana University of Agriculture & Natural Resources (BUAN) and harvested at 3 months after planting (at milk stage). The material was chopped using hand secateurs, treated with additives and ensiled in silos (500ml plastic bottles), excluding air by compaction. After 21 days, samples were evaluated for chemical composition, gross energy and fibre components (ADF, NDF and ADL) using standard methods. *In vitro* gas production was estimated by incubating silage samples with rumen fluid in 100 ml glass syringes. Another set of samples were serially tested for pH and temperature over a period of 0, 2, 4, 7, 14 and 21 days.
There was no significant difference between treatment on pH, temperature and gas production ($P>0.05$), however maize silages showed the lowest pH and highest temperatures compared to sorghum silages. Sorghum silage inoculated with yeast had the highest pH of 4.45 whereas maize silage without additives had the lowest pH of 4.05. Silages without additives had the lowest pH for both crops. Serially measurements showed that pH decreased as time progresses but temperature fluctuated until becoming constant at 26.7°C. Also there was no difference between treatment on dry matter (DM), acid detergent fibre (ADF), neutral detergent fibre (NDF) and gross energy of silages from both crops. There was a difference between treatments ($P<0.05$) on dry matter content, ash, crude protein (CP) and acid detergent lignin (ADL). Sorghum silages had the highest values on dry matter content, ash and ADL whereas maize silages had highest CP value. Silages without additives had high amount of DM content and ADL with sorghum having the highest value (36.73% DM content and 2.22% ADL respectively). The least dry matter content and ADL was from maize silage treated with urea (19.15% and 1.70% respectively). Sorghum silages also had the highest amount of ash (11.77%) while maize had the lowest amounts (9.02%). Maize/yeast silage had the highest CP content (17.86%). Sorghum without additives had the least content of CP (10.16%). This indicate that additives improved silages of both maize and sorghum forages. And local farmers who may not have access to urea feed grade or yeast may use common urea fertilizer as additive and/or brewer's spent yeast from brewery or local beer making to substitute for feed grade urea or yeast respectively.

Keywords: Chemical composition, Maize, Silage, Sorghum, Urea, Yeast

BIUST Research and Innovation Symposium 2019 (RDAIS 2019)
Botswana International University of Science and Technology
Palapye, Botswana, 4 - 7 June 2019

ISSN: 2521-2292

Optimal Considerations Constraints of Hybrid Energy Harvesting System for Seismic Network

[1]Dauda Duncan, [1]Adamu Murtala Zungeru, [1]Mmoloki Mangwala, [2]Bakary Diarra, and [1]Joseph Chuma

[1]Department of Electrical, Computer and Telecommunication Engineering
Botswana International University of Science and Technology
Private Bag 16, Palapye, Botswana

[2]Department of Electrical Engineering, Institute of Applied Sciences, University of Sciences, Techniques and Technologies of Bamako (USTTB), Bamako, Mali

[*]duncan.dauda@studentmail.biust.ac.bw; zungerum@biust.ac.bw; mangwalam@biust.ac.bw; diarrab@biust.ac.bw; chumaj@biust.ac.bw

Abstract

Single energy source and energy bank has not been able to energize seismic network and most often characterized by failure, degrade of reliability and introduction of low frequency noise as well as creation of gaps in the seismic database. An Optimized hybrid energy harvesting system of more than one source delivers a continuous and reliable power supply. Considerations constraints such as a rise in temperature of solar cells, self-discharge and current leakage of energy banks are optimized. Using models of prevailing Maximum Power Point Tracking in PSIM simulating tools, Matlab and Minitab programs. Based on reviews, an optimized hybrid energy harvesting system of photovoltaic and thermoelectric transducers has continuous, reliability, steady, high efficiency and no moving parts so therefore suitable for seismic instrumentation.

Keywords- Solar cells, thermoelectric, energy bank, MPPT

BIUST Research and Innovation Symposium 2019 (RDAIS 2019)
Botswana International University of Science and Technology
Palapye, Botswana, 4 - 7 June 2019
ISSN: 2521-2292

Autonomous Quadrotor Risk Minimization for Law Reinforcement Applications

Onalethata Maswabi
Department of Mechanical, Energy & Industrial Engineering
Botswana International University of Science and Technology, Botswana
magnivecotechb14@gmail.com

Abstract

The focus of the research is to develop an on-board adaptive quadrotor algorithm for localization and navigation system in both GPS accessible and denied locations. The practical implementation is to upgrade police system software for law endorsement during search and rescue, hovering, traffic examinations, target locking and following. The fully functional algorithm is dependent on a inertial measurement unit (IMU), vision-based sensor and a navigation system for precise and reliable coordinates. Thus, some of the favorable characteristics of the system will be online learning and real-time control. The navigation system is also capable of operating without internet and satellite connections by automatically generates accurate satellite orbital data using previous broadcast satellite ephemeris data, traveled ground distance and data logging applications. The motion dynamics, velocity and acceleration of the quadrotor is measured by the IMU sensor. A camera, fore-mentioned as a vision-based sensor is used for motion tracking, object detection, monitoring horizontal motion and speed. The optical flow is computed by using the pyramidal implementation of the Lucas-Kanade algorithm coupled with a rich texture point detector. The GPS sensor computes the position of the robot from connected GPS or downloaded obit data. Using sensor fusion, Kalman filter is used to estimate the position and velocity of the object between camera consecutive frames using data from all sensors. At this early stage, the results of this research cannot be presented as a numerical value but based on the performance evaluation of the overall system. In the meantime the research is ongoing and results are measured based on similar researches.

Keywords: Kalman filter, motion tracking, global positioning system (GPS), quadrotor, optical flow

BIUST Research and Innovation Symposium 2019 (RDAIS 2019)
Botswana International University of Science and Technology
Palapye, Botswana, 4 - 7 June 2019
ISSN: 2521-2292

BIOMETRIC FINGERPRINT RECOGNITION IN FORENSIC SCIENCE; A SMART APPROACH

Botho Modukanele and Onalethata Maswabi
Department of Chemical & Forensic science
Department of Mechanical, Energy & Industrial Engineering
Botswana International University of Science and Technology
Palapye, Botswana
botho.moduks@gmail.com *and* magnivecotechb14@gmail.com

Abstract

One of the objectives of this research is to develop fast, reliable and automated algorithm for pattern recognition, classification and matching of digitized fingerprints. The algorithm employs convolutional neural networks as extractors of peculiar texture patterns by ridge skin impressions of the surface of fingers. The system consists of 3 levels which are used to establish the similarity score between two fingerprints and a database for registering and updating users. Fingerprints for all fingers of both hands and a mugshot will be manually registered into the database with binded personal information like gender, family members, marital status and genetic and other health related information. The functional system will enable crime analysts, health department and immigration offices accessible to information rather than each department being a standalone. In level 1 which is the global structure, we classify fingerprints into 3 categories. We estimate global ridge orientations by computing ridge orientation map that encodes the overall ridge flow pattern using CNN for feature extraction. In level 2 which is the local structure, fingerprints are further classified into 14 categories. The advantage of categorizing fingerprints is to reduce computation time during fingerprint matching. Each category represents a spatial location or shape type of ridge ending or termination. This introduces level 2 feature extraction. We feed the CNN of 200 hidden layers with image blocks from the original image and enhancement filters for removing noise. Level 3 utilizes microscopic level patterns for instance, sweat pore locations, scars and ridge geometric details. This level is dependent in the image quality and type of fingerprint acquisition. Thus, in most of the cases level 2 and 3 are used to establish the similarity score between 2 fingerprints using BOZORTH3 algorithm. So far, we have tested the level 1 feature extractor with a single hidden layer. The performance evaluation of the model was 68.9% for classifying images into 3 categories.

Keywords: Convolutional neural networks(CNN), database, feature extraction, fingerprint

BIUST Research and Innovation Symposium 2019 (RDAIS 2019)
Botswana International University of Science and Technology
Palapye, Botswana, 4 - 7 June 2019
ISSN: 2521-2292

High-level density of K-states in neutron-rich tantalum nuclei

N. Palalani,[1] G.J. Lane,[2] G.D. Dracoulis,[2] F.G. Kondev,[3] A.P. Byrne,[2] M.P. Carpenter,[3] C.J. Chiara,[3] P. Chowdhury,[4] R.O. Hughes,[2] R.V.F. Janssens,[3] T. Lauritsen,[3] C.J. Lister,[3] E. A. McCutchan,[3] D. Seweryniak,[3] I. Stefanescu,[3] H. Wanatabe,[2] and S. Zhu[3]

[1]*Department of Physics, University of Botswana, Gaborone*
[2]*Department of Nuclear Physics, The Australian National University, ACT 0200, Australia*
[3]*Argonne National Laboratory, Argonne, Illinois 60439, USA.*
[4]*Department of Physics, University of Massachusetts Lowe, Lowell, MA 01854, USA*

Nuclei in the region around A=180-190 are generally prolate deformed (rugby-ball like shape) with axial symmetry. The single-particle energy levels in these nuclei are defined by the component, Ω, of the nucleon's angular momentum (j), along the nuclear symmetry axis. These components sum to give a quantum number, K=$\sum_i \Omega_i$, that is norminally conserved. Recent progress in studying the structures of these nuclei has been achieved through population methods such as complete and incomplete fussion reactions, deep-inelastic, fragmentation and particle transfer reactions [1–3]. While the neutron-deficiency side had been accessed via complete and incomplete fussion reactions, the neutron-rich nuclei have been achieved mainly from deep-inelastic, fragmentation and particle transfer reactions. Results have shown that at low excitation energies, the observed excited states in these nuclei are predominantly a competition/coupling between the collective states (rotational and vibrational) and the intrinsic K-states [4–7]. The current presentation will discuss the new results in the context of systematic observations of high-K and collective states across the chain of neutron-rich tantalum isotopes. The experimental measurements used an 840 MeV ^{136}Xe beam from the ATLAS facility at Argonne National laboratory, incident on a ^{186}W target with a gold backing sufficiently thick to stop the recoiling reaction products. The Gammasphere array was used to detect the emitted γ-rays. A range of neutron-rich nuclei were populated in the reactions, including ^{182}Ta and ^{183}Ta. New structures and isomers have been observed in neutron-rich ^{182}Ta and ^{183}Ta. The spins, parities, and configuration were investigated in terms of both the available spectroscopic information as well as self-consistent Lipkin-Nogami pairing calculations. Contrary to what is expected, both the calculations and experimental results suggest a high density of intrinsic states, forming the yrast line at high excitation energy. Limited collective states are observed. A similar pattern in this region has been observed to emerge in neutron-rich tungsten isotopes [8, 9].

[1] R. Broda, J. Phys. G: Nucl. Part. Phys. **32**, R151 (2006).
[2] M. Pfutzner et al Phys. Lett. B **444**, 32 (1998).
[3] G. Lovhoiden et al Phys.Scr. **22**, 203 (1980)
[4] C. Wheldon et al, Eur. Phys. J. A **5**, 353 (1999).
[5] G. J. Lane et al, Phys. Rev. C **80**, 024321 (2009).
[6] T. Shizuma et. al, Eur. Phy. J. A **39**, 263 (2009).
[7] N. Palalani et al, EPJ Web of Conferences **35**, 06004 (2012).
[8] C. Wheldon et al., Eur. Phys. J. A 20, 365 (2004).
[9] G. J. Lane et al., Nuclear structure 2012 conference, unpublished http://ns12.anl.gov/program.shtml

BIUST Research and Innovation Symposium 2019 (RDAIS 2019)
Botswana International University of Science and Technology
Palapye, Botswana, 4 - 7 June 2019
ISSN: 2521-2292

The technical and economic feasibility study to produce chemical Fertilizers in Botswana

Bokamoso K. Phuthego & Prof Paul Agachi

Department of Chemical, Materials & Metallurgical Engineering
Botswana International University of Science & Technology

Private Bag 16, Palapye, Botswana

bokamoso.phuthego@studentmail.biust.ac.bw

agachip@biust.ac.bw

Abstract

The purpose of this study is to assess the techno economic feasibility of starting and operating a chemical fertilizer plant in Botswana. Currently Botswana imports approximately 28,000 tons and 500 tons of Ammonium nitrate and Urea respectively. This is worth a collective total of $12.5million per year. The exploration of coal bed methane (CBM) by Kalahari Energy in central Botswana has yielded positive results so far, and they are confident that they will soon garner a sustainable gas off-take agreement from customers who purchase in bulk. A feasibility study instituted by the government of Botswana estimated natural gas content approaching 196Tcf (5.6 trillion cubic meters) over a 50 000 km^2 area underlain by Karoo carbonaceous sediments and coals. This gas can be reformed by means of steam to produce hydrogen that will subsequently be used to produce ammonia. It is from this ammonia with which a plethora of chemical fertilizers such as Ammonium nitrate, Urea, LAN etc. can be processed. A part of the feasibility study is to search for the possibility of using syngas from coal gasification plant in order to produce ammonia and to compare the results with those obtained from methane reforming. Identification and application of more active catalysts could lead to lowering of process temp and/or pressure necessary to achieve a desired space time yield of products. The plant would be built near Selebi Phikwe, in Central district. Assuming a 340-day capacity factor, the daily capacity of 85.3 tons becomes an annual capacity of 29,000 tons at a cost of $46.5million. Payback period would be 5 years.

Key words; chemical fertilizer, syngas, catalysts

BIUST Research and Innovation Symposium 2019 (RDAIS 2019)
Botswana International University of Science and Technology
Palapye, Botswana, 4 - 7 June 2019

ISSN: 2521-2292

A Comparative Study of the High Fluence Neutron Irradiation Effects on the Optical and Structural Properties of Blue and Green Emitting Plastic Scintillators

Gaogalalwe Mokgatitswane and Chamunorwa Oscar Kureba

Department of Physics and Astronomy
Botswana International University of Science and Technology
Private bag 16, Palapye, Botswana
gaogalalwe.mokgatitswane@studentmail.biust.ac.bw

Abstract

The effects of neutron irradiation on the optical and structural properties of blue UPS-923A and green plastic scintillators were investigated. This study focuses on determining how neutron interactions with plastic scintillators affect their desirable properties of high light output and high optical transmission for high energy physics detectors. Samples were bombarded with neutron beams provided by the IBR-2 nuclear research reactor of the Frank Laboratory of Neutron Physics. Light transmission, light yield and fluorescence measurements were performed to study effects on the optical properties, whilst Raman spectroscopy was conducted to assess structural damage. According to the results obtained, neutron irradiation does influence damage in the material. The disappearance of the Raman peak features in green scintillators at frequencies 1165.8, 1574.7 and 1651.2 cm^{1} revealed significant structural alteration due to neutron bombardment. Losses in light transmission, light yield and fluorescence intensity in the plastic scintillators were observed.

Keywords: Neutron radiation, neutron fluence, scintillator, radiation damage, polystyrene

BIUST Research and Innovation Symposium 2019 (RDAIS 2019)
Botswana International University of Science and Technology
Palapye, Botswana, 4 - 7 June 2019
ISSN: 2521-2292

Anticancer activity of novel ruthenium complexes

Sumbikane Gasebonwe[1], Florence Nareetsile[2], Daphne T. Mapolelo[2], Melvin M. Leteane[3] and David O. Nkwe[1]

[1]Department of Biological Sciences and Biotechnology, Botswana International University of Science and Technology
[2]Department of Chemistry, University of Botswana
[3]Department of Biological Sciences, University of Botswana

Correspondence: nkwed@biust.ac.bw; sumbikane.gasebonwe@studentmail.biust.ac.bw

Abstract

Cancer incidence and mortality are expected to rise by the year 2030. Currently, lack of effective treatment for cancer is one of the contributing factors. Clinical chemotherapy is dominantly reliant on platinum agents such as cisplatin and carboplatin, which have limitations due to drug resistance and toxicity. Here we present a novel ruthenium complex that showed anti-proliferative activity on HeLa cells, a cervical cancer cell line.

As cervical cancer is the most common cancer type in Botswana, ruthenium compounds were tested on HeLa cells. The cells were treated with eight different ruthenium complexes and their ligands. To assess potency of the complexes after treatment, cell viability was measured using the MTT assay. We then determined the amount of the complex required to inhibit cell growth by 50% (IC_{50}). Out of the eight compounds tested, the ruthenium complex $Ru(bbe)(H_2O)Cl_3$ had the highest potency on HeLa cells, with IC_{50} of 52 µM, followed by the bbe ligand with 61 µM. The least potent compound was $RuCl_3(H_2O)$, with IC_{50} of 266 µM.

To understand the mechanism of action of the $Ru(bbe)(H_2O)Cl_3$ complex, apoptosis as the principal cell death mechanism was assessed at different stages: early and late apoptosis. During early apoptosis, phosphatidyl serine (PS) is externalised on the plasma membrane. Therefore, we used Annexin V assay which binds to externalised PS to assess early apoptosis, and PS was qualitatively detected on the plasma membrane of $Ru(bbe)(H_2O)Cl_3$-treated cells. Early apoptosis was further confirmed through the detection of caspase 3, a cell death protease. $Ru(bbe)(H_2O)Cl_3$ increased unit caspase 3 activity by 54 % compared to the control. Finally,

BIUST Research and Innovation Symposium 2019 (RDAIS 2019)
Botswana International University of Science and Technology
Palapye, Botswana, 4 - 7 June 2019
ISSN: 2521-2292

EVALUATION OF SAFFLOWER GENOTYPES FOR GROWTH, YIELD COMPONENTS AND SEED YIELD

Maatla K. Korononeo and Professor Vallantino Emongor

Department of Crop and Soil Science

Botswana University of Agriculture and Natural Resources

Gaborone, Botswana

maatlakagelelo@gmail.com

ABSTRACT

A field experiment was carried out at the Botswana University of Agriculture and Natural Resources content farm, in Sebele which is about 10 km from the city center of Gaborone. The objective of study was to evaluate the effects of safflower genotypes on growth, yield and yield components. The results of the study showed that safflower genotype significantly ($P < 0.05$) increased the yield components flower diameter and seed number/capitulum. However, had no significant ($P > 0.05$) on safflower plant height, branch number, flower number/plant, 100-seed weight and seed yield. The genotype PI 407616-BJ-2131-Turkey had the highest yield of 616.7 kg/ha, but was not significantly ($P > 0.05$) different from the yield of other genotypes in the study. Base on the results it was concluded that safflower has great potential to be grown in Botswana as a multipurpose oilseed crop. It is recommended that this study be repeated because heavy rainfall during the vegetative stage of the crop might have negatively affected the development of safflower because it is a desert plant that requires little water.

Key words: **Safflower, genotype, growth, yield and yield components**

BIUST Research and Innovation Symposium 2019 (RDAIS 2019)
Botswana International University of Science and Technology
Palapye, Botswana, 4 - 7 June 2019
ISSN: 2521-2292

Evaporative Cooling for Botswana: A Case Study

Pradeep K Sahoo
Mechanical, Energy and Industrial Engineering,
Faculty of Engineering, BIUST, Palapye
sahoop@biust.ac.bw

Botswana power consumption in buildings is about 35% of the total electrical energy consumption. Major portion of this energy is consumed by air conditioner for providing comfortable indoor environment. Energy consumption in building rises in typical mid-afternoon summer day. Inevitably, this affects electricity grids' reliability and exerted pressure on public authorities to invest in more power generation capacity. In addition, conventional air conditioning systems contribute to greenhouse gas emission, pollution and carry health risks such as allergies and asthma for building occupants. Hence, there is need to look into air conditioning process to reduce electric energy consumption, in particular the peak load.

Commonly evaporative cooling systems are found in hot and dry climates (e.g., parts of the USA, Middle East, India, Australia etc.) where they operate most effectively. These systems are capable of providing adequate thermal comfort for building occupants and better indoor air quality through displaced ventilation and supply of fresh outdoor air. The principle of water evaporation, to generate a cooling effect through the exchange of sensible and latent between surrounding air and a wet surface, is applied in the design of direct and indirect evaporative cooling systems for thermal comfort application in buildings. As Botswana experiences semi-arid climate, these systems can be used for comfort cooling. Depending on climatic condition, these systems can save up to 75% of energy compared to vapour compression refrigeration (VCR) systems which are being currently used.

A typical evaporative cooling process is shown on psychrometry chart in Fig. 1. Point A refer to outside ambient air (40°C, 12% RH). Theoretically, direct evaporative cooling can produce a temperature of 20°C and 100% RH. Practically, a temperature of 24°C can be achieved, which is ideal for comfort air conditioning.

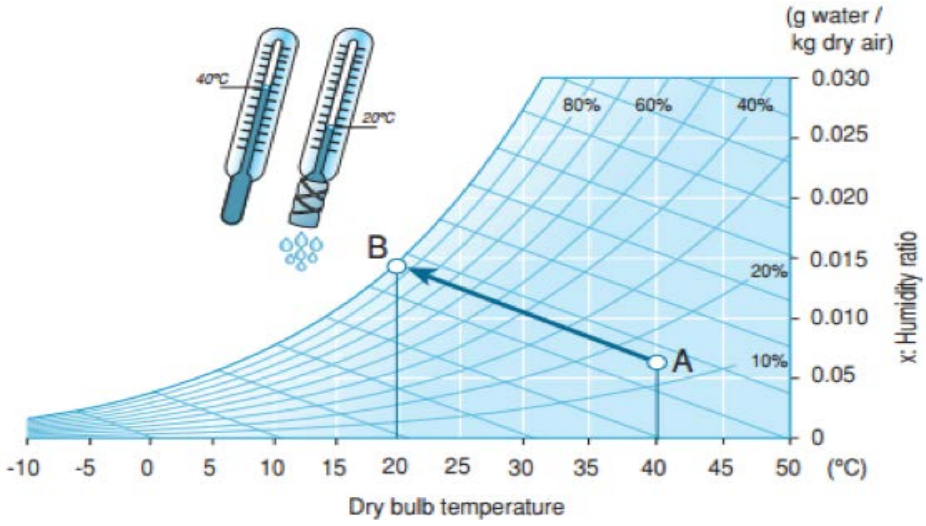


Figure 1. Direct evaporative cooling process on psychrometry chart

Initial investigation shows that such systems will be very useful for Botswana climate.

Keywords: Energy, evaporative cooling.

BIUST Research and Innovation Symposium 2019 (RDAIS 2019)
Botswana International University of Science and Technology
Palapye, Botswana, 4 - 7 June 2019
ISSN: 2521-2292

Program of Activities

ISSN: 2521-2292

Opening Programme

Tuesday, 4 June 2019

RESEARCH & INNOVATION SYMPOSIUM and STEM FESTIVAL 2019

Auditorium, Botswana International University of Science and Technology
Palapye Campus
Tuesday, 4th June 2019
THEME: STEM driven economy: Transforming research into profitable products and services

Director of Ceremonies: Dr Otlhapile Dinakenyane and Dr Peter Eze

08:00 - 08:30	Arrival of Guests and Registration: Led by Ushers
08:30 - 08:35	National Anthem: Led by Palapye Voices
08:35 - 08:40	Opening Prayer: Mrs Gaafele Mochabo
08:40 - 08:45	Introduction of Guests: Deputy District Commissioner, Palapye, Mr Moruti
08:45 - 08:50	Welcome Remarks: Prof. Otlogetswe Totolo, Vice Chancellor
08:50 - 09:00	Overview of the STEM Festival, Research & Innovation Symposium: Dr. Haniso Motlhabane, Director-PUAP
09:00 - 09:05	Music Interlude
09:05 - 09:10	Introduction of Keynote Speaker: District Commissioner, Mr. Rapetse Mathumo
09:10 - 09:25	Keynote Speaker: Hon. Moiseraela Goya, Ass. Minister of Tertiary Education, Research, Science and Technology
09:25 - 09:30	Music Interlude
09:30 - 09:35	Introduction of Guest Speaker: Prof. Otlogetswe Totolo, Vice Chancellor
09:35 - 09:55	Guest Speaker: Mr Albert Milton, Managing Director, Debswana Diamond Mining Company (Pty) Ltd
09:55 - 10:00	Music Interlude
10:00 - 10:20	Keynote Presentation: Mr Tebogo Mogaleemang, Founder & Technical Director, Spectrum Analytics
10:20 - 11:40	Panel Discussions 1. Lieutenant Colonel D.A Dimapo, Botswana Defence Force (BDF) 2. Dr Racious Moatshe - Chief Executive Officer, Local Enterprise Authority (LEA) 3. Mr Meshack Tafa - Deputy Chief Executive Officer, Human Resources Development Council (HRDC) 4. TBA; Morupule Coal Mine
11:40 - 11:45	Vote of Thanks: Distinguished Prof. Dennis Siginer, Deputy Vice Chancellor, Academic Affairs
11:35 - 12:30	Tour of exhibitions by dignitaries
12:30 - 16:00	(See next page)

ISSN: 2521-2292

Program of Activities

Tuesday, 4 June 2019

12:30 - 13:30	**Lunch**		
13:30 - 13:55	**Plenary (Auditorium)** **Speaker: Dr Speech Nelana** **Title: The impact of innovative research on sustainable development**		
Afternoon Talks 14:00 - 15:25	Chemistry, material science, and energy [Physics Seminar Room]	Computing, electrical, and industries [Auditorium]	Life sciences, environment, and physics [Earth and Environment Seminar Room]
14:00 - 14:20	Thomas Frederick Hermanus Wolmarans, Forensic Ballistic	Yame Nkgowe, Gaborone Smart City: Unlocking a knowledge based economy	Lucy Hopkins, BW Scholars
14:20 - 14:35	Micode Mazhani, Melisew Alula and Davison Murape Enhanced peroxidase-like activity of silver nanoparticles doped magnetic nanoparticles for sensitive detection of L-cysteine	Norman Gwangwava Active role of learning institutions in promoting Fourth Industrial Revolution (4IR)	Onthatile Onalenna and Teddie Rahube Assessing the impact of wastewater irrigation on antibiotic resistance dynamics and bacteria species diversity using soil microcosm experiments
14:35 - 14:55	Bashi Thipe Comparison of measured global solar radiation to estimated global radiation using the Liu and Jordan method for the Locality of Gaborone, Botswana	Tshepang Letshwiti, Mompati Molibe, Patrick Mapulane and Nonofo Ditshego SMART energy Meter	Juliet Eze and Teddie Rahube The role of epidemic plasmids in antibiotic resistance dissemination across different environments
14:55 - 15:10	Kevin Nyoni, Leungo Kelebopile and Lesedi Lebogang Dunaliella salina microalgae medium optimization for lipid production using Response Surface methodology.	Unopa Matebesi, Nonofo Ditshego and Gofaone Mogosetso IGZO TFT versus MOSFET	Thatayaone Popego and Peter Eze Estimating the ls factor of the rusle model in a gis based environment for two semi arid watersheds.
15:10 - 15:25	Mmoloki Makoba, László-Zsolt Szabó and Paul Serban Agachi Variations in kinetics of coal pyrolysis at different size ranges and heating rates using a TGA	Natnael Goshu and Semu Kassa Two stage stochastic bilevel programming using stochastic systematic evolutionary(SSE) methods	Keagile Bati and Tebogo E. Kwape In silico evaluation of phytocannabinoids as peroxisome proliferator-activated receptors (PPARs) agonists for type 2 diabetes mellitus therapy.

ISSN: 2521-2292

Program of Activities

Wednesday, 5 June 2019

08:30 - 08:55	**Plenary (Auditorium)** **Speaker: Dr Soumonni Diran** **Title: Inclusive Innovation and Economic Catch-Up: Multi-sectoral Perspectives for Southern Africa**		
Morning Talks 08:30 - 12:30	Chemistry, material science, and energy [Physics Seminar Room]	Computing, electrical, and industries [Auditorium]	Life sciences, environment, and physics [Earth and Environment Seminar Room]
09:00 - 09:20	Ofentse Rice and Tapiwa Pitso, Developer communities and ecosystem capacity building for the 4IR	Mpiping Etsile Nako, Students' Internet Entrepreneurship Intentions: A Comparative Study of University Students in China and Botswana	Bhamini Kamadu, Inspiring Scientists' portraying female role models in science
09:20 - 09:35	Gordon Tinaye Madamombe, Beaven Utete and Abel Olajide Olorunnissola Potential of agro-waste briquetting for domestic heating and cooking as an environmental management strategy in Rushinga, Zimbabwe.	Mhlambululi Mafu Unlocking monetary value from intellectual property at universities and public research institutions	Tsaone Swaabow Thapelo and Rodrigo S. Jamisola Machine learning for maximum and minimum temperature analytics and prediction at local level
09:35 - 09:55	Ndakidzilo Nthoiwa and Einax Mario Thermal performance assessment of a parabolic trough collector prototype system in Palapye, Botswana	Fastel Chipepa, Broderick Oluyede and Makubate Boikanyo The Beta Odd Lindley-G Family of distributions with applications	Analene Montesines-Nagayo, Bindu Pv, Mazna Said Hamdan Al Saidi, Ammar Yousuf Al Farsi, Ammar Said Al Hosni and Rodrigo S. Jamisola Jr. Autonomous Trash Collector Robot with Wireless Charging System in a Campus Environment
09:55 - 10:10	Resego Phiri, O. P. Oladijo and E. T. Akinlabi Effect of deposition temperature on the wear behavior of WC-Co coated mild steel substrate	Tselanngwe Seleka and Rodrigo Jamisola Morphological classification of radio galaxies using machine learning	Oteng Maphane and Jean Baptiste Gatsinzi On the sphere bundle on Grassmannians
10:10 - 10:25	Emmanuel Karabo Mpodi, Zeundjua Tjiparuro and Oduetse Matsebe Development of a dual axis solar tracking concept using morphological analysis	Karabo Bogaisang, Odirile Gamoshe, Dennis Maina and Abid Yahya Anti-poaching system using wireless sensors	Alexander Proyer Diamond genesis: The Ultimate Challenge for a Petrologist?

ISSN: 2521-2292

Program of Activities

Wednesday, 5 June 2019

10:25 - 10:40	Olekile Tibe, Baghali Guys Mathapa and Othusite Madibela Polyphenols and antiparasitic activity from rangelands plants		Tsaone Swaabow Thapelo Recurrent neural networks for prediction of solar radiation - towards the Green Energy
10:40 - 11:05	**Tea/Coffee Break**		
	Chemistry, material science, and energy [Physics Seminar Room]	Computing, electrical, and industries [Auditorium]	Infrastructures, geology, and mining [Earth and Environment Seminar Room]
11:05 - 11:20	James T.P. Matshwele, Sebusi Odisitse and Florence Nareetsile Synthesis and characterization of ruthenium (ii/iii) polypyridyl complexes with antimicrobial properties	Pollard Pako Mogotsi, Thato Phologolo and N Subaschandar Numerical Fluid Mechanics study of effect of rear slant length on the drag of an idealized road vehicle	Kesalopa Gaopale, Rodrigo S Jamisola Jr and Itumeleng Seitshiro Air blast prediction in blasting operation using artificial intelligence technique
11:20 - 11:35	Bao Motshwanaesi, Botsogo Kefalotse, Thebe Kgare, Tsotlhe Leshetla and Tobias Bader Improving energy efficiency in Botswana's hotel sector - a systematic review of energy audit and management principles and previous findings	Kenneth Bogatsu, Thato Phologolo and N Subaschandar Study of effect of tailgates on the drag of an idealised road vehicle using Numerical Fluid Mechanics	Calistus Ramotoroko, Anneke Thiede, Andreas Junge and Elisha Shemang Resistivity surveying in geothermal exploration at a hot spring in Kasane region, northwest of Botswana.
11:35 - 11:50	Kealeboga Motladiile, Tobias Bader, Marvin Smyth, Adrian Pugsley and Jayanta Mondol Energy requirement analysis for the design of solar photovoltaic micro-grids in Botswana - A study of Jamataka village	Suresh Shanmugasundaram interaction design principles in virtual learning tool	Pradeep Sahoo Evaporative cooling for Botswana: A Case Study
11:50 - 12:05	Godiraone Gaedupe, Michelle Matlapeng, Kamogelo Lesole, Ketshephaone Keisang and Tobias Bader Feasibility study on the utilization of solar-photovoltaic technology for water pumping and electrification of an agro-pastoral farm	Suresh Shanmugasundaram Sustainability in Grid Computing	Kesalopa Gaopale, Rodrigo S Jamisola Jr and Itumeleng Seitshiro Application of artificial neural networks to rredict blast-induced ground vibration in a diamond Mine

ISSN: 2521-2292

Program of Activities

Wednesday, 5 June 2019

12:05 - 12:20	Nametso Linda Moumakwa, Eyitayo Olatunde Olakanmi and Tobias Bader Review on performance and processing of natural fibers for thermal insulation purposes	Analene Montesines-Nagayo, Eugene Vega, Omar Rashid Al Maqbali, Ali Khamis Ali Al Kharusi and Rodrigo S. Jamisola Jr. A Smart and Solar-Powered Solid Waste Segregator with Cloud-Based Wireless Monitoring System in a School Campus	Yvette Matshameko and Peter N Eze The Physico-chemical Properties and Geochemical Mass Balance of Two Weathering Soil Profiles in Letlhakeng
12:20 - 12:35	Mushabi Pule, Segolame Phegelo and Tobias Bader A study of energy performance of hotel buildings in Botswana		
12:35 - 13:30	**Lunch Break**		
13:30 - 13:55	**Plenary (Auditorium)** **Speaker: Frank Kienhofer** **Title: The Road to Sustainable Freight Transport**		
14:00 - 15:30	**Poster Session**		

ISSN: 2521-2292

Program of Activities

Thursday, 6 June 2019

08:30 - 08:55	**Plenary (Auditorium)** **Speaker: Prof. Maurice Onyango** **Title: Nanotechnology and Water: Green Coagulants for Water Treatment**		
Thursday Morning Talks 08:30 - 12:25	Chemistry, material science, and energy [Physics Seminar Room]	Computing, electrical, and industries [Auditorium]	Life sciences, environment, and physics [Earth and Environment Seminar Room]
09:00 - 09:20	Senwelo Issacs	Tebogo Mogaleemang, Leveraging Astronomical 'wonder' for STEM education	Bokani Mtengi Gender Equality in STEM
09:20 - 09:35	Nyaladzi Palalani High-level density of K-states in neutron-rich tantalum nuclei	Babedi Kufigwa and Norman Gwangwava Productivity improvement using value stream mapping in a beef abattoir	Kebareng Moalosi-Court and Edward Lungu Optimal portfolios for an investor who receives stochastic income
09:35 - 09:55	Tobias Bader Status of renewable energy in Botswana - part 1: conventional energy supply, solar potential & framework	Valarmathi B, Kavish Pandit, Charan Kumar Pyla, Chellatamilan T and Abid Yahya Classification of e-commerce online auctions and prediction of seller reputation	Amare Gessesse Environmental biotechnology of extremophiles: application of alkaliphiles for the biological treatment of industrial effluents
09:55 - 10:10	Paul Ogbole Peter Forensic Science Practice in Botswana: Prospects and challenges	Utsav Gupta, Valarmathi B, Santhi K and Abid Yahya Classification of patients data to predict signs of diabetic retinopathy	Thatayaone Lucas Gasebonno and Hatson John Boscoh Njagarah Modelling Substance Abuse in Botswana in Presence of Multiple Amelioration Stages and Outpatient Rehabilitation
10:10 - 10:25	Tobias Bader Status of renewable energy in Botswana - part 2: higher education, research and trends	Temitope Fajemilehin, Abid Yahya, Kibet Langat and Jayeola Opadiji Optimizing cognitive radio deployment in cooperative sensing for interference mitigation	Bosa Mosekiemang and Gizaw Mengistu Tsidu Surface water demand and supply of Gaborone City and surrounding areas: Response to climate change and population increase
10:25 - 10:40	Patrick Kandjise, Kesego Petso, Pelonomi Tito and Bokani Mtengi Design of a solar charge controller for DC-load output	Jeet Parikh, Tariku Alemayehu and Janardan Yadav Integrated solar and wind hybrid system with remote monitoring	Onneile Nomsa Keitumetse and Gizaw Mengistu Tsidu Spatio-temporal drought analysis under a changing climate over Botswana using Standardized Precipitation Evapotranspiration Index

ISSN: 2521-2292

Program of Activities

Thursday, 6 June 2019

10:40 - 11:05	**Tea/Coffee Break**		
11:05 - 11:20		Getahun Bekele, Habtu Hailu and Boikanyo Oganeditse Viscosity type Douglas-Rachford Splitting methods for a zero of the sum of a finite family of maximally monotone mappings in Hilbert spaces	Keletso Gorata Masisi and Goabaone Gaobotse A Review: DNA Recombination technology and different expression systems used in the production of recombinant proteins.
11:20 - 11:35		Lone Godfrey Future Kolobe, Adamu Murtala Zungeru and Joseph Chuma Wireless sensor networks based localization and tracking: roadside livestock monitoring system	Matlhogonolo Rakakae and Sachin Shaw Lamellipodial motility of a squared shaped cell - mathematical model
11:35 - 11:50		Peter Gblorso Drone Forensics: How the growing use of drone creates new challenges for Digital Forensics Investigation	Jakob Michael, Tobias Schrag and Tobias Bader Preservation methods for herbarium specimens in Botswana
11:50 - 12:05		Mpho David and Mmoloki Mangwala A Smart Borehole Water Pumping System	Sumbi Gasebonwe and David Nkwe Anticancer activity of ruthenium complexes
12:05 - 12:20		Adrian Pugsley, Samikannu Ravi, Mervyn Smyth, Tobias Badder and Jeet Parikh SolaNetwork - Integrated and affordable solar energy access solutions for socioeconomically diverse rural communities in Botswana	
12:20 - 12:35		Autlwetse Walter Kgomokhumo, Refilwe Phillip, Tshiamo Jacob and Dr Bokani Mtengi Solar powered led streetlights with auto intensity control for remote area electrification	

ISSN: 2521-2292

Program of Activities

Thursday, 6 June 2019

12:35 - 13:30	**Lunch Beak**
13:30 - 13:55	**Plenary (Auditorium)** **Speaker: Mr Paul Ogbole Peter** **Title: Forensic Science practice in Botswana: Prospects and challenges**
14:30 - 15:00	**Big Bang Science**
15:00 - 16:00	**Closing and Prize Giving Ceremony**

ISSN: 2521-2292

Closing Programme

Thursday, 6 June 2019

RESEARCH & INNOVATION SYMPOSIUM and STEM FESTIVAL 2019

Auditorium, Botswana International University of Science and Technology
Palapye Campus
Thursday, 6th June 2019
THEME: STEM driven economy: Transforming research into profitable products and services

Director of Ceremonies: Mr. Donah Lekwati

15:00 - 15:10	Recognition: Dr Haniso Motlhabane
15:10 - 15:15	Feedback from participants, industry/institution
15:00 - 15:20	Feedback from learner participants
15:20 - 15:30	Research and Innovation Team's observation
15:30 - 15:55	Awarding of Prizes: Prof E. Lungu, Acting DVC Research, Development and Innovation
15:55 - 16:05	Vote of Thanks: Prof A. Ochieng, Director, Research, Development and Innovation

ISSN: 2521-2292

Appendices

BIUST Research and Innovation Symposium 2019 (RDAIS 2019)
Botswana International University of Science and Technology
Palapye, Botswana, 4 - 7 June 2019
ISSN: 2521-2292

Reviewers for Topics 1 & 2

Name	Reviews
A. Life sciences, environment, and energy	
Life sciences	
Casper Nyamukondiwa	8
David Nkwe	9
Gaolathe Rantong	9
Goabaone Gaobotse	9
Kabo Masisi	9
Kebaneilwe Lebani	8
Lemme Prica Kebaabetswe	8
Ofentse Mazimba	8
Tebogo Kwape	7
Teddie Rahube	9
Tshepo Pheko	9
Environment	
Gizaw Mengistu Tsidu	10
Gofetamang Ditalelo	8
Gwiranai Danha	8
Moatlhodi Letshwenyo	7
Peter Eze	10
Peter Eliasson	10
Sithabile Tirivarombo	7
Venecio Ultra	15
Wellington Masamba	10
Energy	
Bakary Diarra	9
Bokani Mtengi	7
Cecil Kingondu	7
Leungo Kelebopile	8
Paul Agachi	5
Said Kutua	9
Samikannu Ravi	11
Tobias Bader	7
Moses Tunde Oladiran	3

Name	Reviews
B. Chemistry, material science, and physics	
Chemistry	
Cecil Kingondu	7
Foster Mbaiwa	8
Gwiranai Danha	8
Jens Andersen	11
Melisew Tadele Alula	9
Paul Agachi	5
Sebusi Odisitse	7
Stephen Majoni	9
Wellington Masamba	10
Material Science	
Bokani Mtengi	7
Cecil Kingondu	7
Cosmas Muiva	8
Davison Murape	7
Eyitayo Olatunde Olakanmi	2
Foster Mbaiwa	8
Melisew Tadele Alula	9
Ofentse Mazimba	8
Philip Oladijo	7
Sebusi Odisitse	7
Tshepo Pheko	9
Physics	
Chamunorwa Oscar Kureba	7
George Chimowa	6
Greg Hillhouse	5
Mhlambululi Mafu	8

BIUST Research and Innovation Symposium 2019 (RDAIS 2019)
Botswana International University of Science and Technology
Palapye, Botswana, 4 - 7 June 2019
ISSN: 2521-2292

Reviewers for Topics 3 & 4

Name	Reviews
C. Infrastructures, geology, and mining	
Infrastructures	
Gabatsoswe Lebitsa	7
Goitseone Malumbela	2
Jerome Yendaw	10
Moatlhodi Letshwenyo	7
Selassie Mayunga	7
Victor Mocanu	7
Geology	
Alexander Proyer	7
Ame Thato Selepeng	12
Fulvio Franchi	11
Jerome Yendaw	10
Kazuyasu Shindo	11
Rahul Verma	10
Victor Mocanu	7
Mining	
Alexander Proyer	7
Kazuyasu Shindo	11
Rahul Verma	10
Raymond Suglo	5

Name	Reviews
D. Computations, electrical, and industries	
Computations - Math	
Habtu Zegeye Hailu	12
Jean Baptiste Gatsinzi	11
Sachin Shaw	13
Semu Mitiku Kassa	12
Subaschandar Narayana Rao	9
Zechariah Mushaandja	12
Computations - Computing	
Rodrigo Jamisola	7
Molaletsa Namoshe	10
Hlomani Hlomani	8
Venumadhav Kuthadi	11
Electrical	
Abid Yahya	10
Adamu Murtala Zungeru	8
Bakary Diarra	9
Mmoloki Mangwala	11
Nonofo M. J. Ditshego	6
Samikannu Ravi	11
Venumadhav Kuthadi	11
Industries	
Eyitayo Olatunde Olakanmi	2
Norman Gwangwava	9
Pradip Kumar Sahoo	8
Said Kutua	9
Zeundjua Tjiparuro	8

ISSN: 2521-2292

RDAIS 2019 Working Committees

Custodian: Prof. Ochieng Aoyi
Overall Chair: Prof. Jens E.T. Andersen
Asst. Overall Chair: Dr. Keaboka Sethebe
Program Chair: Prof. Rodrigo S. Jamisola, Jr.
Asst. Program Chair: Ms. Naledi Kefitile

Program Committee
Prof. Rodrigo S. Jamisola, Jr.
Ms. Naledi Kefitile
Ms. Kebadiretse Lefatshe
Ms. Dineo Sebuso
Mr. Ruwona Wiseman

Publicity and Media Committee
Ms. Tsheboeng Ditapole
Mr. Oganne Kenneth
Mr. Gofaone Masisi

Invitation and Budget Committee
Ms. Masego Baliki
Ms. Lediranye Collie Motshidisi

Exhibition and Events (STEM) Committee
Dr. Keaoboka Sethebe
Ms. Leseka Kaelo

ICT Committee
Ms. Kafuti Ngele
Mr. Tshoganetso Ntebogang

Scientific Committee
Dr. Lesedi Lebogang
Dr. Nonofo Ditshego
Dr. Cosmas Muiva
Dr. Nonofo Ditshego
Ms. Mpho Rapoo

Logistics, Protocol and Security Committee
Ms. Kgomotso Seone
Mr. Lopang Jiba Jiba
Mr. Mothusi Maiswe
Ms. Sego Baiphetlhi
Dr. Tshepo Pheko

Sponsors, Merchandise and Awards Committee
Ms. Emmah Sethibe
Dr. Sithabile Tirivarombo
Dr. Cecil Kingondu
Dr. Steven Majoni

Catering Committee
Dr. Tjiparuro Zeundjua
Ms. Magdeline Ditodi
Ms. Tebogo Mogwato
Mr. Dennis Maina

ISSN: 2521-2292

Author Index

A
Agachi, Paul 125
Agachi, Paul Serban 88
Akinlabi, E. T. 15
Al Farsi, Ammar Yousuf 133
Al Hosni, Ammar Said 133
Al Kharusi, Ali Khamis Ali 134
Al Maqbali, Omar Rashid 134
Al Saidi, Mazna Said Hamdan 133
Alemayehu, Tariku 29
Alula, Melisew 78
B
B, Valarmathi 24, 25
Bader, Tobias 43, 51, 52, 53, 56, 58, 60, 61, 77, 87, 90, 91
Bashaga, Godfrey 38
Bati, Keagile 33
Bekele, Getahun 46
Belohlavek, Lukas 111
Bikimane, Rachel Utlwang 66
Binang, Katso 64
Bird, Tharina L. 62
Bitsang, Mooketsi 81
Blenkinsop, Thomas 108
Bogaisang, Karabo 119
Bogatsu, Kenneth 127
Boikanyo, Makubate 98
Bosigo, Romang 74
Boy, Koketso R. 76
C
Champion, Tshoganetso 124
Chigocha, Tapologo 30
Chipepa, Fastel 98
Chipfupi, Elia 5
Chobolo, Leo Lefang 62
Chuma, Joseph 67, 86, 115, 120
D
Danha, Gwiranani 112
David, Mpho 73
Diarra, Bakary 68, 120
Dikgang, Ofentse 43
Dikinya, Oagile 81
Dintwe, Galaletsang 62
Ditalelo, Gofetamang 55
Dithologo, Kegone T. 76
Ditshego, Nonofo 7, 14, 21, 86
Duncan, Dauda 120

ISSN: 2521-2292

E
Eze, Juliet 12
Eze, Peter 32
Eze, Peter N 31
F
Fajemilehin, Temitope 28
Fana, Elliot 42
G
Gabasiane, Tlotlo 112
Gaboitaolelwe, Jwaone 86
Gaedupe, Godiraone 56
Gamoshe, Odirile 119
Gaobotse, Goabaone 54
Gaogane, Tshepho 112
Gaogape, Tiro 113
Gaopale, Kesalopa 40, 41
Gasebonno, Thatayaone Lucas 39
Gasebonwe, 131
Gatsinzi, Jean Baptiste 3
Gblorso, Peter 72
Gessesse, Amare 44
Gonnye, Naledi 62
Goodwell, Modise 62
Goshu, Natnael 23
Gupta, Utsav 25
Gwangwava, Norman 4, 11
Gwebu, Zimele 75
H
Hailu, Habtu 46
Hauzenberger, Christoph 111
I
Itsanang, Banthatile 43
J
Jacob, Tshiamo 84
Jamisola Jr, Rodrigo 133, 134
Jamisola Jr, Rodrigo S 40, 41
Jamisola, Rodrigo 114
Jamisola, Rodrigo S. 94
Julius, Lebogang 50
July, Kushatha Pabalinga 96
Junge, Andreas 95
K
K, Santhi 25
Kabelo, Tshephang Iris 42
Kandjise, Patrick 48
Kassa, Semu 23
Kefalotse, Botsogo 51
Keisang, Ketshephaone 56
Keitumetse, Onneile Nomsa 47
Kelebopile, Leungo 70
Kenyaditswe, Aobakwe 14
Kerileng, Keoagile 85

ISSN: 2521-2292

Kesemang, Monamodi 62
Kgare, Thebe 51
Kgomokhumo, Autlwetse Walter 84
Kgosiemang, Dimpho 27
Kingondu, Cecil 59
Kolobe, Lone Godfrey Future 67
Koolopile, Edward 129
Kootswetse, Emmanuel 101
Korononeo, Maatla 132
Kufigwa, Babedi 4
Kureba, Chamunorwa Oscar 130
Kurusa, Seth 14
Kwape, Tebogo E. 33

L

Langat, Kibet 28
Lebani, Kebaneilwe 26, 42
Lebogang, Lesedi 70
Lebogang, Mothusi 103
Lefadola, Oarabile 89
Legodimo, Moemedi 117
Lepodise, Lucia 74
Leshetla, Tsotlhe 51
Lesole, Kamogelo 56
Letshwenyo, Tshepho 87
Letshwiti, Tshepang 7
Letsile, Bogadi Pako 66
Lungu, Edward 8

M

Mabutho, Otsile James 83
Madamombe, Gordon Tinaye 5
Madibela, Othusite 19
Madibela, Othusitse 117
Mafu, Mhlambululi 92
Maina, Dennis 119
Makatane, Boitumelo Elizabeth 87
Makati, Tlamelo 27
Makgope, Onkabetse Dennies Omphile 76
Makoba, Mmoloki 88
Malete, Thabo 37
Mangwala, Mmoloki 73, 120
Maniki, Naledi 116
Manyiwa, Trust 89, 97
Maphane, Oteng 3
Maphane, Phalaneng 34
Mapolelo, Daphne 50
Mapulane, Patrick 7
Mario, Einax 6
Marumo, Otlaatla 82
Masamba, Wellington 36
Masenga, Wangu 69
Mashaba, Thabiso 80
Masisi, Keletso Gorata 54

ISSN: 2521-2292

Masu, Bernum 93
Masutlha, Lesego Lilian 18
Maswabi, Onalethata 121, 122
Matebesi, Unopa 21
Mathapa, Baghali Guys 19, 20
Matlapeng, Michelle 56
Matsebe, Oduetse 17
Matshameko, Yvette 31
Matshwele, James T.P. 49
Matsuokwane, Lame 116
Mazhani, Micode 78
Mazimba, Ofentse 18
Mbaiwa, Dr. Foster 16
Mbedzi, Olebogeng 75
Mengistu Tsidu, Gizaw 35
Michael, Jakob 61
Mmemo, Obakeng 43
Mmusi, Keene 13
Moalosi-Court, Kebareng 8
Modukanele, Botho 122
Moganane, Boago 81
Mogatsaseno, Neo 65
Mogosetso, Gofaone 21
Mogotsi, Pollard Pako 126
Mohutsiwa, Lucky Odirile 113
Moilwa, Kagiso 37
Moitoi, Annah Janet 10
Mokgatitswane, Gaogalalwe 130
Mokgethe, Bakang 37
Mokgosi, Serwalo 100
Mokoka, Tshepiso 87
Mokomo, Thabo 101
Molebatsi, Lefika 103
Molibe, Mompati 7
Mondol, Jayanta 53
Moni, Nayna Ann 68
Montesines-Nagayo, Analene 133, 134
Moore, Andrew 108
Morake, Gorata Pearl 66
Mosate, Moses 82
Mosekiemang, Bosa 35
Mosetlhi, Bothepha 81
Mosoboloko, Lame K 82
Mosweu, Kenosi 43
Motladiile, Kealeboga 53
Motlhabane, Taboka 52
Motlhanka, Koketso 26
Motshwanaesi, Bao 51
Motswedi, Kennedy 83
Moumakwa, Nametso Linda 58
Mpodi, Emmanuel Karabo 17
Mtengi, Bokani 48

ISSN: 2521-2292

Mtengi, Dr Bokani 84
Muiva, Cosmas 74
Mukoka, Leungo Daddie 62
Murape, Davison 78
N
Nareetsile, Florence 49, 50
Nermark, Fiona 117
Njagarah, Hatson John Boscoh 22, 39
Ntesang, Keene B. 103
Nthoiwa, Ndakidzilo 6
Nthusang, Pearl 57
Nyoni, Kevin 70
O
Odisitse, Sebusi 13, 49
Odumetse, Obakeng 14
Oganeditse, Boikanyo 46
Oladijo, O. P. 15
Olakanmi, Eyitayo Olatunde 58
Olorunnissola, Abel Olajide 5
Oluyede, Broderick 98
Onalenna, Onthatile 9
Opadiji, Jayeola 28
P
Paakanyo, Katso Rosalie 45
Padiso, Tumelo 71
Paganotti, Giacomo 69
Palalani, Nyaladzi 123
Pandit, Kavish 24
Parikh, Jeet 29, 77
Paul Ogbole Peter, 99
Petso, Kesego 48
Phalaagae, Pendukeni 115
Phegelo, Segolame 60
Pheko-Ofitlhile, Tshepo 36
Phillip, Refilwe 84
Phiri, Resego 15
Phologolo, Thato 126, 127, 128, 129
Phuthego, Bokamoso 125
Phuthego, Douglas Gobe 102
Popego, Thatayaone 32
Proyer, Alexander 104, 105, 106, 107, 108, 111
Pugsley, Adrian 53, 77
Pule, Mushabi 60
Pv, Bindu 133
Pyla, Charan Kumar 24
R
Radipodi, Mpho 55
Rahube, Katlego Seleofeng 87
Rahube, Teddie 9, 12
Rakakae, Matlhogonolo 63
Ramontsho, Gosatla Kelebogile 83

ISSN: 2521-2292

Ramotoroko, Calistus 95
Rathedi, Maemo 113
Ravi, Samikannu 77, 83
Robert, Lasiwe 109
S
Sahoo, Pradeep 135
Samikannu, Ravi 29
Samuel, Nonofo 16
Schrag, Tobias 61
Sebikiri, Kenaleone 93
Sefako, Gaopalelwe 116
Seitshiro, Itumeleng 40, 41
Sekopo, Emmanuel 62
Seleka, Tselanngwe 114
Sephiri, Oteng 93
Serame, Eniah 36
Setuwe, Boitshwarelo 100
Shanmugasundaram, Suresh 1, 2
Shaw, Sachin 10, 38, 63
Shemang, Elisha 95
Sichilongo, Associate Professor Kwenga 16
Sichilongo, Kwenga 65, 69, 71
Sigauke, Morelyn 22
Sigweni, Boyce 68, 115
Smarts, Tagala 27
Smyth, Mervyn 53, 77
Subaschandar, N 124, 126, 127, 128, 129
Szabó, László-Zsolt 88
T
T, Chellatamilan 24
Takuwa, David 64
Telekelo, Kebalebile Oteng 30
Thaolang, Leaname 30
Thapelo, Tsaone Swaabow 94, 110, 118
Thibedi, Mmilili 113
Thiede, Anneke 95
Thipe, Bashi 79
Thuto, Mmoloki 117
Tibe, Olekile 19, 20
Tiro, Bakang 20
Tito, Pelonomi 48
Tjiparuro, Zeundjua 17
Tlotleng, Kaloso Mpho 82
Tsheole, Tshiamo 57
Tsidu, Gizaw Mengistu 47
Tsima, Gaopalelwe 93
U
Ude, Albert 101
Ultra Jr, Venecio 97
Ultra, Venecio Jr 89
Ultra, Venecio U. Jr 96

ISSN: 2521-2292

Utete, Beaven 5
V
Vega, Eugene 134
Venecio, Ultra 100
Vryburg, Maikano 37
Y
Yadav, Janardan 29
Yahya, Abid 24, 25, 28, 119
Yendaw, Jerome A. 45
Yudovskaya, Marina 108
Z
Zhou, Nerve 26, 62
Zungeru, Adamu Murtala 67, 86, 103, 115, 120